UNIVERSITY OF SHEFFIELD

DEPARTMENT OF CIVIL AND STRUCTURAL ENGINEERING

THE ANALYSIS AND DESIGN OF INFLATABLE HYDRAULIC STRUCTURES

by

ALAA H. AL-SHAMI
B.Sc., M.E.(W.R.D.)

A thesis submitted to the
University of Sheffield
for the Degree of
Doctor of Philosophy

September 1982

TEXT BOUND CLOSE TO THE SPINE IN THE ORIGINAL THESIS

PAGE NUMBERS ARE CLOSE TO THE EDGE OF THE PAGE.

SOME ARE CUT OFF

DAMAGED TEXT IN ORIGINAL

To my Dear Wife .

ACKNOWLEDGEMENTS

This research was carried out in the Department of Civil and Structural Engineering of the University of Sheffield under the supervision of Dr. F.A. Johnson.

The author wishes to thank Dr. F.A. Johnson for his guidance, helpful advice and encouragement and excellent supervision throughout the project.

Professor T.H. Hanna is thanked for permission to carry out research in the Department of Civil and Structural Engineering.

Grateful thanks are also due to the departmental technical staff, in particular Mr. G. Brown, for his assistance in the construction of the experimental apparatus.

The operators and staff of the University of Sheffield Computing Service are thanked for their helpfulness and advice.

Financial support was provided by the Ministry of Irrigation, state organization of Tharthar project, Iraq, to whom the author is indebted.

Finally the author wishes to thank Mrs. J. Czerny for typing this thesis.

SUMMARY

The range of possible uses of inflatable hydraulic structures is very great provided a suitable design and analysis technique is available.

The object of this project was to study both theoretically and experimentally the behaviour and performance of inflatable hydraulic structures under both hydrostatic and hydrodynamic conditions for dams inflated with air, water and a combination of the two.

The theoretical anslysis was based on a finite element approach to design a dam under different inflation fluids in order to find the dam parameters of tension, profile of the dam, upstream slope, and elongation of the material under both hydrostatic and hydrodynamic conditions.

A series of models of different sizes were constructed and tested under both hydrostatic and hydrodynamic conditions. A comparison of different output parameters was carried out between the experimental and theoretical results showing a good relationship between the two.

Relationships were derived so that the length of the membrane could be found for the design of a dam to satisfy particular conditions.

A new formula was derived for calculating the rate of flow and coefficient of discharge for all three types of inflation allowing the application of inflatable dam as a device for measuring discharge.

A range of computer programs was written for the analysis and design of all dams based on the finite element approach.

This work was restricted to single anchor dams with the anchor located on the upstream side.

CONTENTS

LIST OF FIGURES

CHAPTER 5.

Page

CHAPTER 8.

LIST OF TABLES

NOTATION

A	cross-sectional area of the channel.
A'	cross-sectional area of the membrane material.
a, a_1	constant.
$\bar{a}$	acceleration.
B	length of the base width of the dam.
B_1	length of the base toward the upstream side.
B_2	length of the base toward the downstream side.
$B\ell$	new length of the element.
b	breadth of sharp crest rectangular weir.
C	dimension coefficient of discharge.
C_1, C_2, C_3, C_4	polynomial coefficients.
C_f	constant.
C_2	constant of integration.
C_D	dimensionless coefficient of discharge.
D	difference between the upstream head and the maximum height of dam.
$d\omega$	depth of fluid inside the dam.
E	normal elliptic integrals of the second kind.
$\hat{E}$	complete elliptic integrals of the second kind.
F	normal elliptic integrals of the first kind.
$\hat{F}$	complete elliptic integrals of the first kind.
F_a	internal air force.
F_a	gravity force.
f	extension ratio of the membrane under load.
f_1, f_2, f_3, f_4	constant.
$f(x)$	analytical function describing the shape of the dam.

g	acceleration of gravity.
H	overflow head.
H'	pressure head along the base.
H_D	maximum height of dam.
H_p	total pressure head.
H_s	depth and silt to be considered.
h_1	depth of water from the centre of element of the upstream side to the free water surface.
h_2	depth of fluid from the centre of the element to the face of the fluid surface inside the dam.
h_3	depth of silt from the centre of element to the face surface of the silt in the upstream side.
h_4	depth of water from the centre of the element to the free surface water level of the downstream side.
h_d	depth of water on the downstream side.
h_e	depth of water over the crest of the dam.
h_u	maximum upstream hydrostatic depth.
K	constant.
L_m	scale ratio of model.
L_p	scale ratio of prototype.
L_r	ratio of L_m/L_p.
ℓ	length of element.
M	mass.
m	constant.
NN	number of nodes.
n	number of element.
n_1	numerical exponent.

p	resultant of internal pressure.
p_a	internal air pressure.
p_i	internal pressure.
p_o	external pressure.
p_r	pressure at an arbitrary point of the membrane of the downstream face.
p_s	upstream silt force.
Q	discharge.
q	flow per unit width.
R	radius of curvature.
R_1	upstream hydrostatic force.
R_2	internal fluid force.
R_3	downstream hydrostatic force.
Re	Reynolds number.
S	total length of the perimeter length of the dam.
S_1	length of the perimeter toward the upstream side.
S_2	length of the perimeter toward the downstream side.
T	horizontal force acting on the dam per unit length (equation 2.2).
T'	force per unit length in a horizontal section of the fabric.
T_1	ultimate tension of the membrane material.
T_A	initial tension at the node x_I, y_I
T_B	tension at the node, xII,yII.
t	thickness of the material.
V	velocity of approach.
V_p	vertical component of the tension per unit length at an arbitrary point (P).

W	horizontal component of water force (equation 2.8).
w	weight of the membrane per unit area.
w_1	dry weight of solid particles.
w_f	weight of element.
w_s	weight of silt submerged.
x,y	co-ordinates.
y_I	vertical co-ordinate of the lower node.
y_{II}	vertical co-ordinate of the upper node.
α	proportional factor.
β	the membrane upstream slope.
γ	specific weight of water.
γ_1	specific weight of fluid inside the dam.
ΔF	difference in the hydrostatic force.
ΔL	elongation of the element.
ε	x/H_D
η	y/H_D
θ	inclination of the membrane in the downstream face.
θ_i	slope of element at node n.
θ_A	slope of the element at x_I, y_I.
θ_β	slope of the element at x_{II},y_{II}.
μ	fluid viscosity.
σ	stress in the fabric.
ϕ	downstream fabric angle at the anchor point.
ψ	defined by equation 2.25
ψ'	upstream slope of the fabric outside of the dam (fig.8.1).
ψ_o	value of ψ at downstream toe.
ψ_1	value of ψ at crest.

CHAPTER 1.

INTRODUCTION

1.1 General.

The concept of fabric hyraulic structures is a relatively new idea and has a wide range of water engineering applications.

The simplest and most common type of inflatable hydraulic structure consists of a single sheet of rubberised fabric folded into a tubular shaped bag which is then sealed in place during installation. The bag is attached by one fixed end toward the upstream side by means of anchor bolts set in a reinforced concrete slab.

This type of structure was originally developed as an adjustable gate to control water levels in rivers and reservoirs. It can be more economical and practical than a conventional steel gate system which requires large concrete abutments and foundations.

In general, according to Connor (1), the cost of an inflatable structure installation varies between one to two thirds of the cost of an alternative steel gate.

The design techniques for inflatable hydraulic structures has been developed for many different considerations and assumptions but is still limited.

The object of this study is to develop a design technique for a dam with a wide range of applications.

Due to the lack of information on the effects of upstream and downstream head with relation to the type of inflation fluids and materials many failures have occurred during dam operations. Limited attention has been given to the theoretical analysis of inflatable structures. The early work on this concept has been carried out by Anwar (2), Owiwara (3), Harrison (4), Binnie (5), Parbery (6) and Alwan (7).

The theoretical analyses developed by the above investigators all have limitations, for example (1) not considering the base length; (2) limiting internal pressurehead to not more than the height of the dams; (3) not considering the weight and thickness of the material (i.e., properties of the materials); (4) using only one type of inflation fluid. The aim of this work was to overcome many of these limitations and hence to have a wider range of application of the method.

In this project a theoretical analysis has been developed using the finite element approach with a computer solution in order to analyse a dam.

In this analysis the possibility of a silt pressure has been considered as a static load on the upstream face of the dam. The theoretical development is discussed in detail in Chapter 4 for static conditions and Chapter 5 discusses the analysis of a dam under hydrodynamic conditions.

A comparison of the theoretical and experimental work is discussed in detail in Chapter 6. When using an inflatable structure as a flow measuring structure it is necessary to determine the coefficient of discharge. The coefficient of discharge is determined experimentally and a series of relationships are given to compute the coefficient of discharge for different types of inflation as detailed in Chapter 7.

The design for the length of the membrane is calculated theoretically with respect to a water inflated case, while the design of the length of the membrane for air or (air+water) cases are found experimentally, and are detailed in Chapter 8.

Chapter 9 is a general discussion and recommendations for further studies on this type of structure are made.

1.2 Applications of Inflatable Hydraulic Structures.

An ever increasing demand for water use and control in most countries of the world requires the use of economic and simple structures in design

and construction. Inflatable hydraulic structures offer such an alternative solution to traditional structures for many such uses.

The following description refers to the more important ones.

1.2.1 Increasing the capacity of existing dams.

Inflatable hydraulic structures can be used to extend the height of an existing dam to increase the storage capacity, by placing the inflatable structure on the top of the crest of the spillway to achieve the required elevation. An example of the extension of a spillway crest is in the Koomboolomba dam of the Tully falls hydro-electric power project in Australia (8) as illustrated in Fig. 1.1.

1.2.2 Inflatable weir structures for the period of construction of a project.

Inflatable hydraulic structures can be used as temporary weir controls during the period of construction of a project, therefore by this arrangement the cost of temporary works can be reduced. This practice has been adopted in Pakistan in the temporary work for the construction of Mangla dam (9) which included an inflatable weir with three inflatable hydraulic structures to regulate the tail water level at the outlet of the tunnels used for the river diversion. The arrangement is illustrated in Fig.1.2.

1.2.3 Flood control.

The purpose of flood mitigation schemes is to reduce the damage caused by flooding and due to the low cost and flexibility of operation inflatable hydraulic structures have found considerable use on such schemes. An example of such a use is in Australia in New South Wales (1).

1.2.4 Controlling the water table.

An inflatable structure has been made in the South of the Netherlands (10) in order to prevent lowering of the ground water table and thus preventing the agricultural land from drying out.

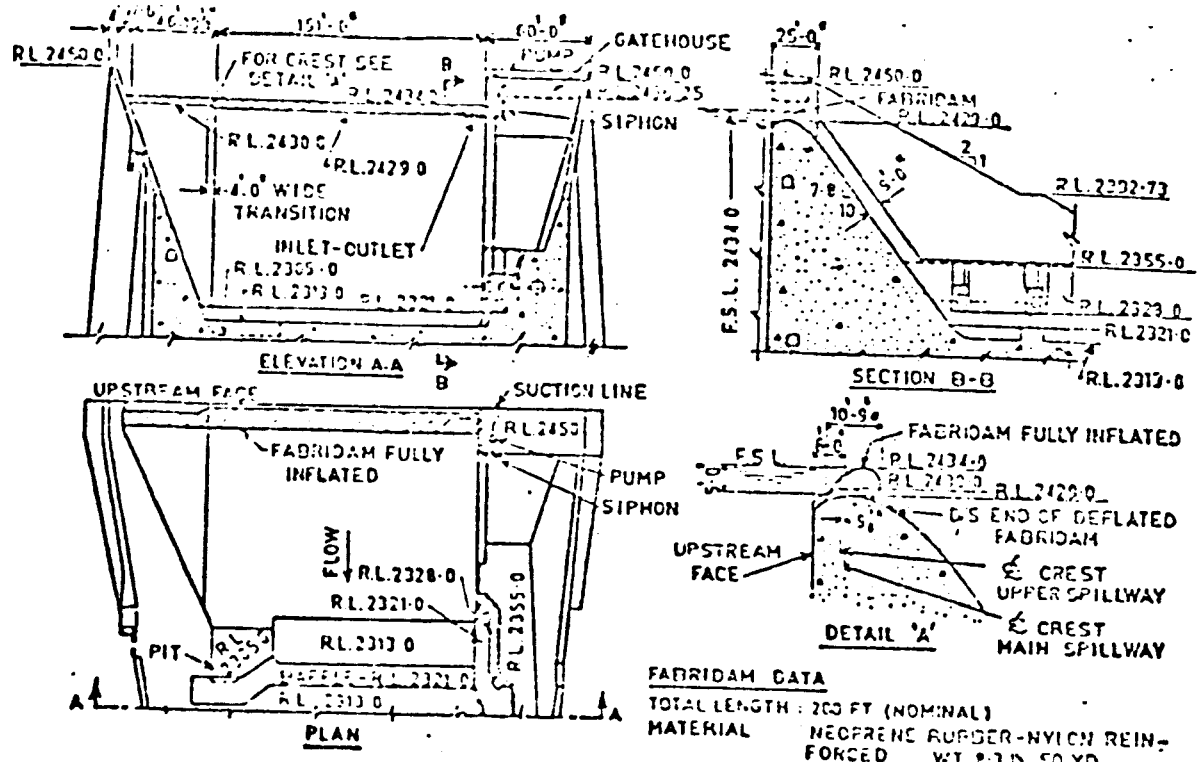

FABRIDAM DATA

TOTAL LENGTH : 200 FT (NOMINAL)

MATERIAL : NEOPRENE RUBBER-NYLON REINFORCED WT 8·0 D SQ.YD. THICKNESS 0·135" BUTYL RUBBER SKIN.

INFLATION : INFLATED WITH WATER TO HEAD 7·4 FT. ABOVE R.L. 2429·0

DEFLATION : AUTOMATIC WHEN FABRIDAM HEAD EXCEEDS 7·6 FT.

FIG. (1-1) INCREASING THE EXISTING HEIGHT OF DAM

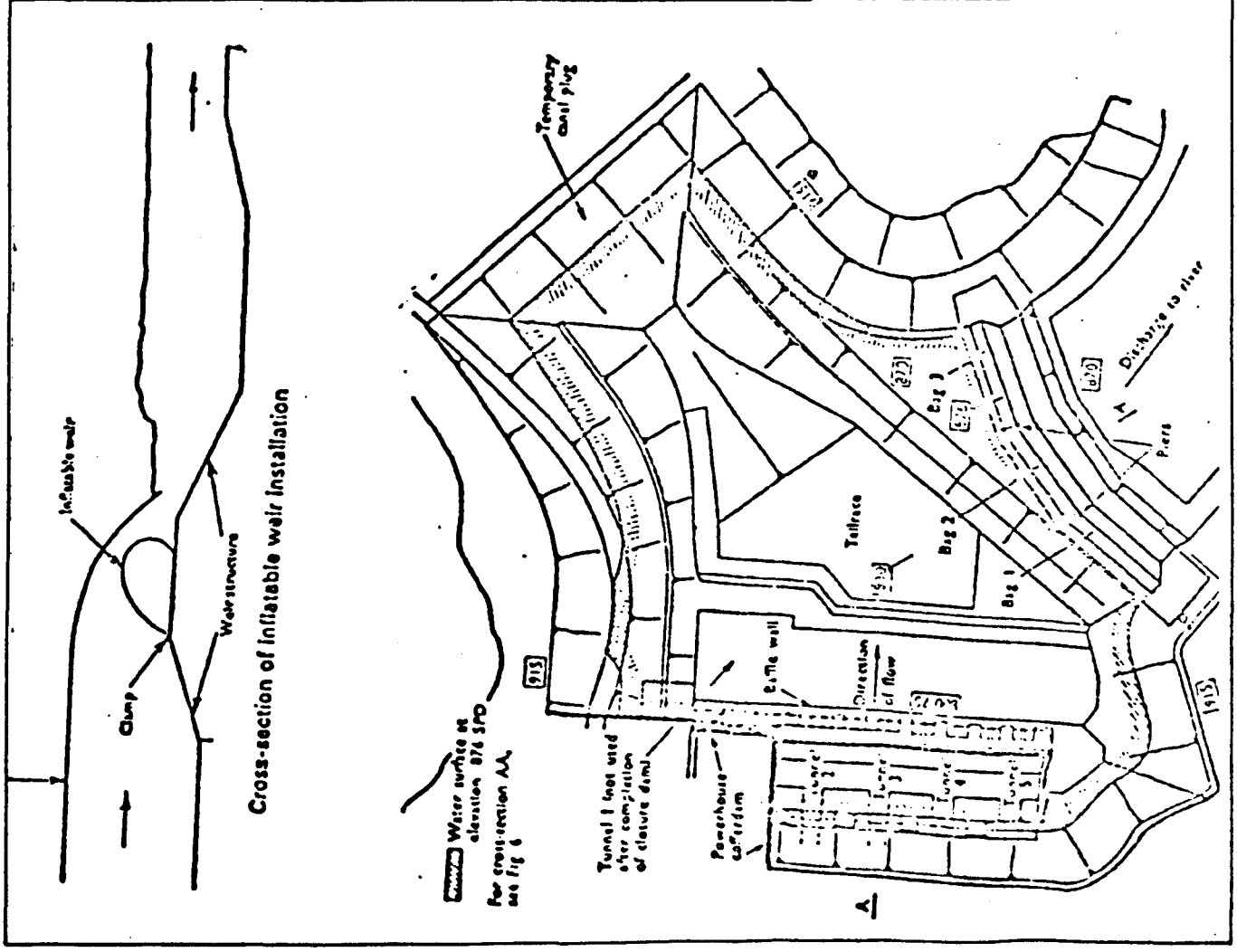

FIG. (1-2) INFLATABLE STRUCTURES FOR CONSTRUCTION PERIODS

1.2.5 Other possible uses of inflatable structures.

Inflatable structures can be used for other purposes in addition to those listed above.

1. To raise river water levels in the dry season by constructing a weir across a river to maintain the required water level. This solution was adopted in England by the construction of an inflatable weir on the River Avon (11) and the River Allen near Wibborne. Fig.1.3 shows the inflatable weir on the River Allen.

2. Inflatable fabric structures can be used as cofferdams to protect the banks of rivers and reservoirs during renovation work (12). Fig.1.4 illustrates an inflatable structure placed on the bank of a river to allow the repair of a concrete revetment.

3. Diversion control in irrigation works to replace flashboards and sluice gates (13).

4. Extending the level of the embankment along rivers to prevent flooding of adjacent low land areas during periods of high tide.

1.3 Economics of Inflatable Structures.

One of the main reasons for constructing an inflatable hydraulic structure is the low cost compared with a conventional structure. Investigations were made to compare the alternatives on the Tuckambid floodway scheme in New South Wales (1). The preliminary studies showed that the capital cost of the fabridam was approximately 50% of the cost of the cheapest steel gates available and also the service life of the inflatable structure was estimated as 20 years. When it becomes necessary to replace the fabric the cost was estimated as only about one third to one half of the price for the complete installation which was less than the maintenance cost of a steel structure over a 20 year period.

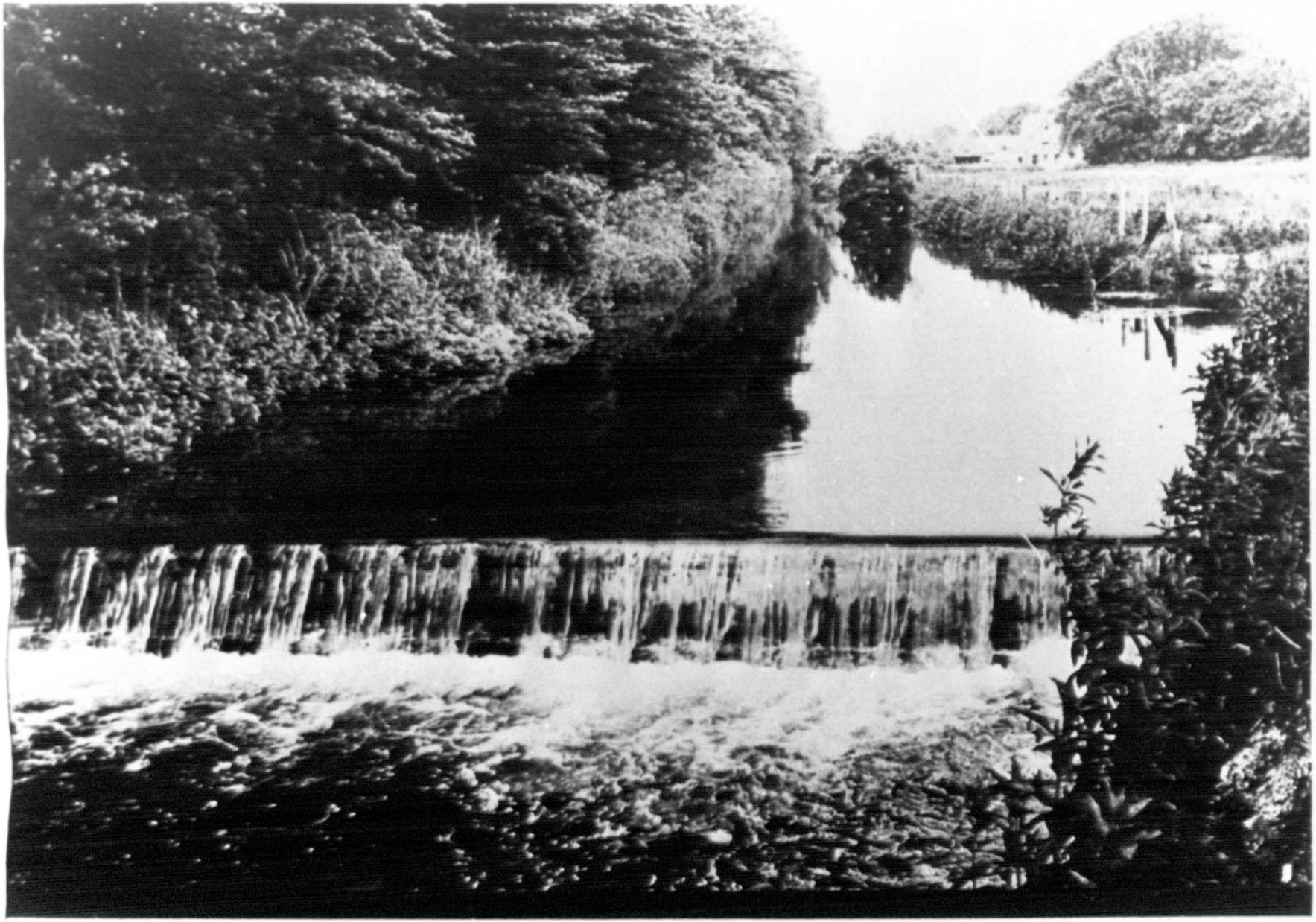

Variable height weir on the River Allen near Wimborne. One of seven used during the summer to maintain water levels.

FIG. (1-3) INFLATABLE WEIR TO MAINTAIN SUMMER WATER LEVELS

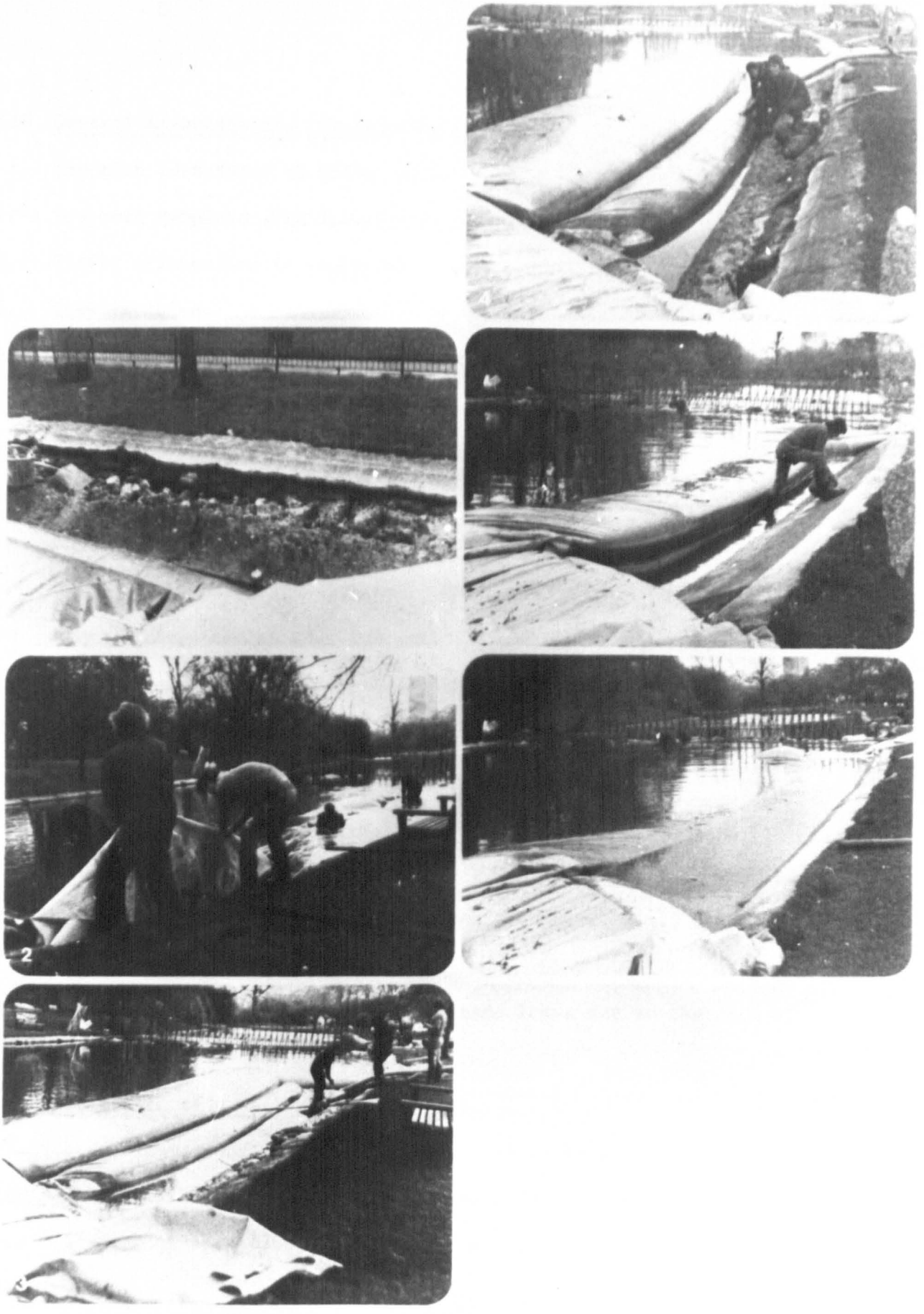

FIG. (1-4) CONCRETE REVETMENT FOR THE RIVER BANK

1.4 General Advantage and Disadvantage of Inflatable Hydraulic Structures.

The main advantages of using inflatable structures are as below:

1. low cost compared with conventional structure (See 1.3);
2. little maintenance is required;
3. easy erection;
4. during a flood the dam can be deflated, so that it offers no resistance to the water flow and debris;
5. easy water level control, particularly with two way flow access in tidal reaches;
6. ice build up can be controlled in that as the thickness of ice increases a dam can be partially deflated; the ice will then break up and float away reducing the risk of ice jams.

The disadvantages of this kind of structure are as follows:

1. service life of the structure is not likely to exceed 20 years;
2. the fabric material is vulnerable to vandalism;
3. for high flows the structure is not suitable;
4. it has been claimed that the fabric is not suitable for installation when it is subject to continuous dynamic loading, e.g., substantial and continued overflow of water;
5. not suitable in water with high sediment loads due to the risk of abrasion.

1.5 Development of a New Design Technique.

The development of a new design technique in this study consists of finding the length of membrane required and then to analyse the structure over the range of operational parameters to overcome the limitations of other techniques.

The length of the membrane is designed for a maximum proportional factor alpha by assuming the maximum upstream head required. The total length is

calculated with respect to equations determined both theoretically and experimentally for different types of inflation fluids. The analysis is carried out to find the maximum height of dam for the maximum upstream head for a given proportional factor.

Finding the maximum upstream head equal to the maximum height of the dam (for maximum proportional factor) the length of the membrane can be determined. Details of this procedure are given in Chapter 8.

Additional analysis has been carried out for different proportional factors (i.e., 1.0, 1.2, 1.4, 1.6, 1.8, 2.0, 2.2, 2.5) for a water inflated dam with constant length of membrane, the analysis has also been carried out for different inflation fluids i.e., water, air and the combination of the two (air+water). Analysis has also been carried out for different design lengths of membrane with different proportional factors. All of these analyses were achieved using a computer program (IHSIP) which is based on the finite element method. The main output parameters are:-

1. Tension along the membrane.
2. Upstream slope (at the anchor point).
3. Cross-sectional profile of the membrane.
4. Maximum dam height.
5. Cross sectional area.
6. Elongation of the membrane.

For dynamic conditions the length of membrane is based on the same design methods as for the static condition and the analysis is carried out for dams under different over flow heads to find the same output parameters as for static conditions. The details of this part of the study are given in Chapter 5. For dynamic conditions a technique for calculating the coefficient of discharge has been developed and is detailed in Chapter 7.

Two types of materials were used in this study (material type I and II), see Table 3.1, and the details of the material properties are shown in detail in Chapter 3.

The inflation fluids used are water, air and a combination of the two as these fluids are most likely to be used in practice mainly due to their ease of availability, but the computer program developed can consider different fluids of known specific weight.

The work is also solely related to single anchor systems as this type of system is the one that has received least attention and yet is the easiest to instal.

CHAPTER 2.

REVIEW OF PREVIOUS WORK.

2.1 General Historical Review.

The idea of an inflatable hydraulic structure was first used in 1957 by N.M. Ibertson (13) the Chief Engineer for the Los Angeles Department of Water and Power. This collapsible dam consisted of a flexible tube achored along its length to a concrete floor. The first of this type was installed at the end of a wooden dam and was 5 feet high and 90 feet long. A larger size dam was then designed as a large tube or bag, tear-drop in section. This tube, fabricated by the Firestone Tyre and Rubber Company, was 30 feet in circumference and 150 feet long. Fig.2.1 shows the details of the first dam.

Later this type of dam was widely used in the U.S.A. under the trade name "Fabridam" operating mostly under hydrostatic conditions (no-overflow). The dams were usually inflated with water, but sometimes inflated with air or water and air and deflated when not required.

In Pakistan a fabridam was used in 1965 for diversion work (9) for an irrigation project to maintain the water level in a tunnel (see Fig.1.2). Unfortunately this installation failed after a short period of operation and it is believed that this resulted from the dam having operated most of the time under vibration conditions (14).

In 1967 Schofield (15) suggested and carried out some tests on a model of a type of flexible wall to be used as a temporary flood controlling device for the river Thames. The main early use has been for flood control or irrigation purposes mainly in Australia, U.S.A. (16) and Hong Kong (17).

2.2 Construction of Inflatable Prototype Structures.

An inflatable dam is usually constructed from sheets of rubberised fabric folded in a tubular shape and fastened to a reinforced concrete slab

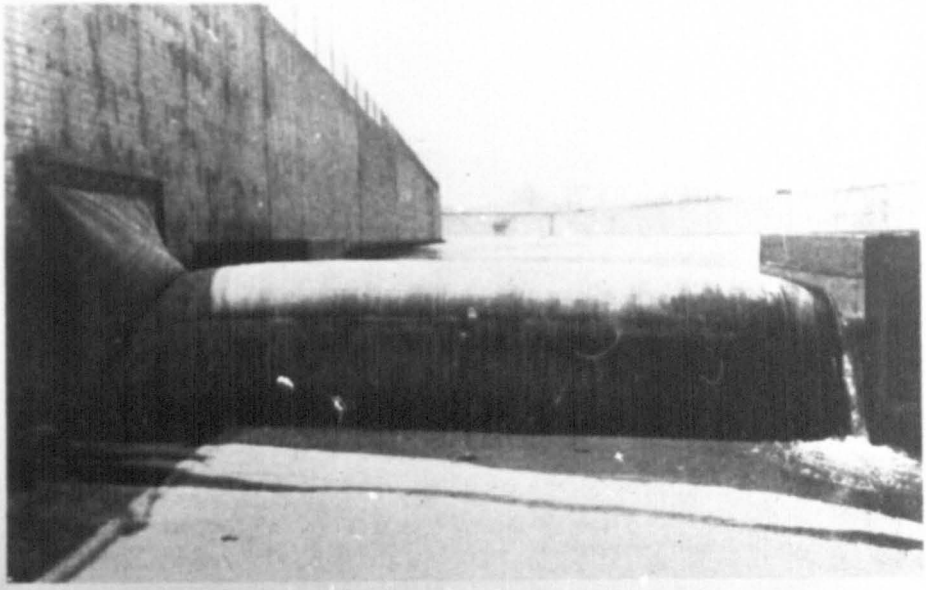

Prototype dam was installed at one end of the wooden dam in 1957 to find out whether this type of collapsible structure would be feasible. Prototype was 20 ft long and operated at a height of 5 ft.

Giant nylon bag coated with neoprene backs up the water in Los Angeles River to replenish underground basins. This structure is 150 ft long and 6 ft high. It takes about 25 min and 50,000 gal of water to inflate it. A period of only 10 min is required to collapse the dam automatically in case of flood conditions.

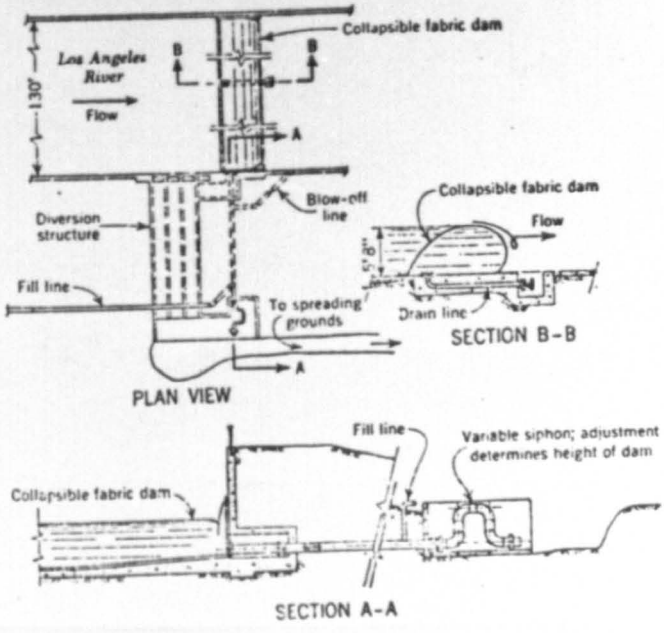

Collapsible dam is inflated with water from a pipe connection through the channel wall. Under flood conditions, the water pressure inside the dam rises to a predetermined height, the siphon primes and deflates the dam.

FIG. (2-1) FIRST INFLATABLE DAM INSTALLED IN LOS ANGELES

with structural steel members (18), clamps or anchor bolts either or both on the upstream and downstream sides. The main parts of an inflatable structure are:

1. The fabric material.
2. The clamping system.
3. The control system (for inflation and deflation).

2.2.1 The fabric material.

Usually the fabric material is constructed from high strength nylon. There are many different types of fabric available in the way of weaves, cord, counts, weight and breaking strength although other materials could replace nylon such as metal fabrics.

The properties of materials that can be used are summarised in Table 2.1 this list being prepared by Clare (14). Materials such as bolyl, rubber, Heoprene, Hypalon, polythene and p.v.c. have all been used successfully in marine environments. Neoprene compounds have proved to be the best type of coating and their weathering characteristics are excellent. The life expectancy of such materials has been determined to be in the region of 20 years. Hypolon can be used as another coating on the Heoprene, since it has very good resistance to abrasion.

2.2.2 The clamping systems.

Inflatable fabric structures are usually fixed with either one or two ends restrained by means of anchor systems or clamped to a concrete slab.

Fig.2.2 shows the anchor bolt designed by the Firestone Tyre and Rubber Company (19) which they used on the upstream side of a dam in a single anchor system. This study relates to dams fixed only on the upstream edge. One of the high elements of the cost of construction is the anchor system and also by constructing a single system of anchor bolts it will assist the fabric to settle on the base without causing any obstruction to the flow during the

	Nefylate	Butyl	Hypalon	Natural Rubber	Neoprene	Nitrite	BR	Poly-propylene	Poly-urethane	PVC	Poly-thene	SBR	Silicone	Thiorol
Specific gravity	1.09	0.92	1.10	0.93	1.23	1.00	1.00	0.90	1.05	1.25-1.50	0.92-0.96	0.94	1.25	1.35
Tensile strength (kN/m^2)	10342	5516-17237	> 13790	5516-31027	5516-20685	5516-17237	22064	28959-37922	Up to 48265	41370	6895-15858	5516-27580	2758-6895	4137-10342
Tensile Elongation (%)	-	< 800	< 500	500	650-850	200-600	335	50-600	500	200-450	50-800	450	200-350	200-350
Tear strength	M	M	M	FH	H	M	M	M	VH	H	VH	M	L	L
Abrasion resistance	M	M	H	H	H	M	VH	H	VH	H	VH	H	L	L
Heat resistance	H	M	FH	FL	FH	M-FH	M	H	FH	FL	FL	FL	VH	L
Cold resistance	FL	H	M	H	FH	L-M	VH	L	M	VL	VH	H	VH	H
Working temp. range (^{o}C)	-	-50 to +125	-	-55 to +70	-20 to +120	-20 to +120	-75 to +110	- to +150	-	-15 to + 78	-	-45 to 100	-90 to +250	-50 to +95
Ageing resistance general	VH	H	VH	M	H	H	M	H	H	VH	H	M-FH	H	H
Resistance to sunlight	H	H	H	L	H	M	L	H	H	H	M	L	H	M
Resistance to ozone and corona	VH	M-H	H	M	FH-H	L-M	VL	H	VH	VH	M	L-M	H	H
Resistance to flame	L	L	H	L	H	L-M	L	L	FH	H	L	L	H	L
Resistance to water	M	FH-H	H	H	M	M	H	H	FL	M	H	M-H	M	M
Adhesion to fabrics	-	FH	FH	H	H	FH	FH	-	FH	M	-	FH	M	L
Resistance to flexing	-	M	M	M	VH	VH	VH	VH	VH	M	M	H	-	-

KEY

VL = Very Low
L = Low
FL = Fairly Low
M = Medium
FH = Fairly High
H = High
VH = Very High

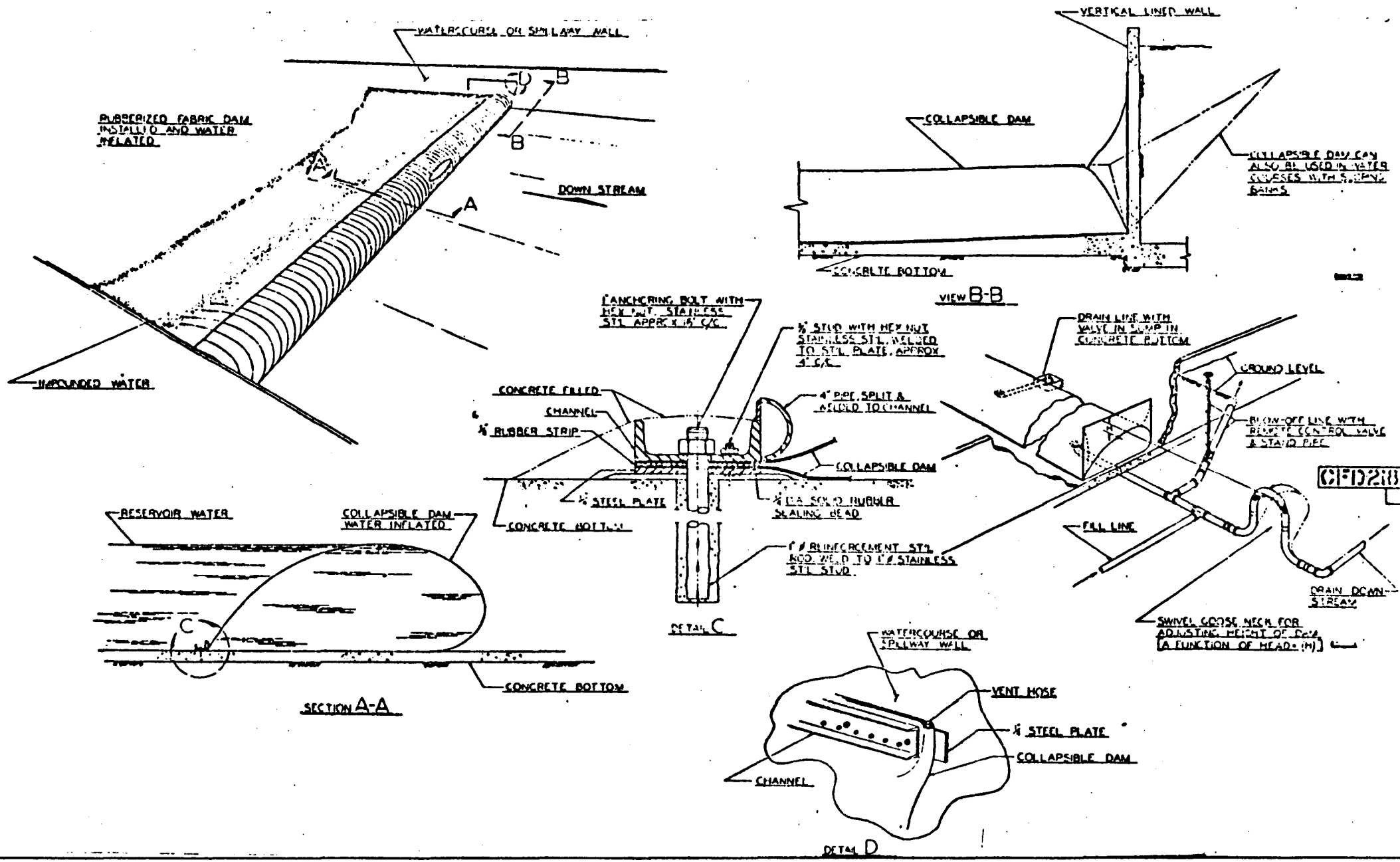

FIG.(2-2) DETAILS OF THE ANCHOR BOLT SYSTEM

deflation condition and minimise the risk of puncturing the fabric by parts of the downstream anchor system. The single system of anchors may help to increase the life of a fabric structure. Alternatively an upstream sheet attached to the dam and lying upstream can rely on the hydrostatic pressure to hold the dam in place although this is likely to be limited to small structures.

2.2.3 The control operation system.

The successful operation of an inflatable fabric structure depends on the pressure inflation and control devices consisting of,for a water inflated dam, a water level control system and for other types a pumping system for the inflation or deflation of the dam.

The control system used on the water inflated Koombooloomba fabric dam (8) is illustrated in Fig.2.3A. This consisted of forming the main header pipe used for filling and emptying into a siphon at an elevation just above the slab and equivalent to the internal pressure in the bag when fully inflated. As the pressure inside the fabridam increased with rising head, water deflation commenced and proceeded by siphonic action.

The controlling system used for the Los Angeles dam (1) (see Fig.2.1) incorporated automatic inflation and needed 10 mins. for complete deflation in the case of a flood. The system consisted of a siphon installed in a spreading basin channel and connected through an 18" pipe to water inside the dam which controlled the pressure.

The practice used for the control operation system in the Mangala dam (9) is illustrated in Fig.2.3B and included pumps and valves for water and a blower for air was installed in the abutment of the weir; the pumps could be used to inflate or deflate the bags. Siphons were also used as protection against over inflation of the bag.

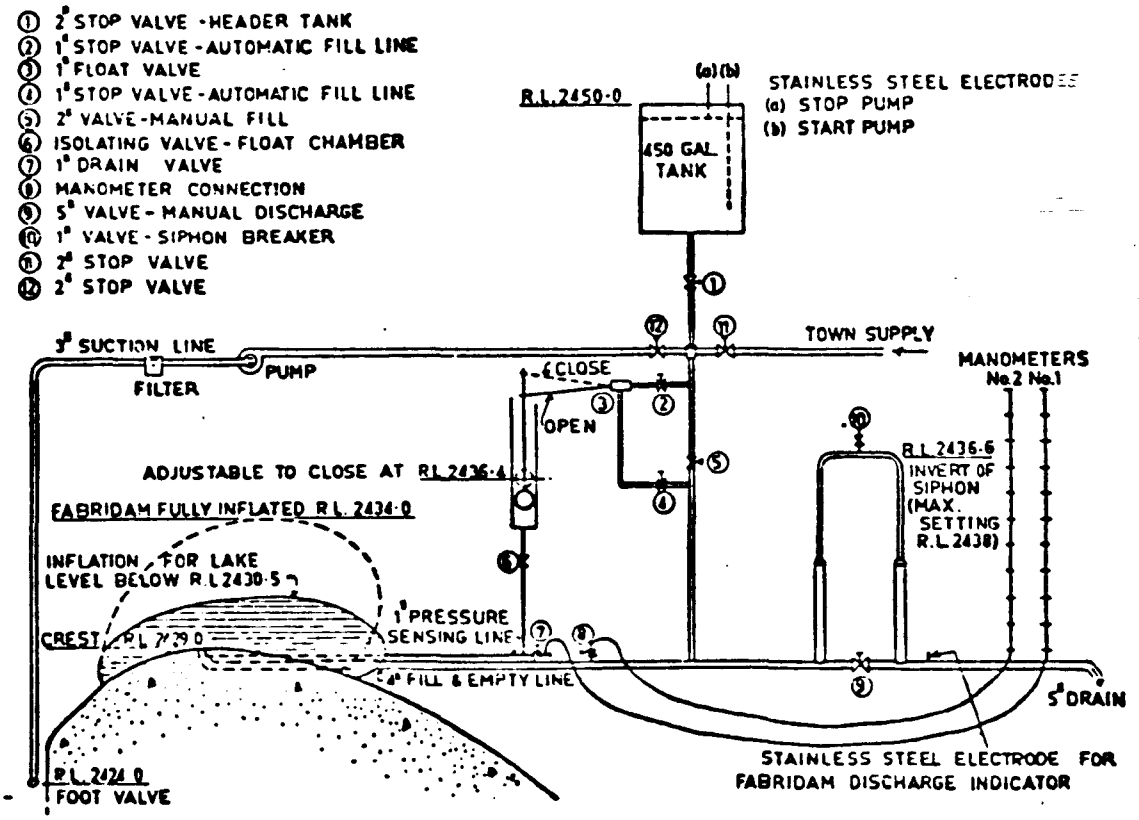

Fabridam Schematic Arrangement, showing Operating Settings of Siphon and Float Valve.

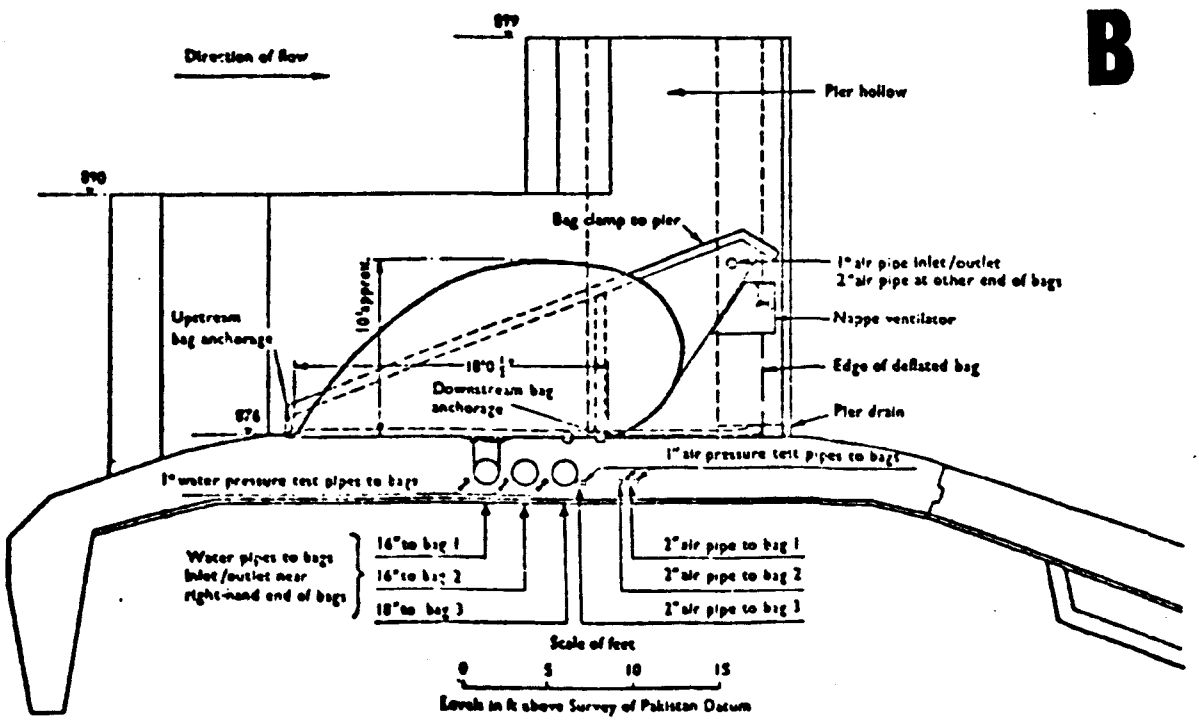

Cross-section of inflatable weir

FIG.(2-3) THE CONTROL SYSTEM ARRANGEMENT

2.3 Construction of Inflatable Model Structures.

In many instances it is very important to study the problems of inflatable dams from model tests. Most previous work on inflatable dams has incorporated the construction and testing of models to check dam behaviour under different conditions. Baker (20) used a (1/20) scale sectional model 0.46 m wide to check the performance of the fabridam to be used in the Mangala Schemes, in Pakistan to maintain the water level in the diversion tunnels.

The model used was of a total perimeter equal to 0.60 m and was clamped to the model concrete sill on two longitudinal lines of 0.16 m length.

The ratio of the perimeter length to the nominal height was 4.9 and the ratio of the base length to the nominal height equal to 1.3. The material used was a thin flexible rubberised cloth.

Shepherd (8) constructed a model for the Koombooloomba fabridam to check the general hydraulic behaviour and the stability of the fabridam extension when installed on the crest and to determine what effect the fabridam would have on the discharge characteristics of the dam and in particular the discharge capacity. Two different materials were used, a lightweight uncoated nylon material and a nylon fabric coated with neoprene.

Anwar (2), Kunihiro Owiwara (3), Stodulka (21), Clare (14) and Alwan (7) all built models to compare experimental results with their theoretical analyses for the profiles.

A description of each of the above models is given in Table 2.2.

2.4 Theoretical Analyses of Previous Investigators.

A theoretical analysis technique was first published in 1967 by Anwar (2). The aim of this work was to determine the behaviour of the upstream and downstream faces of air and water inflated dams under hydrostatic conditions and also to consider the dynamic condition for an air inflated structure. The analysis required certain assumptions to be made in order to determine the

Table 2.2 Properties of Model Materials.

No.	Investigator	Type of Material	Size of model			Thickness in mm	Weight Kg/m^3	Tensile strength KN/m	Purpose of the Models
			width (m)	height (m)	perimeter (m)				
1	Baker	Rubber and cloth	0.1587 0.2223	0.122 0.170	0.5969 0.706	1.58	-	-	Checking the following 1.Discharge and U/S water level. 2. Tension in the fabric. 3. Shape of the dam.
2	Shepherd	1. Uncoated nylon 2. Neoprene coated nylon	0.061	0.03	-	-	0.081 0.221		To test the operation of the Koombooloomba dam.
3	Kunitiro Owiwara et al.	Consists of two sheets of 0.01 inside and covered by 0.05 vinyl sheet inside	0.4	-	0.5	-	-	-	To check the theoretical analysis.
4	Anwar	Commercial polythene	0.61	0.3-0.23	-	0.254	0.239	1.927 4.201	To check the theoretical analysis
5	Stodulka	Nylon fabric	0.305	0.305	0.965	-	0.221	-	1.To check the theoretical analysis 2.To investigate the coefficient of discharge

Continued .....

Table 2.2 Continued.

No.	Investigator	Type of Material	Size of model			Thickness in mm	Weight Kg/m^3	Tensile strength KN/m	Purpose of the Models
			width (m)	height (m)	perimeter (m)				
6	Clare	1) Polythene 2) Rubber 3) Rubber insert 4) Combination of rubber and rubber insert. 5) Rubber backed canvas.	0.254 0.203	0.156 0.254	1.016 1.016	0.254 0.792 0.695 0.381		3.854 6.008 6.739 3.678	1. To check the theoretical analysis 2. To investigate the vibration of the dam. 3. To investigate the coefficient of discharge.
7	Alwan	N.T. Fabric	1.03	0.300	0.787	0.36	0.391	27.36	To check the theoretical analysis

behaviour of the upstream and downstream faces of the dam.

In 1970 Owiwara et al. (3) also worked on the analysis of dam behaviour for both static and dynamic conditions for air and water inflated conditions. The result of the analysis was in the form of elliptic integrals for the static conditions, which is similar to Anawar analysis.

Also in 1970 Harrison (4) developed a method based on a finite element technique to be used on dams under static condition and inflated by air or water or a combination of air and water.

In 1972 Binnie (5) also analysed a dam under static conditions to find the relationship between the internal pressure, height, base width and length of the perimeter of the dam. This analysis was a development of the Anwar method.

Parbery (6) published a paper concerning the analysis of an inflatable dam inflated by air or water, the analysis taking the form of differential equations. A numerical method was used to find the shape of the dam and tension in the membrane. In 1978 a paper published by Parbery (22) detailed the analysis of an inflatable dam under static loads for an air inflated condition, and the analysis was based on the approach of Binnie (5).

These different analysis techniques are detailed in the following sections.

2.4.1 Theoretical analysis of Anwar's method.

Anwar worked out the theoretical shape of an inflatable dam in air inflated cases for both the no-overflow and overflow condition and for water inflated case for the no-overflow condition only. In all these cases the analysis required the following assumptions.

1. A weightless material and constant tension along the membrane.
2. The downstream head equal to zero.
3. The membrane length and base length are ignored.

4. The maximum upstream head is equal to the maximum height of the dam.

5. The dam is constructed on a horizontal slab.

On the basis of the above general assumptions the theoretical approach required specific assumptions depending on the specific inflation condition considered.

2.4.1.1 Analysis under hydrostatic conditions.

2.4.1.1.1 Air inflated structure.

i) Tension in the membrane.

Fig.2.4A represents the air inflated case under hydrostatic conditions. In this case Anwar considered the air pressure inside the dam is proportional to the maximum upstream head i.e. the maximum height of the dam H_D can be represented by the following equation

$$P_1 - P_2 = \alpha \rho g H_D \quad \ldots\ldots \quad 2.1$$

where

P_1-P_2 = internal pressure.

α = proportional factor.

ρ = density of water.

g = acceleration of gravity.

H_D = maximum height of dam.

By assuming that the downstream face of che dam is a semi circular curve of a diameter equal to the maximum height of the dam (H_D) and assuming that the base length and perimeter have no effect, then the horizontal force T (Fig.2.4A) acting on the dam for a unit length can be shown to be equal to

$$T = \frac{1}{2} (P_1-P_2) H_D \quad \ldots\ldots \quad 2.2$$

ii) Shape of the dam.

The shape of the dam is represented by the profile of the membrane under the effect of the maximum upstream head, and internal pressure head.

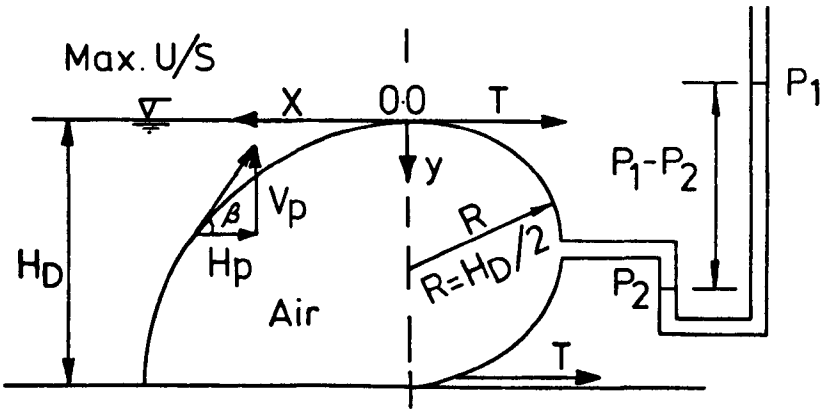

(A) Air inflated condition (no – overflow)

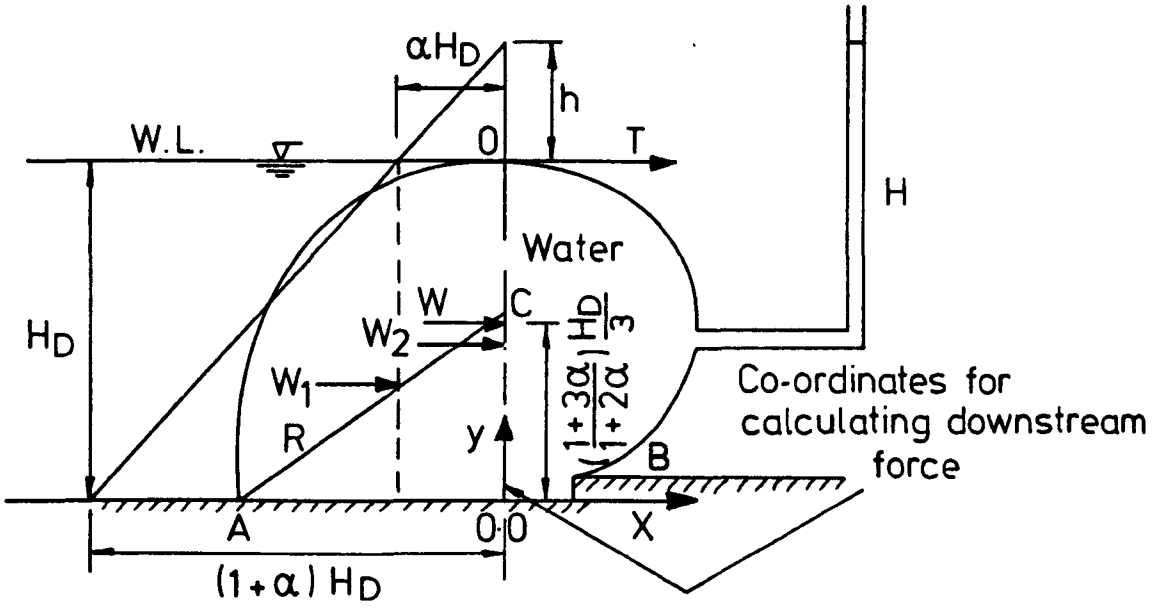

(B) Water inflated condition (no-overflow)

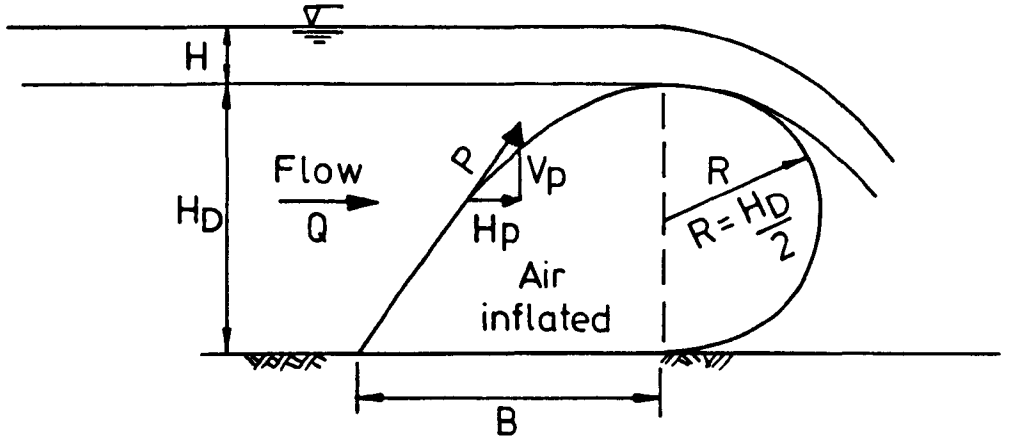

(C) Air inflated condition (with-overflow)

FIG. (2-4) ANALYSIS OF AN INFLATABLE DAM BY ANWAR

Hence to find the profile of the dam, the profile equations are worked out separately for the upstream face and downstream face and depend mainly on the type of inflation fluid.

a) Upstream face of the dam.

From Fig.2.4A the upstream slope of the membrane at any arbitrary point (p) is represented by the following

$$\text{Tan}\beta = \frac{Vp}{Hp} \qquad \ldots\ldots \qquad 2.3$$

where β = the membrane upstream slope.

Hp = horizontal component of the tension in the membrane per unit length at an arbitrary point (p).

Vp = vertical component of the tension per unit length at at arbitrary point (p)

The values of Hp and Vp at an arbitrary point (p) per unit length are given by

$$H_p = \frac{1}{2} \propto \rho g (H_D)^2 + \frac{1}{2} \rho g y^2 - \propto \rho g H_D y \qquad \ldots\ldots \qquad 2.4$$

$$V_p = \rho g \int f(x)\, dx - \propto \rho g (H_D)\, x \qquad \ldots\ldots \qquad 2.5$$

In which x, y are the co-ordinates of the point (p) and f(x) is an analytical function describing the shape of the dam. Substituting equations 2.4 and 2.5 into equation 2.3 gives the general equation of the shape of the upstream profile.

$$\frac{x}{H_D} = \sqrt{2\alpha} \left\{ 2 \hat{E} \left[\frac{\sqrt{\alpha}}{2} - \hat{F} \left(\frac{\sqrt{\alpha}}{2} \right) \right] - E \left(\arccos \frac{\eta}{\alpha} - 1 \right), \frac{\sqrt{\alpha}}{2} \right]$$

$$+ \frac{1}{F} F \left[\arccos \left(\frac{\eta}{\alpha} - 1 \right), \frac{\sqrt{\alpha}}{2} \right] \} \qquad \ldots\ldots \qquad 2.6$$

in which

$$\eta = \frac{y}{H_D}$$

where

F, E are the elliptic integrals of the first and second kind respectively and $\hat{F}$, $\hat{E}$ represent the complete elliptic integrals of the first and second kind respectively.

b) Downstream face of the dam.

The downstream profile for an air inflated dam with zero downstream head is a semi circle with a diameter equal to the maximum height of the dam as the tension is constant around the membrane as shown in Fig.2.4A.

2.4.1.1.2 Water inflated structure.

i) Tension.

In order to find the tension in the membrane the following assumptions are made:

1. The anchor point B in Fig.2.4B on the downstream face of the dam is higher than the upstream face anchor.

2. The downstream face lays tangential to the horizontal base at (B).

3. The differential pressure head is proportional to the maximum storage head, i.e.

$$h = \alpha H_D \quad \ldots\ldots \quad 2.7$$

where

h = differential pressure head.

On the basis of the above assumption the tension of the membrane can be calculated by taking the moment at (0,0), see Fig.2.4B and since the horizontal component of the water force is

$$W = \frac{1+2\alpha}{2} \rho g H_D^2 \quad \ldots\ldots \quad 2.8$$

and this force has a line of action equal to $(\frac{1+3\alpha}{1+2\alpha}) \frac{H_D}{3}$ above the base, then the tension at the top of the crest is

$$T = (\frac{1+3\alpha}{6}) \rho g H_D^2 \quad \ldots\ldots \quad 2.9$$

ii) Shape of the dam.

The shape of the dam represents the profiles of the upstream and downstream faces and these profiles are different from those of air inflated dams.

a) Upstream profile.

The differential equation for the upstream profile is obtained by using the same concept of that for an air inflated case. The horizontal and vertical components of the hydrostatic forces acting on an arbitrary point p in Fig.2.4B for a unit length are

$$H_p = \frac{1+3\alpha}{6} \rho g (H_D)^2 - \alpha \rho g y \quad \ldots\ldots \quad 2.10$$

$$V_p = - \alpha \rho g (H_D) x \quad \ldots\ldots \quad 2.11$$

The shape at the point (p) can be written as

$$\tan\beta = \frac{V_p}{H_p} = \frac{-\alpha \rho g (H_D) x}{\frac{1+3\alpha}{6} \rho g (H_D)^2 - \alpha \rho g y} \quad \ldots\ldots \quad 2.12$$

The general solution of the above equation gives the shape of the upstream face and can be written as follows

$$(\eta^3 + \varepsilon^2) = \left(\frac{1+3\alpha}{3\alpha}\right) \eta \quad \ldots\ldots \quad 2.13$$

$$\eta = y/H_D, \quad \varepsilon = \frac{x}{H_D}$$

Equation (2.13) represents a circle with radius $(1+3\alpha)/6$ and is tangential to the x-axis at the origin.

b) Downstream profile.

The downstream profile is obtained from the following relationship:

$$T = P_r R \quad \ldots\ldots \quad 2.14$$

where T is the tension in the membrane as given in equation 2.2, P_r is the pressure at an arbitrary point of the membrane on the downstream face and is given by:

$$P_r = \rho g [(1+\alpha H_D - y] \quad \ldots\ldots \quad 2.15$$

R is the radius of curvature and is given in the form

$$R = [1 + (dy/dx)^2)]^{3/2} / \frac{d^2y}{dx^2} \quad \ldots\ldots \quad 2.16$$

Substituting T, P_r and R in equation 2.14, the solution may be written as:

$$\varepsilon + C_2 = \sqrt{2a_1+\delta}\ E(K_1,\phi) - \frac{\delta}{\sqrt{2a_1+\delta}}\ F(K_1,\phi) \quad \ldots\ldots \quad 2.17$$

where

$$\varepsilon = \frac{x}{H_D}, \quad a_1 = \frac{1+3\alpha}{6}$$

$$\delta = \alpha^2 - \alpha - 1/3$$

Substituting the above values in equation 2.16 and the following equation can be derived

$$\frac{x}{H_D} + C_2 = \alpha E(K_1,\phi) - (\alpha - 1 - \frac{1}{3\alpha}) F(K_1,\phi) \quad \ldots\ldots \quad 2.18$$

in which C_2 is a constant of integration and F, E are the elliptic integrals of the first and second kind.

2.4.1.2 Analysis under hydrodynamic conditions.

The analysis of this condition by Anwar only applied when the dam was inflated with air and the main parameters studied were the tension and the shape of the profile. In his study the solution was idealized by considering that the fluid flow jetted off the crest as shown in Fig.2.4C. The theoretical concept for finding the profile and tension are similar to the hydrostatic condition of an air inflated case (see Section 2.4.1.1.1) except that allowance is made in the analysis of the upstream profile for an approach velocity and higher static pressure due to an increased head.

2.4.2 Theoretical analysis of Kunihiro Owiwara et al.

In this section the investigation for both the theoretical and experimental work for hydrostatic and dynamic conditions for both air and water inflated cases is given.

2.4.2.1 Analysis under hydrostatic conditions.

2.4.2.1.1 Air Inflated Structure.

i) Tension in the membrane.

The basic equation used to find the tension in the circumference of the dam is as follows (see Fig.2.5).

$$T = (P_i - P_o)\, R \qquad \ldots\ldots \qquad (2.18)$$

P_i = Internal pressure.

P_o = External pressure.

R = Radius of curvature as defined in equation 2.16.

ii) Shape of the dam.

a) Down stream face.

The main equation used to find the shape of the down stream face of the dam is

$$(\eta_1)^2 + (\varepsilon_1)^2 = \left(\frac{2T}{2\rho g H_D}\right) \eta_1 \qquad \ldots\ldots \qquad (2.19)$$

where

$$\eta_1 = \frac{y_1}{H_D}, \qquad \varepsilon_1 = \frac{x_1}{H_D}$$

b) Upstream face of the dam.

The shape of the upstream face is derived using elliptic integrals of the first and second kind as in the Anwar results. The equation is as follows:

$$\varepsilon_2 = \sqrt{2\alpha}\left\{ E\left[\frac{\sqrt{\alpha}}{2}, \arccos\left(1 - \frac{\eta_1}{\alpha}\right)\right] - E\left[\frac{\sqrt{\alpha}}{2}, 0\right) - \frac{1}{2} F\left[\frac{\sqrt{\alpha}}{2}, \arccos\left(1 - \frac{\eta_1}{\alpha}\right)\right] + \frac{1}{2} F\left[\frac{\sqrt{\alpha}}{2}, 0\right] \qquad \ldots. \qquad (2.20)$$

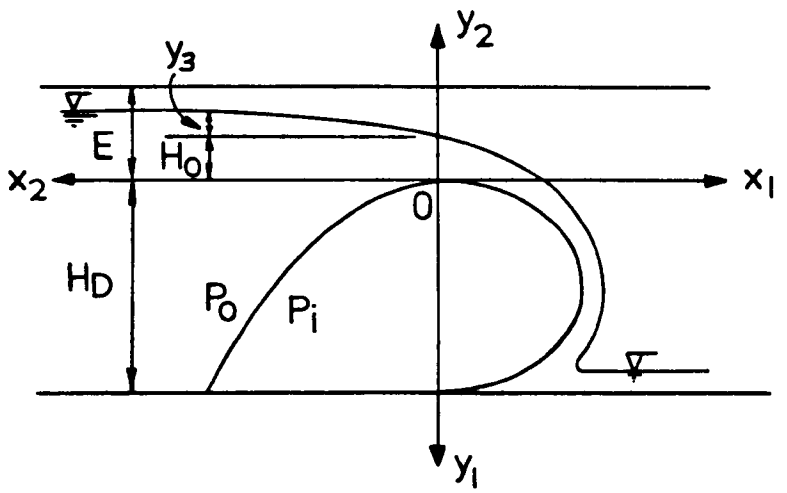

FIG.(2-5) DAM ANALYSIS BY OWIWARA

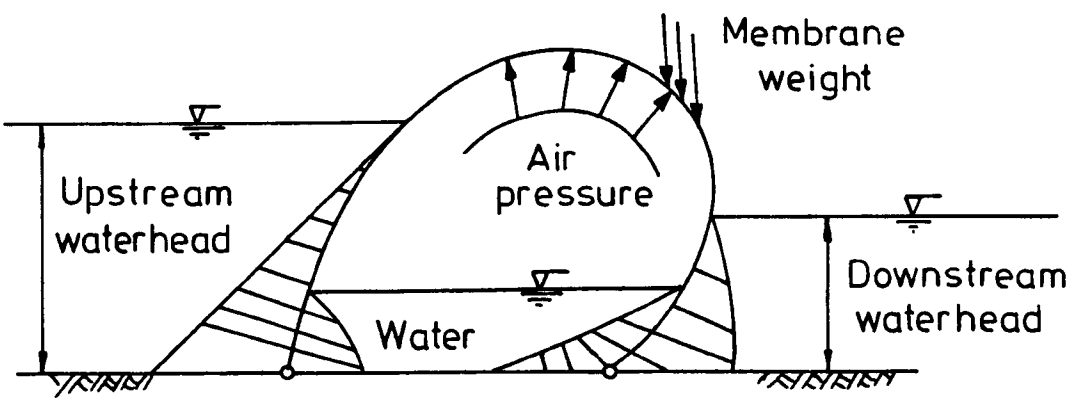

(A) Forces acting on the membrane for dam analysis by Harrison

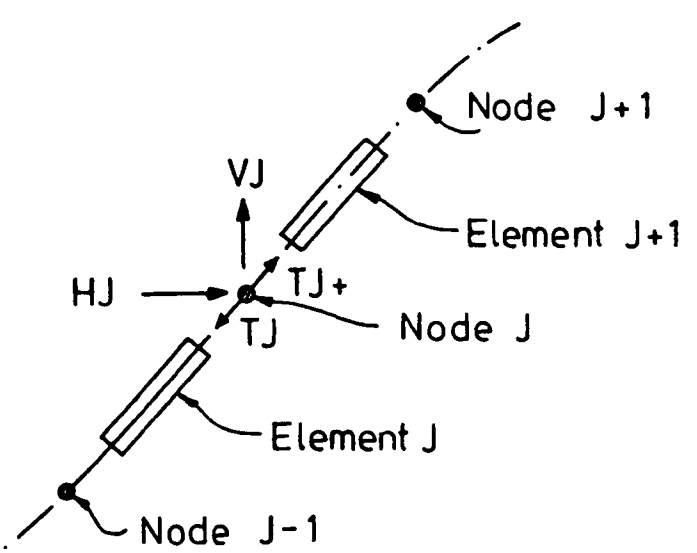

(B) Forces acting on nodes

FIG. (2-6) DAM ANALYSIS BY HARRISON

where F, E are both elliptic integrals of the first and second kind.

2.4.2.1.2 Water Inflated Structure.

For the water inflated condition the derived equations for the down stream and upstream profiles are worked out under different assumptions. These equations are different from the Anwar analysis, but the form of the downstream equation requires the use of elliptic integrals.

2.4.2.2 Analysis under hydrodynamic conditions.

The shape of the curved surface in the case with overflow has to be solved with relation to the internal and external pressure, but since the external pressure varies with the condition of flow, it is necessary to consider the effect of the flow on the dam. Hence the analysis considered separately the flow condition at the upstream and down stream faces.

i) Upstream face.

The analysis is similar to the previous analysis for static conditions for both air or water but the following additional assumptions are made.

1. The specific energy is constant.
2. The flow at all sections will be uniform.
3. Ignore the friction along the membrane.
4. Static water pressure only is operating.

By making these assumptions the investigator found two equations for the profile for the upstream face for both air and water inflated cases.

ii) Down stream face.

In the downstream case the flow descending over the curved surface is subjected to both a centrifugal force and to the weight of the water.

For the down stream face in the state of equilibrium the external force per unit length of the dam can be written as

$$- P_o \, R \, d\theta = \rho \frac{v^2}{R} \, R \, d\theta \, h - \rho R \, d\theta \, hg \, \text{Sin} \, \theta \quad \ldots\ldots \quad 2.21$$

Since the flow volume (q) at the central point on the dam is already known and can obtain, hence

v = flow speed = q/h.

q = flow per unit width.

h = depth of flow on the down stream face.

θ = inclination of the membrane on the D/S face.

R = radius of curvature.

Two equations for the down stream profiles for air and water inflated conditions are found subject to the following assumptions:

1. The flow speed over the dam surface will not vary greatly from the mean flow speed.

2. The water depth on the dam surface is approximately constant.

3. Compared with the centrifugal force the weight of water on the dam is negligible.

2.4.3 Theoretical Analysis of Harrison's method.

The theoretical method developed by Harrison (14) in 1970 allowed the upstream and downstream tension and the profile of the dam to be found. The method is applicable for structures inflated by air or water and is based on the following assumptions.

1. The behaviour of the three dimensional structure can be represented reasonably by the behaviour of a two dimensional transverse section of unit width.

2. The perimeter of the dam is composed of a finite number of small straight elements and loads act on the nodes of each element.

In this analysis the weight of the material is considered and it is necessary to specify the perimeter length, base length together with the thickness and elastic modulus of the material. The loads acting on the dam are as shown in fig.2.6 and are upstream water head, internal pressure head, downstream water head and membrane weight.

2.4.3.1 Method of obtaining the profile and membrane tension.

To obtain the profile and tension in the membrane, the profile is divided into n elements giving n+1 nodes. The forces acting on a particular node are as shown in fig. 2.6. The tension and profile of the dam can be found by assuming initial values of tension and slope for the first element of the upstream face of the membrane. The loads acting on each node due to the hydrostatic pressure are calculated in order to find the tension in the element and the co-ordinates of the nodes. This procedure is followed around the whole membrane to find the shape of the dam.

In some cases the co-ordinates of the last node do not coincide with co-ordinates of the downstream anchor point. The procedure for determining the co-ordinate of the nodes of the profile, therefore needs to be repeated with adjusted values of initial tension and slope for the first element to eliminate this mis-close.

A development of the above technique as detailed in Chapter 4 is used for the conditions of one end fixed used in this work.

2.4.4 Theoretical analysis of Binnie's method.

Binnie (5) in 1972 analysed a dam inflated by water and derived a relationship between the internal pressure and the height of the dam, the base width and the length of the curved perimeter of the dam were considered, while the ends effects were ignored. This analysis was based on the distortion of a strut into a curve known as the elastica (23).

2.4.4.1 Shape of the Dam.

a. Downstream profile analysis.

From the expression of radial equilibrium, see fig.2.7

$$- T^2 \, d\theta = (H-g) \, ds \qquad \ldots\ldots \qquad 2.22$$

where

$T^2 = \frac{T'}{pg}$, T' equals the tension in the membrane

H = pressure head in base of dam.

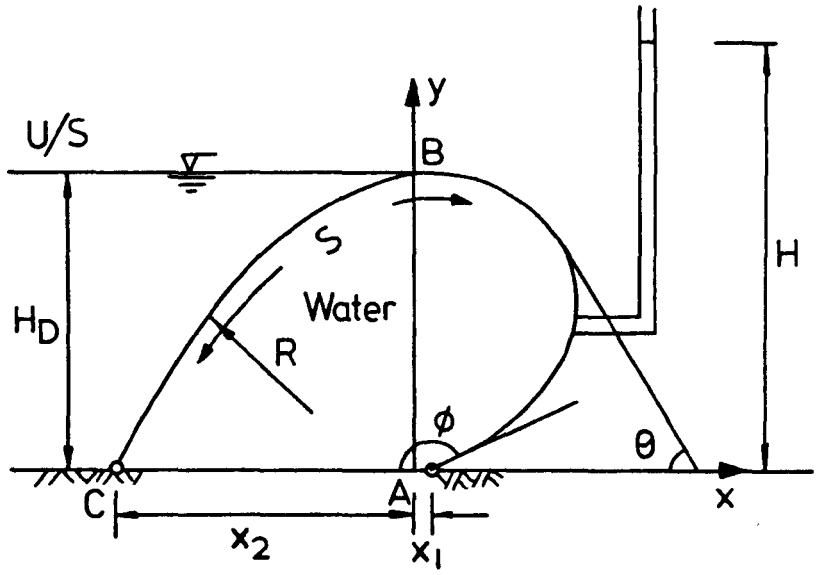

FIG. (2-7) DAM ANALYSIS OF BINNIE

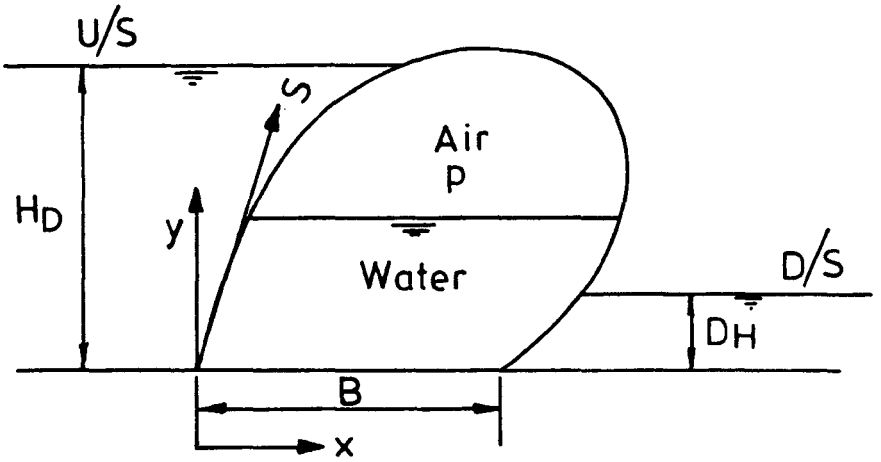

(A) Dam analysis of Parbery

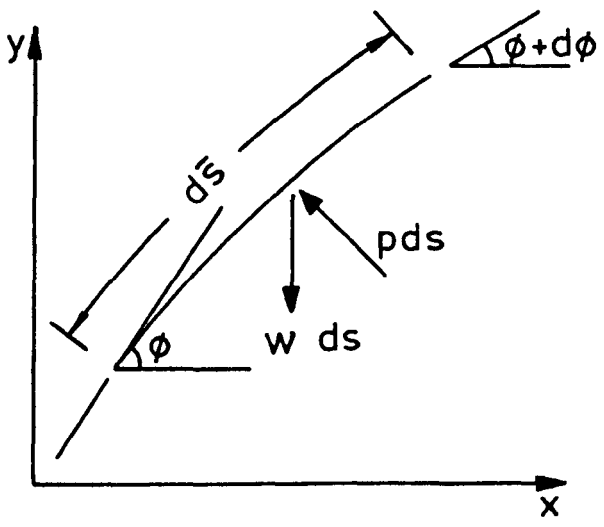

(B) Load on element

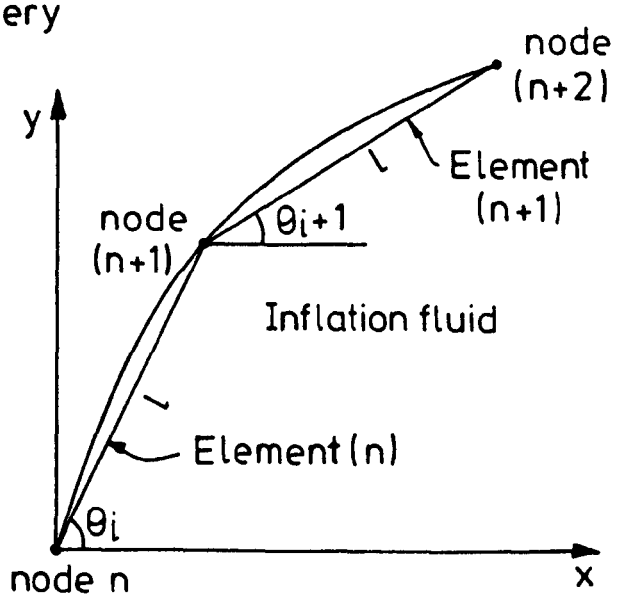

(C) Analysis method

FIG. (2-8) PARBERY'S ANALYSIS OF A DAM UNDER HYDROSTATIC CONDITIONS

The expression of the downstream profile is

$$\frac{X_1}{T} = F(K,\psi_1) - F(K,\psi_o) - 2\{E(C,\psi_1) - E(K,\psi_o)\} \quad \ldots\ldots \quad 2.23$$

where

F and E are the elliptic integrals of first and second kind respectively and K and ψ are constant. To simplify the equation, K and ψ are related by the expression

$$K = \left[\frac{H^2}{4T^2} + \cos^2\frac{\phi}{2}\right]^{\frac{1}{2}} \quad \ldots\ldots \quad 2.24$$

and $$K \sin\psi = \cos\frac{\theta}{2} \quad \ldots\ldots \quad 2.25$$

where

ϕ is the downstream fabric angle at the anchor point

θ is the slope of the fabric on the downstream side.

From fig.2.7

At point A $\theta = \phi, \quad \psi = \psi_o$

$$K \sin\psi_o = \cos\phi/2 \quad \ldots\ldots \quad 2.26$$

At point B

$\theta = 0, \quad \psi = \psi_1$

$$K \sin\psi = 1 \quad \ldots\ldots \quad 2.27$$

where

ψ is defined in equation (2.25)

ψ_o = value of ψ at downstream toe

ψ_1 = value of ψ at crest.

The ordinates of this curve are given by the following expression

$$H_D/T = 2K(\cos\psi_o - \cos\psi) \quad \ldots\ldots \quad 2.28$$

and the expression which gives the length of the membrane on the downstream side is

$$S_2/T = \int_{\psi_o}^{\psi} \frac{1}{(1-K^2 \sin^2 \psi)^{\frac{1}{2}}} \quad \ldots\ldots \quad 2.29$$

The pressure head was written in the following form

$$H/T = 2K \cos \psi_o \quad \ldots\ldots \quad 2.30$$

Equations 2.28 and 2.30 are plotted for different values of (K) downstream anchor slope (ψ_o) as shown in fig.2.9. Values of K should be greater than 1.0 (i.e. transformation to modulus of elliptics integrals should be done from greater than one to less than one).

The length of the downstream base is given by the following equation

$$\frac{X_2}{T} = F(K,\psi) - F(K,\psi_o) - 2\{E(K,\psi) - E(K,\psi_o)\} \quad \ldots\ldots \quad 2.31$$

where F, E are the elliptic integrals of the first and second kind.

b) Upstream face of the dam.

The equation for the upstream side is an arc of constant radius because of the constant pressure difference ($H-H_D$) and is given by

$$R = -\frac{dS}{d\theta} \quad \ldots\ldots \quad 2.32$$

From equation 2.22 and 2.32 the radius of the upstream face can be written as

$$\frac{T}{R} = \frac{H}{T} - \frac{H_D}{T} \quad \ldots\ldots \quad 2.33$$

The length of the curve BC, see fig.2.7, is given by

$$S_1 = R\beta \quad \ldots\ldots \quad 2.34$$

where

$$\cos \beta = \frac{R - H_D}{R} \quad \ldots\ldots \quad 2.34$$

and the base length of the upstream side is given by

$$\frac{X_1}{T} = \frac{R}{T} \sin \beta \quad \ldots\ldots \quad 2.35$$

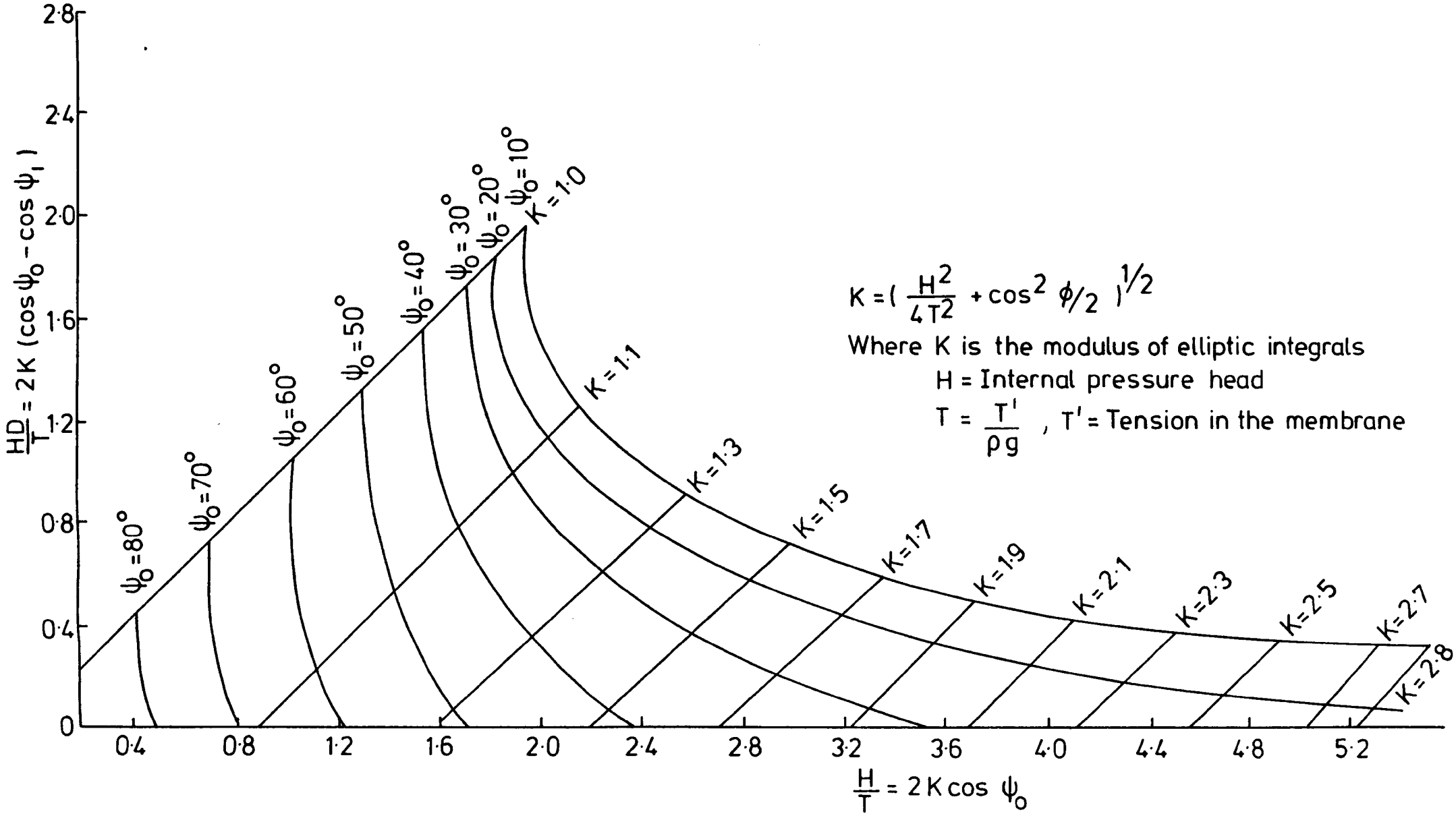

FIG. (2-9) VARIATION IN THE HEIGHT OF THE DAM WITH THE PRESSURE HEAD FOR DIFFERENT MODULUS OF ELLIPTIC INTEGRALS

2.4.5 Theoretical analysis of Clare's Method.

The analysis carried out by Clare (14) on a series of model tests to compare the mathematical analysis for the shape of the water inflated fabric tube with the experimental profiles. The mathematical analysis was almost similar to Binnie (5) approach. Clare investigated the Mangela dam failure by constructing a model dam to observe the behaviour for different operating characteristics.

2.4.6 Theoretical analysis of Parbery's Method.

In 1977 Parbery (6) derived a differential equation for the equilibrium of an inflatable structure the method dealing with the analysis of air, water and (air + water) inflation conditions under hydrostatic states. The analyses allowed determination of the tension and the shape of the dam profile.

2.4.6.1 Method of analysis.

The analysis is carried out on a membrane divided into n straight elements givine (n+1) nodes. The resultant forces acting on each element due to internal and external pressures are determined in order to calculate the tension and slope of the first element as shown in fig.2.8.

For loads acting on the elemental strip ds' of unit width, where p is the resultant internal pressure and T is the tension per unit width (assuming forces in the tangential direction) then

$$\frac{dT}{ds'} = w \sin \phi \qquad \ldots\ldots \qquad 2.37$$

where s' is the distance along the perimeter in the loaded state.

and $dy/ds = \sin \phi$ 2.38

hence

$$T = T_o + wy \qquad \ldots\ldots \qquad 2.39$$

where

T = tension in the membrane per unit width.

T_o = T(0) initial tension in the membrane of the origin (upstream anchor).

w = weight of the membrane per unit area.

y = co-ordinate position.

The initial tension and slope of the first element are calculated from a set of differential equations and by assuming the behaviour of the stress strain relationship of the membrane to be linear.

The differential equations of equilibrium are:

$$\frac{d\phi}{ds'} = \frac{f}{T_o + wy} (P - w \cos \phi) \quad \ldots\ldots \quad 2.40$$

$$\frac{dx}{ds'} = f \cos \phi \quad \ldots\ldots \quad 2.41$$

$$\frac{dy}{ds'} = f \sin \phi \quad \ldots\ldots \quad 2.42$$

with boundary conditions

$$x(0) = x(0) = 0 \quad \ldots\ldots \quad 2.43$$

$$x(L) = B, \; y(L) = 0 \quad \ldots\ldots \quad 2.44$$

where

ϕ = inclination of the tangent in the s' direction to the horizontal (see fig.2.8).

s' = the length along the unstretched perimeter.

f = extension ratio of the membrane under load.

P = resultant of internal pressure.

x, y = co-ordinates of an arbitrary point on the profile.

Equations 2.40, 2.41 and 2.42 are solved by using the Runge-Kutta method with estimated values of $\phi(0)$ and which can be refined by using the Newton-Raphson method.

If the membrane is assumed weightless and inextensible and the pressure is assumed constant, equation 2.40 will represent the arc of a circle the co-ordinates of the points on the profile are given by

$$x = \ell \{\cos \theta_i [2 - \frac{7}{12} (\frac{pL}{T})^2 + \frac{pL}{T} \sin \theta_i\} \quad \ldots\ldots \quad 2.45$$

$$y = \ell \{\sin \theta_i [2 - \frac{7}{12} (\frac{pL}{T})^2 - \frac{pL}{T} \cos \theta_i\} \quad \ldots\ldots \quad 2.46$$

where θ_i = slope of element.

ℓ = length of element.

2.4.7 Theoretical analysis of Alwan's Method.

In 1979 Alwan (7) studied the inflatable dam for different inflation fluids and under static and dynamic cases. This study was carried out to analyse a dam with two ends fixed by developing the Harrison method. The developed method considered the variation of the stress-strain relationship as non-linear and the length of the membrane was designed for a particular dam by assuming a constant radius of curvature in the upstream and downstream face.

2.5 Comparison of different analysis techniques.

The comparison of the different methods of previous investigators can be made under three main headings.

1. Condition of flow (static or dynamic).
2. Type of inflation fluid.
3. Design considerations and assumptions.

On the basis of the above points, table 2.3 is produced to show the comparison of the different methods of analysis by the different investigators.

In addition to the difference between the techniques shown in table 2.3, additional comments are presented according to the type of inflation fluid.

1. Water inflated condition.

Analysis techniques developed by Anwar, Kunihiro et al. and Binnie all given the upstream face of the dam is part of a circle, but the downstream face is related to the elliptic integrals and each method gives a profile.

In the Binnie analysis the results of the modulus of the elliptic integrals is greater than one whereas normally it should be less than one and

Table 2.3 Comparison of Previous Works.

No.	Condition	Anwar H.O.	Kunihiro Owiwora et al.	H.B. Harrison	A.M. Binnie and Clare	R.D. Parbery	A.D. Alwan
		1	2	3	4	5	6
1	Condition of Flow	1. Static 2. Dynamic	1. Static 2. Dynamic	Static	Static	Static	1. Static 2. Dynamic
2.	Type of Inflation Fluid	1. Water 2. Air	1. Water 2. Air	1. Water 2. (Air + Water)	Water	1. Air 2. Air + Water	1. Air 2. Water 3. Air + Water
3.	Design considerations and assumptions	1. Weightless material. 2. Constant tension. 3. No restriction of the base length 4. Upstream head equal to the max. height of the dam. 5. Downstream head equal to zero. 6. Stress-strain relationship is not considered.	1. Weightless material 2. Constant tension. 3. Consider the base and length of membrane. 4. Upstream head equal to the max.height of the dam. 5. Downstream head equal to zero. 6. Stress-strain relationship is not considered.	1. Consider the weight and thickness of the material 2. Tension is not constant along the membrane. 3. The upstream head is not necessarily equal to the max.height of the dam. 4. Downstream head may equal to zero or greater than zero. 5. Base length and perimeter length is considered. 6. Stress-strain Relationship have been considered.	1.Weightless material. 2.Constant tension along the membrane 3.Upstream head equal to max. height of the dam. 4.Downstream head equal to zero. 5.Base length and length of perimeter is considered. 6.Stress-strain relationship is not considered.	1. Weightless material. 2. Constant tension along the membrane 3. Upstream head less than the max.height of the dam. 4. Downstream head may equal to zero or greater than zero. 5. Base length and total length have been considered. 6.Stress-strain relationship have been considered	1.Consider the weight and thickness of the material. 2.Tension is not constant along the membrane. 3.The upstream head is not necessarily equal to the max.height of the dam. 4.Downstream head may equal to zero or greater than zero. 5.Base length and perimeter length is considered. 6.Stress-strain relationship have been considered.

in this case it is necessary to use spacial inversion formula (24) to transfer the value of the modulus of elliptic integrals to less than one.

2. Air inflated condition.

In the case of air inflated dams the results of Anwar, Kunihiro et al. and Parbery all give the shape of the upstream face as related to the elliptic integrals but the downstream face with zero downstream head is part of a circle. They give formulae in different forms.

In the case of dynamic condition both Anwar and Kunihiro have worked out the shape of the dam for air inflated dams but the results are different.

The Harrison and Alwan methods use a different approach by using the finite element technique to find the profile of the dam by considering the weight and thickness of the material. The analysis is achieved by a computer program the main output are tension, slopes and cross-sectional profile of the membrane.

2.6 Developing a new technique of analysis.

All previous work has related to double anchor systems whereas in this study a new technique based on the Harrison technique is developed applicable to a single anchor system.

1. The dam is considered to be fixed at one end only at the upstream face of the dam.

2. The effect of silt pressure on the upstream face of the dam is considered.

3. A non-linear relationship in the stress-strain relationship of the material is allowed.

4. The analysis applies to both hydrostatic and hydrodynamic conditions.

In this analysis the length of the membrane is designed according to different proportional factors whereas in the Harrison method the length of the membrane is assumed or uses the trial and error method to select a certain length to satisfy the other parameters (i.e., upstream head, internal pressure, downstream head).

CHAPTER 3.

EXPERIMENTAL WORK FOR STATIC CONDITIONS.

3.1 Introduction.

The object of the experimental work is to check the behaviour of the inflatable structure as given by the theoretical calculations, and to verify the design technique as realistic.

The maximum size of the mode used was limited by the maximum upstream head that could be contained within the tank used for the test. The details of the calculations for the length of the material to give this size of dam are given in Chapter 8.

Dams using inflation fluids of water, air and a combination of both were tested although the initial design was based on a water inflated dam.

The maximum upstream head for static conditions was 0.230 m for a maximum proportional factor equal to 2.5 and the length of material for this dam was 0.80 m. Different lengths were used to determine patterns of behaviour and different materials used to assess the significance of material properties.

A detailed description of the construction of the models and inflation apparatus is given in this chapter. A technique for measuring the cross sectional profile is also detailed in this chapter. This allowed a comparison of the measured profiles with those obtained from the computer program as described in Chapter 6.

3.2.1 Model Tank.

A rectangular tank in which the inflatable models were installed was 4267 mm long x 1030 mm wide x 380 mm deep constructed from 10 mm thick clear perspex. The tank incorporated a 12.5 mm thick perspex hinged gate for controlling the down stream level below the model. The flow from the tank passed into a rectangular galvanized steel channel, 220 mm wide and 250 mm deep with a rectangular sharp crested weir installed at the downstream end to allow

flow measurement for the tests in the hydrodynamic condition. The weir was calibrated by the volumetric method by collecting known volumes in known time in a tank 3040 mm long x 1219 mm wide x 711 mm deep.

The water supply system was completely self contained and was circulated by a centrifugal pump of 30 ℓ/s maximum flow rate supplied to the tank through a 100 mm diameter delivery pipe which divided into two 50 mm diameter flexible pipes feeding the upstream end of the tank. The details of this arrangement are shown in fig. 3.1 and fig. 3.2A.

3.2.2 Air Inflation Apparatus.

The apparatus used for air inflation of the dams is shown in fig.3.2B and 3.3B.

The air lines system was connected to the model structures by 8 mm plastic pipe into the upstream face of the dam on the lower side. The pipe was kept loose in the vicinity of the model dam in order to minimize any effect the pipe may have on the dam.

The air was supplied from an existing laboratory compressed air supply system with a maximum air pressure of 10.0 KN/m^2.

Referring to figs. 3.2B and 3.3B the apparatus consisted of the following items:

Valve No. 1. main valve used as an initial control of the air pressure from the compressor to the apparatus.

Valve No. 2. coarse pressure control.

Valve No. 3. used to release air from the system (safety valve).

Valve No. 4. fine pressure control valve.

Valve No. 5. control valve to isolate the gauges from the model dam under test.

Valve No. 6. used to isolate the air pressure inside the model from the apparatus system.

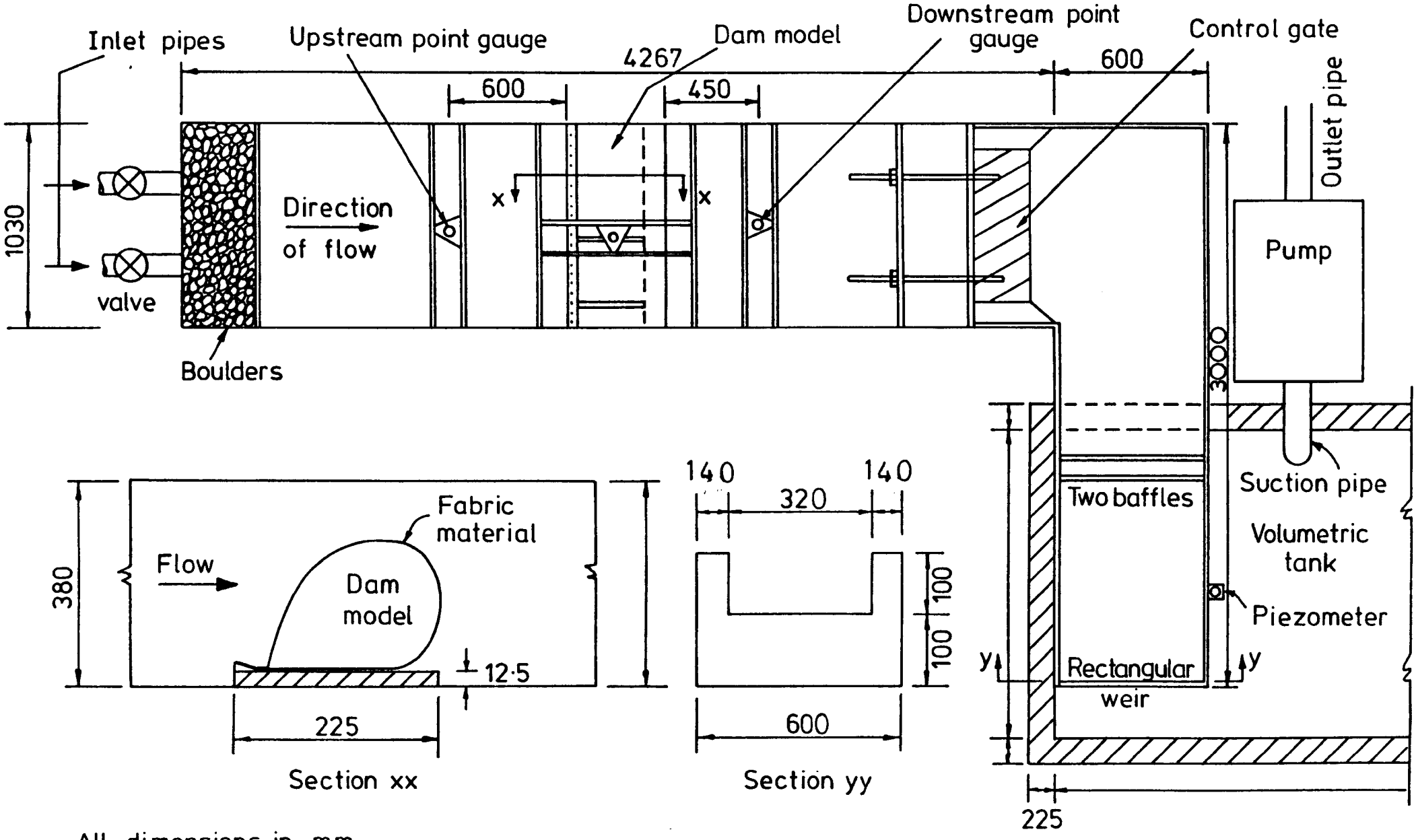

FIG. (3·1) DIAGRAM OF TEST TANK

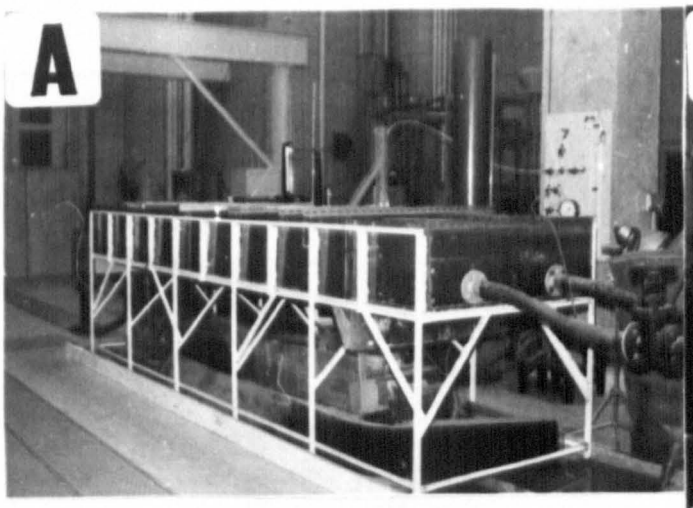

A– Test tank

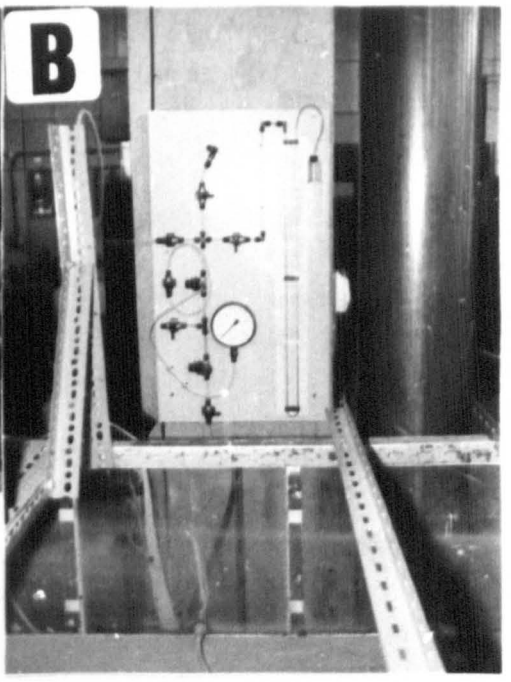

B– Air inflation apparatus

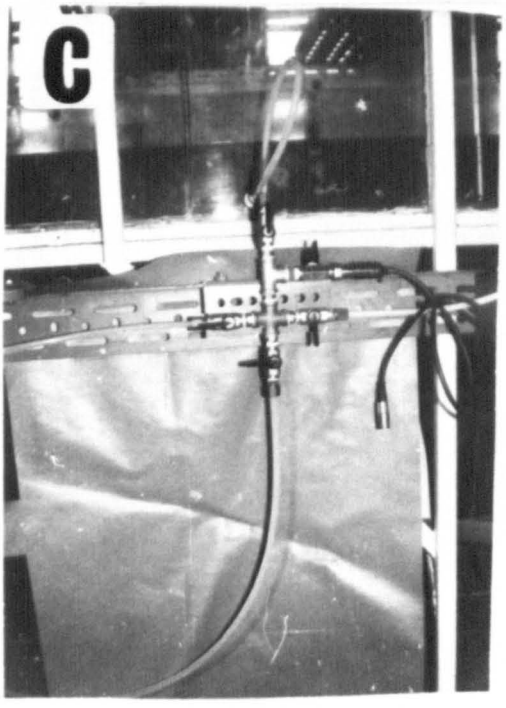

C – Control valves

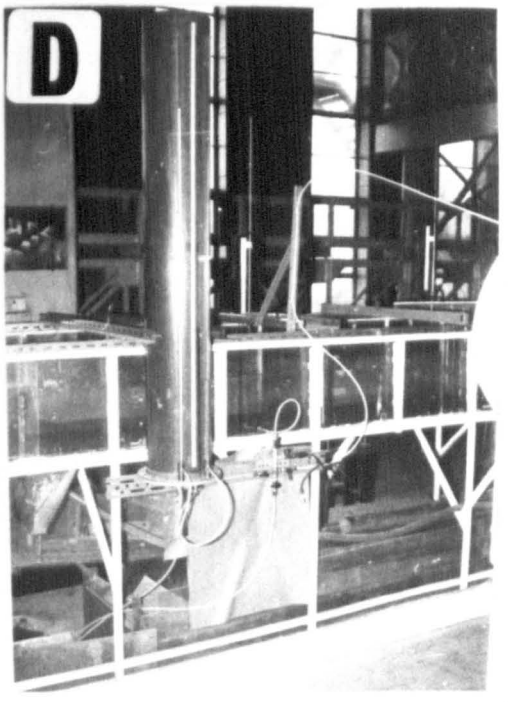

D – Water inflation apparatus

FIG. (3-2) LABORATORY APPARATUS

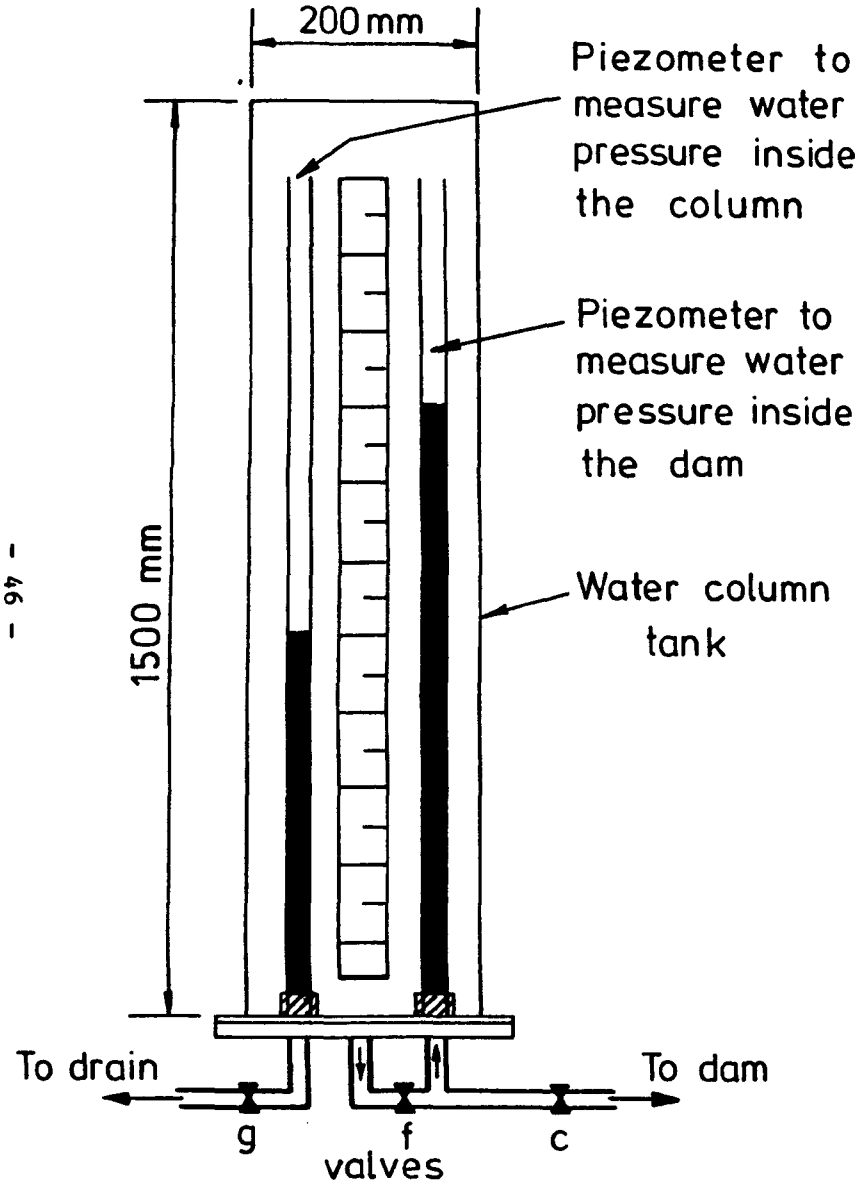

(A) Water inflation apparatus

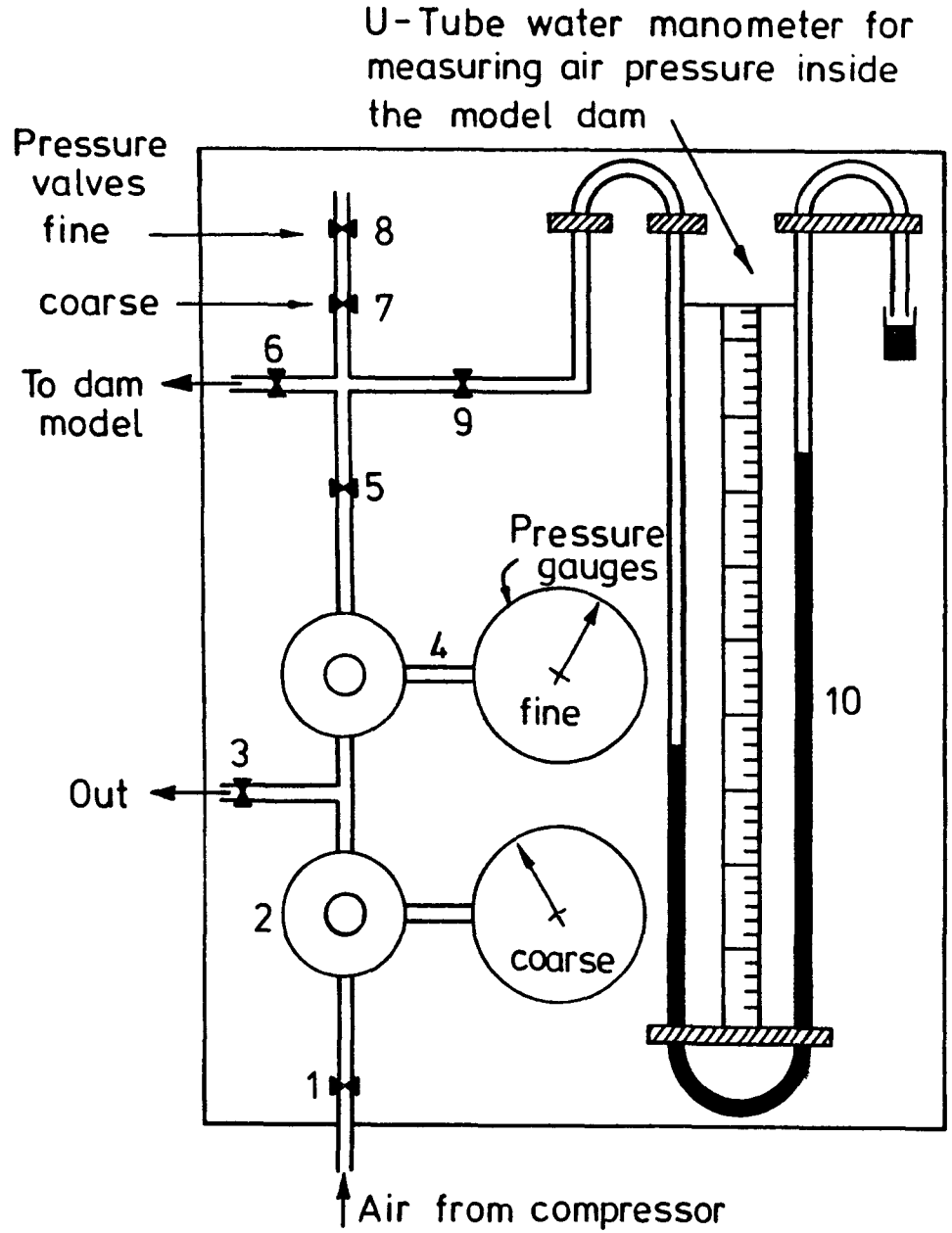

(B) Air inflation apparatus

FIG (3·3) INFLATION APPARATUS

Valve No. 7. coarse pressure control valve for air pressure inside the model.

Valve No. 8. fine pressure control valve for air pressure.

Valve No. 9. valve used to prevent high air pressures removing the water from the manometer.

3.2.2.1 Operation of air inflation system.

The sequence of operation for inflating a model using this air system was as follows:

1. Before starting the inflation procedure all valves in the system were closed.

2. Open valves 7, 8 and 9 in order to release the air inside the manometer and to adjust the U-tube manometer to atmospheric pressure.

3. Close valves 7, 8 and 9.

4. Open coarse pressure control valve No. 2, then Valve No. 1 and in this case it was necessary to open the fine control valve No. 4 until the dial gauge read 2.2 bars and then by this arrangement the air started to inflate the model.

5. By opening valves 5 and 6 this allowed the air to pass through the plastic pipe to inflate the model dam until a required pressure was reached and then valve 5 was closed.

6. To read the pressure head inside the dam valve No. 9 was opened and the air pressure registered on the U-tube manometer and the difference in level in the tubes could be used to determine the pressure head.

7. To lower the pressure inside the dam, valve No. 7 was opened and by using the fine pressure control valve No. 8 to release air from inside the model, the pressure could be reduced down to the required level.

A second system of control valves was placed near the dam to allow variations in the type of inflation fluid (i.e. air or water) in the dam. This system shown in fig. 3.2C and fig.3.4 consisted of the following parts:

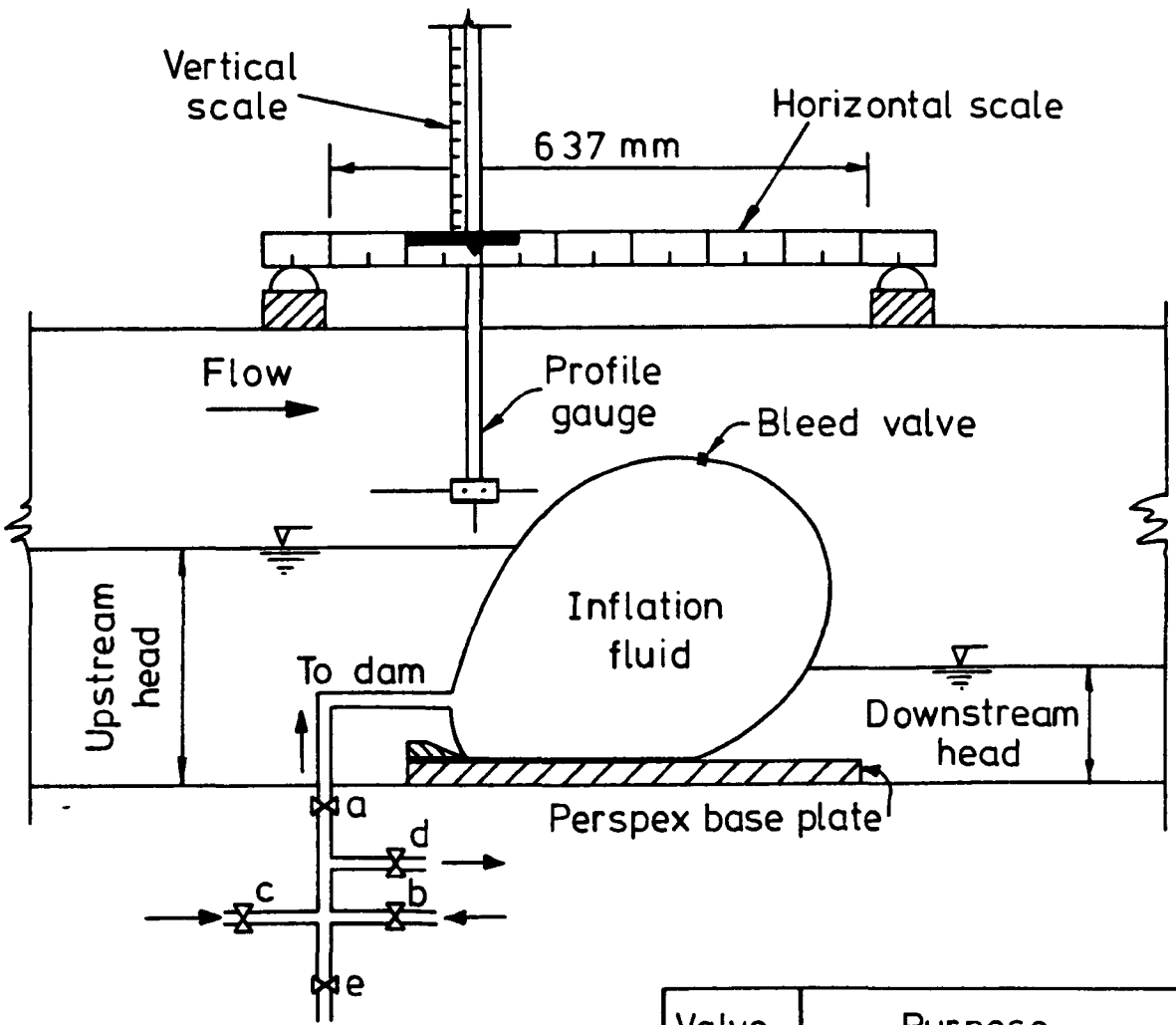

Valve	Purpose
a	Main control valve in the dam model
d	Pressure transducer connected to data logger
b	Control valve for air pressure
c	Control valve for water pressure
e	Valve used for deflation

FIG. (3-4) MAIN CONTROL VALVES TO MODEL DAM

a. main control valve in the dam,

b. control valve for air inflation,

c. control valve for water inflation,

d. valve to pressure transducer,

e. deflation valve.

3.2.3 Water Inflation Apparatus.

A column 200 mm in diameter by 1500 mm high made of plastic was used to create a water inflation system. Two piezometer tubes were connected to this column one to measure the pressure head inside the model structure and the other to measure the depth of water inside the column. Two valves were attached to the bottom of the column, one to supply the model structure with water (valve f, fig.3.3A) and the second valve (g) to lower the water or to drain the column. The arrangement is illustrated in figs. 3.2D and 3.3A.

3.2.3.1 Operation of the water inflation apparatus.

In order to inflate a model structure with water, it was necessary to use the water column and control valves as shown in figs. 3.2D, 3.3A and 3.4 in the following way.

1. The bleed valve in the model dam was opened so that any air inside the dam was removed.

2. Close valves d, b, and e (fig.3.4) and open valves a and c.

3. Open valve f (fig.3.3A); this allowed water inflation to commence.

4. When the pressure head reached approximately the required value: the bleed valve was closed and then continued inflation of the dam with water was made until the required pressure was reached, then valve (f) was closed, and pressure head in the model dam measured from the piezometer on the column.

3.2.4 Depth and Profile Gauges.

3.2.4.1 Point gauges.

Two point gauges were installed in the test tank as shown in fig. 3.1, one 600 mm from the upstream face of the dam model and the other 450 mm down stream of the down stream edge of the base.

A third point gauge was used in the volumetric tank to measure the depth of water in this tank during the calibration of the rectangular weir. The accuracy of all point gauge measurements was within ± 0.5 mm.

3.2.4.2 Profile gauge.

The profile gauge was used to measure the profile of the dam and was constructed so that measurements could be both round a profile and transversely along the model. The range of movement of the gauge across the dam was 637 mm. Fig.3.4 illustrates the profile gauge and the technique of the measurement is explained in detail in Sec. 3.6.1. This gauge consisted of three arms, the vertical arm was used to measure the crest profile, the short horizontal arm to measure the profile of the upstream face of the dam and the long horizontal arm to measure the profile of the downstream face of the model. The accuracy of measurements using this gauge was within ± 0.1 mm.

3.3 Model Materials.

One aim of this study was to use different types of material to ascertain material property significance in the behaviour of a dam. The main parameters in the selection of the type of material were high tensile strength and high flexibility. Any difficulties with materials used in models constructed by other workers are not detailed by them. It was therefore necessary to contact a number of manufacturers to find suitable materials, and the following materials were eventually selected.

1. N.T. Fabric. This material was available from "Flexible Structure Ltd." Company (25) and had been used by the company for dams comprising a water filled tube clamped to a concrete foundation for raising the level of river water during drought conditions.

2. 'Story Butylite'. This material was suggested by Butyl Products Limited (26), the recommendation being based on the fact that it was a high quality synthetic rubber membrane manufactured under static test control

conditions to ensure reliable performance and life expectancy. The manufacturers maintained that it has excellent weathering, water and chemical resistance in addition to elastic recovery, puncture resistance, and a wide temperature range for practical application (i.e. 40°C to 140°C), and this material was considered suitable for the fabrication of dams.

For this study only these two materials were used although other materials were suggested by manufacturers but were considered unsuitable because of high elongation of the material, low flexibility and low tensile strength.

3.3.1 Properties of the materials.

The properties of the materials selected and used in this study are given in table 3.1.

Table 3.1 Material properties.

Type	Materials	Thickness mm	Weight Kg/m^2	Tensile strength (KN/m)	Max. breaking load (KN)
I	N.T. Fabric	0.36	0.391	29.20	0.73
II	Butylite	0.455	0.502	26.0	0.65

In order to find the stress-strain relationship tests of the tensile strength according to B.S. 3424, 3411, 2576 (27,28,29) were carried out by taking several specimens 25 mm wide x 200 mm long from different positions of the fabric material and testing these in a tensometer machine as shown in fig.3.5. The tests were carried out at normal room temperature in the range (10-25°C). The measurements made were the elongations of the material for a series of load increments up to failure of the strip.

The results of these tests were analysed using a least square polynomial method to find the relationship between the stress and strain. An existing

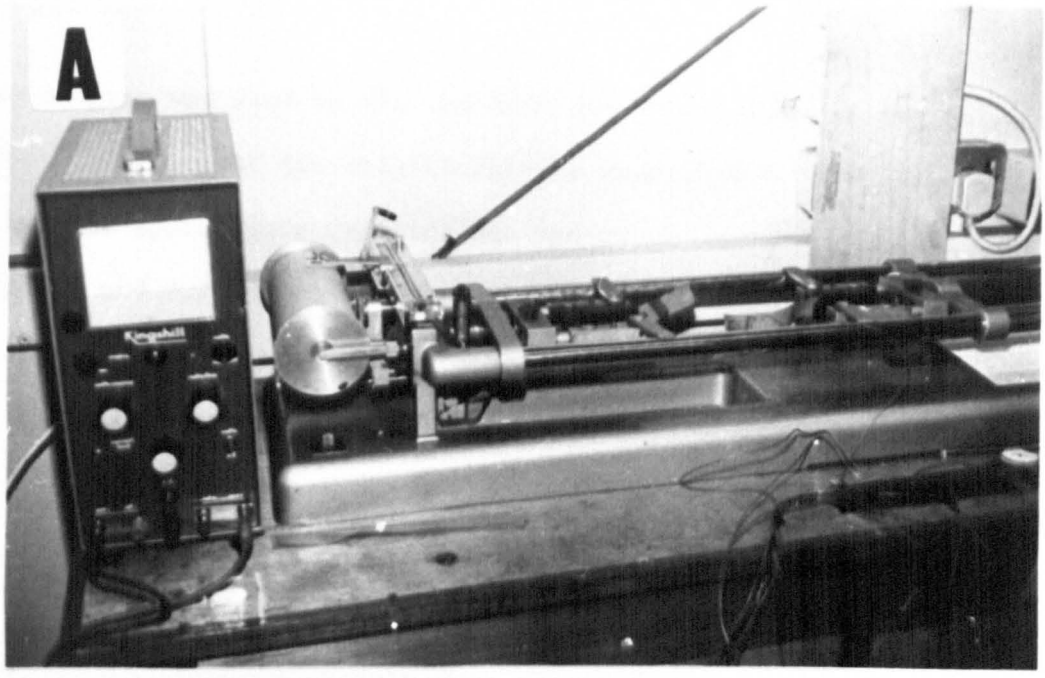

A - Tensometer for tensile tests on materials

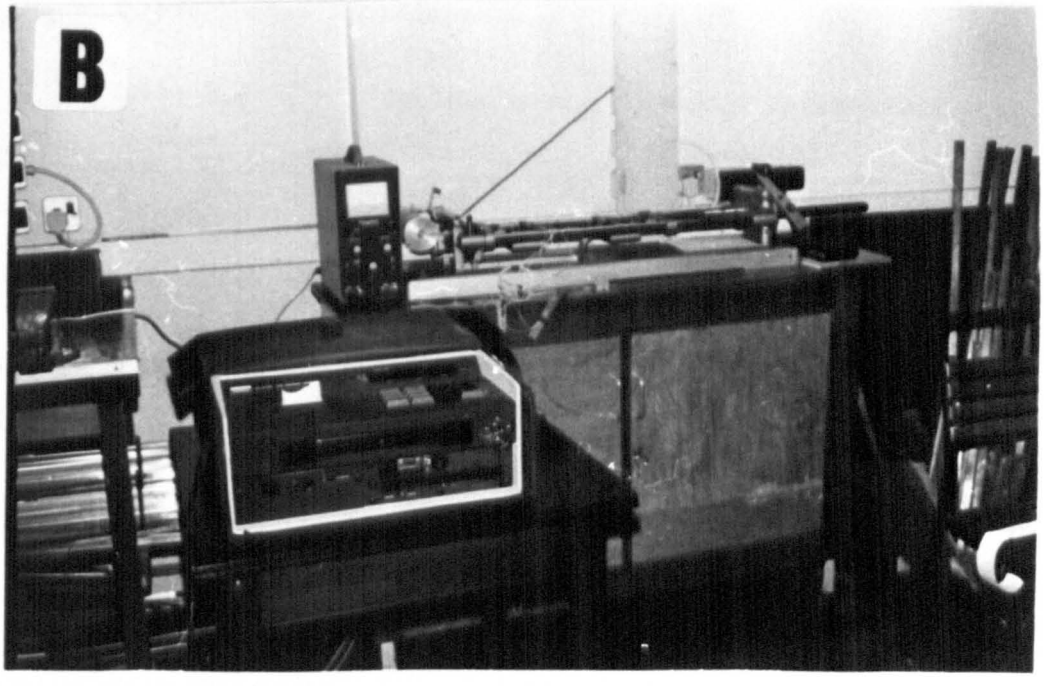

B— Data logger

FIG. (3-5) MATERIAL - TENSILE TESTS

computer program was used to fit the data and the results of the polynomial curve fitting show that the relationship is described by a third degree polynomial and the appropriate coefficients are given in table 3.2.

Fig.3.6 and 3.7 show the stress-strain relationship for the materials Type I and Type II. The form of the equation obtained by the polynomial fitting method is as follows:

$$\varepsilon = C_1 + C_2 \sigma + C_3 \sigma^2 + C_4 \sigma^3 \quad \ldots\ldots \quad 3.1$$

where

ε = strain in the fabric = $\frac{\Delta L}{L}$

ΔL = elongation of the fabric.

L = original length of the fabric strip m.

σ = stress in the fabric (KN/m^2)

C_1, C_2, C_3, C_4 = polynomial coefficients.

Table 3.2 Coefficients polynomial curve fitting.

Type	Materials	C_1	C_2	C_3	C_4
I	N.T. Fabric	0.40638E-02	0.85447E-05	-0.11483E-09	0.66118E-15
II	Butylite	0.34260E-02	0.85838E-05	-0.12976E-09	0.82579E-15

3.4 Model Design.

The length of the material required for the model dam was determined according to the theoretical analysis as detailed in Chapter 8 and was based on the following considerations.

1. Upstream head equal to the maximum height of the dam.
2. Downstream head equal to zero.
3. Inflation fluid used is water.

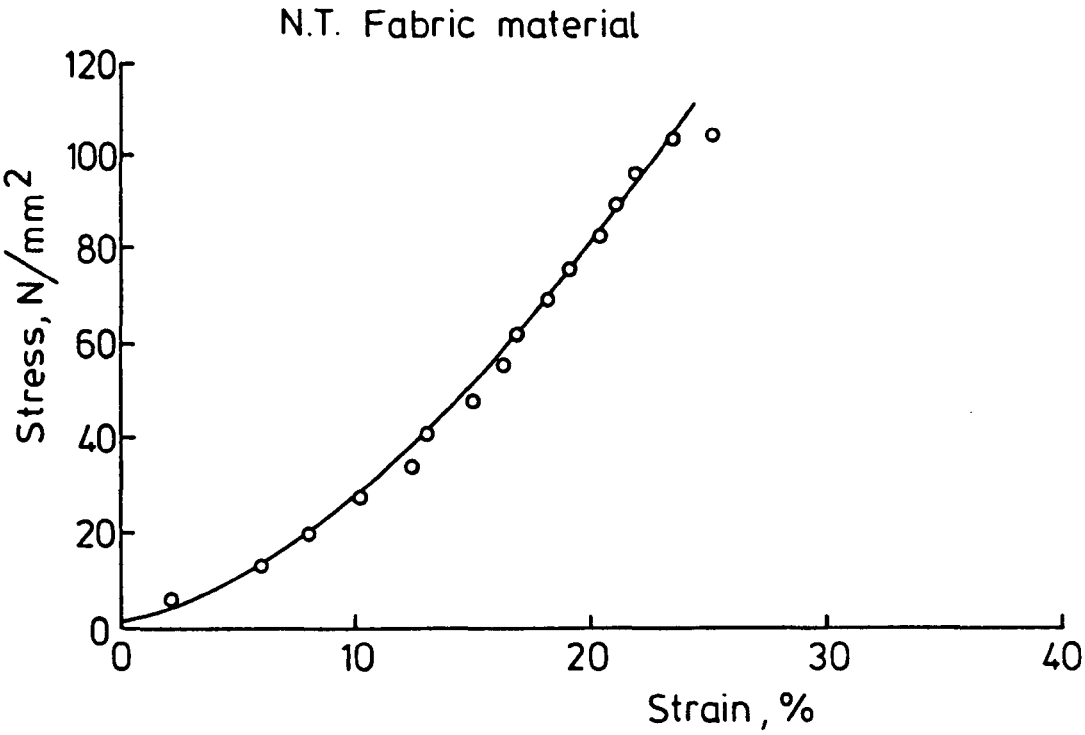

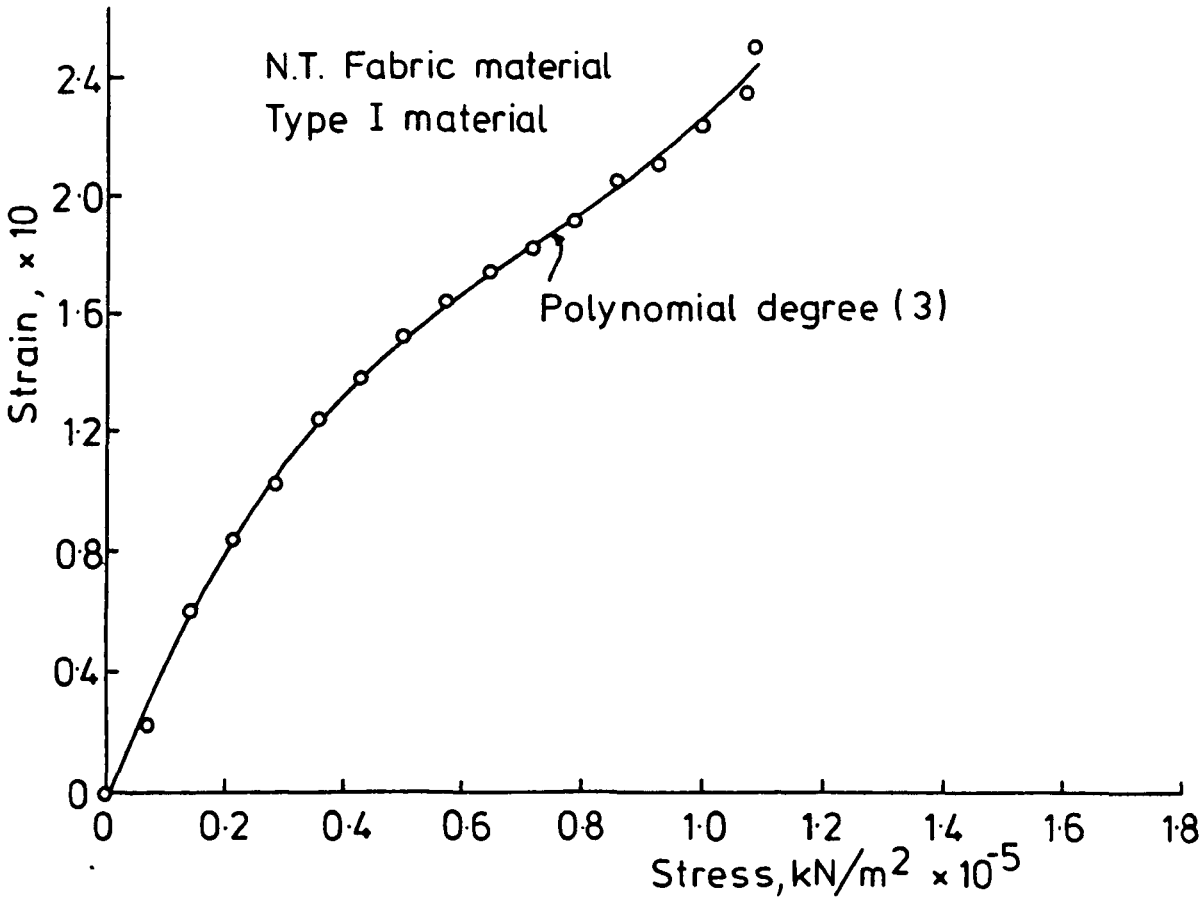

FIG. (3·6) STRESS-STRAIN RELATIONSHIP FOR N.T.FABRIC MATERIAL

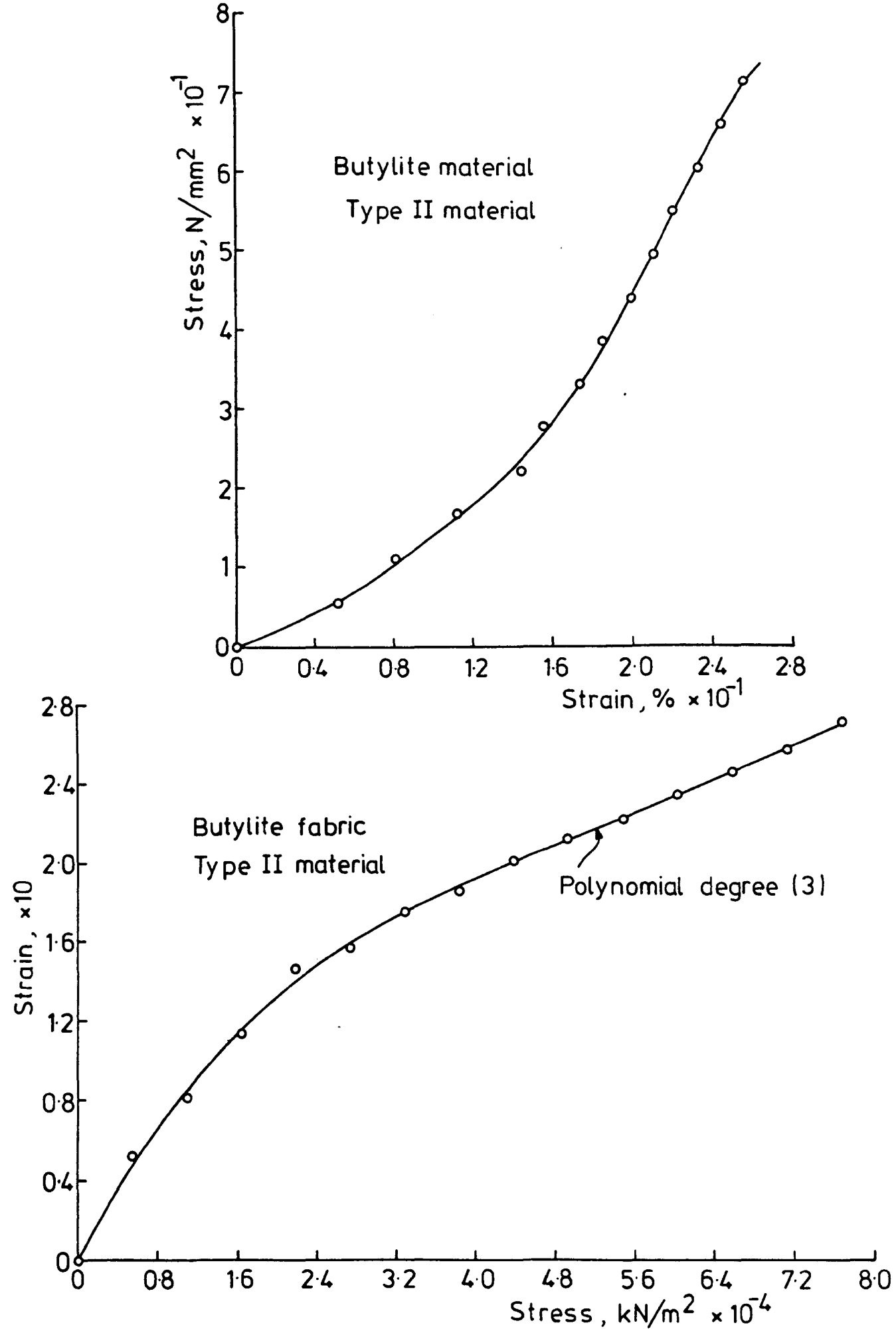

FIG.(3·7) STRESS – STRAIN RELATIONSHIPS FOR BUTYLITE FABRIC MATERIAL

From these considerations the maximum U/S head of the model dam was equal to 0.230 and maximum pressure head equal to 0.80 m for a maximum proportional factor equal to 2.5. The minimum total length of the membrane was found equal to 0.80 m including the minimum base length of the membrane equal to 0.126 m.

As shown in Chapter 8 the length of the dam membrane is initially calculated by ignoring the weight and thickness of the membrane and by considering a constant tension along the membrane. Once the initial length is found the dam is then analysed by using the program (IHSIP) to find the maximum height of dam for the maximum upstream head used and considering the weight and thickness of the material. Fig.3.8 illustrates the output of the program (IHSIP) for minimum and maximum proportional factors (1.0-2.5) for a dam inflated with water.

3.5 Construction of the Dam Model.

The basic components of a dam model are as follows:

1. Bag construction.
2. Base of the model.
3. Anchoring arrangement.
4. Inflation technique.
5. End constraints.

The details of the above components are explained in the following sections.

3.5.1 Bag construction.

The same technique applied for both the materials used. A dam was constructed by cutting a single rectangular sheet of length 1500 mm (Sec.5.3.5) but the width of the sheet varied depending on the storage head (maximum upstream head).

The single rectangular sheet was punched with two 14 mm holes, one located at a distance of 275 mm from the side of the sheet. An internal

U/S HEAD	=	0.2297	METER
D/S HEAD	=	0.0000	METER
AIR PRESSURE	=	0.0000	KN/SQ.M
WATER PRESSURE	=	0.7959	M.W.G.
ORIGINAL LENGTH	=	0.8000	METER
NEW LENGTH	=	0.8143	METER
U/S TENSION	=	0.6163	KN/M
U/S SLOPE	=	153.5459	DEGREE
D/S TENSION	=	0.8708	KN/M
BASE LENGTH	=	0.1259	METER
MAX. HEIGHT	=	0.2397	METER
ALFA	=	2.5000	
AREA	=	0.0520	METER SQ
SILT DEPTH,HS	=	0.0000	METER

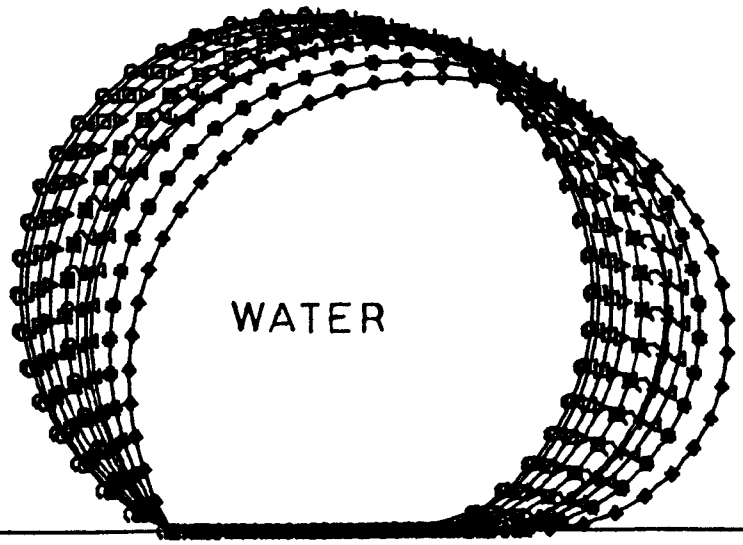

FIG.(3-8) THE OUTPUT PROFILES UNDER HYDROSTATIC CONDITION USING COMPUTER PROGRAM (IHSIP)

threaded brass tube of 13 mm outside diameter and sealed with a washer in order to allow the connection of the inflation pipe to the model was fastened through this hole.

The second hole was located on the crest of the dam near the side of the tank. This hole contained the bleed valve. Fig.3.9 illustrates the details of a single sheet for model construction.

Sealing of the bag was achieved by using an adhesive glue material "Dunlop 1310". The overlap required was found to be 25 mm from a series of tests on the tensile strength of 10, 15 and 25 mm overlaps. The 25 mm overlap gave a bond strength equal to 2.5 KN/m.

15 mm wide strips of silver foil were fixed at distances of 360 and 750 mm from the side of the bag around the profile before fixing the dam in the test tank. These silver foil strips were used in the measurement of the profile of the dam. The procedure for the sealing of a bag is described below and illustrated in figs. 3.9 and 3.10.

1. Cut the sheet according to the design dimensions and punch the required holes for the outlet and inlet pipes.
2. Seal the side AB (fig. 3.9 and fig. 3.10B) to side CD to form a tube.
3. Seal the side AC of the tube.
4. Fit the bleed valve and the inlet valve.
5. Seal the side BD of the tube.
6. Fix the silver foil strips around the tube.

At this stage the tube dam was ready for fixing in the test tank and the inlet pipe (for air or water) was connected to the dam.

3.5.2 Base of the model.

The model dam was anchored at one edge of a perspex base 12.5 mm deep x 325 mm long which was of sufficient length to allow the dam to spread on the base under pressures or even in the deflation condition. Fig.3.9 illustrates the details of the base of the model.

All dimensions in mm

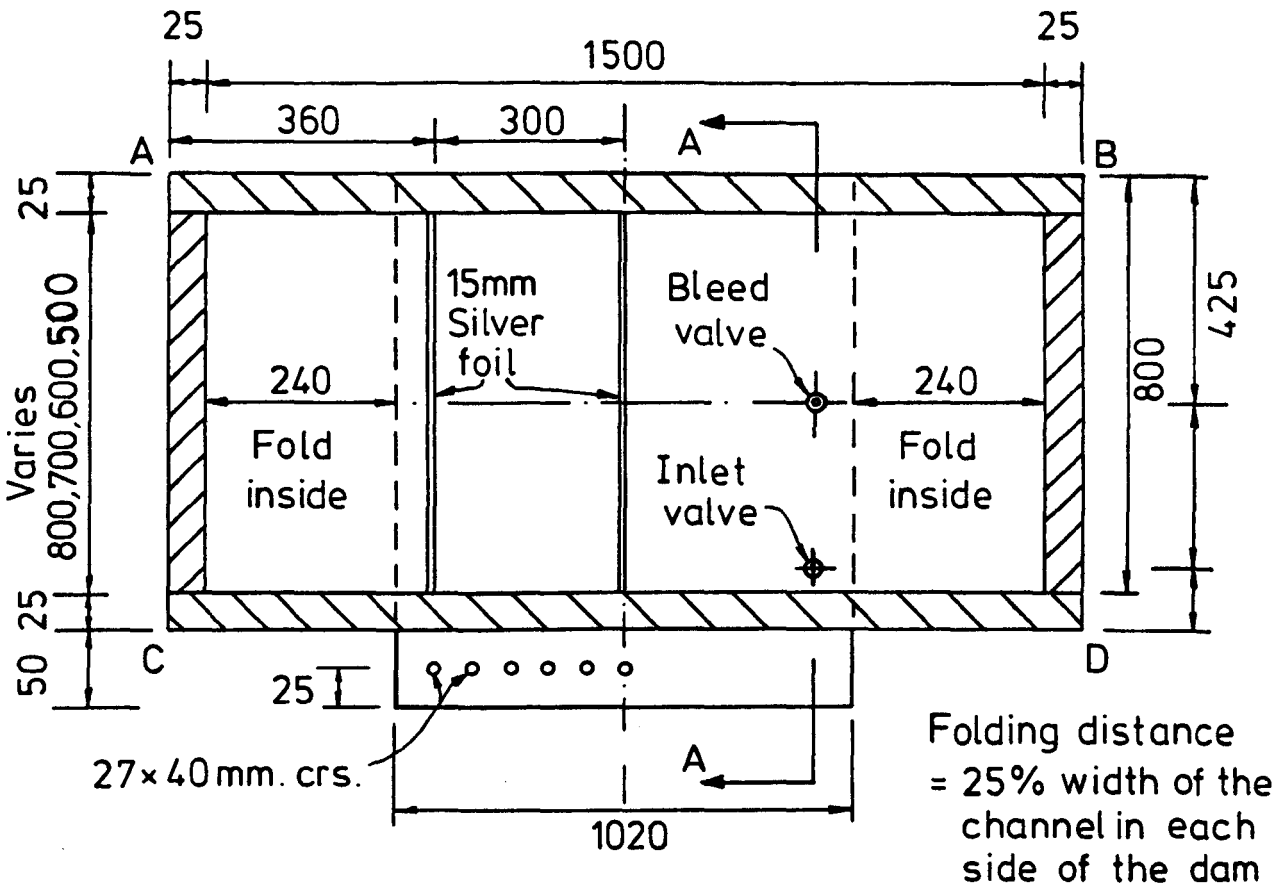

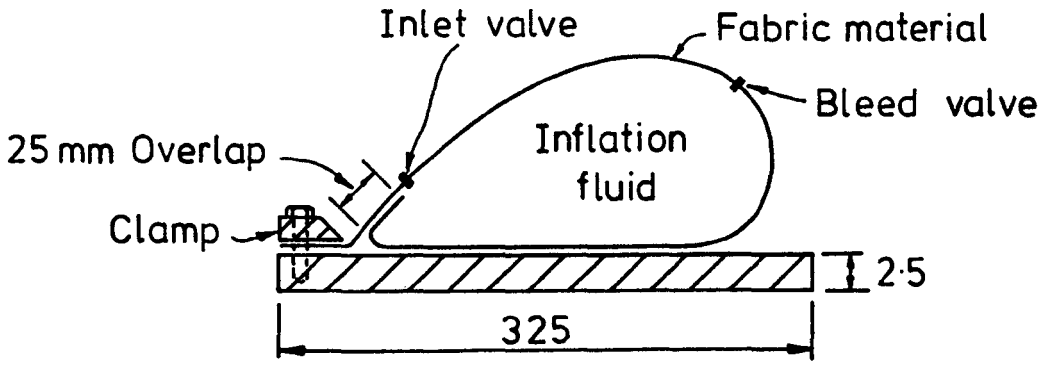

Section AA Inflation condition

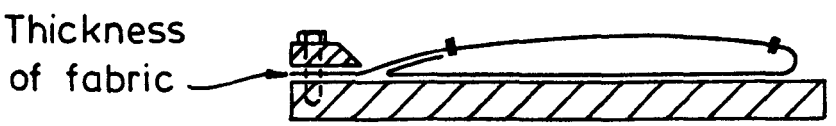

Section AA Deflation condition

FIG. (3-9) SINGLE SHEET DAM CONSTRUCTION

A – Single sheet

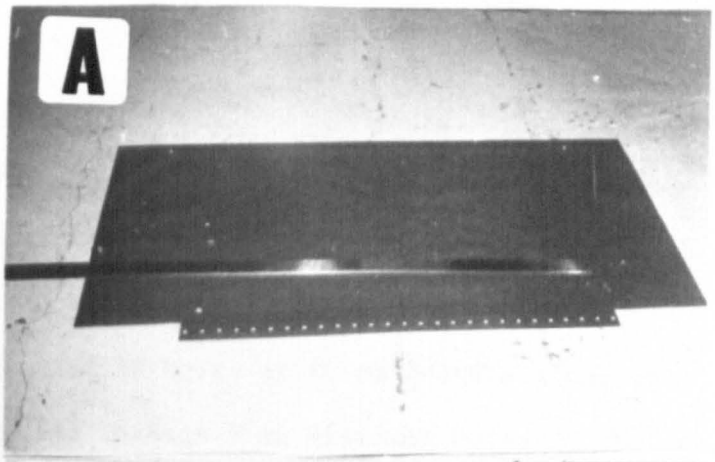

B – Tube sealing

C – Completed tube

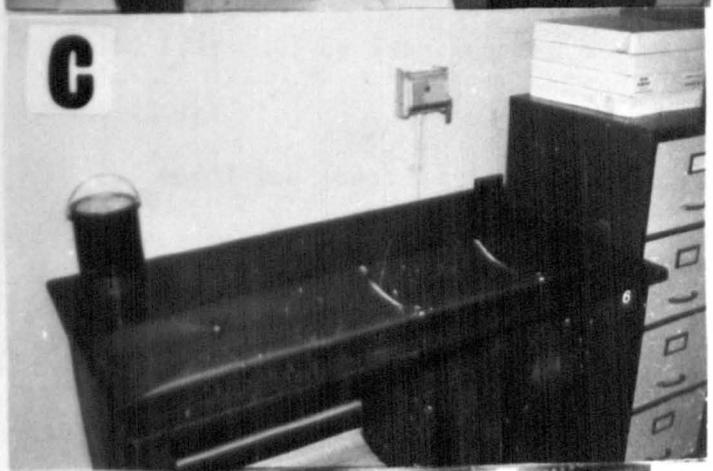

D – Fixing the tube
in the test tank

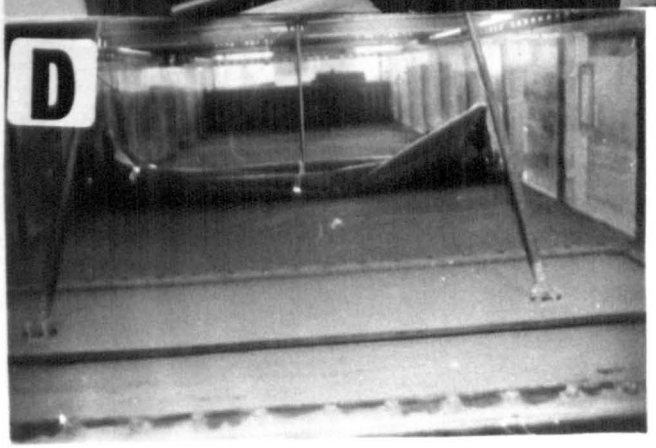

FIG.(3-10) STEPS IN THE CONSTRUCTION OF AN INFLATABLE DAM MODEL

3.5.3 Anchoring arrangement.

Anchoring of the bag to the base was achieved by clamping the 30 mm flaps between the upstream edge of the base and a perspex strip 8 mm thick along the transverse length of the dam (width of the test tank).

The clamping system consisted of 27 bolts at 40 mm centers along the edge. The 7 mm bolts were inserted through 7 mm diameter holes in the perspex strip. An illustration of this arrangement is given in fig.3.9.

3.5.4 Inflation Technique.

The inflation of the model was either by water, air or a combination of both (air + water).

Inflation by air was made by connecting the valve b (see fig.3.4) with valve No. 6 in the air apparatus system (see fig.3.3.B), with an 8 mm diameter nylon pipe. Air was supplied from the air compressor to the air control system and then to the controlling valve (fig.3.4) by adopting the sequence of valve operations described in Section 3.2.2.1.

In the case of water inflation, the model was supplied with water through the valve c and by opening valve f in the water column (see fig.3.3A). Again the sequence of valve operations has been detailed in Section 3.2.3.1.

Inflation by both air and water was achieved by using the procedure for water inflation to inflate the model to the required internal depth, then inflating the model with air with the same procedure for an air inflated model and then measuring and adjusting the pressure head using the peizometer and valves on the water column.

A pressure transducer was connected to valve (d) and connected to the data logger and thus was also used to measure the pressures in the dam especially in the case of a small change in the pressure inside the dam. The pressure transducer was used especially for the dynamic conditions when the

changes of the pressure inside the dam cannot find it by the manometer reading. The pressure transducer registered the reading on the data logger. The detail of using the pressure transducer is shown in Chapter 5.

3.5.5 End Constraints.

In order to keep the dam stable under different inflation fluids, the ends of the dam were made with extra width that was folded inside the dam during the inflation.

The folded length (extra width) was chosen by trying different folded lengths in order to find the most suitable length to give minimum leakage of water at the ends and for the dam to be stable during the operation.

It was found experimentally that the best folded length was equal to 1/4 the width of the dam on each side.

Hence the width of the fabric w_f which can be used to build a dam in a particular channel of width b is:

$$w_f = b + 2\,\frac{1}{4}\,b$$

$$\text{or} \quad w_f = 1.5\,b \qquad \ldots\ldots \qquad 3.2$$

3.6 Testing of a Model.

The purpose of the model tests was to check the theoretical work and prediction of the behaviour of an inflatable dam.

For the three different inflation conditions, three dams all of the same size were built and three dams of different sizes were also built for each condition of inflation to avoid using a particular dam again after elongation had occurred when high pressures had been applied.

The series of tests were divided into three parts for each type of inflation fluid for the total length equal to 0.80 m those covering low pressures (low proportional factor), medium pressures and high pressures (high proportional factor).

For water inflated dams, the tests were carried out from a lowest pressure of 370 mm to a highest pressure equal to 800 mm and with the downstream heads equal to 0.0,0.1 m. The test program is shown in table 3.3.

Air inflated dams were tested under pressures from a lowest pressure of 2.8 KN/m^2 to a highest pressure equal to 5.73 KN/m^2 for the downstream heads equal to 0 and 0.1 m. Details of the test program are shown in table 3.4.

Similar tests were done for the (air + water) inflated dam under a lowest pressure of 1.5 KN/m^2 to a highest pressure equal to 3.96 KN/m^2 by keeping the depth of water inside the dam equal to 0.158 m. The tests were carried out for the downstream heads equal to 0.0, 0.04, 0.1 m. The details of the tests are given in table 3.5.

3.6.1 Profile Measuring Technique.

The profiles of the inflatable models were measured using a profile point gauge as illustrated in fig.3.11. A small test meter was connected with the dam so that when the profile point gauge came into contact with the silver foil, the test meter indicated a full deflection, and from this indication, the reading of the dam profile can be taken.

3.6.1.1 Procedure for measuring a profile.

1. Place the point profile gauge at point A as illustrated in fig.3.11 so that the initial reading of the horizontal and vertical co-ordinate can be taken. (In this arrangement the initial readings were 0.0 and 180 mm for the vertical and horizontal co-ordinates respectively.)

2. Inflate the dam with a particular pressure head for a certain type of fluid and readings of the profile of the upstream side were taken by raising the point gauge every 20 mm using the short pin arm at position (1) as illustrated in fig.3.11.

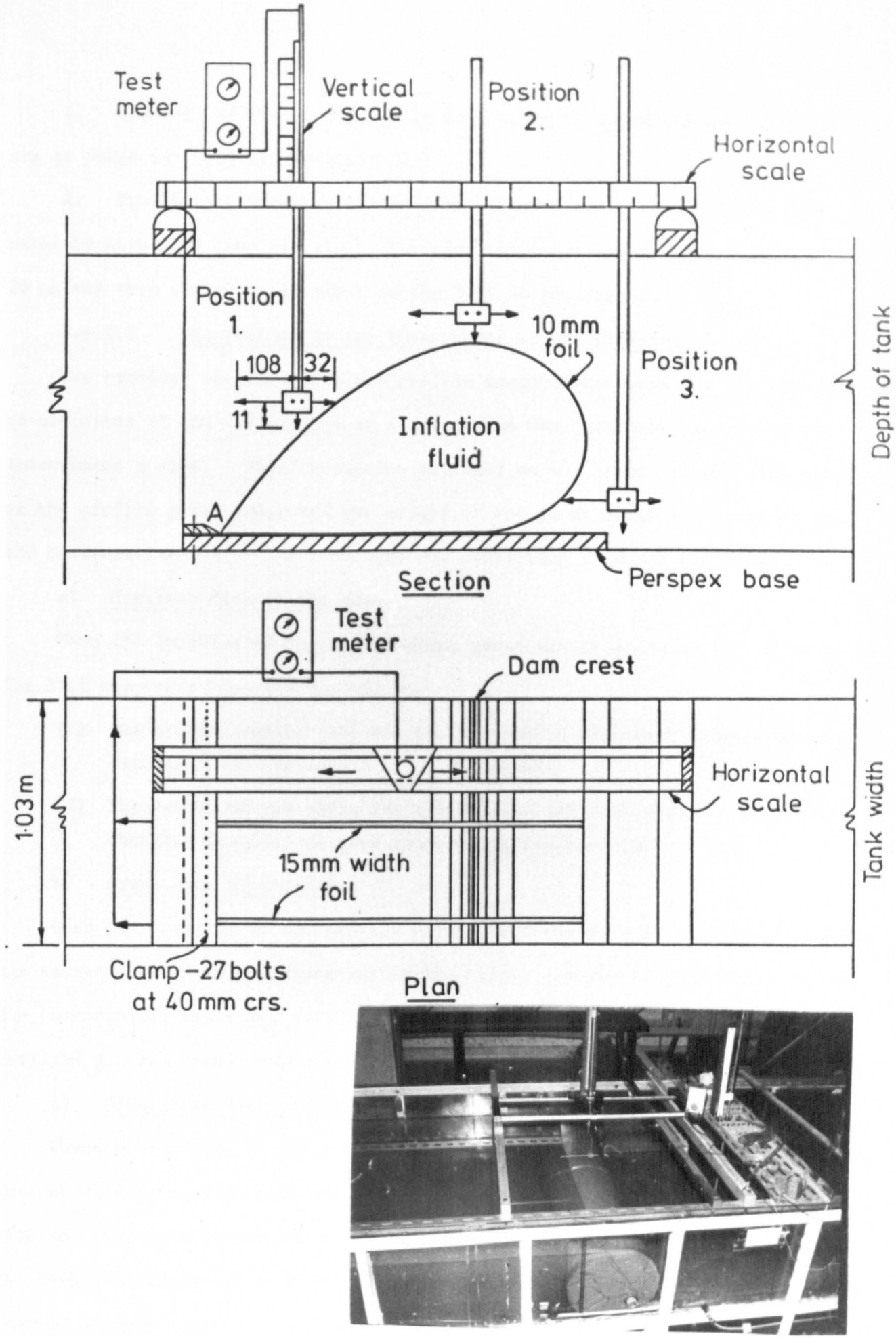

FIG.(3-11) PROFILE MEASURING TECHNIQUE

3. Readings of the crest profile were taken by using the vertical pin arm as shown in fig.3.11, position 2.

4. Profile measurements of the downstream side of the model dam were taken by using the long pin arm by lowering the point profile gauge every 20 mm and this technique is shown in fig.3.11 at position 3.

3.6.1.2 Correction to the measurement of the profiles.

The readings recorded from the profile measurements were not the actual co-ordinates of the dam profile as a correction was necessary because of the measurement system. This correction depended on the length of the pins arms of the profile point gauge and the origin of the point gauge with respect to the horizontal scale. The procedure for correction is described below.

a) Upstream face of the dam.

When the location of the profile point gauge was at position (1) as shown in fig.3.11 the correction was as follows:

(1) The origin reading (180 mm) was subtracted from each horizontal reading (this applied to all conditions).

(2) The length of the short arm pin (32 mm) was then added to the value obtained from (1) to give the correct co-ordinate.

b) Crest face of the dam.

When the location of the profile point gauge was at position (2), fig.3.11, the correction was made by subtracting the origin reading from each horizontal x - co-ordinate, while the vertical y - co-ordinate measured by using the vertical pin arm remain unchanged.

c) Downstream face of the dam.

When the location of the profile point gauge was at position (3), fig.3.11, the correction could be made by (1) subtracting the origin x - co-ordinate (180 mm) from each horizontal x - co-ordinate as before and (2) subtracting the long pin arm length equal to 108 mm from the value from (1) to give the correct x co-ordinate.

After the corrections had been made to measured points, dam profiles could be plotted. A computer program (EW) was used to plot the profiles determined in the experimental investigation.

The accuracy of the measurements was within ± 0.1 mm for the vertical reading and within ± 0.5 mm for the horizontal scale reading. The greater accuracy for the vertical reading was due to using the additional vernier scale attached to the profile point gauge. This increased accuracy was desirable because when the dam was inflated with high pressure and under overflow condition, the changes in the profiles were very small and the accuracy of the vertical gauge allowed measurement of these small changes in the profiles.

3.6.2 Water Inflated Models.

Six models of water inflated dams were built as detailed in table 3.3. Three were for tests on membranes of length equal to 800 mm and the other three on membrane lengths of 500, 600, 1000 mm.

Table 3.3 Tests of water inflated models.

Model No.	Test No.	Proportional factor	Max. U/S head (mm)	D/S head (mm)	Water pressure head (mm)	Total length (mm)
1	1	1.0	188	0.0	373	800
	2	1.2	200	0.0	430	800
2	3	1.6	216	0.0	560	800
	4	2.5	230	0.0	800	800
3	5	1.0	188	100	370	800
	6	1.6	216	100	560	800
4	7	1.5	131	0.0	320	500
5	8	1.2	148	0.0	320	600
6	9	1.0	236	0.0	467	1000

Profiles of all the dam models were measured experimentally and examples of the typical profiles are illustrated in fig.3.12 for pressures equal to 370 mm and 560 mm under maximum upstream heads of 188 mm and 216 mm respectively with downstream head equal to zero.

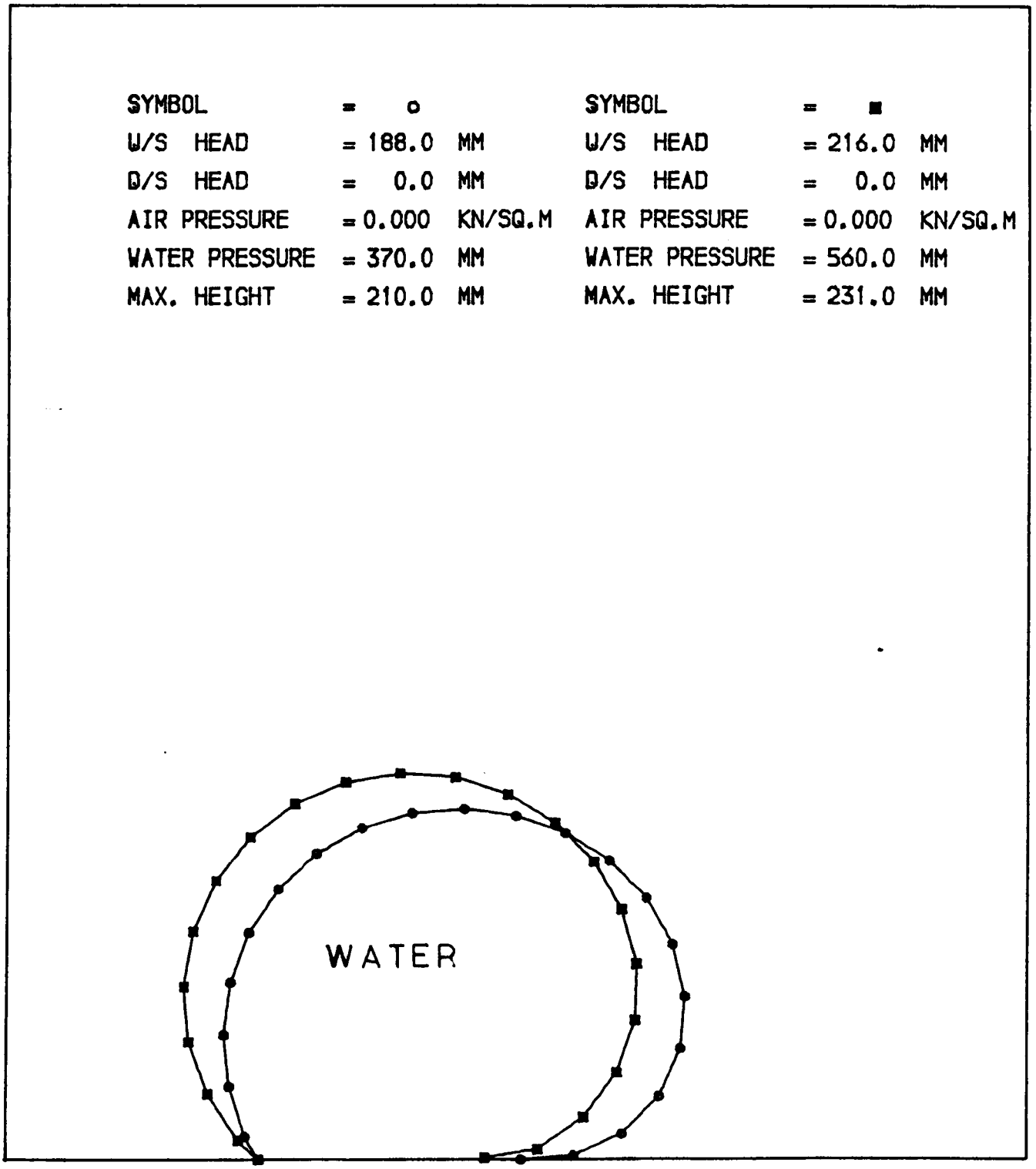

FIG. (3-12) TYPICAL EXPERIMENTAL PROFILES OF WATER INFLATED DAMS

It was observed that with the pressure equal to 370 mm the dam was in a condition with minimum leakage of water at the ends of the dam. For pressure heads greater than this value the effect of any minor distortion was diminished as the dam became more rigid. Fig.3.13 shows the model of a water inflated dam under test, while fig.3.14 shows the condition of a deflated dam with gradually decreasing height and water falling over the crest.

3.6.3 Air Inflated Models.

Six models were made and tested under different pressure heads and maximum upstream heads (i.e. different proportional factors). The test program was as shown in table 3.4.

Table 3.4 Tests of Air Inflated Models.

Model No.	Test No.	Proportional factor	Max.U/S head (mm)	D/S head (mm)	Air pressure KN/m^2	Length of membrane (mm)
1	1	0.4	241	0.0	3.40	800
	2	0.75	252	0.0	4.42	800
	3	0.8	254	0.0	4.56	800
2	4	1.0	257	0.0	3.15	800
	5	1.1	258	0.0	3.43	800
3	6	0.4	242	100	3.40	800
	7	0.8	254	100	4.36	800
	8	1.1	259	100	5.40	800
4	9	0.8	160	0.0	2.85	500
5	10	0.8	190	0.0	3.42	600
6	11	0.8	222	0.0	4.00	700

Tests were carried out on three models with a membrane length equal to 800 mm and three with lengths of 500, 600, 700 mm respectively.

For all models the profiles were measured and then plotted using the computer program (EW). An example of such experimental plots is shown in fig.3.15 for pressures equal to 3.4 and 5.4 KN/m^2.

Below a proportional factor of 0.4 the internal air pressure was not sufficient to eliminate significant distortion and leakage took place but as the

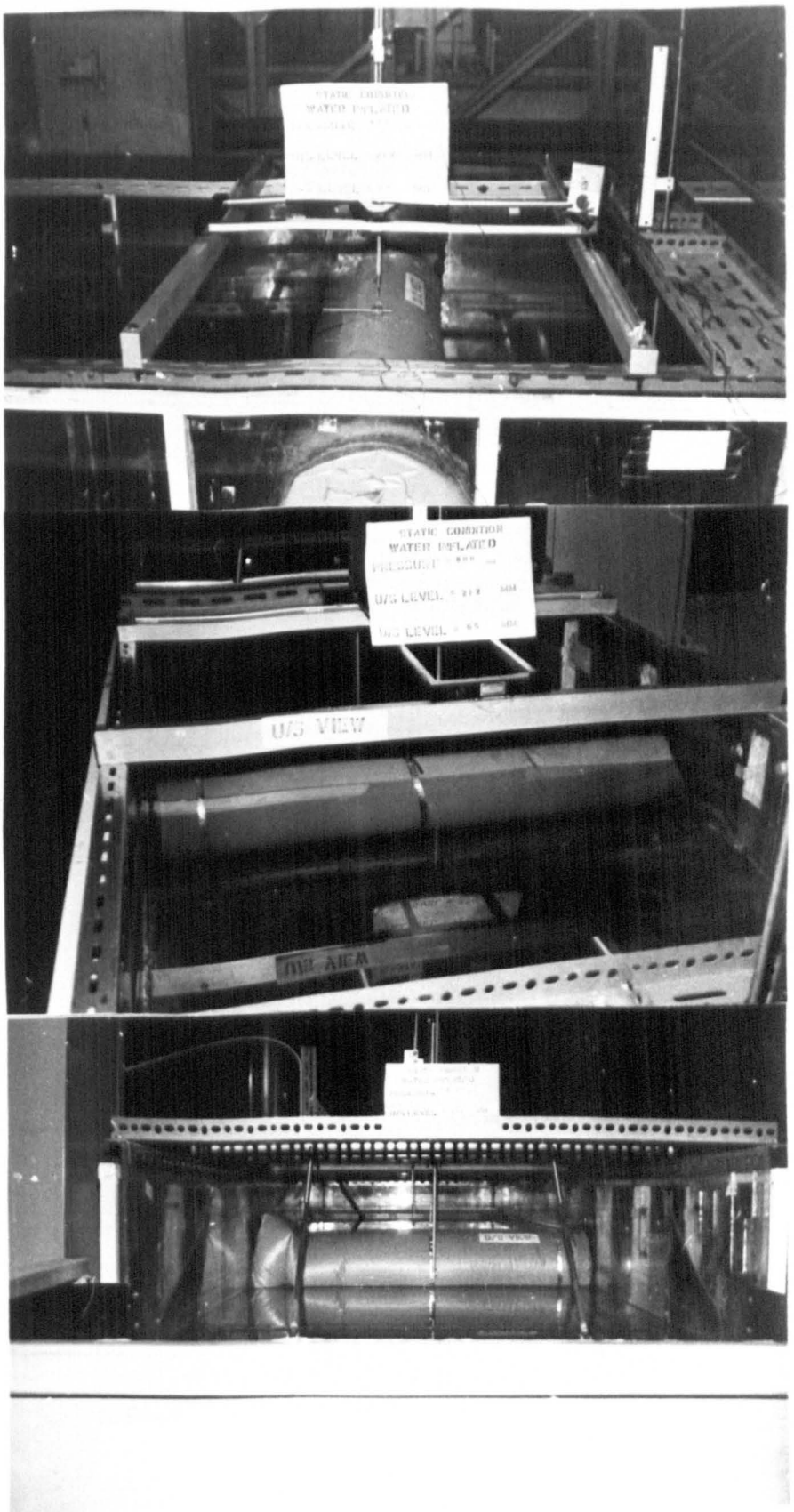

FIG.(3-13) WATER INFLATED MODEL UNDER TEST

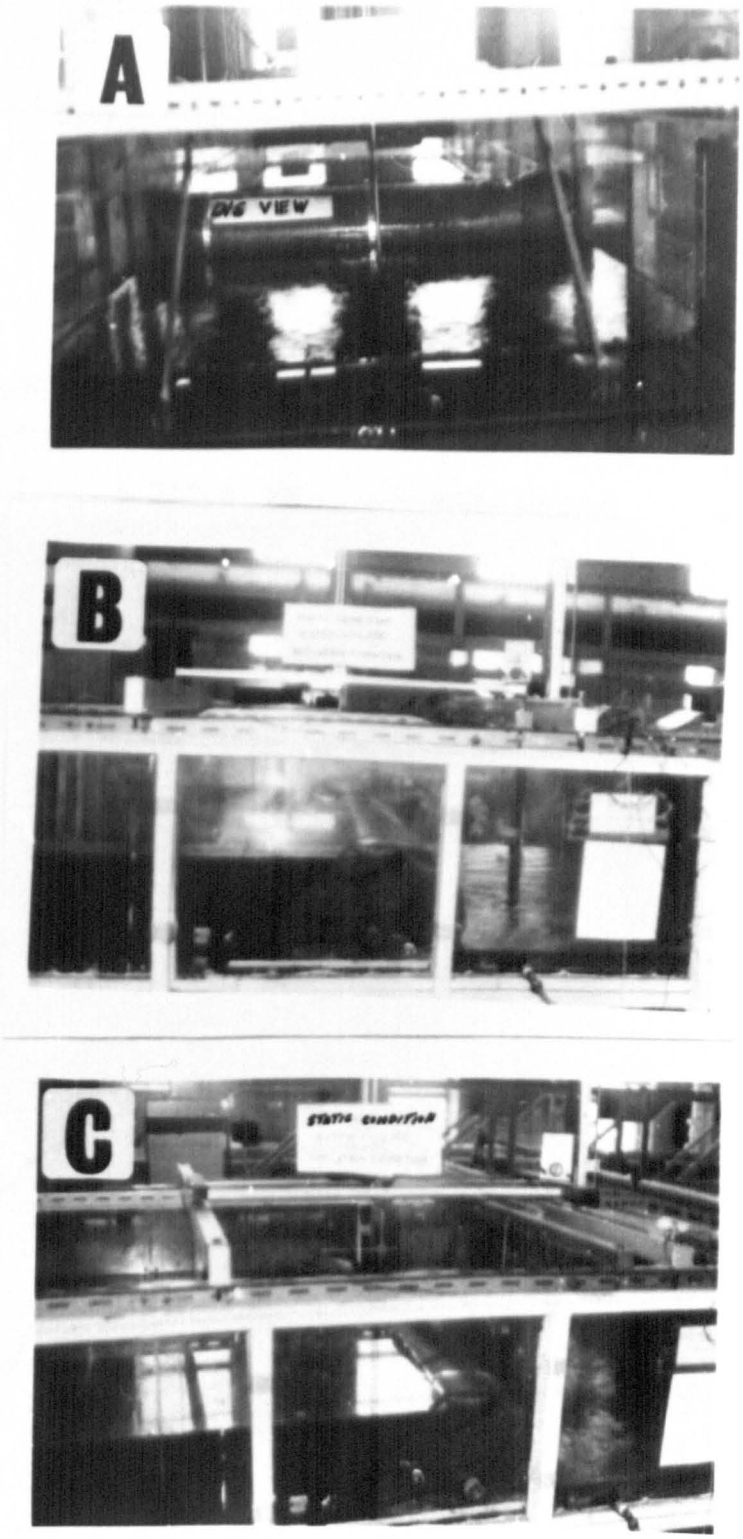

FIG. (3-14) WATER DEFLATION CONDITION

SYMBOL	=	o	SYMBOL	=	■
U/S HEAD	= 241.0	MM	U/S HEAD	= 259.0	MM
D/S HEAD	= 0.0	MM	D/S HEAD	= 100.0	MM
AIR PRESSURE	= 3.400	KN/SQ.M	AIR PRESSURE	= 5.400	KN/SQ.M
WATER PRESSURE	= 0.0	MM	WATER PRESSURE	= 0.0	MM
MAX. HEIGHT	= 242.0	MM	MAX. HEIGHT	= 260.0	MM

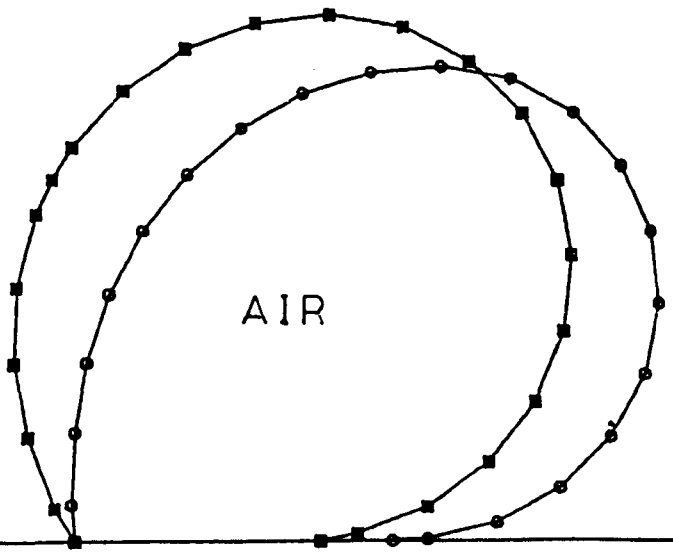

FIG(3-15) TYPICAL EXPERIMENTAL PROFILES OF AIR INFLATED DAM

air pressure increased the dam became more rigid and for a proportional factor greater than 1.2 distortion was eliminated altogether under maximum upstream head.

Fig.3.16 illustrates the laboratory test of an air inflated model for a pressure equal to 5.286 KN/m^2.

During deflation all dams deflated gradually resulting in a v-notch developing on one side of the dam. This resulted from the upstream head acting on the internal air pressure during deflation in addition to deflation that would occur just by opening the release valve without any upstream head.

The v-notch probably occurred on one side rather than the centre of the dam as a result of non-symmetry in the construction of the model and unequal end effects.

An illustration of a deflation effect is shown in sequence in fig.3.17.

3.6.4 (Air + Water) Inflated Models.

The tests for (air + water) models were carried out on six dams with the total length of membrane equal to 800 mm for three models and three with the lengths of membrane equal to 500, 600, 700 mm. The details of the tests are given in table 3.5.

Table 3.5 Tests of (Air + Water) Inflated Models.

Model No.	Test No.	Proportional factor	Max.U/S head (mm)	D/S Head (mm)	Air pressure KN/m^2	Water pressure (mm)	Length of membrane (mm)
1	1	0.6	195	0.0	1.536	158	800
	2	0.8	200	0.0	2.000	158	800
	3	0.9	203	100	2.247	158	800
2	4	1.0	206	0.0	2.500	158	800
	5	1.5	215	0.0	3.715	158	800
3	6	0.7	198	40	1.755	158	800
	7	1.5	215	40	3.715	158	800
4	8	0.8	125.5	0.0	1.231	100	500
5	9	0.7	148	0.0	1.292	120	600
6	10	0.7	173.2	0.0	1.510	140	700

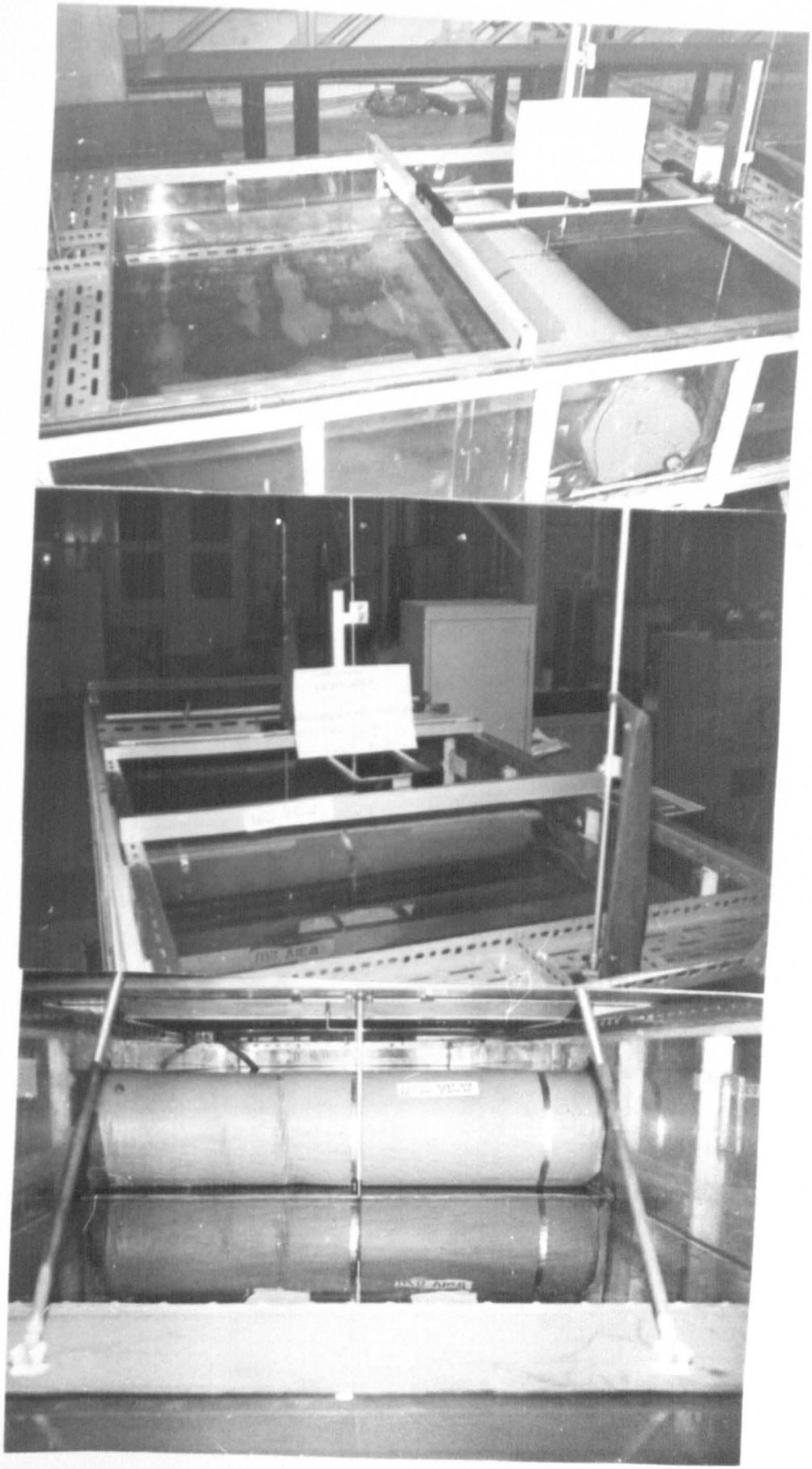

FIG. (3-16) AIR INFLATED MODEL UNDER TEST

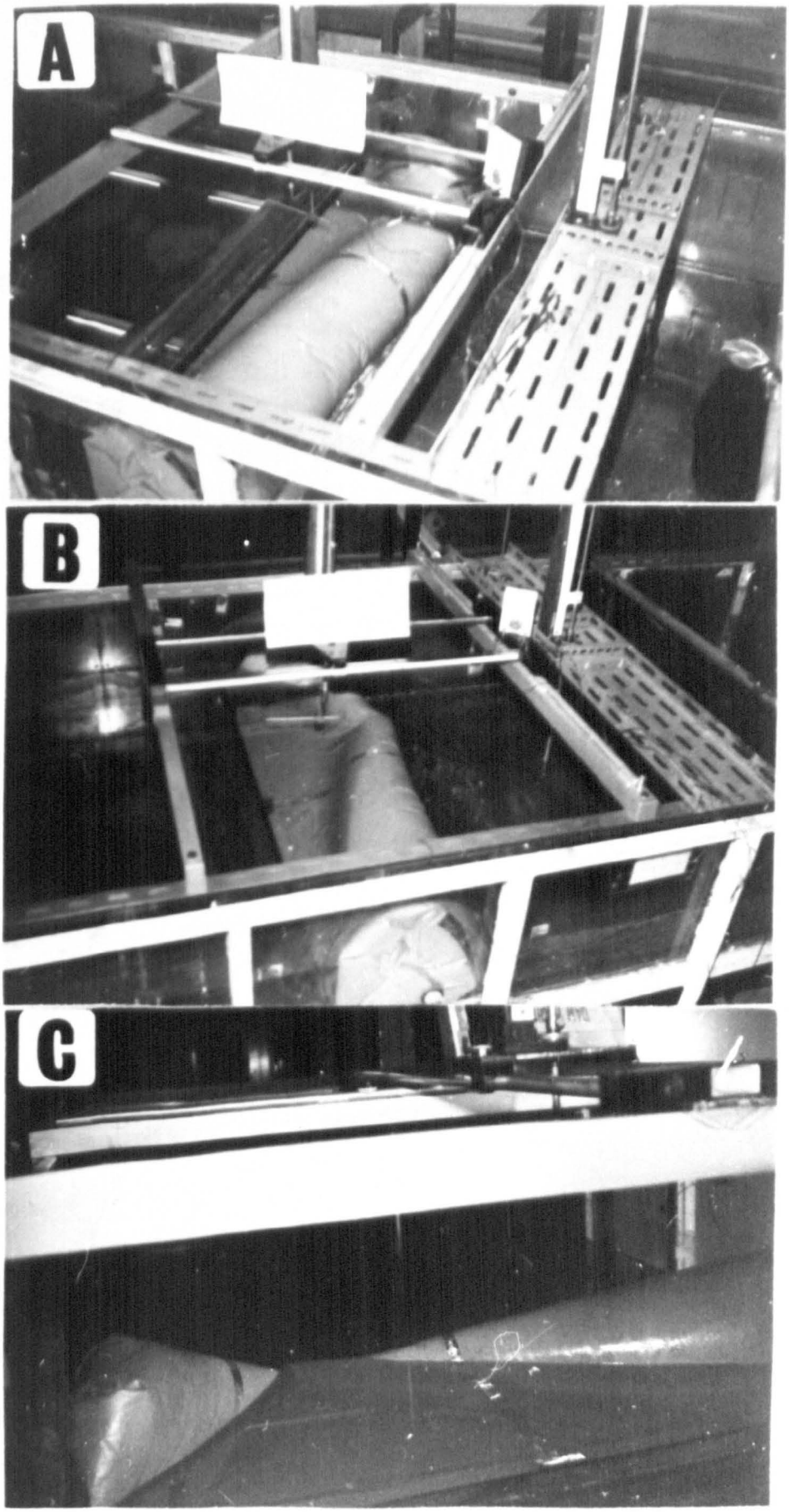

FIG.(3-17) AIR DEFLATION CONDITIONS

SYMBOL	=	o	SYMBOL	=	■
U/S HEAD	= 195.0	MM	U/S HEAD	= 206.0	MM
D/S HEAD	= 0.0	MM	D/S HEAD	= 0.0	MM
AIR PRESSURE	= 1.536	KN/SQ.M	AIR PRESSURE	= 2.500	KN/SQ.M
WATER PRESSURE	= 158.0	MM	WATER PRESSURE	= 158.0	MM
MAX. HEIGHT	= 195.0	MM	MAX. HEIGHT	= 206.0	MM

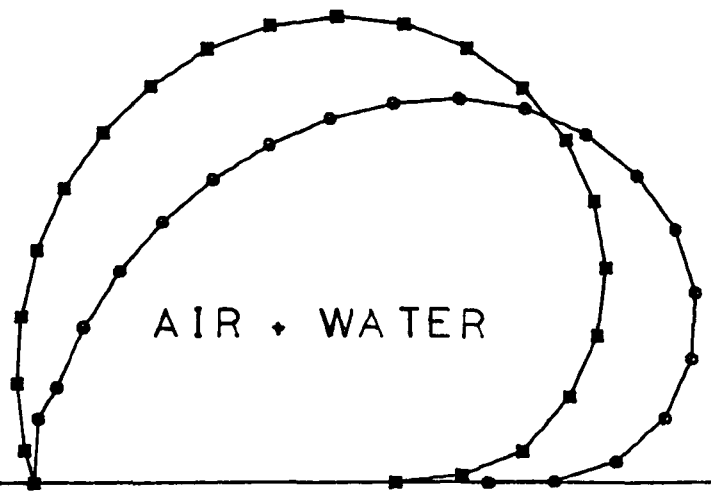

FIG. (3-18) TYPICAL EXPERIMENTAL PROFILES OF AIR + WATER INFLATED DAMS

Profiles of the dams were measured for all tests and an example of the computer plot of the results is shown in fig.3.18, for air pressures equal to 1.536 KN/m^2 and 2.5 KN/m^2 and depth of water inside the dams equal to 158 mm for all models of 800 mm length of membrane (i.e. 75% of maximum height of the dam).

It was observed when a dam was inflated with water to more than 50% of the maximum height the deflation condition was similar to a water inflated dam (see fig.3.14) whilst if the dam was inflated with water to less than 50% of the maximum height the deflation squence was similar to the air inflated condition as shown in fig.3.17.

The comparison between the profiles determined experimentally and theoretically is discussed in Chapter 6.

From the experimental work of the different inflation fluids it was observed that for a particular internal pressure head, the maximum downstream head equal to 50% of the maximum height of a dam which can give a constant base width of a dam.

CHAPTER 4.

THE DEVELOPMENT OF THEORETICAL ANALYSIS OF INFLATABLE HYDRAULIC STRUCTURES UNDER STATIC CONDITIONS.

4.1 Introduction.

The analysis of inflatable hydraulic structures under static conditions has been studied by several investigators as described in Chapter 2, each using a different approach and making different assumptions in order to find solutions. These solutions are generally long mathematical equations restricted by conditions which may not be practical over a wide range of applications.

In this study it was decided to use the Harrison (4) approach and to develop his method by considering the condition of an inflatable structure fixed at the upstream side only which means that the dam can be flat on the downstream side with the downstream angle approaching to zero (21). This consideration has been assumed by other investigators (2,14) for dams fixed at two points which is not valid.

In this analysis consideration of the possibility of a depth of sediment on the upstream side of the dam has been made to observe the effect on the different parameters of the dam.

The length of material was designed under maximum proportional factor equal to 2.5 for water inflated condition in order to find the minimum length of material to hold the maximum head required. Other inflation conditions are considered later. The details of the design are given in Chapter 8.

A computer program was written for the analysis of a dam under different combinations of inflation pressure (from low proportional factor equal to 1.0 to the maximum proportional factor equal to 2.5), downstream head and silt pressure. The length of the material can be found with respect to the maximum proportional factor to be chosen for certain dams. Separate subroutines were

used to compute the initial tension and slope (detail in Sec.4.3.2). The program was also developed to take account of the dynamic condition of loading.

The program can analyse a dam under different conditions of inflation fluid for a wide range of proportional factors alpha.

The main output parameters of the program (IHSIP) are as follows:-

1. Tension along the membrane of the structure.
2. Upstream slope.
3. Elongation of the material.
4. Profile of the dam (shape).
5. Cross-sectional area of the profile.

A subroutine was developed in order to plot the profile of the dam under the developed conditions of inflation.

A comparison of the results obtained from the experimental and theoretical work is detailed in Chapter 6.

4.2 Details of the analysis.

The analysis developed is based on the Harrison (4) method to analyse the inflatable structures to determine the tension along the membrane, the slopes and the profile of the dam.

The analysis carried out by Harrison (4) depends on three main assumptions to analyse the stresses in the membrane of the structure and these are briefly listed below.

a) The behaviour of the three dimensional structure can be represented by the behaviour of a two dimensional transverse section of unit width.

b) The perimeter of the cross-section of the inflatable structure is composed of a finite number of small straight elements and the static loads are acting on the nodes of each element.

c) The material of the dam is elastic and that the stress-strain relationship of the material can be assumed to be linear.

4.2.1 Application of the Harrison Method.

The Harrison method can be used on a dam with two anchors at the upstream and downstream edge respectively, i.e. the downstream angle is not equal to zero. This technique also requires a trial and error solution to find the following parameters:

1. Length of material, 2. Base width, 3. Internal pressure,

and to obtain the best solution to find all the above parameters considerable computer time is needed.

The range of application of the method is limited to the static condition i.e. the dam can be used only for the storage condition and not for overflow conditions. This therefore places a severe limitation on the application of the method to practical problems.

4.2.2 Modification of the Harrison Method.

The Harrison method has been developed to consider an inflatable structure fixed only at the upstream edge and to allow for the downstream angle tending to zero (21) with the material flat,i.e. tangential on the base. A second modification considers the effect of a static force on the upstream face representing a silt load.

A third modification allows the design of the length of material required under a certain proportional factor alpha, so it is possible to design the length of the material and pressure head. Chapter 8 shows the details of the design length of material for different conditions of inflation fluid and inflation pressure.

In this analysis non-linear stress-strain relationships are taken into consideration based on the test behaviour of the material. The new length of the material due to elongation caused by the effect of the loads, i.e.

upstream head, internal pressure head,silt pressure and downstream head can be found from the stress-strain relationship as shown in detail in Chapter 3.

In this technique a subroutine "Initial" can be used to compute the initial tension and slope based on the proportional factor as start values in the analysis compared with the difficult and time consuming approach of the Harrison method.

In this study it is assumed that the effect of the variation of air and water temperature on the material properties is so small that it can be ignored as the air temperature range in the laboratory varied between (15-25)^{o}C for air and (11-20)^{o}C for water.

4.3 The analysis of an inflatable Hydraulic Structure.

4.3.1 Forces Acting on the Dam.

The forces acting on an inflatable structure are the maximum upstream head, downstream head, silt pressure on the upstream face, the inflated air pressure, water pressure and the weight of the material of the dam, and downstream head on the downstream face, these are shown diagrammatically in fig.4.1.

The method of analysis is based on dividing the total length of the material into (n) number of elements giving (n+1) number of nodes. The loads acting on each element are based on the location of the particular element within the dam itself, as some elements are influenced by the upstream head and the silt pressure, whilst other elements are only influenced by the downstream head. All the elements are affected by the internal pressure head, but some elements are flat on the base under the influence of the internal pressure head.

The loads are transmitted from one element to the next by analysing the loads in the first element and progressively continuing the analysis to the last element.

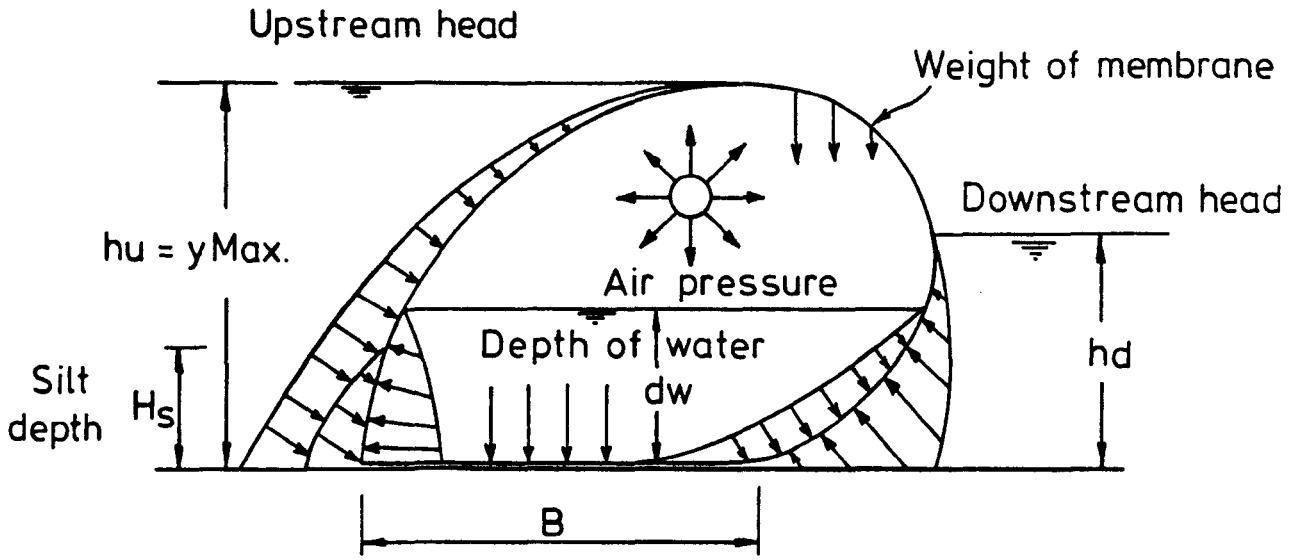

(a) Forces acting on a dam

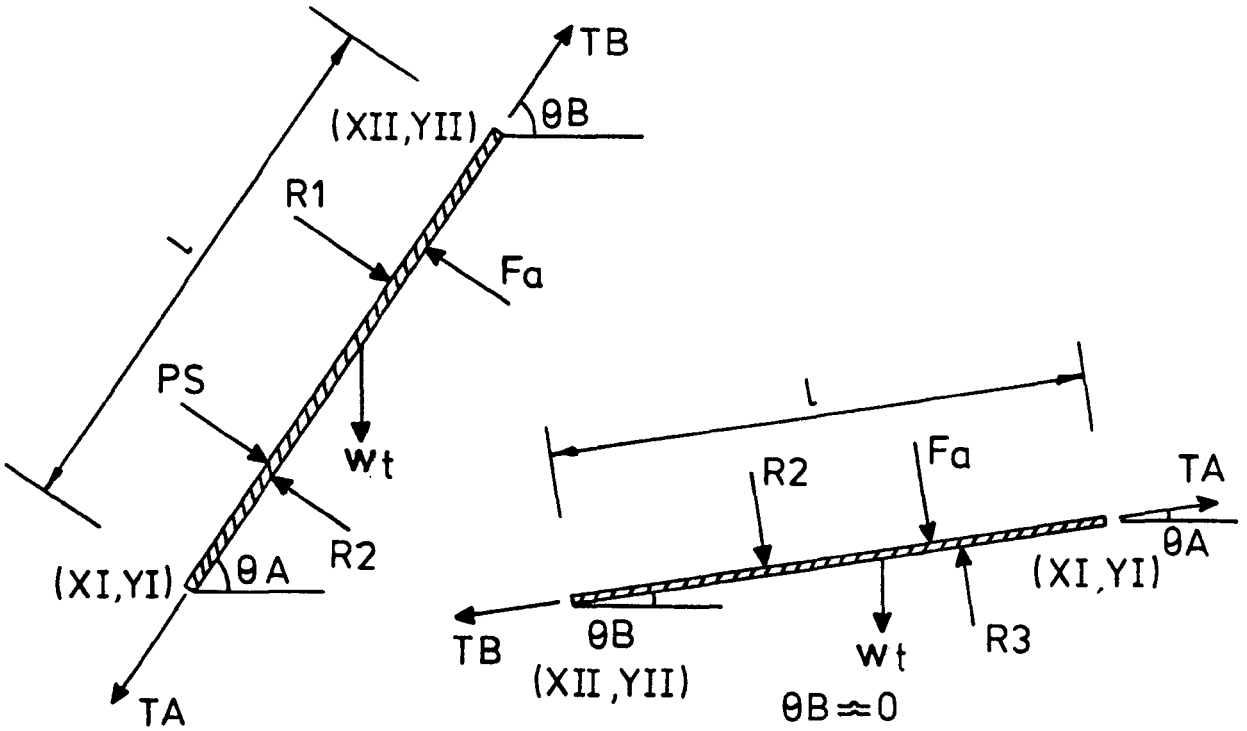

Upstream element Downstream element

(b) Forces acting on an element

FIG.(4-1) FORCES ACTING ON A DAM

Fig.4.1B shows the forces acting on the upstream and downstream face of the dam per unit width.

The techniques to find the forces are shown below, these depending on whether it is an upstream or downstream element. The following equations assume that water is the liquid both internally and externally creating forces. If other inflation liquids are used the appropriate value of specific weight must be used.

4.3.1.1 Upstream elements.

The forces acting on an upstream element are listed below.

1. $R_1 = \gamma h_1 \ell$ 4.1

where R_1 = upstream hydrostatic force.

γ = specific weight of the water.

h_1 = depth of water from the centre of the element to the free water surface, i.e.

$h_1 = (y_{II} - y_I)/2 + (h_u - y_{II})$

y_I = vertical co-ordinate of the lower node.

y_{II} = vertical co-ordinate of the upper node.

h_u = maximum upstream hydrostatic depth.

ℓ = length of the element.

2. $F_a = P_a \times \ell$ 4.2

where F_a = internal air force.

P_a = internal air pressure in KN/m^2.

3. $R_2 = \gamma_1 h_2 \ell$ 4.3

where R_2 = internal fluid force.

h_2 = depth of fluid from the centre of the element to the free water surface, i.e.

$h_2 = (y_{II}-y_I)/2 + (d_w - y_{II})$ on the upstream side

or $h_2 = (y_I - y_{II})/2 + (d_w - y_I)$ on the downstream side

d_w = depth of fluid inside the dam.

γ_1 = specific weight of fluid inside the dam.

4. $w = w_t \times \ell$ 4.4

where w = weight of the membrane.

w_t = weight of the element per unit area.

5. The silt load is calculated by using the Rankine (30) equations and shown below are the details of using this equation.

$p_s = W_s\, h_3\, \ell\, C_f$ 4.5

where p_s = upstream silt force.

W_s = weight of silt submerged equal to

$$W_s = \frac{W_1\,(\rho_s - 1)}{\rho_s}$$

where W_1 = 1600 Kg/m^3 the assumed dry weight of solid particles of silt material

ρ_s = 2.6 (specific gravity of solid particles of the silt material.

$$C_f = \frac{1 - \sin \eta}{1 + \sin \eta}$$

η = 30^o angle of internal friction for sand or clay.

h_3 = depth of silt from the centre of element to the free surface of the silt, i.e.

$h_3 = (y_{II} - y_I)/2 + (H_s - y_{II})$

where H_s = depth of silt to be considered.

Knowing the relevant properties of the water, air and the material, the forces on each element can be calculated from the horizontal and vertical equilibrium equation (4.6) and (4.7).

Horizontal equilibrium

$$T_B \cos \theta B = (F_a + R_2 - R_1 - P_s) \sin \theta_A + T_A \cos \theta_A \quad \ldots\ldots \quad (4.6)$$

Vertical equilibrium

$$T_B \sin \theta B = T_A \sin \theta A + (P_s + R_1 - F_a - R_2) \cos \theta_A + W \quad \ldots\ldots \quad 4.7$$

To find the values of T_B and θ_B for the second node it is necessary to assume values of T_A and θ_A for the first node. Based on these it is now possible to find all other values of tension and slope of the other elements in sequence as detailed in Section 4.3.3.

4.3.1.2 Downstream elements.

The analysis for the downstream elements is similar to that for the upstream elements except that the forces P_s (equation 4.5) and R_1 (equation 4.1) are equal to zero and it is necessary to take into account the effect of the downstream head as given by

$$R_3 = \gamma h_4 \ell \quad \ldots\ldots \quad 4.8$$

where

R_3 = downstream hydrostatic force.

h_4 = depth of water from the centre of the element to the free surface level i.e.

$h_4 = (y_I - y_{II})/2 + (h_d - y_I)$, where

h_d = depth of water on the downstream side.

4.3.2 Initial values of tension and slope.

On the basis of previous work (2,14) the tension for the membranes is assumed constant along the length of the dam, by assuming a weightless material and the details of this analysis are given in Chapter 8. The relationship between tension and slope are found with respect to the proportional factor and can be used as initial values of tension and slope for the first element. It was found that this technique of obtaining the initial values of tension and slope was acceptable. The relationships used are

$$T(\text{initial}) = \rho g \left(\frac{1+2\alpha}{4}\right) H_D^2 \quad \ldots\ldots \quad 4.9$$

and

$$\text{slope(initial)} = \psi = \cos^{-1}\frac{2\alpha-1}{1+2\alpha} \quad \ldots\ldots \quad 4.10$$

These equations are explained in Chapter 8.

On the basis of the above equations the subroutine "Initial" was used to find the initial value of tension and slope.

4.3.3 Procedure for finding the co-ordinate positions of the profile.

Once the initial value of the tension and slope are computed by using equations (4.9) and (4.10), the value of the tension and slope in the next node can be calculated from equation (4.6) and (4.7) by considering the hydrostatic load applied to the first element. The elongation of the element can be computed by using the stress-strain relationships of the material, so that the new co-ordinates of the next node can be determined. The analysis of the second element can be made by using the results of tension and slope of the first element and the process can then be repeated for all elements. Using this method the co-ordinates of the profile can be found along the membrane. The details of this technique are explained below with reference to fig. 4.2.

1. Divide the length of the membrane into (n) elements as shown in fig. 4.2 step (1).
2. Obtain the initial estimates of tension and slope for the first element using the subroutine "Initial".
3. Find the elongation of the element using the equation for the stress-strain relationship. The stresses can be calculated from the following expression:

$$\text{stress} = \frac{T_{(J)}}{t} \quad \ldots\ldots \quad 4.11$$

where t = thickness of the membrane.

As the co-ordinates of the first nodes are known (usually assumed 0.0), so the co-ordinates of the second node (J) can be calculated from equations (4.12) and (4.13), see also fig.4.2, step (4).

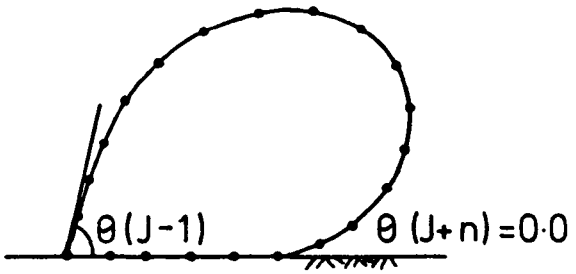

Step 1.

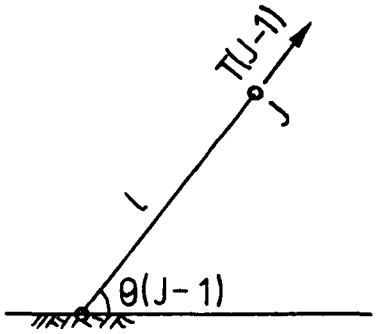

Step 2.

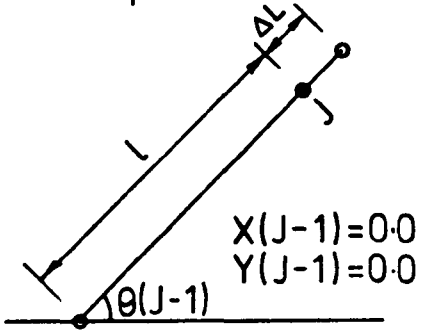

Step 3.

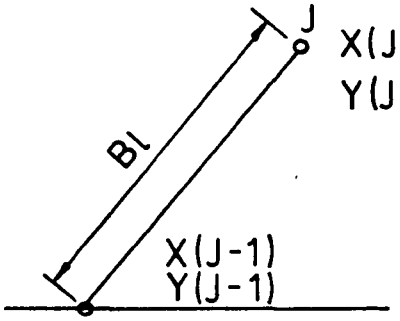

Step 4.

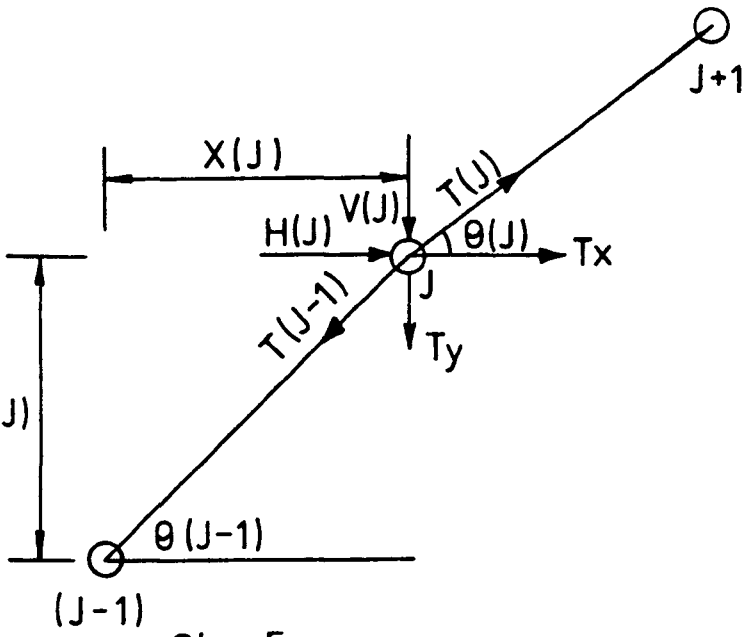

Step 5.

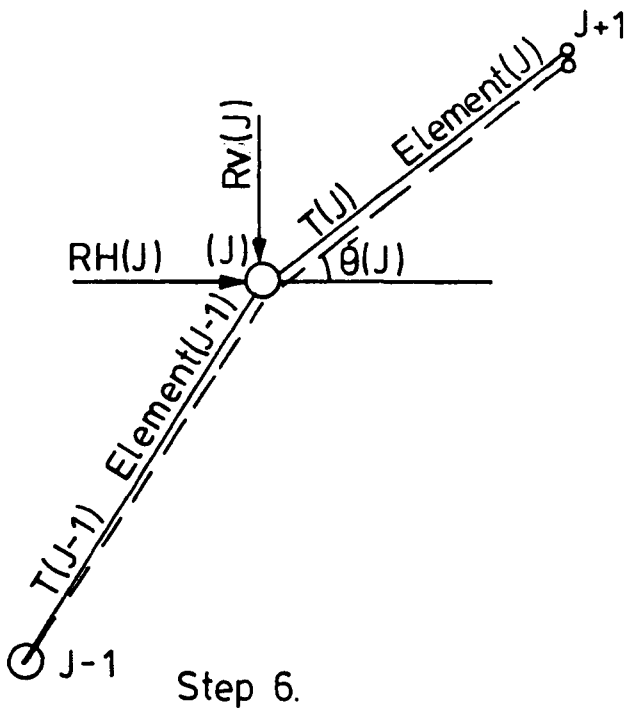

Step 6.

$$TX = T(J-1)\cos(J-1) - H(J)$$

$$TY = T(J-1)\sin(J-1) - V(J)$$

$$\tan\theta(J) = \frac{TY}{TX}$$

$$T(J) = [(TX)^2 + (TY)^2]^{1/2}$$

$$[V(J-1) + V(J)]/2 = RV(J)$$

$$[H(J-1) + H(J)]/2 = RH(J)$$

$$\tan\bar{\theta}(J) = \frac{RV(J)}{RH(J)}$$

$$\bar{T}(J) = [(RV(J))^2 + (RH(J))^2]^{1/2}$$

FIG.(4-2) PROCEDURE FOR FINDING THE PROFILE AND TENSION ALONG THE MEMBRANE

$$X_{(J)} = B_{\ell} \cos(J-1) \quad \ldots\ldots \quad 4.12$$

$$Y_{(J)} = B_{\ell} \sin(J-1) \quad \ldots\ldots \quad 4.13$$

where $B_{\ell} = \ell + \Delta\ell$

B_{ℓ} = new length of the element

ℓ = original length of the element

ΔL = elongation of the element

and ΔL can be calculated by equation 4.11 and equation of the stress-strain relationships as shown in Chapter 3 for the particular material used.

5. The forces acting on the element (J-1) can be found from equations (4.1), (4.2), (4.3), (4.4), (4.5) and the horizontal and vertical component of the forces can be determined i.e. H(J), V(J).

6. From the equilibrium equation at the node (J), the horizontal and vertical component TY, TX of the tension T(J) in the next element are determined and the angle θ(J) is found from the two force components TX,TY, so that the preliminary value for the co-ordinate of the node (J+1) can be calculated as shown in fig. (4.2) step (5).

7. The forces acting at the node (J) are now adjusted by finding a better estimate for the co-ordinate of the node (J) and (J+1) by taking the average of the vertical and horizontal forces of the element (J+1)and element (J) to find the new adjusted value of T'(J) as shown in fig.4.2 step (6).

This method is repeated for each element of the membrane to find the co-ordinates of the profile of the dam and the tension.

It was noticed that in some cases, the downstream slope of the membrane is not tangential with the base and may not satisfy the design base length, this condition is called the mis-close which is due to the estimate of initial values of tension and slope and is reduced by using the Netwen-iteration method to minimize the mis-close so that the membrane is tangential to the base with the downstream slope approaching to zero.

4.3.4 Newton Iteration Method.

The Newton Method of iteration has been used to adjust the assumed initial values of tension and slope in the first element to minimize the mis-close. The technique is as described by Whittaker and Robinson (31) and applied in a similar approach to that by O'Brien, Francis and Harrison (32,33,34) to analyse the suspension of a cable. The procedure for adjusting the initial value of tension and slope is shown in fig.4.3. It is necessary to place a limit on the number of iterations to minimize the amount of computer use.

The Newton Iteration method is applied by increasing the tension by a small amount (δT) and the new mis-close of x, y with respect to (T) may be evaluated as illustrated in fig. 4.3b. The procedure can be repeated for the slope by increasing the slope θ by ($\delta\theta$) and hence the x, y mis-close can be calculated with respect to θ as illustrated in fig. 4.3c. The procedure is repeated for various values of δT, $\delta\theta$, to minimize the mis-close within the specified allowable mis-close and the fabric will then be tangential to the floor with the downstream slope approaching to zero.

The adjusted values of T and θ of the first element are determined numerically from the expression

$$T(\text{improved}) = T - \left[X \frac{\partial y}{\partial \theta} - Y \frac{\partial x}{\partial \theta}\right] / Z$$

$$\theta(\text{improved}) = \theta - \left[Y \frac{\partial x}{\partial T} - X \frac{\partial y}{\partial T}\right] / Z$$

$$Z = \frac{\partial x}{\partial T} \cdot \frac{\partial y}{\partial \theta} - \frac{\partial y}{\partial T} \cdot \frac{\partial x}{\partial \theta}$$

and the above equation can be represented in the general form:

$$\begin{bmatrix} T(\text{improved}) \\ \theta(\text{improved}) \end{bmatrix} = \begin{bmatrix} T \\ \theta \end{bmatrix} - \begin{bmatrix} \frac{\partial x}{\partial T} & \frac{\partial x}{\partial \theta} \\ \frac{\partial y}{\partial T} & \frac{\partial y}{\partial \theta} \end{bmatrix}^{-1} \begin{bmatrix} x \\ y \end{bmatrix}$$

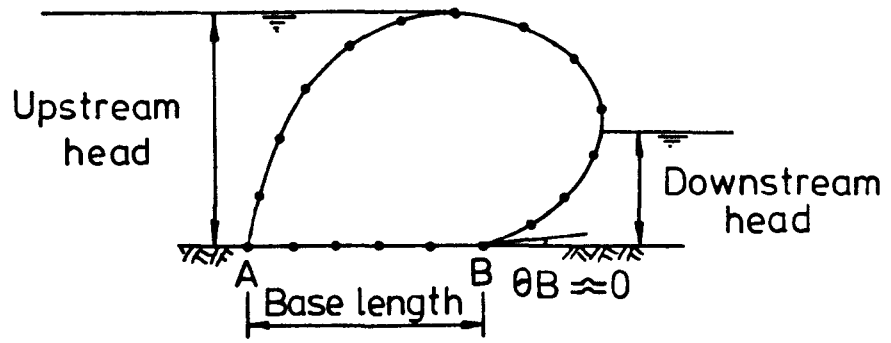

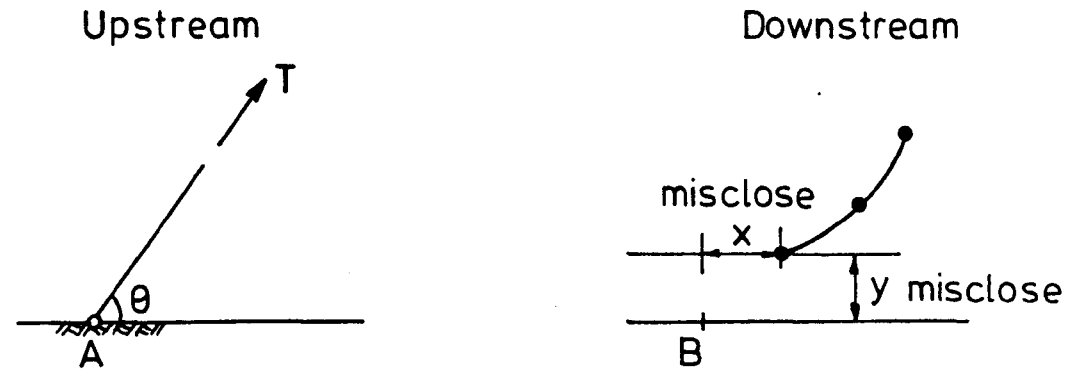

(a) Analyse for T, θ

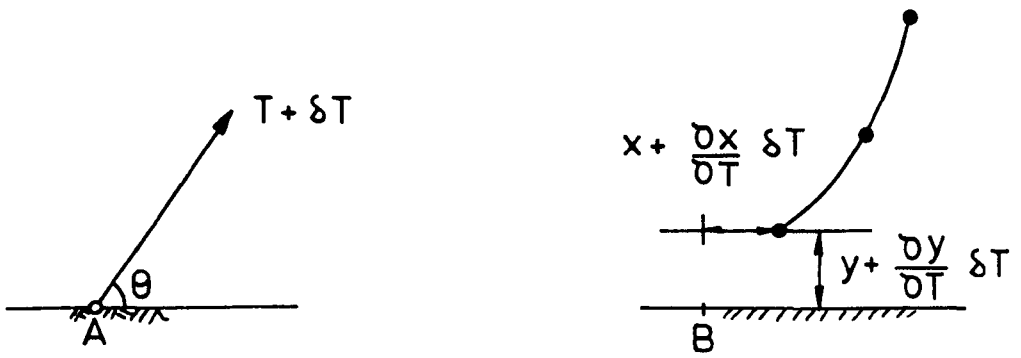

(b) Analyse with T increased
T+δT, θ

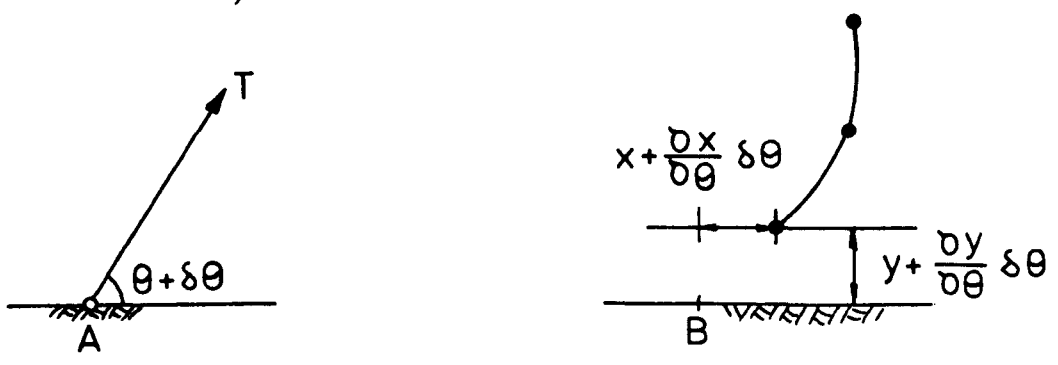

(c) Analyse with θ increased
θ+δθ, T

FIG.(4-3) ADJUSTMENT OF THE INITIAL ESTIMATES OF THE TENSION AND SLOPE TO MINIMISE THE MISCLOSE

4.4 Computer programs.

4.4.1 General.

In this study the analysis was carried out on the ICL 1906S computer at the University of Sheffield.

The computer library (NAG FLIB) was used to provide subroutines to help with the analysis and computer plots of the profiles of the dam using an available graphical output.

The program was written in FORTRAN IV language and a complete list of the program and a guide to its uses is available in the Department of Civil and Structural Engineering of the University of Sheffield.

4.4.2 Main analysis program.

The first program developed was under file name (IHS) to analyse a dam with one end fixed but a modified program was developed to consider the effect of silt on the upstream side and was stored under file name (IHSIP). The computation of the design length of the material was incorporated in the main program. Finding this length of material was based on the proportional factor alpha as described in detail in Chapter 8. Also the subroutine "Initial" was incorporated in the main program to find the initial value of tension and slope to be used.

The programe was therefore capable of calculating initial values of tension and slope rather than adopting limited error solutions as required in Harrison's original method.

A later modification allowed the program to be used for analysis in the dynamic condition of loading and stored under the file name (DYIHSP). In this program the overflow head, coefficient of discharge and discharge can be calculated.

4.4.2.1 The program (IHSIP).

The program was developed to analyse theoretically an inflatable hydraulic structure under hydrostatic conditions of load for different inflation fluids.

The results of the analysis gave values of the profile of the membrane, tension along the membrane, elongation of the material and the cross-sectional area of the dam section. The analysis was carried out for air, water and a combination of both as inflation fluids.

The input for the analysis consisted of 8 cards as detailed in Section (4.4.2.2).

4.4.2.2 Input cards.

In program (IHSIP) the following details on the eight cards are required:

CARD NO. 1. The number of structures to be analysed.

CARD NO. 2. The number of elements and the number of nodes to be considered.

CARD NO. 3. Properties of the material and the inflation fluid.
1. Thickness of the membrane, 2. Weight of the membrane per unit area, 3. Specific gravity of the inflation fluids.

CARD NO. 4. Coefficients of the stress-strain relationship.

CARD NO. 5. Design considerations:

1. Maximum upstream head.
2. Allowable mis-close.
3. Condition of the analysis, NTYPE:-
   NTYPE = 1 static, NTYPE = 2, dynamic.
4. Calculating the maximum height of dam, MHEAD.
   MHEAD = 0 if required, MHEAD = 1 if not required.
5. Profile plot requirement, NPLOT.
   NPLOT = 1 required, NPLOT = 2 not required.
6. Type of inflation fluid, NKIND.
   NKIND = 1 Air, NKIND = 2 Water, NKIND = 3 (Air+Water)

CARD NO. 6. The co-ordinates of the first element of the dam (i.e. anchor point) normally equal to (0,0).

CARD NO. 7. The load condition:
1. Upstream head, 2. Downstream head,
3. Proportional factor alpha, 4. Percentage of the depth of water inside the dam with respect to the maximum height of the dam. 4. Depth of silt on the upstream face of the dam.

CARD NO. 8. Horizontal and vertical scale to plot profile scale.

The following table represents the arrangement of the cards as required by program (IHSIP).

Table 4.1 Notation for the input cards.

CARD NO.	Notation of the input data.
1	NS
2	NEL, NN
3	A, W, GAMMA
4	C_1, C_2, C_3, C_4
5	HD, AC, NTYPE, MHEAD, NPLOT, NKIND
6	X(I), Y(I), 0.0, 0.0
7	UH, DH, ALFA, RA, HS
8	SCALEX, SCALEY

4.4.2.3 Output parameters of the program (IHSIP).

The output of the program (IHSIP) is as follows:

1. Number of iterations.
2. Original design length of the membrane.
3. New length of the membrane (stretch length).
4. Maximum height of the dam.
5. Length of the base.
6. Cross-sectional area.
7. Design air pressure.
8. Design water pressure.
9. x, y co-ordinates of each element (profile of the dam).
10. Tension of the membrane for all elements.
11. The slope of each element along the profile of the dam.

4.4.3 Range of application of the program IHSIP.

The program (IHSIP) can be run for a range of values of the proportional factor alpha depending on the type of the inflation fluid.

For the water inflated condition the proportional factor range is (1.0 - 2.5) and for the air inflated condition (0.2 - 1.2). For (air + water) inflation with a water depth equal to 75% of the maximum height, the proportional factor ranges from (0.6 - 1.6). These limiting values of the proportional factor are found from the experimental work and for these values the dam will be stable. The values of the proportional factor are found from a relationship based on the differential pressure head as a proportion of the maximum storage head, i.e. $\alpha = h/H_D$ or $= \frac{H-H_D}{H_D}$ as shown in fig.2.4B of the analysis of Anwar (2), where (H) represents the total pressure head, and H_D is the maximum storage head.

The analysis was performed for a series of depths of downstream head and silt depth for different proportional factors in order to find out the effect on the output parameters.

In this study the maximum depth of silt was arbitrarily chosen as 0.05 m (for all inflation fluids), a spatial study is needed to find the maximum depth of silt that can be tolerated at the upstream face under different conditions of inflation fluids.

The flow chart shown in fig. 4.4 for the program (IHSIP) details the general outline of the operation of the program. Figs. 4.5, 4.6 and 4.7 show typical graphical output for air, water and (air + water) inflated dams respectively.

4.5 Influence of number of elements.

To assess the significance in the analysis of the choice of the number of elements, analyses were carried out for numbers ranging between 20 to 180 elements. From the results given in table (4.2) it can be seen that increasing

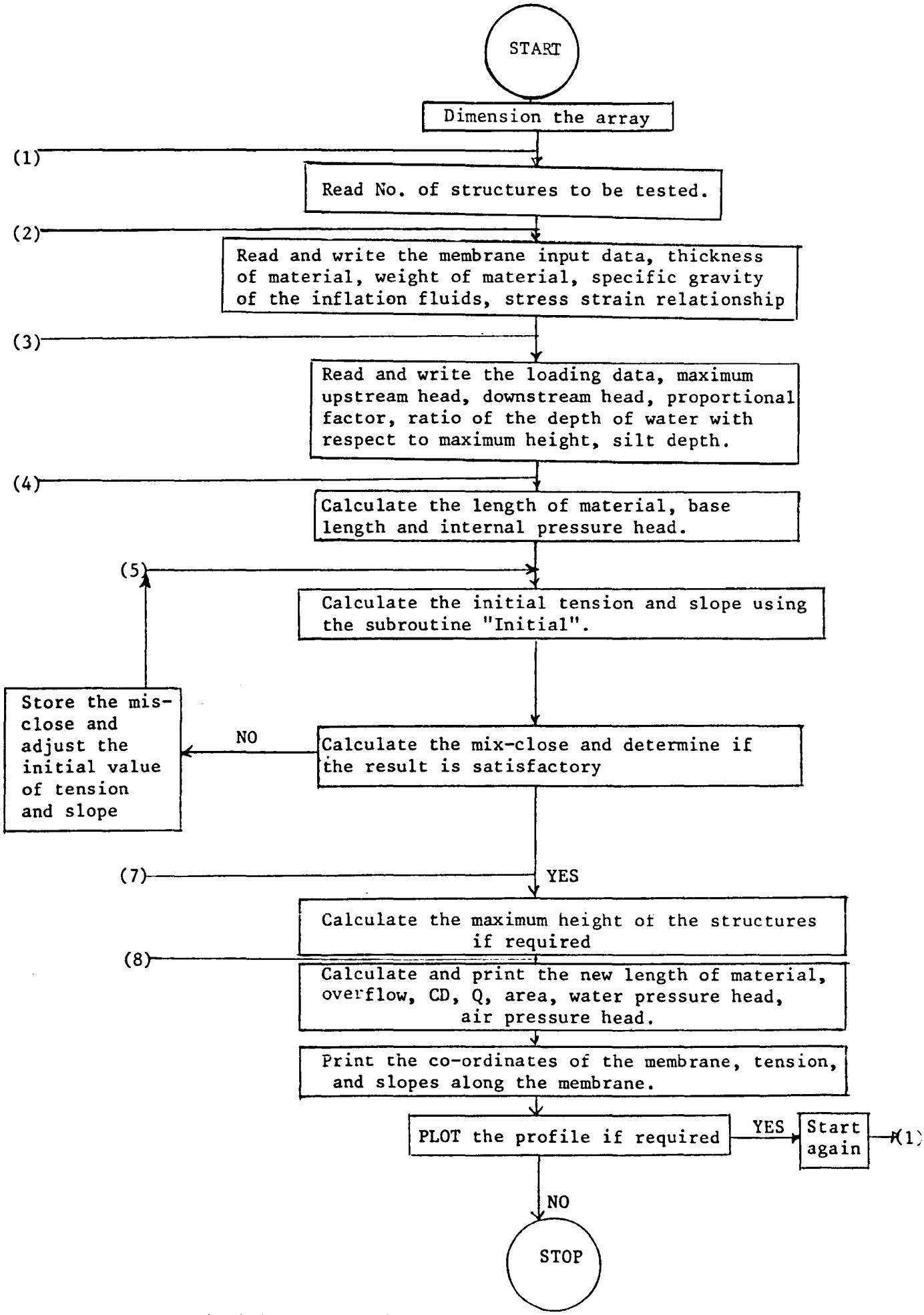

Fig.4.4 Flow Chart for the program (IHSIP).

U/S HEAD	=	0.2575	METER
D/S HEAD	=	0.0000	METER
AIR PRESSURE	=	5.1500	KN/SQ.M
WATER PRESSURE	=	0.0000	M.W.G.
ORIGINAL LENGTH	=	0.8008	METER
NEW LENGTH	=	0.8122	METER
U/S TENSION	=	0.4742	KN/M
U/S SLOPE	=	110.7642	DEGREE
D/S TENSION	=	0.6483	KN/M
BASE LENGTH	=	0.1272	METER
ALFA	=	1.0000	
AREA	=	0.0496	METER SQ
SILT DEPTH, HS	=	0.0500	METER

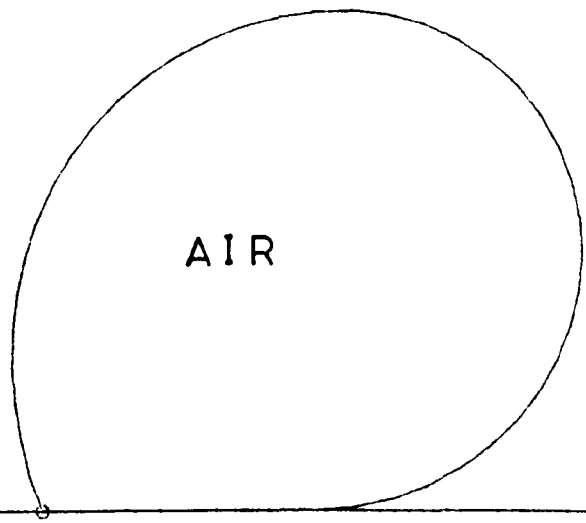

FIG. (4-5) OUTPUT FOR AN AIR INFLATED STRUCTURE

U/S HEAD	=	0.1979	METER
D/S HEAD	=	0.0400	METER
AIR PRESSURE	=	0.0000	KN/SQ.M
WATER PRESSURE	=	0.4308	M.W.G.
ORIGINAL LENGTH	=	0.8000	METER
NEW LENGTH	=	0.8072	METER
U/S TENSION	=	0.2650	KN/M
U/S SLOPE	=	116.6357	DEGREE
D/S TENSION	=	0.3628	KN/M
BASE LENGTH	=	0.1648	METER
ALFA	=	1.2000	
AREA	=	0.0487	METER SQ
SILT DEPTH, HS	=	0.0000	METER

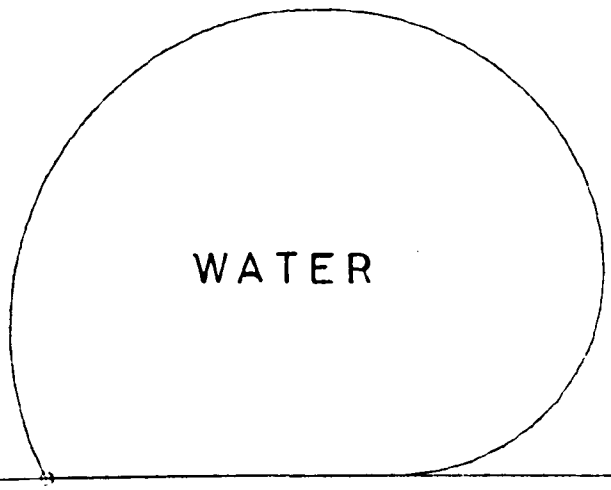

FIG. (4-6) OUTPUT FOR A WATER INFLATED STRUCTURE

U/S HEAD	=	0.2009	METER
D/S HEAD	=	0.0000	METER
AIR PRESSURE	=	2.0019	KN/SQ.M
WATER PRESSURE	=	0.1575	M.W.G.
ORIGINAL LENGTH	=	0.8000	METER
NEW LENGTH	=	0.8046	METER
U/S TENSION	=	0.2201	KN/M
U/S SLOPE	=	96.9950	DEGREE
D/S TENSION	=	0.2895	KN/M
BASE LENGTH	=	0.1928	METER
ALFA	=	0.8000	
AREA	=	0.0467	METER SQ
SILT DEPTH,HS	=	0.0000	METER

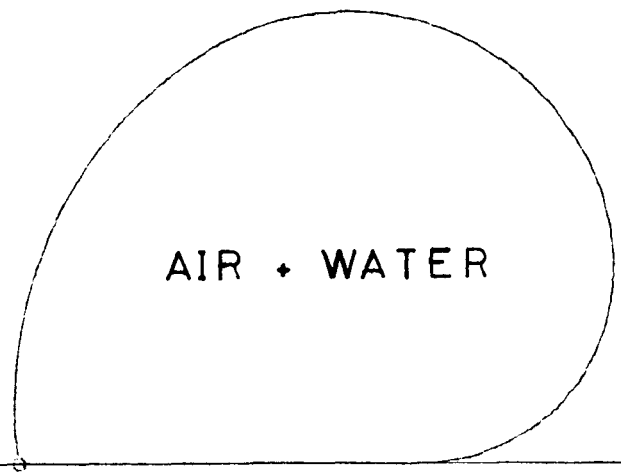

FIG.(4-7) OUTPUT FOR AN AIR+WATER INFLATED STRUCTURE

the number of elements reduces the calculated maximum height of the dam although this effect is small for elements in excess of 50.

The data is for the behaviour of a water inflated dam with proportional factor alpha equal to 1.0 and the original length of membrane equal to 0.80 m.

Table 4.2.
Effect of number of elements on maximum height of dam.

No.	No.of elements	Max.Height (m)	Average tension (Kn/m)	Upstream slope degree
1	20	0.21150	0.2510	120.35
2	30	0.21100	0.2520	120.70
3	40	0.21080	0.2522	121.03
4	50	0.21075	0.2524	121.19
5	60	0.21075	0.2526	121.30
6	80	0.21075	0.2530	121.79
7	100	0.21075	0.2531	122.10
8	140	0.21075	0.2533	122.34
9	160	0.21070	0.2536	122.65
10	180	0.21030	0.2538	122.98

Also it shows that the calculated tension increases with increasing number of elements as does the upstream angle at the anchorage.

It can be seen from table 4.2 that for element numbers in excess of 50 the variation in these parameters for greater element values are very small.

Similar behaviour was also noticed in the case of the dams inflated with air and (air + water).

This conclusion was also reached by Harrison (35).

Fig.4.8 illustrates the print out for water and air inflated dams with initial length of membrane equal to 0.80 m and analysis under 50 elements.

4.6 The effect of operational factors.

. The operational factors affecting the dam are as follows:

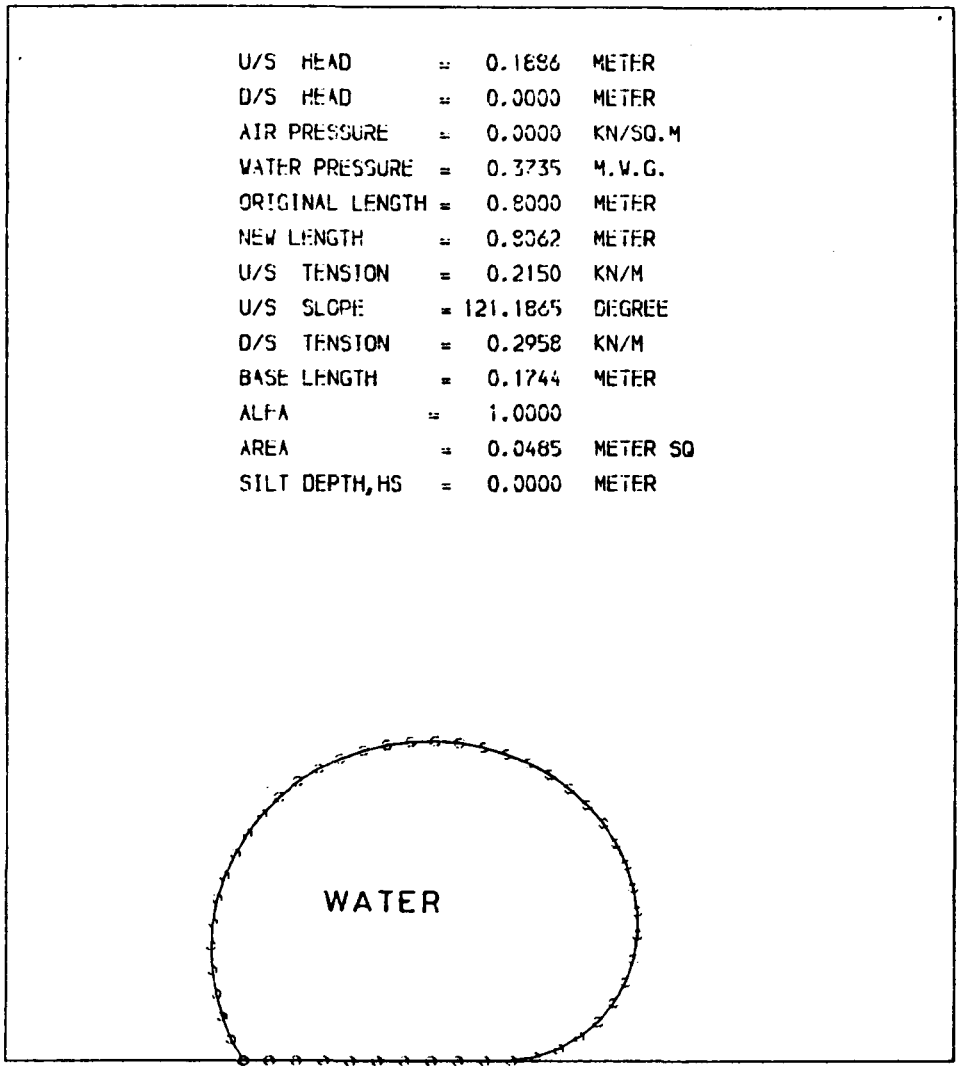

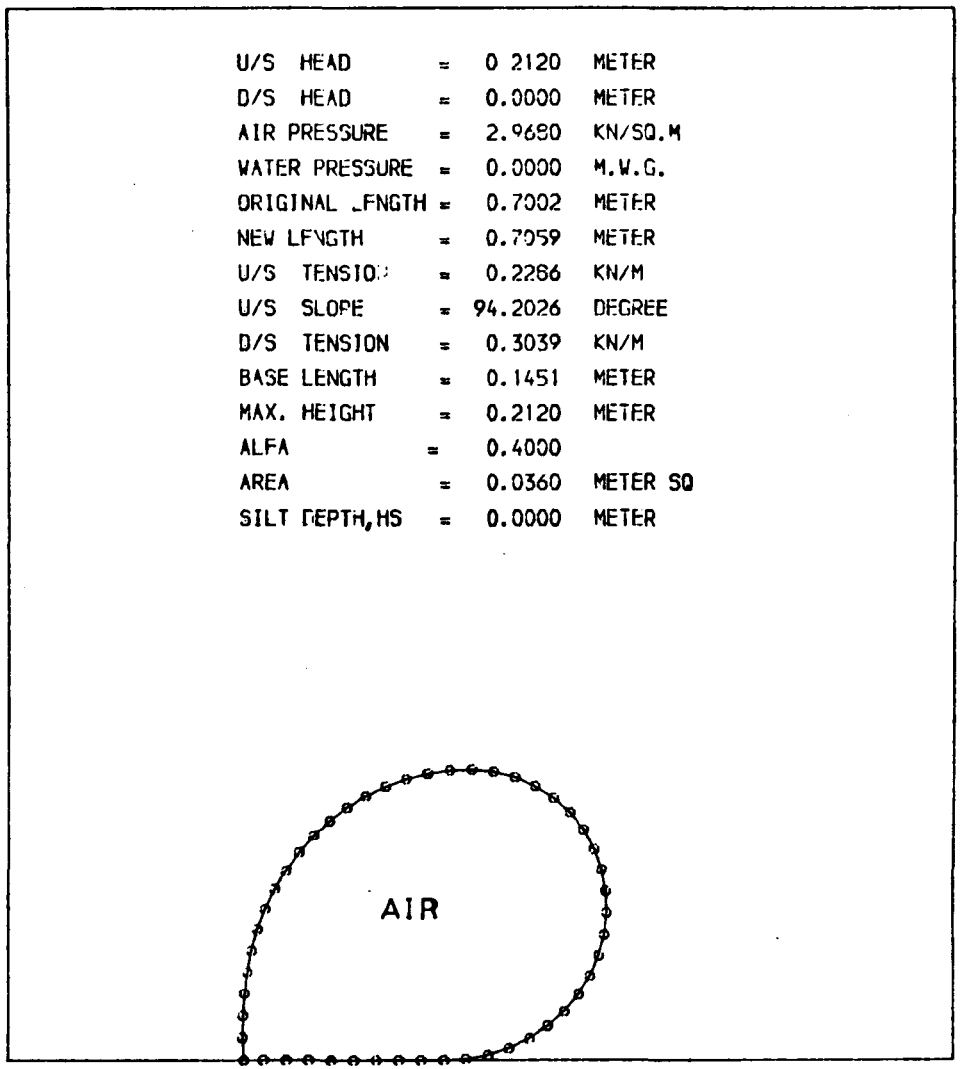

FIG.4-8 WATER AND AIR INFLATED STRUCTURES WITH 50 NUMBER OF ELEMENTS

1. The proportional factor.

2. Maximum upstream head.

3. Downstream head.

4. Depth of the silt on the upstream face.

For different proportional factors (α) (ranges of alpha are given in Section 4.4.3) and under the maximum upstream head, the following conditions have been assumed to study the behaviour of the output parameter (see Sec. 4.4.2.3) on an inflatable dam.

1. Downstream head = 0.0 ; depth of silt = 0.0.

2. Downstream head = 0.0 ; depth of silt = 0.05 m.

3. Downstream head = 0.1m ; depth of silt = 0.0.

4. Downstream head = 0.1m ; depth of silt = 0.05 m.

The following output parameters were found from the program (IHSIP) for different ranges of proportional factor.

1. Upstream and downstream tension.

2. Upstream slope.

3. Maximum height of dam.

4. Elongation of the material.

5. Cross-sectional area of the dam.

Table 4.3 shows the ranges of the proportional factors under maximum upstream head for the different inflation fluids.

From the study carried out, the results of the output parameters found are described in the following sections.

4.6.1 Tension.

The tension in the membrane was calculated for each element and the average of the tensions in the upstream elements found as the upstream tension and similarly for finding the downstream tension. The tension was calculated

Table 4.3 Condition of analysis for different inflation fluids.

WATER Inflated					AIR Inflated					(AIR+WATER) Inflated				
No.	Propl. factor (α)	Max. U/S Head m	D/S Head m	Silt Depth m	No.	Propl. factor (α)	Max. U/S Head m	D/S Head m	Silt Depth m	No.	Propl. factor (α)	Max. U/S Head m	D/S Head m	Silt Depth m
1	1.0	0.1886	0.0-0.1	0.0-0.05	1	0.2	0.231	0.0-0.10	0.0-0.05	1	0.6	0.1944	0.0-0.1	0.0-0.05
2	1.2	0.1978	0.0-0.1	0.0-0.05	2	0.3	0.238	0.0-0.10	0.0-0.05	2	0.7	0.1979	0.0-0.1	0.0-0.05
3	1.4	0.2085	0.0-0.1	0.0-0.05	3	0.4	0.2425	0.0-0.10	0.0-0.05	2	0.8	0.2009	0.0-0.1	0.0-0.05
4	1.5	0.2094	0.0-0.1	0.0-0.05	4	0.5	0.246	0.0-0.10	0.0-0.05	4	0.9	0.2035	0.0-0.1	0.0-0.05
5	1.6	0.2160	0.0-0.1	0.0-0.05	5	0.6	0.249	0.0-0.10	0.0-0.05	5	1.0	0.2060	0.0-0.1	0.0-0.05
6	1.8	0.2192	0.0-0.1	0.0-0.05	6	0.7	0.2526	0.0-0.10	0.0-0.05	6	1.2	0.210	0.0-0.1	0.0-0.05
7	2.0	0.2226	0.0-0.1	0.0-0.05	7	0.8	0.2536	0.0-0.10	0.0-0.05	7	1.3	0.212	0.0-0.1	0.0-0.05
8	2.2	0.2257	0.0-0.1	0.0-0.05	8	1.0	0.2575	0.0-0.10	0.0-0.05	8	1.4	0.213	0.0-0.1	0.0-0.05
9	2.4	0.2284	0.0-0.1	0.0-0.05	9	1.1	0.2590	0.0-0.10	0.0-0.05	9	1.5	0.215	0.0-0.1	0.0-0.05
10	2.5	0.2297	0.0-0.1	0.0-0.05	10	1.2	0.2604	0.0-0.10	0.0-0.05	10	1.6	0.216	0.0-0.1	0.0-0.05

for different proportional factors and under the maximum upstream heads listed in table 4.3 for different inflation fluids.

4.6.1.1 Upstream tension.

The upstream tension for the air inflated dam increases almost linearly as the proportional factor increases for all conditions.

The tension for the air inflated dam for the case of the downstream head equal to zero and a zero depth of silt is more than with the effect of a silt depth e.g. the tension for the proportional factor equal to 0.80 under zero downstream head and zero silt depth, is equal to 0.4212 Kn/m, while the tension for the same proportional factor but under zero downstream head and 0.05 m silt depth the tension is equal to 0.418 Kn/m.

The reduction of the tension with a particular proportional factor for the condition of downstream head equal to zero and with silt depth equal to 0.05 m relative to the tension for the condition of zero downstream head and zero silt depth is due to the reduction of the resultant force T(J) of the vertical and horizontal components acting on the elements.

The case of increasing tension with increasing the proportional factors or decreasing tension with decreasing the proportional factors under all conditions of downstream head (0.0-0.1) and silt depth (0.0-0.05) is due to the force (F_a) which causes an increase in the resultant of the force with an increase in the proportional factor and decrease in the resultant of the forces with low proportional factors.

The above behaviour of the upstream tension under the different load condition is the same for the different dams under different inflation fluids and these effects are shown in fig. 4.9, 4.10, and 4.11 for air, water and (air + water) inflated structures respectively.

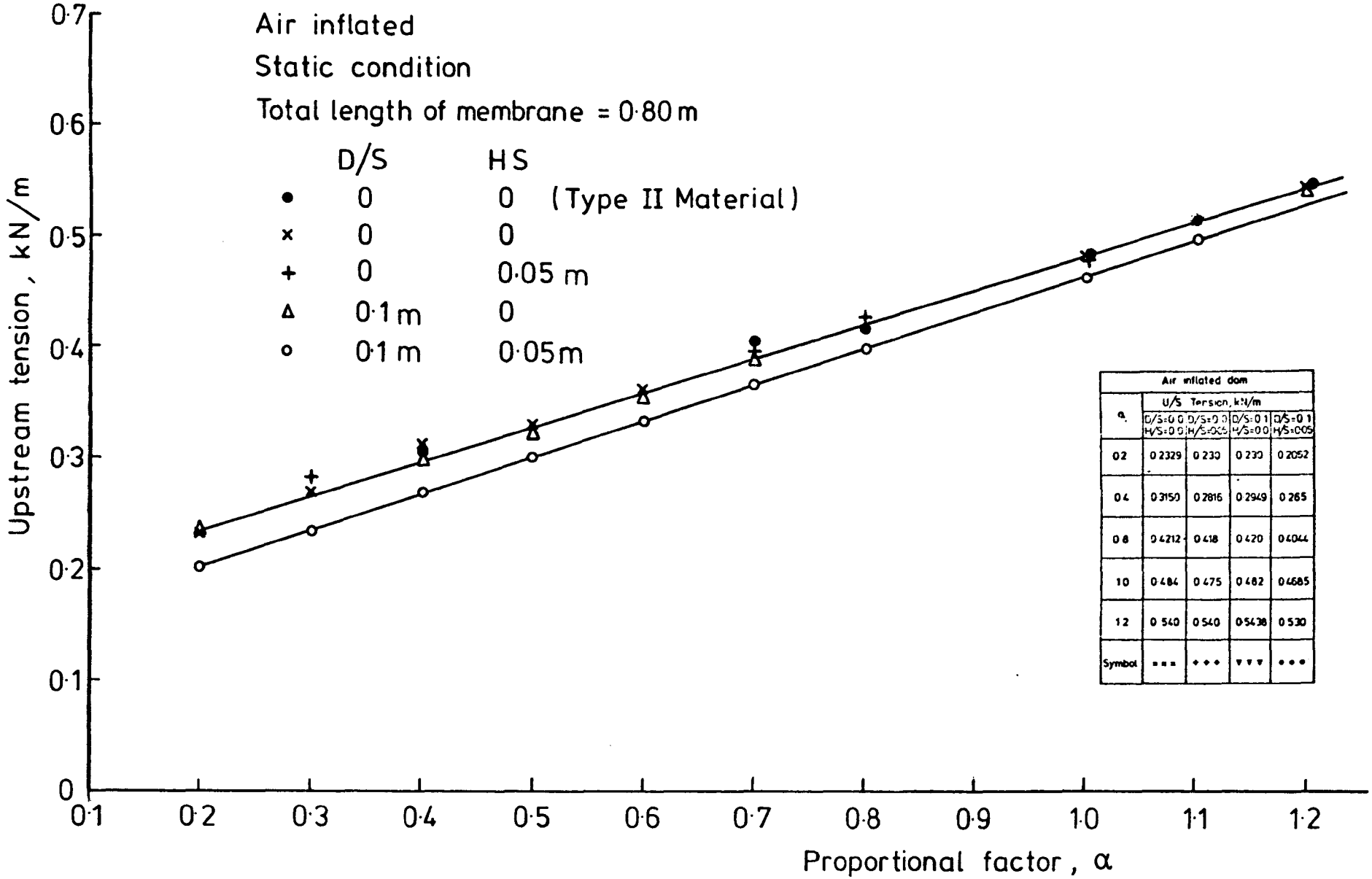

Air inflated dom				
α	U/S Tension, kN/m			
	D/S=0 0 H/S=0 0	D/S=0 0 H/S=0·05	D/S=0·1 H/S=0 0	D/S=0·1 H/S=0·05
0·2	0·2329	0·230	0·230	0·2052
0·4	0·3150	0·2816	0·2949	0·265
0·8	0·4212	0·418	0·420	0·4044
1·0	0·484	0·475	0·482	0·4685
1·2	0·540	0·540	0·5438	0·530
Symbol	▪ ▪ ▪	◆ ◆ ◆	▼ ▼ ▼	● ● ●

FIG.(4-9) UPSTREAM TENSION Vs. DIFFERENT PROPORTIONAL FACTORS FOR AN AIR INFLATED STRUCTURE

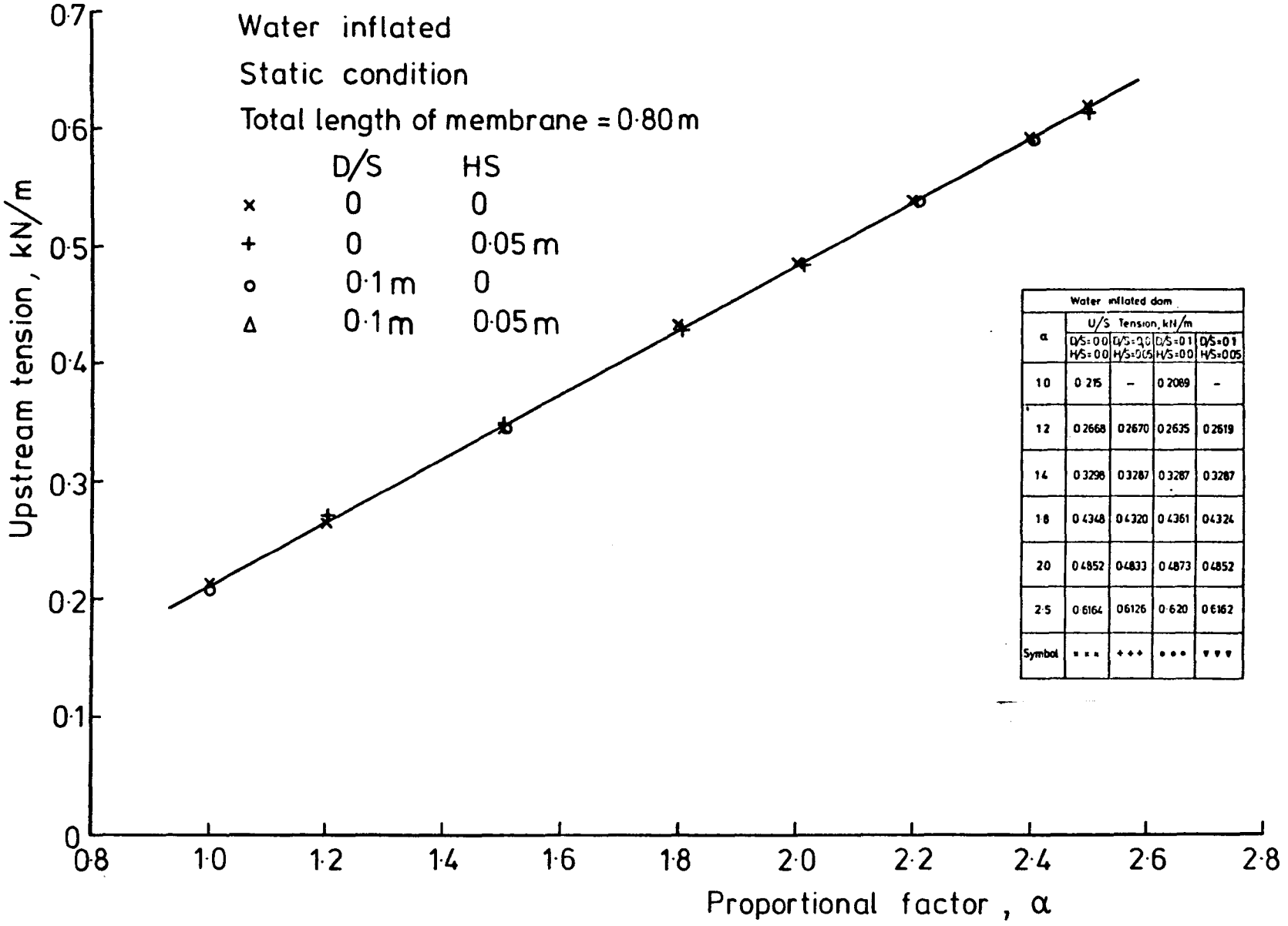

Water inflated dam				
α	U/S Tension, kN/m			
	D/S=0·0 H/S=0·0	D/S=0·0 H/S=0·05	D/S=0·1 H/S=0·0	D/S=0·1 H/S=0·05
1·0	0·215	–	0·2089	–
1·2	0·2668	0·2670	0·2635	0·2619
1·4	0·3298	0·3287	0·3287	0·3287
1·8	0·4348	0·4320	0·4361	0·4324
2·0	0·4852	0·4833	0·4873	0·4852
2·5	0·6164	0·6126	0·620	0·6162
Symbol	× × ×	+ + +	o o o	▼ ▼ ▼

FIG. (4-10) UPSTREAM TENSION Vs. DIFFERENT PROPORTIONAL FACTORS FOR A WATER INFLATED STRUCTURE

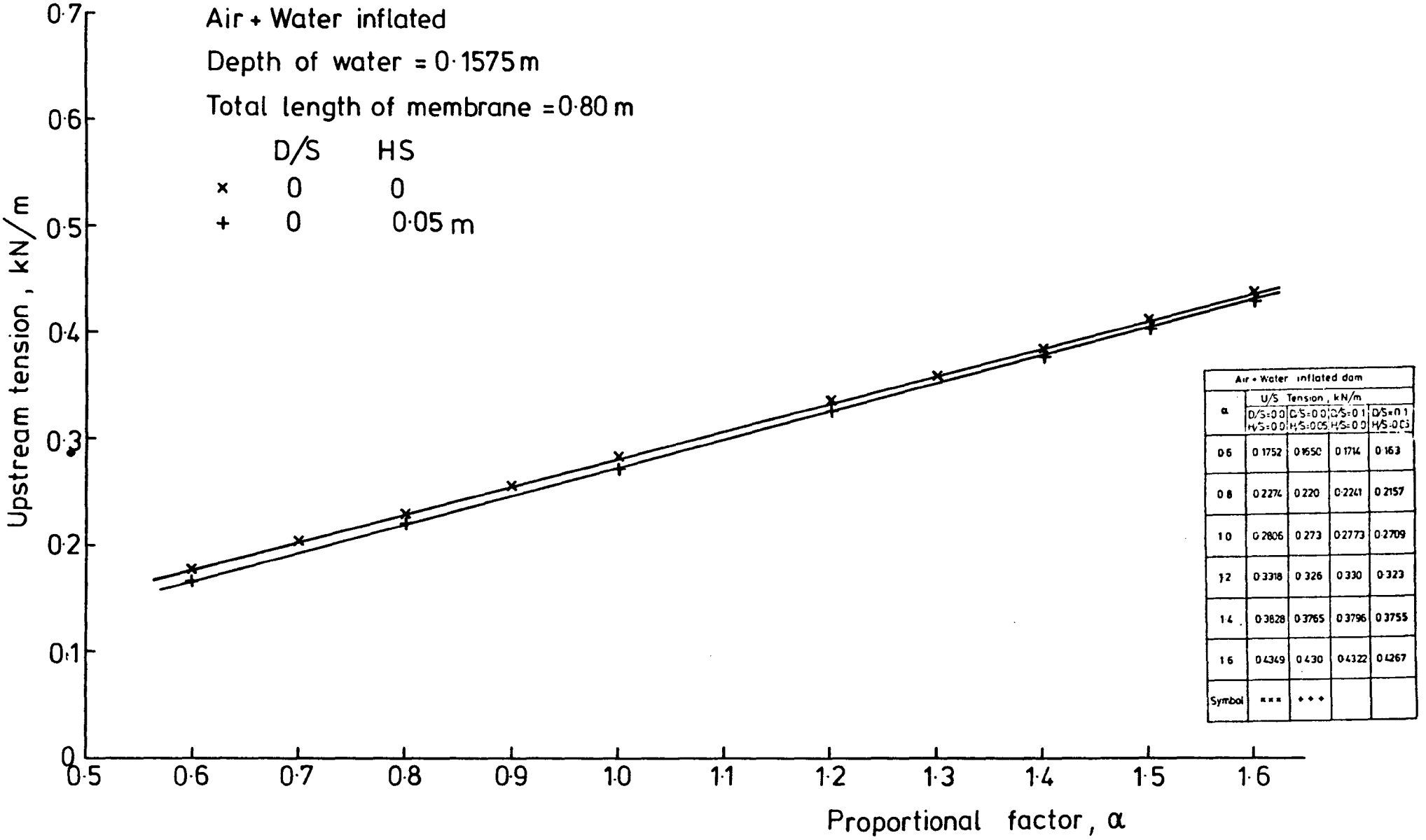

Air + Water inflated dam				
α	U/S Tension , kN/m			
	D/S=0·0 H/S=0·0	D/S=0·0 H/S=0·05	D/S=0·1 H/S=0·0	D/S=0·1 H/S=0·05
0·6	0·1752	0·1650	0·1714	0·163
0·8	0·2274	0·220	0·2241	0·2157
1·0	0·2806	0·273	0·2773	0·2709
1·2	0·3318	0·326	0·330	0·323
1·4	0·3828	0·3765	0·3796	0·3755
1·6	0·4349	0·430	0·4322	0·4267
Symbol	×××	•••		

FIG. (4-11) UPSTREAM TENSION Vs. DIFFERENT PROPORTIONAL FACTORS FOR AIR + WATER INFLATED STRUCTURE

4.6.1.2 Downstream tension.

The tension on the downstream side is greater than the upstream side for all proportional factors.

The tension calculated for different conditions (as for the upstream tension) shows that the tension under the condition of downstream head equal to zero and zero silt is greater than the condition of zero downstream head and with a silt depth equal to 0.05 m. Also the tension is greater for the condition of downstream head equal to 0.1 m and silt depth equal to zero than the condition of downstream head equal to 0.10 m and with a silt depth equal to 0.05 m. The pattern of behaviour of the downstream tension is the same for all types of the inflation fluids.

The reduction of the tension for the downstream head equal to 0.10 and silt depth equal to 0.05 m relative to the tension for the condition of the downstream head equal to 0.10 and zero silt depth is due to the reduction of the resultant of the force T(J). This reduction in the downstream tension under the above conditions is a similar behaviour as found for the upstream tension under the same conditions.

The behaviour of the downstream tension with respect to different proportional factors and under different load conditions (D/S = 0.0,0.1), (H_s = 0.0, 0.05)for air, water and (air + water) inflated structures are shown in fig.4.12, 4.13 and 4.14 respectively.

4.6.2 Upstream slope.

The upstream slope is defined as the angle of inclination of the first element of the membrane to the base level (starting on the upstream side).

The upstream slope was calculated for different conditions of downstream (D/S = 0.0, 0.01) and silt depth (H_s = 0.0, 0.05) for different types of inflation fluids. Consider the air inflated structure of the downstream

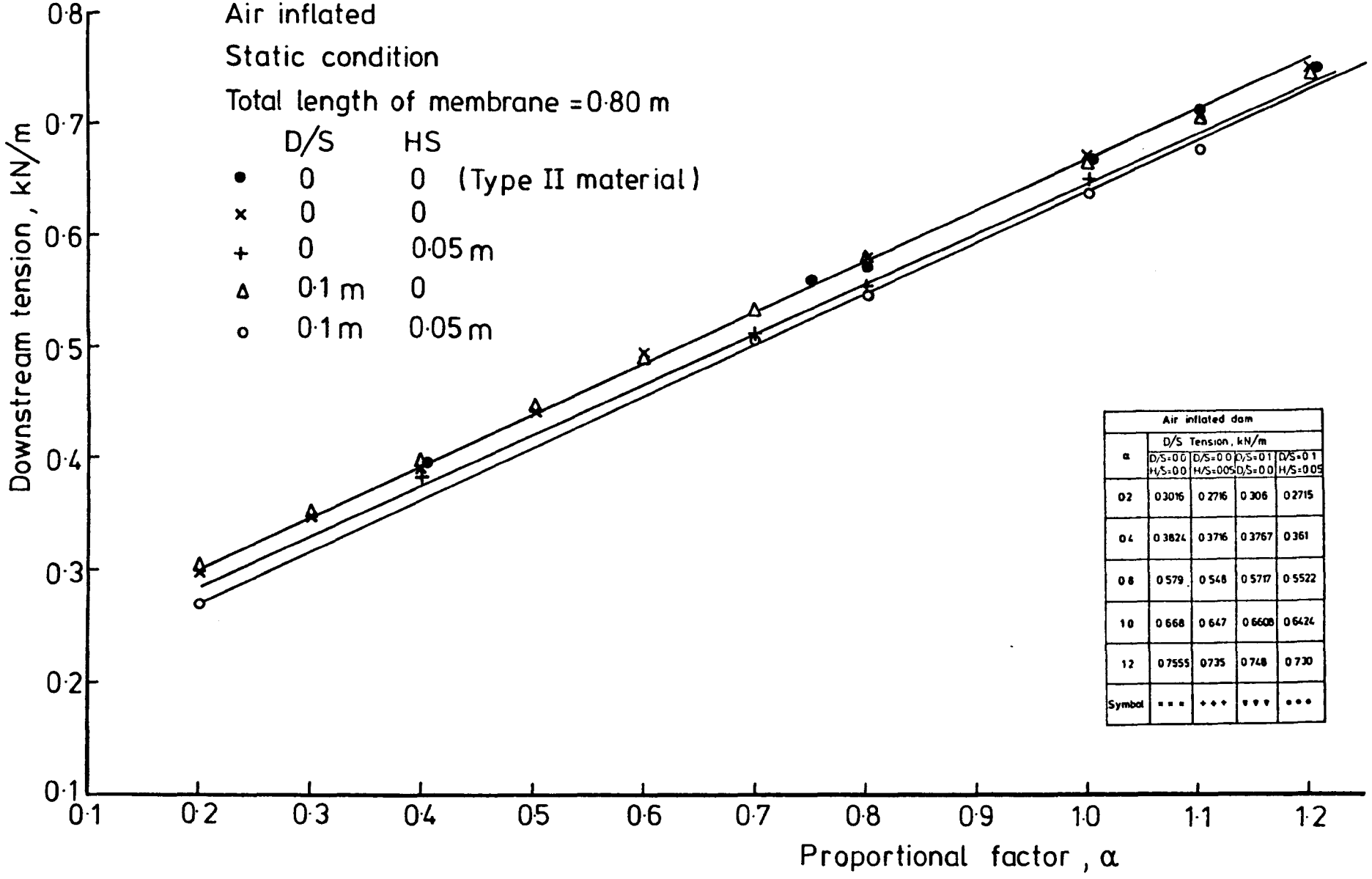

Air inflated dam				
α	D/S Tension, kN/m			
	D/S=0·0 H/S=0·0	D/S=0·0 H/S=0·05	D/S=0·1 H/S=0·0	D/S=0·1 H/S=0·05
0·2	0·3016	0·2716	0·306	0·2715
0·4	0·3824	0·3716	0·3767	0·361
0·8	0·579	0·548	0·5717	0·5522
1·0	0·668	0·647	0·6608	0·6424
1·2	0·7555	0·735	0·748	0·730
Symbol	• • •	+ + +	▾ ▾ ▾	• • •

FIG.(4-12) DOWNSTREAM TENSION Vs DIFFERENT PROPORTIONAL FACTORS FOR AIR INFLATED STRUCTURE

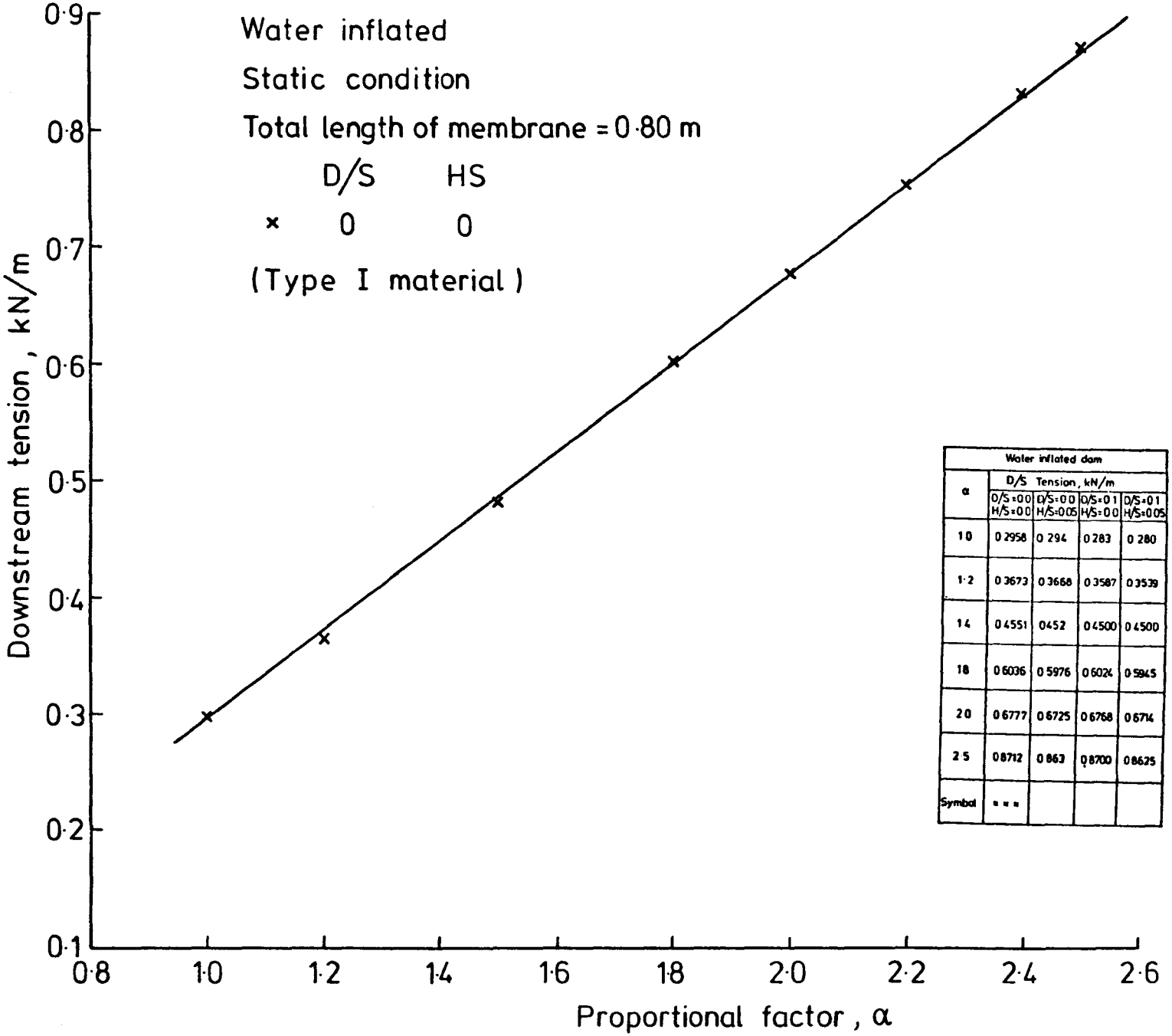

Water inflated dam				
α	D/S Tension, kN/m			
	D/S=0·0 H/S=0·0	D/S=0·0 H/S=0·05	D/S=0·1 H/S=0·0	D/S=0·1 H/S=0·05
1·0	0·2958	0·294	0·283	0·280
1·2	0·3673	0·3668	0·3587	0·3539
1·4	0·4551	0·452	0·4500	0·4500
1·8	0·6036	0·5976	0·6024	0·5945
2·0	0·6777	0·6725	0·6768	0·6714
2·5	0·8712	0·863	0·8700	0·8625
Symbol	× × ×			

FIG. (4-13) DOWNSTREAM TENSION Vs. DIFFERENT PROPORTIONAL FACTORS FOR WATER INFLATED STRUCTURE

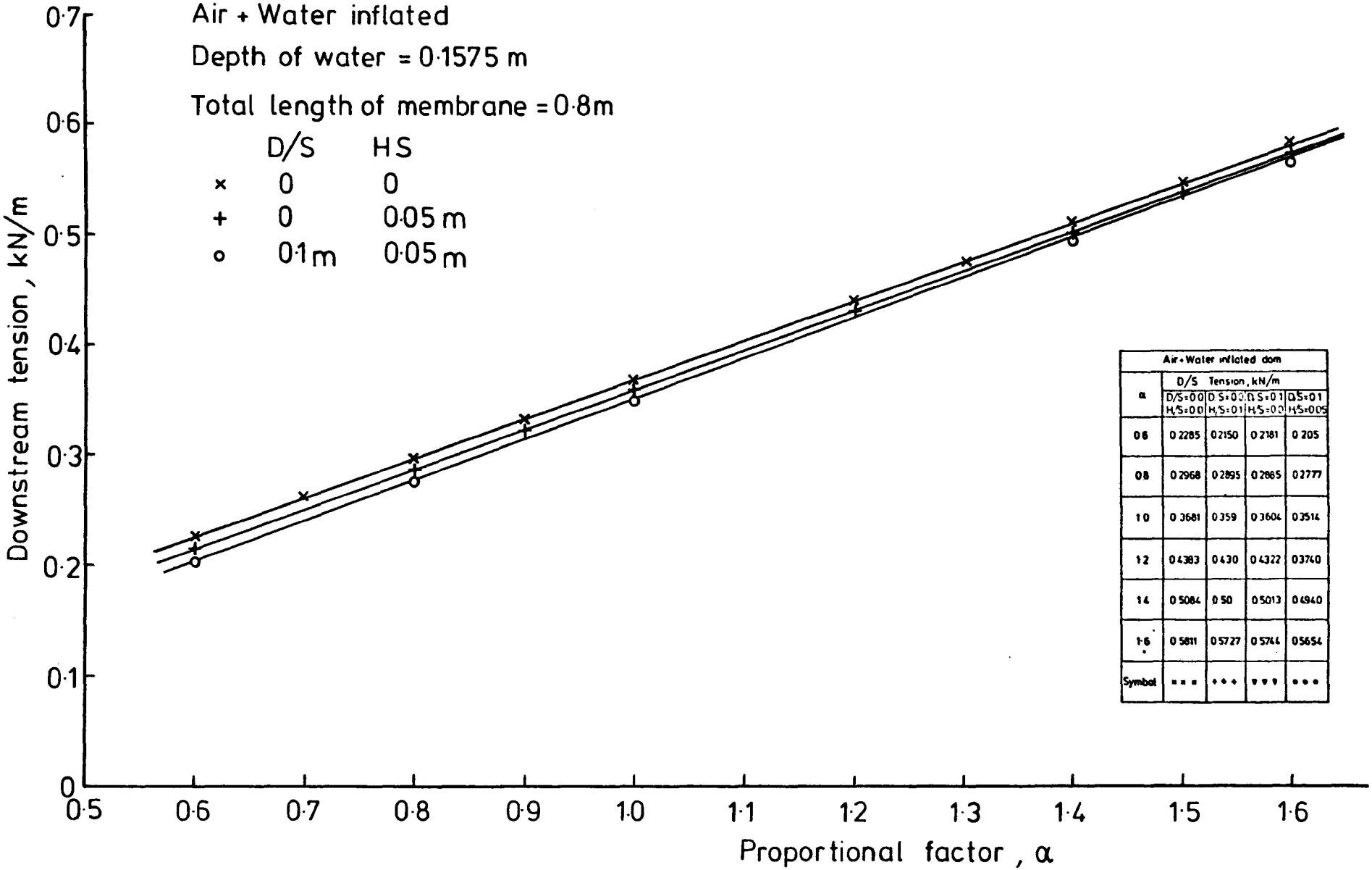

Air+Water inflated dam				
α	D/S Tension, kN/m			
	D/S=0·0 H/S=0·0	D/S=0·0 H/S=0·1	D/S=0·1 H/S=0·0	D/S=0·1 H/S=0·05
0·8	0·2285	0·2150	0·2181	0·205
0·8	0·2968	0·2895	0·2865	0·2777
1·0	0·3681	0·359	0·3604	0·3514
1·2	0·4383	0·430	0·4322	0·3740
1·4	0·5084	0·50	0·5013	0·4940
1·6	0·5811	0·5727	0·5744	0·5654
Symbol	▪ ▪ ▪	♦ ♦ ♦	▾ ▾ ▾	• • •

FIG. (4-14) DOWNSTREAM TENSION Vs. DIFFERENT PROPORTIONAL FACTORS FOR AIR + WATER INFLATED STRUCTURE

head equal to zero and zero silt depth, the upstream slope ranged from 80^{o} to 125^{o} as the proportional factor increased from 0.2 to 1.2 while these variations of the slope will be greater if the downstream head increases from zero to 0.10 m and it was found the variation is from 88^{o} to 127^{o} under the same variation of the proportional factors.

The degree of variation of the upstream slope changes as the proportional factor increases from 0.2 to 1.2, i.e. the rate of increase of the upstream slope for low proportional factors is higher than for high proportional factors, e.g. the difference in an increase in the upstream slope from $\alpha = 0.2$ to $\alpha = 0.3$ is 5 degrees while the difference in the upstream slope from $\alpha = 1.1$ to $\alpha = 1.2$ is 2.63 degrees.

The variation of the upstream slope with downstream head equal to zero and with depth of silt equal to 0.05 m does not follow the above behaviour. The variation of the upstream slope is changed from 55 degrees to 120 degrees as the proportional factor increases from 0.2 to 1.2

The higher reduction in the upstream slope is due to the distortion of the dam toward the downstream side as a result of the silt effect on the upstream face of the dam. Fig.4.15 shows the behaviour of the upstream slope under different proportional factors for an air inflated structure. From fig.4.15 it can be seen that the maximum upstream slope of the dam is for the condition of downstream head equal to 0.1 m and with the silt depth equal to zero. The minimum upstream slope occurs when the downstream head is equal to zero and with silt depth equal to 0.05 m for all proportional factors varying from 0.2 to 1.2.

The pattern of behaviour is similar for a dam inflated with water, but the values of the upstream slopes are greater than for an air inflated structure. Also the variation of the upstream slope for an (air + water) inflated structure

is similar to both the air and water inflated structures, but the values of the upstream slope depend on the depth of water inside the dam.

Figs. 4.16 and 4.17 show the variation of the upstream slope for different values of the proportional factor for water and (air + water) inflated structures respectively.

A detailed comparison between different inflation fluids for the upstream slopes is given in Chapter 6.

4.6.3 Elongation.

The increase in the length of the material in excess of the original length results from elongation. The required original length of the material is calculated according to the maximum upstream head for maximum proportional factor for water inflated structures (α = 2.5),and the new length of the material can be found from the strain-stress relationships under the applied loads. The establishments of the stress-strain relationships of TYPE I and TYPE II materials was explained in detail in Chapter 3.

The stretching of the material is due to the effect of the loads, i.e. maximum upstream head, downstream head, internal pressure head, silt depth and self weight of the material.

Elongation of the material is also affected by the properties of the material, in particular the thickness of the material used (see equation 4.11), and a spacial study was carried out with respect to the effect of the thickness of the material (Section 4.8.3).

The variation of elongation was investigated for a constant thickness (t = 0.36 mm) of material under different conditions (D/S = 0.0,0.1) (H_s = 0.0, 0.05) for different ranges of proportional factors for different inflation fluids. The results show that the elongation increases with increasing proportional factor for all conditions of downstream head and silt

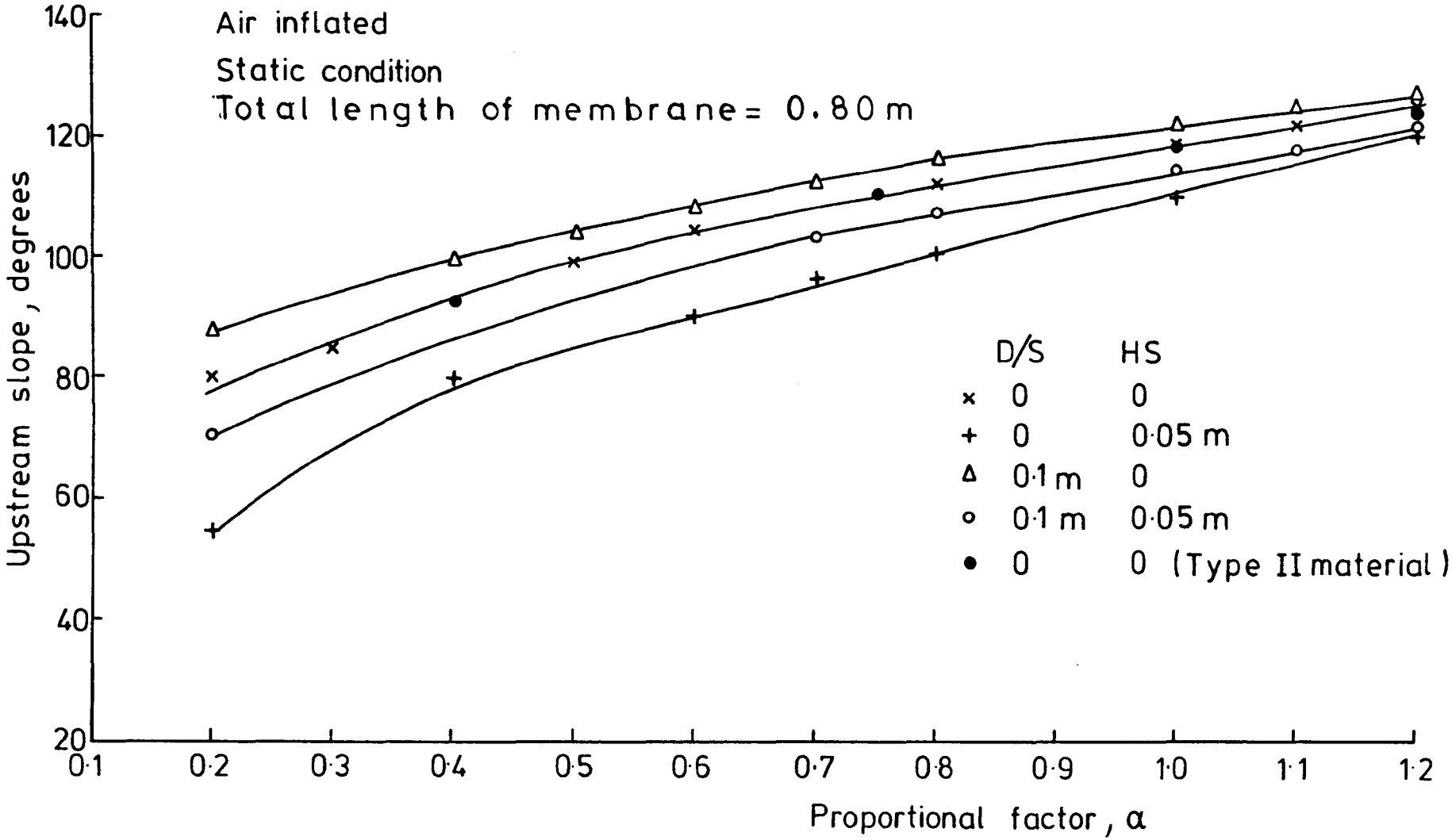

FIG.(4-15) UPSTREAM SLOPE Vs. DIFFERENT PROPORTIONAL FACTORS FOR AIR INFLATED STRUCTURE

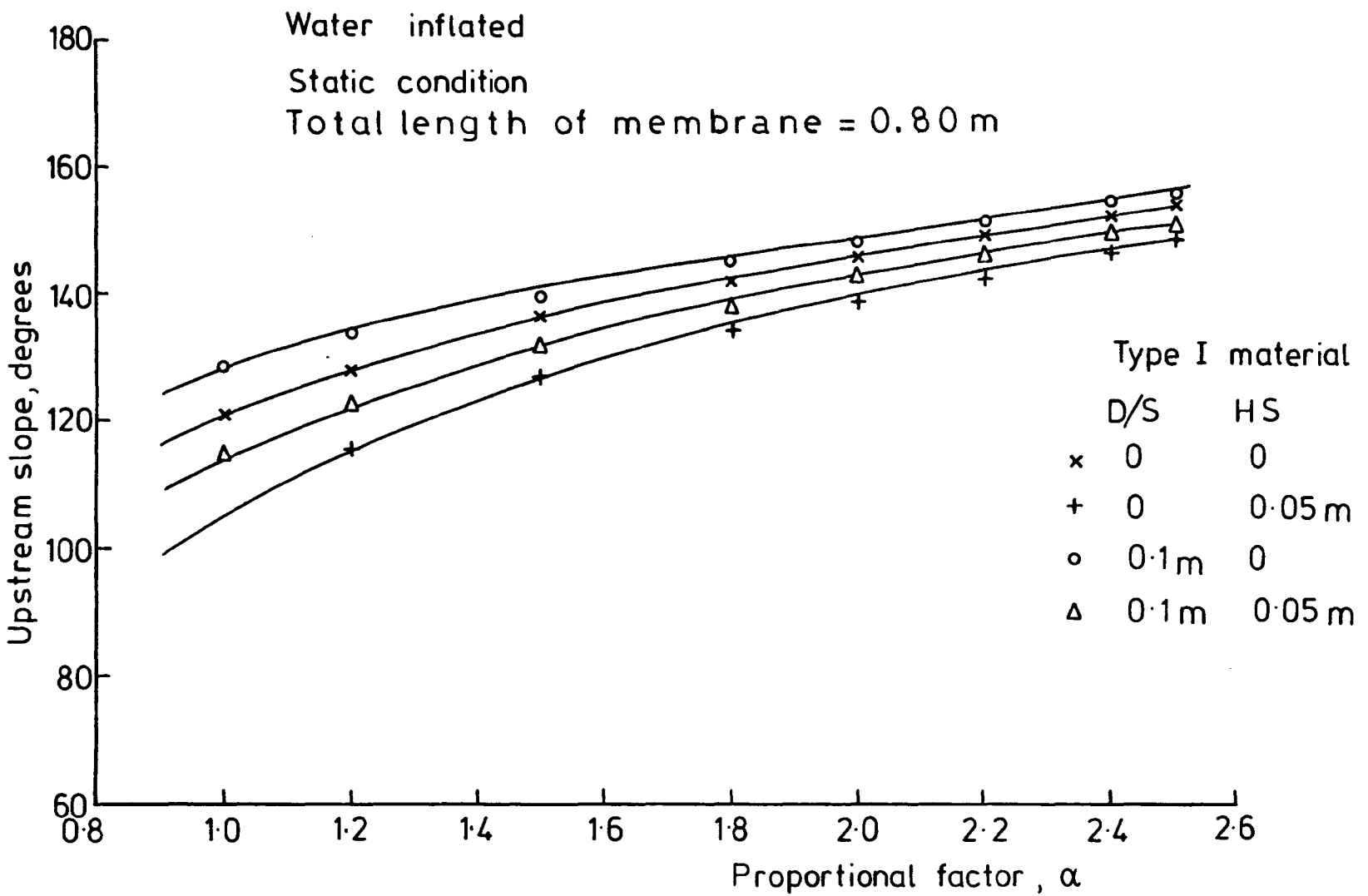

FIG. (4-16) UPSTREAM SLOPE Vs. DIFFERENT PROPORTIONAL FACTORS FOR WATER INFLATED STRUCTURE

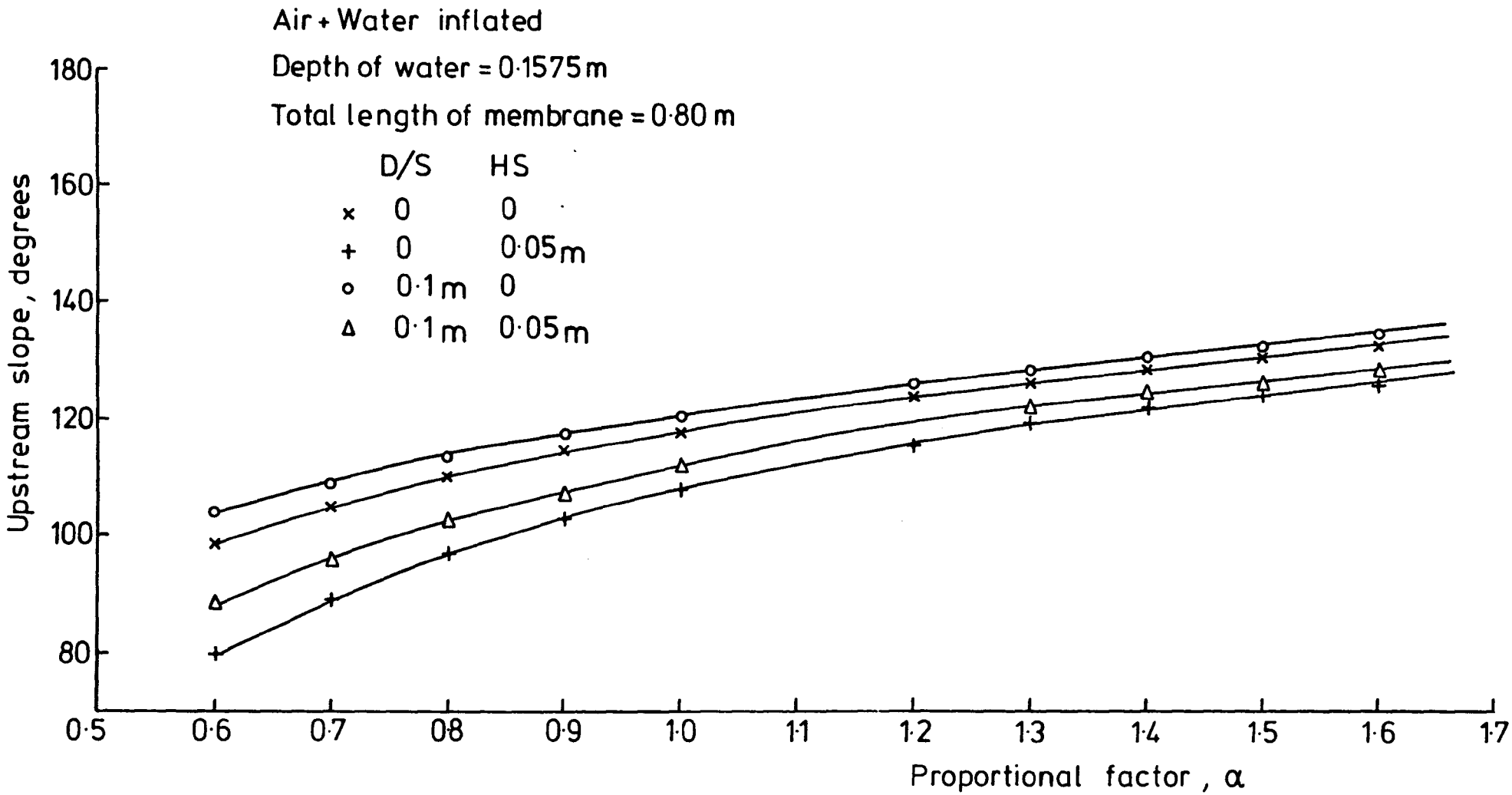

FIG. (4-17) UPSTREAM SLOPE Vs. DIFFERENT PROPORTIONAL FACTORS FOR AIR + WATER INFLATED STRUCTURE

depth. The variation of the elongation for different proportional factors for air inflated structures is represented in fig.4.18 from which one can see that the maximum elongation occurs for the condition of downstream head equal to zero and zero silt depth while the minimum elongation occurs for the condition of downstream head equal to 0.1 m and 0.05 m of silt pressure.

A similar behaviour for the variation of elongation was found for the type II material for the condition of downstream head equal to zero and zero silt depth as shown in fig. 4.18.

The variation in the elongation of the materials is similar for the water inflated structures if the maximum and minimum elongation occurring when the downstream head is equal to zero with zero silt depth and with downstream head equal to 0.1 with silt depth equal to 0.05 m respectively as the proportional factors increase from 1.0 to 2.5. Fig.4.19 shows the variation of the elongation of the material when the structure is inflated with water.

A similar pattern for the variation of the elongation is found for the (air + water) inflated structure as shown in fig.4.20.

From the above results then the elongation is a maximum under the condition of downstream head equal to zero and zero silt depth which coincides with the conditions for greater tension.

4.6.4 Cross-sectional area.

The area of the cross section of the inflatable structures was computed for different proportional factors under downstream head equal to (D/S = 0.0,0.1) and silt effect equal to H_s =(0.0, 0.05). The area was computed from the following relationship:

$$\text{Area} = \sum_{NN=2}^{NN} [(y(J) + y(j-1)] \cdot [x(J) - x(J-1)]/2 \quad .... \quad 4.14$$

where y(J), x(J) are the co-ordinate of the nodes.

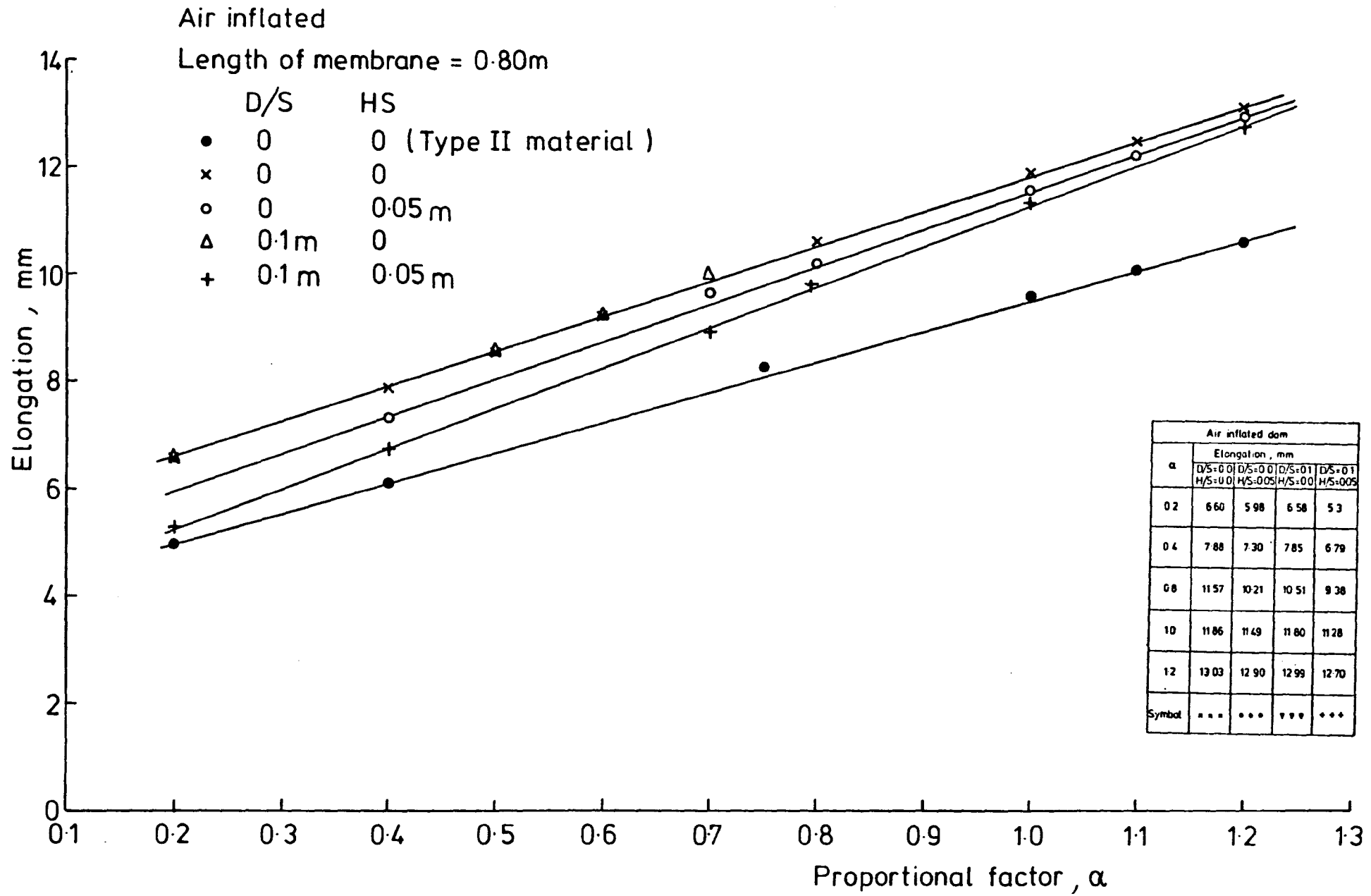

Air inflated dam				
α	Elongation , mm			
	D/S=0 0 H/S=0 0	D/S=0 0 H/S=0 05	D/S=0 1 H/S=0 0	D/S=0 1 H/S=0 05
0 2	6 60	5 98	6 58	5 3
0 4	7 88	7 30	7 85	6 79
0 8	11 57	10 21	10 51	9 38
1 0	11 86	11 49	11 80	11 28
1 2	13 03	12 90	12 99	12 70
Symbol	▪ ▪ ▪	● ● ●	▼ ▼ ▼	◆ ◆ ◆

FIG. (4-18) ELONGATION OF THE MEMBRANE Vs. DIFFERENT PROPORTIONAL FACTORS FOR AIR INFLATED STRUCTURE

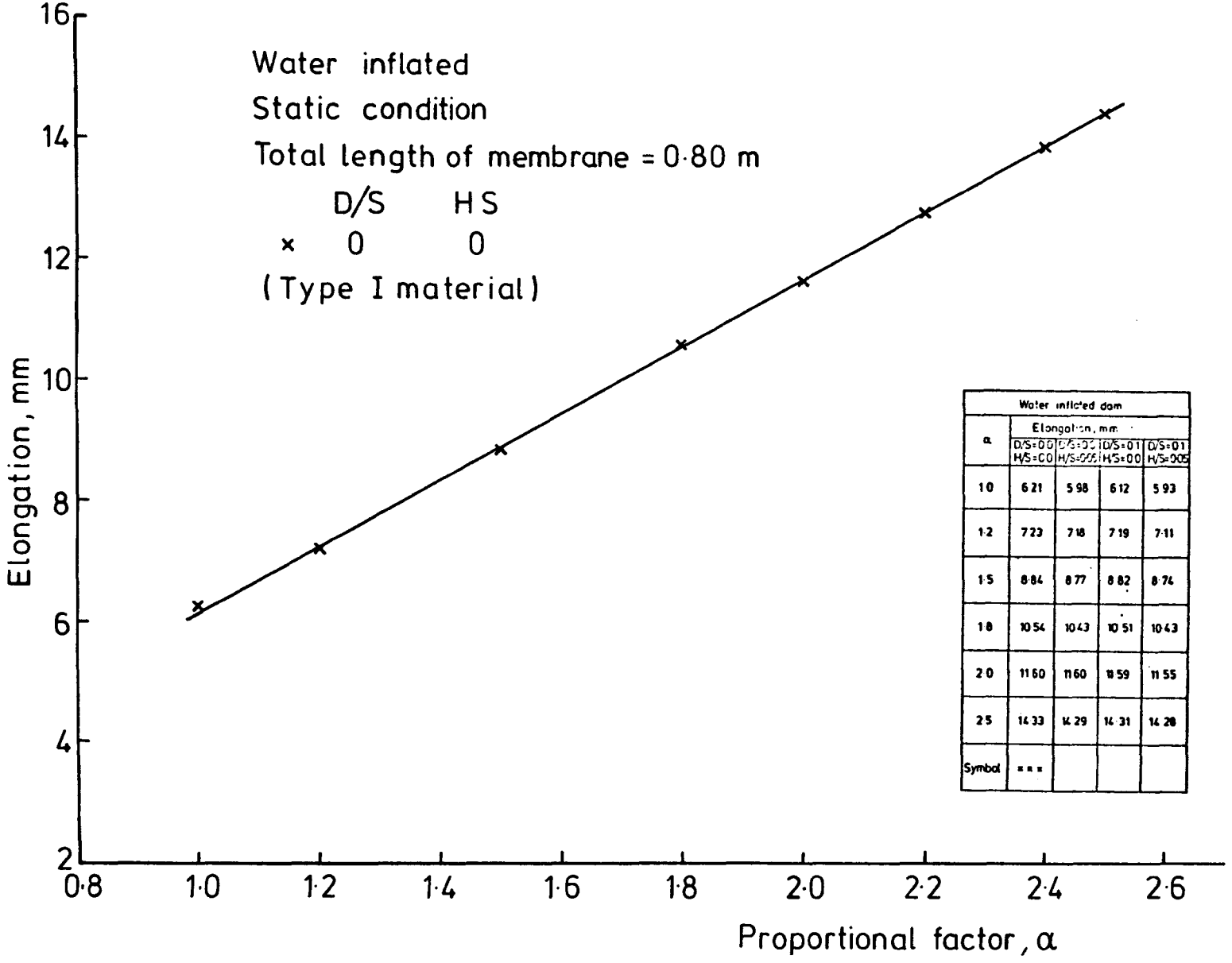

Water inflated dam				
α	Elongation, mm			
	D/S=0.0 H/S=0.0	D/S=0.0 H/S=0.05	D/S=0.1 H/S=0.0	D/S=0.1 H/S=0.05
1.0	6.21	5.98	6.12	5.93
1.2	7.23	7.18	7.19	7.11
1.5	8.84	8.77	8.82	8.74
1.8	10.54	10.43	10.51	10.43
2.0	11.60	11.60	11.59	11.55
2.5	14.33	14.29	14.31	14.28
Symbol	× × ×			

FIG.(4-19) ELONGATION OF THE MEMBRANE Vs. DIFFERENT PROPORTIONAL FACTORS FOR WATER INFLATED STRUCTURE

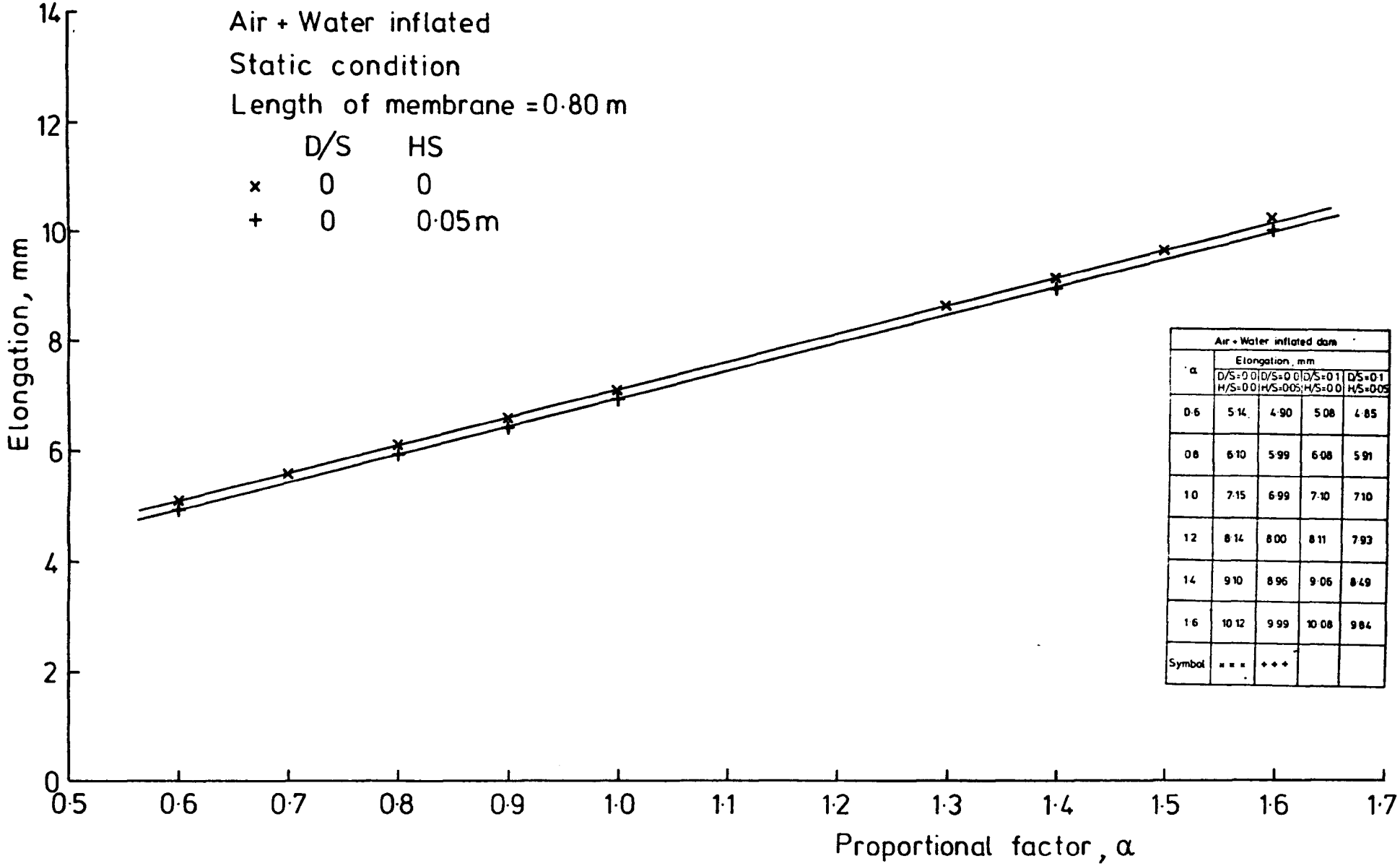

Air + Water inflated dam				
α	Elongation, mm			
	D/S=0 0 H/S=0 0	D/S=0 0 H/S=0 05	D/S=0 1 H/S=0 0	D/S=0 1 H/S=0 05
0·6	5 14	4·90	5 08	4 85
0 8	6 10	5 99	6 08	5 91
1 0	7 15	6 99	7 10	7 10
1 2	8 14	8 00	8 11	7 93
1 4	9 10	8 96	9 06	8 49
1 6	10 12	9 99	10 08	9 84
Symbol	× × ×	+ + +		

FIG. (4-20) ELONGATION OF THE MEMBRANE Vs. DIFFERENT PROPORTIONAL FACTORS FOR AIR + WATER INFLATED STRUCTURE

The cross-sectional area increases for increasing proportional factor alpha for all conditions of downstream head and silt depth, and for the different types of inflation fluids. The maximum cross-sectional area occurs when the downstream head is equal to 0.10 m and zero silt depth whilst the minimum area is the condition of zero downstream head and with silt depth equal to 0.05 m on the upstream face. Fig.4.21 illustrates the variation of area with respect to different proportional factors (0.2-1.2) for an air inflated structure.

The cross-sectional area also depends on the behaviour of the elongation of the material, i.e. high strain material will stretch to give high elongation giving a higher dam which results in an increase in the cross-sectional area. The cross-sectional areas for different materials (TYPE I, TYPE II) are shown in fig.4.21 for air inflated and under downstream head equal to zero and zero silt, the resulting cross-sectional area of type I material is less than the cross-sectional area of type II material under the same conditions, the difference being due to the differences in the elongation of the two materials.

The variation of the cross-sectional area for a water inflated structure is similar to the air inflated structure but for high proportional factor ($\alpha > 2.2$) the cross-sectional area is approximately constant.

Fig.4.22 shows the variation of the cross-sectional area for a water inflated structure for different downstream heads (D/S = 0.0, 0.1) and silt depths (H_s = 0.0, 0.05 m). The maximum cross-sectional area occurs at a downstream head equal to 0.10 m and silt depth equal to zero whilst the minimum cross-sectional area is when the downstream head is equal to zero and with the silt depth equal to 0.05 m.

The cross-sectional area of the (air + water) inflated structure is almost similar to the water inflated structure. The cross-sectional area is dependent on the depth of water inside the dam. The variation of the cross-

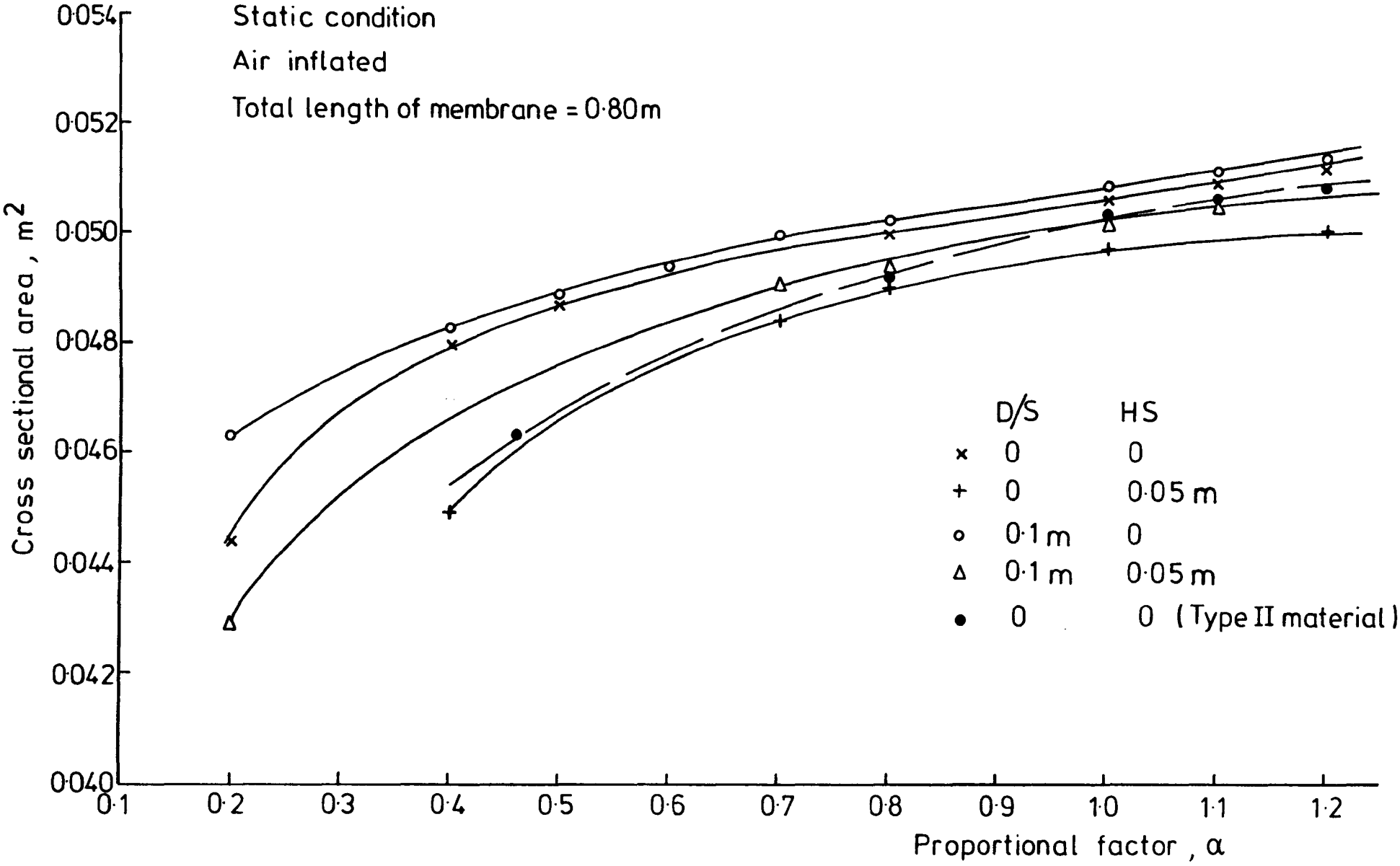

FIG. (4-21) CROSS SECTIONAL AREA Vs. DIFFERENT PROPORTIONAL FACTORS FOR AIR INFLATED STRUCTURE

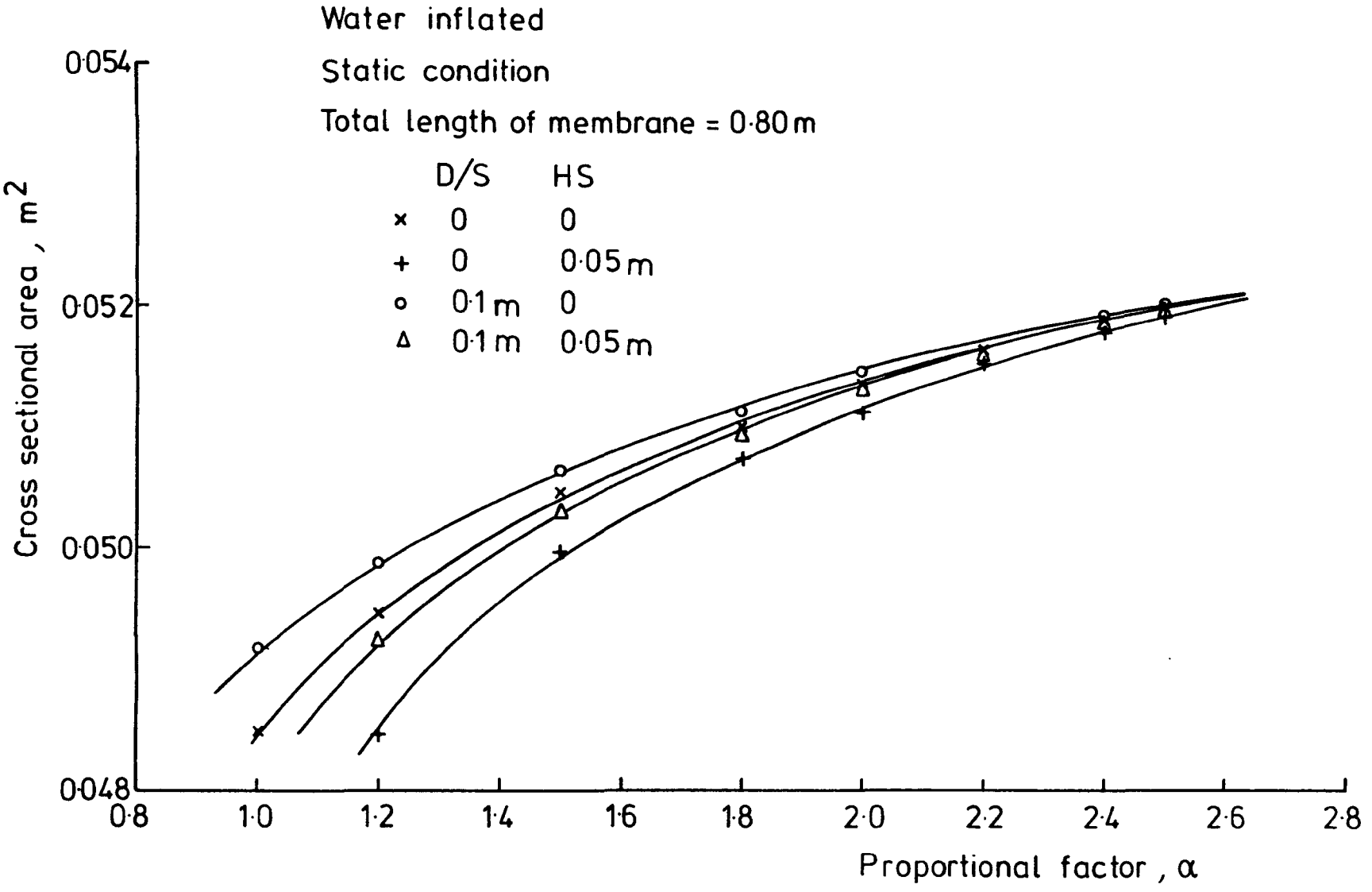

FIG.(4-22) CROSS SECTIONAL AREA Vs DIFFERENT PROPORTIONAL FACTORS FOR WATER INFLATED STRUCTURE

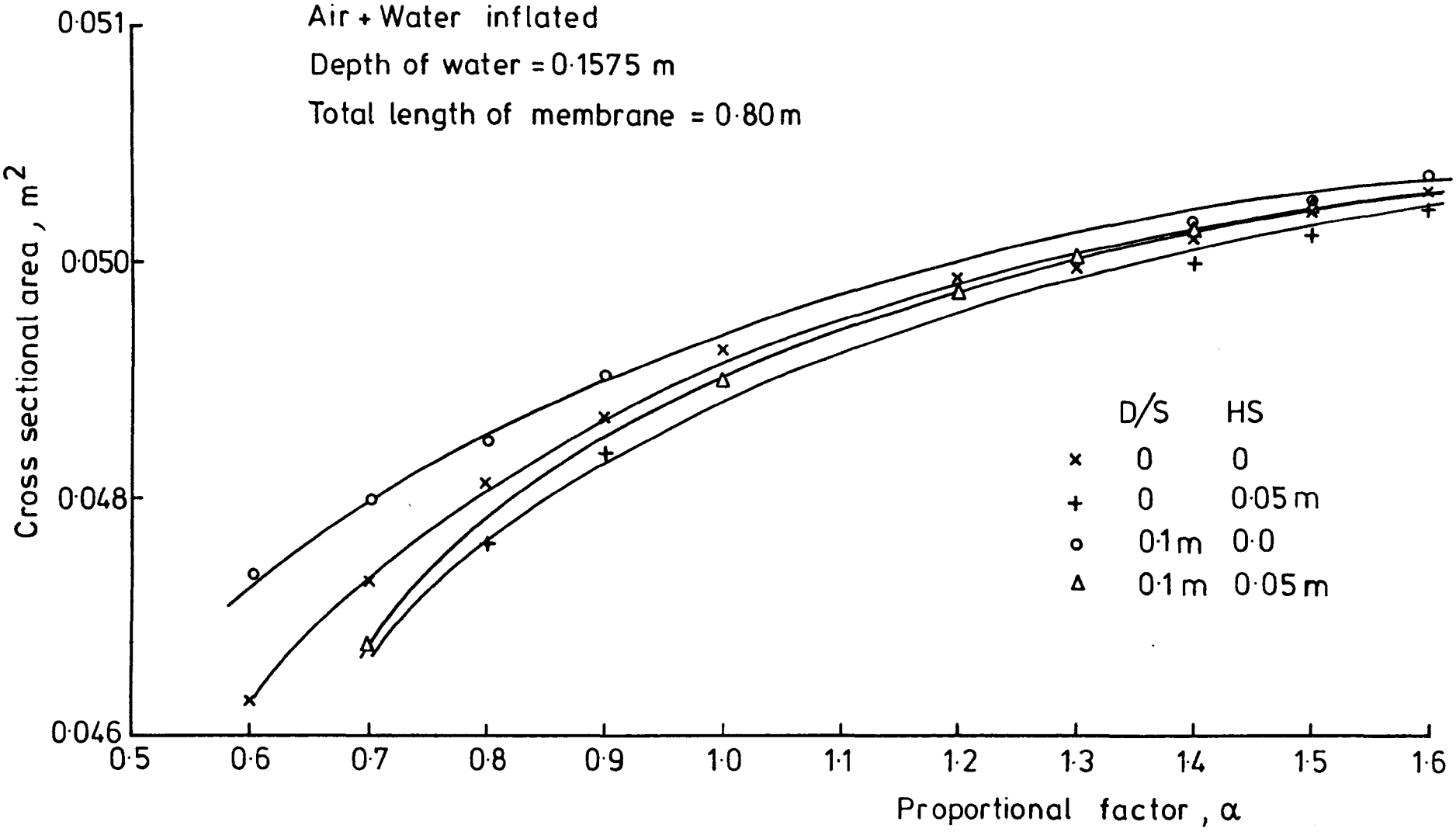

FIG.(4-23) CROSS SECTIONAL AREA Vs. DIFFERENT PROPORTIONAL FACTORS FOR AIR + WATER INFLATED STRUCTURE

sectional area will be close to the variation of water inflated structure if the depth of water inside is high, whilst the variation will be close to that of an air inflated structure if the depth of water is low.

Fig.4.23 shows the variation of the cross-sectional area of the dam for different proportional factors for different conditions of downstream head and silt depths on the upstream face.

The different typical profile's behaviour under different conditions of downstream head and silt depth were shown in figs. 4.24, 4.25 and 4.26 for the dams inflated with air, water and (air + water) respectively.

4.6.5 Maximum dam height.

The maximum y(J) co-ordinate of the nodes around the membrane under different loading gives the maximum crest height of the dam. The maximum height increases as the proportional factor increases and the maximum height will be approximately constant for high proportional factor ($\alpha > 2.4$) for water inflated structures.

The maximum height of an air inflated dam is when downstream head is equal to 0.10 m and with zero silt depth whilst the minimum height is when the downstream head is equal to zero and with 0.05 m silt depth. The rate of increase in the maximum height is higher for low proportional factor than increases in the maximum height for high proportional factors, e.g., the maximum height for an air inflated structure under zero downstream head and zero silt depth increased from 0.23m to 0.24 m as the proportional factor increased from 0.2 to 0.3 whilst the maximum height of the dam increased from 0.259 m to 0.260 m as the proportional factor increased from 1.1 to 1.2.

The maximum height of the dam is not dependent only on the internal pressure head, upstream head, downstream head and silt pressure, but also depends on the thickness of the material. Details of this effect are given in

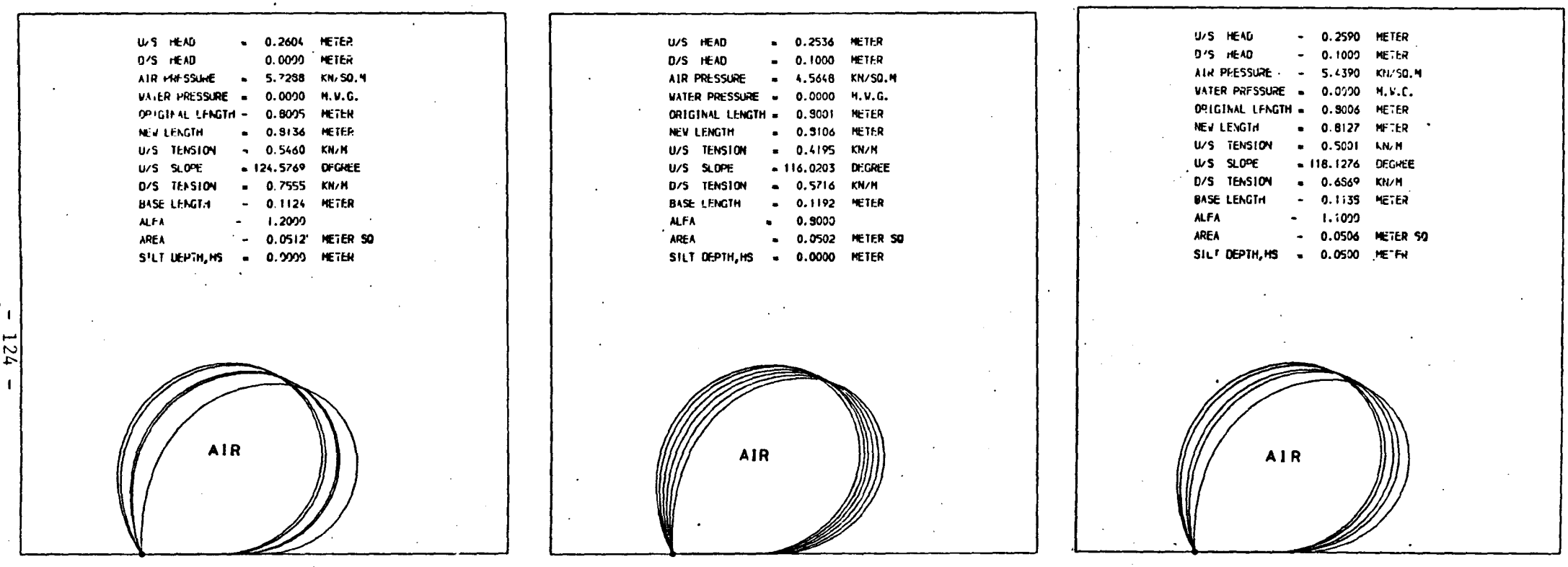

FIG. (4-24) TYPICAL PROFILE BEHAVIOUR OF AN AIR INFLATED STRUCTURE UNDER DIFFERENT PROPORTIONAL FACTORS

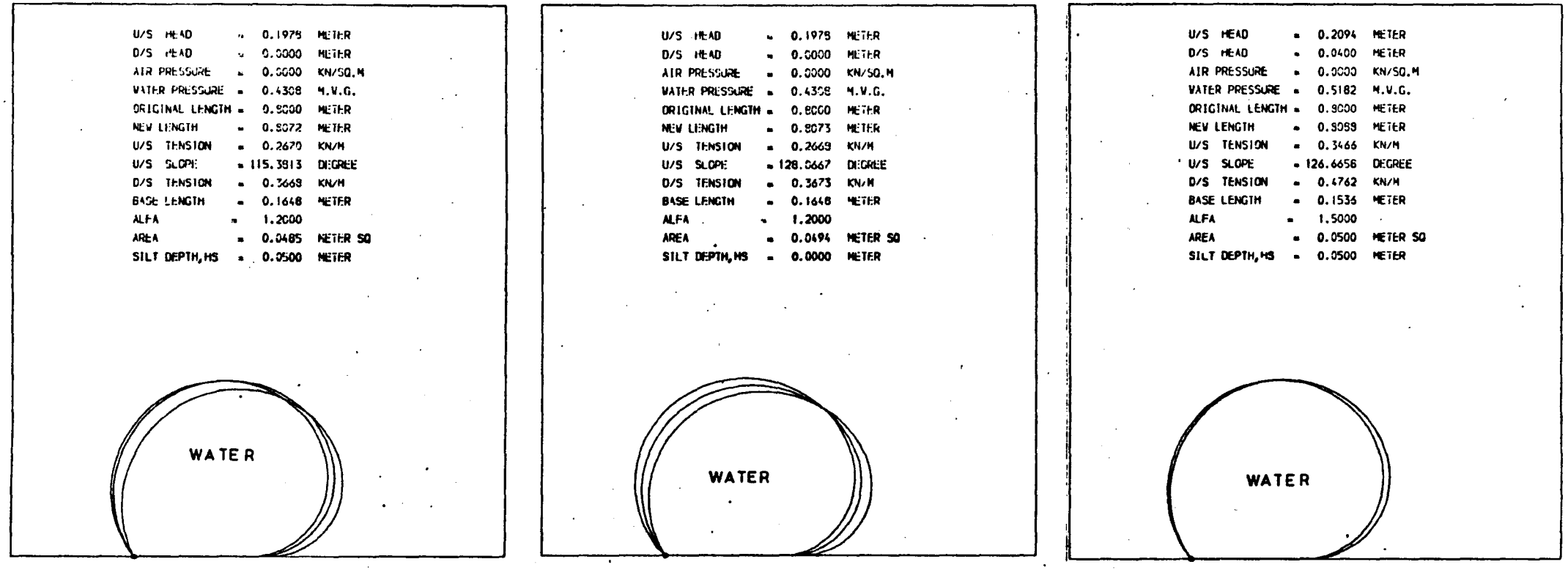

FIG. (4-25) TYPICAL PROFILE BEHAVIOUR OF WATER INFLATED STRUCTURE UNDER DIFFERENT PROPORTIONAL FACTORS

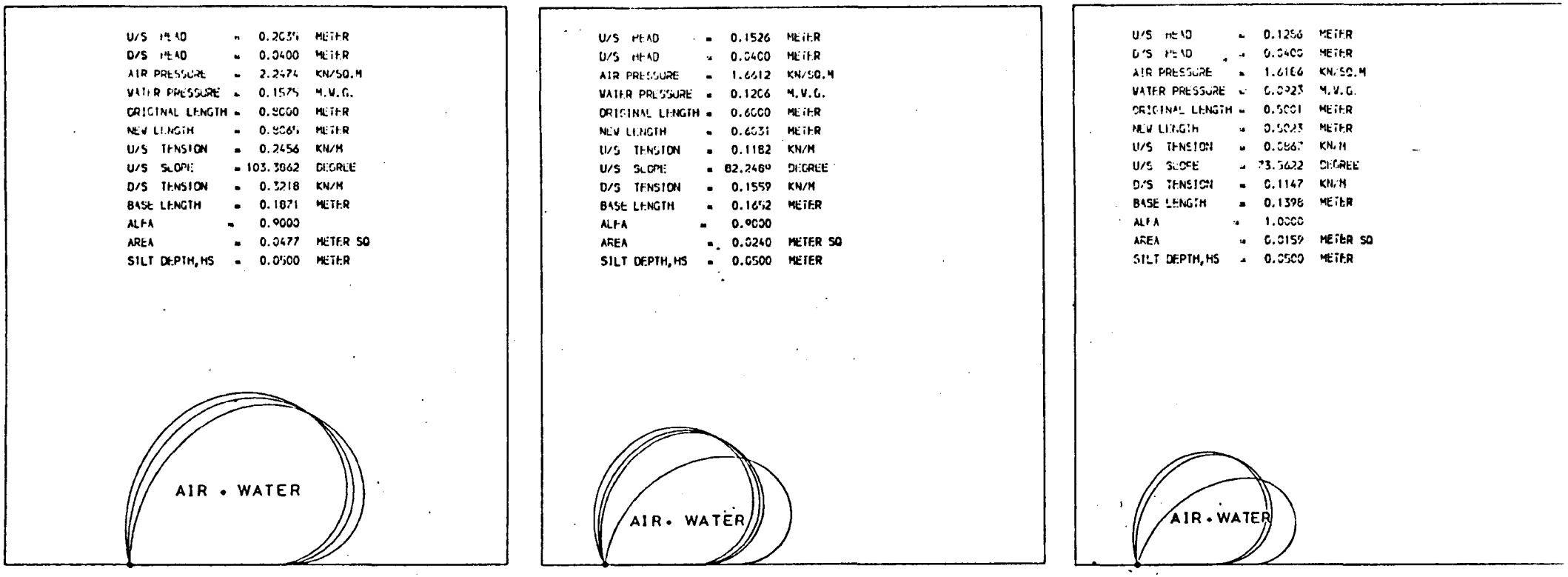

FIG.(4-26) TYPICAL PROFILE BEHAVIOUR OF AN AIR+WATER INFLATED STRUCTURE UNDER DIFFERENT PROPORTIONAL FACTORS

Sec. 4.8.3. Fig.4.27 shows the variation of the maximum height of a dam for different proportional factors under different conditions of downstream head and silt depth. From this variation it can be seen that the type I material with downstream head equal to zero and zero silt depth is higher than for the type II material under the same condition, the differences being due to the thickness of the material.

In the case of a water inflated dam the variation of the maximum height of the dam is similar to the air inflated case, i.e. the maximum height is when the downstream head is equal to 0.1 m and zero silt depth. Fig.4.28 shows the variation of maximum height of the dam for different proportional factors under different downstream heads and silt depths.

In the case of the (air + water) inflated structure, the maximum height of the dam is similar to the water inflated structure as can be seen from fig.4.29 which illustrates that the rate of change in the maximum height under the condition of downstream head equal to 0.1 m and silt depth equal to 0.05 m is similar to the rate of change in the maximum height of the dam under condition of downstream head equal to 0.10 m and zero depth of silt as the proportional factor increases from 1.2 to 1.6.

As far as the maximum height and minimum height of the dam are concerned for this type of inflation, the variations are similar to the previous cases, i.e. the maximum height of the dam occurs for a downstream head equal to 0.1 m and zero silt pressure whilst the minimum height is when the downstream head is zero and with a silt depth equal to 0.05 m.

4.7 Effect of the initial length of the membrane.

The length of the perimeter of the membrane has a major effect on the output parameters of the dam i.e. tension, maximum upstream head, maximum height of dam, and cross-sectional area. In this study the length of the

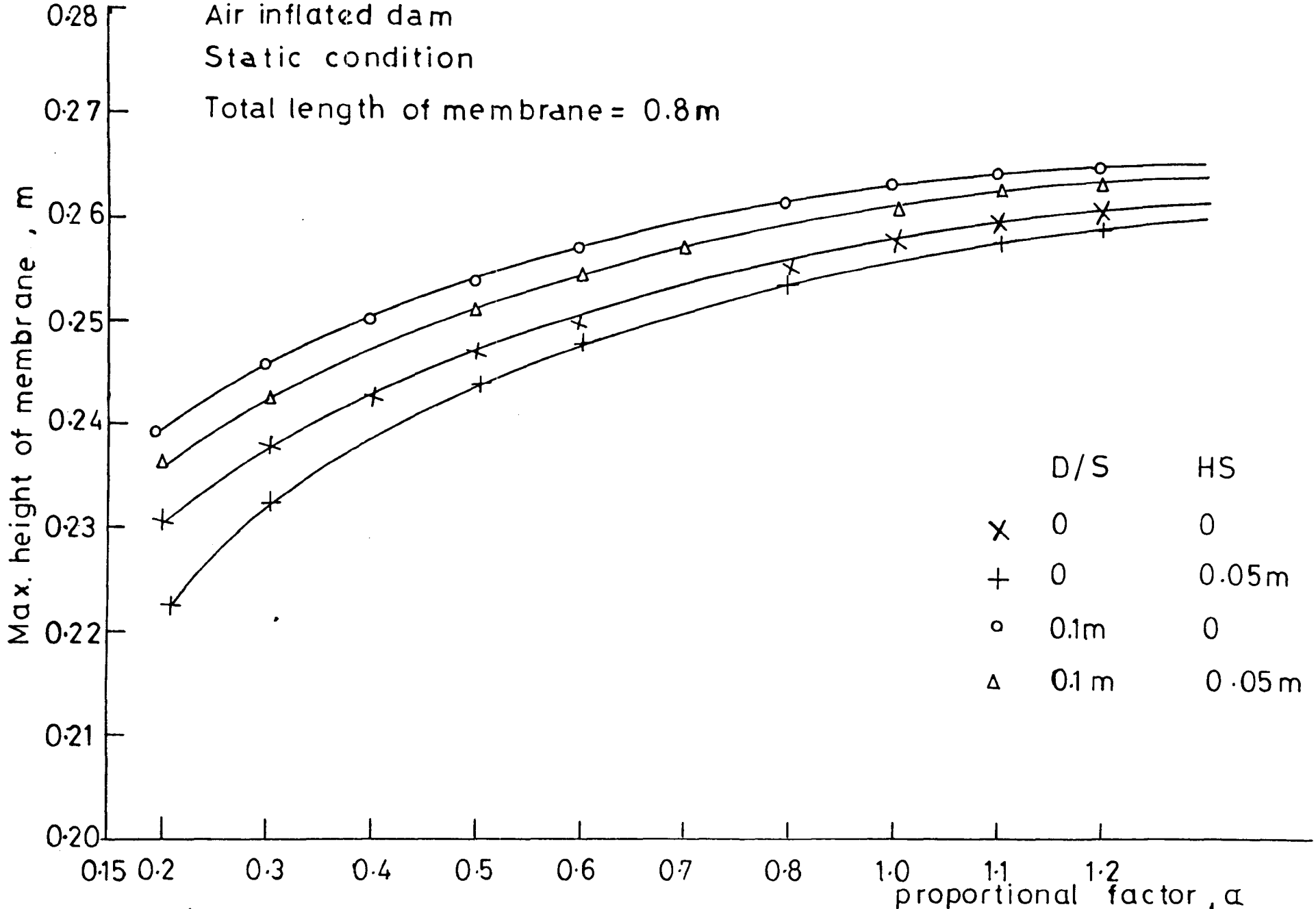

FIG.(4-27) MAXIMUM DAM HEIGHT Vs. DIFFERENT PROPORTIONAL FACTORS FOR AIR INFLATED STRUCTURE

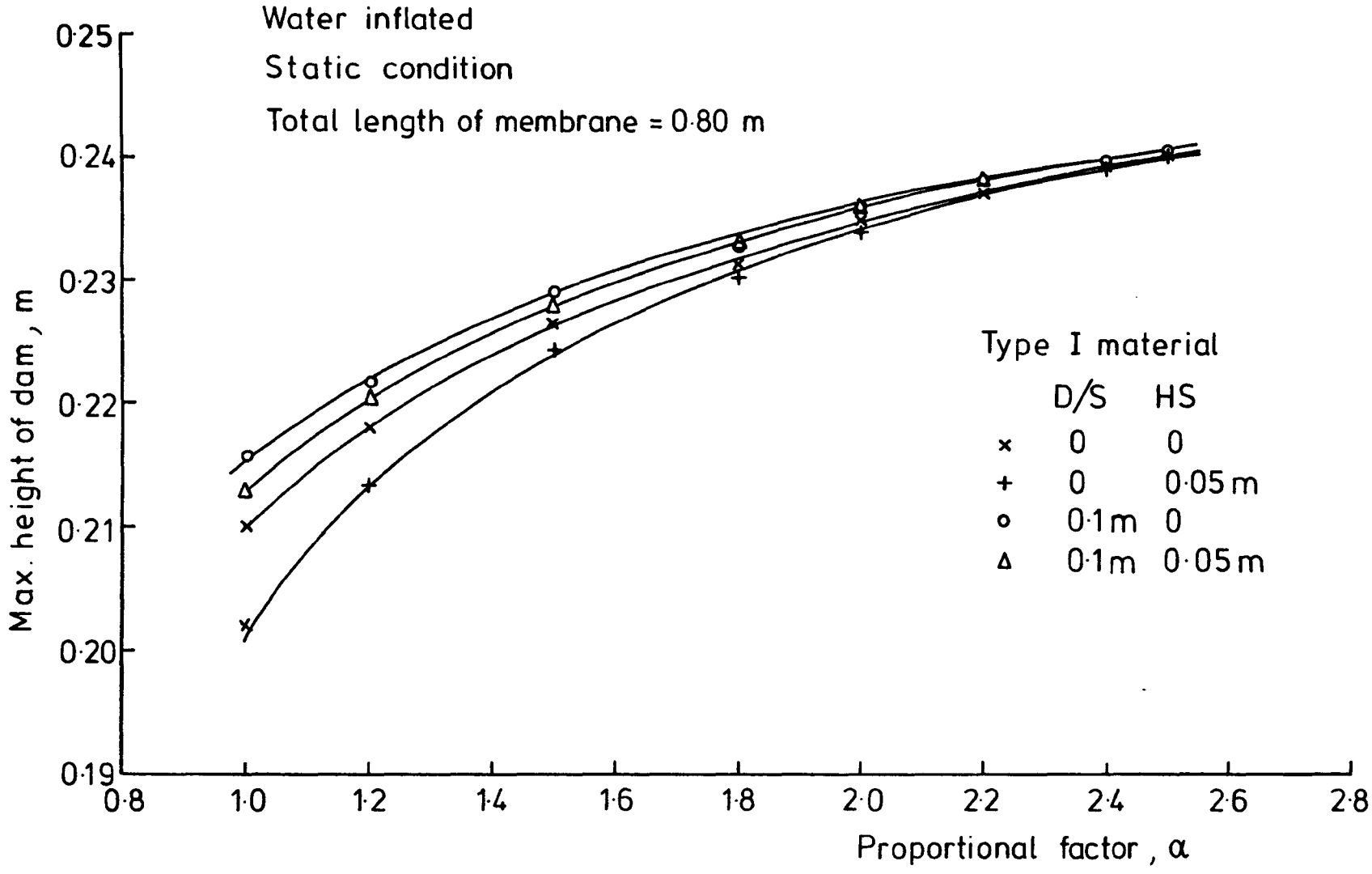

FIG.(4-28) MAXIMUM HEIGHT OF DAM Vs. DIFFERENT PROPORTIONAL FACTORS FOR WATER INFLATED STRUCTURE

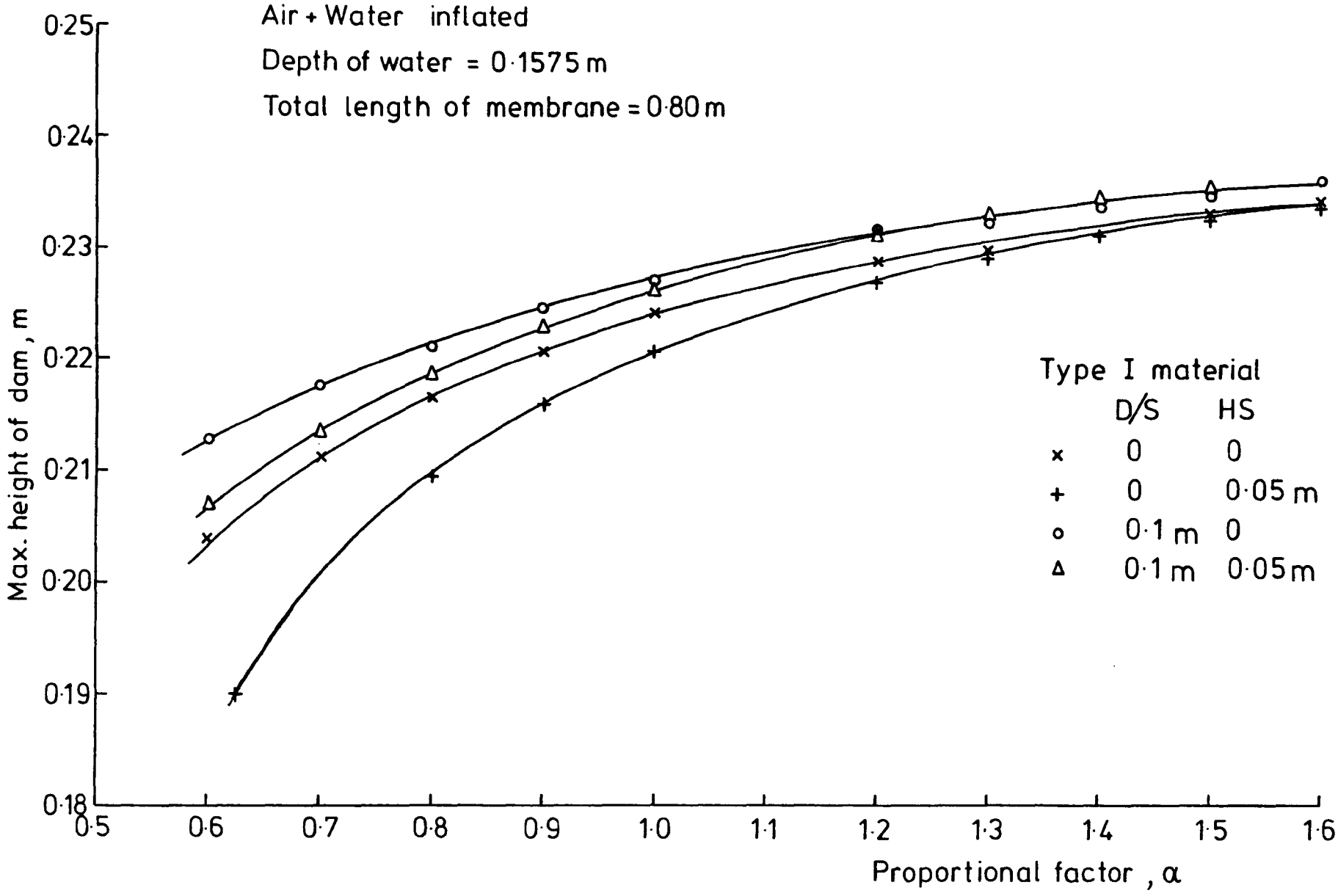

FIG.(4-29) MAXIMUM DAM HEIGHT Vs. DIFFERENT PROPORTIONAL FACTORS FOR AIR + WATER INFLATED STRUCTURE

membrane is found from the relationship as detailed in Chapter 8. The lengths tested were 0.50, 0.60, 0.70,0.80, 1.0 m under zero downstream head and zero silt depth for maximum upstream head for different inflation fluids under different proportional factors. This study of varying the length gave information on the effect on the following parameters:

1. Tension.
2. Upstream slope.
3. Elongation of the membrane.
4. Cross-sectional area.
5. Maximum height of the dam.

4.7.1 Tension.

The tension in each element was calculated around the membrane and the average tension of the upstream face found as the average of the tension in the upstream elements and similarly for the downstream force. The tension was calculated for different inflation fluids, i.e., air, water and the combination of both for different proportional factors.

4.7.1.1 Upstream tension.

Variations in the upstream tensions are proportional to the length of the membrane, with increasing length of the membrane, tension increases for all the proportional factors for an air inflated structure, i.e., (α = 0.3, 0.4, 0.5, 0.8, 1.0 and 1.2). Fig.4.30 illustrates this variation of tension with different length of membrane.

From the above result one can conclude that a membrane which can be used for a small dam may not be suitable for a large dam as the tension may be higher and hence may exceed the breaking strength of the material.

A similar pattern of behaviour exists for the variation of tension with respect to the different length of membrane for the water inflated structure.

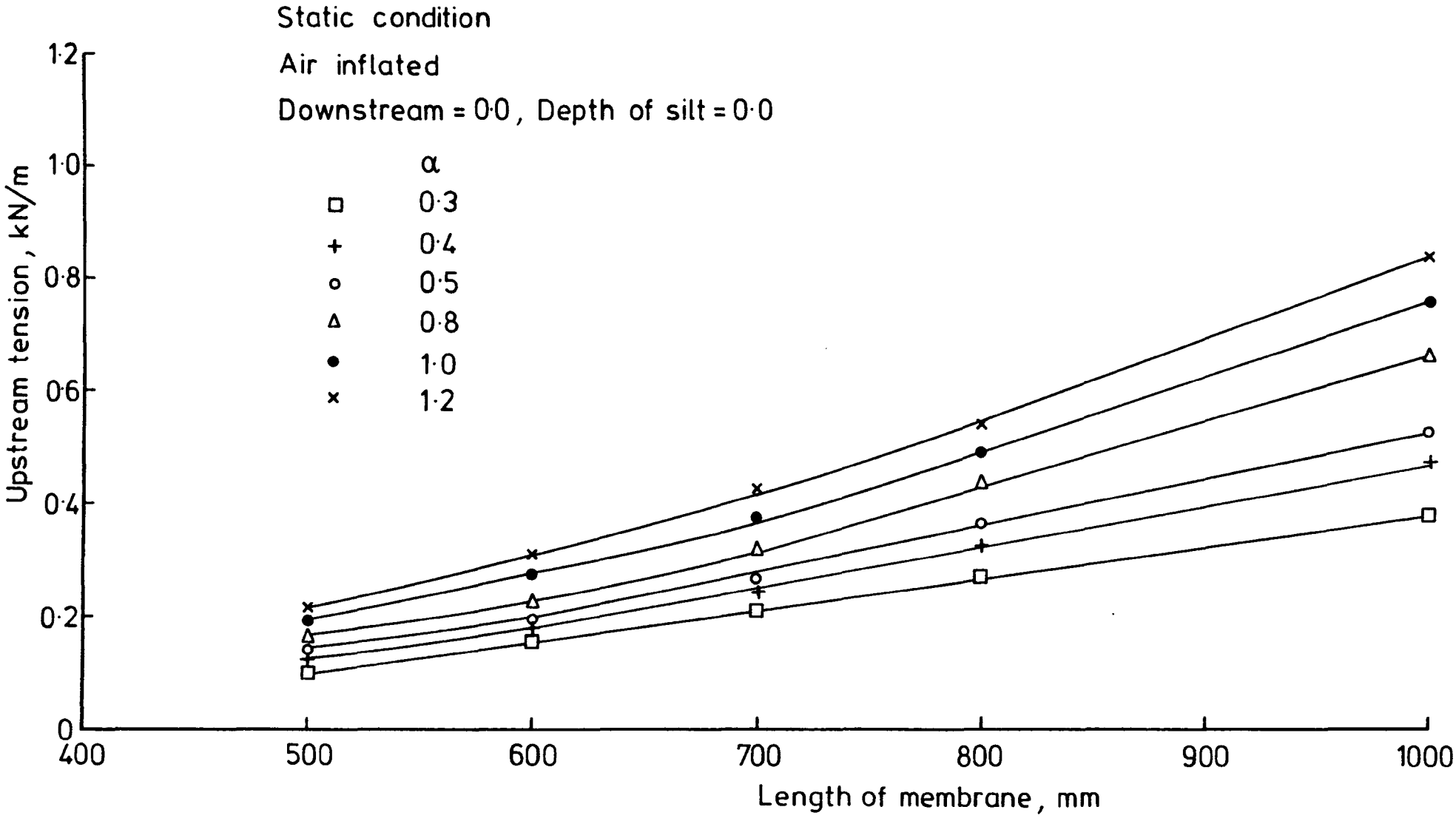

FIG.(4-30) UPSTREAM TENSION Vs. DIFFERENT LENGTH OF MEMBRANE FOR AIR INFLATED STRUCTURE

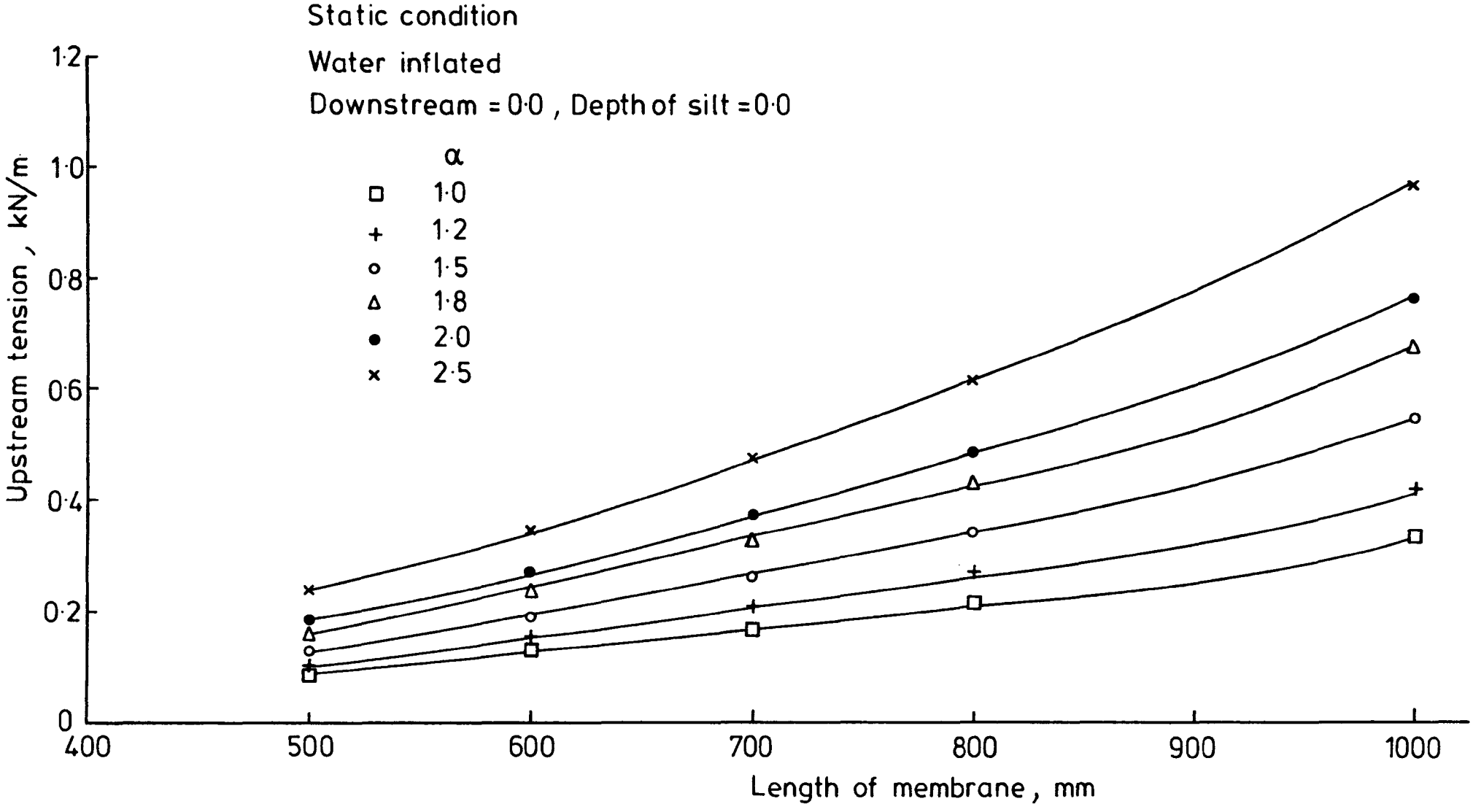

FIG. (4-31) UPSTREAM TENSION Vs. DIFFERENT LENGTH OF MEMBRANE FOR WATER INFLATED STRUCTURE

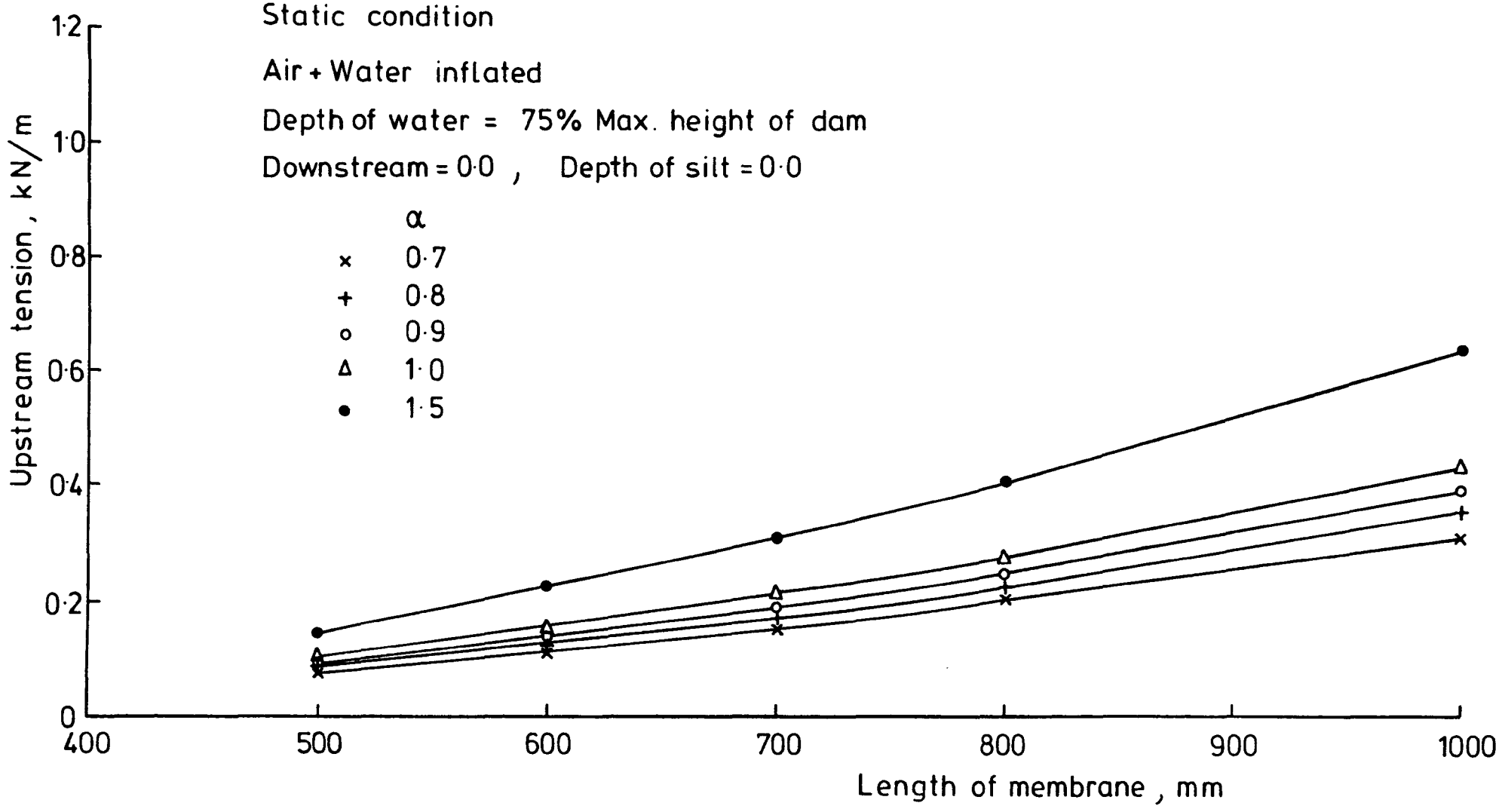

FIG. (4-32) UPSTREAM TENSION Vs. DIFFERENT LENGTH OF MEMBRANE FOR AIR + WATER INFLATED STRUCTURE

Fig.4.31 illustrates the variation of tension with different lengths of membrane. The variation of tension increases with increasing the length of the membrane for different proportional factors (1.0, 1.2, 1.5, 1.8, 2.0, 2.5).

So far as the (air+water) inflated structure is concerned, the variation of tension with respect to the different length of membrane is similar to the previous cases of inflation. Fig.4.32 illustrates the variation of tension with different length of membrane for an (air+water) inflated structure under different proportional factors (i.e., α = 0.7, 0.8, 0.9, 1.0 and 1.5).

The above result was also found by Parbery (22), who states that the profile length has a direct effect on the tension.

4.7.1.2 Downstream tension.

Variation of the downstream tension is similar to that of the upstream tension as the length of the membrane increases, the downstream tension increases.

For the air inflated structure, the downstream tension was calculated for the same conditions as the upstream tension. Fig.4.33 illustrates the variation of downstream tension with respect to different lengths of membrane.

The variation of the downstream tension for water inflated structures and (air+water) inflated structures follow a similar pattern to the variation of the air inflated structure and fig. 4.34 and fig. 4.35 represent these variations.

4.7.2 Upstream slope.

From fig.4.36 it can be seen that there is no significant variation of upstream slopes with the length of membrane for particular proportional factor. This is better illustrated by the profiles for different lengths of membrane plotted for proportional factors alpha equal to 0.8 and 1.0 as in fig.4.37. The profiles have been plotted for lengths equal to 0.50, 0.60, 0.70, 0.80, 1.0 m and it is seen that the upstream slope is constant for all dams for a particular proportional factor.

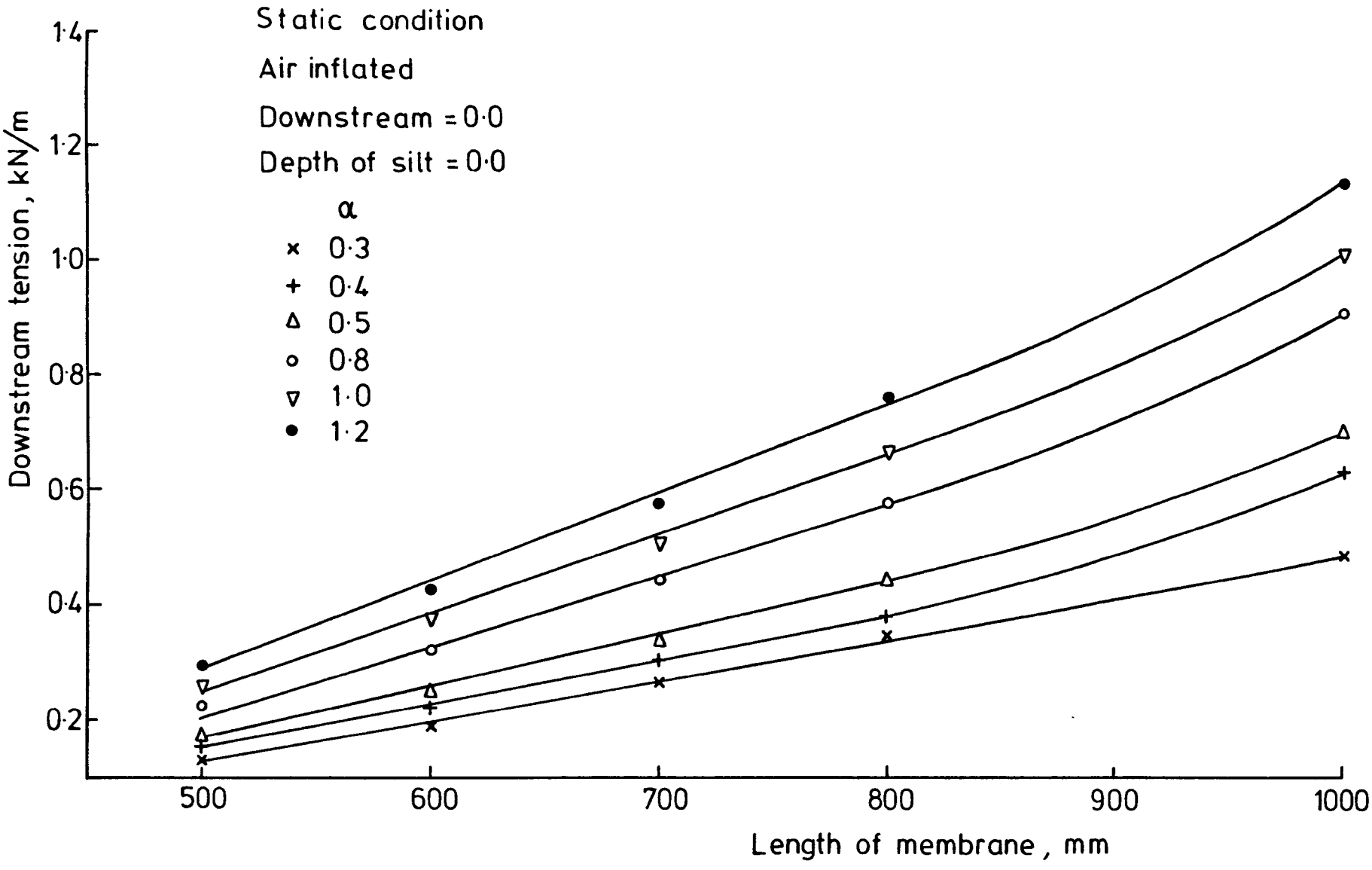

FIG. (4-33) DOWNSTREAM TENSION Vs. DIFFERENT LENGTH OF MEMBRANE FOR AIR INFLATED STRUCTURE

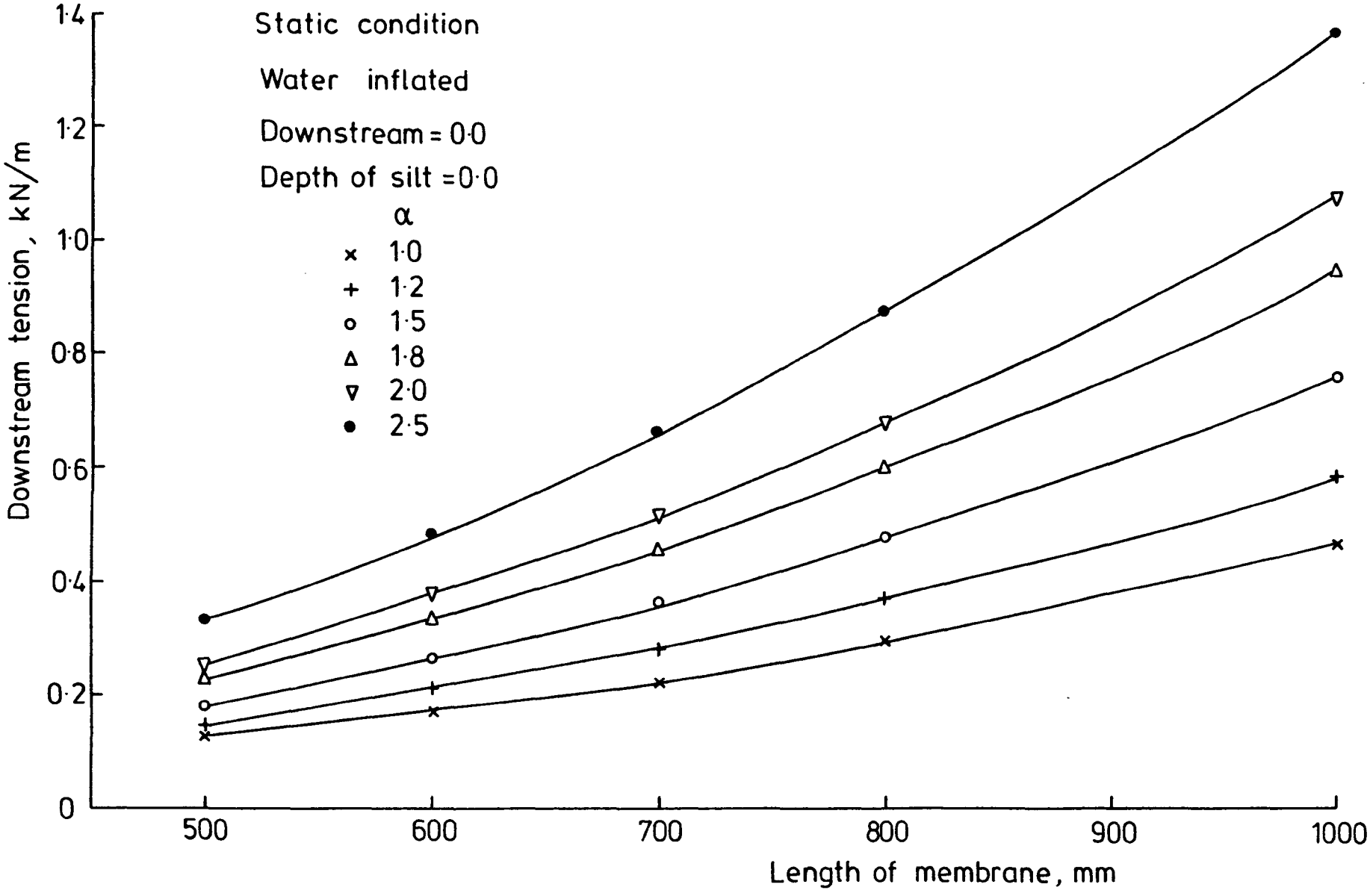

FIG.(4-34) DOWNSTREAM TENSION Vs. DIFFERENT LENGTH OF MEMBRANE FOR WATER INFLATED STRUCTURE

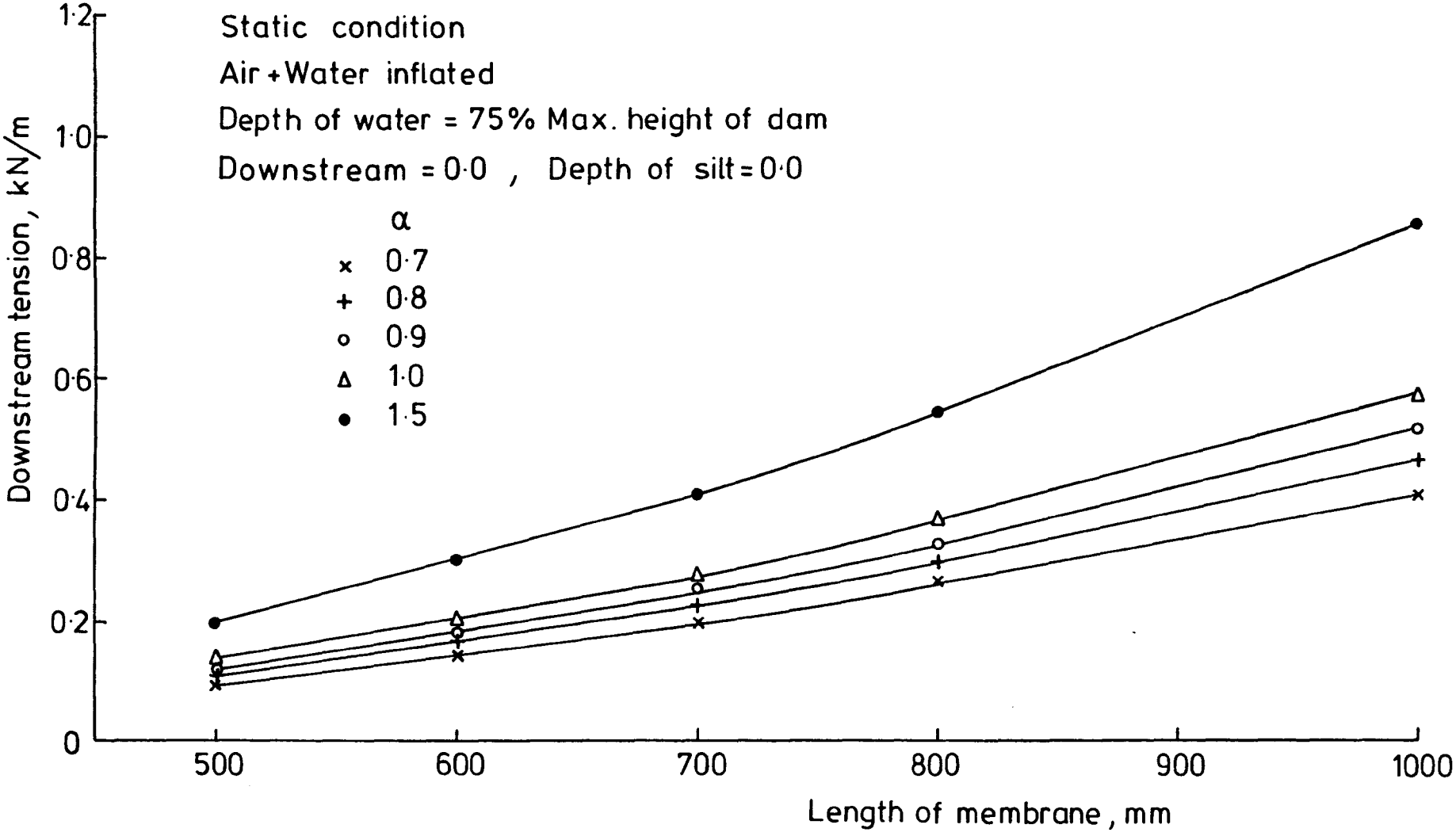

FIG. (4-35) DOWNSTREAM TENSION Vs. DIFFERENT LENGTH OF MEMBRANE FOR AIR + WATER INFLATED STRUCTURE

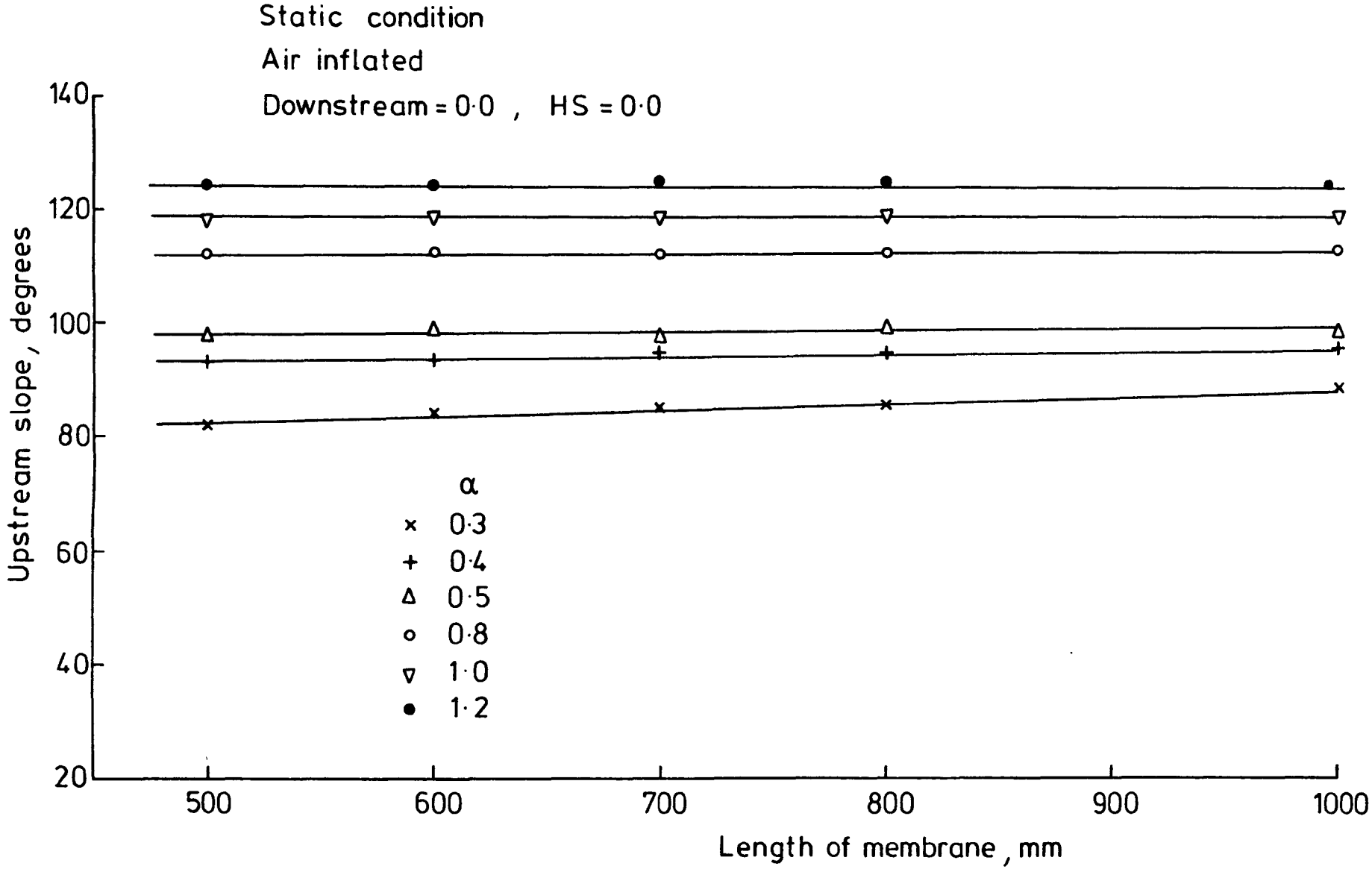

FIG.(4-36) UPSTREAM SLOPE Vs. DIFFERENT LENGTH OF MEMBRANE FOR AIR INFLATED STRUCTURE

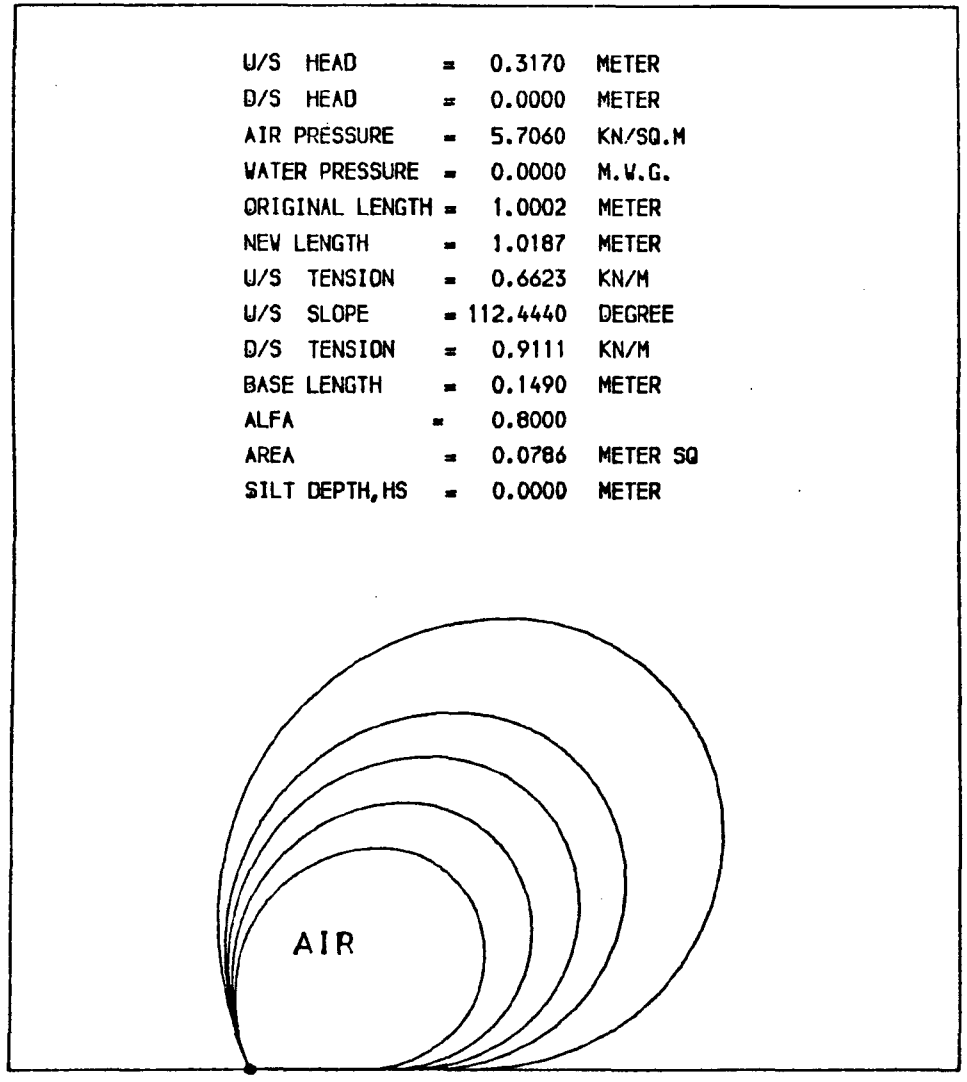

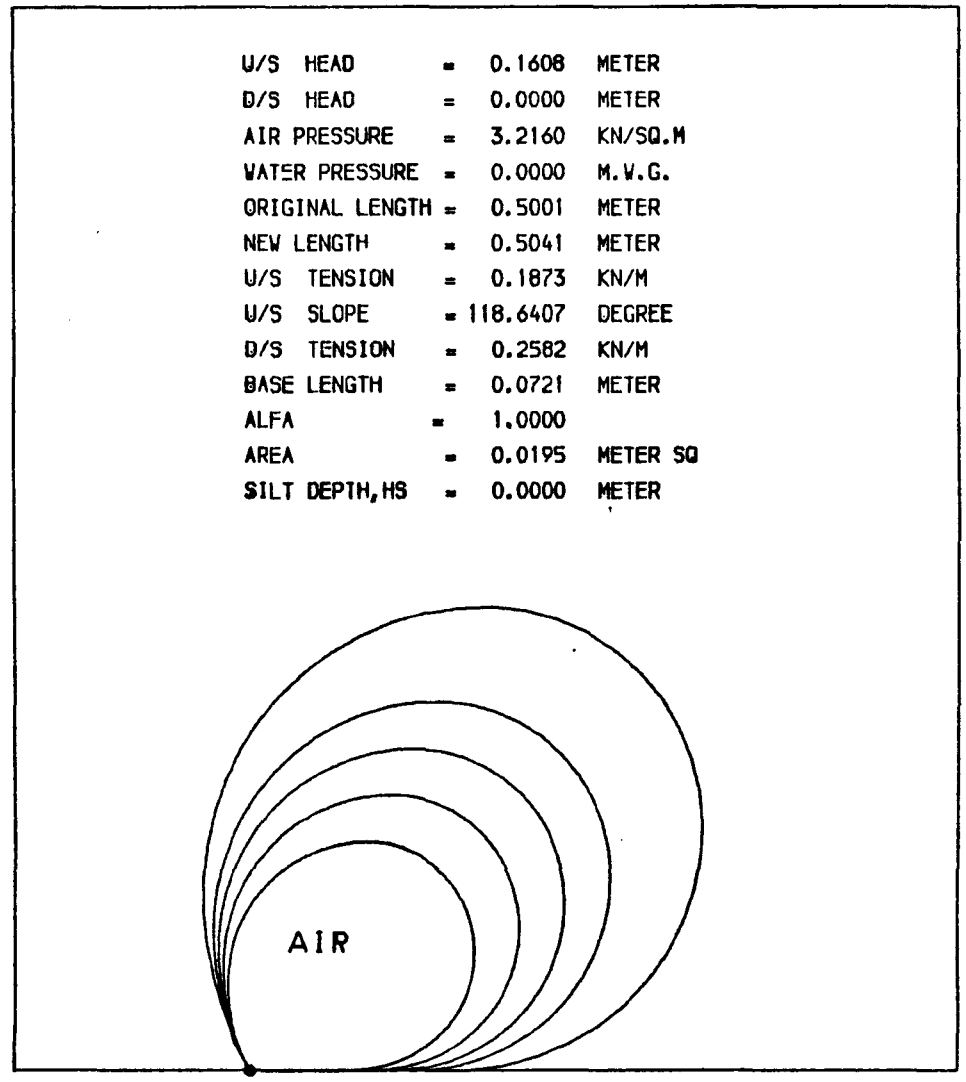

FIG. (4-37) PROFILE BEHAVIOUR OF DIFFERENT LENGTHS OF MEMBRANE FOR AN AIR INFLATED STRUCTURE FOR THE SAME PROPORTIONAL FACTOR

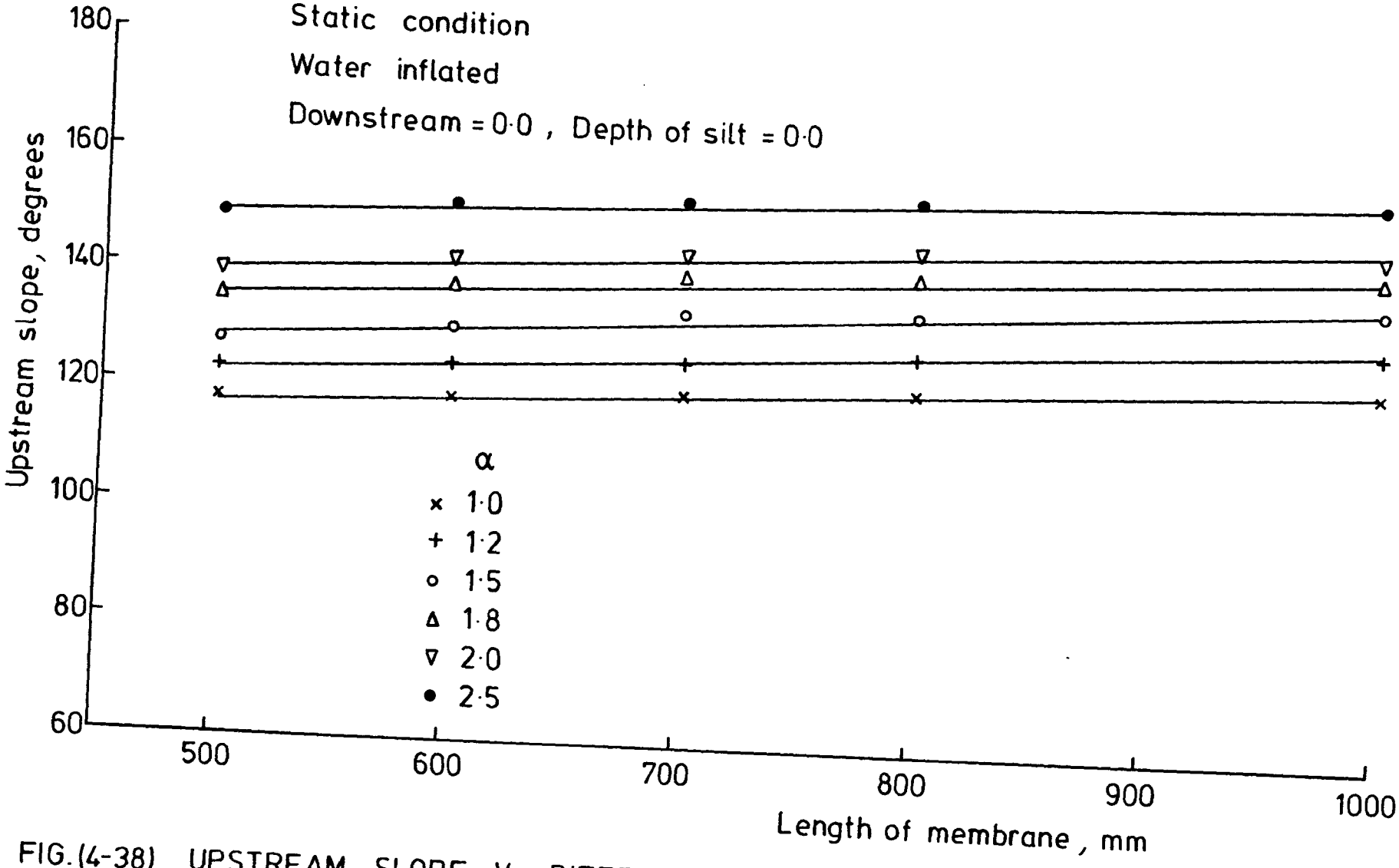

FIG.(4-38) UPSTREAM SLOPE Vs. DIFFERENT LENGTH OF MEMBRANE FOR WATER INFLATED STRUCTURE

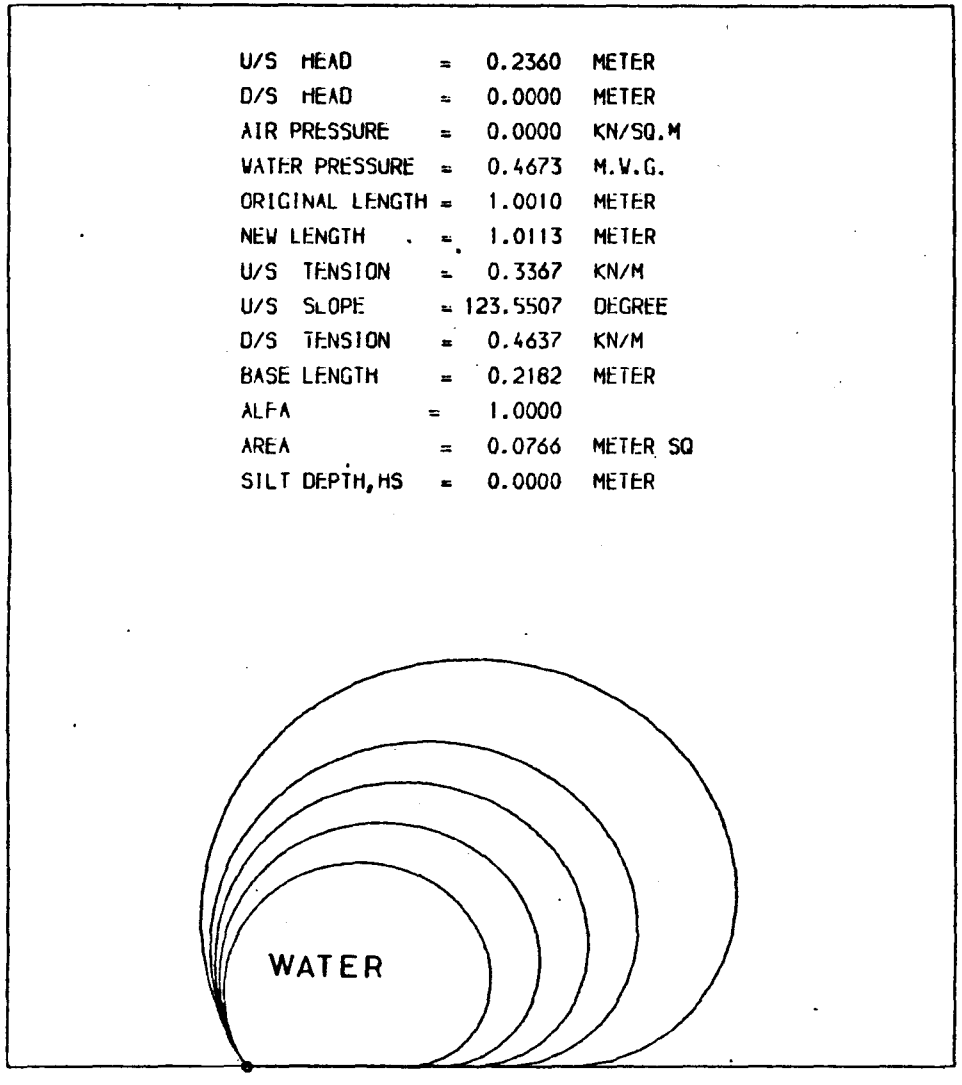

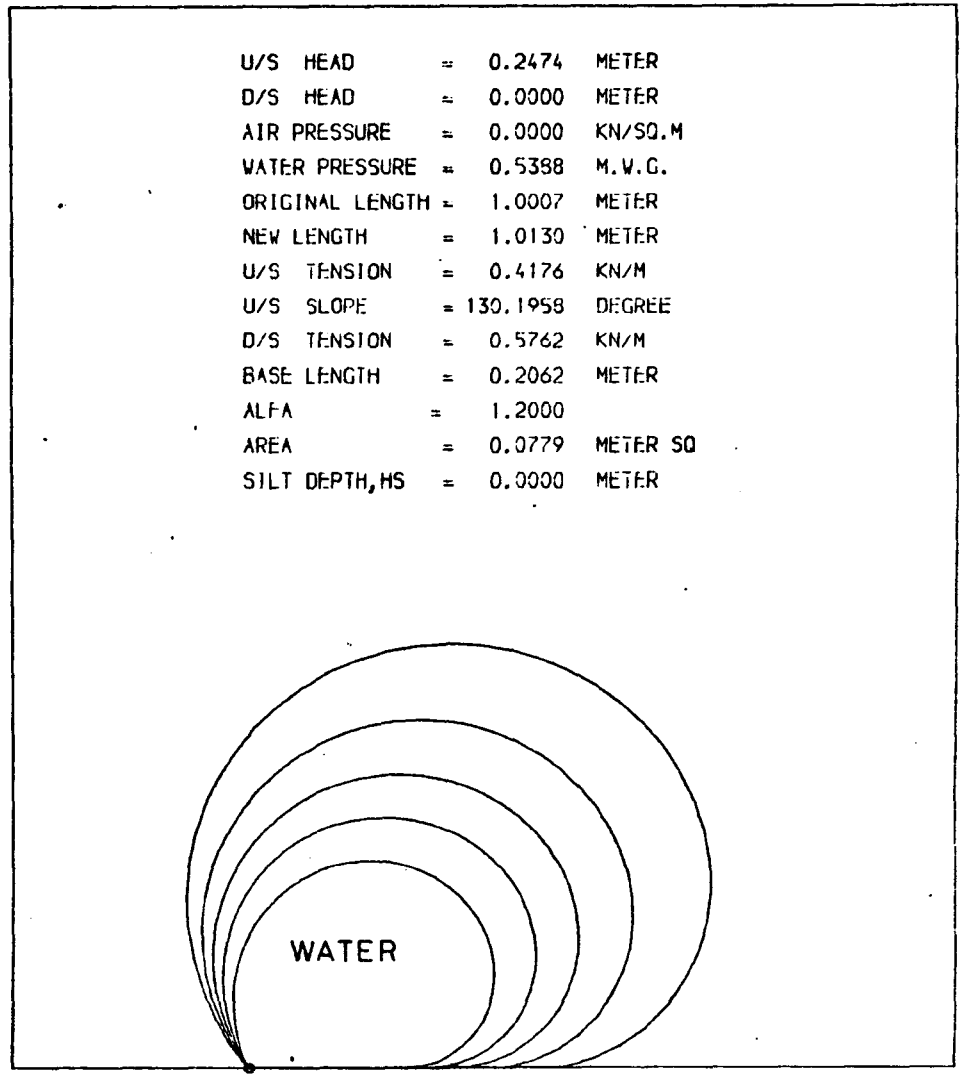

FIG.(4-39) PROFILE BEHAVIOUR OF DIFFERENT LENGTHS OF MEMBRANE FOR A WATER INFLATED STRUCTURE FOR SAME PROPORTIONAL FACTOR

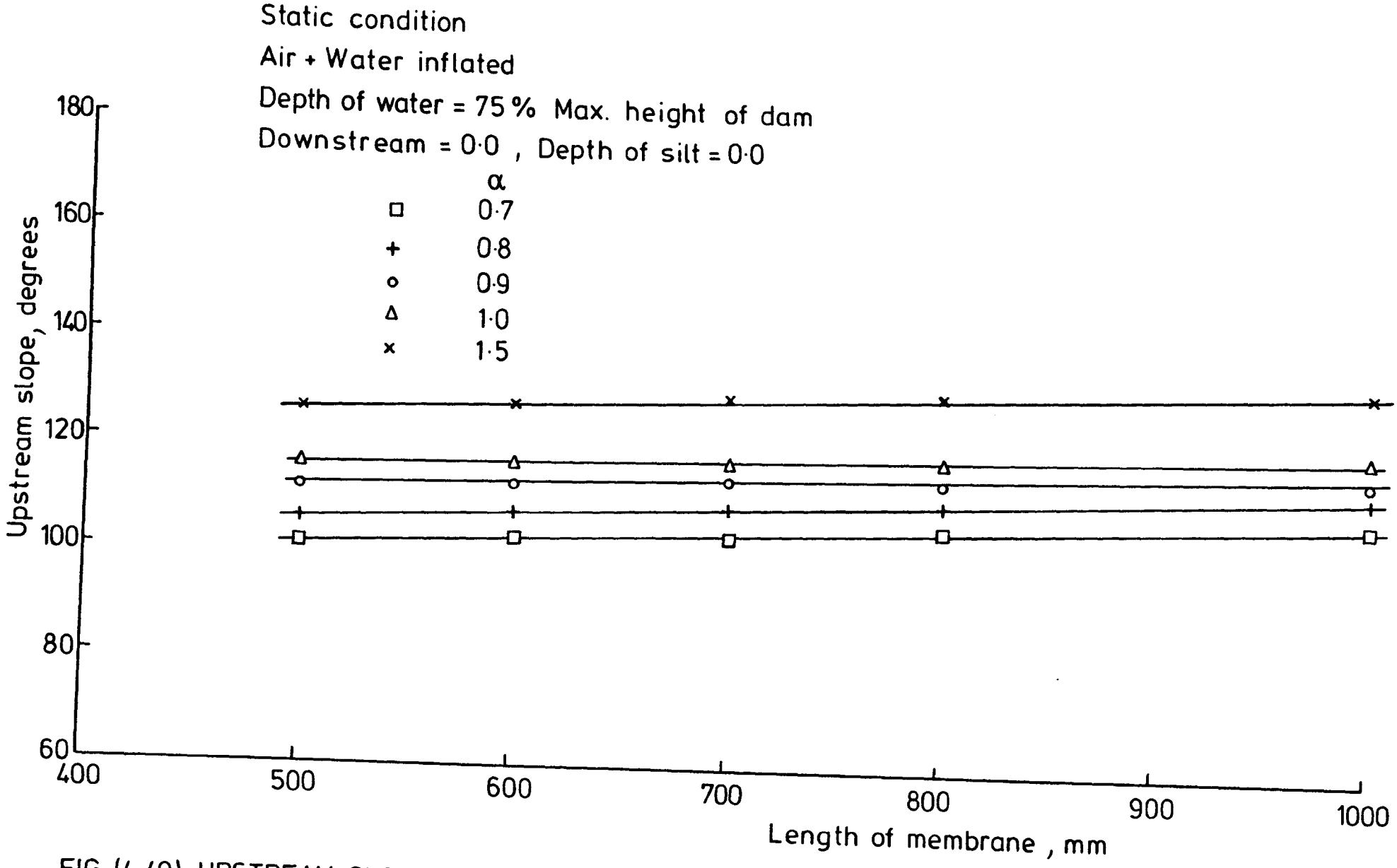

FIG. (4-40) UPSTREAM SLOPE Vs. DIFFERENT LENGTH OF MEMBRANE FOR AIR + WATER INFLATED STRUCTURE

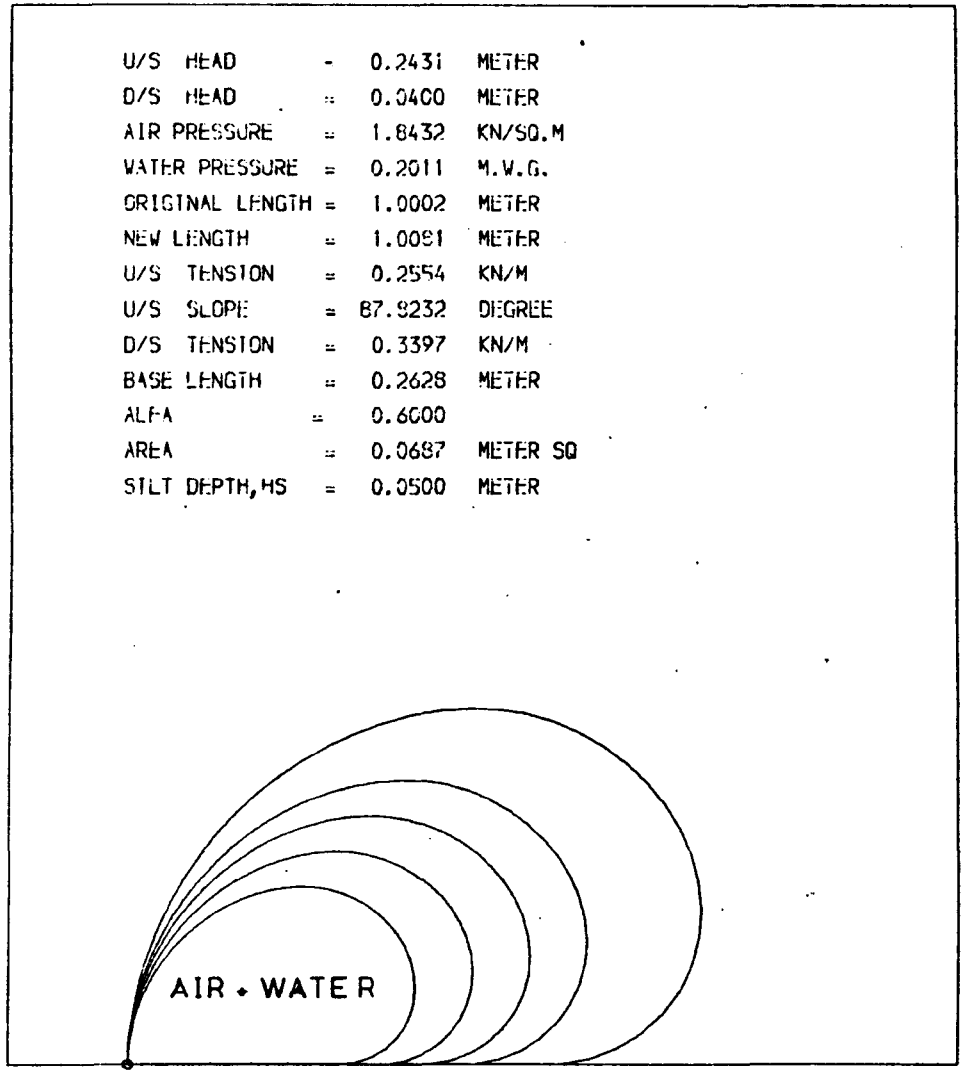

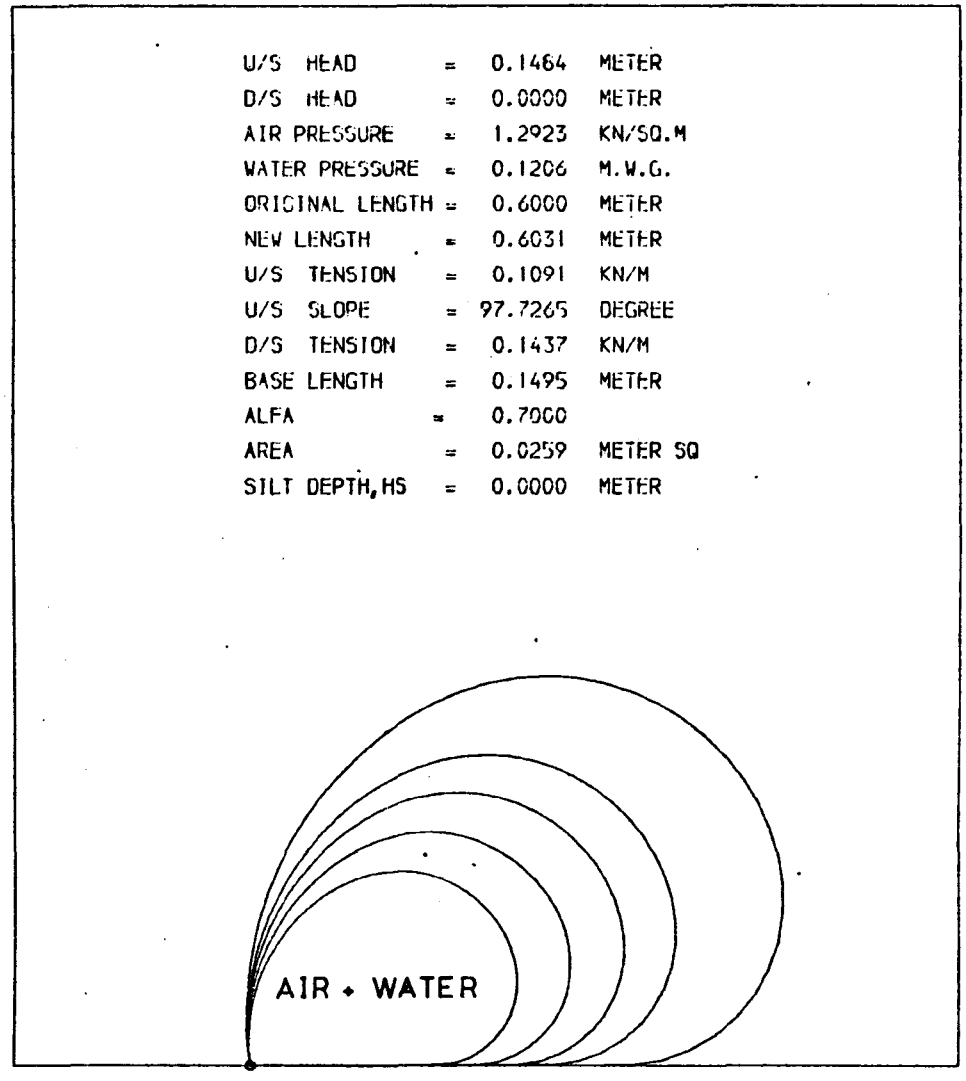

FIG.(4-41) PROFILE BEHAVIOUR OF DIFFERENT LENGTHS OF MEMBRANE FOR AN AIR + WATER INFLATED STRUCTURE FOR SAME PROPORTIONAL FACTOR

The behaviour of the upstream slope for the water inflated condition is also the same as can be seen in fig.4.38.

Similarly, the profiles for different lengths have been plotted for a proportional factors equal to 1.0,1.2 as shown in fig.4.39. Fig.4.40 shows the behaviour of the upstream slope for an (air+water) inflated structure for proportional factors of 0.7, 0.8, 0.9, 1.0 and 1.5. The profiles for different lengths have been plotted for the proportional factors equal to 0.6 and 0.7 as shown in fig. 4.41.

4.7.3 Elongation.

The elongation of the membrane for different initial lengths increases with increasing length of the membrane for all proportional factors as shown in fig.4.42 for an air inflated structure under different proportional factors and with downstream head equal to zero and with zero silt depth.

The behaviour of a water inflated structure is similar to the air inflated structure, i.e. the elongation increases with increasing the length of the membrane as shown in fig. 4.43 and also for the (air+water) inflated structure as shown in fig. 4.44.

These values of elongation are only for the Type I material and depend on the stress-strain relationship.

This means that the elongation is dependent on the properties of the material used.

4.7.4 Cross-sectional area.

The cross-sectional area of the profile for different lengths was computed for different proportional factors and the cross-sectional area can be seen to increase with increasing length of the membrane for all proportional factors as shown in fig.4.45 for the air inflated structure and proportional factors of 0.3, 0.4, 0.5, 0.8, 1.0. Similarly in fig. 4.46 and fig.4.47 the cross-

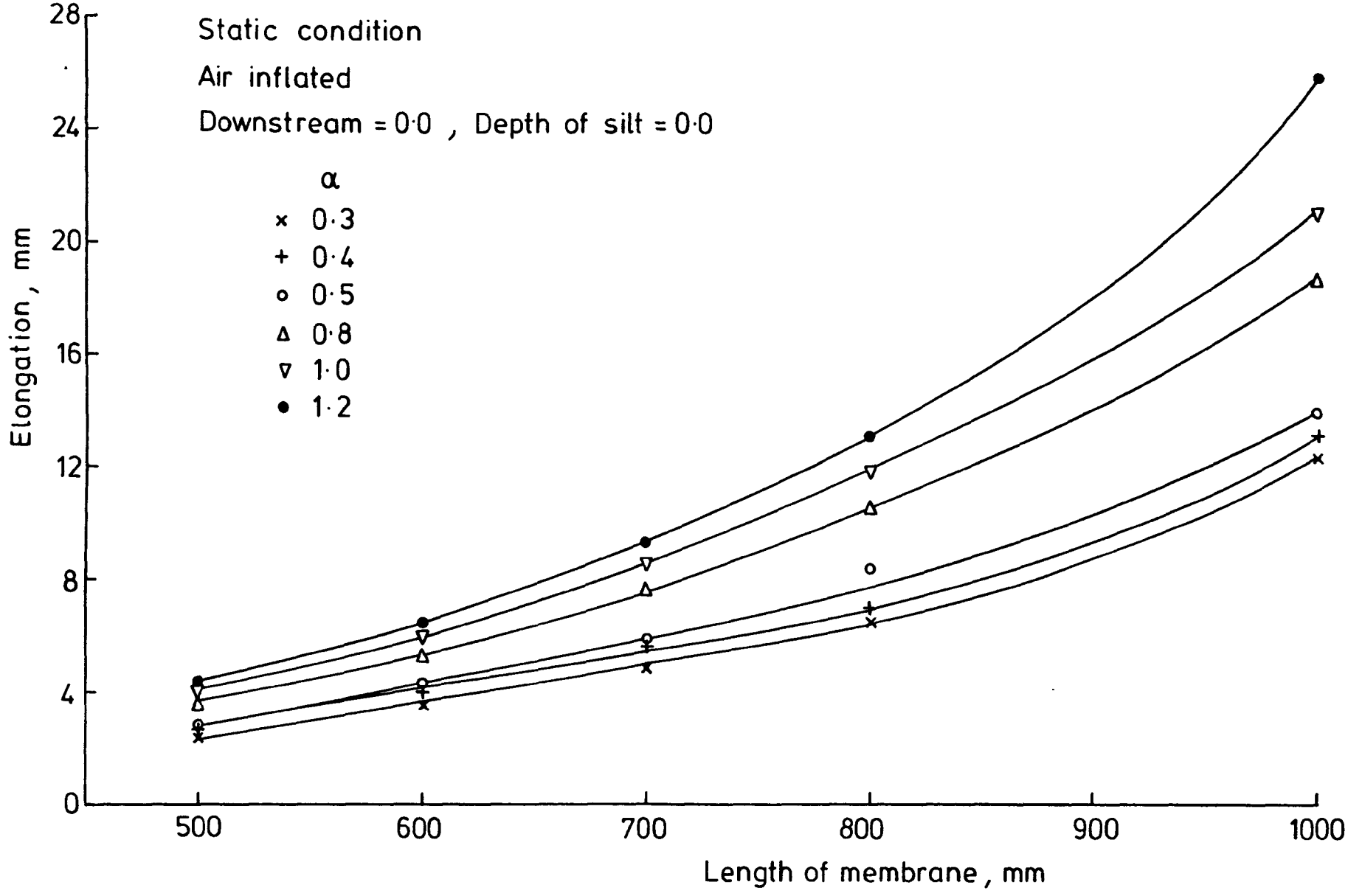

FIG. (4-42) ELONGATION Vs. DIFFERENT LENGTH OF MEMBRANE FOR AIR INFLATED STRUCTURE

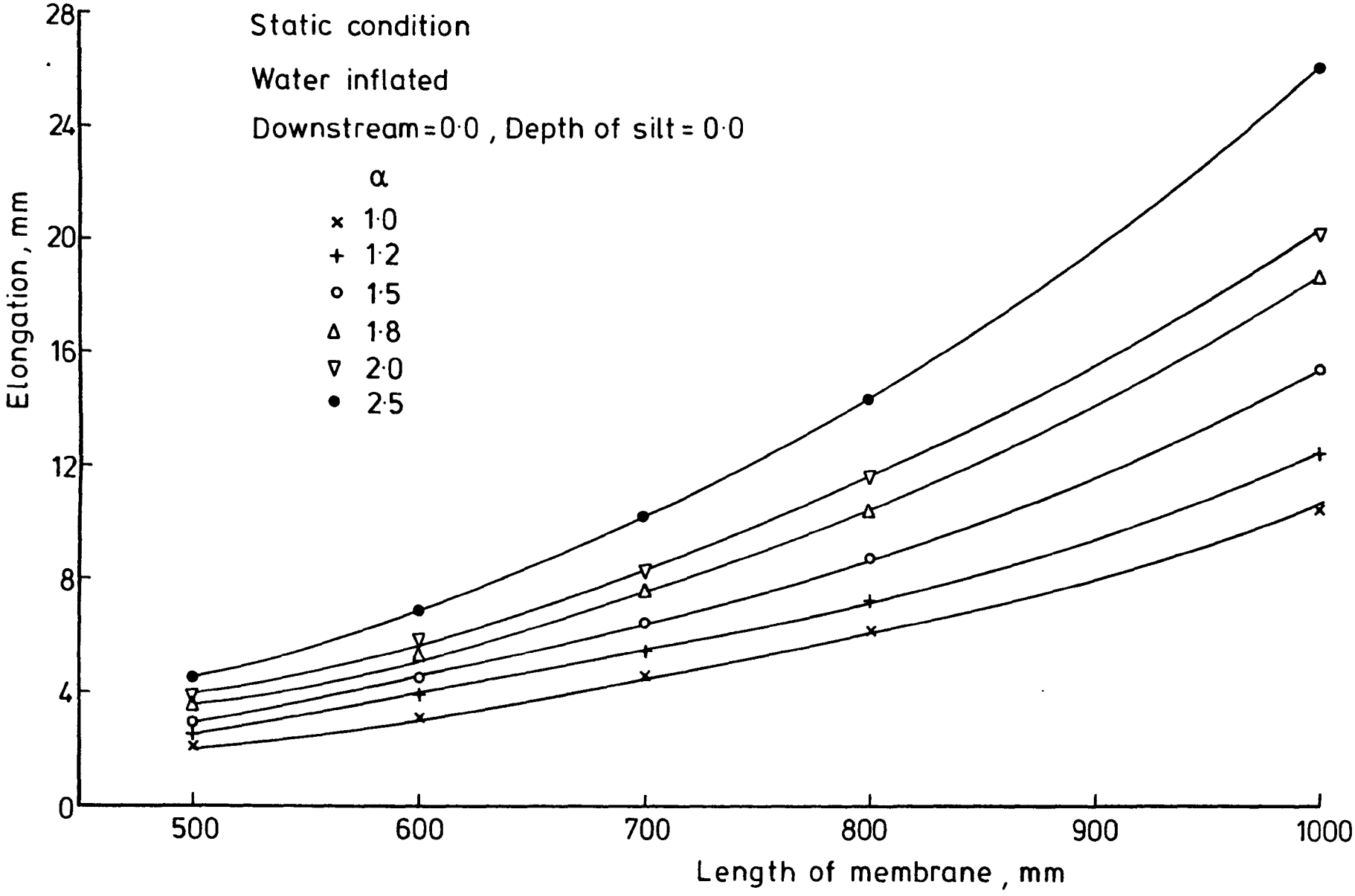

FIG. (4-43) ELONGATION Vs. DIFFERENT LENGTH OF MEMBRANE FOR WATER INFLATED STRUCTURE

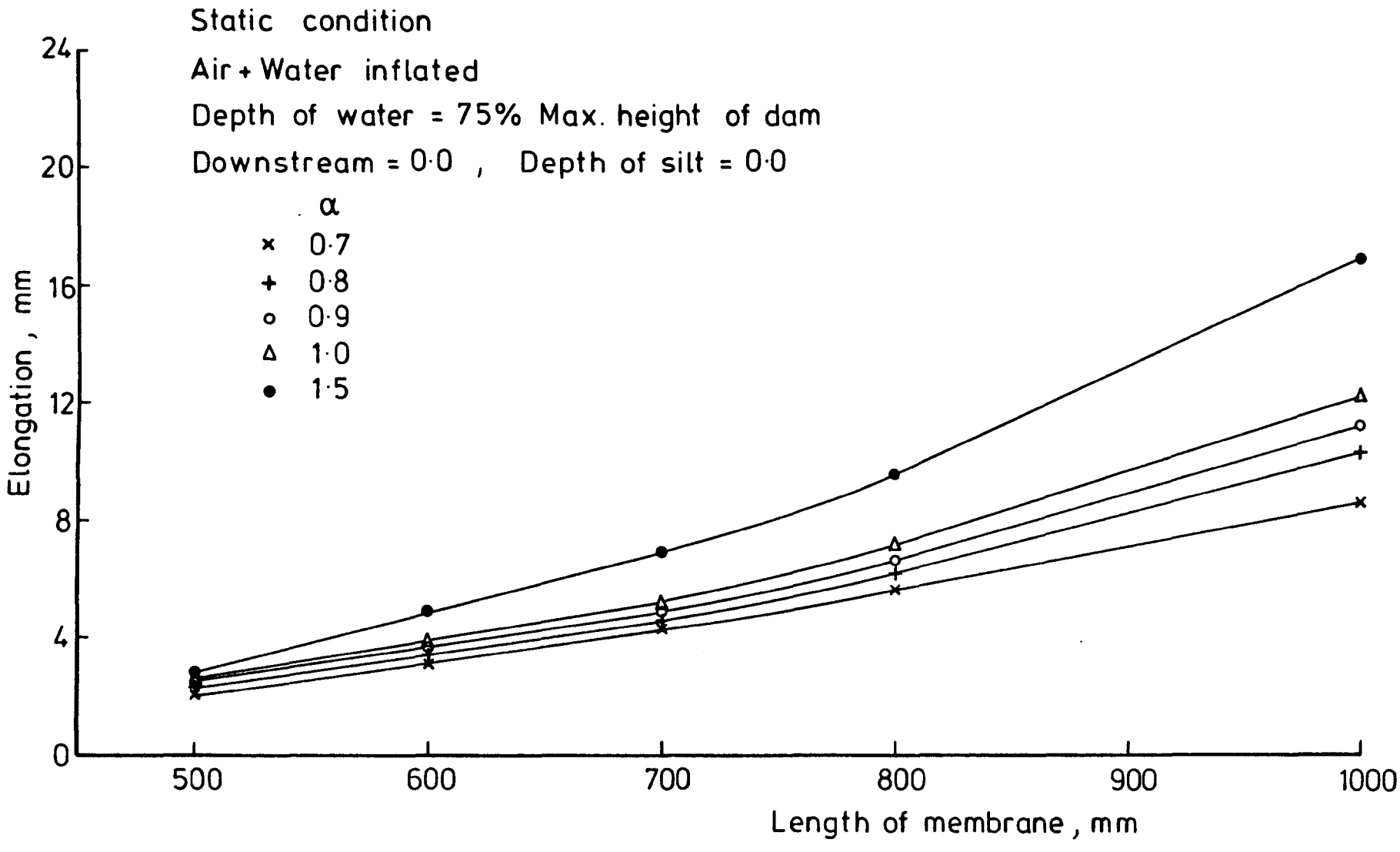

FIG. (4-44) ELONGATION Vs. DIFFERENT LENGTH OF MEMBRANE FOR AIR + WATER INFLATED STRUCTURE

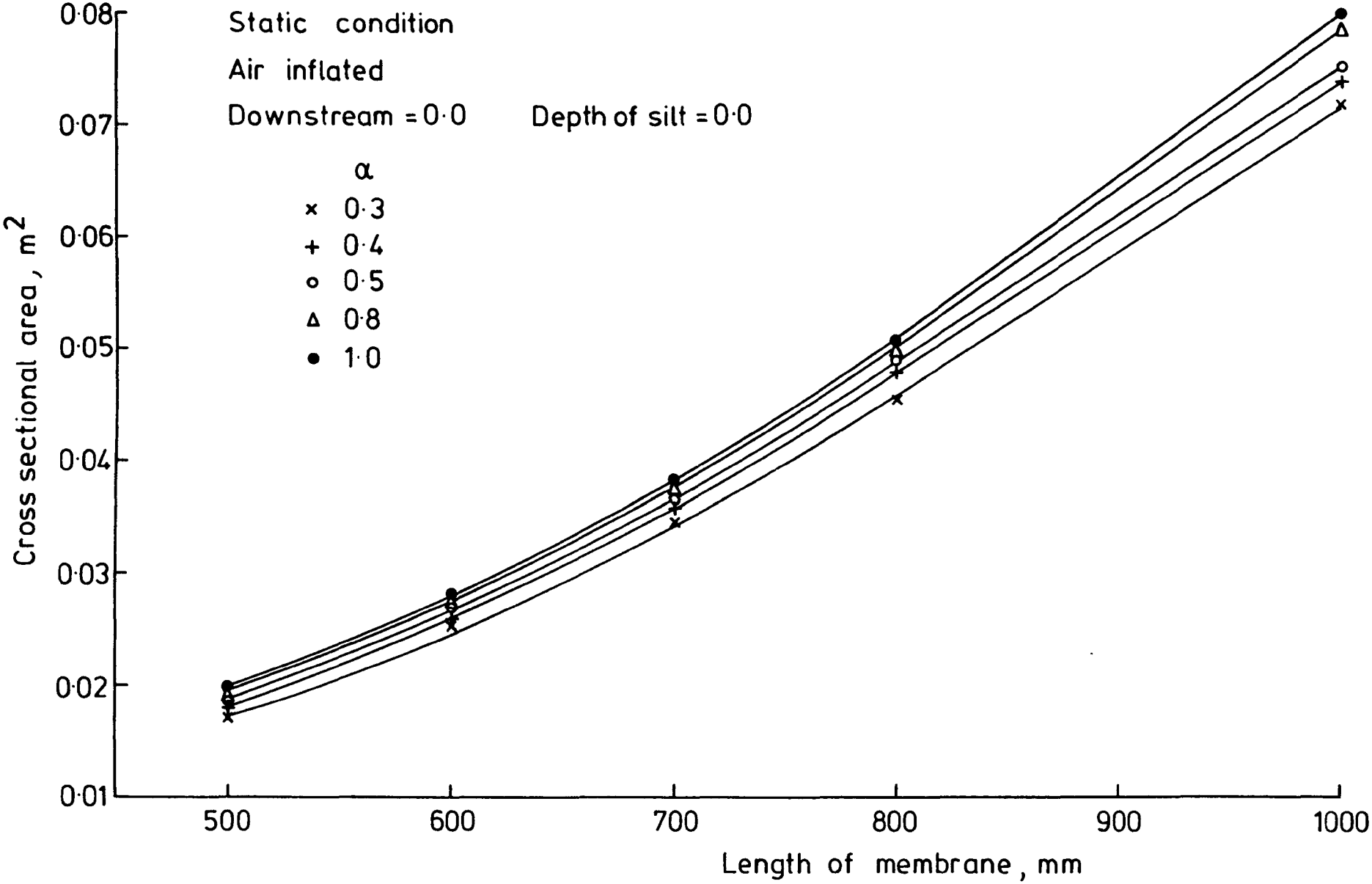

FIG. (4-45) CROSS SECTIONAL AREA Vs. DIFFERENT LENGTH OF MEMBRANE FOR AIR INFLATED STRUCTURE

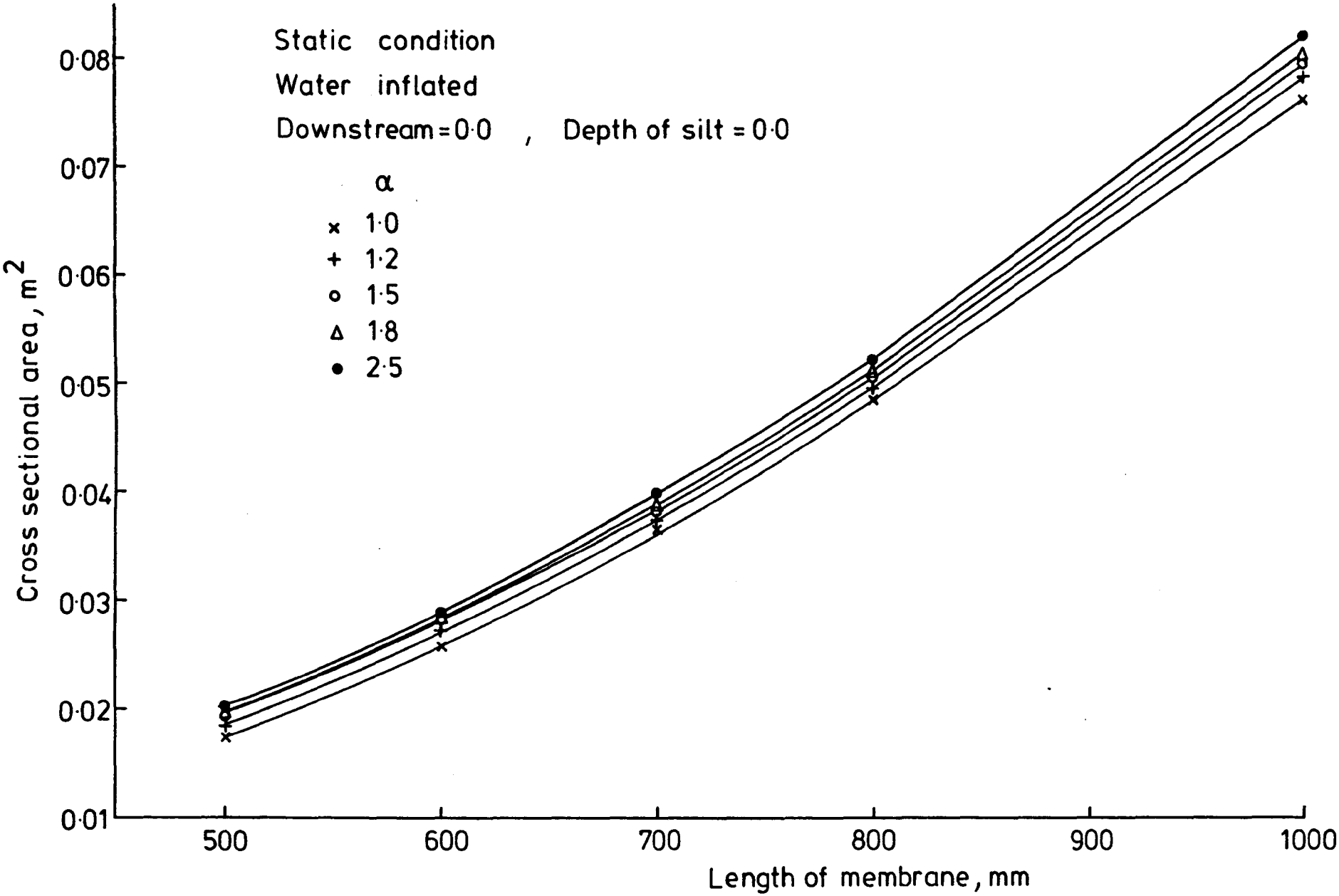

FIG. (4-46) CROSS SECTIONAL AREA Vs. DIFFERENT LENGTH OF MEMBRANE FOR WATER INFLATED STRUCTURE

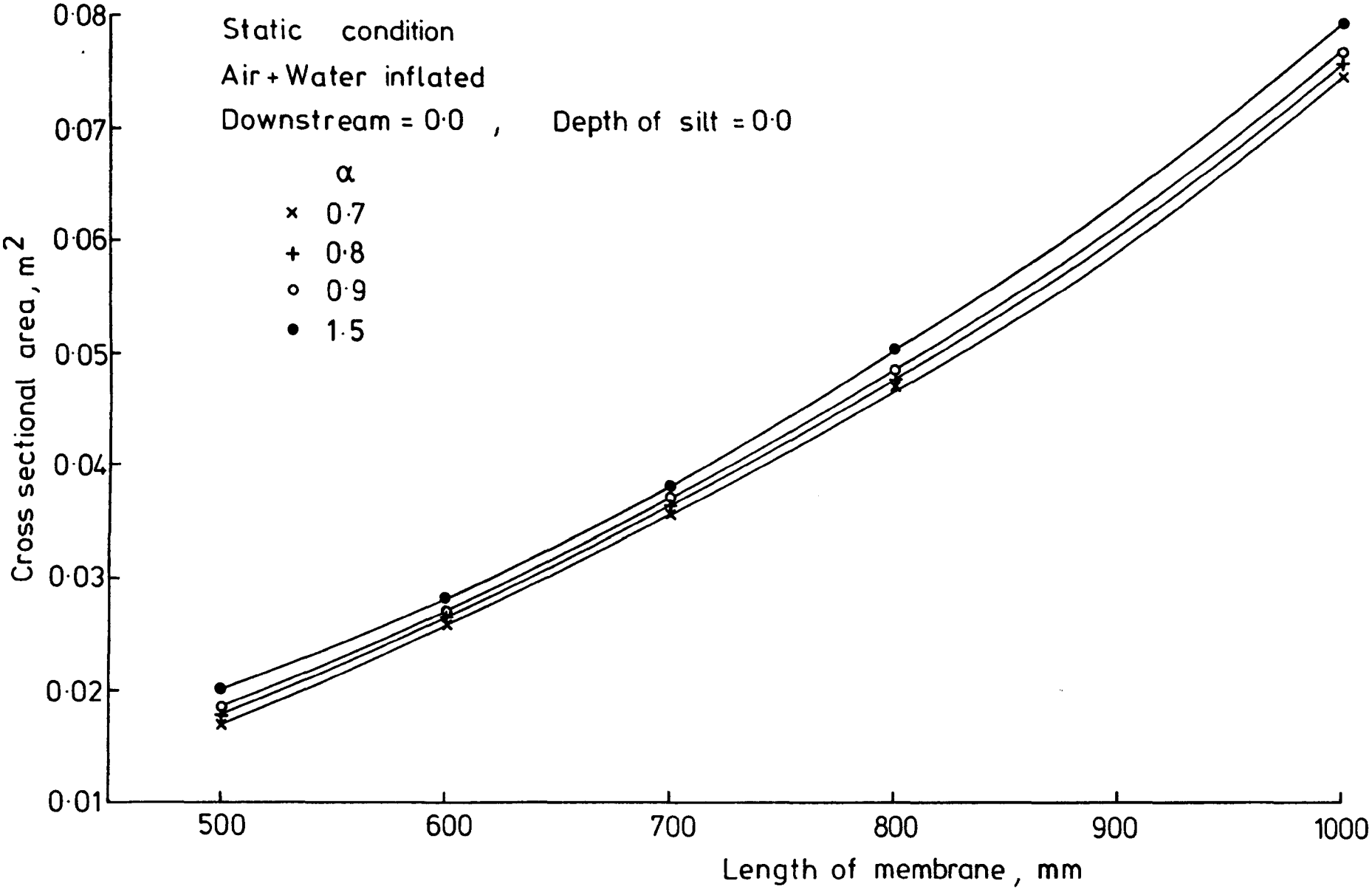

FIG.(4-47) CROSS SECTIONAL AREA Vs. DIFFERENT LENGTH OF MEMBRANE FOR AIR + WATER INFLATED STRUCTURE

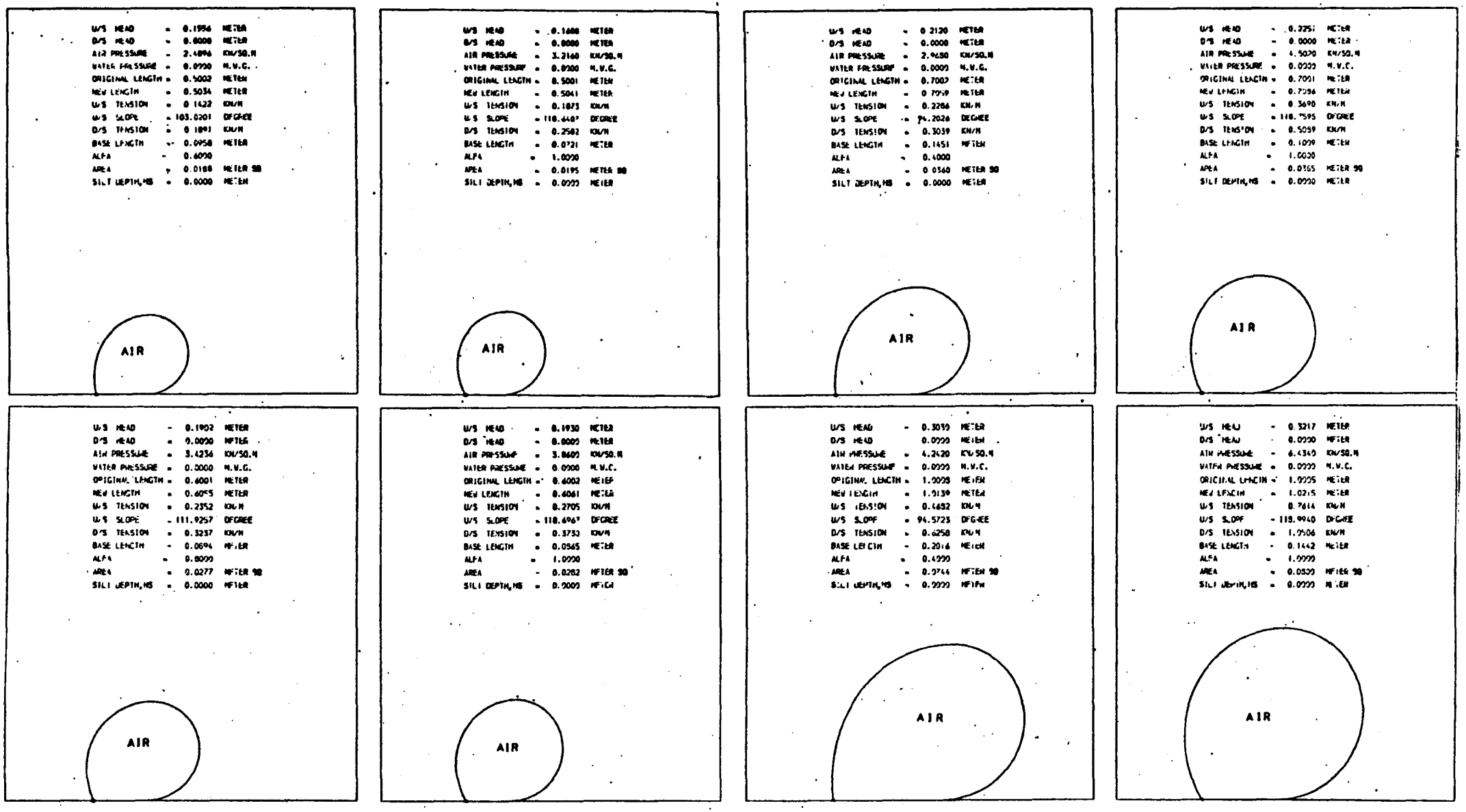

FIG.(4-48) TYPICAL PROFILE BEHAVIOUR OF AN AIR INFLATED STRUCTURE OF DIFFERENT LENGTHS OF MEMBRANE

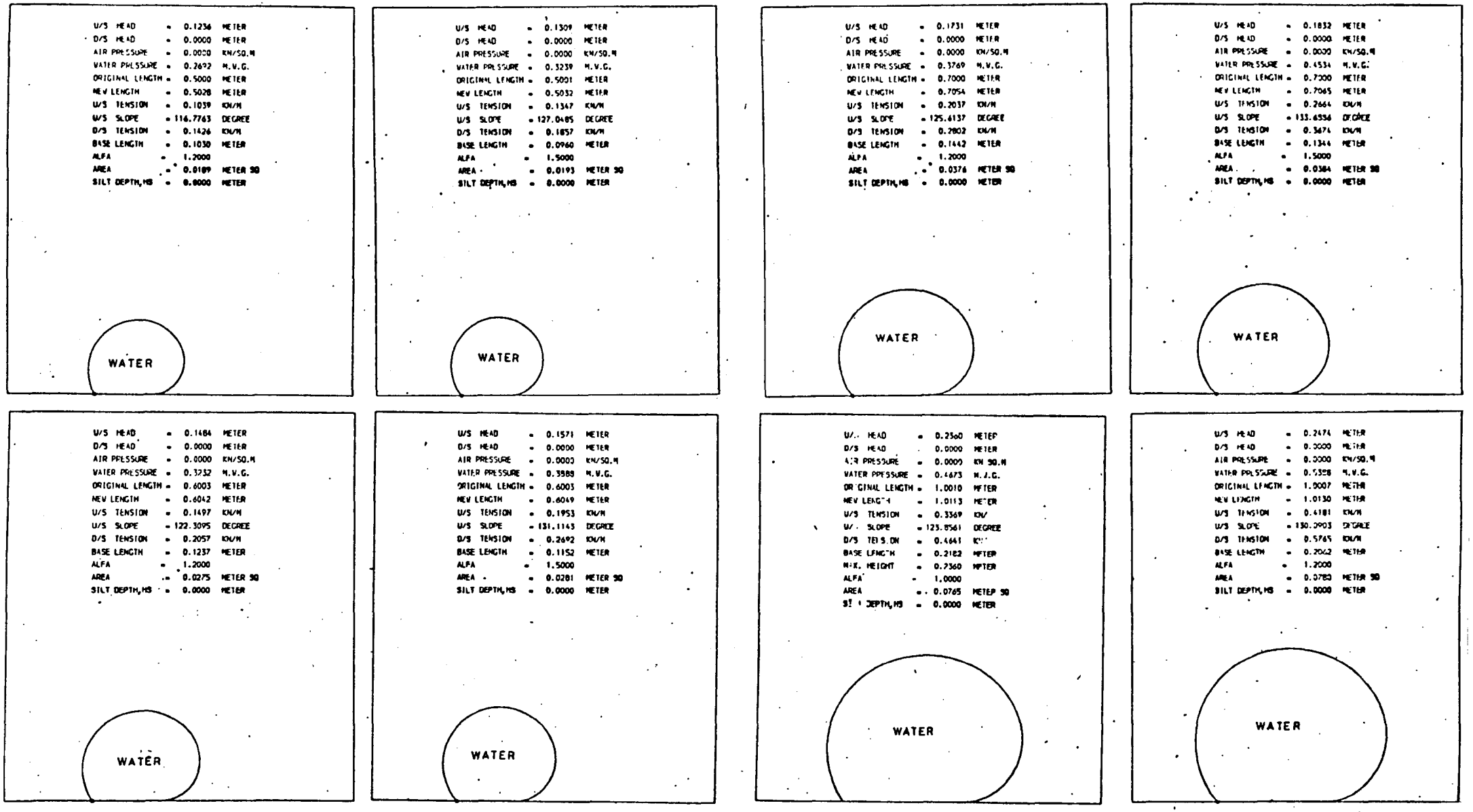

FIG.(4-49) TYPICAL PROFILE BEHAVIOUR OF WATER INFLATED STRUCTURE OF DIFFERENT LENGTHS OF MEMBRANE

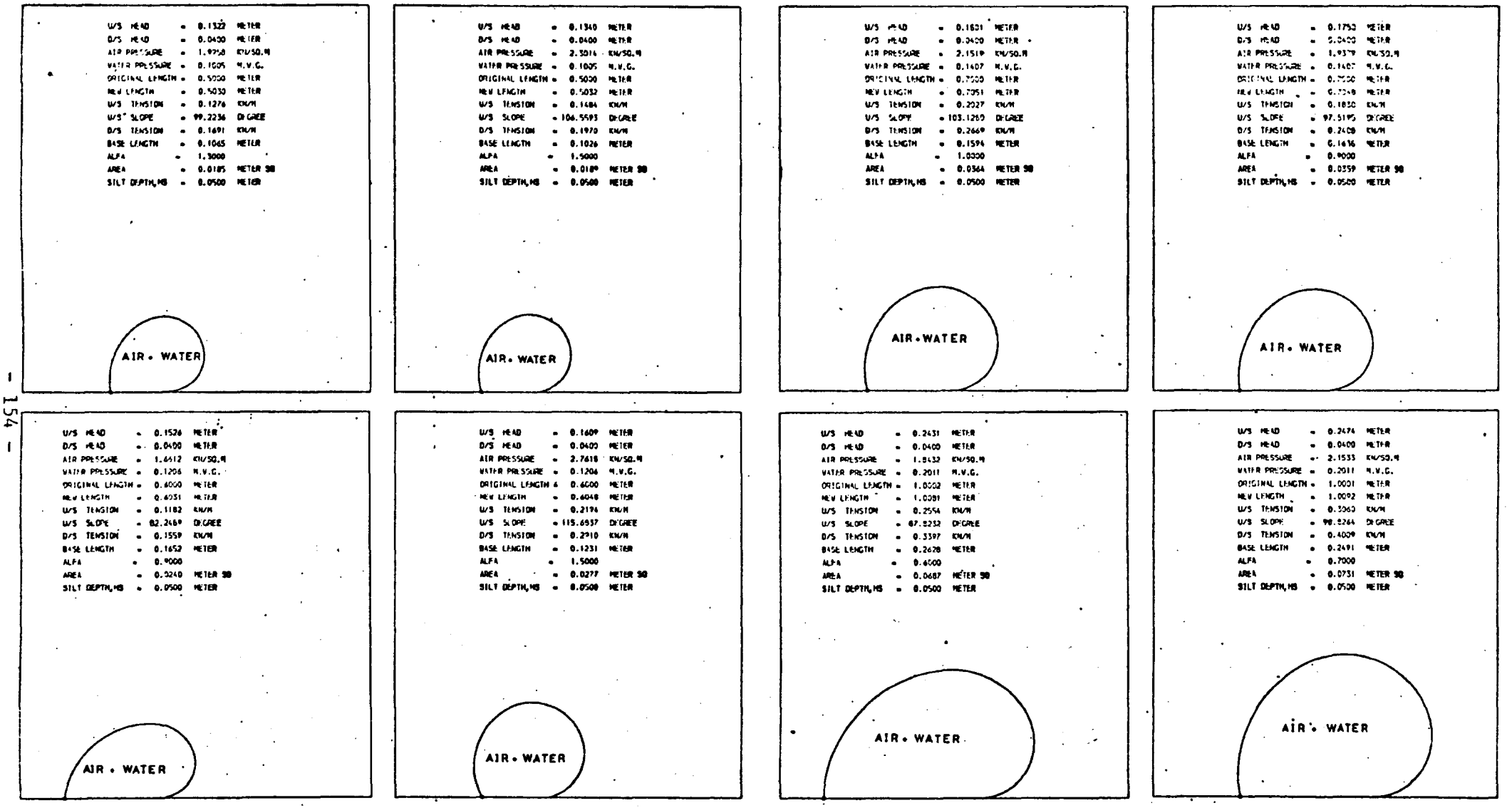

FIG. (4-50) TYPICAL PROFILE BEHAVIOUR OF AN AIR+WATER INFLATED STRUCTURE OF DIFFERENT LENGTH OF MEMBRANE

sectional area of the water inflated and (air+water) structures give variations of the same type. For all three cases the conditions are for a downstream head equal to zero and zero silt depth. The different typical profile behaviour of the dams of different lengths of membrane under different proportional factor are shown in fig.4.48, 4.49 and 4.50 for air, water and (air+water) inflation fluids respectively.

4.7.5 Maximum dam height.

The maximum height of the dam is calculated as the maximum y(J) co-ordinate of the nodes around the membrane. The maximum height for an air inflated structure is illustrated in fig. 4.51 for proportional factors equal to 0.3, 0.4, 0.5, 0.8, 1.0, 1.2. The increment in the maximum height between the proportional factor equal to 0.3 and 0.4 is greater than the increment of the maximum height for proportional factors equal to 1.0 and for all variations of length of the membrane i.e. from length of membrane equal to 0.50 m to 1.0 m.

Similar patterns of variation of the maximum height with respect to different lengths of membrane for a water inflated structure are illustrated in fig.4.52. The variation of the maximum height is calculated for proportional factors equal to (1.0, 1.2, 1.5, 1.8,2.0, 2.5) and, the results show that the increment in the maximum height for the proportional factor equal 1.0 to 1.2 is more than the increment in the maximum height when the proportional factor increases from 2.0 to 2.5.

Variations of the maximum height of the (air+water) inflated structure are of a similar form to the previous cases as represented in fig.4.53. The greater the depth of water inside the dam, the less will be the maximum height of the dam. The depth of water taken was equal to 75% of the maximum dam height. The maximum height is calculated for the proportional factors 0.7, 0.8, 0.9, 1.0 and 1.5.

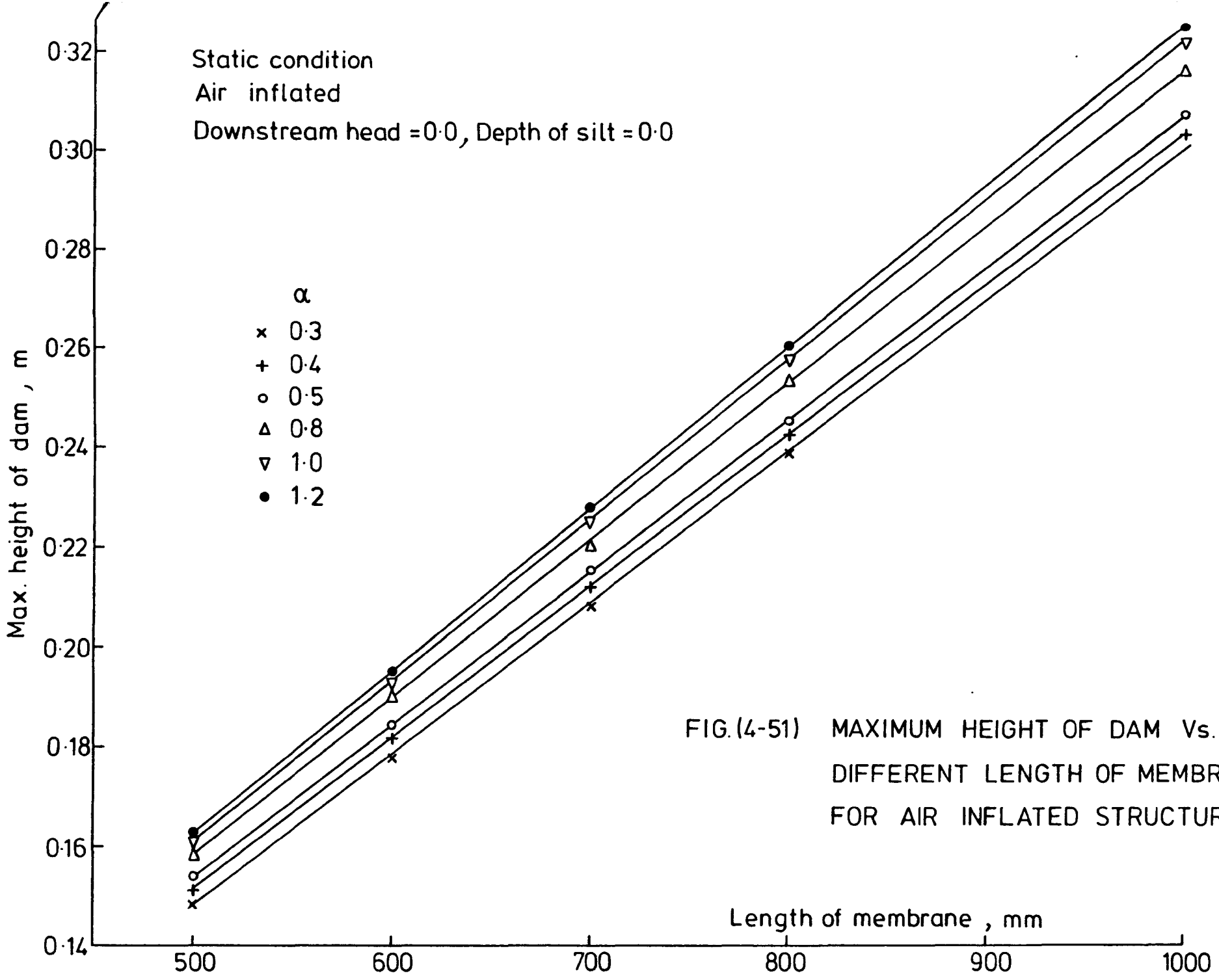

FIG. (4-51) MAXIMUM HEIGHT OF DAM Vs. DIFFERENT LENGTH OF MEMBRANE FOR AIR INFLATED STRUCTURE

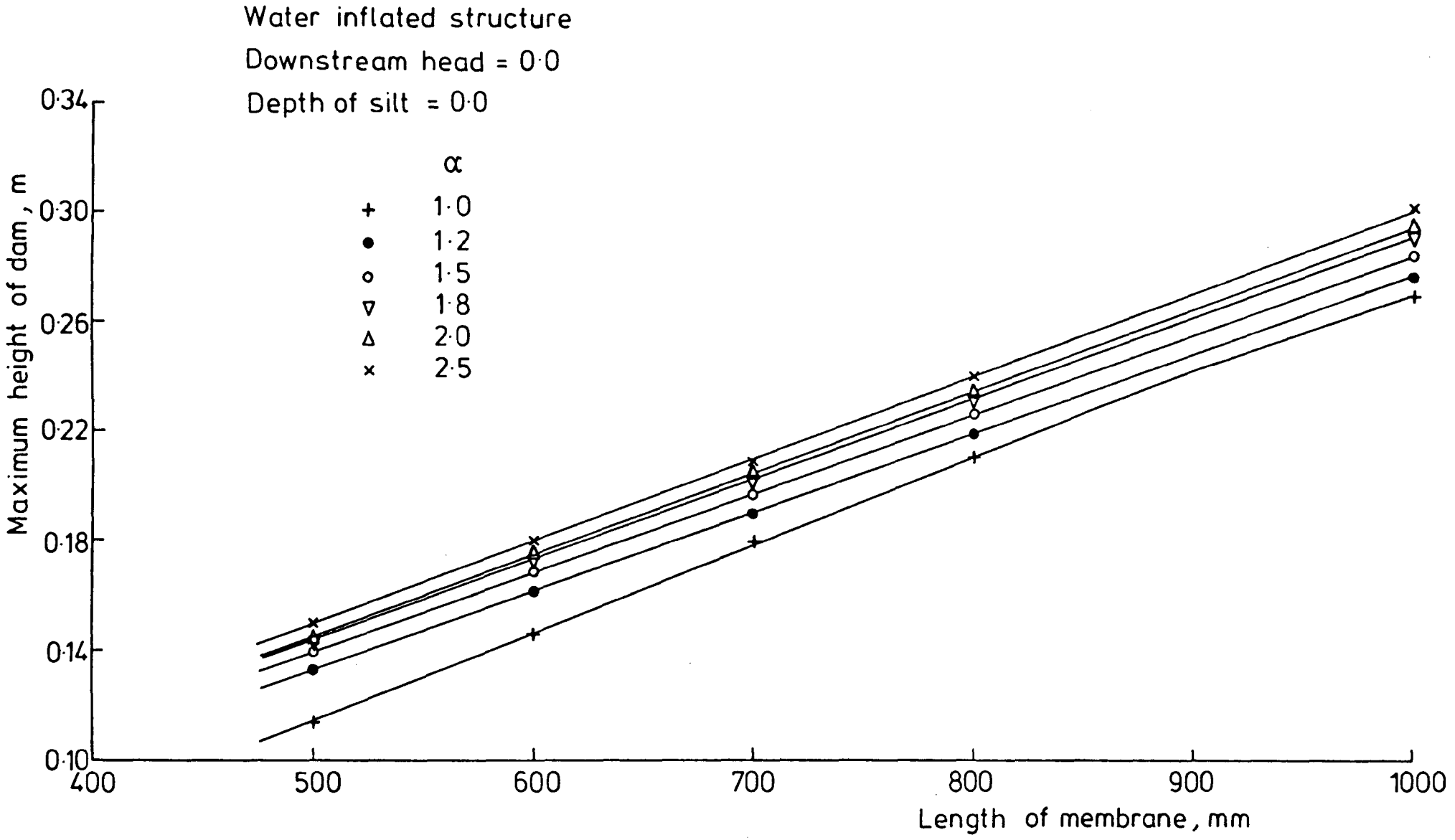

FIG. (4-52) MAXIMUM HEIGHT OF DAM Vs. DIFFERENT LENGTH OF MEMBRANE FOR WATER INFLATED STRUCTURE

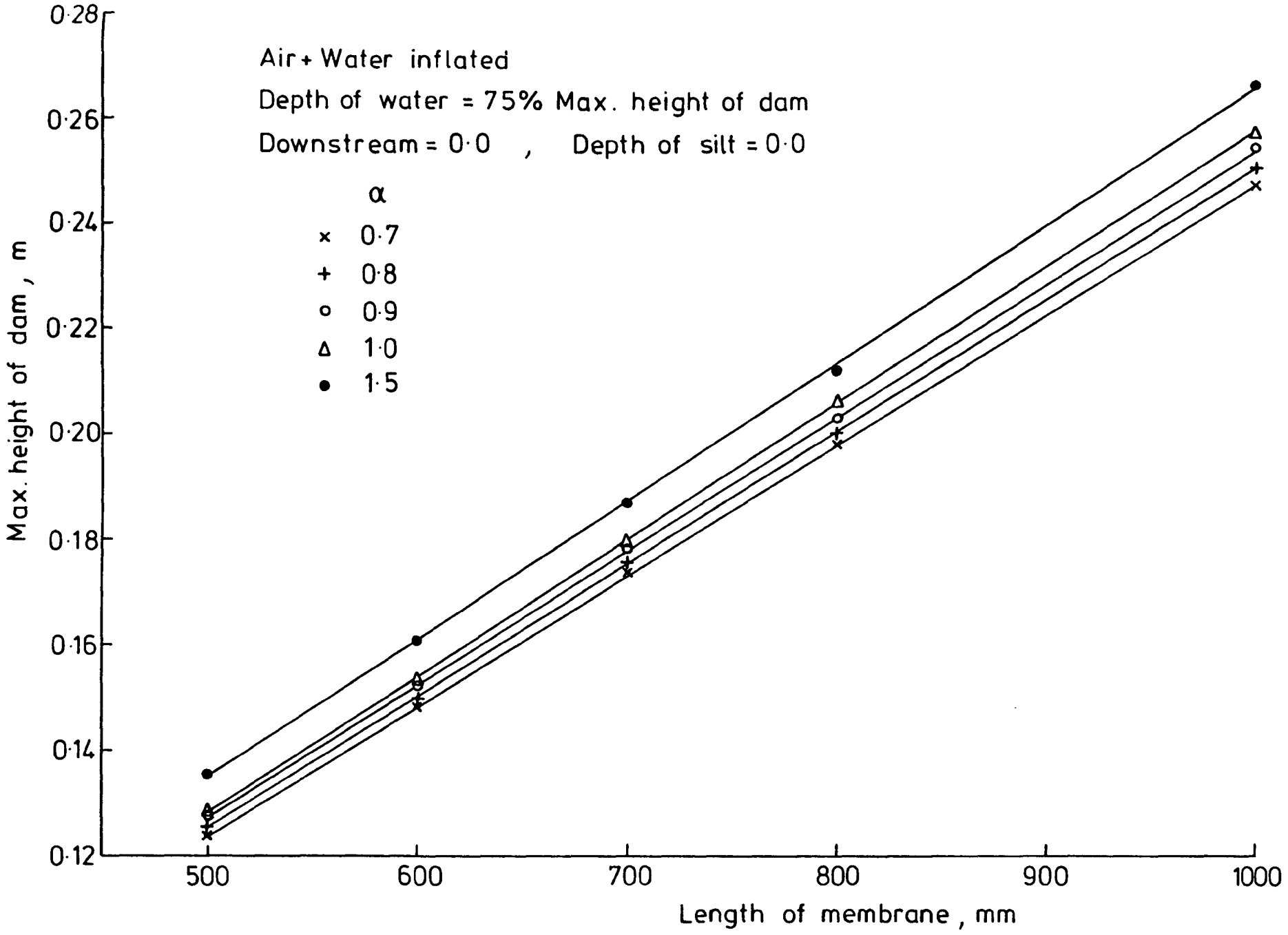

FIG.(4-53) MAXIMUM HEIGHT OF DAM Vs. DIFFERENT LENGTH OF MEMBRANE FOR AIR + WATER INFLATED STRUCTURE

4.8 Effect of weight and thickness of the membrane on the output parameters.

4.8.1 General.

The variation of the weight and thickness of the membrane have been considered to see the effect on the output parameters (i.e., tension, upstream slope, maximum height, elongation, area, and the profile of the dam.

Different thicknesses and weights have been assumed for the same stress strain relationship for Type I material and the analysis was carried out for an air inflated structure for proportional factors equal to 0.75 and 0.5 and under the conditions of downstream head equal to zero and zero silt depth and also under downstream head equal to 0.1 m and 0.05 m silt depth.

A similar analysis was carried out for the water inflated structure for the proportional factor equal to 1.0 and 1.2 under same condition of downstream head and silt depth.

4.8.2 Effect of weight of membrane.

Different weights of membrane have been taken to establish the effect on the output parameters (Sec.4.8.1) for air inflated and water inflated structures. Weights of membrane of 0.15 Kg/m^2 to 0.50 Kg/m^2, were considered and it was found out that tension decreased from 0.4063 KN/m to 0.4054 KN/m i.e. the difference in tension equal to 0.009 KN/m for a different in weight equal to 0.35 Kg/m^2.

Downstream tension, upstream slope, maximum height, elongation and area all decrease with increasing the weight of the membrane. These decreases however are very small for both air or water inflated structures.

Table 4.4 shows the effects of the weights of the membrane on the output parameters for air inflated structure for the proportional factors equal to 0.75 and 0.5.

The variation of all output parameters with changing weights of the membrane is similar to air inflated for water inflated structures and these

variations are represented in table 4.5. Profiles for different weights of membrane do not show any visible differences and are illustrated in fig. 4.54 for both air and water inflated structures.

4.8.3 Effect of thickness of membrane.

Different thicknesses have been assumed ranging from 0.04 mm to 0.5 mm to find the effect on the output parameters. Although the thickness was changed the other properties of type I material were assumed constant.

The variation of the thickness was carried out for the air inflated and water inflated structures under different downstream head and silt depths.

The effect of changing thickness is more significant than changing the weight of the membrane and the variation is particularly high in the elongation of the membrane reflected in the maximum height of the dam for both air inflated and water inflated structures.

Table 4.6 illustrates the variation of the output parameters as the thicknesses of the membrane change for an air inflated structure for proportional factors equal to 0.75 and 0.5 and Table 4.7 illustrates the variation of the output parameter as the thicknesses change for water inflated structures for the proportional factors equal to 1.0 and 1.2.

The profiles of the dam of different thickness are shown in fig.4.55 for the air inflated structure and water inflated structure.

U/S HEAD	=	0.2460	METER
D/S HEAD	=	0.1000	METER
AIR PRESSURE	=	3.6900	KN/SQ.M
WATER PRESSURE	=	0.0000	M.W.G.
ORIGINAL LENGTH	=	0.8005	METER
NEW LENGTH	=	0.8088	METER
U/S TENSION	=	0.3095	KN/M
U/S SLOPE	=	94.3066	DEGREE
D/S TENSION	=	0.4189	KN/M
BASE LENGTH	=	0.1306	METER
ALFA	=	0.5000	
AREA	=	0.0473	METER SQ
SILT DEPTH,HS	=	0.0500	METER

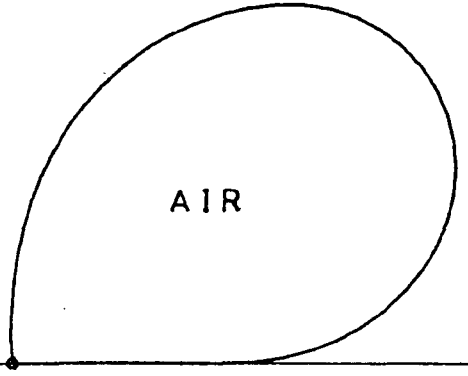

U/S HEAD	=	0.1986	METER
D/S HEAD	=	0.0000	METER
AIR PRESSURE	=	0.0000	KN/SQ.M
WATER PRESSURE	=	0.3735	M.W.G.
ORIGINAL LENGTH	=	0.8000	METER
NEW LENGTH	=	0.8062	METER
U/S TENSION	=	0.2155	KN/M
U/S SLOPE	=	120.5126	DEGREE
D/S TENSION	=	0.2961	KN/M
BASE LENGTH	=	0.1744	METER
MAX. HEIGHT	=	0.1856	METER
ALFA	=	1.0000	
AREA	=	0.0484	METER SQ
SILT DEPTH,HS	=	0.0000	METER

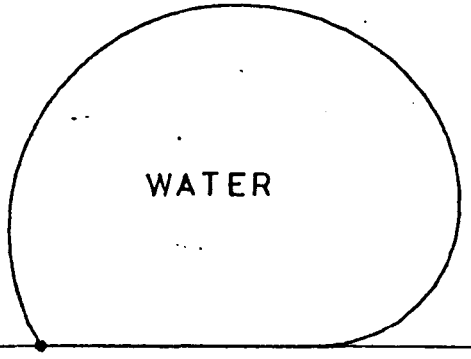

FIG.(4-54) PROFILES FOR DIFFERENT WEIGHTS OF MEMBRANE FOR AN AIR INFLATED AND A WATER INFLATED STRUCTURE

U/S HEAD	=	0.2460	METER
D/S HEAD	=	0.1000	METER
AIR PRESSURE	=	3.6900	KN/SQ.M
WATER PRESSURE	=	0.0000	M.W.G.
ORIGINAL LENGTH	=	0.8005	METER
NEW LENGTH	=	0.8165	METER
U/S TENSION	=	0.3124	KN/M
U/S SLOPE	=	94.7457	DEGREE
D/S TENSION	=	0.4237	KN/M
BASE LENGTH	=	0.1301	METER
ALFA	=	0.5000	
AREA	=	0.0483	METER SQ
SILT DEPTH,HS	=	0.0500	METER

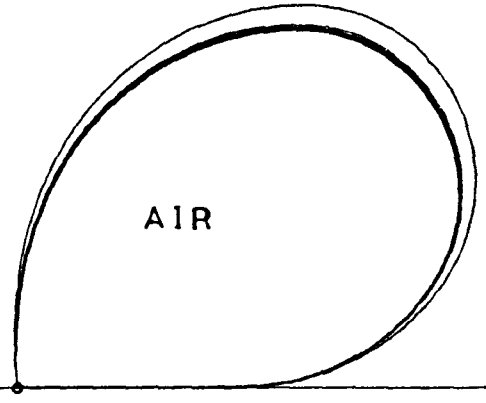

U/S HEAD	=	0.1978	METER
D/S HEAD	=	0.0400	METER
AIR PRESSURE	=	0.0000	KN/SQ.M
WATER PRESSURE	=	0.4308	M.W.G.
ORIGINAL LENGTH	=	0.8000	METER
NEW LENGTH	=	0.8092	METER
U/S TENSION	=	0.2653	KN/M
U/S SLOPE	=	116.1355	DEGREE
D/S TENSION	=	0.3635	KN/M
BASE LENGTH	=	0.1648	METER
ALFA	=	1.2000	
AREA	=	0.0488	METER SQ
SILT DEPTH,HS	=	0.0500	METER

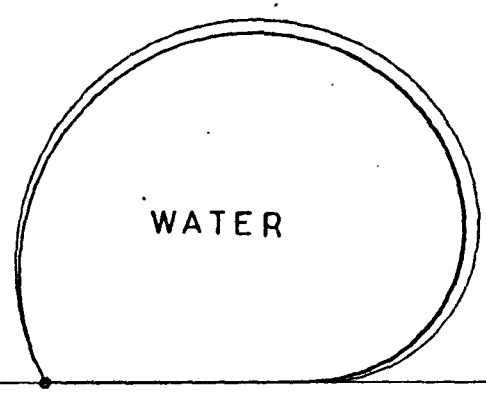

FIG.(4-55) PROFILES FOR DIFFERENT THICKNESS OF MEMBRANE FOR AN AIR INFLATED AND A WATER INFLATED STRUCTURE

Air Inflated - Table 4.4

Effect of weight of membrane on the other parameters.

No.	Weight Kg/m^2	Propl. factor α	U/S Head m	D/S Head (m)	H_s depth of silt (m)	U/S Tension KN/m	D/S Tension KN/m	Press. KN/m^2	Max. Height m	Area m^2	U/S slope degree	Elongation mm
1	0.15	0.75	0.2526	0.0	0.0	0.4063	0.5582	4.4205	0.2536	0.04957	110.46	10.24
2	0.20	0.75	0.2526	0.0	0.0	0.4062	0.5581	4.4205	0.2535	0.04957	110.45	10.24
3	0.25	0.75	0.2526	0.0	0.0	0.4061	0.5579	4.4205	0.2534	0.04957	110.44	10.24
4	0.30	0.75	0.2526	0.0	0.0	0.4059	0.5578	4.4205	0.2533	0.04956	110.44	10.24
5	*0.35	0.75	0.2526	0.0	0.0	0.4058	0.5577	4.4205	0.2532	0.04956	110.43	10.24
6	*0.391	0.75	0.2526	0.0	0.0	0.4057	0.5576	4.4205	0.2532	0.04956	110.42	10.24
7	0.40	0.75	0.2526	0.0	0.0	0.4057	0.5576	4.4205	0.2532	0.04956	110.42	10.24
8	0.45	0.75	0.2526	0.0	0.0	0.4036	0.5575	4.4205	0.2532	0.04956	110.41	10.23
9	0.50	0.75	0.2526	0.0	0.0	0.4054	0.25573	4.4205	0.2532	0.04955	110.40	10.23
1	0.15	0.50	0.246	0.10	0.05	0.3095	0.4189	3.690	0.24653	0.04730	94.31	8.29
2	0.20	0.50	0.246	0.10	0.05	0.3095	0.4188	3.690	0.24652	0.04730	94.29	8.28
3	0.25	0.50	0.246	0.10	0.05	0.3093	0.4187	3.690	0.24651	0.04730	94.28	8.28
4	0.30	0.50	0.246	0.10	0.05	0.3092	0.4185	3.690	0.24648	0.04729	94.26	8.28
5	*0.35	0.50	0.246	0.10	0.05	0.3091	0.4184	3.690	0.24645	0.04729	94.25	8.27
6	*0.391	0.50	0.246	0.10	0.05	0.3090	0.4183	3.690	0.24663	0.04729	94.23	8.27
7	0.40	0.50	0.246	0.10	0.05	0.3090	0.4183	3.690	0.21642	0.04729	94.23	8.27
8	0.45	0.50	0.246	0.10	0.05	0.3089	0.4181	3.690	0.24638	0.04728	94.22	8.27
9	0.50	0.50	0.246	0.10	0.05	0.3088	0.4180	3.690	0.24635	0.04728	94.20	8.27

* Weight of the material Type I.

Water Inflated - Table 4.5

Effect of weight of membrane on the other parameters.

No.	Weight Kg/m^2	Propl. factor α	U/S Head m	D/S Head (m)	H_s depth of silt (m)	U/S Tension KN/m	D/S Tension KN/m	Max. Height m	Press. KN/m^2	Area m^2	U/S slope degree	Elongation mm
1	0.15	1.0	0.18862	0.0	0.0	0.2155	0.2961	0.21009	0.3734	0.04813	120.51	6.21
2	0.20	1.0	0.18862	0.0	0.0	0.2154	0.2961	0.21006	0.3734	0.04842	120.51	6.21
3	0.25	1.0	0.18862	0.0	0.0	0.2153	0.2960	0.21003	0.3734	0.04842	120.51	6.21
4	0.30	1.0	0.18862	0.0	0.0	0.2152	0.2959	0.20949	0.3734	0.04842	120.51	6.21
5	0.35	1.0	0.18862	0.0	0.0	0.2151	0.2958	0.20996	0.3734	0.04841	120.51	6.21
6	*0.39	1.0	0.18862	0.0	0.0	0.2131	0.2957	0.20994	0.3734	0.04840	120.50	6.20
7	0.40	1.0	0.18862	0.0	0.0	0.2151	0.2955	0.20993	0.3734	0.08840	120.49	6.20
8	0.45	1.0	0.18862	0.0	0.0	0.2150	0.2452	0.20989	0.3734	0.04839	120.48	6.19
9	0.50	1.0	0.18862	0.0	0.0	0.2149	0.2949	0.20986	0.3734	0.04838	120.48	6.18
1	0.15	1.2	0.19779	0.040	0.05	0.2655	0.3631	0.21491	0.431	0.04862	116.06	7.15
2	0.20	1.2	0.19779	0.040	0.05	0.2654	0.3631	0.21487	0.431	0.04862	116.05	7.15
3	0.25	1.2	0.19779	0.040	0.05	0.2653	0.3630	0.21484	0.431	0.04862	116.05	7.15
4	0.30	1.2	0.19779	0.040	0.05	0.2652	0.3629	0.21481	0.431	0.04862	116.04	7.15
5	*0.39	1.2	0.19779	0.040	0.05	0.2651	0.3628	0.21480	0.431	0.04862	116.03	7.15
6	0.45	1.2	0.19779	0.040	0.05	0.2650	0.3627	0.21478	0.431	0.04862	116.02	7.14
7	0.50	1.2	0.19779	0.040	0.05	0.2699	0.3626	0.21475	0.431	0.04861	116.01	7.14

Table 4.6

Effect of thickness of material on other parameter for Air Inflated.

No.	Thickness mm	α	U/S Head (m)	D/S Head (m)	H_s silt depth (m)	U/S Tension kn/m	D/S Tension kn/m	Max. Height (m)	Area m^2	U/S slope degree	Press. kn/m^2	Elongation mm
1	0.15	0.75	0.2526	0.0	0.0	0.4115	0.5661	0.2558	0.05085	110.73	4.4205	20.51
2	0.20	0.75	0.2526	0.0	0.0	0.4090	0.5625	0.2580	0.05030	110.60	4.4205	16.13
3	0.25	0.75	0.2526	0.0	0.0	0.4075	0.5603	0.2548	0.04997	110.52	4.4205	13.49
4	0.30	0.75	0.2526	0.0	0.0	0.4065	0.5588	0.2543	0.04974	110.46	4.4205	11.72
5	0.35	0.75	0.2526	0.0	0.0	0.4058	0.5578	0.2538	0.04958	110.45	4.4205	10.45
6	*0.36	0.75	0.2526	0.0	0.0	0.4055	0.5575	0.2526	0.04951	110.41	4.4205	9.92
7	0.40	0.75	0.2526	0.0	0.0	0.4053	0.5570	0.2523	0.04947	110.40	4.4205	9.49
8	0.45	0.75	0.2526	0.0	0.0	0.4049	0.5564	0.2523	0.04937	110.38	4.4205	8.75
9	0.50	0.75	0.2526	0.0	0.0	0.4045	0.5559	0.2520	0.04930	110.36	4.4205	8.15
1	0.04	0.50	0.246	0.1	0.05	0.3310	0.4470	0.2620	0.05260	95.94	3.69	49.89
2	0.15	0.50	0.246	0.1	0.05	0.3124	0.4237	0.2510	0.04826	94.75	3.69	15.98
3	0.20	0.50	0.246	0.1	0.05	0.3112	0.4213	0.2490	0.04783	94.42	3.69	12.67
4	0.25	0.50	0.246	0.1	0.05	0.3102	0.4199	0.2485	0.04759	94.34	3.69	10.70
5	0.30	0.50	0.246	0.1	0.05	0.3096	0.4190	0.2473	0.04742	94.28	3.69	9.38
6	0.35	0.50	0.246	0.1	0.05	0.3091	0.4184	0.2465	0.04731	94.24	3.69	8.43
7	*0.36	0.50	0.246	0.1	0.05	0.3090	0.4182	0.2462	0.04728	94.23	3.69	8.33
8	0.40	0.50	0.246	0.1	0.05	0.3088	0.4179	0.2461	0.04722	94.21	3.69	7.72
9	0.45	0.50	0.246	0.1	0.05	0.3085	0.4175	0.2460	0.04715	94.10	3.69	7.17
10	0.50	0.50	0.246	0.1	0.05	0.3083	0.4172	0.2460	0.04710	94.17	3.69	6.72

*Thickness of the material Type I.

Table 4.7

Effect of thickness of material on other parameter for Water Inflated.

No.	Thickness mm	α	U/S Head (m)	D/S Head (m)	H_s silt depth (m)	U/S Tension kn/m	D/S Tension kn/m	Max. Height (m)	Area m^2	U/S slope degree	Press. kn/m^2	Elongation mm
1	0.15	1.0	0.1886	0.0	0.0	0.2155	0.2972	0.21103	0.04901	120.75	0.3734	11.26
2	0.20	1.0	0.1886	0.0	0.0	0.2153	0.2966	0.21057	0.04875	120.64	0.3734	9.11
3	0.25	1.0	0.1886	0.0	0.0	0.2152	0.2962	0.21028	0.04860	120.58	0.3734	7.80
4	0.30	1.0	0.1886	0.0	0.0	0.2151	0.2959	0.21009	0.04890	120.53	0.3734	6.93
5	0.35	1.0	0.1886	0.0	0.0	0.2151	0.2956	0.20996	0.04842	120.50	0.3734	6.31
6	*0.36	1.0	0.1886	0.0	0.0	0.2151	0.2956	0.20996	0.04841	120.49	0.3734	6.30
7	0.40	1.0	0.1886	0.0	0.0	0.2150	0.2955	0.20985	0.04836	120.47	0.3734	5.84
8	0.45	1.0	0.1886	0.0	0.0	0.2150	0.2953	0.20477	0.04831	120.45	0.3734	5.47
9	0.5	1.0	0.1886	0.0	0.0	0.2150	0.2952	0.20471	0.04828	120.43	0.3734	5.18
1	0.04	1.2	0.19779	0.04	0.05	0.2728	0.3705	0.22293	0.05265	117.71	0.431	39.94
2	0.15	1.2	0.14779	0.04	0.05	0.2657	0.3640	0.21530	0.04895	116.22	0.431	12.65
3	0.20	1.2	0.19779	0.04	0.05	0.2655	0.3637	0.21526	0.04890	116.18	0.431	10.15
4	0.25	1.2	0.19779	0.04	0.05	0.2653	0.3635	0.21522	0.04885	116.14	0.431	9.14
5	0.30	1.2	0.19779	0.04	0.05	0.2632	0.3631	0.21496	0.04872	116.08	0.431	8.05
6	*0.36	1.2	0.19779	0.04	0.05	0.2650	0.3628	0.21480	0.04870	116.06	0.431	7.89
7	0.45	1.2	0.19779	0.04	0.05	0.2648	0.3621	0.21477	0.04856	116.02	0.431	6.24
8	0.50	1.2	0.19779	0.04	0.05	0.2644	0.3617	0.21470	0.04851	115.98	0.431	5.87

CHAPTER 5.

THE ANALYSIS OF AN INFLATABLE HYDRAULIC STRUCTURE UNDER HYDRODYNAMIC CONDITIONS.

5.1 Introduction.

The analysis of an inflatable hydraulic structure under hydrodynamic conditions is more complicated than for the hydrostatic analysis. It is necessary to include in this analysis parameters additional to the effect of the upstream head, downstream head and internal pressure head. These additional parameters to be considered in the analysis are, on the upstream side the effect of the specific energy and on the downstream side the effect of the centrifugal force.

Very few investigators have studied theoretically this condition for inflatable hydraulic structures. Anwar (2) in 1967 studied an inflatable hydraulic structure for the case of a hydrodynamic condition. This study was for a dam inflated with air and he determined a mathematical solution (see Chapter 2) to find the profile of the upstream face only with no indication of a solution for the shape of the downstream face nor for the shape with overflow in the case when the internal pressure is due to inflation with water.

Kunihiro Iwiwara (3) also studied a dam under hydrodynamic conditions but this solution depends on a number of assumptions as detailed in Chapter 2.

Investigators who have made an experimental study of inflatable hydraulic structures under hydrodynamic conditions are Baker (20), Shepherd (8) and Stodulka (21).

This chapter deals with the analysis of an inflatable hydraulic structure under hydrodynamic condition by using the technique of dividing the design length of the membrane into a specified number of elements and considering the effect of all forces on each element in turn.

A computer program was developed from that used in the case of static conditions the results from the program giving, tension, slopes, area, maximum height and the profile of the dam. Plotting of the profile is also included in the output from the program if required.

Experiments on different dams have been performed in order to check the theoretical profile and the tension in the membrane by fixing strain gauges inside the dam.

5.2 Design of the dam model.

The same basis for the design of the inflatable hydraulic structure under static conditions was used to design the length of the membrane. As the technique mentions in Chapter 8 the length of the material is based on the maximum proportional factor assumed to be considered and since this proportional factor is in relation to maximum storage head and the differential pressure head the relationship is as follows:

$$h = \alpha H_D \quad \ldots\ldots \quad 5.1$$

where h = differential pressure head inside the dam.

α = proportional factor.

H_D = maximum height of the dam.

The above equation is used in order to find the length of the membrane, the detail being given in Chapter 8.

In the preliminary study of the hydrodynamic condition created by allowing overflow to occur over the dam designed for the static condition it was noticed that as the overflow increased for a particular proportional factor alpha, the pressure inside the dam increased. However, the maximum overflow head has been considered up to the condition that the dam just starts to oscillate, and in this condition the internal pressure head is not significantly changed. Therefore it is considered that the criteria for the design length of the

membrane for the dynamic condition could be assumed to be similar to that for static condition as shown in table 5.1. This conclusion was also reached by Anwar (2) and Clare (14) as a result of their experiments.

Table 5.1 Criteria for design length of membrane in order to test the dam under different overflow.

Type of inflation fluid	Max. proportional factor	Max. U/S (m)	Length of membrane (m)	Length of base (m)	Pressure	
					Air (KN/m)	Water (m)
1. Water	2.5	0.2297	0.800	0.1259	-	0.800
2. Air	1.2	0.2604	0.800	0.1124	5.728	-
3. Air+ Water	1.6	0.216	0.800	0.1615	3.944	0.1575

For those conditions the dams were analysed under different overflows in order to find the effect of overflow head on the different output parameters (see Sec. 5.7).

A computer program (DYIHSIP) was used to analyse the dams in the hydraulic condition to find the magnitude of various parameters with respect to different overflow heads.

5.2.1 Construction of the model.

The construction of the models was as already described in Chapter 3 and the bags were constructed from two different materials with properties as shown in table 3.1. Also the systems used for inflation were the same as for the static condition except that the pressure created by the overflow was measured by a pressure transducer connected to a data logger. The pressure transducer was calibrated for both air and water pressures.

In addition to the dam with a total length equal to 0.80 m, dams were tested with different material lengths in order to establish the behaviour of such dams.

5.3 Experimental Work.

Tests on the dams inflated by air, water and (air+water) for different design lengths of membrane were carried out as follows:-

1. A dam was tested for different overflow and downstream heads with different proportional factors in order to find the profile of the sections, upstream slopes and area of the sections.

2. The overflow was measured up to the limit when vibration occurred this being observed by a pick-up vibration technique.

3. The tension around the profile was measured using strain gauges fixed inside the dam.

5.3.1 Shape of the dam.

5.3.1.1 Profile measurement.

The profile measurements were made in exactly the same way as for a dam under static conditions of loading as described in Section 3.6.1 of Chapter 3.

Using this technique the profile of the dam could be measured. However, during the measurements it was noticed that when lowering the point gauge into the water the test meter indicated a half deflection as water is a conductor of electricity, but the profile measurement was only made when the reading on the test meter was a full scale deflection indicating contact between the point gauge and the foil.

5.3.1.2 Measuring the shape of the dams.

The shapes of the dams were measured under different overflows for different proportional factors with various inflation fluids. The test program is shown in table 5.2. The overflow head was found by subtracting the maximum height of the dam from the upstream head and the discharge was calculated from the calibration curve,details of which are given in Chapter 7.

Typical profiles as measured experimentally for air, water and (air+water) inflated under different overflows are shown in fig.5.1. A computer program (EW) was used to plot these profiles.

Table 5.2 Experimental test program.

Type of Infl.	No.	Propl. factor	U/S Head m	D/S Head m	Max. dam height m	Water Press. m	Air Press. KN/m^2	Overflow head mm	Discharge ℓ/s
Water	1	1.2	0.221	0.0	0.21	0.436	0.0	11	1.79
			0.228	0.0	0.206	0.436	0.0	22	5.18
			0.233	0.0	0.205	0.436	0.0	25	7.95
	2	1.4	0.230	0.0	0.223	0.300	0.0	7	0.90
			0.236	0.0	0.221	0.500	0.0	15	3.10
			0.241	0.0	0.218	0.500	0.0	23	5.53
			0.251	0.0	0.215	0.500	0.0	35	11.30
	3	2.5	0.241	0.0	0.240	0.800	0.0	2.0	0.11
			0.248	0.0	0.239	0.800	0.0	9.0	1.15
			0.256	0.0	0.238	0.800	0.0	18.0	3.45
			0.258	0.0	0.238	0.800	0.0	20.0	4.07
	1	1.2	0.221	0.04	0.2122	0.435	0.0	8.8	1.30
			0.227	0.04	0.2093	0.435	0.0	16.7	3.82
			0.233	0.04	0.2061	0.435	0.0	26.9	7.30
	2	1.4	0.230	0.04	0.2234	0.500	0.0	9.6	0.73
			0.236	0.04	0.2217	0.500	0.0	14.3	2.730
			0.242	0.04	0.2196	0.500	0.0	22.4	5.55
			0.252	0.04	0.2155	0.500	0.0	36.5	12.12
			0.255	0.04	0.2149	0.500	0.0	40.11	14.11
Air	1	0.6	0.253	0.0	0.224	0.0	3.484	29	9.75
			0.256	0.0	0.224	0.0	3.984	32	11.9
			0.262	0.0	0.222	0.0	3.984	42	18.01
	2	1.0	0.258	0.0	0.240	0.0	5.15	18	4.28
			0.265	0.0	0.241	0.0	3.15	27.0	8.47
			0.268	0.0	0.237	0.0	5.15	28	8.81
			0.273	0.0	0.235	0.0	5.15	38.4	14.78
	3	1.2	0.263	0.0	0.2610	0.0	5.73	2.0	0.11
			0.272	0.0	0.2595	0.0	5.73	12.5	2.12
			0.288	0.0	0.2583	0.0	5.73	29.7	8.44
Air+Water	1	0.8	0.218	0.0	0.209	0.1575	2.040	9	1.46
			0.230	0.0	0.199	0.1575	2.040	31	11.42
			0.233	0.0	0.198	0.1575	2.04	35.4	14.78
	2	1.0	0.226	0.0	0.214	0.1575	2.04	12	2.23
			0.242	0.0	0.213	0.1575	2.04	29	9.21
			0.248	0.0	0.2078	0.1575	2.04	40.2	16.15

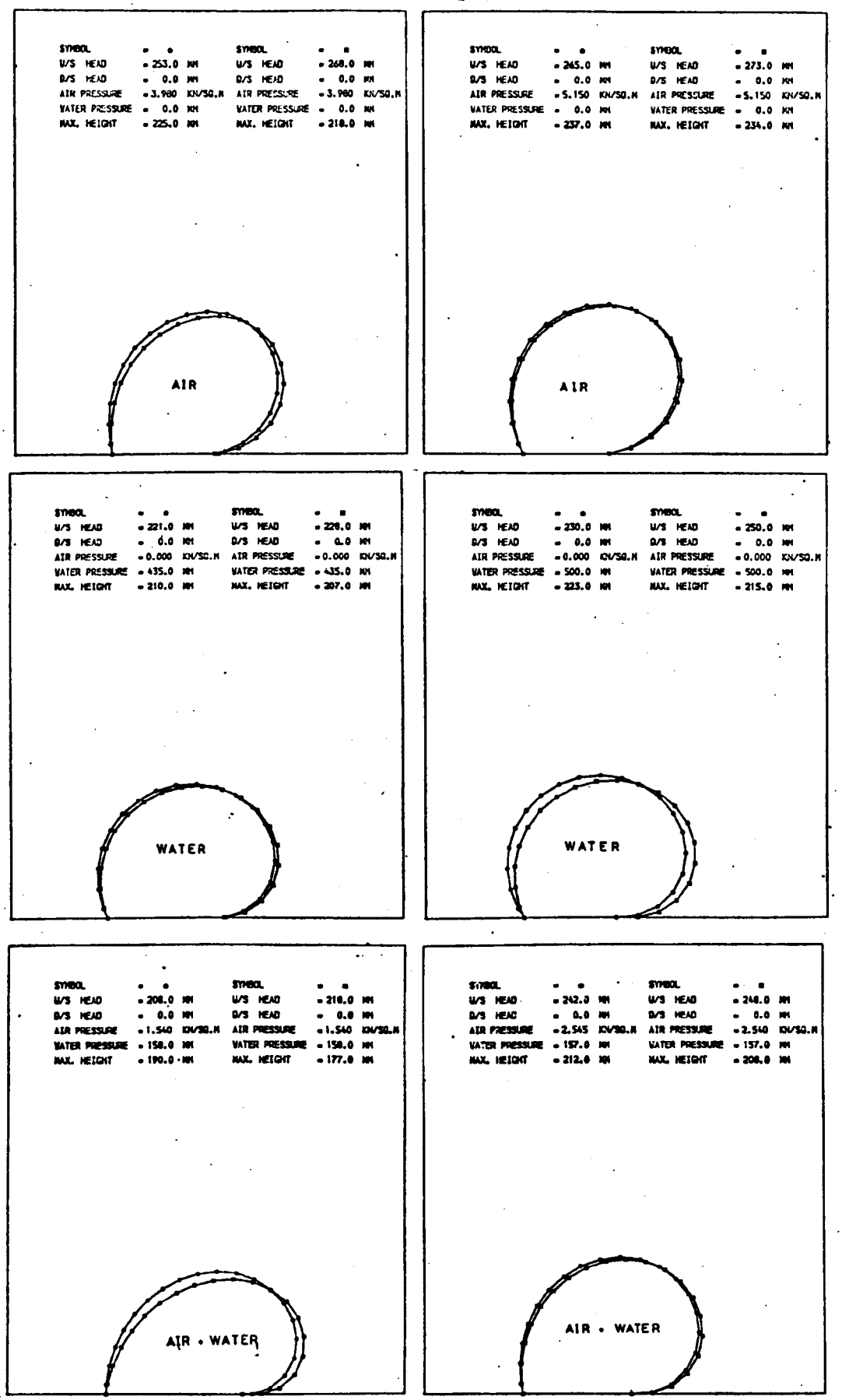

FIG. (5-1) DIFFERENT TYPICAL EXPERIMENTAL PROFILES FOR DIFFERENT INFLATION FLUIDS

5.3.2 Overflow head limit.

At a particular overflow oscillation of the nappe started due to an alternating force which was created by the motion of the air trapped in the space beneath the nappe causing vibration. The oscillation of the nappe affected the downstream membrane face causing the dam to vibrate. This phenomenon of vibration was initally noticed during high flow rates. Once started reduction could only be achieved by

1. Decreasing the overflow.
2. Aerating the nappe by inserting two pipes on both sides of the downstream face close to the dam.
3. Vibration could also be reduced by tapping the model by hand or by using a trip rod of 8 mm diameter on the top near the crest to prevent the backward and forward movement of the crest.

In this section the experiments concentrated on the limiting range of overflows to those below which vibration occurred

The limit to the overflow before the vibration started was found by using a proximity vibration pick-up device which clamped on the top of a small aluminium channel fixed on the top of the crest of the dam with a (1-3) mm gap between the needle of the vibration pick-up and the aluminium channel. The proximity vibration pick-up was connected to a transducer oscillator and oscilloscope.

The arrangement of this set up is shown in figs. 5.2 and 5.3 and to operate the system, the dam was inflated with particular pressure and water allowed to flow over the crest. The overflow was increased until it was found that the oscilloscope screen gave a vertical displacement, i.e., the vibration onset for this particular overflow.

This method was used by allowing different overflows and once the vibration started, the overflow was not allowed to increase above the onset

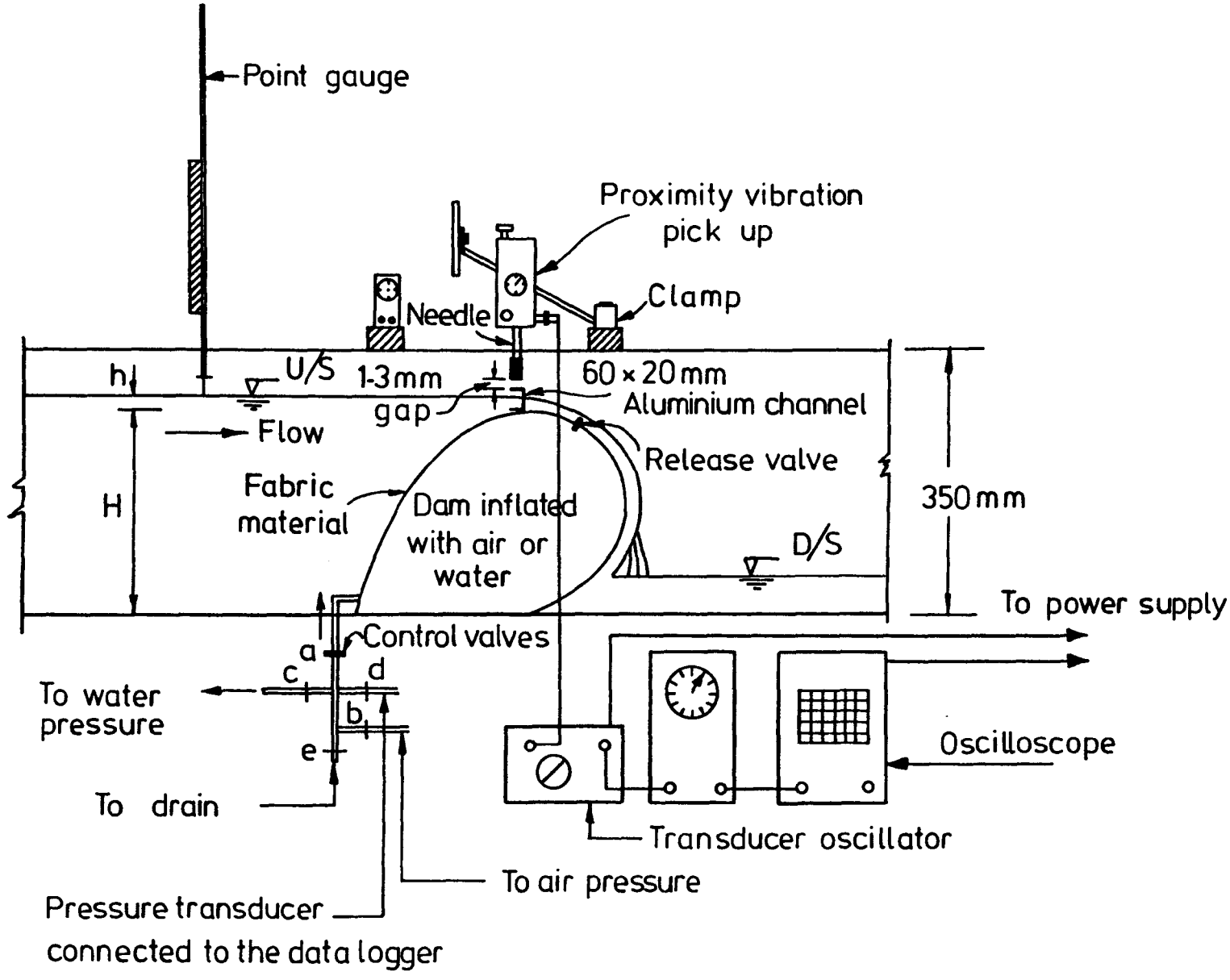

FIG. (5-2) APPARATUS USED FOR INDICATION OF THE VIBRATION

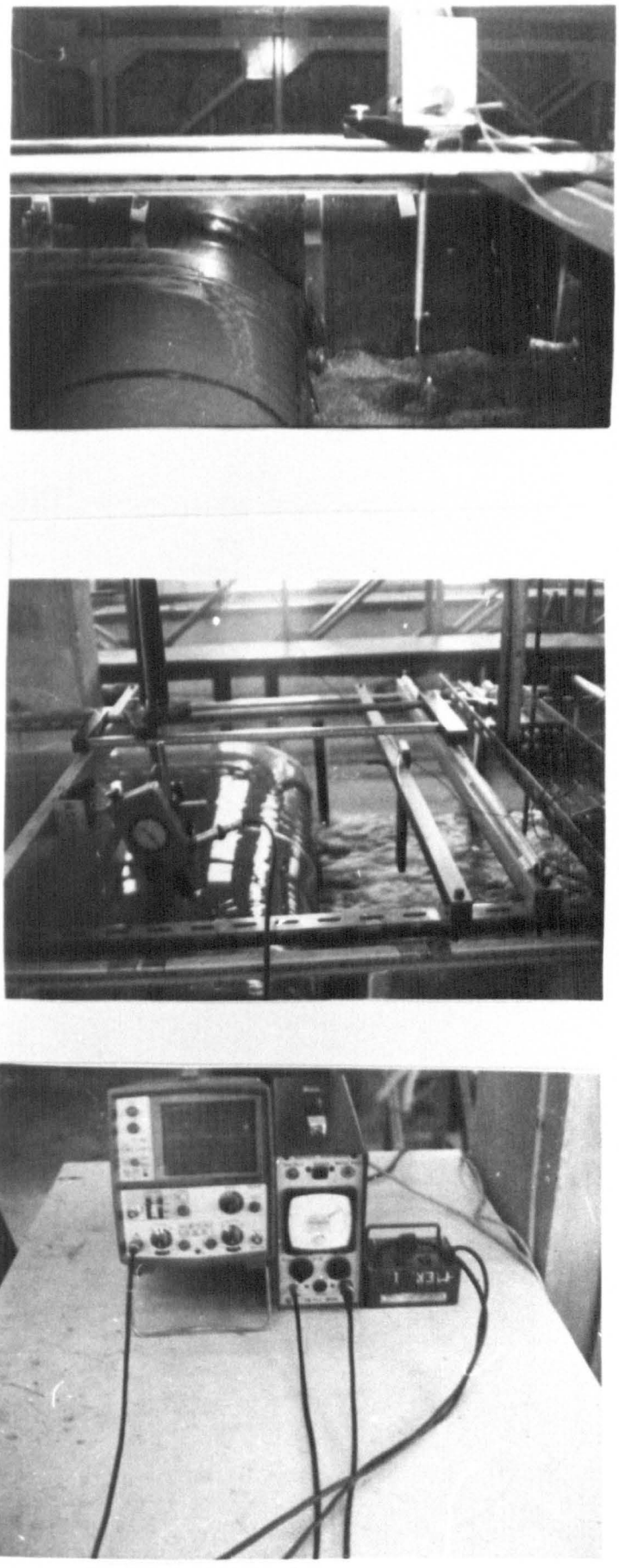

FIG.(5-3) SET UP OF APPROXIMITY VIBRATION PICK UP

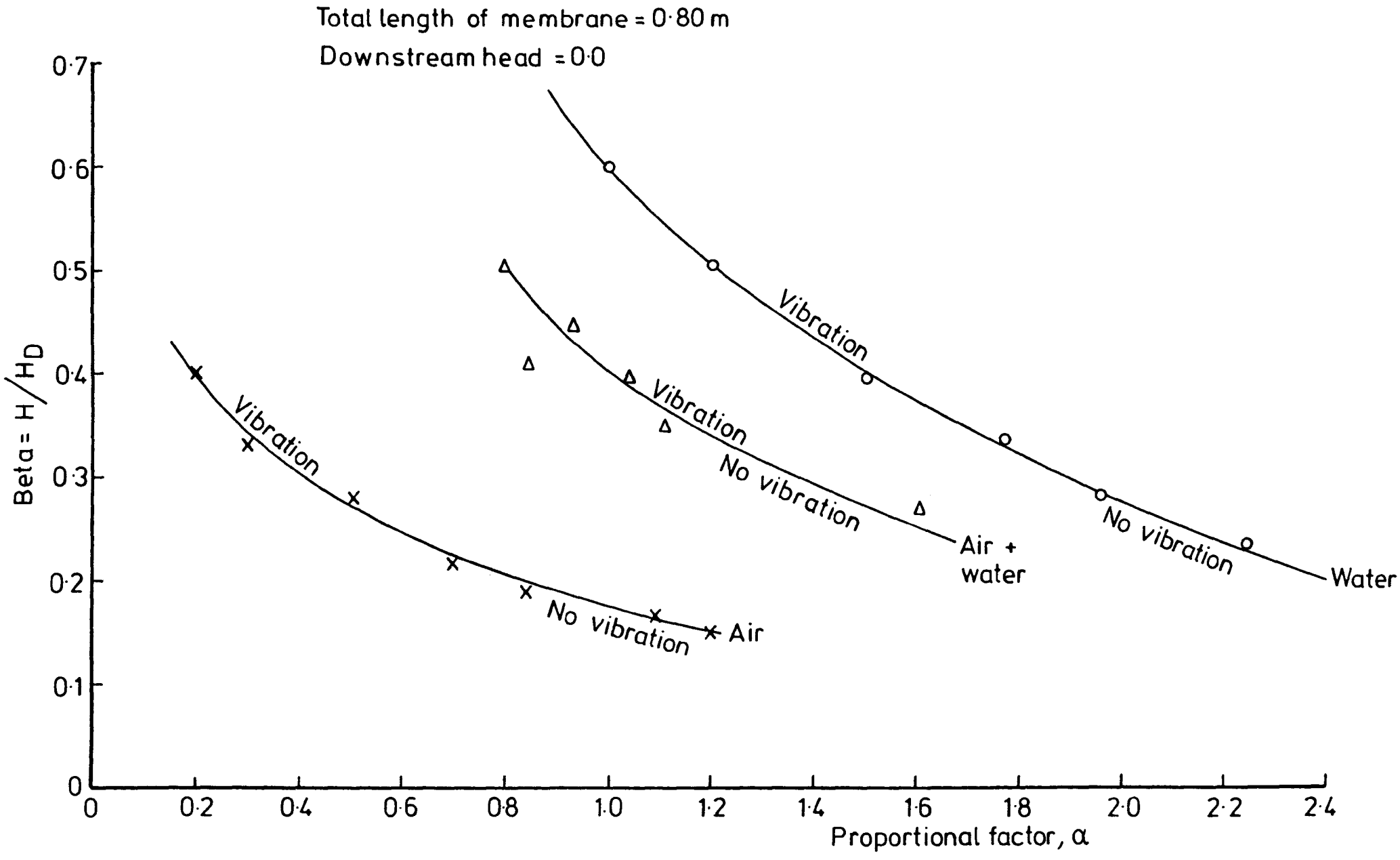

FIG.(5-4) MAXIMUM POSSIBLE NON-DIMENSIONAL OVERFLOW Vs PROPORTIONAL FACTOR FROM EXPERIMENTAL OBSERVATION

of vibration value. This procedure was carried out for dams under different proportional factors and for different inflation fluids.

A graph was plotted between the results of the ratio of the maximum overflow head just before vibration and maximum dam height, i.e. (H/H_D) and the different proportional factors, and this procedure was carried out for dams under different inflation fluids, i.e., air, water and (air+water).

Fig.5.4 shows the result of the limit of the overflow head just before the onset of vibration.

The pressure inside the dam was measured by using a pressure transducer connected to a data logger, the pressure transducer used was a Type PDCR 10 with a maximum capacity of 10 psi with a temperature error less than ± 0.3% according to the information listed from the supply company. A calibration of the pressure transducer was made for both air and water pressures and the results of the calibration can be seen in fig.5.5.

5.4 Measuring the Tension In the Membrane.

5.4.1 Strain gauges installation.

Two sets of experiments were carried out to measure the tension in the membrane by using strain gauges. The first experiment involved attaching strain gauges (Type KYOWA gauges) which were suitable for measuring the strain in high elongation materials. The strain gauges were fixed in four groups of cells, each cell consisting of two strain gauges working as active strain gauges and connected with two other strain gauges as dummy gauges kept outside the dam but in conditions similar to the active gauges by keeping the dummy strain gauges in a container of water. The four cells were distributed around the perimeter of the dam. One cell was fixed on the upstream face, two cells fixed on the crest of the dam and the fourth cell fixed on the downstream face of the dam. The strain gauges were attached to the dam using

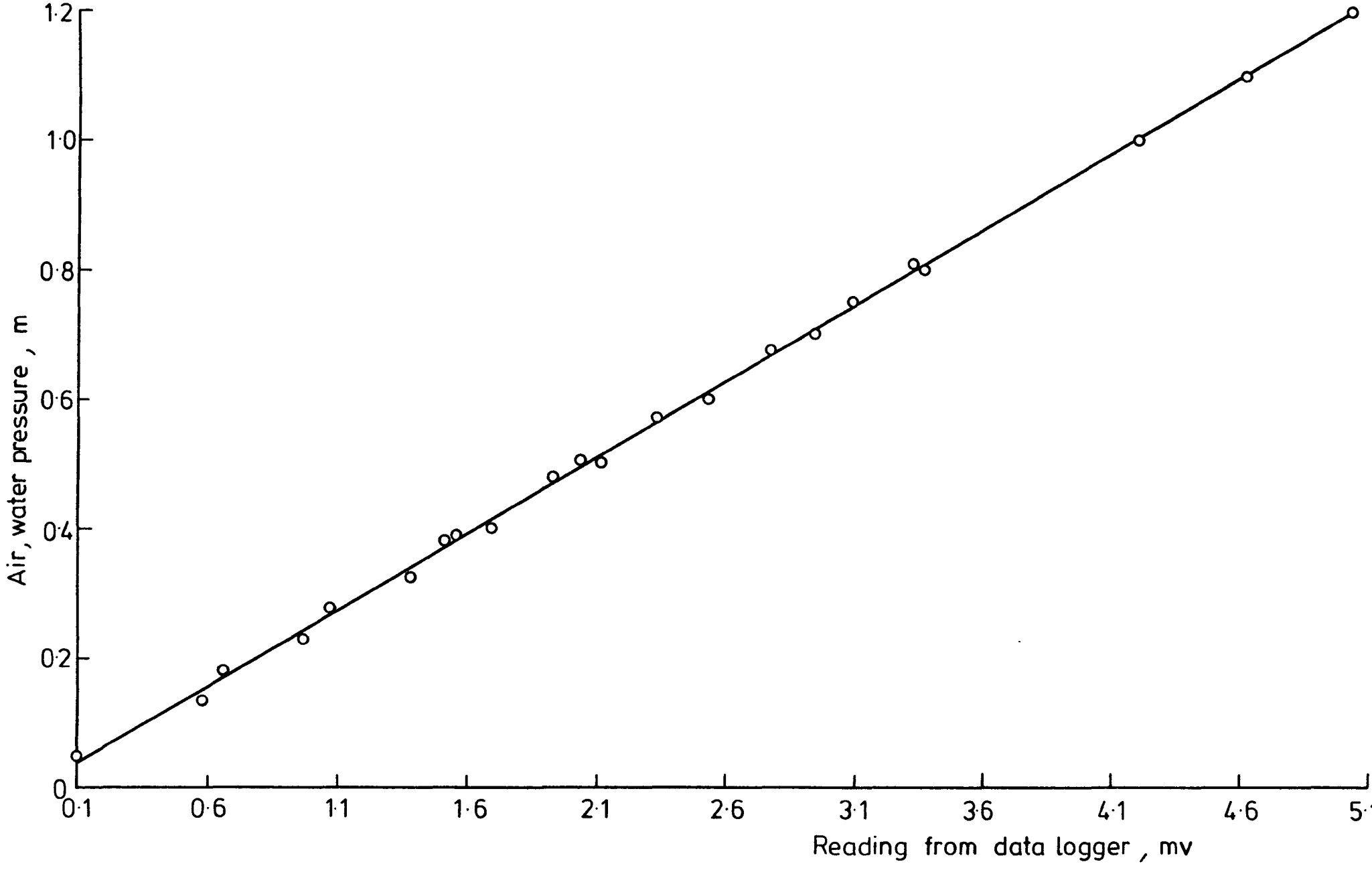

FIG.(5-5) CALIBRATION OF THE PRESSURE TRANSDUCER FOR AN AIR,WATER INFLATED DAM

a cement type (CC-ISA) as recommended by the company and in accordance with the instructions provided. The gauges were attached after the dam tube was folded and then the gauges were covered with two layers of sealer, i.e, IVI-spray electrical sealar, to prevent the water coming into direct contact with the strain gauges. After installation of all four groups, tests could be started by connecting to a data logger, the tension in the membrane being recorded in the data logger as millivolts.

It was found that when the level of the water was below the level of the strain gauges, the tension results give good agreement but once the water rose above the level of the strain gauges, the readings were not satisfactory.

This initial arrangement of strain gauges on the inflatable dam is shown in fig.5.6 and 5.7 but due to the above problem an alternative technique was developed to eliminate this effect of water on the strain gauges.

This second arrangement involved sticking the strain gauges inside the tube to avoid the effect of water on the strain gauges. This was carried out before the dam was folded.

The strain gauges were mounted in two rows, the first row in the centre consisting of seven cells each cell containing four strain gauges connected to form a "Wheatstone Bridge" (47) as shown in fig.5.8. All the cells were attached 100 mm from each other. Each strain gauge required two 0.25 mm diameter wires so that each cell was connected to 8 wires. These 8 wires were connected as a Wheatstone Bridge resulting in four wires from each cell which were taken out of the dam through the valve B as shown in fig.5.8.

A second row of strain gauges was attached close to the sides of the dam in the form of three cells 200 mm apart and wired in a similar pattern to the first row.

All the cells of strain gauges were glued to the dam using the adhesive cement mentioned earlier.

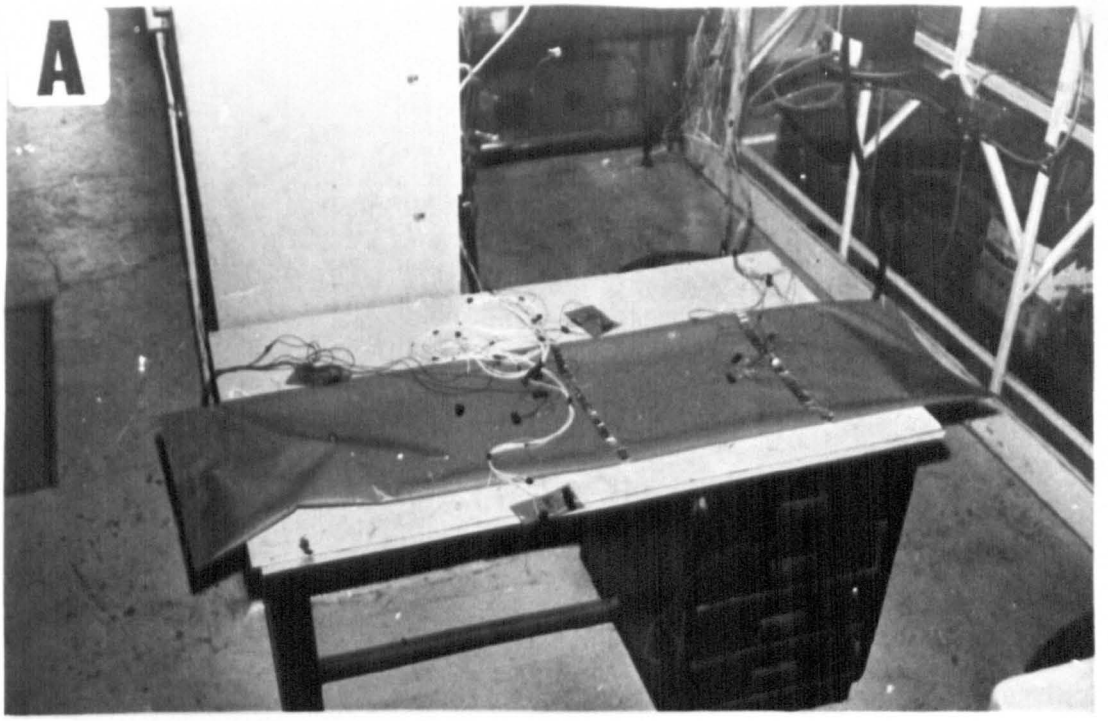

(a) Strain gauges attached before the dam is fixed in the test tank

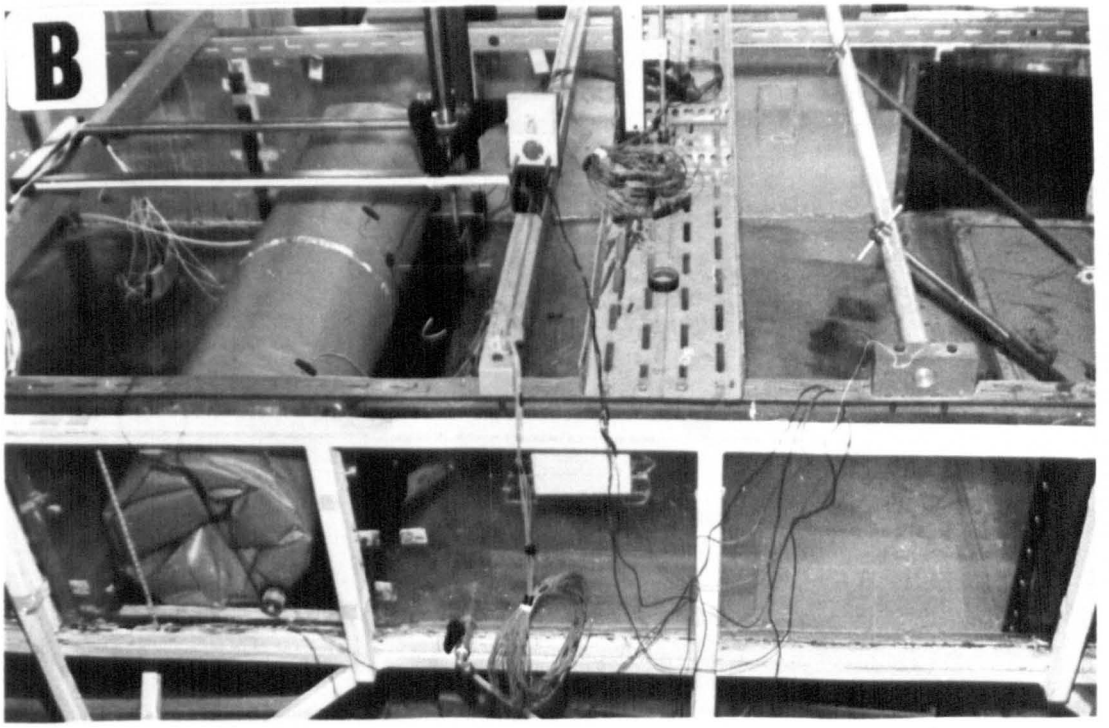

(b) Strain gauges after fixing the dam in the test tank

FIG. (5-6) STRAIN GAUGES ATTACHED TO THE INFLATABLE DAM – FIRST METHOD

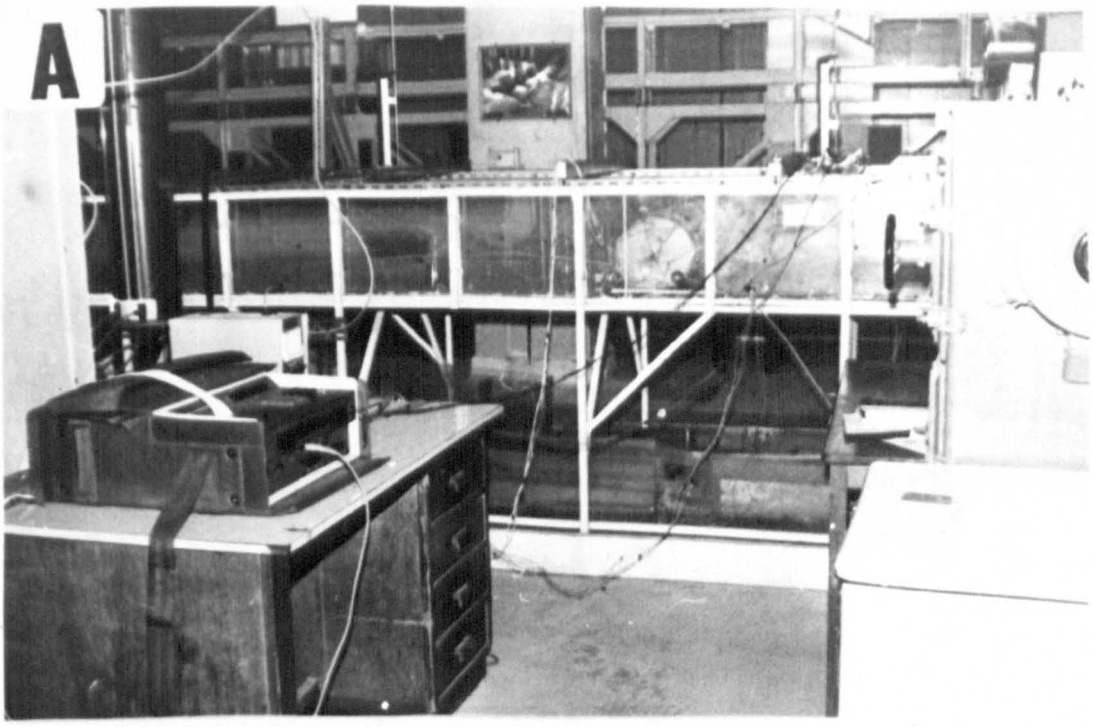

(a) Dam under test

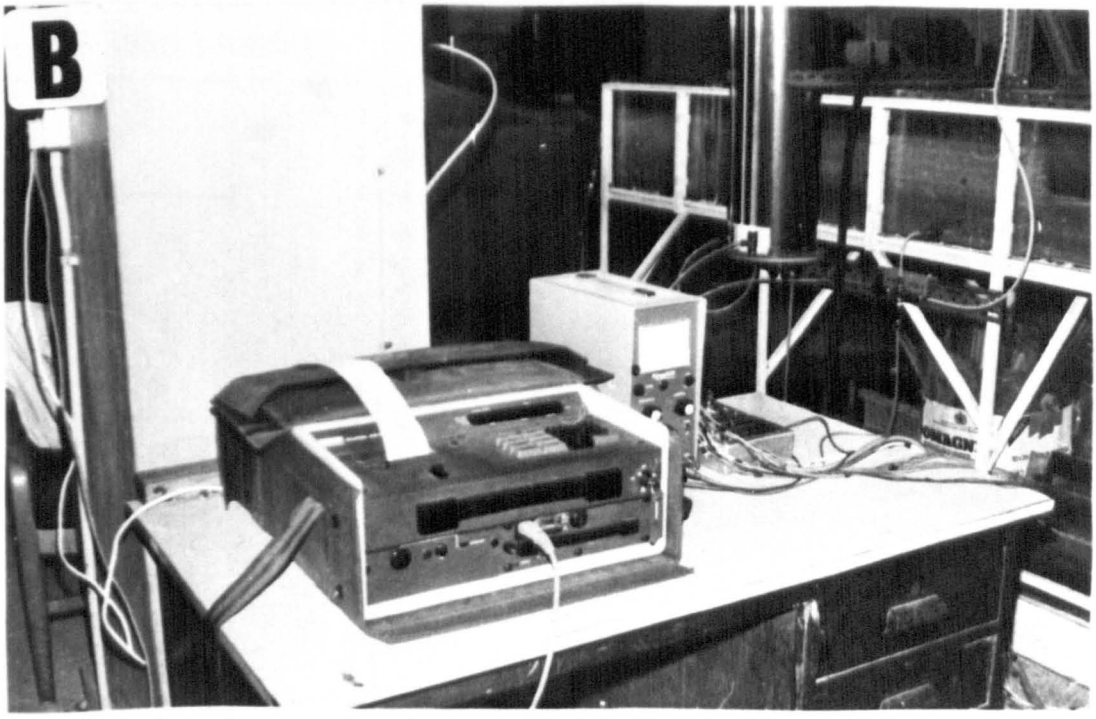

(b) Recording the results on the data logger

FIG.(5-7) AN INFLATABLE DAM UNDER TEST

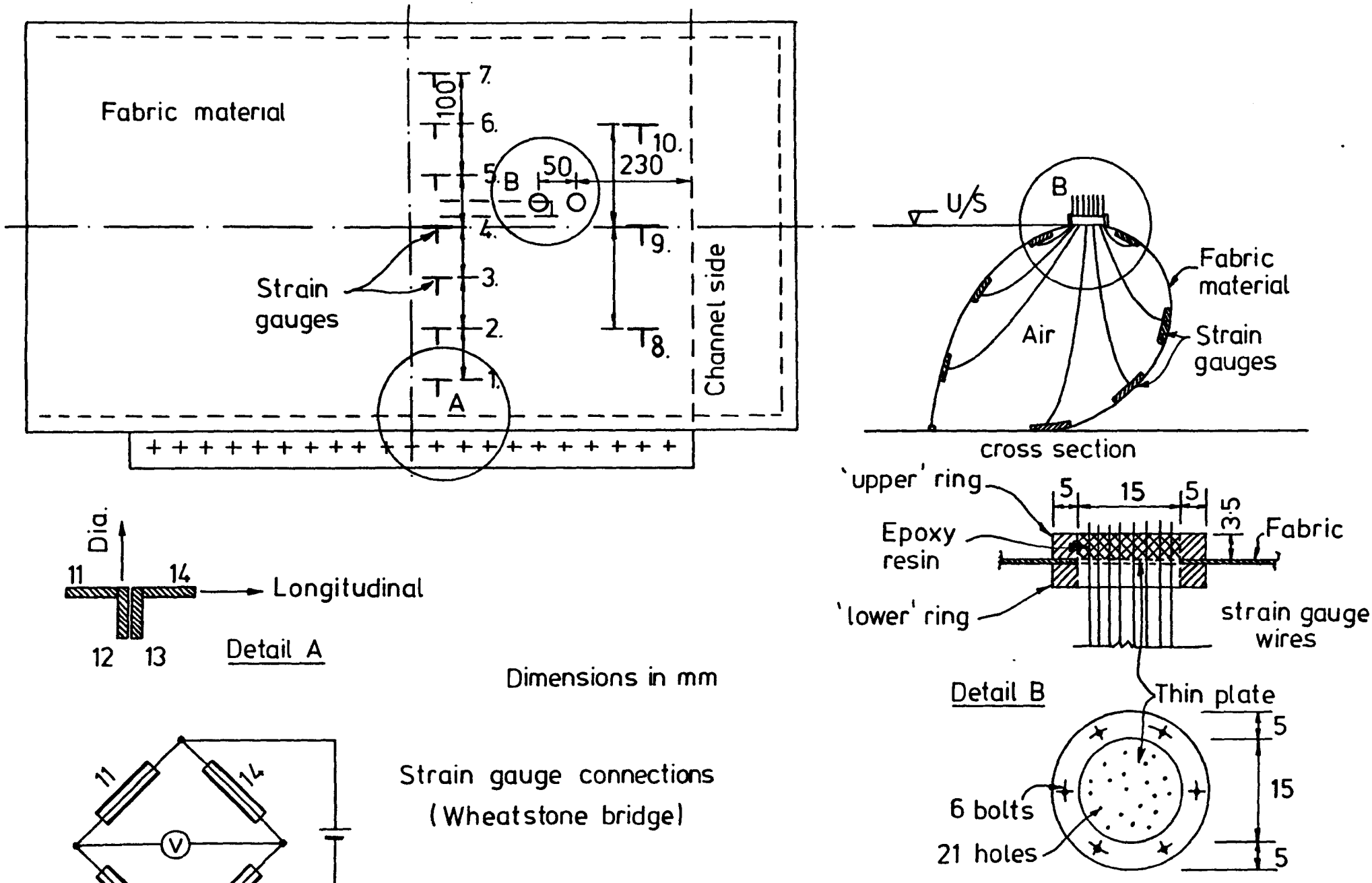

FIG.(5·8) DETAILS–ATTACHMENT OF STRAIN GAUGES (SECOND METHOD)

A total of 40 wires emerged from the dam and these were divided into two groups to pass from the tube through two valves designed and installed for this purpose and installed at distances of 230 mm and 280 mm from the ends of the side test tank located on the top of the dam crest. These two valves consisted of two rings 3.5 mm thick and sandwiched in between was a thin plate with twenty one holes to allow the wires to pass to the outside of the tube. One ring was fitted inside the tube and the other to the outside and these were joined by 6 bolts.

Once all the wires were passed through the holes each wire was checked to ensure that it was loose inside the dam to prevent any tension in the wire affecting the inflation of the dam. Once satisfied of this condition, the top ring outside the tube was filled with 5 minute "Epoxy" compound to prevent the leakage of water into the dam and also to prevent any deflation of the dam during a test.

This arrangement is shown in detail in figs. 5.8 and 5.9.

5.4.2 Stability and calibration of the strain gauges.

Before commencing the tests two points were considered. The first was to check the stability of the strain gauges both before and after folding the tube. This was done by using the data logger to take readings from the strain gauges every hour for two days. The maximum differences for all cells was ± 0.015 mv equivalent to 2% and this was probably due to a change in individual temperature throughout the test period. In view of this very small change the stability was considered acceptable.

The second point was the calibration of the strain gauges which was carried out using two different methods.

Firstly, the calibration was achieved by taking a specimen of the dam material and attaching one cell of strain gauges. The specimen was prepared

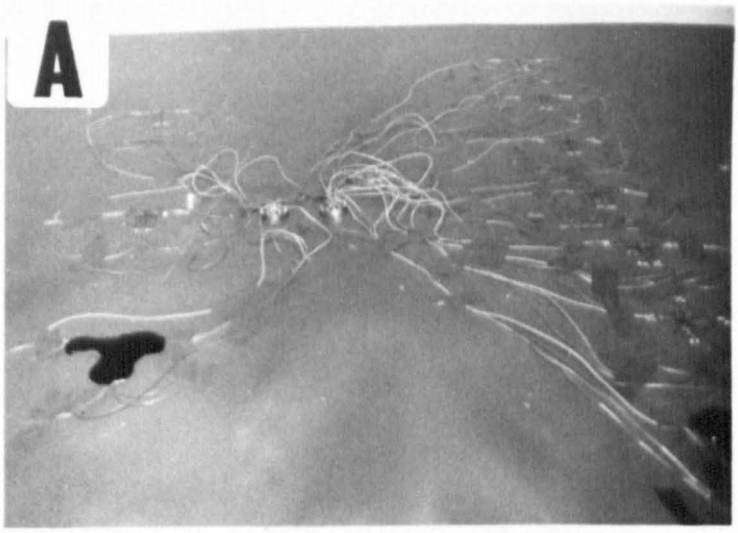

(a) Sticking the gauges before folding the tube

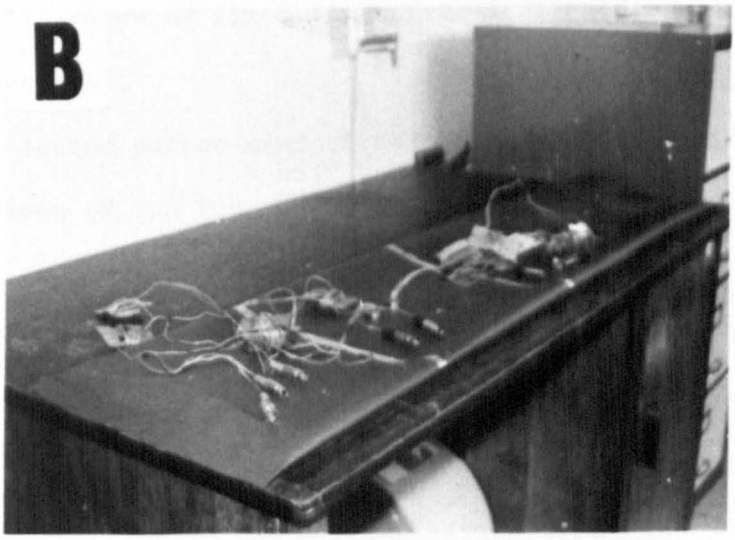

(b) Wires from the strain gauges after folding the tube dam

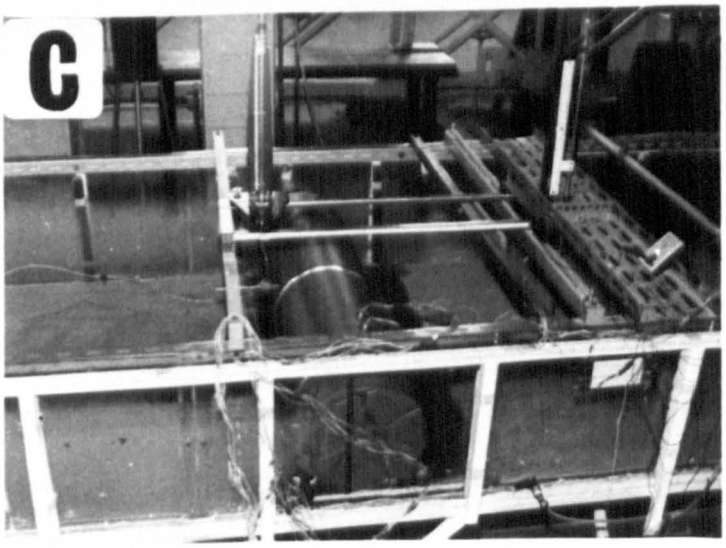

(c) Wires from the valves after fixing the dam in the test tank

FIG. (5-9) ARRANGEMENT FOR INSTALLING THE STRAIN GAUGES INSIDE DAM TUBE

according to the British Standard, BS 2576-1977 (29) and was fitted in a tensometer machine to find the tension under different loadings. Four specimens were used and the readings from the data logger in mv were plotted against tension in the membrane in KN/m. It was found that for small loading the tensometer could not be adjusted to give small reliable readings and therefore this system could only be used satisfactorily to find the breaking strength and tension in the high load ranges. The arrangement of the tensometer is shown in fig.3.5, Chapter 3 as used to find the breaking strength of the material.

A second method used to calibrate the strain gauges was to take (100x200mm) specimens of the two different materials and to suspend these from a hook and by using different weights hung from the bottom of the specimen as shown in fig. 5.10 to find the strain in the material, and hence the tension in KN/m.

From each increment of loads, readings of the data logger were taken in mv and this continued until the breaking strength of the material was reached.

The results of the above readings i.e. loads and readings of the data logger in mv were plotted to find the relationship between tension in the membrane and the reading from the data logger in (mv). A subroutine (EOZADF) was used to fit the data based on the Chebyshev-series. The results of the best polynomial fits are shown in fig.5.11 for the different materials and the different methods of testing.

5.4.3 Results of the tension test.

The test program for measuring the tension in the membrane was only applied to the air inflated condition as this gave higher tensions than for the other conditions of inflation considered. Two different pressures were used for two different conditions, one with the downstream head equal to zero and the second with the downstream head equal to 100 mm. Five different overflow heads were used for each condition. Readings from the data logger of the

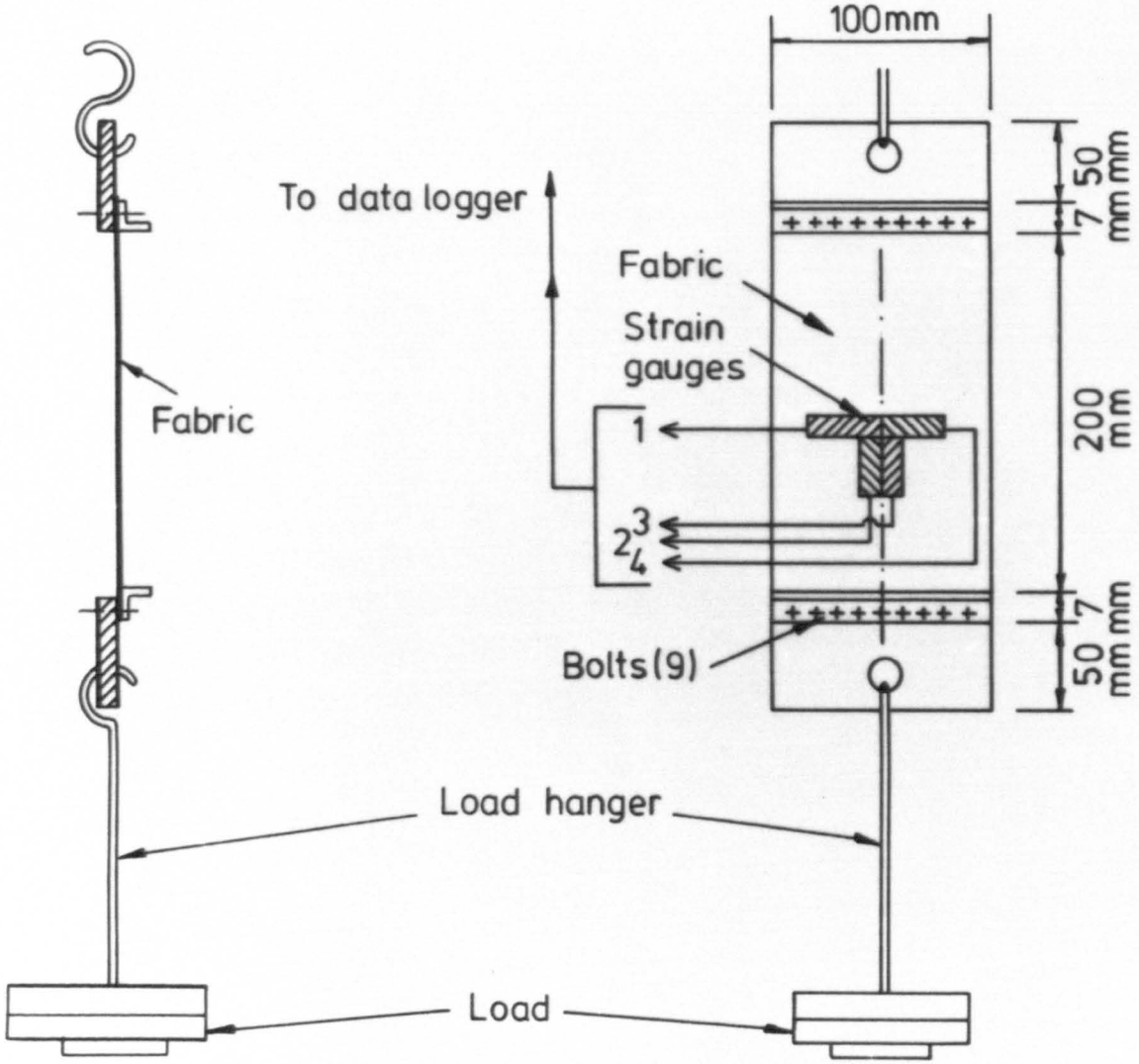

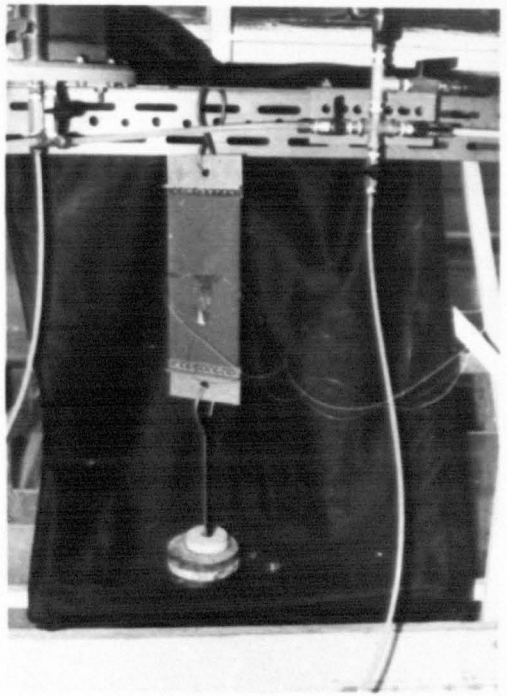

FIG (5-10) CALIBRATION OF STRAIN GAUGES BY THE SUSPENDED LOAD METHOD

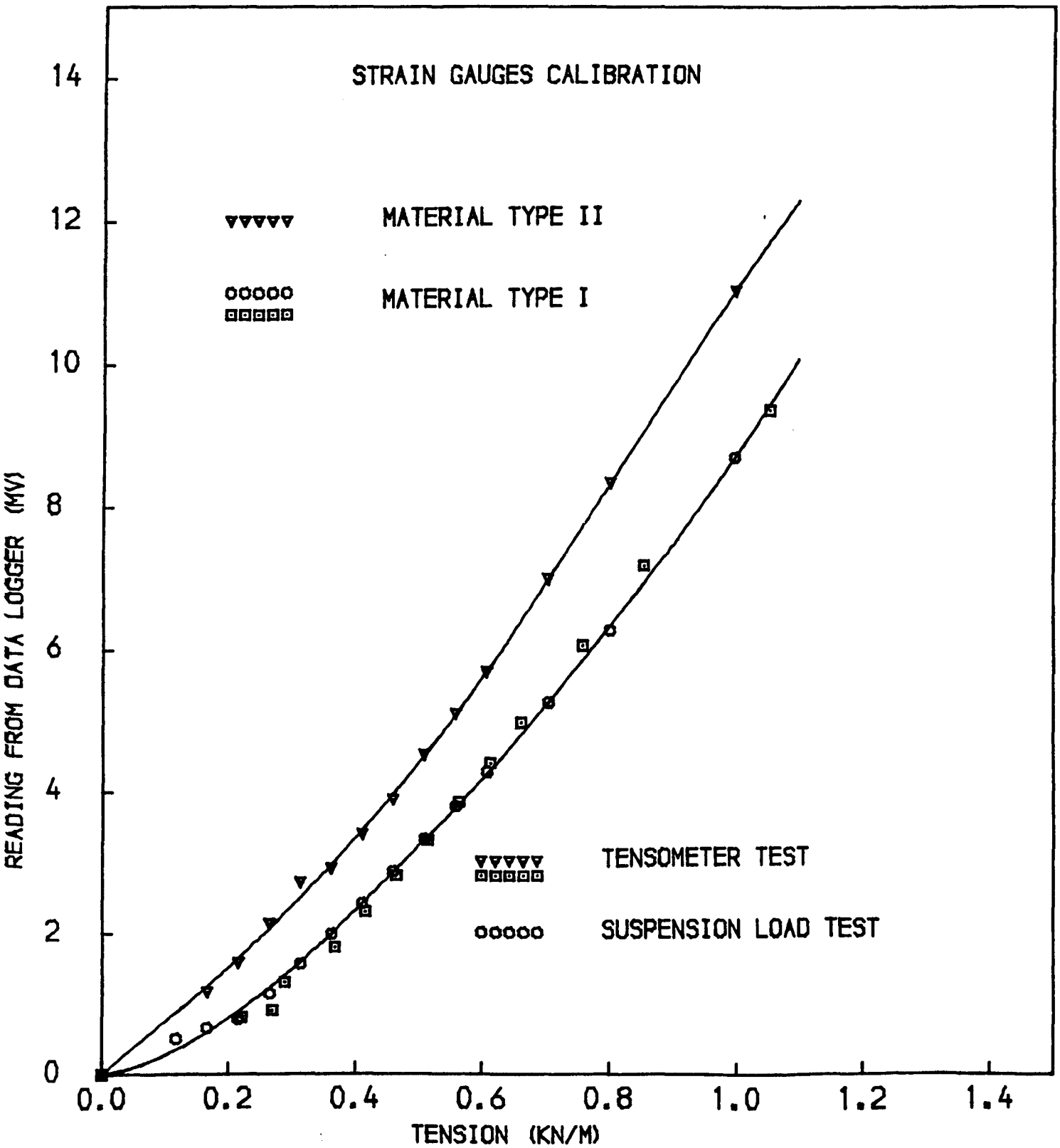

FIG(5-11) STRAIN GAUGES CALIBRATION

strain gauge cells were taken every 10 minutes with each overflow head running for one hour to give six readings for each cell and by averaging these readings the tension was found from the calibration curve, fig.5.11.

Tables 5.3 and 5.4 show the average tension for each cell for each condition.

Comparison between the tension found by experiment and those found theoretically is discussed in Chapter 6 and the above tables only show the results of the tests. Fig.5.12 shows an air inflated dam under a tension test.

5.5 Behaviour of an inflatable dam.

5.5.1 Behaviour of an air inflated dam.

To study the behaviour of an air inflated dam under different overflows a dam was built of total membrane length equal to 0.60 m and tested under two air pressures of 3.355 KN/m^2 and 5.1 KN/m^2. The study was carried out under different overflows for downstream heads of 70, 90, 100, 120, 140 mm. It was observed that for a particular air pressure the height of the dam decreased with increasing overflow (increasing the rate of flow) with an overflow resulting in a distortion of the dam toward the downstream side and a lowering of the crest. This pattern of behaviour was found for both the air pressures and all the different downstream heads. Fig.5.13 shows this pattern of behaviour for different air pressure and different downstream heads. Also it was noticed that for the dam with an internal air pressure equal to 3.355 KN/m^2 under a downstream head equal to 140 mm, the maximum height of the dam was equal to 0.187 m whilst for a dam with an internal air pressure equal to 5.1 KN/m^2 under the same downstream head, the maximum height of the dam was equal to 0.186 m. This behaviour shows that under certain downstream heads that for a dam under a low internal pressure, the maximum height can be more than the same dam inflated with a higher pressure and this is clearly

Table 5.3 Results of the test for the tension for an air inflated dam with D/S = 0.

Dam Information							Pressure transducer channel (0)	Section at Centre of the dam							Section at End		
								Part (1) Upstream face			Part (2) Crest face		Part (3) Downstream face		U/S face	Crest face	D/S face
No. of test	Alpha	U/S Head (m)	D/S Head (m)	Max. Height of dam (m)	Over-flow Head (mm)	Disch. Q ℓ/s	Equivalent pressure g/m^2 in KN/m	Cell (1)	Cell (2)	Cell (3)	Cell (4)	Cell (5)	Cell (6)	Cell (7)	Cell (8)	Cell (9)	Cell (10)
								Ten. KN/m	Ten. KN/m	Ten. KN/m	Ten. KN/m	Ten. KN/m	Ten. KN/m	Ten. KN/m	Ten. KN/m	Ten. KN/m	Ten. KN/m
1	0.6	0.253	0.0	0.2247	28.3	10.02	3.984	0.368	0.771	0.382	0.393	0.429	0.4383	0.475	0.368	0.41	0.480
2		0.256	0.0	0.2246	31.4	11.82	3.984	0.360	0.362	0.375	0.394	0.402	0.437	0.476	0.366	0.43	0.440
3		0.262	0.0	0.222	40.0	17.80	3.984	0.357	0.360	0.373	0.384	0.397	0.432	0.470	0.360	0.41	0.430
4		0.268	0.0	0.218	50.0	26.05	3.984	0.355	0.358	0.368	0.377	0.391	0.425	0.463	0.358	0.401	0.430
5		0.270	0.0	0.201	*69.0	49.36	3.984	0.360	0.363	0.369	0.376	0.389	0.43	0.45	0.365	0.392	0.455
1	1.2	0.263	0.0	0.243	20.0	5.11	5.728	0.541	0.58	0.61	0.60	0.63	0.69	0.735	0.548	0.62	0.745
2		0.266	0.0	0.2427	23.3	6.526	5.728	0.540	0.56	0.59	0.60	0.635	0.688	0.733	01740	0.628	0.742
3		0.272	0.0	0.240	32.0	10.99	5.728	0.550	0.56	0.58	0.60	0.630	0.68	0.73	0.555	0.62	0.742
4		0.275	0.0	0.2398	35.0	12.69	5.728	0.540	0.55	0.58	0.60	0.62	0.67	0.72	0.55	0.61	0.74
5		0.278	0.0	0.2388	39.2	15.297	5.728	0.540	0.55	0.575	0.60	0.62	0.67	0.74	0.56	0.60	0.74

*Vibration started.

Table 5.4 Results of the test for the tension for an air inflated dam with D/S = 0.1 m.

Dam Information							Pressure transducer channel (0)	Section at Centre of the dam							Section at End		
								Part (1) Upstream face			Part (2) Crest face		Part (3) Downstream face		U/S face	Crest face	D/S face
No. of test	Alpha	U/S Head (m)	D/S Head (m)	Max. Height of dam (m)	Over-flow Head (mm)	Disch. Q ℓ/s	Equivalent pressure in KN/m^2	Cell (1)	Cell (12)	Cell (3)	Cell (4)	Cell (5)	Cell (6)	Cell (7)	Cell (8)	Cell (9)	Cell (10)
								Ten. KN/m	Ten. KN/m	Ten. KN/m	Ten. KN/m	Ten. KN/m	Ten. KN/m	Ten. KN/m	Ten. KN/m	Ten. KN/m	Ten. KN/m
1	0.6	0.263	0.1	0.231	32.0	11.68	3.984	0.350	0.36	0.37	0.40	0.42	0.44	0.46	0.356	0.42	0.47
2		0.268	0.1	0.228	40.0	17.00	3.984	0.346	0.35	0.36	0.37	0.39	0.43	0.47	0.35	0.40	0.47
3		0.271	0.1	0.226	45.0	20.78	3.984	0.34	0.35	0.36	0.37	0.39	0.42	0.46	0.34	0.39	0.47
4		.279	0.1	0.223	*56.0	30.05	3.984	0.33	0.34	0.35	0.36	0.38	0.42	0.45	0.335	0.38	0.46
1	1.2	0.264	0.1	0.248	16.0	3.47	5.728	0.55	0.56	0.59	0.61	0.64	0.69	0.74	0.555	0.65	0.75
2		0.268	0.1	0.247	21.0	5.38	5.728	0.54	0.55	0.58	0.60	0.63	0.68	0.73	0.56	0.63	0.73
3		0.2725	0.1	0.246	26.5	7.39	5.728	0.53	0.54	0.58	0.59	0.63	0.675	0.73	0.55	0.58	0.68
4		0.2777	0.1	0.2451	32.6	10.95	5.728	0.53	0.54	0.58	0.59	0.62	0.67	0.720	0.54	0.61	0.68
5		0.281	0.1	0.244	37.0	13.49	5.728	0.53	0.54	0.57	0.60	0.59	0.67	0.71	0.540	0.59	0.70

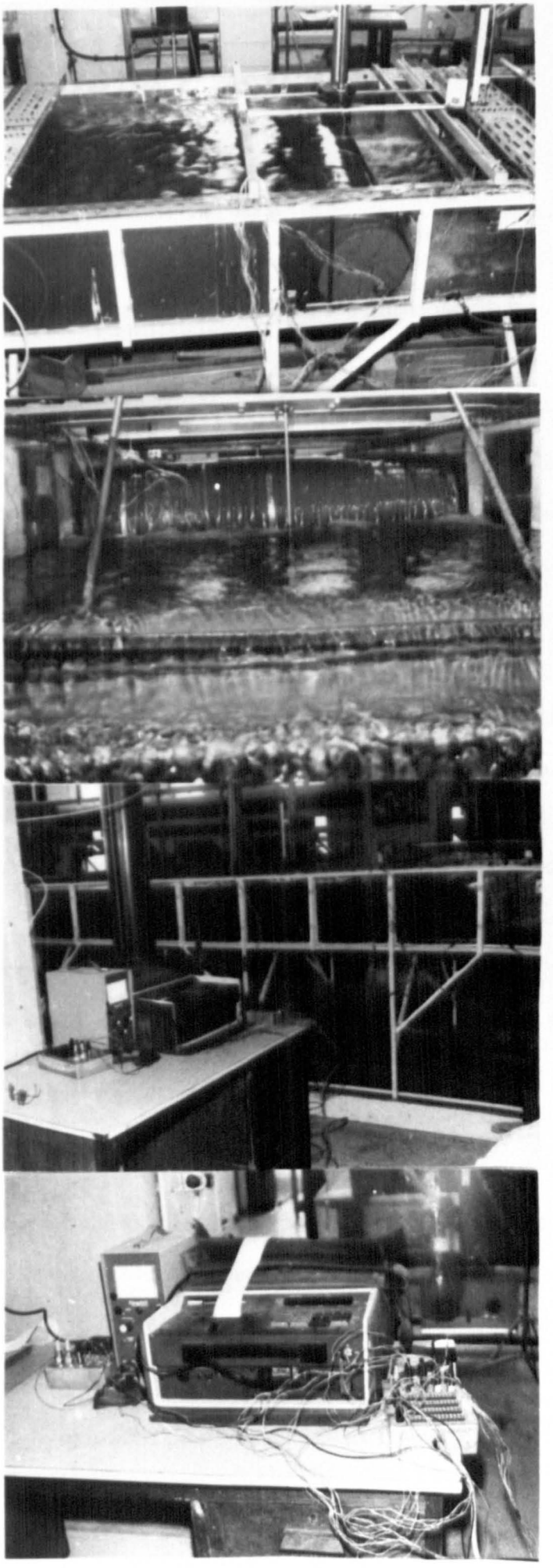

FIG.(5-12) INFLATABLE DAM INFLATED BY AIR UNDER TEST TO MEASURE THE TENSION USING STRAIN GAUGES

reflected in fig.5.13. This behaviour was not found in the case when the downstream head was lowered from 140 mm to 120 mm. This means that it is possible to get a high dam with low internal pressure, which results in a low tension in the material by increasing the downstream head.

5.5.2 Behaviour of water inflated dam.

In order to study the behaviour of a water inflated dam, two internal water pressures of 330 mm and 600mm were used for different downstream heads. The variation in the downstream head was over the same range as for the air inflated condition. It was noticed that the dam height increased with increasing downstream head and also that the height of the dam decreased with increasing the overflow head for a constant downstream head.

The behaviour of the dam with an internal pressure head equal to 330 mm and the downstream head equal to 100 mm and increasing the overflow from 25 to 30 mm was such that the crest height reduced by 5.10 mm whilst when the downstream head was equal to 140 mm the reduction in the height of the crest was equal to 1.4 mm. When the pressure inside the dam increased to 600 mm with all other conditions kept constant the result was that a reduction at 0.7 mm for the downstream head equal to 100 mm and 0.5 mm for the downstream head equal to 140 mm.

It was also observed that when the overflow head was equal to 25 mm, a dam of 330 mm internal pressure head and under a downstream head equal to 100 mm, the maximum height was 155.3 mm whilst the height rose to 161.0 mm for the condition of downstream head equal to 140 mm with the same overflow head, giving a dam height increase of 5.7 mm. This condition can be repeated by changing the pressure head to 600 mm and keeping the other conditions constant the maximum height of the dam with downstream head equal to 100 mm is 169 mm whilst the maximum height of the dam with downstream head equal to 140 mm is 172 mm, and hence the crest height increased by 3 mm. The results

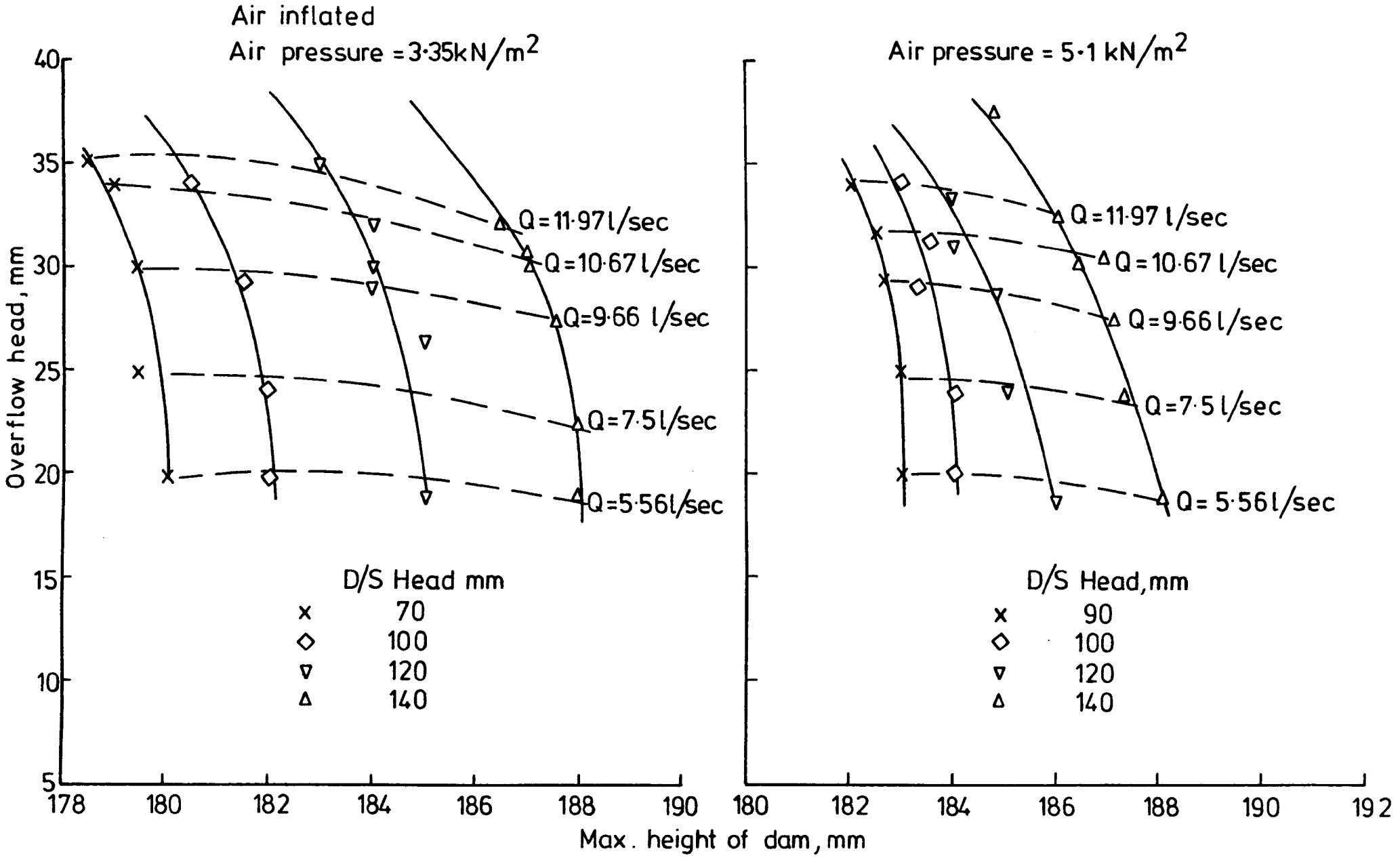

FIG. (5-13) MAXIMUM HEIGHT OF DAM Vs. DIFFERENT OVERFLOW HEADS FOR AN AIR INFLATED STRUCTURE

show that the rate of increase in height of the crest is higher for low internal pressures and low for high internal pressure with increasing downstream head.

Hence the height of the dam depends mainly on the internal pressure head, downstream head and the overflow head.

The behaviour of a water inflated dam with different overflows and downstream heads is shown in fig.5.14.

5.5.3 Behaviour of an (air+water) inflated dam.

The behaviour of an (air+water) inflated dam was similar to the previous conditions for both air and water inflated dams, but the rate of change of the crest height was different depending on the depth of water inside the dam. In this study two dams with different depths of water inside but both with a total internal pressure head equal to 600 mm were used to observe the behaviour of the two cases as follows.

For the dam with an internal water depth equal to 15 percent of the maximum height of the dam an overflow head equal to 25 mm and a downstream head equal to 100 mm the height was equal to 178.1 mm. The maximum height for the same condition but changing the downstream head to 140 mm was 181.6 mm, when all the above conditions were kept constant but the depth of water inside the dam was changed to 75 percent of the maximum height, the results showed that the maximum height with the downstream head equal to 100 mm was 171 mm while the crest height was 174.3 mm for a downstream head equal to 140 mm. The crest height of the dam reduced by 7.1 mm with the downstream head equal to 100 mm and reduced by 7.33 mm with the downstream head equal to 140 mm. This difference was due to changing the depth of water inside the dam from 15 to 75 percent.

Fig.5.15 shows in detail the above behaviour for the dam inflated with air and with different internal water depths and fig.5.16 shows a dam inflated with air under observation.

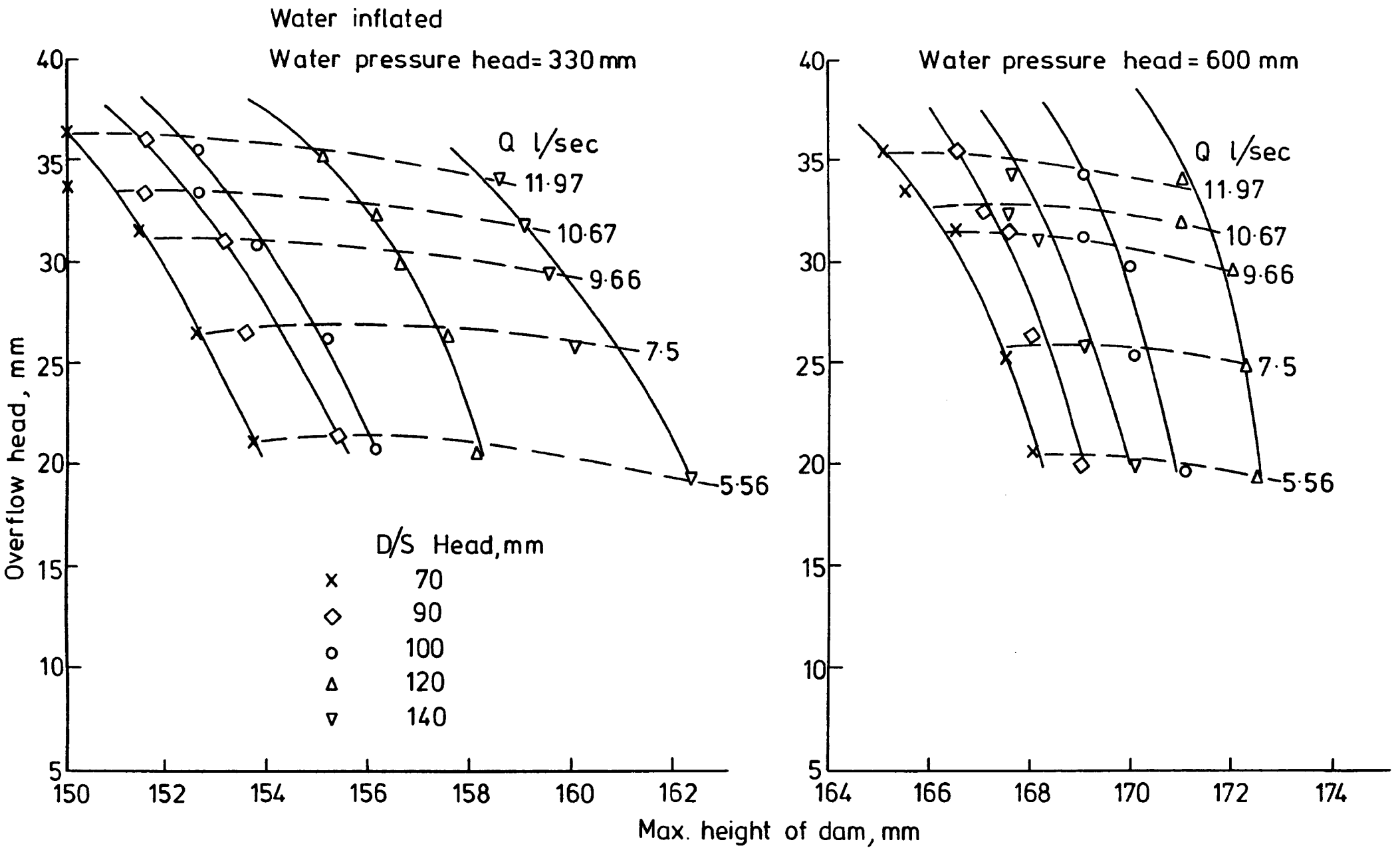

FIG. (5-14) MAXIMUM HEIGHT OF DAM Vs. DIFFERENT OVERFLOW HEADS FOR A WATER INFLATED STRUCTURE

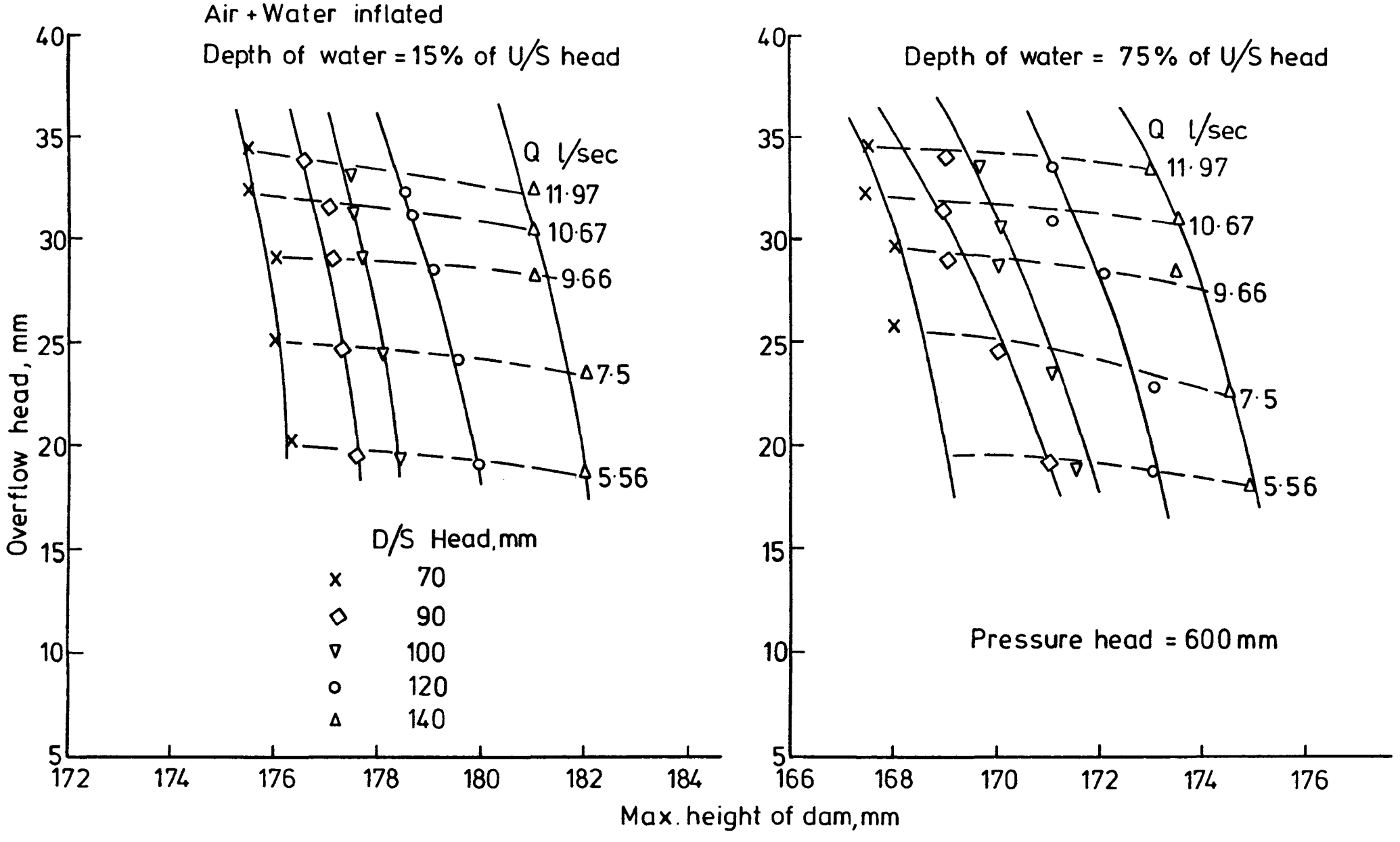

FIG.(5-15) MAXIMUM HEIGHT OF DAM Vs. DIFFERENT OVERFLOW HEADS FOR AN AIR + WATER INFLATED STRUCTURE

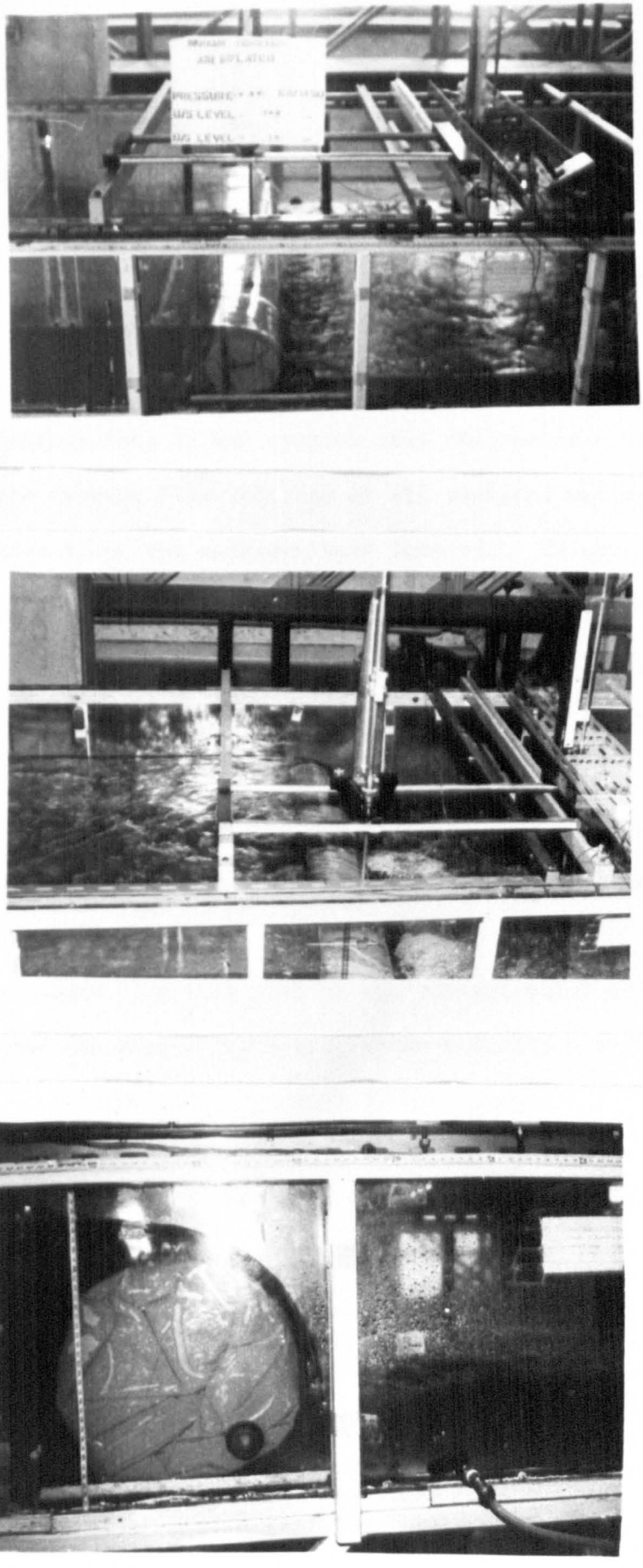

FIG. (5-16) AIR INFLATED DAM UNDER OBSERVATION

5.6 Theoretical Analysis.

The inflatable hydraulic structure under hydrodynamic conditions has been analysed in order to find the tension, slope, elongation, cross-sectional area, maximum height and profile of the dam in a similar way to that adopted for static conditions.

On the upstream face it was assumed that the specific energy was constant and the average flow velocity at all sections was constant and frictional forces along the membrane were ignored. It was considered that only the static water pressure was operating (3). On the downstream face the flow was considered as passing down the lower surface of the dam without giving rise to any break away at all and this condition assumed the flow to be fully aerated.

Naturally due to the fact that the flow descends over a curved surface, the flow is influenced by both a centrifugal force and the self weight of water.

Since the volume flow rate (36) at the control point on the dam is already known one can obtain the average flow velocity v as the following:

$$v = q/h_e \qquad 5.2$$

by assuming the flow over the dam surface has uniform flow velocity.

In this study the depth of water on the surface of the dam on the downstream face is approximately constant and it was found experimentally that this depth was related to the overflow head.

It was found experimentally and from fig.5.17 that the depth of water over the crest (h_e) was equal to 0.69 of the overflow head (H) and this result was obtained by examining different heads for different inflation pressures for all inflation conditions.

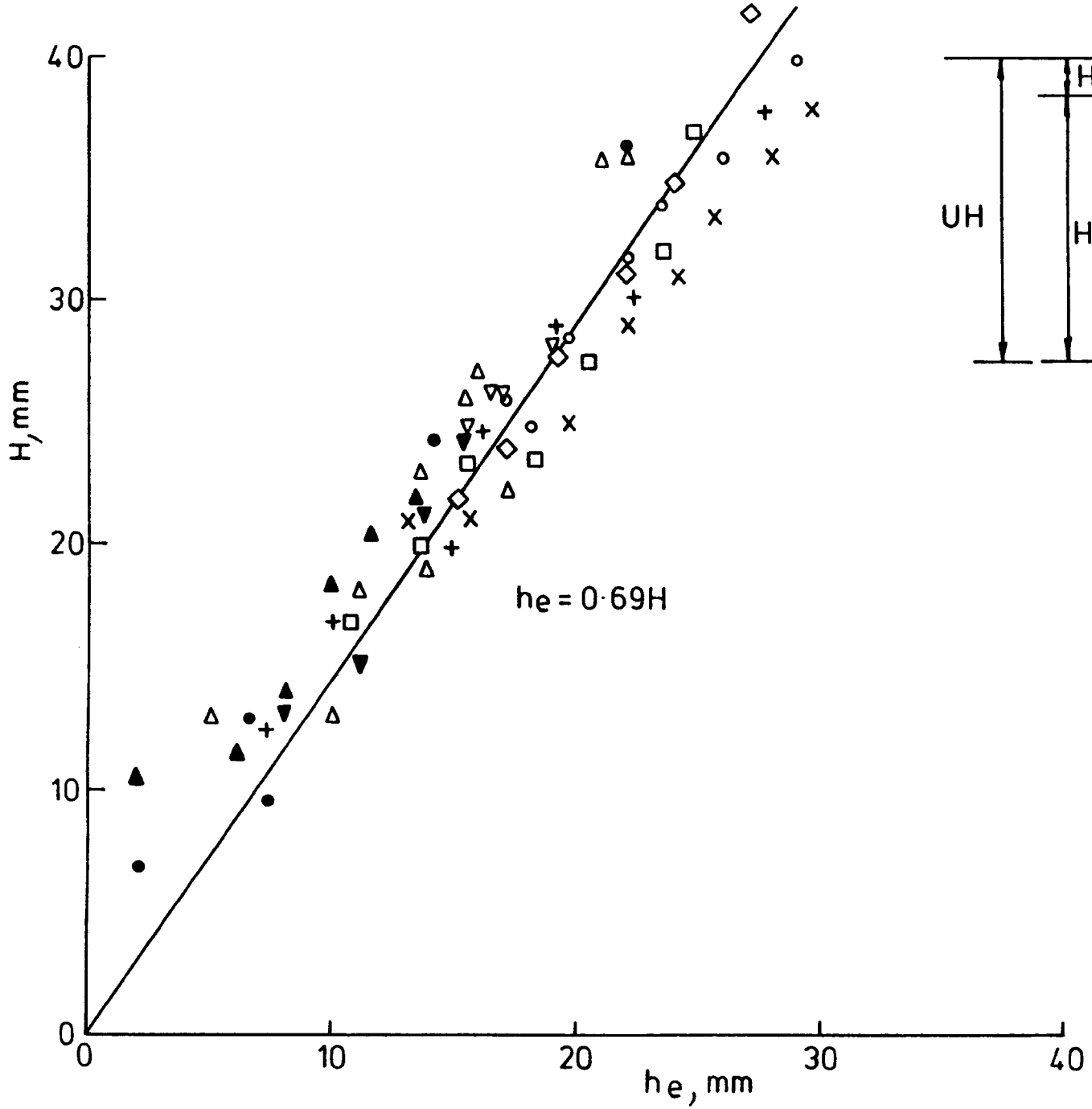

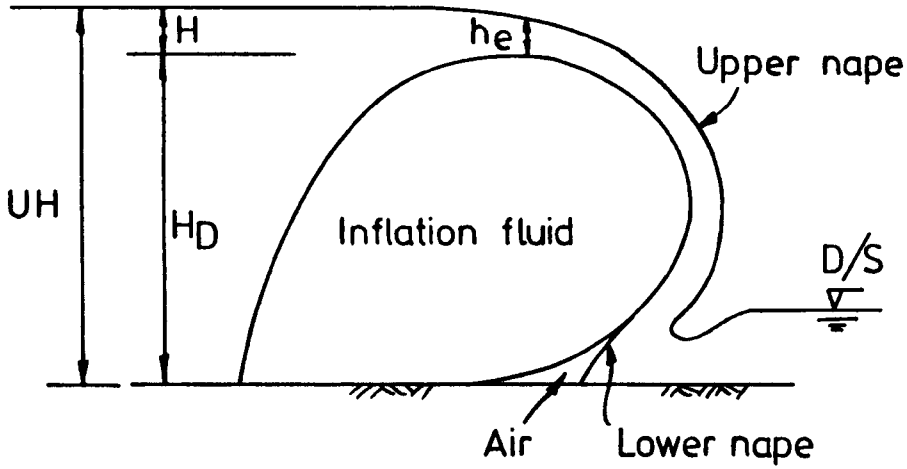

	Inflation pressures	
	Air, kN/m	Water, mm
x	4·46	0
o	5·05	0
◇	6·64	0
▽	0·0	688
●	0·0	443
+	0·0	276
△	5·886	100
▼	4·159	100
□	3·355	100

FIG. (5-17) OVERFLOW HEAD (H) Vs. DEPTH OF WATER OVER THE CREST (h_e)

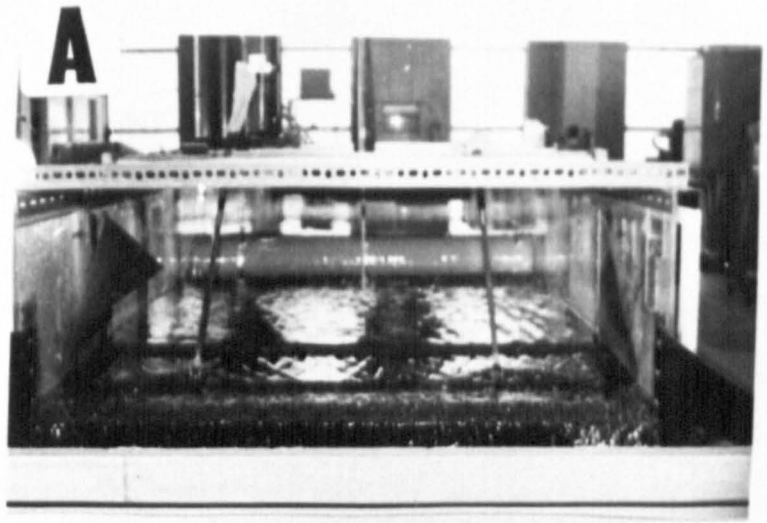

(a) Low flow

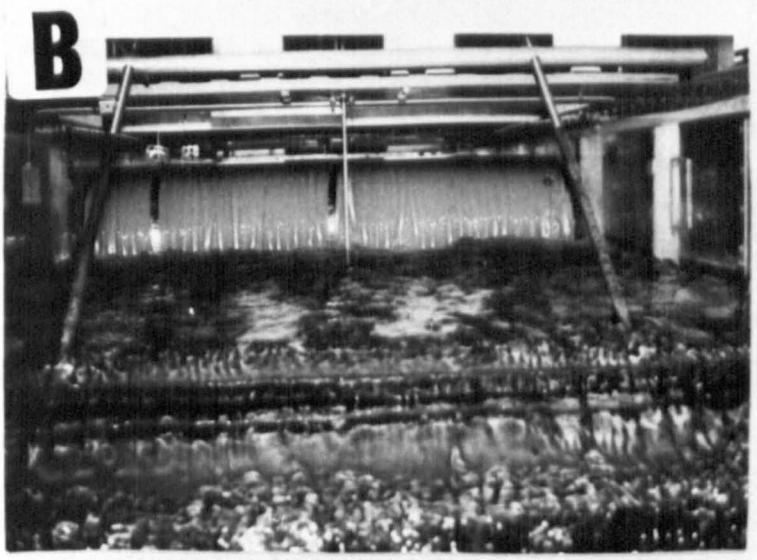

(b) High flow

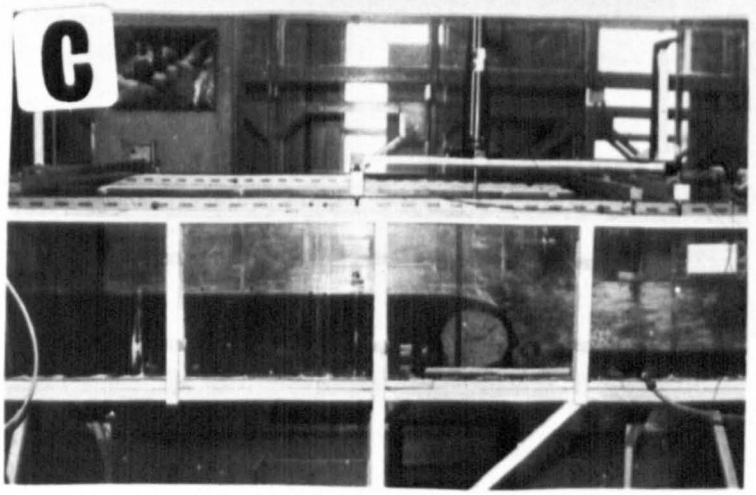

(c) Variation of the overflow head (H) with depth of water over the crest (he) see FIG.(5-17)

FIG.(5-18) BEHAVIOUR OF THE FLOW OVER THE CREST

On the basis of these results which can be seen in fig.5.17 and fig. 5.18, the depth of water on the downstream face of the dam was considered in order to find the effect of the centrifugal force and the self weight of water.

As mentioned earlier the analysis of the hydrodynamic condition was similar to the hydrostatic condition which required dividing the membrane into (n) elements with (n+1) nodes. The magnitude and location of the loads acting on each element due to upstream head, downstream head, internal pressure, weight of membrane and the centrifugal force were analysed, on each element in order to find the resultant of the forces on each element. From this procedure the shape of the dam can be determined. The analysis of the forces on an element are shown in fig.5.19 A. The co-ordinates of the final element did not always coincide with the base width resulting in a mis-close. This mis-close was overcome by the same procedure as in the static condition by using the Newton-Iteration method (31) to correct the tension and slope of the first element on the upstream side.

This procedure was repeated to minimize the mis-close to within acceptable limits. It was noticed that for an air inflated dam under ten different overflows the maximum error of mis-close was 0.3 mm and minimum mis-close was 0.01 mm and these were found from a maximum number of iterations of 5 and a minimum number of iterations of 2. An increase in the number of iterations increased the time required on the computer, so the smaller the number of iterations the better.

A computer program for the static condition (IHSIP) was modified for use in the hydrodynamic condition (DYIHSIP). The program of the dynamic condition used the same number of cards as shown in table 4.1, Chapter 4, except Card Number 5 which was changed to the form NTYPE = 1 to NTYPE = 2 in order to analyse a dam under hydrodynamic condition. Fig.5.19B shows water and air inflated dams analysed under 50 number of elements.

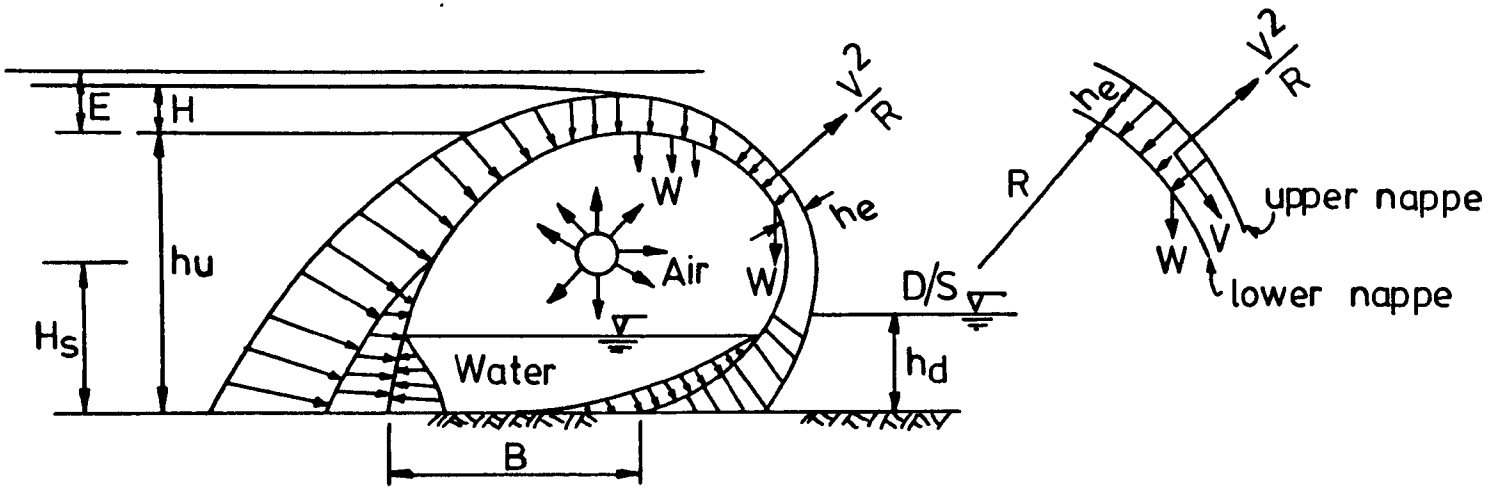

FIG. FORCES ACTING ON A DAM

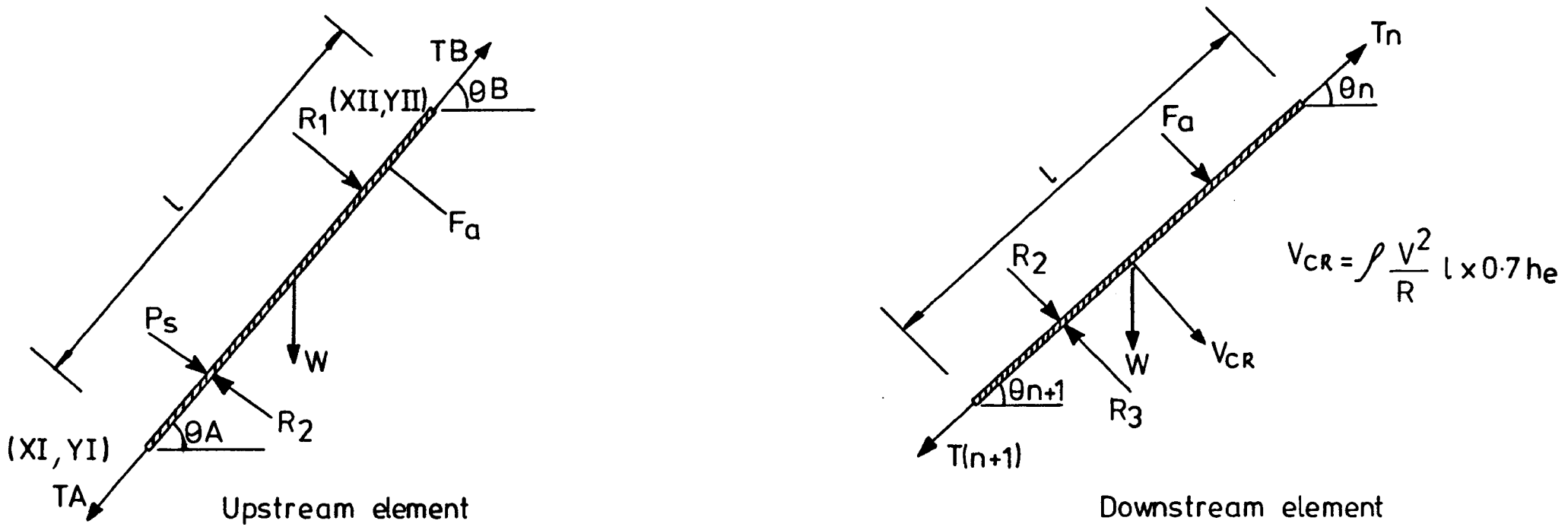

FIG.(5-19A) FORCES ACTING ON INDIVIDUAL ELEMENTS

U/S HEAD	=	0.2460	METER
D.S HEAD	=	0.0400	METER
AIR PRESSURE	=	0.0000	KN/SQ.M
WATER PRESSURE	=	0.5004	M.W.G.
ORIGINAL LENGTH	=	0.8007	METER
NEW LENGTH	=	0.8191	METER
U/S TENSION	=	0.3252	KN/M
U/S SLOPE	=	116.8034	DEGREE
D S TENSION	=	0.4467	KN/M
BASE LENGTH	=	0.1635	METER
MAX. HEIGHT	=	0.2176	METER
ALFA	=	1.4000	
AREA	=	0.0501	METER SQ
SILT DEPTH,HS	=	0.0000	METER
OVERFLOW HEAD	=	0.0304	METER
CD	=	0.3776	
RATE OF FLOW	=	9.1363	LET/SEC

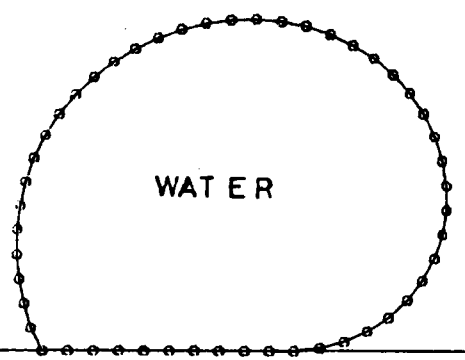

U/S HEAD	=	0.2590	METER
D/S HEAD	=	0.0000	METER
AIR PRESSURE	=	3.9840	KN/SQ.M
WATER PRESSURE	=	0.0000	M.W.G.
ORIGINAL LENGTH	=	0.8005	METER
NEW LENGTH	=	0.8096	METER
U/S TENSION	=	0.3600	KN/M
U/S SLOPE	=	99.6847	DEGREE
D/S TENSION	=	0.4850	KN/M
BASE LENGTH	=	0.1362	METER
MAX. HEIGHT	=	0.2231	METER
ALFA	=	0.6000	
AREA	=	0.0481	METER SQ
SILT DEPTH,HS	=	0.0000	METER
OVERFLOW HEAD	=	0.0359	METER
CD	=	0.3980	
RATE OF FLOW	=	14.7915	LET/SEC

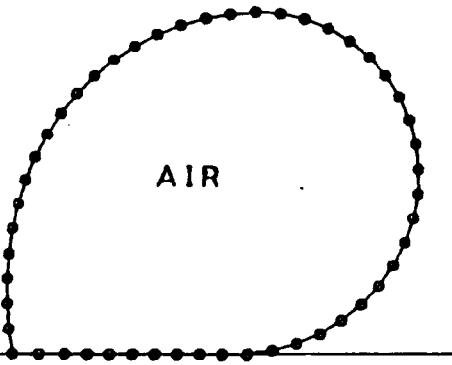

FIG. 5·19B OUTPUT OF WATER INFLATED DAM FOR 50 NUMBER OF ELEMENTS USING PROGRAM DYIHSIP

From the study of the behaviour of the flow over the crest for different conditions and for different inflation fluids a range of calibration equations were obtained to calculate the rate of flow and coefficient of discharge (detail in Chapter 7).

The program (DYIHSIP) calculated the rate of flow and coefficient of discharge in order to use this in the analysis for the dam shape and the following points needed to be considered.

1. Analyse the dam by only considering the static forces on the upstream and downstream faces.

2. Calculate the rate of flow and radius of curvature from the initial analysis by finding the ratio (H/H_D) for the particular proportional factor and type of inflation fluid.

3. Re-analyse the dam to consider the effect of the centrifugal force on the downstream force after calculating the rate of flow.

4. Using the iteration method minimize the mis-close and then find the shape of the dam and final maximum height of dam.

Fig.5.20 A, B and C shows the output of the program (DYIHSIP) for dams inflated with air, water and (air+water) respectively and under different overflow heads ranges between 14 to 56 mm.

5.7 Effect of the operational parameters on different output parameters.

The main operational parameters of an inflatable hydraulic structure under hydrodynamic conditions are

1. Overflow head (difference between the upstream head and maximum height of dam).
2. Downstream head.
3. Silt depth.
4. Internal pressure head.

U/S HEAD	=	0.2650	METER
D/S HEAD	=	0.1000	METER
AIR PRESSURE	=	5.4390	KN/SQ.M
WATER PRESSURE	=	0.0000	M.W.G.
ORIGINAL LENGTH	=	0.8006	METER
NEW LENGTH	=	0.8127	METER
U/S TENSION	=	0.4963	KN/M
U/S SLOPE	=	116.3637	DEGREE
D/S TENSION	=	0.6820	KN/M
BASE LENGTH	=	0.1136	METER
MAX. HEIGHT	=	0.2403	METER
ALFA	=	1.1000	
AREA	=	0.0504	METER SQ
SILT DEPTH,HS	=	0.0500	METER
OVERFLOW HEAD	=	0.0247	METER
CD	=	0.3789	
RATE OF FLOW	=	7.2960	LET/SEC

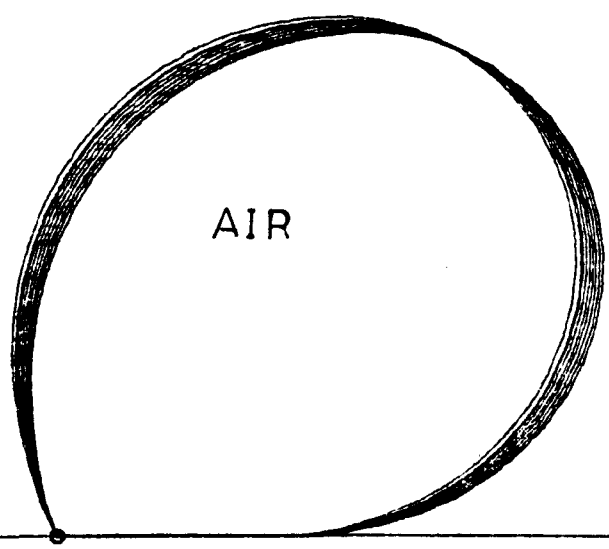

FIG.(5-20A) OUTPUT OF AN AIR INFLATED DAM UNDER DIFFERENT OVERFLOW HEADS

U/S HEAD	=	0.2290	METER
D/S HEAD	=	0.0000	METER
AIR PRESSURE	=	0.0000	KN/SQ.M
WATER PRESSURE	=	0.5235	M.W.G.
ORICINAL LENGTH	=	0.8000	METER
NEW LENGTH	=	0.8087	METER
U/S TENSION	=	0.3435	KN/M
U/S SLOPE	=	116.9433	DEGREE
D/S TENSION	=	0.4768	KN/M
BASE LENGTH	=	0.1536	METER
MAX. HEIGHT	=	0.2151	METER
ALFA	=	1.5000	
AREA	=	0.0468	METER SQ
SILT DEPTH,HS	=	0.0500	METER
OVERFLOW HEAD	=	0.0139	METER
CD	=	0.3568	
RATE OF FLOW	=	2.7039	LET/SEC

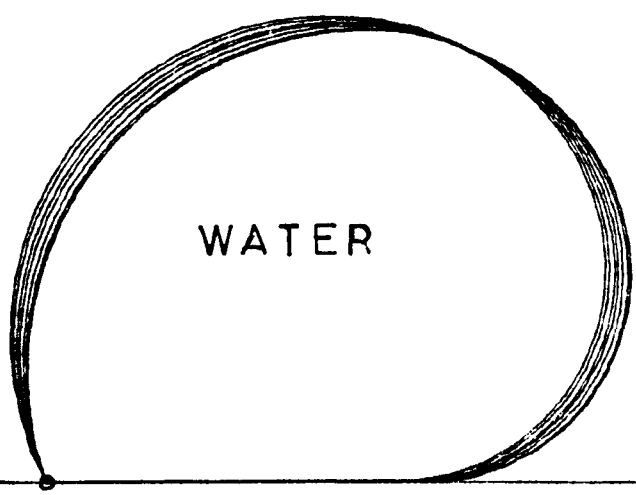

FIG. (5-20B) OUTPUT OF A WATER INFLATED DAM UNDER DIFFERENT OVERFLOW HEADS

U/S HEAD	=	0.2390	METER
D/S HEAD	=	0.1000	METER
AIR PRESSURE	=	2.5450	KN/SQ.M
WATER PRESSURE	=	0.1575	M.W.G.
ORIGINAL LENGTH	=	0.8009	METER
NEW LENGTH	=	0.8075	METER
U/S TENSION	=	0.2503	KN/M
U/S SLOPE	=	97.1483	DEGREE
D/S TENSION	=	0.3293	KN/M
BASE LENGTH	=	0.1824	METER
MAX. HEIGHT	=	0.2113	METER
ALFA	=	1.0000	
AREA	=	0.0469	METER SQ
SILT DEPTH,HS	=	0.0500	METER
OVERFLOW HEAD	=	0.0277	METER
CD	=	0.3731	
RATE OF FLOW	=	8.9215	LET/SEC

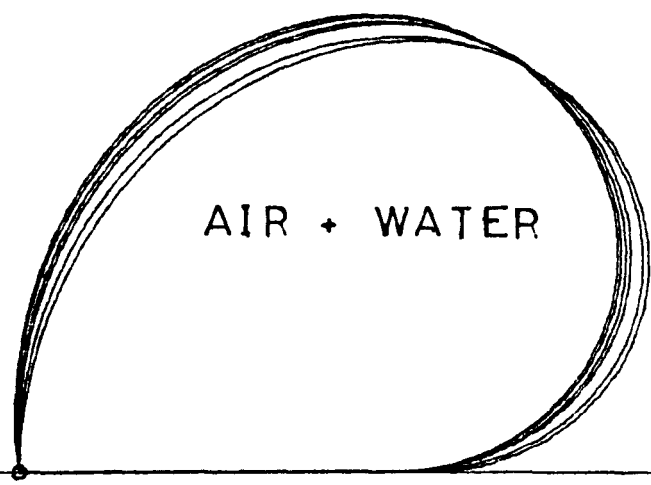

FIG. (5-20C) OUTPUT OF AN AIR+WATER INFLATED DAM UNDER DIFFERENT OVERFLOW HEADS

The above operation of parameters have to be known in order to find the output from the program (DYIHSIP) which are represented by the following parameters.

1. Tension.
2. Upstream slope.
3. Elongation of the membrane.
4. Maximum height of dam.
5. Cross-sectional area and profiles of the dam.

In this analysis type I material was used with design length equal to 0.80 m and the results are discussion in the following sections.

5.7.1 Tension.

The study of the behaviour of the upstream tension and downstream tension for the dam under different overflows showed that the tension increased with increasing the proportional factor alpha and that the tension in the upstream face was less than the downstream face. However the tension decreased with an increase in the overflow. This pattern of behaviour was the same for the different inflation fluid as shown in fig.5.21 and fig.5.22 for the upstream and downstream tension under different conditions of downstream heads and silt pressure for an air dam. Fig.5.23 shows the variation of the upstream tension and downstream tension for a water inflated dam and fig. 5.24 shows the variation of the upstream and downstream tension for an (air+water) inflated dam.

The tension found considered the effect of silt on the upstream face of the dam and the effect of different downstream heads. The results show that for all three conditions of inflation fluids, tension decreased with increasing the downstream head and also tension was reduced by increasing the depth of silt on the upstream face of the dam.

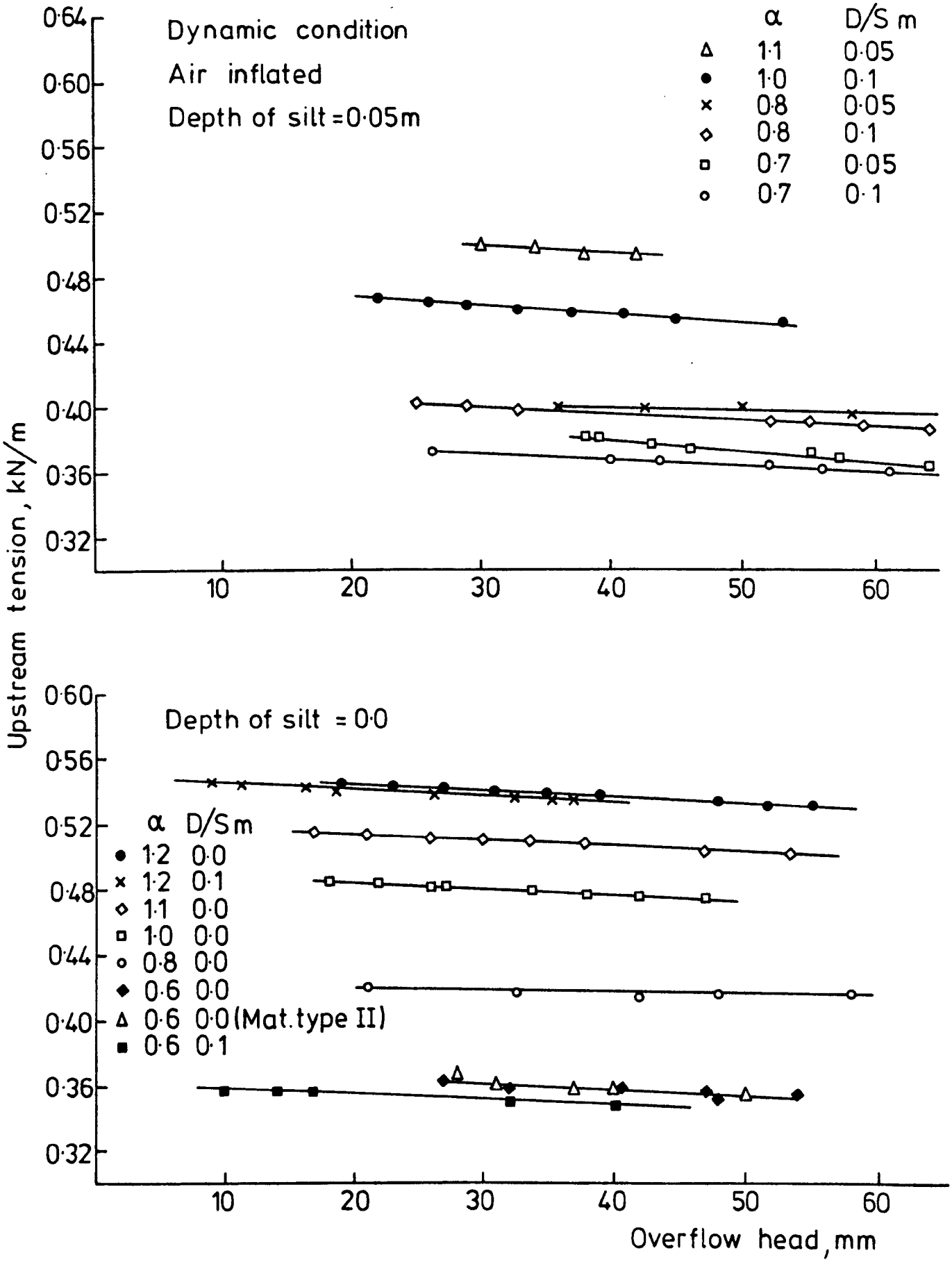

FIG. (5-21) UPSTREAM TENSION Vs. DIFFERENT OVERFLOW HEADS FOR AN AIR INFLATED STRUCTURE

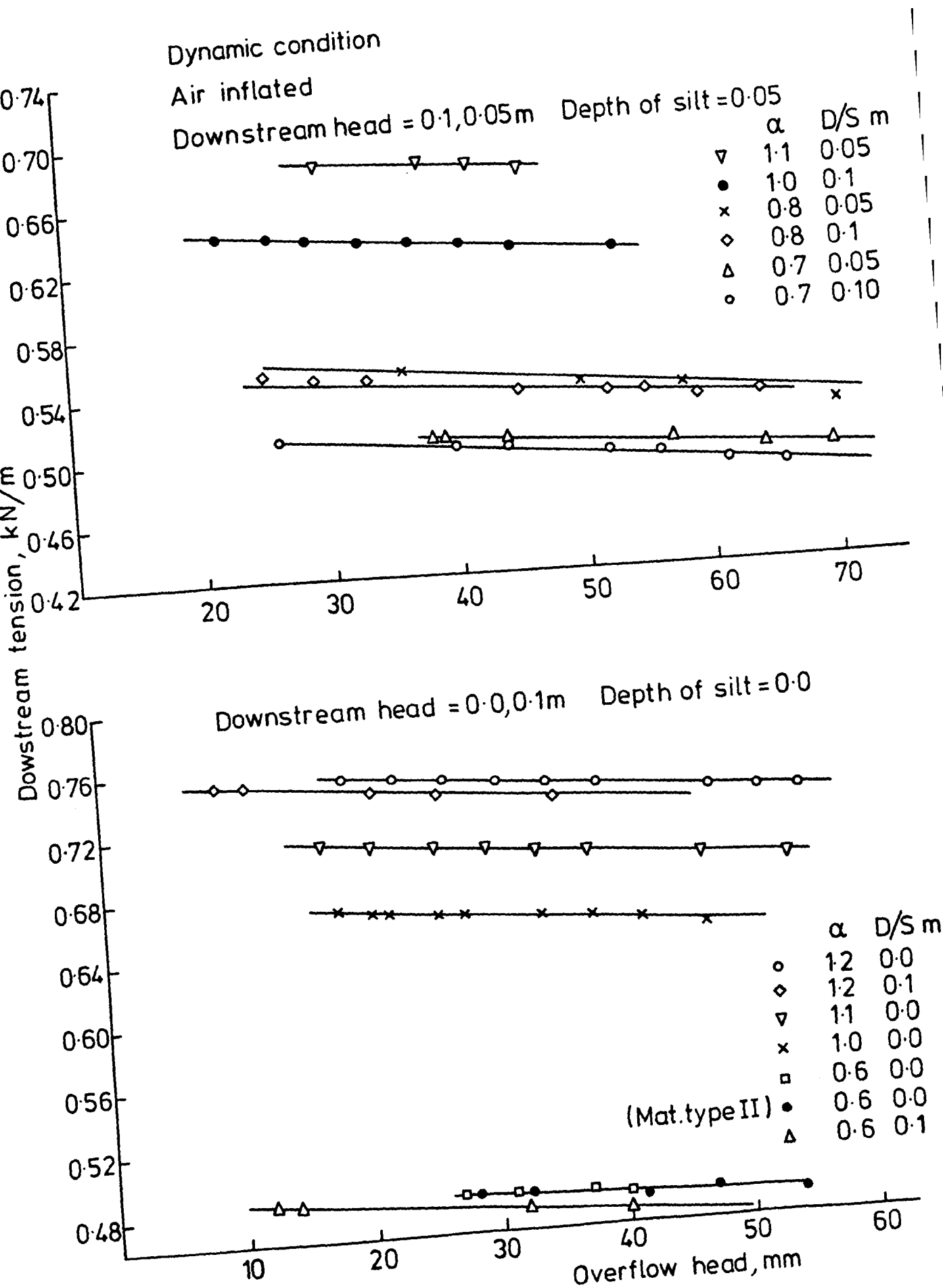

FIG. (5-22) DOWNSTREAM TENSION Vs. DIFFERENT OVERFLOW HEADS FOR AN AIR INFLATED STRUCTURE

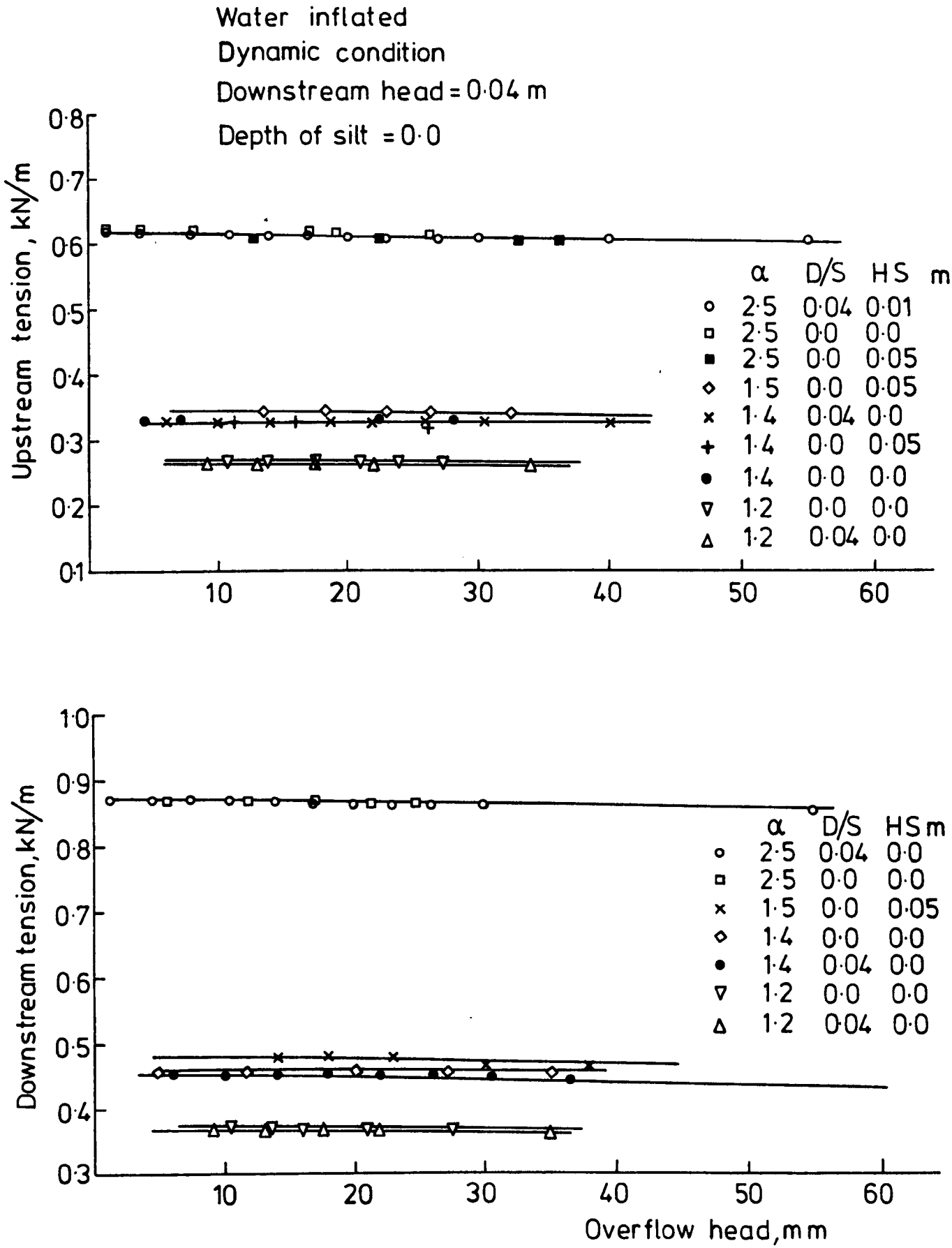

FIG. (5-23) UPSTREAM AND DOWNSTREAM TENSION Vs. DIFFERENT OVERFLOW HEADS FOR WATER INFLATED STRUCTURE

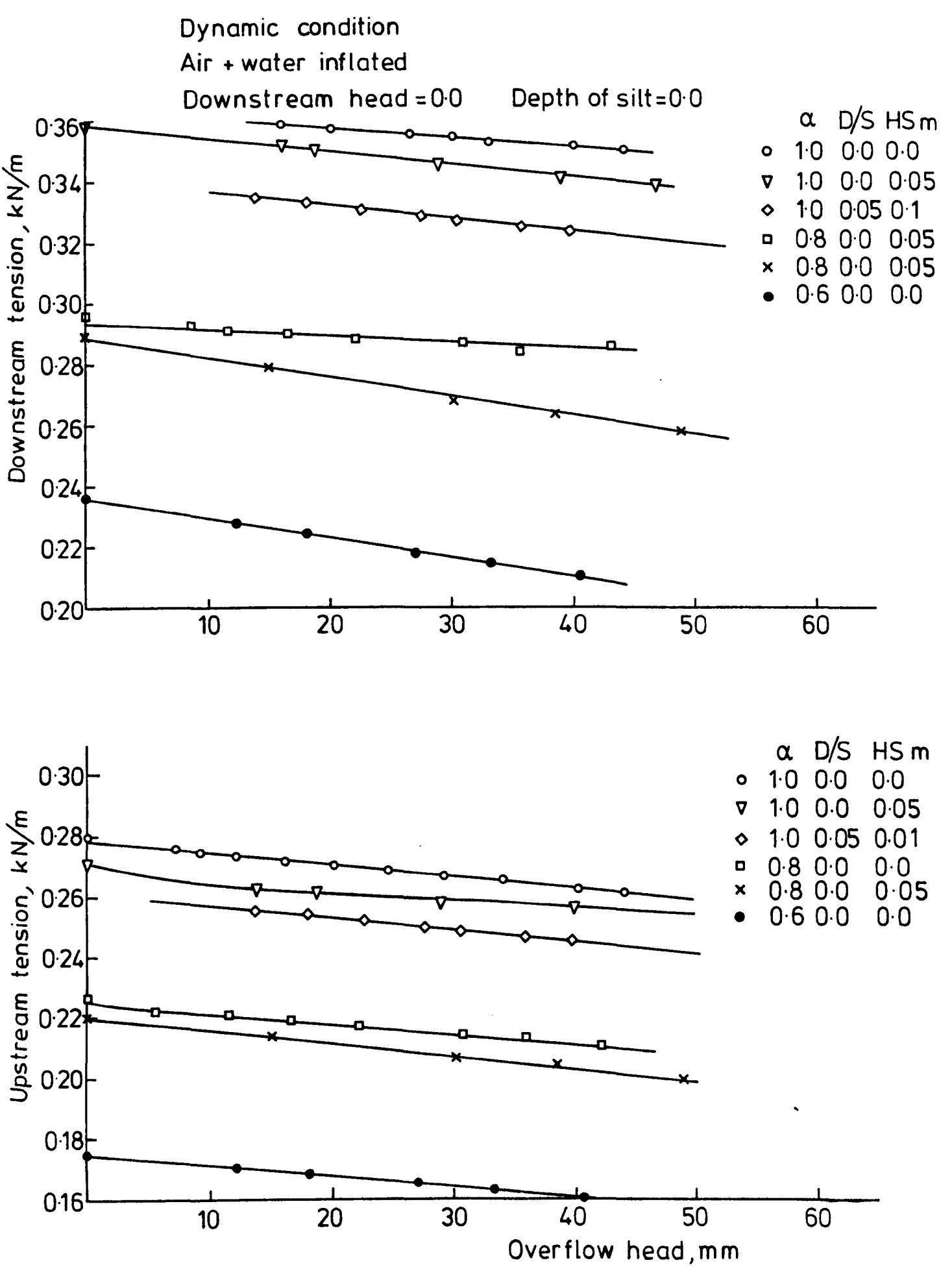

FIG. (5-24) UPSTREAM AND DOWNSTREAM TENSION Vs. DIFFERENT OVERFLOW HEADS FOR AN AIR+WATER INFLATED STRUCTURE

The reduction in tension when increasing the overflow head has been observed in the experimental work shown in table 5.3 and 5.4 measured using strain gauges inside an air inflated dam for the conditions of downstream head equal to zero and 0.10 m respectively.

The phenomenon of decreasing tension with increasing the overflow was also observed by Stodulka (37) in his experimental work.

5.7.2 Upstream slope.

The upstream slope of the dam decreased as the overflow head increased for all three conditions of inflation, but the slope of the upstream face increased as the proportional factor increased. When the downstream head and silt pressure were taken into consideration the upstream slope increased with increasing downstream head while the upstream slope decreased as the effect of silt pressure on the upstream face of the dam was considered. Fig.5.25 shows the variation of the upstream slope with different overflow heads for an air inflated dam and fig.5.26 shows the variation of the upstream slope with different overflows for a water inflated dam. When considering different downstream heads and silt pressures it was found that for a proportional factor equal to 2.5 and for a downstream head equal to zero and zero silt the upstream was always the same for all overflows due to the high internal pressure. The downstream head when increased to 40 mm still did not result in any change in slope. Fig.5.27 shows the variations of the upstream slope with different overflows for a dam inflated with (air+ water) and under different conditions of downstream head and silt pressure. The behaviour shown is similar to both and and water inflated conditions.

5.7.3 The elongation of the dam material and maximum height of dam.

The reduction in the tension with increasing overflow head also resulted in a smaller elongation of the material but the magnitude of the

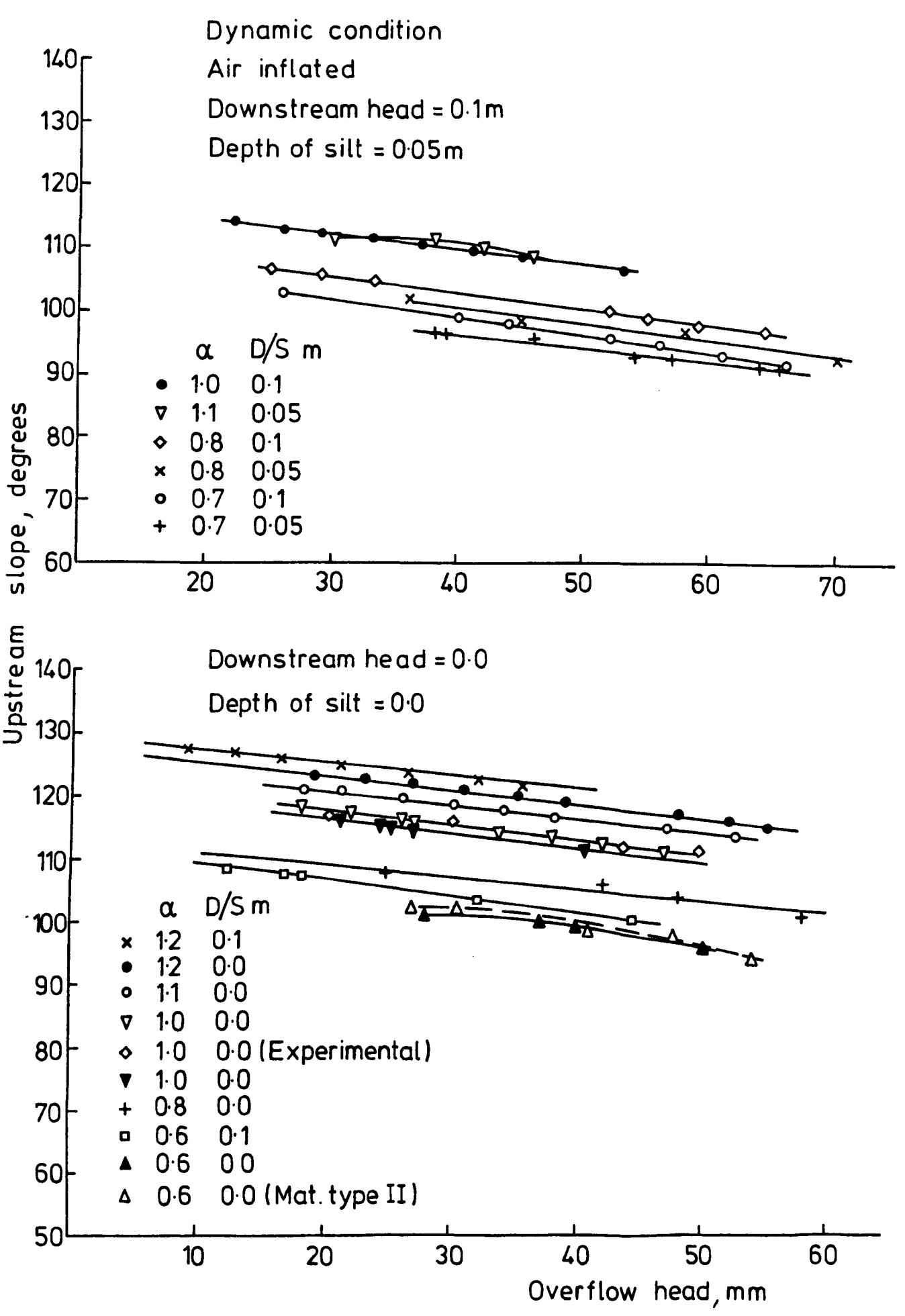

FIG. (5-25) UPSTREAM SLOPE Vs. DIFFERENT OVERFLOW HEADS FOR AN AIR INFLATED STRUCTURE

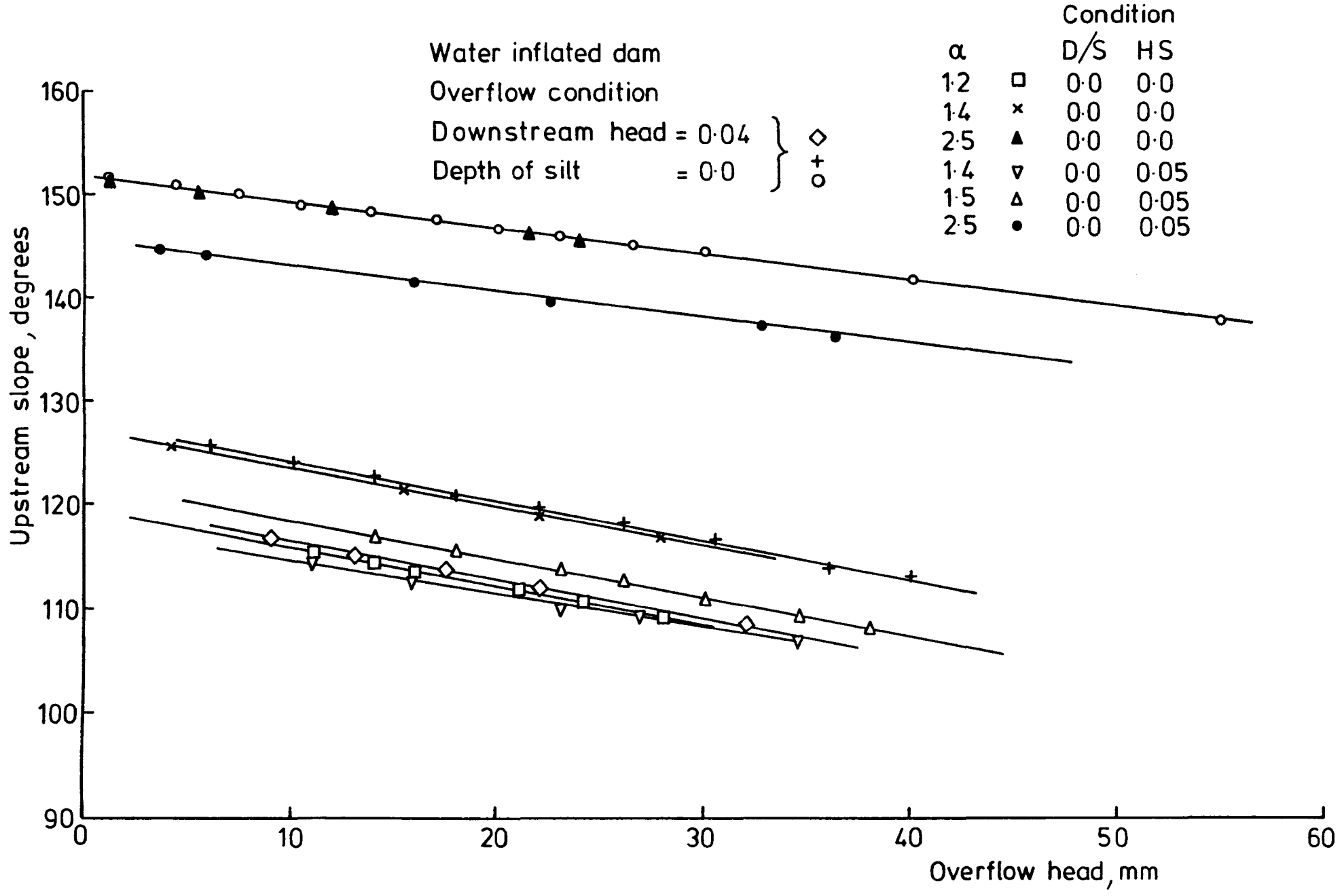

FIG.(5-26) UPSTREAM SLOPE Vs OVERFLOW HEAD FOR WATER INFLATED STRUCTURE

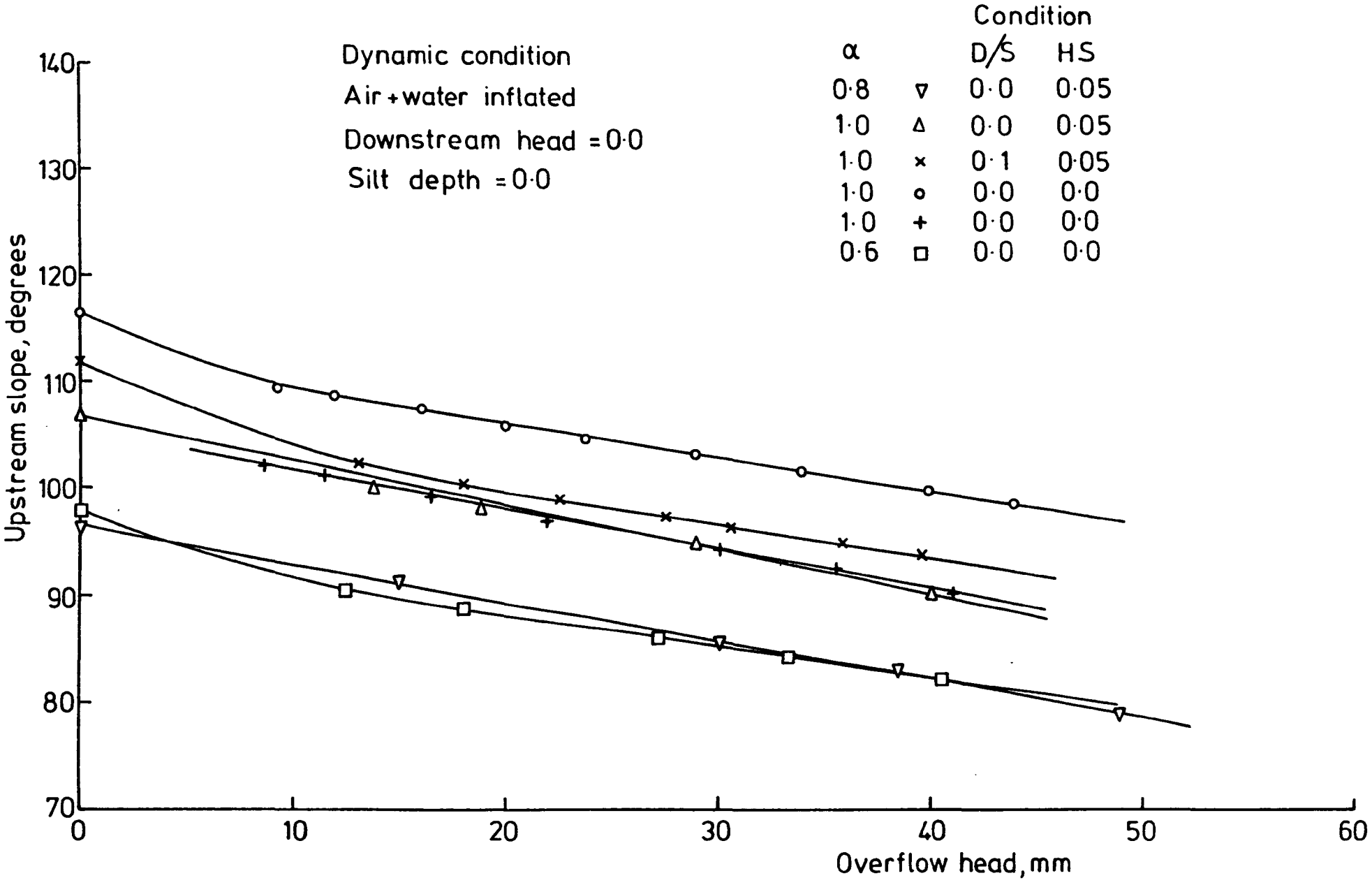

FIG. (5-27) UPSTREAM SLOPE Vs. DIFFERENT OVERFLOW HEADS FOR AN AIR+WATER INFLATED STRUCTURE

elongation of the material changed with respect to the proportional factor, downstream head and the silt pressure. For a low proportional factor the elongation was less than for a high proportional factor under the same overflow and downstream head and with no silt pressure. These changes are shown in fig.5.28 for an air inflated dam for different conditions of downstream head and silt pressure. The behaviour was similar for the case of water and (air+water) inflated dams, i.e. the elongation was less for low proportional factors and higher for high proportional factors as shown in fig.5.29 and fig.5.30.

The effect of silt on the upstream face was to cause a reduction in the elongation and also a decrease in the maximum height i.e. the dam was distorted to the downstream side. It was also observed that a dam inflated with air with a proportional factor equal to 0.6 and with downstream head equal to 100 mm, the maximum height was higher than a dam inflated with air with a proportional factor equal to 1.0 and with downstream head equal to zero and even with silt depth equal to 30 mm. This behaviour was also found experimentally as described. Section 5.5 and fig. 5.31 shows the variation of the maximum height of a dam for the air inflated condition.

Fig.5.32 shows the behaviour of the maximum height with respect to different overflows for the condition of a water inflated dam and shows that the maximum height increased with increasing downstream head and vice versa the maximum height of the dam reduced if the silt was included on the upstream face, and this behaviour was similar to the condition of an (air+water) inflated dam as shown in fig.5.33.

5.7.4 Cross-sectional area and profile of the dam.

The cross-sectional areas were calculated according to the equation 4.14 in Section 4.6.4 for different proportional factors under different overflow

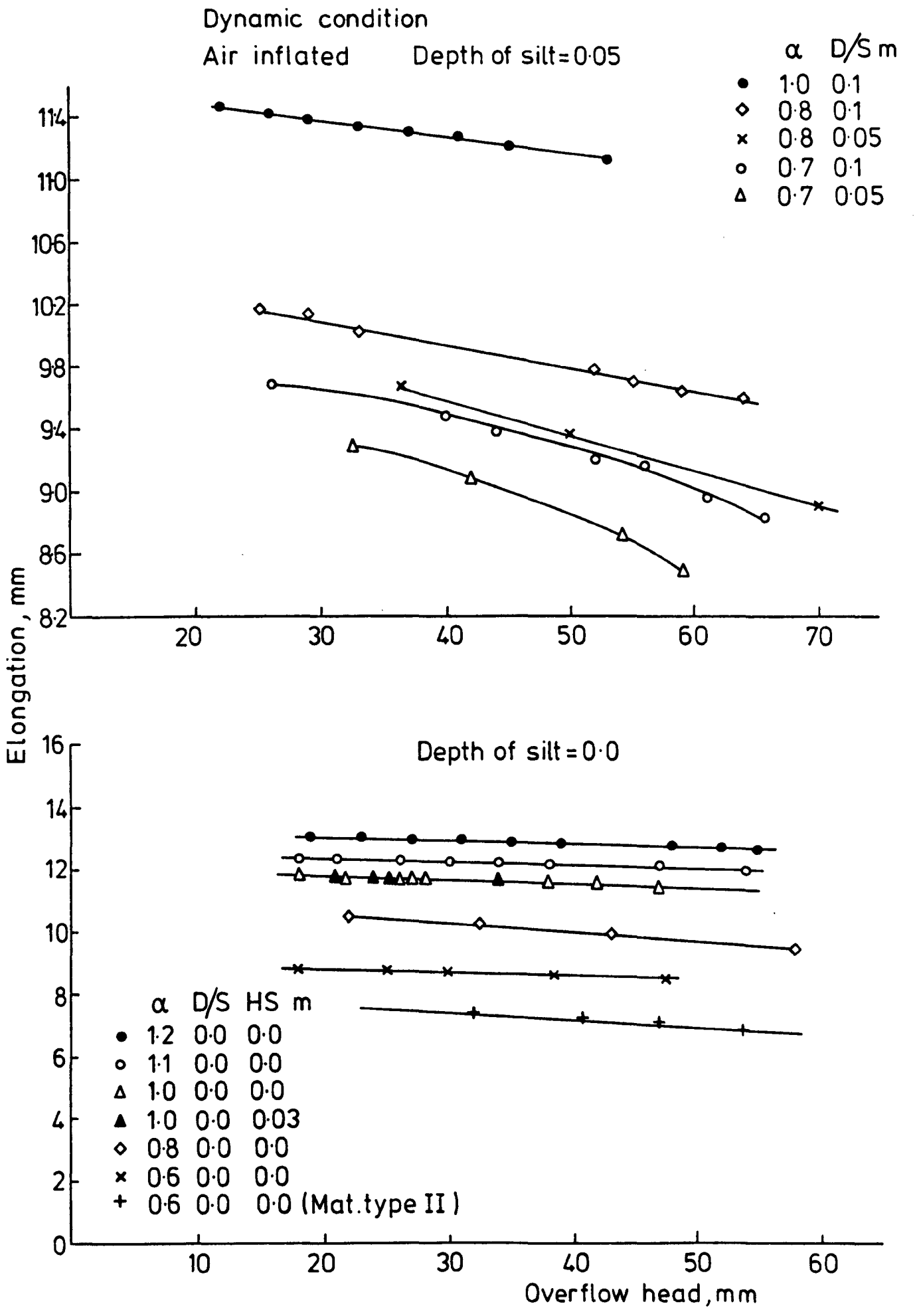

FIG.(5-28) ELONGATION Vs. DIFFERENT OVERFLOW HEADS FOR AN AIR INFLATED STRUCTURE

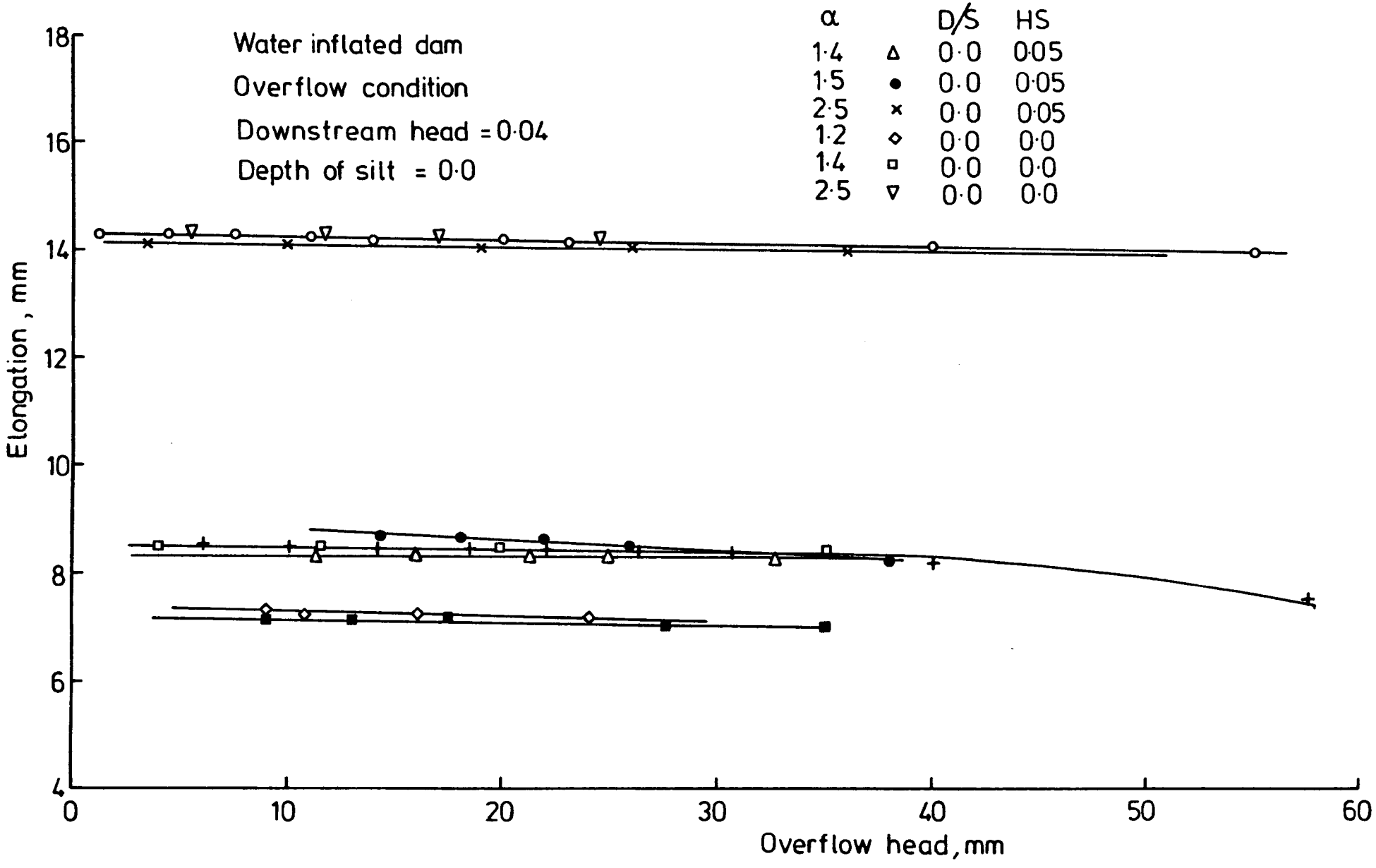

FIG. (5-29) ELONGATION Vs DIFFERENT OVERFLOW HEADS FOR WATER INFLATED STRUCTURE

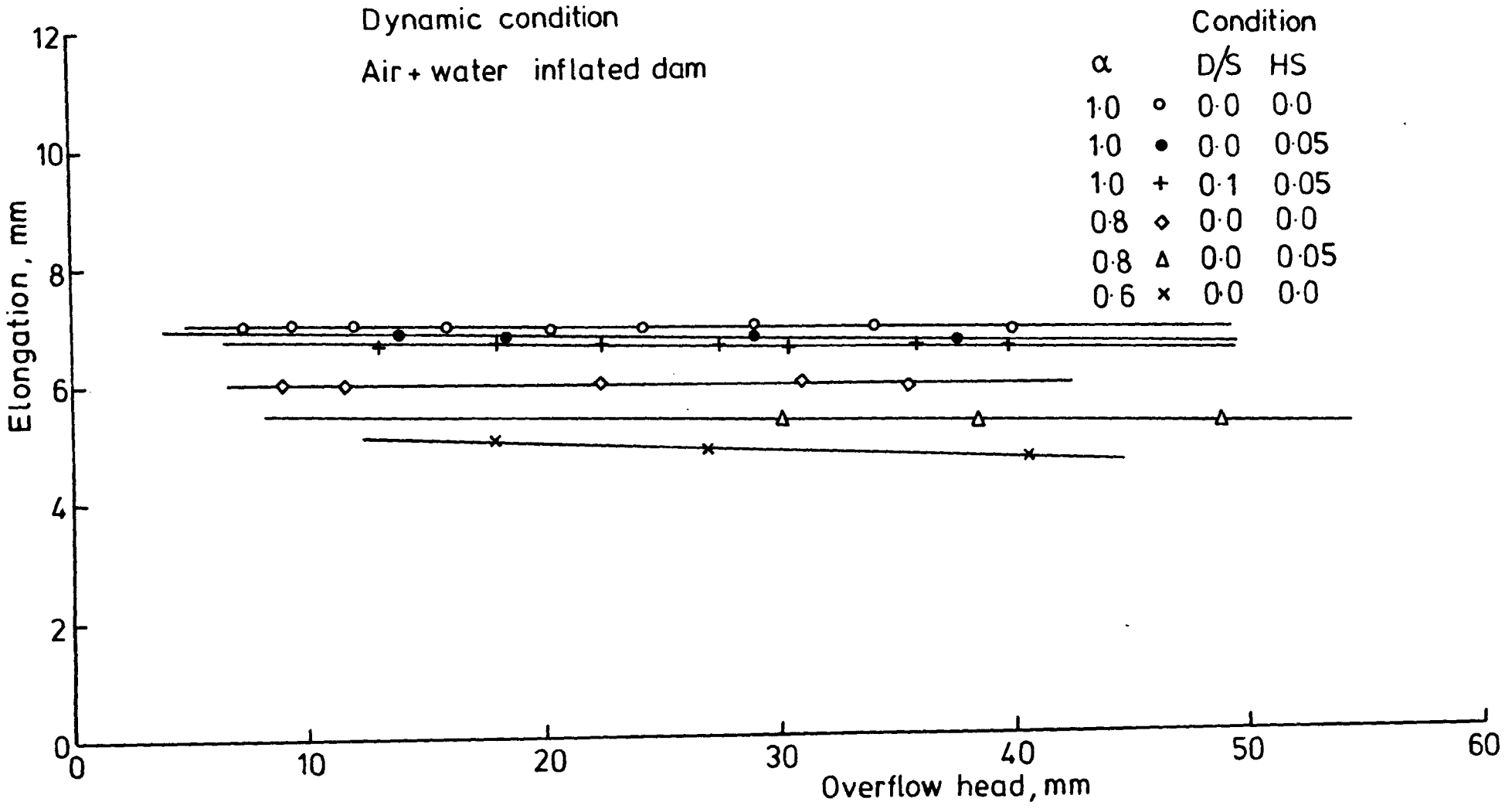

FIG. (5-30) ELONGATION Vs. DIFFERENT OVERFLOW HEADS FOR AN AIR+WATER INFLATED STRUCTURE

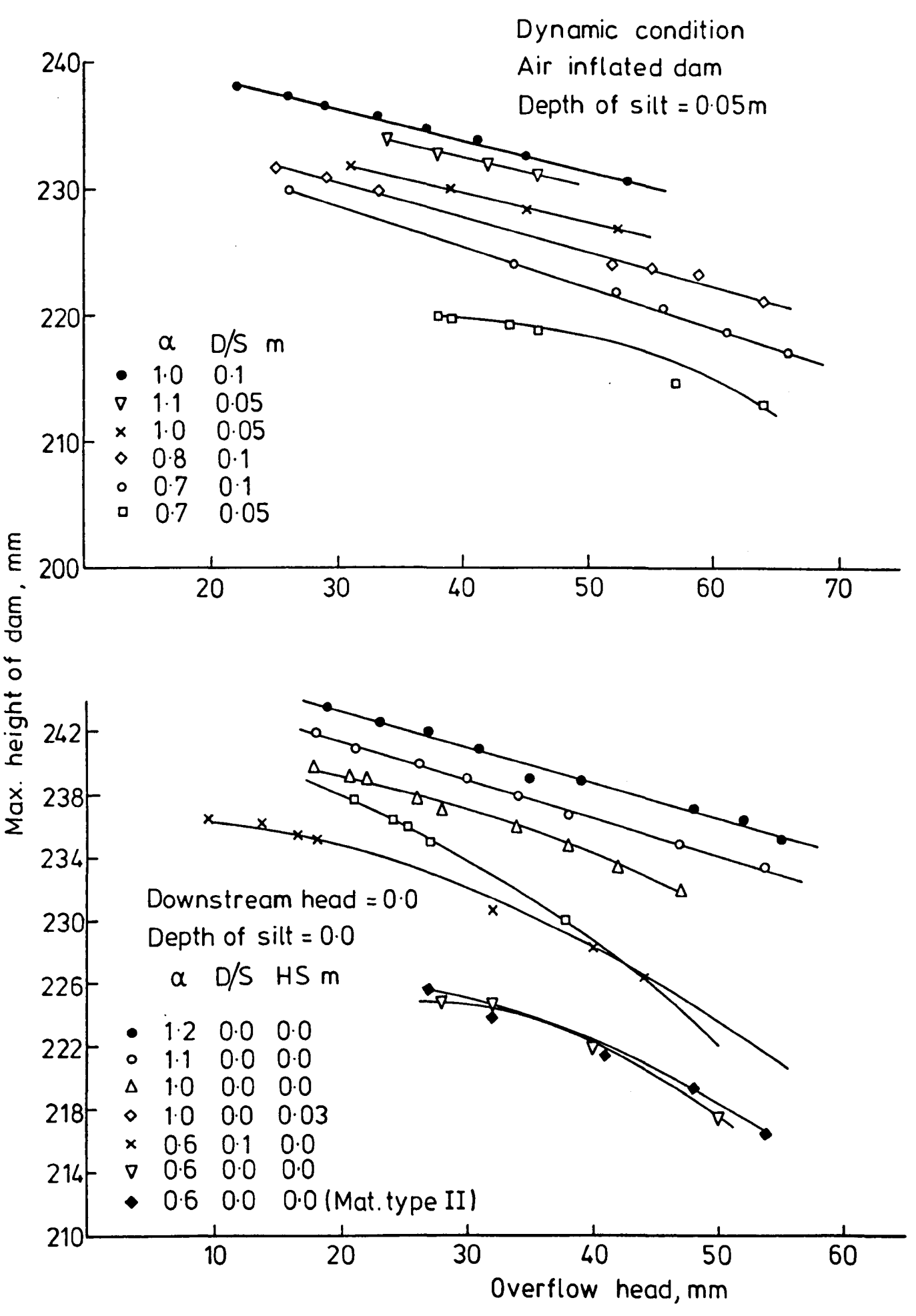

FIG. (5-31) MAXIMUM HEIGHT OF DAM Vs. DIFFERENT OVERFLOW HEADS FOR AN AIR INFLATED DAM

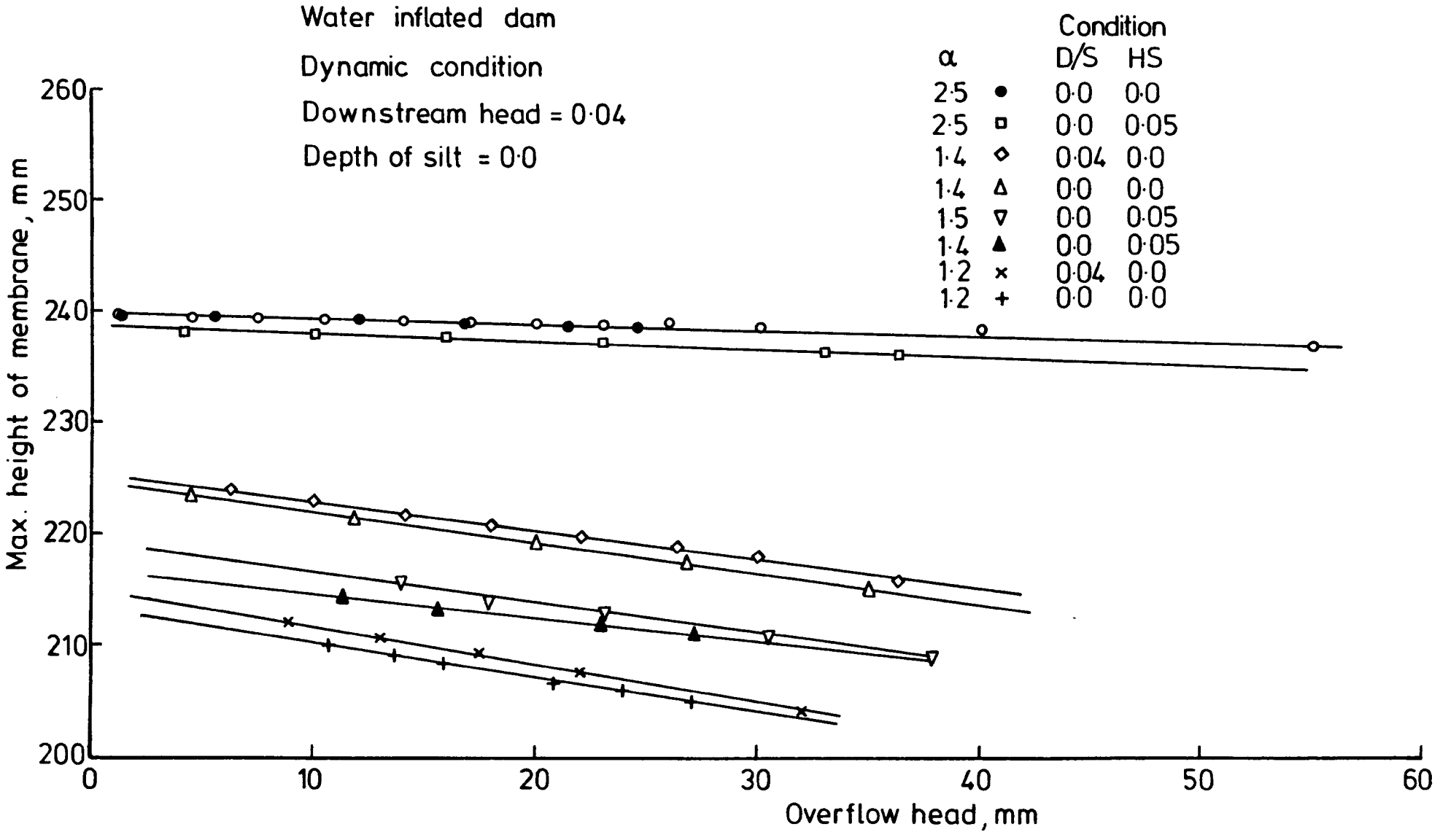

FIG. (5-32) MAXIMUM HEIGHT OF DAM Vs DIFFERENT OVERFLOW HEADS FOR WATER INFLATED STRUCTURE

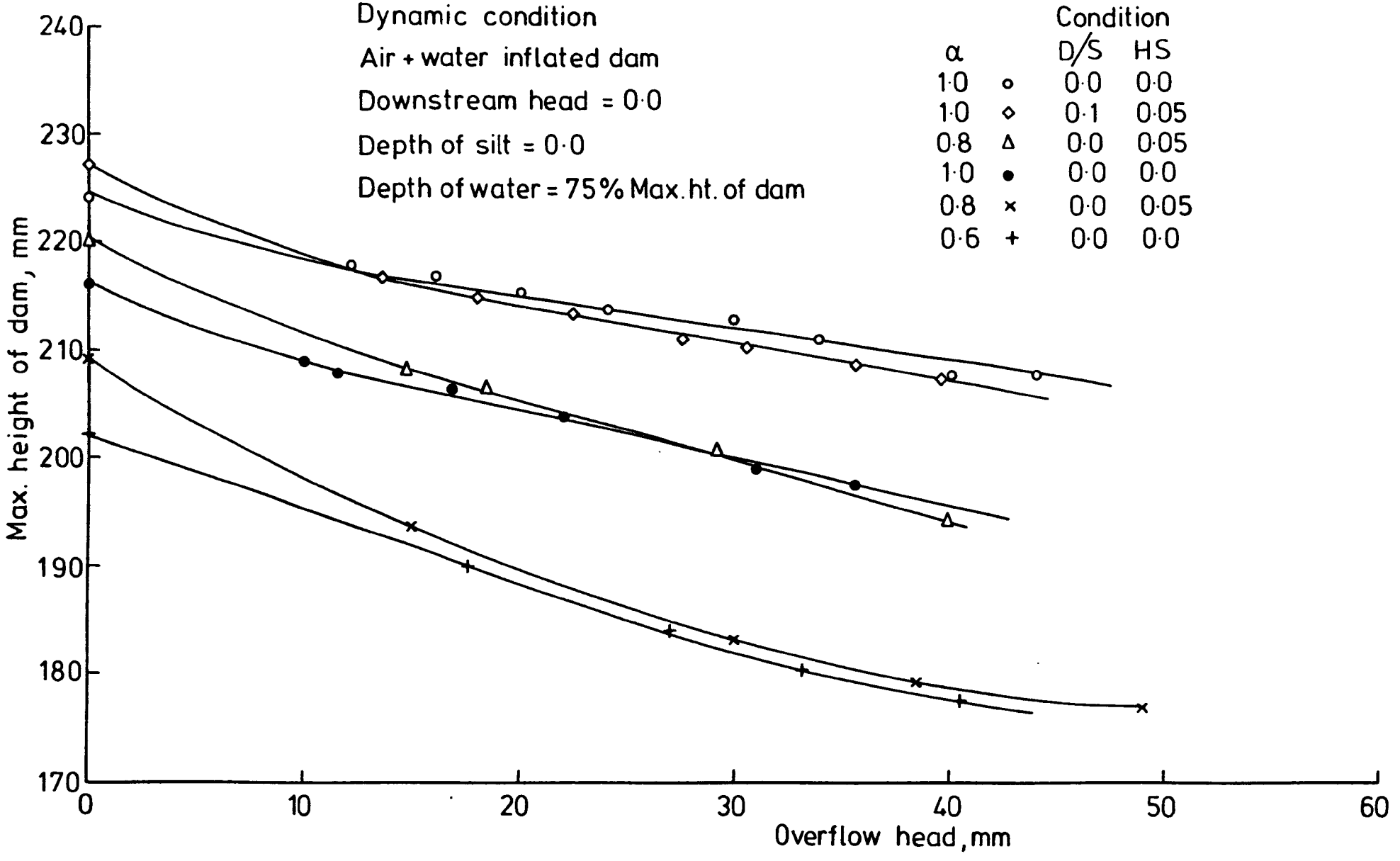

FIG. 5-33 MAXIMUM HEIGHT OF DAM Vs. DIFFERENT OVERFLOW HEADS FOR AN AIR + WATER INFLATED DAM

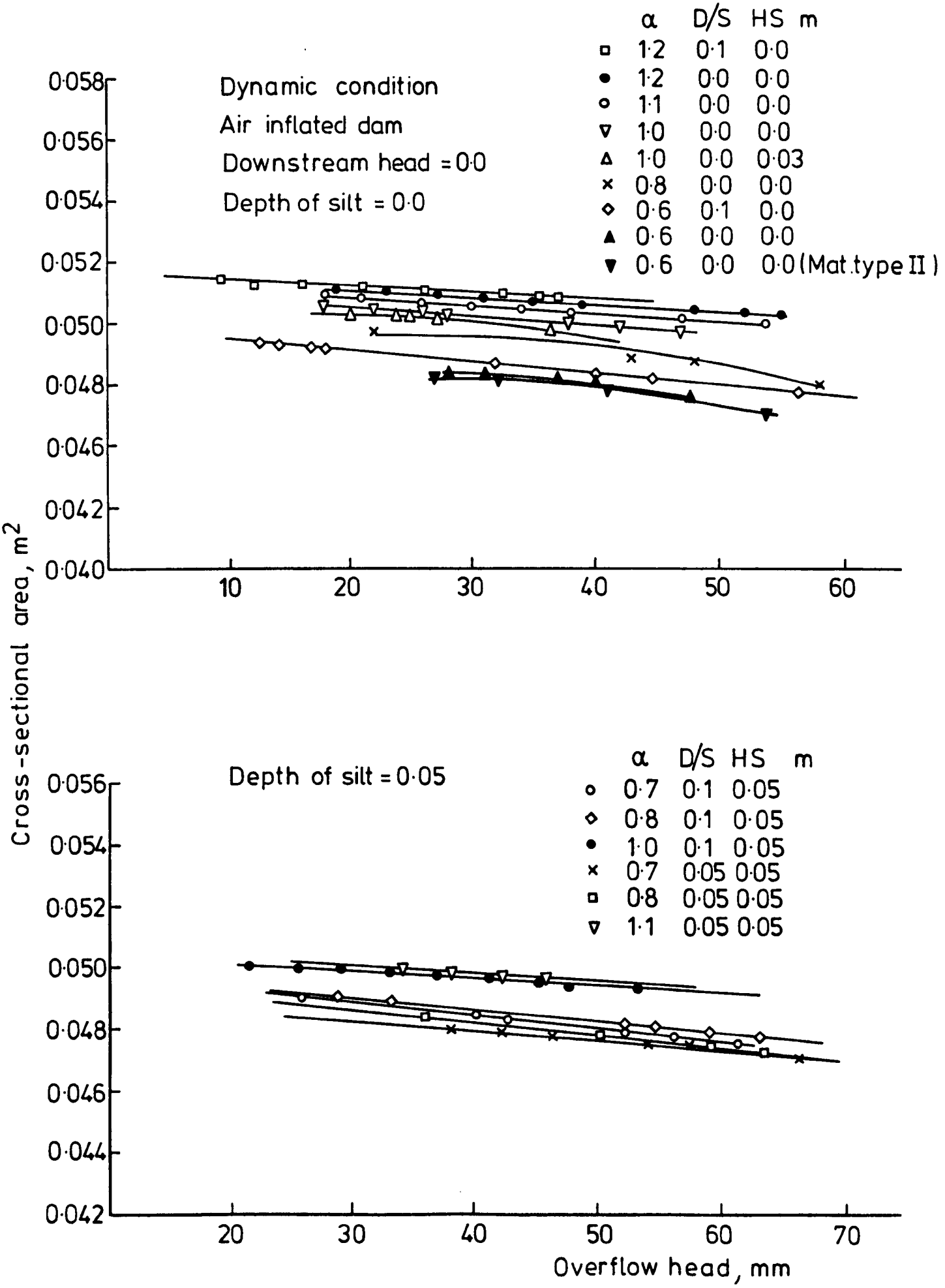

FIG. (5-34) CROSS SECTIONAL AREA Vs. DIFFERENT OVERFLOW HEADS FOR AN AIR INFLATED STRUCTURE

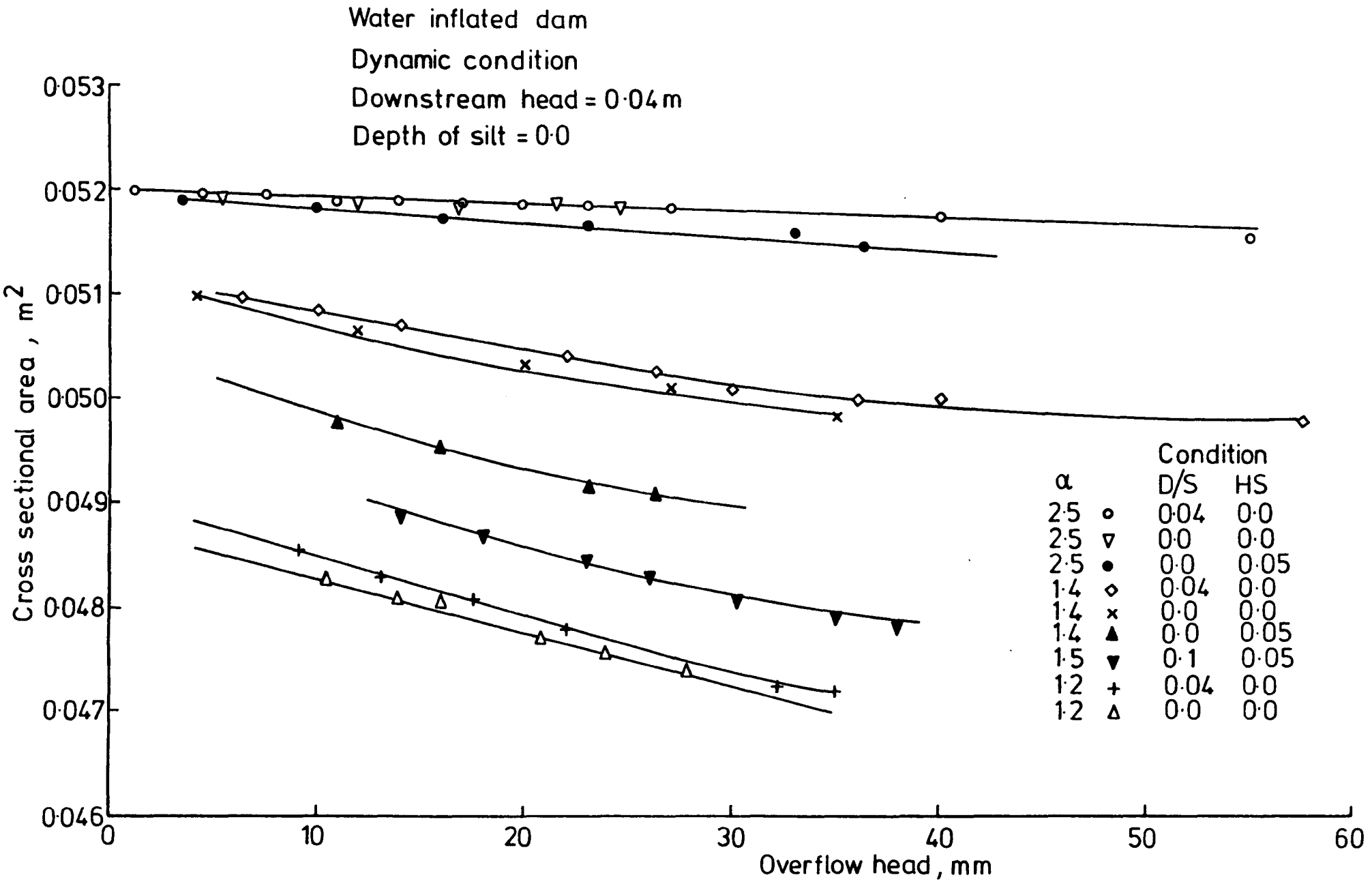

FIG.(5-35) CROSS SECTIONAL AREA Vs. DIFFERENT OVERFLOW HEADS FOR A WATER INFLATED STRUCTURE

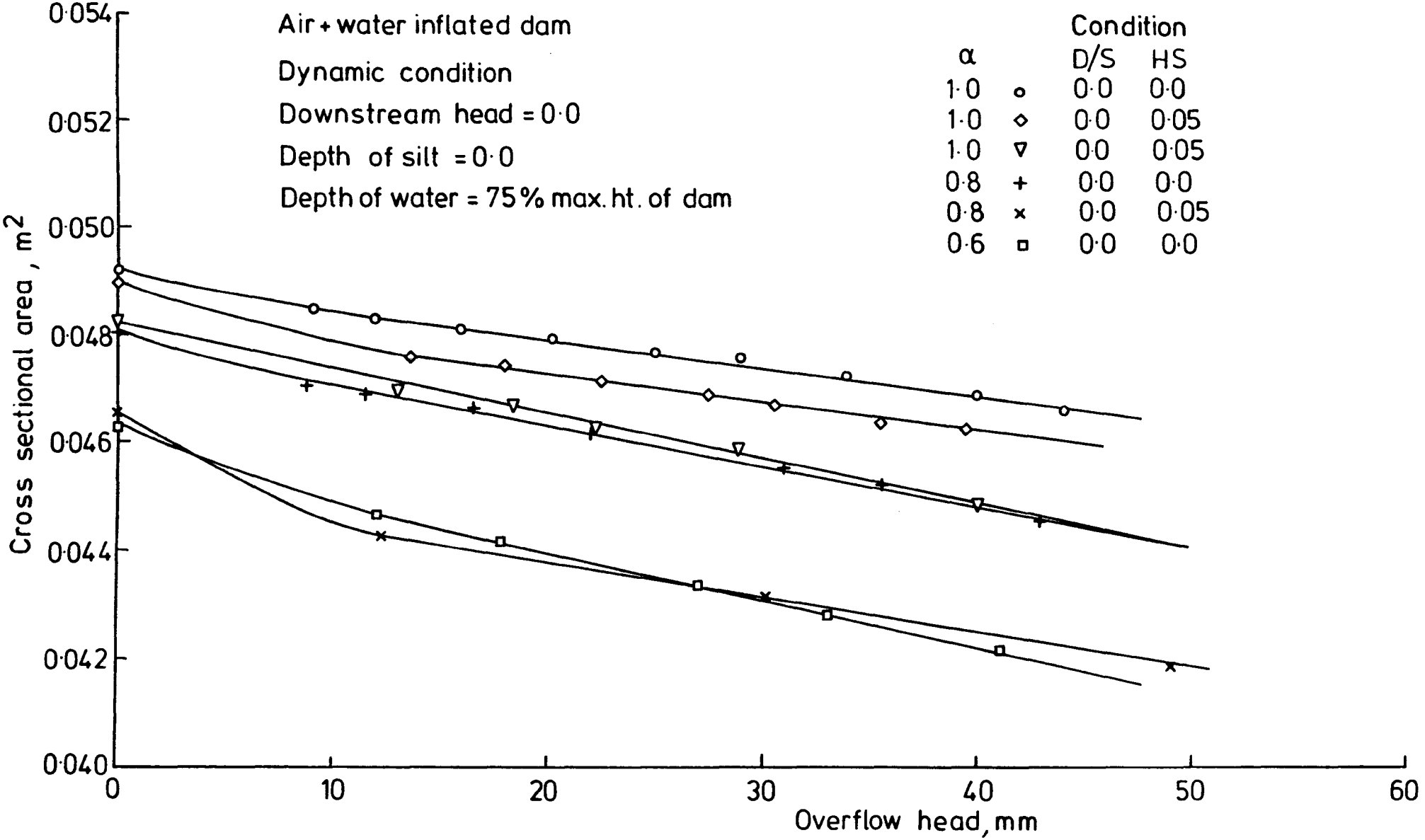

FIG. (5-36) CROSS SECTIONAL AREA Vs. DIFFERENT OVERFLOW HEADS FOR AN AIR + WATER INFLATED STRUCTURE

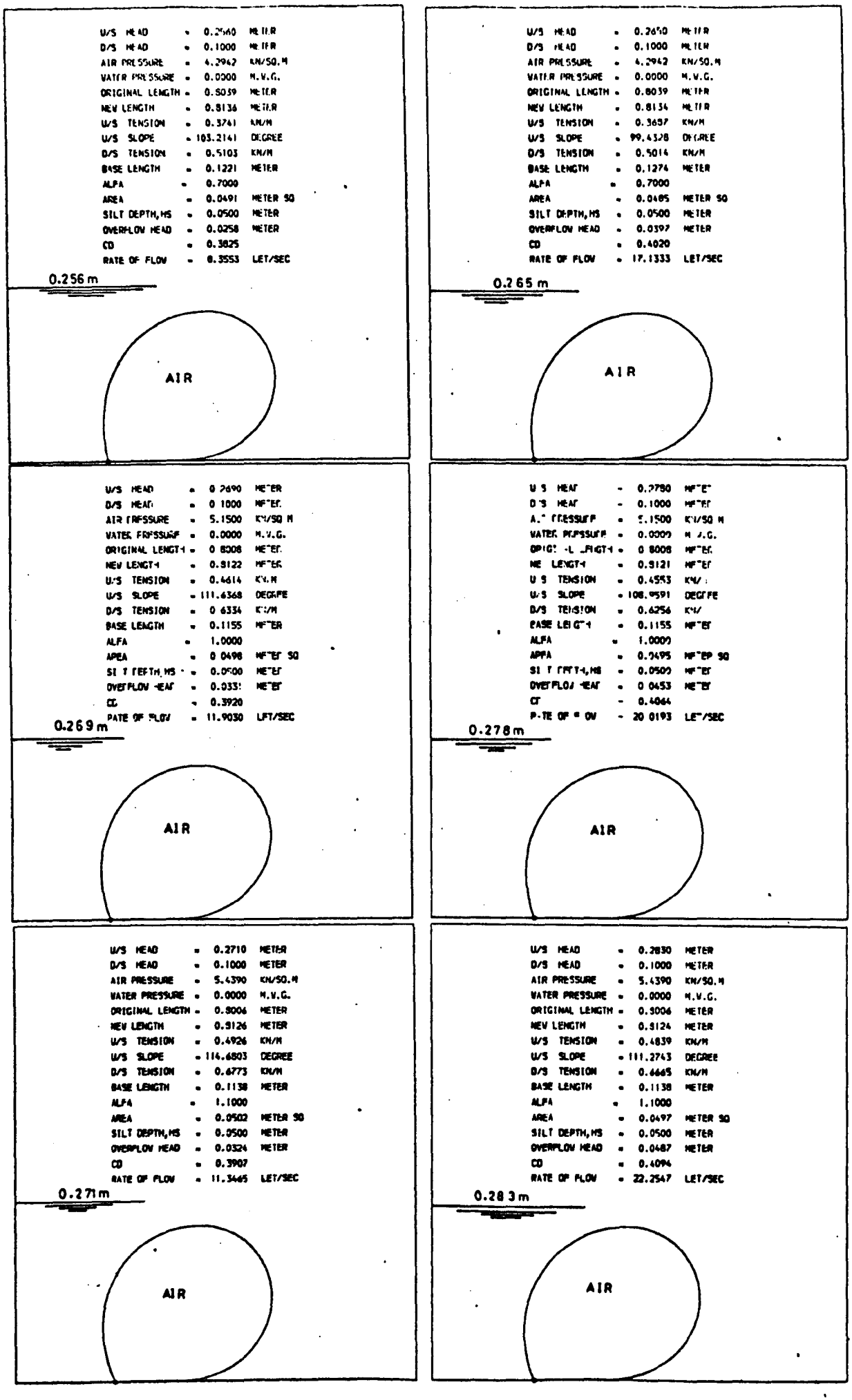

FIG.(5-37) TYPICAL PROFILES OF DIFFERENT OVERFLOW HEADS FOR AN AIR INFLATED STRUCTURE

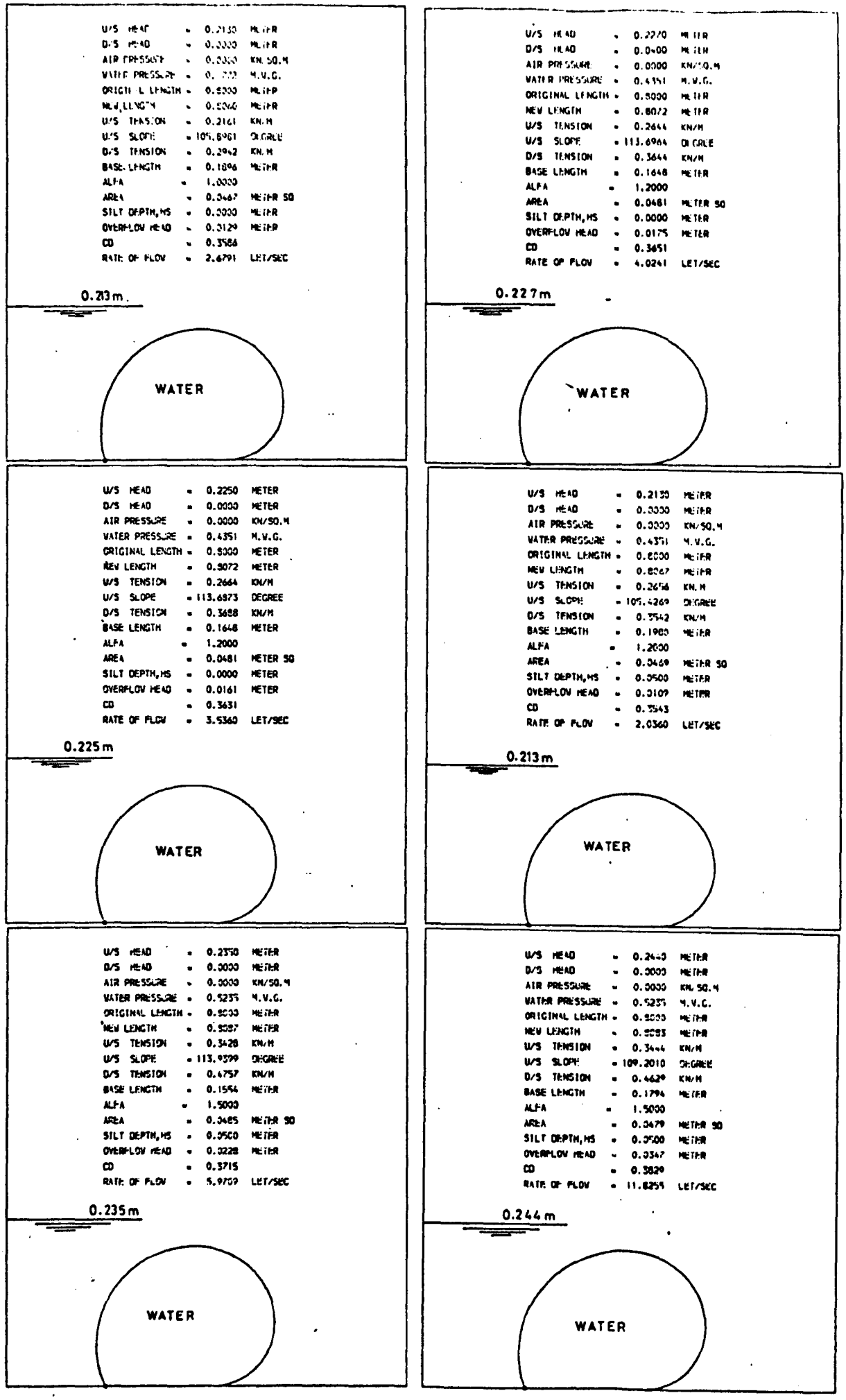

FIG.(5-38) TYPICAL PROFILES OF DIFFERENT OVERFLOW HEADS FOR A WATER INFLATED STRUCTURE

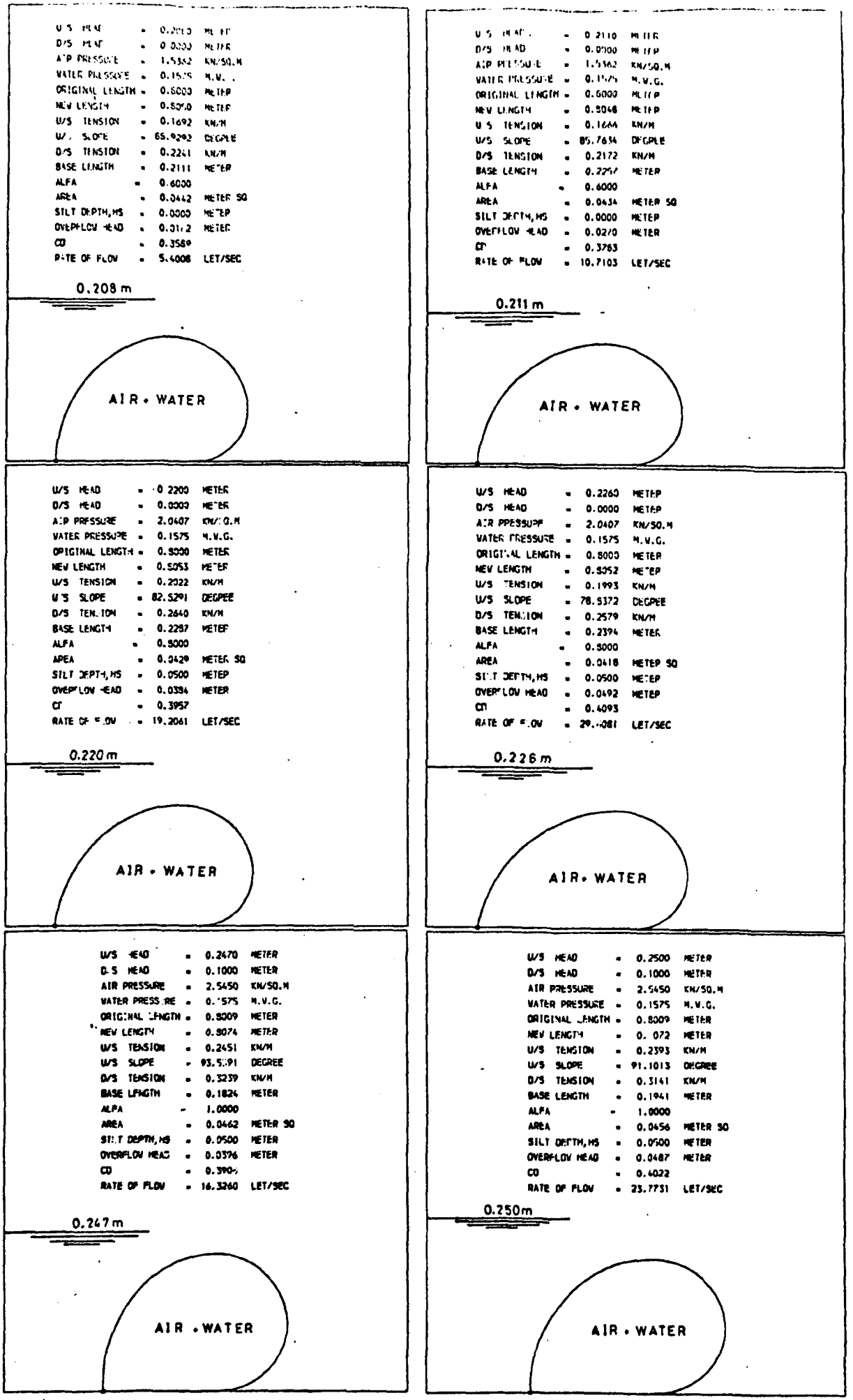

FIG.(5-39) TYPICAL PROFILES OF DIFFERENT OVERFLOW HEADS FOR AN AIR+WATER INFLATED STRUCTURE

heads and the cross-sectional area was also determined experimentally by plotting the profile of the dam using the program (EW) and by using the same equation in order to calculate the area. The results of the theoretical cross-sectional area are compared with the experimental results in Chapter 6.

This analysis showed that the cross-sectional area decreased with increasing the overflow head for all conditions of inflation and for all proportional factors. This behaviour was different when the effect of downstream head and silt pressure was considered as the cross-sectional area increased with increasing of the downstream head, while the cross-sectional area decreased with an increasing effect of silt pressure.

The behaviour of the cross-sectional areas with respect to the different proportional factors and under different overflow heads for air, water and (air+water) inflated are shown in figs. 5.34, 5.35 and 5.36 respectively.

Different profiles under different overflow heads and for different proportional factors are shown in fig.5.37, 5.38 and 5.39 for air, water and (air+water) inflated dams respectively.

5.8 Summary.

This chapter has concentrated on dams inflated with different inflation fluids under hydrodynamic conditions and studied both experimentally and theoretically.

The main experimental work was to find the maximum overflow head over the dam before vibration started and to determine the fabric tension experimentally by using strain gauges inside the dam.

The behaviour of the dam was studied under different overflow heads under different inflation fluids.

Analysing the dam theoretically was done by using the same technique developed for the static condition except to take into consideration additional forces on the downstream face.

CHAPTER 6.

COMPARISON BETWEEN THEORETICAL AND EXPERIMENTAL WORK.

6.1 General.

The comparison of the different results from the experimental and theoretical work is detailed in this chapter. A comparison between the experimental and theoretical work was made for the following parameters.

1. Profiles of a dam for both the static and dynamic conditions.
2. Average upstream and downstream tensions.
3. Upstream slopes.
4. Maximum height of a dam.
5. Cross-sectional area.

The comparison of theoretical work was also made for dams which had been inflated with different fluids. The main parameters compared are as follows: 1. Tension, 2. Upstream slope, 3. Elongation, 4. Maximum height of dam, 5. Cross-sectional area.

Additional to the above, a comparison was also made for the different materials which were used for the construction of the dams.

6.2 Comparison of experimental and theoretical work.

6.2.1 Profile of the dam.

The comparison of the profiles for the dams obtained from the theoretical and experimental work was carried out by calculating the average of the straight line distance of co-ordinate points from the anchor point for both the theoretical and experimental work in order to find the percentage differences between the two. These details of the comparisons are arranged in table 6.1 for different dams under different inflation fluids for static conditions.

The comparison shows that the maximum percentage differences between the experimental and theoretical work was only 1.3 which was considered acceptable for the range of characteristics studied.

Table 6.1 A comparison of the profiles of dams obtained from experimental and theoretical work for static conditions.

Test No.	Propl. factor α	Orig. length (m)	Air Press. KN/m^2	Water Press. (m)	U/S Head (m)	D/S Head (m)	Average distances		% Diff.
							Theor-etical	Experi-mental	
1	0.75	0.800	4.421	-	0.253	0.0	0.202	0.201	0.5
2	1.1	0.800	5.439	-	0.259	0.0	0.198	0.147	0.61
3	1.0	0.800	-	0.373	0.189	0.0	0.200	0.199	0.4
4	1.0	1.000	-	0.467	0.236	0.0	0.250	0.248	0.61
5	1.2	0.800	-	0.431	0.198	0.0	0.197	0.195	0.72
6	0.6	0.800	1.621	0.146	0.195	0.0	0.208	0.208	0.0
7	0.7	0.600	1.292	0.121	0.148	0.0	0.158	0.156	1.3
8	0.8	0.500	1.23	0.10	0.126	0.0	0.131	0.130	0.77

Table 6.2 Comparison of the profiles of dams obtained from experimental and theoretical work for hydrodynamic conditions.

Test No.	Propl. factor α	Orig. length (m)	Air Press. KN/m^2	Water Press (m)	U/S Head (m)	D/S Head (m)	Average distances		% Diff.
							Theor-etical	Experi-mental	
1	0.6	0.800	3.984	0.0	0.262	0.0	0.208	0.206	1.0
2	1.0	0.800	5.150	0.0	0.265	0.0	0.200	0.199	0.5
3	1.2	0.800	0.0	0.435	0.228	0.0	0.204	0.203	0.7
4	1.2	0.800	0.0	0.435	0.239	0.04	0.207	0.203	1.97
5	0.8	0.800	2.041	0.157	0.233	0.0	0.214	0.213	0.2
6	1.0	0.800	2.545	0.157	0.248	0.0	0.211	0.210	0.4

Profiles from the experimental and theoretical work were plotted using a computer program "COMPARE" and are shown in figs. 6.1, 6.2 and 6.3 for air, water and (air+water) inflated dams respectively. The comparison of the plotted profiles covers aproportional factors - of 0.75 and 1.1 for air inflated dams, 1.0 and 1.2 for the water inflated dams and o.6 to 0.8 for (air+water) inflated dams.

The profiles were also compared in the same way for the hydrodynamic condition and the results are shown in table 6.2. The maximum percentage difference between the theoretical and the experimental results was equal to 2.0.

This percentage difference for the dynamic condition is higher than for the static condition due to the effect of the overflow causing a vibration of the fabric of the dam resulting in a difficulty in measuring the profile as accurately as for the static condition.

Fig.6.4 shows different profiles for the experimental and theoretical work for air, water and (air+water) inflated structures under hydrodynamic conditions.

6.2.2 Comparison of the results of the output parameters for static conditions.

The main output parameters which have been compared are as follows:

1. Average upstream and downstream tensions.
2. Upstream slopes.
3. Maximum height of dam.
4. Cross-sectional area.

The results for the comparison of the above parameters are arranged in table 6.3 for different dams and different inflation fluids.

The average upstream and downstream tension were only available for air inflated dams and the results show that the maximum difference between the

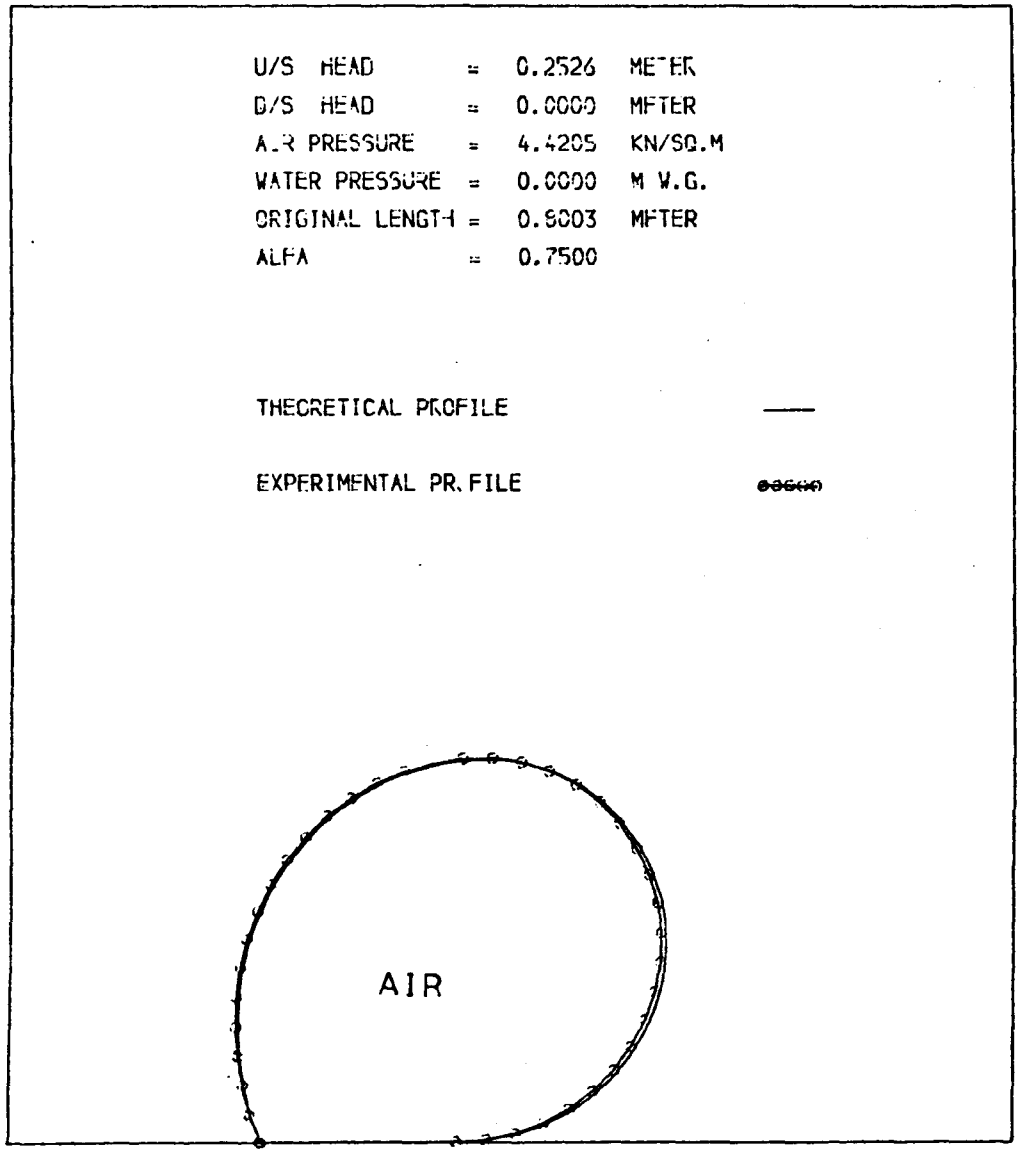

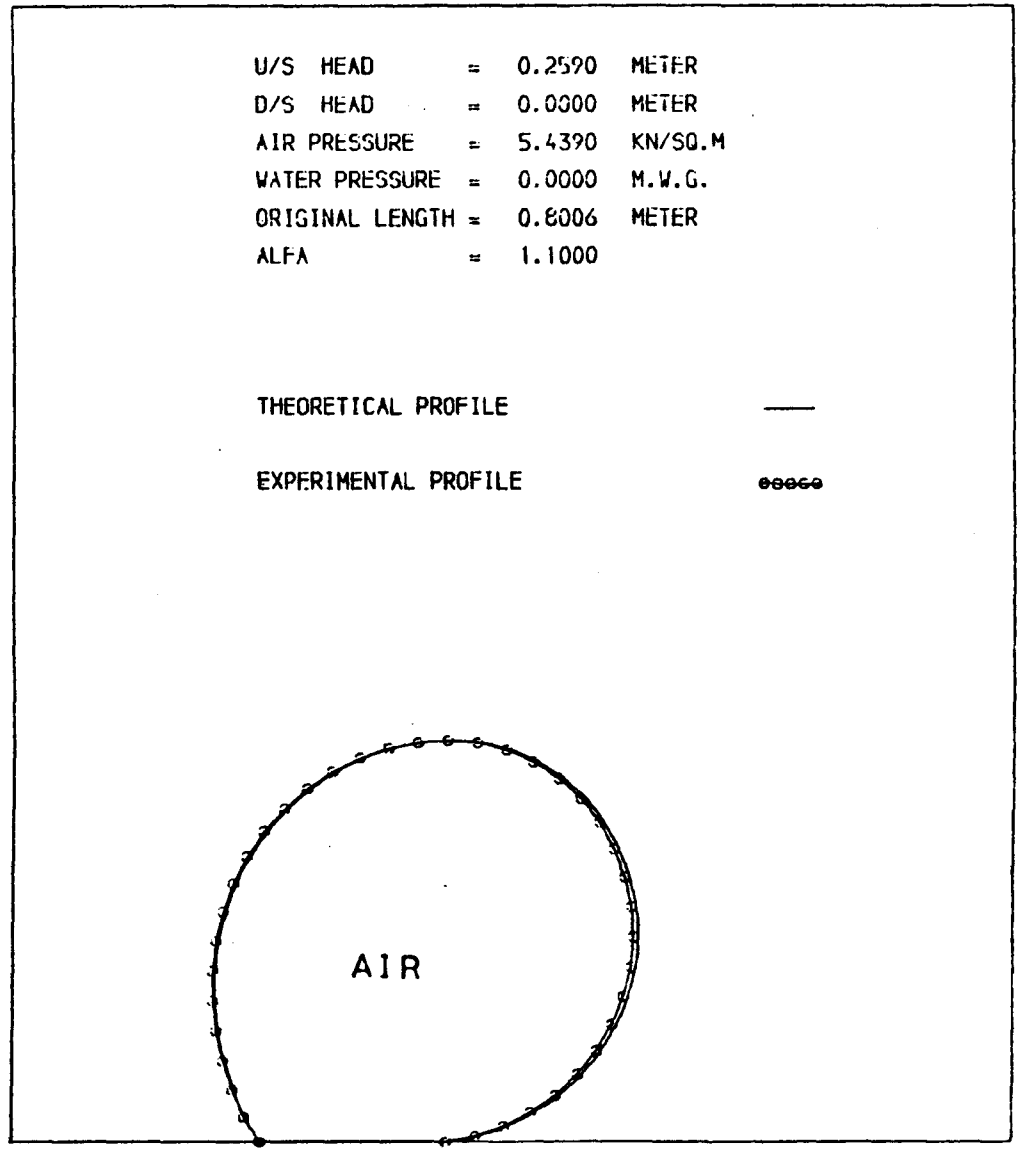

FIG.(6-1) COMPARISON BETWEEN EXPERIMENTAL AND THEORETICAL PROFILES OF A TYPICAL AIR INFLATED STRUCTURE FOR STATIC CONDITION

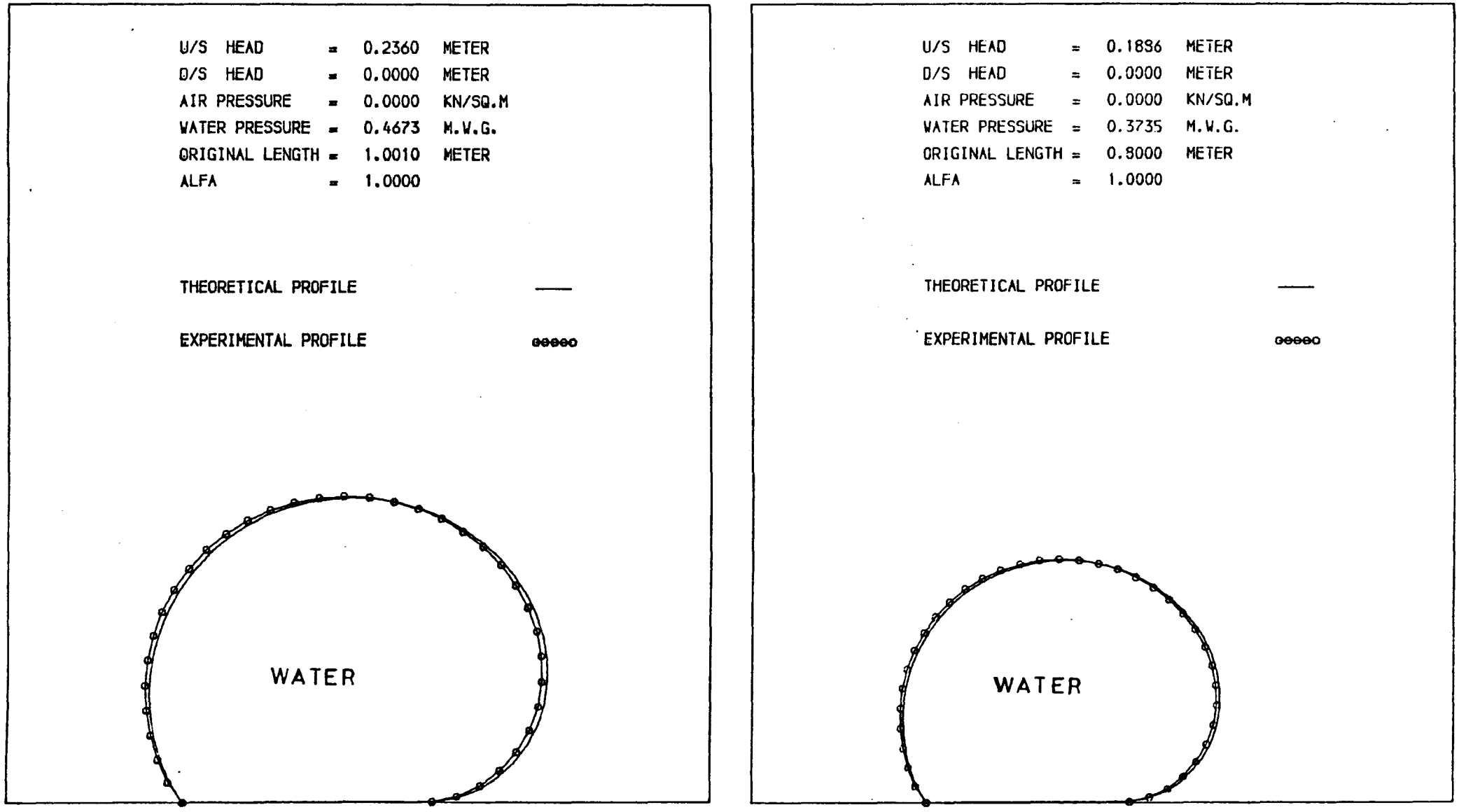

FIG. (6-2) COMPARISON BETWEEN EXPERIMENTAL AND THEORETICAL PROFILES OF A TYPICAL WATER INFLATED STRUCTURE FOR STATIC CONDITION

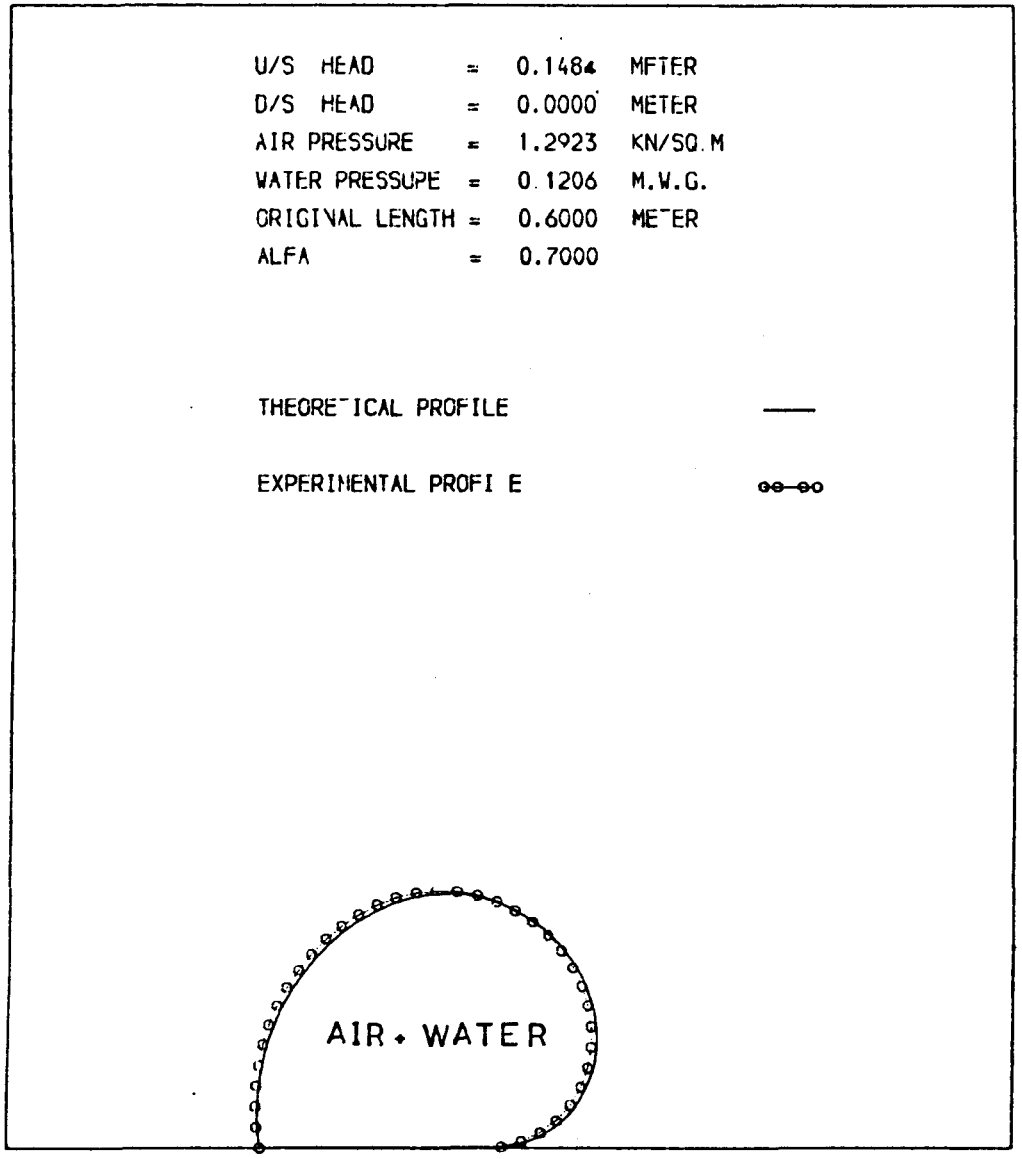

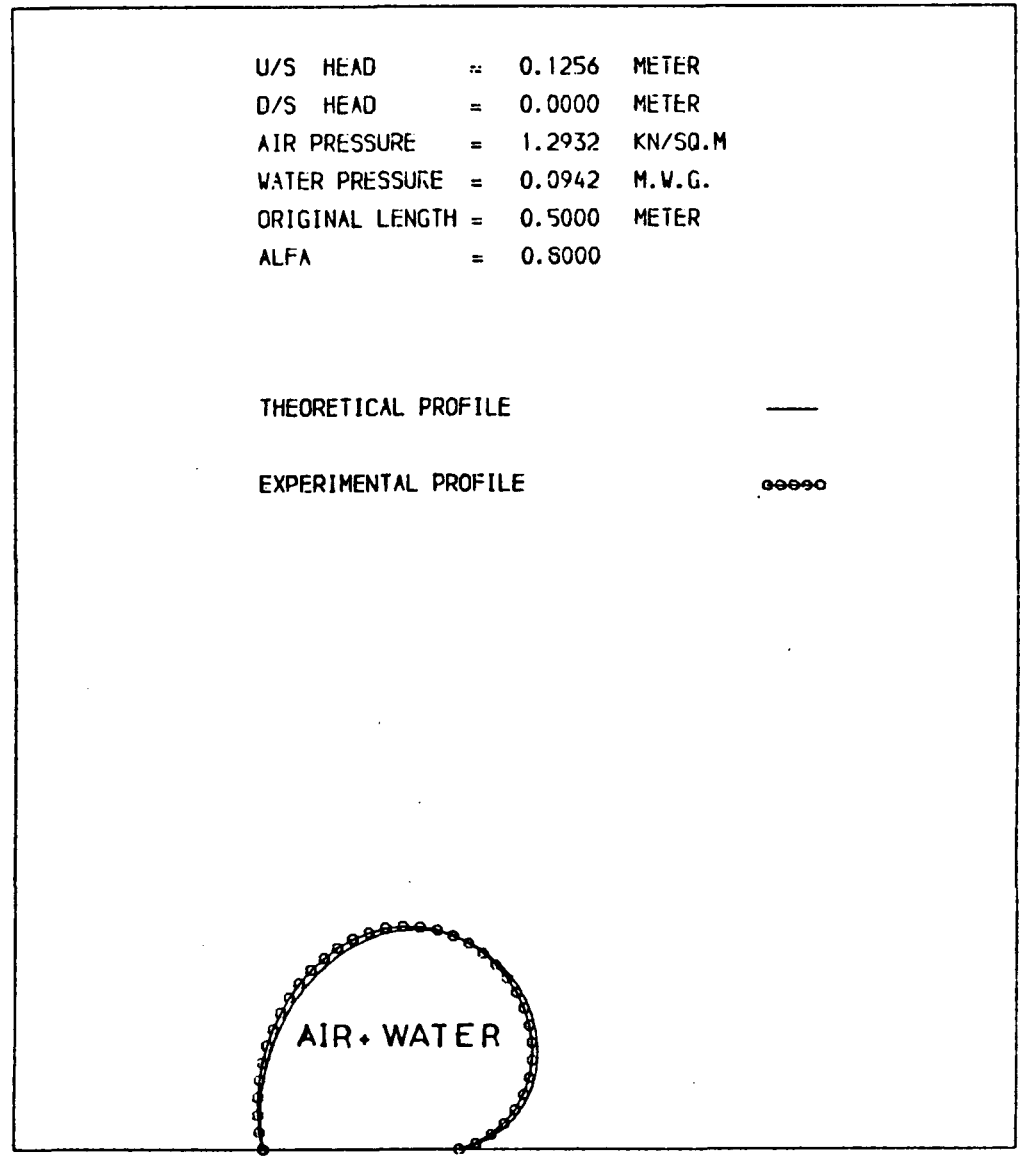

FIG.(6-3) COMPARISON BETWEEN EXPERIMENTAL AND THEORETICAL PROFILES OF A TYPICAL AIR+WATER INFLATED STRUCTURE FOR STATIC CONDITION

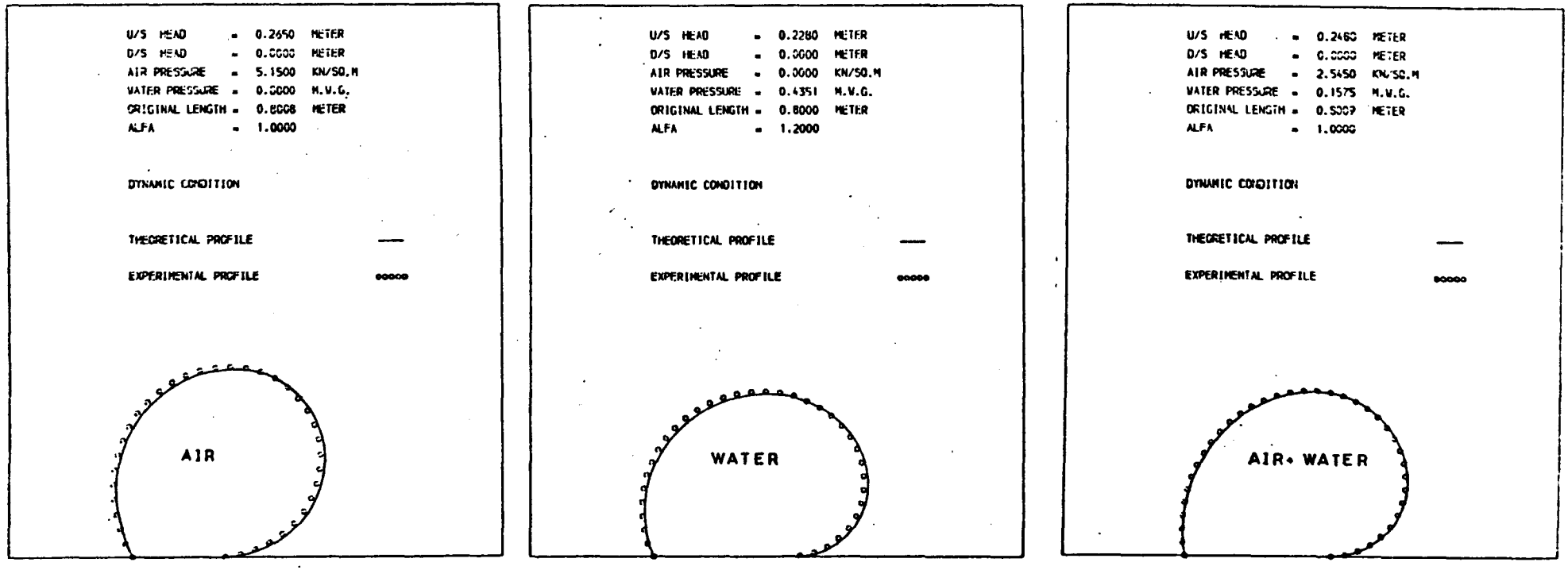

FIG. (6-4) COMPARISON BETWEEN EXPERIMENTAL AND THEORETICAL PROFILES OF A TYPICAL AIR, WATER AND AIR+WATER INFLATED STRUCTURE FOR HYDRODYNAMIC CONDITION

Table 6.3 Comparison between theoretical and experimental work of the output parameters.

Type No. Type of Inflation	No. of test	Proportional factor	Original length of material (m)	U/S Head (m)	D/S Head (m)	Air pressure KN/m^2	Water pressure (m)	Average U/S and D/S Tension KN/m			U/S Slope degree			Max. height of dam (m)			Cross-sectional area m^2		
								Theoret-ical	Exptl.	% Diff.	Theoret-ical	Exptl.	% Diff	Theoret-ical	Exptl.	% Diff.	Theoret-ical	Exptl.	% Diff.
1 Air	1	0.4	0.80	0.242	0.0	3.40	0.0	0.339	0.322	5.3	82.4	83.5	0.3	0.245	0.243	1.0	0.0439	0.0432	1.6
	2	0.75	0.80	0.253	0.0	4.42	0.0	0.454	0.480	0.8	110.52	111.42	0.8	0.256	0.255	0.6	0.0499	0.0496	0.7
	3	1.0	0.80	0.257	0.0	5.15	0.0	0.576	0.570	1.1	118.84	118.95	0.1	0.258	0.258	0.0	0.0506	0.0501	1.0
	4	1.1	0.80	0.259	0.0	5.44	0.0	0.518	0.511	1.36	121.85	122.73	0.7	0.253	0.254	0.4	0.0514	0.0505	1.86
	5	1.2	0.80	0.260	0.0	5.73	0.0	0.651	0.633	2.8	124.51	124.8	0.2	0.261	0.260	0.2	0.0512	0.0510	0.33
2 Water	6	1.0	0.80	0.188	0.0	0.0	0.373				121.23	123.43	1.8	0.21	0.211	0.5	0.0486	0.0500	2.8
	7	1.0	1.00	0.236	0.0	0.0	0.467				121.9	122.60	0.6	0.264	0.266	0.8	0.0767	0.0768	0.2
	8	1.2	0.80	0.197	0.0	0.0	0.431				128.31	131.05	2.1	0.218	0.219	0.5	0.0496	0.0498	0.5
3 Air+Water	9	0.6	0.80	0.194	0.0	1.62	0.146				101.14	102.19	1.0	0.211	0.211	0.0	0.0471	0.0471	0.0
	10	0.7	0.60	0.148	0.0	1.29	0.120				98.35	101.80	2.8	0.154	0.156	1.3	0.0261	0.0268	2.7
	11	0.8	0.5	0.126	0.0	1.23	0.100				99.32	102.30	3.0	0.131	0.133	1.5	0.0182	0.0184	1.1

experimental and theoretical work was 5.3% for a proportional factor equal to 0.4. This high difference between the experimental and the theoretical tensions is due to the fact that a dam with such a low proportional factor is not stable and the end conditions cannot prevent the leakage of water from the upstream side.

The comparison of the other output parameter, i.e. upstream slope, maximum height and cross-sectional area shows acceptable results with the maximum differences between the experimental and theoretical work equivalent to 3.0, 1.5 and 2.8 percent respectively, the differences probably due mainly to experimental error.

6.2.3 Comparison between experimental and theoretical work of tension for the hydrodynamic condition.

The experimental technique for measuring the tension by using strain gauges attached inside the dam is explained in detail in Section 5.4, Chapter 5., and the results of the experiment are given in table 5.3 and 5.4.

In this section a comparison is made between the tensions found by the theoretical and experimental work for the hydrodynamic condition. The results of this comparison are arranged in tables 6.4 and 6.5 for a dam inflated with air and for the conditions of downstream heads equal to 0.0 and 0.1.m.

The comparison is divided into three parts depending on the location of the strain gauges inside the dam.

Part (1) relates to the cells 1, 2 and 3 fitted on the upstream face.

Part (2) relates fo the cells 4 and 5 fitted on the crest face.

Part (3) relates to the cells 6 and 7 fitted on the downstream face.

Additional to the above, a comparison was also carried out for the total average tension around the membrane length of the dam. Table 6.4 shows the

comparison of this tension for an air inflated dam with downstream head equal to zero, and the results of the comparison indicate that the maximum difference between the experimental and theoretical work was equal to + 4.7 percent occurring on the crest face, while the maximum difference between the theoretical and the experimental work for the condition of downstream head equal to 0.10 m was + 5.5 percent again this occurring on the crest face.

The main reason for the high differences between the experimental and theoretical results in the region of the crest face was due to the effect of the flow over the crest and down the downstream face. In some cases the flow over the crest will not be uniform along the dam which has been assumed in the theoretical analysis. Such differences between the theoretical and experimental results for the upstream region did not occur due to a stable static head on the upstream face of the dam.

The details of the comparison for the tension are shown in tables 6.4 and 6.5 for proportional factors equal to 0.6 and 1.2 with downstream heads equal to 0.0 and 0.1 m. The range of variation of the tension between the theoretical and experimental results was -3.0 to +4.7% for the condition of downstream head equal to zero whilst the range of variation was -1.8 to +5.5% for the condition of downstream head equal to 0.1 m.

The maximum difference percentage between the theoretical and experimental average of the total tension around the membrane were 2.5 for the condition of downstream head equal to zero and 2.9 for the condition of the downstream head equal to 0.1 m.

6.3 Comparison of the theoretical results between dams inflated with different inflation fluids.

Dams of different inflation fluids were compared by considering the main output parameters with different internal pressures. This comparison was made for different conditions of downstream head and silt pressures and with a total length of membrane equal to 0.8 m.

Table 6.4 Comparison of the tension obtained from experimental and theoretical work for an Air Inflated Dam with downstream head = 0.0

Dam Details								Section at the centre of the dam									
								Part (1) Upstream face				Part (2) Crest face			Part (3) Downstream face			Total aver % diff.
								Tension in KN/m										
Proportional factor	Test No.	U/S Head (m)	D/S Head (m)	Max. Height (m)	Over flow Head mm	Disch. Q ℓ/s	Press. KN/m^2	Cell (1) Exp. / Theor.	Cell (2) Exp. / Theor.	Cell (3) Exp. / Theor.	% diff	Cell (4) Exp. / Theor.	Cell (5) Exp. / Theor.	% diff	Cell (6) Exp. / Theor.	Cell (7) Exp. / Theor.	% diff	
0.6	1	0.253	0.0	0.2247	28.3	10.02	3.984	0.368 0.366	0.371 0.371	0.382 0.382	+0.0	0.382 0.382	0.343 0.398	+3.6	0.438 0.462	0.475 0.484	+3.5	+2.0
	2	0.256	0.0	0.2246	31.4	11.82	3.984	0.360 0.360	0.362 0.365	0.375 0.377	+0.4	0.386 0.394	0.402 0.410	+2.0	0.437 0.440	0.478 0.479	+0.6	+1.0
	3	0.262	0.0	0.222	40.0	17.80	3.984	0.357 0.357	0.360 0.362	0.373 0.373	+0.3	0.384 0.388	0.397 0.422	+3.6	0.432 0.456	0.470 0.475	+3.2	+2.3
	4	0.268	0.0	0.218	50.0	26.05	3.984	0.355 0.353	0.358 0.357	0.368 0.367	-0.3	0.377 0.383	0.391 0.416	+4.0	0.425 0.451	0.463 0.469	+3.6	+2.2
1.2	1	0.263	0.0	0.243	20.0	5.11	5.728	0.541 0.545	0.580 0.555	0.610 0.580	-3.0	0.600 0.619	0.630 0.669	+4.7	0.690 0.719	0.735 0.754	+3.3	+1.2
	2	0.266	0.0	0.2427	23.3	6.526	5.728	0.540 0.543	0.560 0.557	0.590 0.583	-0.4	0.600 0.616	0.635 0.666	+3.7	0.688 0.717	0.733 0.752	+3.3	+2.0
	3	0.272	0.0	0.240	32.0	10.99	5.728	0.550 0.539	0.560 0.553	0.580 0.579	-1.1	0.600 0.611	0.630 0.635	+1.3	0.680 0.662	0.73 0.73	+1.3	+0.5
	4	0.275	0.0	0.2398	35.0	12.69	5.728	0.540 0.538	0.550 0.551	0.580 0.577	-0.4	0.600 0.608	0.620 0.660	+4.0	0.670 0.710	0.72 0.74	+4.3	+2.5
	5	0.278	0.0	0.2388	39.2	15.297	5.728	0.540 0.536	0.550 0.549	0.575 0.575	-0.4	0.600 0.606	0.620 0.657	+3.5	0.670 0.708	0.74 0.743	+2.9	+1.8

Table 6.5 Comparison of the tension obtained from experimental and theoretical work for an Air Inflated Dam with downstream head = 0.1

Dam Details								Section at the centre of the dam										
								Part (1) Upstream face				Part (2) Crest face			Part (3) Downstream face			Total aver. % diff.
								Tension in KN/m										
Proportional factor	No. of test	U/S Head (m)	D/S Head (m)	Max. Height (m)	Over flow Head mm	Disch. Q ℓ/s	Press. KN/m2	Cell (1) Exp. / Theor.	Cell (2) Exp. / Theor.	Cell (3) Exp. / Theor.	% diff.	Cell (4) Exp. / Theor.	Cell (5) Exp. / Theor.	% diff.	Cell (6) Exp. / Theor.	Cell (7) Exp. / Theor.	% diff	
0.6	1	0.263	0.1	0.231	32.0	11.68	3.484	0.350 0.358	0.360 0.354	0.370 0.366	-1.1	0.400 0.388	0.420 0.419	-1.6	0.435 0.458	0.460 0.473	+4.0	+0.5
	2	0.268	0.1	0.228	40.0	17.00	3.984	0.346 0.344	0.350 0.349	0.363 0.361	-0.6	0.370 0.378	0.390 0.415	+1.7	0.430 0.450	0.465 0.468	+2.6	+1.8
	3	0.271	0.1	0.226	45.0	20.78	3.984	0.340 0.342	0.350 0.347	0.360 0.359	-0.2	0.370 0.380	0.390 0.412	+4.2	0.420 0.448	0.460 0.465	+3.8	+2.4
1.2	1	0.264	0.1	0.248	16.0	3.47	5.728	0.550 0.542	0.560 0.556	0.590 0.583	-1.8	0.610 0.616	0.640 0.617	+4.3	0.690 0.720	0.740 0.746	+2.5	+1.1
	2	0.268	0.1	0.247	21.0	5.38	5.728	0.540 0.539	0.550 0.553	0.580 0.580	-0.06	0.600 0.613	0.630 0.664	+3.8	0.680 0.714	0.730 0.743	+3.3	+2.1
	3	0.273	0.1	0.246	26.5	7.39	5.728	0.530 0.537	0.540 0.553	0.580 0.576	+1.2	0.590 0.609	0.625 0.660	+4.4	0.675 0.711	0.725 0.739	+3.6	+2.9
	4	0.278	0.1	0.245	32.6	10.015	5.728	0.530 0.535	0.539 0.547	0.577 0.573	+0.5	0.590 0.605	0.620 0.656	+4.2	0.670 0.707	0.720 0.735	+3.8	+2.6
	5	0.281	0.1	0.244	37.0	13.49	5.728	0.525 0.533	0.540 0.545	0.570 0.571	+0.8	0.600 0.602	0.590 0.653	+5.5	0.670 0.704	0.710 0.733	+4.1	+0.8

The main output parameters compared are

(1) Tension, (2) Upstream slope, (3) Elongation, (4) Maximum height of dam and (5) Cross-sectional area.

6.3.1 Tension.

The tension in the membrane of the dam under different inflation fluids was compared for both the upstream and downstream faces. The results show that the tension in an air inflated dam for a particular internal pressure head is more than the tension of the same dam if inflated with water to the same internal pressure head. If the dam is inflated with (air+water) the values of the tension are lower than the tension for the air inflated dam but higher than for dams inflated with water. The ranges of values of the tension for a dam inflated with (air+water) depends on the depth of water inside the dam. A high depth of water results in the tension approaching the tension for a dam inflated with water only or if the depth of water inside the dam is low the resulting tension is close to the tension for a dam inflated with air only.

Since in this investigation the depth of water inside a dam inflated by (air+water) was equivalent to 75 percent of the maximum height of the dam, the resulting tension was close to the tension of a dam inflated with water only.

The theoretical variation of the upstream and downstream tension are plotted with different internal pressure heads for air, water and (air+water) inflated dams and under different downstream heads and silt pressures and these results are shown in figs. 6.5, 6.6, 6.7 and 6.8.

6.3.2 Upstream slope.

The upstream slope increased with increasing internal pressure head for all cases of inflation fluids and for all conditions of downstream head and silt depth.

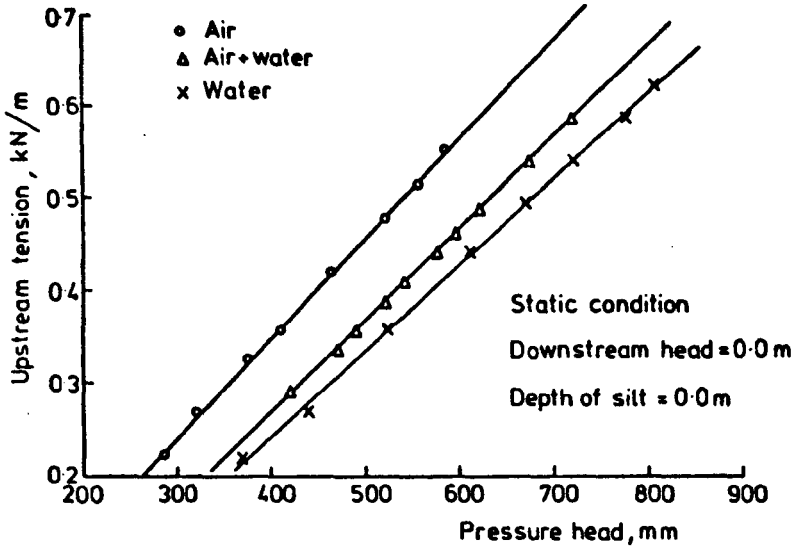

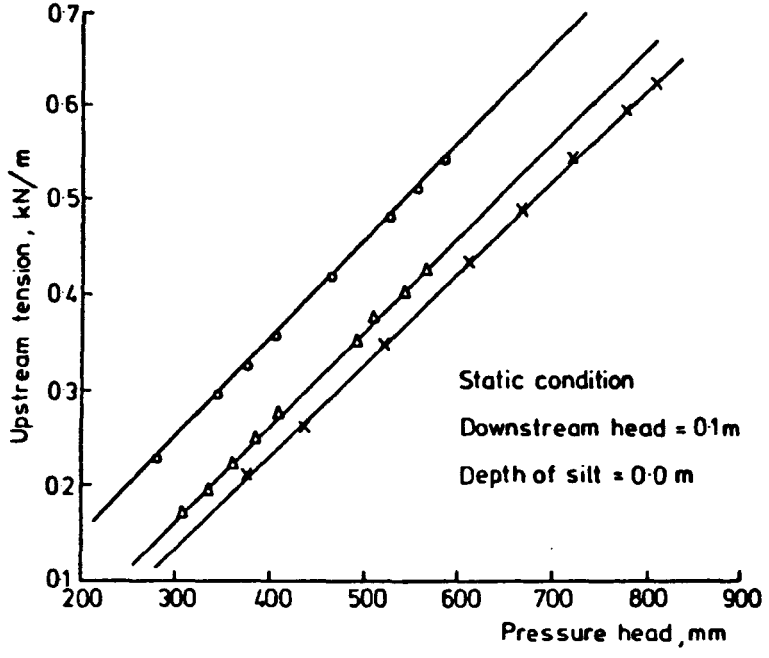

FIG. 6-5. UPSTREAM TENSION Vs PRESSURE HEAD FOR DIFFERENT INFLATION FLUIDS

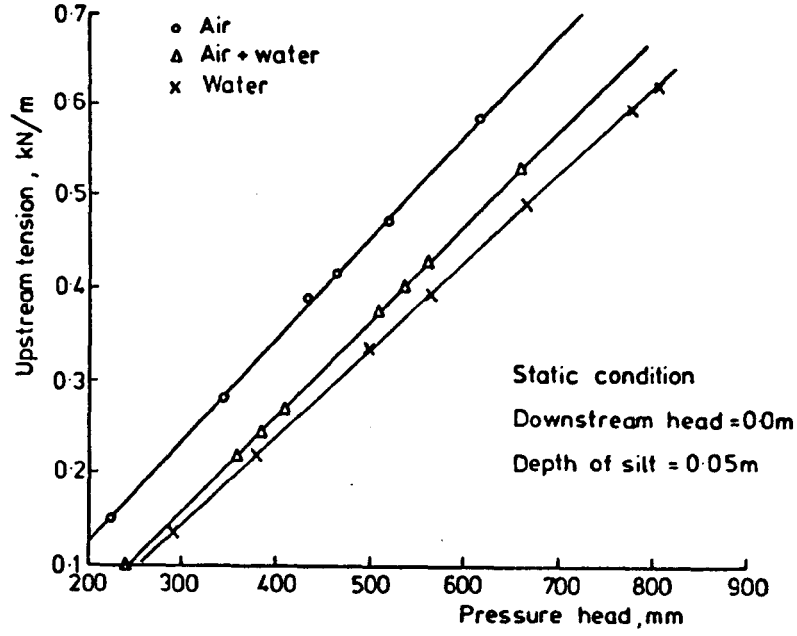

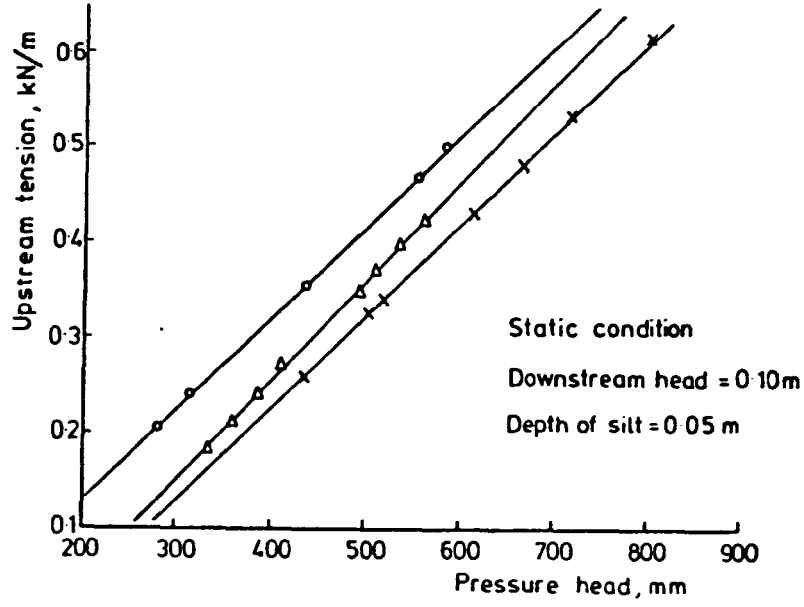

FIG. 6-6. UPSTREAM TENSION Vs. PRESSURE HEAD FOR DIFFERENT INFLATION FLUIDS

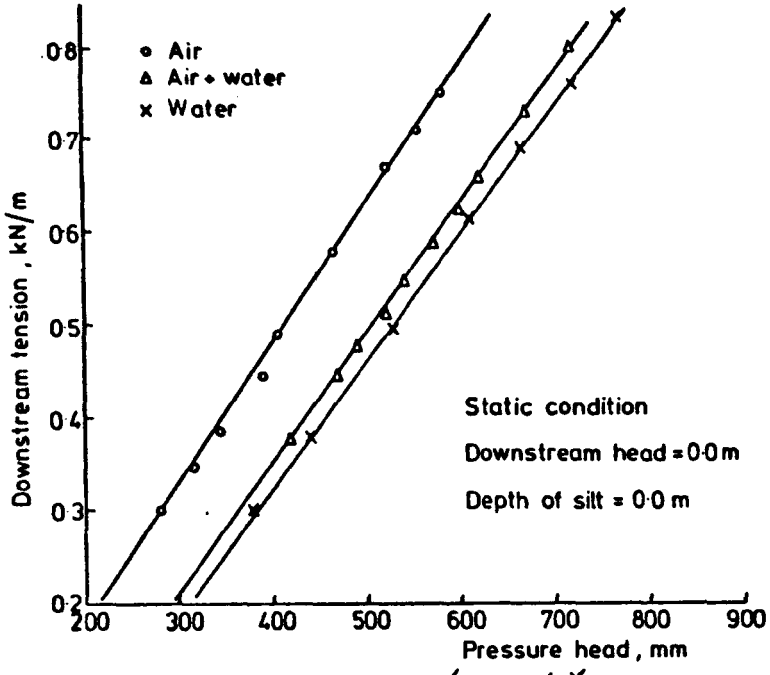

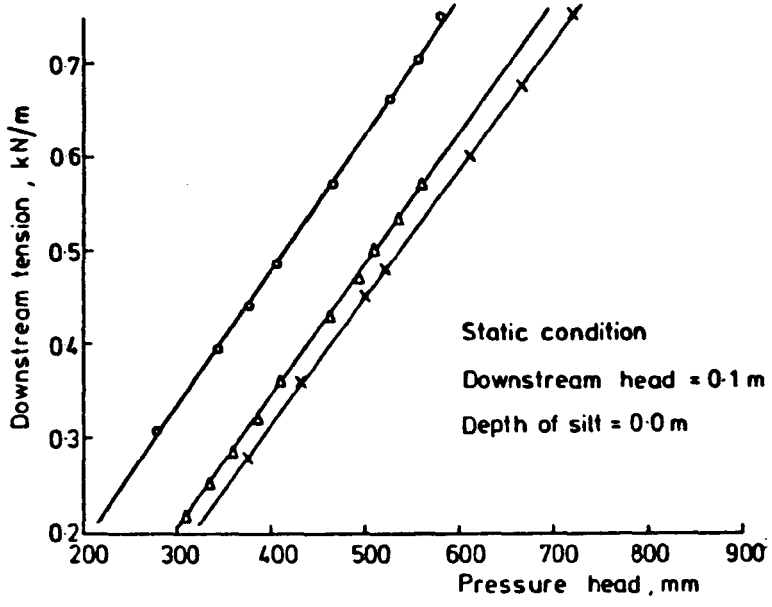

FIG 6·7. DOWNSTREAM TENSION Vs. PRESSURE HEAD FOR DIFFERENT INFLATION FLUIDS

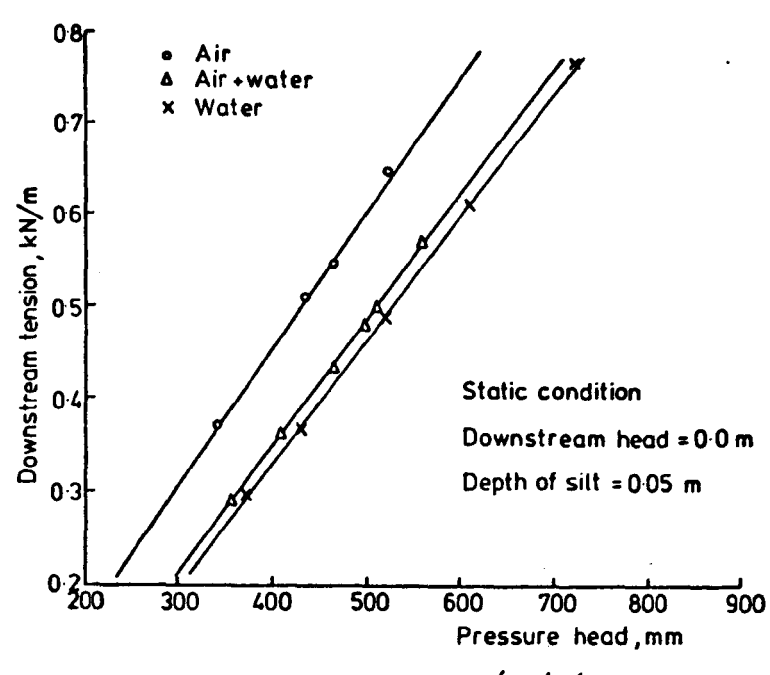

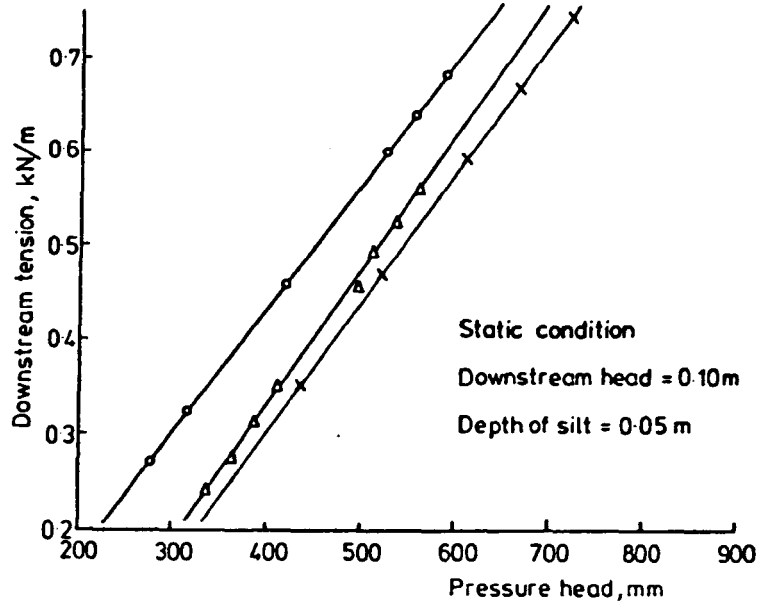

FIG. 6·8. DOWNSTREAM TENSION Vs PRESSURE HEAD FOR DIFFERENT INFLATION FLUIDS

The results show that the upstream slope for a water inflated dam are higher than for the equivalent air inflated dam for a particular pressure head for all conditions of downstream head and silt depth.

As one might expect the upstream slope for a dam inflated with (air+water) is less than the upstream slope of a water inflated dam and higher than for an air inflated dam. The values of the upstream slope for a dam inflated with (air+water) also depend on the depth of water inside the dam.

The details of the comparison of the upstream slope with different inflation fluids under different downstream heads and silt depths are shown in figs. 6.9 and 6.10.

6.3.3 Elongation of the material.

Since the results show that the tension for an air inflated dam is higher than the tension of an equivalent water inflated dam the elongation should be higher for the air inflated dam for all conditions of downstream head and silt depth. Elongation for a dam inflated with (air+water) should be between the values of the elongation found for the above two conditions.

These values also depend on the depth of water inside the dam. The details of the elongation for air, water and (air+water) inflated dams and under different conditions of downstream and silt depth are shown in fig. 6.11 and 6.12.

These show that the above comments on the elongation are true.

6.3.4 Maximum height of dam.

The maximum height of a dam increased as the internal pressure increased for all conditions of downstream head and silt depths.

The highest maximum height for a particular internal pressure head was when the dam was inflated with air whilst the lowest height was for a dam inflated with water for the same internal pressure head. A dam inflated with (air+water) gave the maximum height of the dam in between the values for the

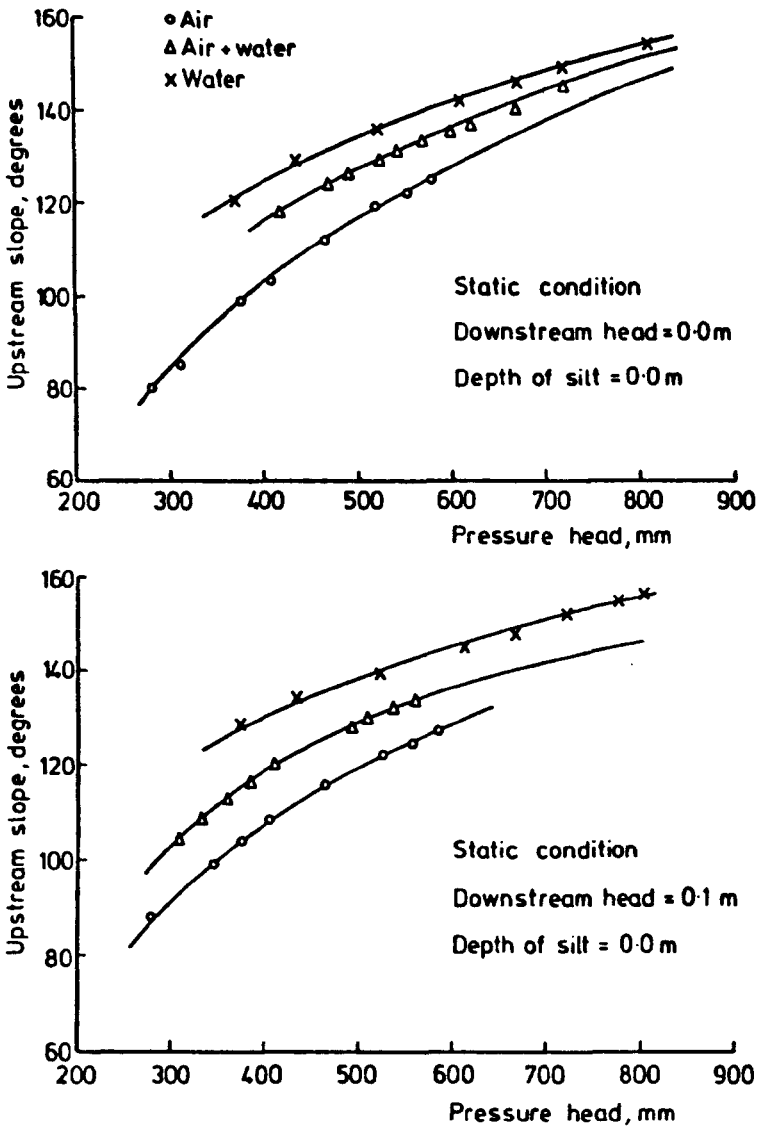

FIG 6-9. UPSTREAM SLOPE Vs. PRESSURE HEAD FOR DIFFERENT INFLATION FLUIDS

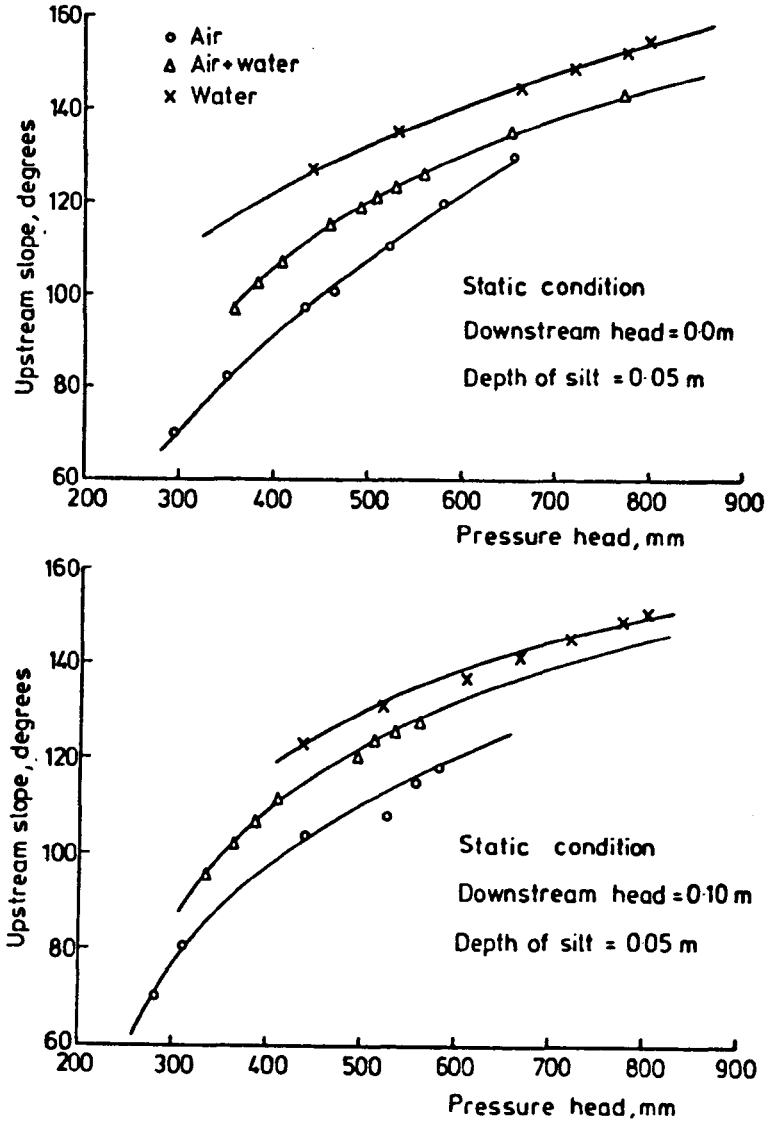

FIG. 6-10. UPSTREAM SLOPE Vs PRESSURE HEAD FOR DIFFERENT INFLATION FLUIDS

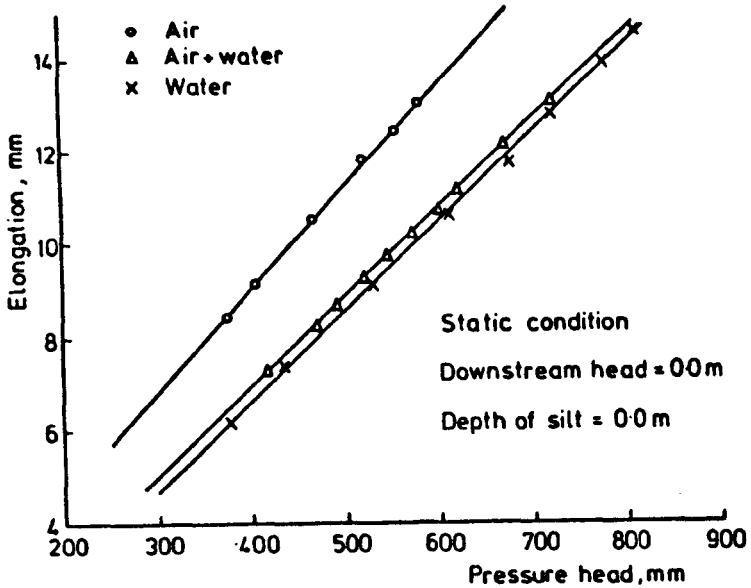

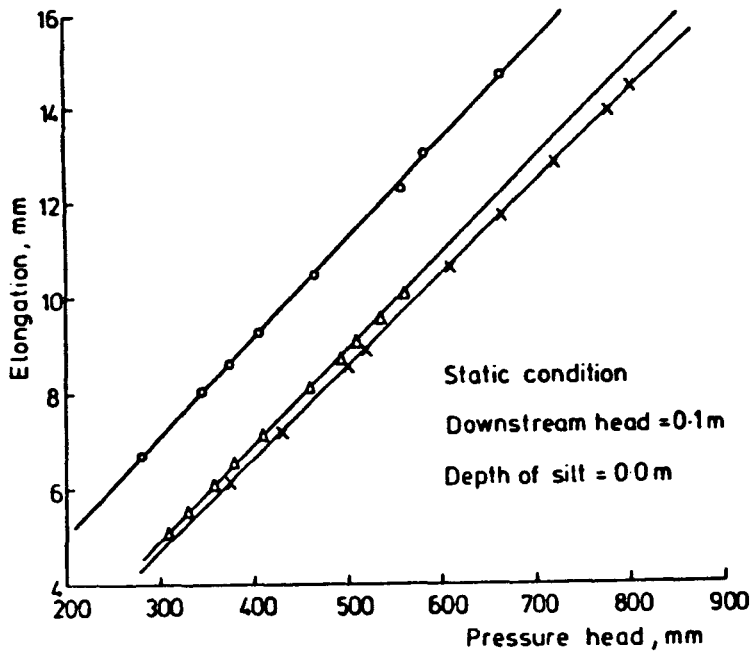

FIG.6-11 ELONGATION Vs PRESSURE HEAD FOR DIFFERENT INFLATION FLUIDS

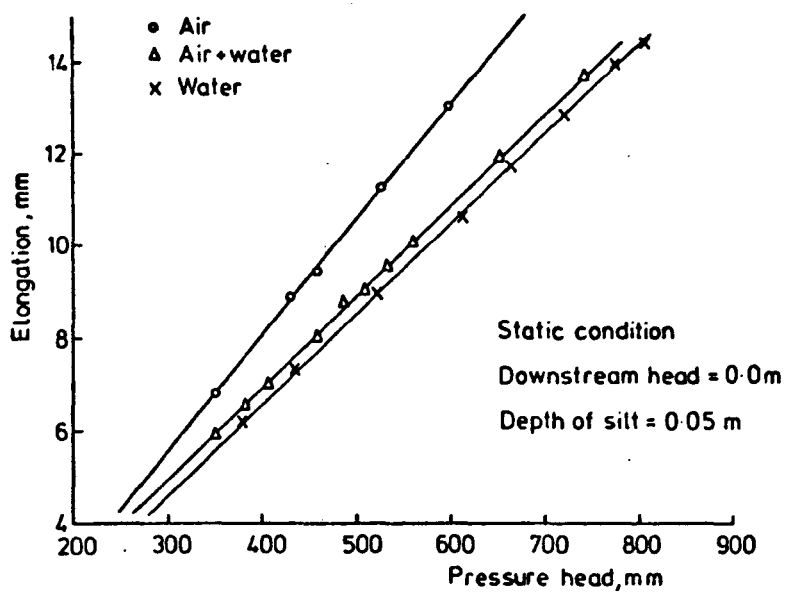

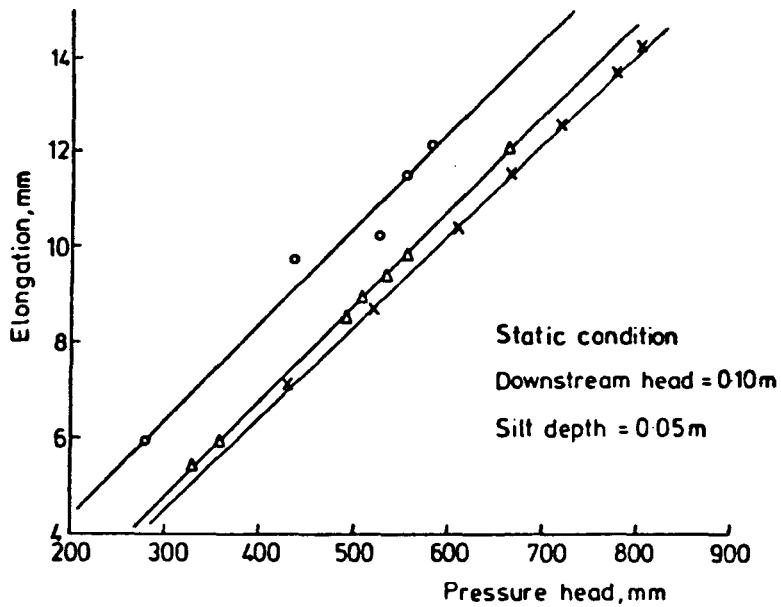

FIG.6-12.ELONGATION Vs. PRESSURE HEAD FOR DIFFERENT INFLATION FLUIDS

water and air inflated dams and also the maximum height depended on the depth of water inside the dam. Fig.6.13 shows the maximum height of dams under different inflation fluids for the condition of a downstream head equal to 0.1 m and silt depths equal to 0.0 and 0.05 m.

6.3.5 Cross-sectional area.

The cross-sectional area increased as the internal pressure heads increased for all inflation fluids and different conditions of downstream head and silt depth.

The cross-sectional areas for water inflated dams were higher than for air inflated dams while the cross-sectional area for an (air+water) inflated dam was higher than an air inflated dam and lower than a water inflated dam.

In the case of downstream depth equal to 0.0 and silt depth equal to 0.0 the cross-sectional area of an air inflated dam increased more than an (air+water) dam when the internal pressure head increased to 500 mm this being due to the higher elongation occurring in the air inflated dam. Moreover the air inflated dam gave a higher cross-sectional area than an (air+water) inflated dam for low pressure head (i.e. 200-300 mm) for the condition of downstream head equal to 0.1 m and zero silt depth, this result being due to the effect of the downstream head pushing the dam toward the upstream position.

The cross-sectional area was approximately constant for high pressure heads for all the dams inflated with different inflation fluids for the condition of downstream head equal to 0.0 and with silt depth equal to 0.05 m.

Figs. 6.14 and 6.15 show the variation of the cross-sectional area of the dams for different inflation fluids under different conditions of downstream head and silt depths.

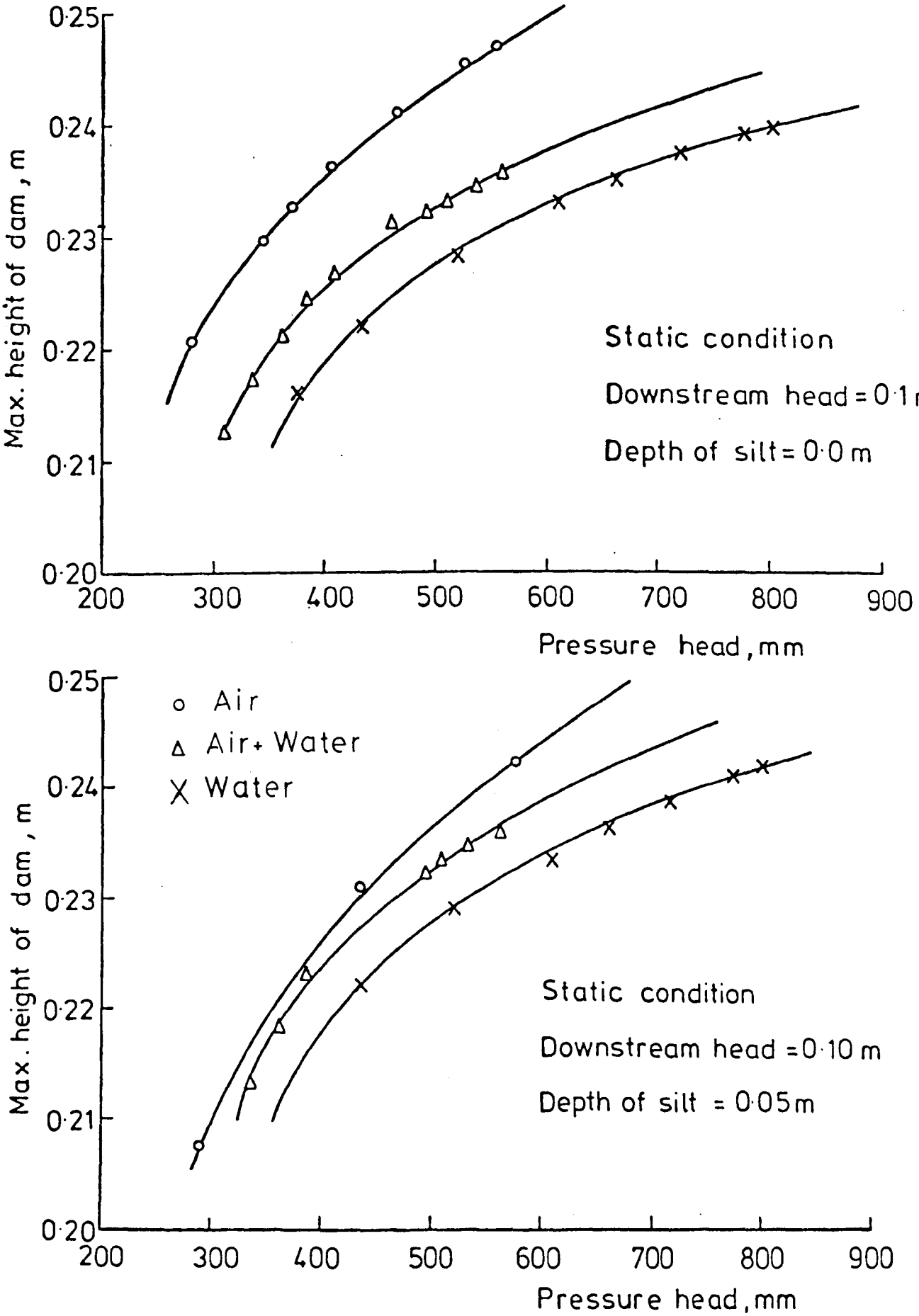

FIG.6-13. MAXIMUM HEIGHT OF DAM Vs. PRESSURE HEAD FOR DIFFERENT INFLATION FLUIDS

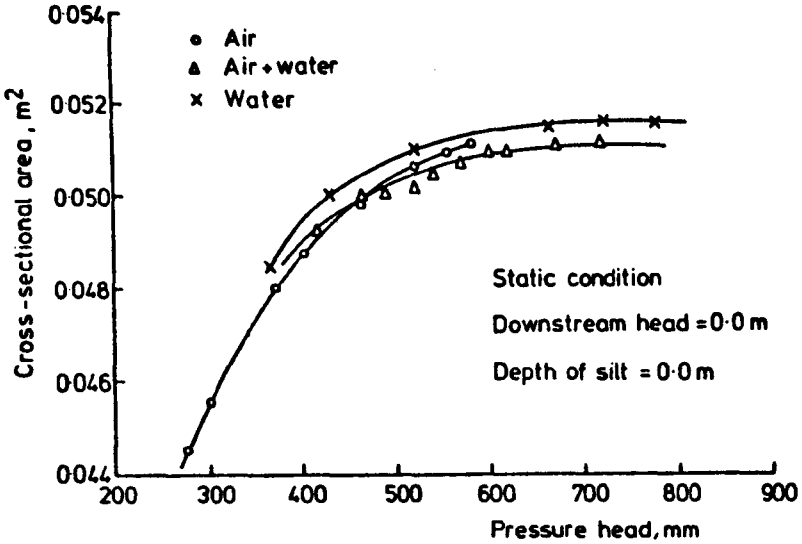

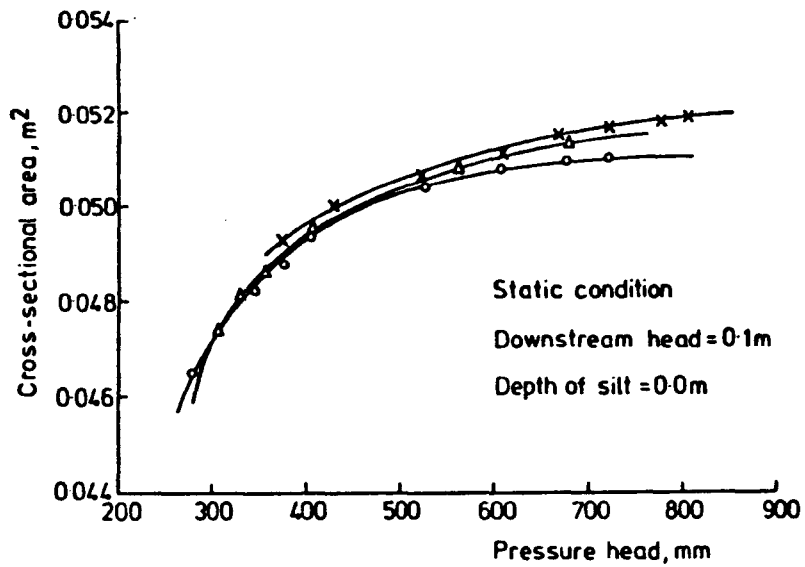

FIG. 6-14. CROSS-SECTIONAL AREA Vs. PRESSURE HEAD FOR DIFFERENT INFLATION FLUIDS

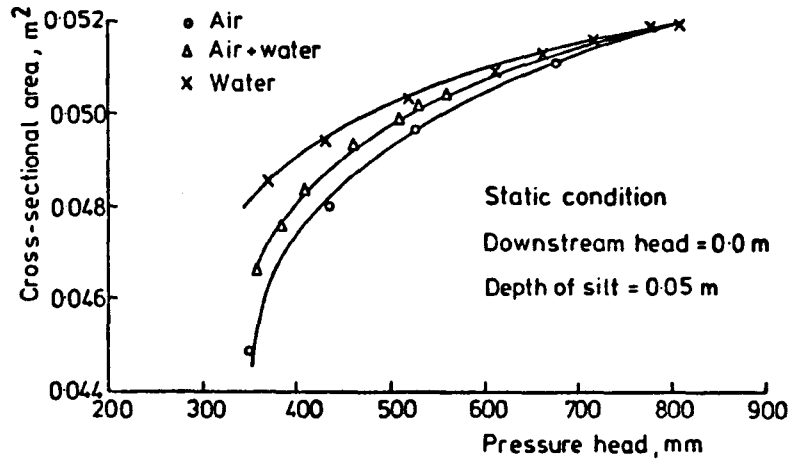

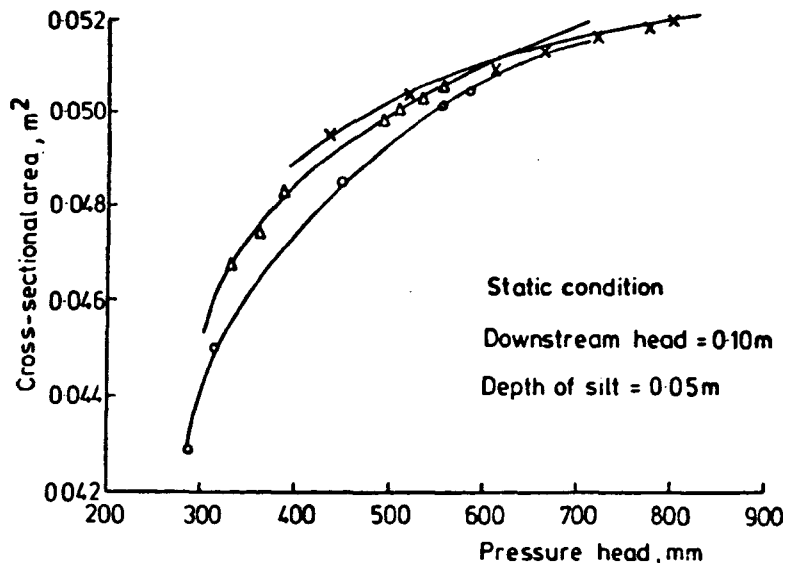

FIG. 6-15. CROSS-SECTIONAL AREA Vs. PRESSURE HEAD FOR DIFFERENT INFLATION FLUIDS

6.4 Comparison of the theoretical results of dams constructed from different materials.

The resulting output parameters depend also on the type of material used for the construction of a dam.

In this study two types of material were used, type I and type II, the details of the properties being given in table 3.1, Chapter 3.

Results of the comparison of using these two materials are given in table 6.6. These results show that the values of the output parameters for the type I material are higher than output parameters for the type II material. The differences are mainly due to the variation in the thickness of the material and the behaviour of the stress-strain relationship. The effect of the weight of the material was not significant on the output parameter and this conclusion was found in Chapter 4, tables 4.4 and 4.5, while the thickness can be considered a significant parameter in the output parameter (see table 4.6 and 4.7). Hence, since the thickness of material type I is less than the thickness of the material type II, the value of the output parameters of the type I material are higher than for the type II material. Increasing the thickness of the material will decrease the tension in the membrane but it will decrease the flexibility of the material which effects the construction of the dam. Therefore the chosen material should be of high flexibility and high strength for ease of construction and strong to avoid any damage due to high pressure heads. Table 6.6 shows the details of the comparison of material type I and material type II, and fig. 6.16 shows different profiles of dams under different inflation fluids for the two materials.

6.5 Summary.

In this chapter a comparison of the theoretical and experimental work was made and the results were satisfactory.

Table 6.6 Comparison of Material Type I and Type II for different output parameters under the same conditions.

Type No.	Type of Inflation	No. of Test	Propl. factor	U/S (m)	D/S (m)	H_s (m)	U/S Tension KN/m		D/S Tension KN/m		U/S Slope degree		Elongation (mm)		Cross Sectional Area m^2	
							Type I Mat.	Type II Mat.	Type I Mat.	Type II Mat.	Type I Mat.	Type II Mat.	Type I Mat.	Type II Mat.	Type I Mat.	Type II Mat.
1	Air	1	0.4	0.2425	0.0	0.0	0.315	0.303	0.402	0.396	93.16	92.97	6.7	6.1	0.0476	0.0469
		2	0.8	0.2536	0.0	0.0	0.421	0.416	0.579	0.513	112.42	112.23	10.57	8.5	0.0498	0.0491
		3	1.0	0.2575	0.0	0.0	0.484	0.483	0.668	0.666	118.84	188.75	11.86	9.59	0.0506	0.0503
		4	1.1	0.2590	0.0	0.0	0.515	0.513	0.712	0.709	121.88	121.63	12.02	10.09	0.0509	0.0506
		5	1.2	0.2609	0.0	0.0	0.546	0.594	0.756	0.753	124.51	124.20	13.03	10.57	0.0512	0.0509
2	Water	1	1.0	0.1886	0.0	0.0	0.215	0.214	0.296	0.295	121.19	121.2	6.21	5.06	0.0480	0.0483
		2	1.2	0.1978	0.0	0.0	0.267	0.266	0.367	0.367	128.07	127.96	7.23	5.88	0.0494	0.0492
		3	1.4	0.2085	0.0	0.0	0.330	0.329	0.455	0.454	133.27	133.64	8.56	6.93	0.0515	0.0512
2	Air+Water	1	0.8	0.2000	0.04	0.05	0.218	0.218	0.286	0.285	97.65	98.19	5.94	4.84	0.0466	0.0465
		2	0.9	0.2035	0.04	0.05	0.246	0.245	0.322	0.321	103.39	103.86	6.47	5.27	0.0477	0.0476

U/S HEAD = 0.2956 METER
D/S HEAD = 0.0000 METER
AIR PRESSURE = 4.5648 KN/SQ.M
WATER PRESSURE = 0.0000 M.V.G.
ORIGINAL LENGTH = 0.5001 METER
NEW LENGTH = 0.5107 METER
U/S TENSION = 0.4212 KN/M
U/S SLOPE = 112.3571 DEGREE
D/S TENSION = 0.5742 KN/M
BASE LENGTH = 0.1192 METER
ALFA = 0.8000
AREA = 0.0498 METER SQ
SILT DEPTH,MS = 0.0000 METER

Material type I

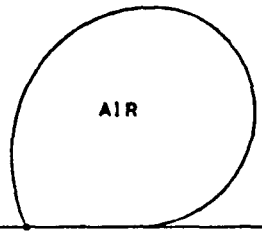

U/S HEAD = 0.2956 METER
D/S HEAD = 0.0000 METER
AIR PRESSURE = 4.5448 KN/SQ.M
WATER PRESSURE = 0.0000 M.V.G.
ORIGINAL LENGTH = 0.8001 METER
NEW LENGTH = 0.8086 METER
U/S TENSION = 0.6197 KN/M
U/S SLOPE = 112.2327 DEGREE
D/S TENSION = 0.5773 KN/M
BASE LENGTH = 0.1192 METER
ALFA = 0.8000
AREA = 0.0495 METER SQ
SILT DEPTH,MS = 0.0000 METER

Material type II

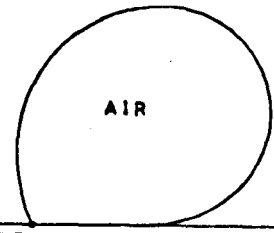

U/S HEAD = 0.1886 METER
D/S HEAD = 0.0000 METER
AIR PRESSURE = 0.0000 KN/SQ.M
WATER PRESSURE = 0.3735 M.V.G.
ORIGINAL LENGTH = 0.8000 METER
NEW LENGTH = 0.8062 METER
U/S TENSION = 0.2151 KN/M
U/S SLOPE = 120.4894 DEGREE
D/S TENSION = 0.2956 KN/M
BASE LENGTH = 0.1750 METER
ALFA = 1.0000
AREA = 0.0484 METER SQ
SILT DEPTH,MS = 0.0000 METER

Material type I

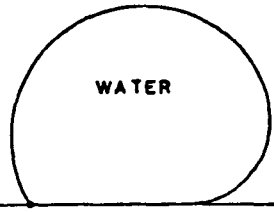

U S HEAD = 0.1886 METER
D/S HEAD = 0.0000 METER
AIR PRESSURE = 0.0000 KN/SQ.M
WATER PRESSURE = 0.3735 M.V.G.
ORIGINAL LENGTH = 0.8000 METER
NEW LENGTH = 0.8051 METER
U/S TENSION = 0.2148 KN/M
U S SLOPE = 120.4279 DEGREE
D S TENSION = 0.2944 KN/M
BASE LENGTH = 0.1767 METER
ALFA = 1.0000
AREA = 0.0482 METER SQ
SILT DEPTH,MS = 0.0000 METER

Material type II

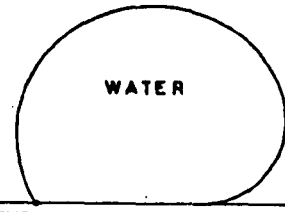

U/S HEAD = 0.2004 METER
D/S HEAD = 0.0400 METER
AIR PRESSURE = 1.9931 KN SQ.M
WATER PRESSURE = 0.1575 M.V.G.
ORIGINAL LENGTH = 0.7980 METER
NEW LENGTH = 0.8040 METER
U/S TENSION = 0.2181 KN/M
U SLOPE = 97.6496 DEGREE
D/S TENSION = 0.2857 KN
BASE LENGTH = 0.1923 METER
ALFA = 0.8000
AREA = 0.0466 METER SQ
SILT DEPTH,MS = 0.0500 METER

Material type I

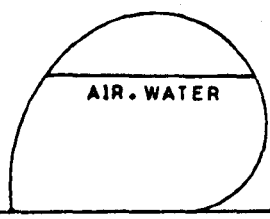

U/S HEAD = 0.2004 METER
D/S HEAD = 0.0400 METER
AIR PRESSURE = 1.993 KN SQ.M
WATER PRESSURE = 0.1575 M.V.G.
ORIGINAL LENGTH = 0.7980 METER
NEW LENGTH = 0.8079 METER
U S TENSION = 0.2180 KN M
U S SLOPE = 98.1919 DEGREE
D S TENSION = 0.2854 KN/M
BASE LENGTH = 0.1923 METER
ALFA = 0.8000
AREA = 0.0465 METER SQ
SILT DEPTH,MS = 0.0000 METER

Material type II

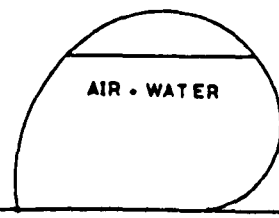

FIG. (6-16) PROFILES FOR THE DIFFERENT MATERIALS USED IN THE PROJECT

Also a comparison was carried out for the results of the output parameter found theoretically for dams inflated with different inflation fluids.

A comparison of using different materials has been carried out and it was concluded that the thickness of the material has a significant effect on the output parameters.

CHAPTER 7.

DISCHARGE COEFFICIENTS FOR INFLATABLE STRUCTURES.

7.1 Introduction.

The coefficient of discharge for different types of structure varies depending on the type of structure, i.e. broad crested weir, sharp crested weir, sills, spillways.

For inflatable structures it is necessary to find the coefficient of discharge for different values of the proportional factor and also for different inflation fluids.

Several investigators have carried out experimental work to find the coefficient of discharge. Baker (20) and Clare (14) determined the coefficient of discharge (C_D) from experimental work for a water inflated dam by using the following equation:

$$C = \frac{q}{H^{3/2}} \quad \ldots\ldots \quad 7.1$$

where q = discharge per unit width ($ft^3/s/ft$).

H = overflow head in ft.

C = coefficient of discharge in $ft^{\frac{1}{2}}/sec$.

Both of the above investigators found the values of C to range between 3.1 for low flows and 4.1 for high flows.

Equation 7.1 is not dimensionless as the values of C include the term $\sqrt{2g}$, hence the dimensionless coefficient (38) can be found by the following relationship:

$$C_D = C/\sqrt{2g} \quad \ldots\ldots \quad 7.2$$

where C_D = dimensionless coefficient of discharge.

g = acceleration due to gravity.

Therefore the coefficient of discharge in dimensionless form ranges between 0.386 for low heads up to 0.510 for high flows.

Anwar (2) and Stodulka (21) determined the coefficient of discharge by using the following equation:

$$C_D = \frac{q}{\sqrt{2g}\, H^{1.5}} \quad \ldots\ldots \quad 7.3$$

The results for the coefficient of discharge determined by Anwar were in the range 0.35 for a low proportional factor to 0.5 for high proportional factors.

Stodulka's investigations gave coefficient of discharges in the ranges 0.25 to 0.40 for a range of low to moderate flows of 0.074 $m^3/s/m$. but no mention was given of the range of the proportional factors used for the dam.

In this study attempts have been made to find a relationship between discharge and the coefficient of discharge data from the experimental work in order to develop an equation for other similar structures.

These calibration equations were worked out for different inflation fluids (air, water, and the combination of the two) and under different proportional factors alpha.

This chapter also includes a comparison of the values found by different investigators with those found from the calibration equation and also the main factors affecting the coefficient of discharge.

7.2 Discharge Measurement.

In order to measure the discharge flowing over the inflatable structure, a rectangular sharp crested weir was placed at the end of a rectangular channel connected to the outlet of the test tank as shown in fig.7.1A, B, C.

1. Rectangular channel.

This channel was connected to the test tank and incorporated the rectangular sharp crested weir. The channel was made from 1.5 mm galvanised

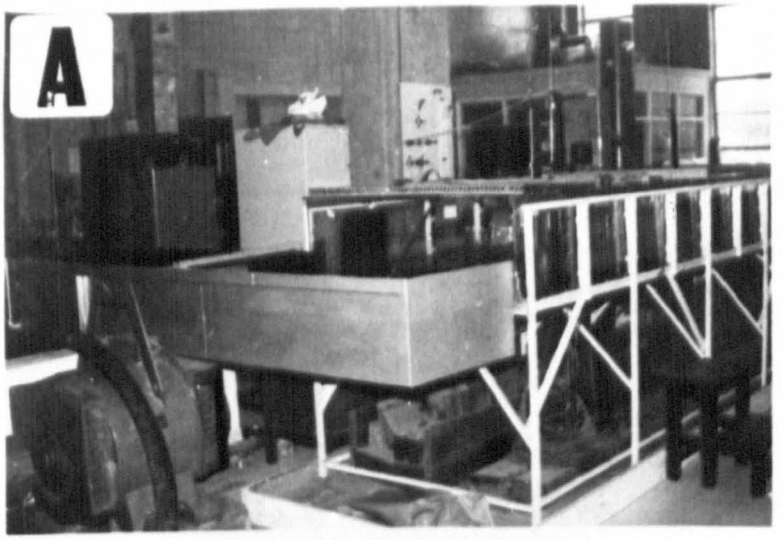

Rectangular channel

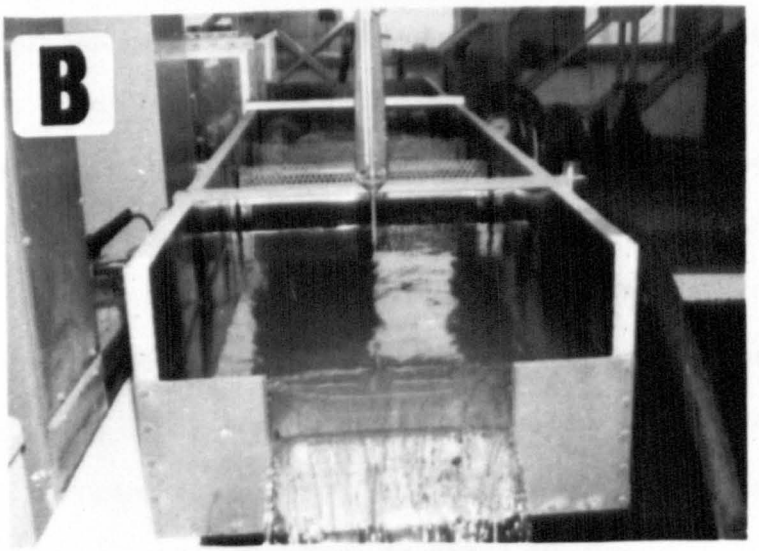

Rectangular sharp crested weir

Volumetric tank

FIG. (7-1) FLOW MEASUREMENT SYSTEM

steel sheet and was 3000 mm long, 600 mm wide and 350 mm deep. 1000 mm upstream of the weir two baffle plates were fitted across the flow, each baffle consisting of three layers of hexagonal aluminium mesh, 16 mm thick. The two baffles were placed 400 mm apart. These baffles were used to create uniform flow across the section and hence improve the accuracy of the flow measurements.

2. Sharp crested weir.

The sharp crested rectangular weir was fitted at the end of the channel. The weir plate was made from 5 mm thick brass and was designed according to BS 3680 (39) part 4. The rectangular crested weir can be seen in fig.7.1B.

3. Volumetric tank.

A tank of dimensions (3040 mm x 1219 mm x 711 mm) was used to measure volumes of water collected in different time intervals in order to find the stage - discharge relationship for the rectangular weir by the volumetric calibration technique. A point gauge was used to measure the depth of water in the tank, while the head over the weir was measured by means of a piezometer tube connected to the rectangular channel 400 mm upstream of the weir. The volumetric tank is shown in fig.7.1C.

7.2.1 Calibration of the weir.

The general equation relating stage and discharge for a rectangular sharp crested weir is shown in equation 7.4 (48).

$$Q = \frac{2}{3}\sqrt{2g}\ b\ C_D\ H_r^{3/2} \quad \ldots\ldots \quad 7.4$$

where Q = discharge (M^3/s).

b = breadth (m).

g = acceleration due to gravity (m/s^2).

C_D = coefficient of discharge.

H_r = head of water above the crest level (m).

For the maximum design discharge of 18 ℓ/s and maximum allowable head over the weir of 97 mm with a crest height of 100 mm, the necessary breadth of the wrie was evaluated using equation 7.4 as 320 mm assuming the coefficient of discharge is equal to 0.63.

By considering $\frac{2}{3}\sqrt{2g}\ b\ C_D$ of equation 7.4 as a coefficient K this gave a theoretical stage discharge relationship

$$Q = 0.596\ H_r^{3/2} \quad \ldots\ldots \quad 7.5$$

By finding the time for known volumes to accumulate in the measuring tank (see fig.7.1C) for different steady conditions of discharge and head over the weir it was possible to obtain an experimentally derived relationship between the head and the discharge.

Fig.7.2 shows a plot of $H_r^{3/2}$ against the discharge Q and from this relationship a value of K of 0.583 was found by using a computer program to find the best fit line. This gave an experimentally derived equation

$$Q = 0.583\ H_r^{3/2} \quad \ldots\ldots \quad 7.6$$

This difference in the K values in equation 7.5 and 7.6 is probably due to the estimated value of C_D in equation 7.4 together with the scale of the weir being outside the limitations of the British Standard. In view of the difference in the K values the volumetric calibration equation was used in all future work.

7.3 Experimental model test.

The coefficients of discharge were found experimentally for the inflatable hydraulic structures for different inflation fluids under different proportional factors, with different downstream heads. The test program for the discharge coefficient is shown in table 7.1. The overflow over the dam was measured from low to high heads as shown in table 7.1.

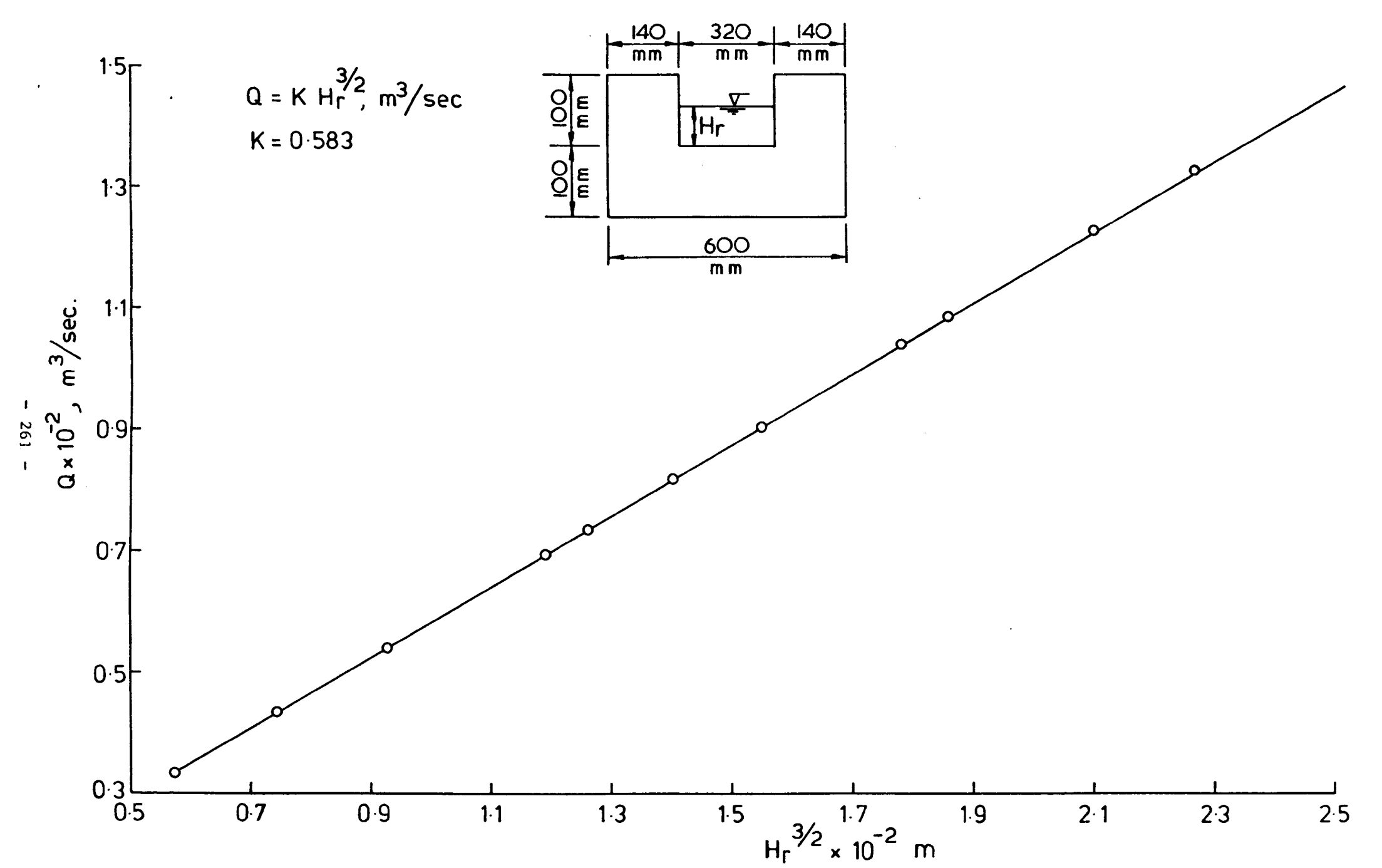

FIG. 7-2 CALIBRATION CURVE FOR THE RECTANGULAR SHARP-CRESTED WEIR

Table 7.1 Test program for the coefficient of discharge determinations.

No.	Type of inflation fluid	Proportional factor	Overflow head mm		Downstream head mm	
			Min.	Max.	Min.	Max.
1	Air	0.4	12.00	30.00	0.0	100
		0.6	18.00	32.50	0.0	100
		0.8	21.00	43.00	0.0	100
		1.0	18.13	47.40	0.0	100
		1.2	19.14	47.90	0.0	100
		0.8	12.54	44.57	0.0	100
		1.2	8.95	36.70	0.0	100
2	Water	0.8	18.00	46.00	0.0	100
		1.0	12.00	35.00	0.0	100
		1.2	10.72	27.75	0.0	100
		1.5	14.00	38.00	0.0	100
		2.5	3.45	24.62	0.0	100
		2.5	4.52	39.89	0.0	100
3	Air+Water	0.6	18.17	40.58	0.0	100
		0.8	8.64	42.96	0.0	100
		1.0	7.22	44.10	0.0	100
		1.5	6.00	35.00	0.0	100
		1.8	8.00	40.00	0.0	100
		1.0	16.50	42.25	0.0	100

7.4 Characteristics of flow over the crest.

From observations during the experimental work for the inflatable hydraulic structures for different inflation fluids it was noted that there was a limit to the overflow head beyond which the dam started to oscillate backwards and forwards and this phenomenon has been explained in Section (5.3.2).

For the head over the crest before exceeding the limit beyond which the dam started to vibrate, the nappe was almost in complete contact with the surface of the dam. Fig.7.3 shows the flow of the nappe before the separation for low and high rates of flow.

The lower nappe separation from the membrane may produce a negative pressure underneath the nappe due to the removal of air by the overfalling jet. This negative pressure will cause undesirable effects on the nappe behaviour.

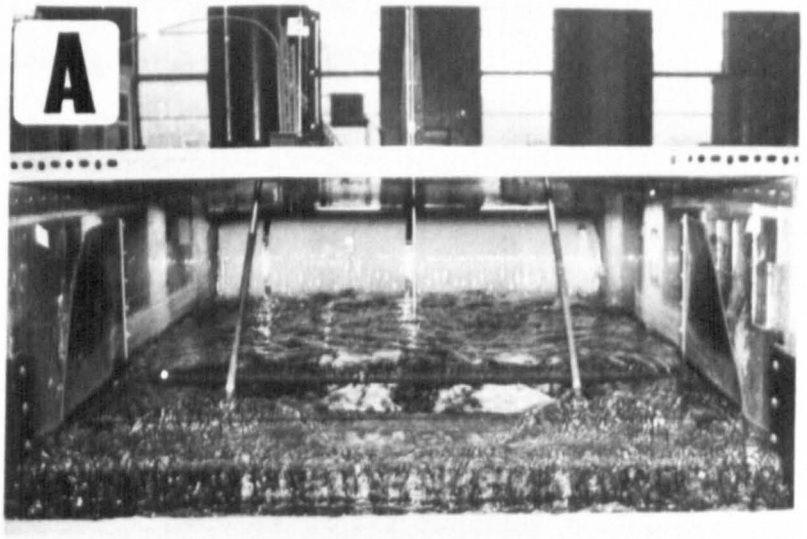

(a) Low flow

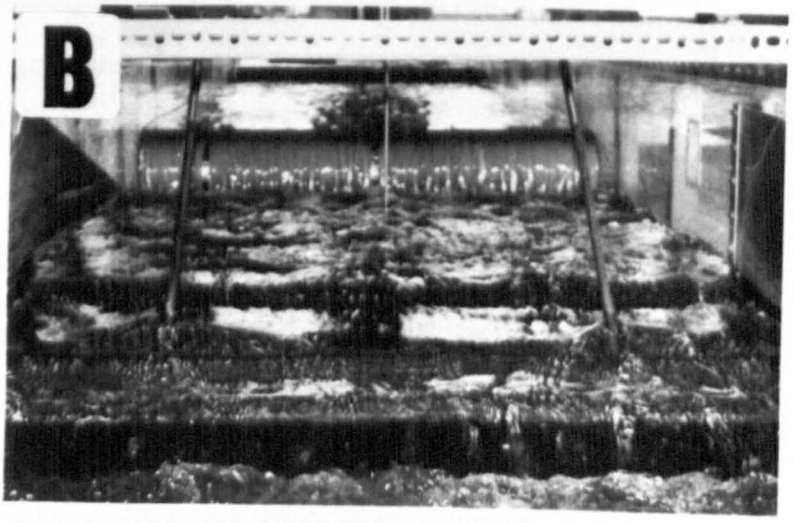

(b) Flow before seperation of the nappe

FIG. (7-3) BEHAVIOUR OF THE FLOW OVER THE CREST

Chow (40) illustrated the effect of the separation of the nappe which caused the following effects:

1. Increase in pressure difference on the crest of the dam.
2. Change in the shape of the nappe.
3. Increase in the discharge.
4. Unstable performance of the dam.

The above points have been studied by Hickoy (41) and on the basis of experimental tests to avoid this effect on the spillway of a dam he developed an equation to find the quantity of air required for aeration of the nappe.

In this technique aeration of the nappe was achieved by inserting two glass pipes on both outer edges of the downstream side to allow atmospheric pressure to be created under the nappe. The two pipes were of diameters equal to 12 mm and bent to an L shape.

With the relation to the downstream head, it was observed that the negative pressure decreased as the downstream head increased.

7.5 Coefficient of discharge for an inflatable dam.

The coefficient of discharge was determined experimentally under different inflation pressures and for different inflation fluids and it was found that the coefficient of discharge changes as the proportional factor changes and when the proportional factor changes, the shape of the crest of the dam changes.

Hence it was considered that the coefficient of discharge C_D changes with respect to the following parameters:

$$C_D = \emptyset\ (\alpha, H, H_D, v, \mu, \rho) \quad \ldots\ldots \qquad 7.7$$

where

C_D = coefficient of discharge.

α = proportional factor.

H = overflow head.

H_D = maximum height of dam.

v = velocity of approach.

μ = fluid viscosity.

ρ = fluid density.

Applying Rayleigh's method (42) of dimensional analysis, these variables can be re-grouped as follows:

$$C_D = f_1 (\alpha, H_D, H, v, u, \rho) \quad \ldots\ldots 7.8$$

or

$$C_D = f_2 \left(\frac{H}{H_D}\right)^a (Re)^c \quad \ldots\ldots 7.9$$

The second parameter of equation 7.9 represents the Reynolds number which Rao (43) has extensively investigated and concluded in the case of an uncontracted sharp crested weir, the effect of Reynolds number has been found to be insignificant.

Hence equation 7.9 can be written in the following form

$$C_D = f_3 \left(\frac{H}{H_D}\right)^a \quad \ldots\ldots 7.10$$

Since the discharge Q is a function of the coefficient of discharge C_D, one can derive a second equation which represents the discharge function in terms of the ratio $\left(\frac{H}{H_D}\right)$ or

$$Q = f_4 \left(\frac{H}{H_D}\right)^{a_1} \quad \ldots\ldots 7.11$$

By taking logs of both sides of equation 7.10 and 7.11, then

$$\log C_D = \log f_3 + a \log \left(\frac{H}{H_D}\right) \quad \ldots\ldots 7.12$$

$$\log Q = \log f_4 + a_1 \log \left(\frac{H}{H_D}\right) \quad \ldots\ldots 7.13$$

and equation 7.12 and 7.13 represent linear relationships between log C_D, log Q and log $\left(\frac{H}{H_D}\right)$ with slopes of a and a_1 respectively.

In this analysis, the coefficient of discharge was computed using equation 7.3 for different proportional factors and the discharge was found by using the calibration curve for the rectangular sharp crested weir for different heads of flow over the inflatable dam.

The results of the coefficient of discharge with the discharge found by the measurement are plotted on log-log scales for different inflation fluids and the coefficients of the equations 7.10 and 7.11 were found by using the least square method. A computer program was used for this purpose. The program can also plot the results of the best fit equations.

Fig. 7.4 - 7.9 represent the results of the analysis for the discharge and coefficient of discharge for different inflation fluids.

Coefficients of equations 7.10 and 7.11 are arranged in table 7.2 for the different inflation fluids.

All the data for different inflation fluids was plotted in order to find the overall best fit equation for both the discharge and the coefficient of discharge. These equations 7.13 and 7.14 are illustrated graphically in fig.7.10 and 7.11. These equations were called the combined equations.

$$q = 186.84\left(\frac{H}{H_D}\right)^{1.5047} \quad \text{.....} \quad 7.13$$

$$C_D = 0.46\left(\frac{H}{H_D}\right)^{0.095} \quad \text{.....} \quad 7.14$$

The values for the coefficient of discharge (C_D) are plotted with different discharges found from the calibration curve, fig. 7.2, under different ratios of (H/H_D). The theoretical line of discharge and the coefficient of discharge of the equations which are found for water, air and air+water inflated dams are also plotted together with the combined equations 7.13 and 7.14.

These graphical plots are shown in fig.7.12, 7.13 and 7.14.

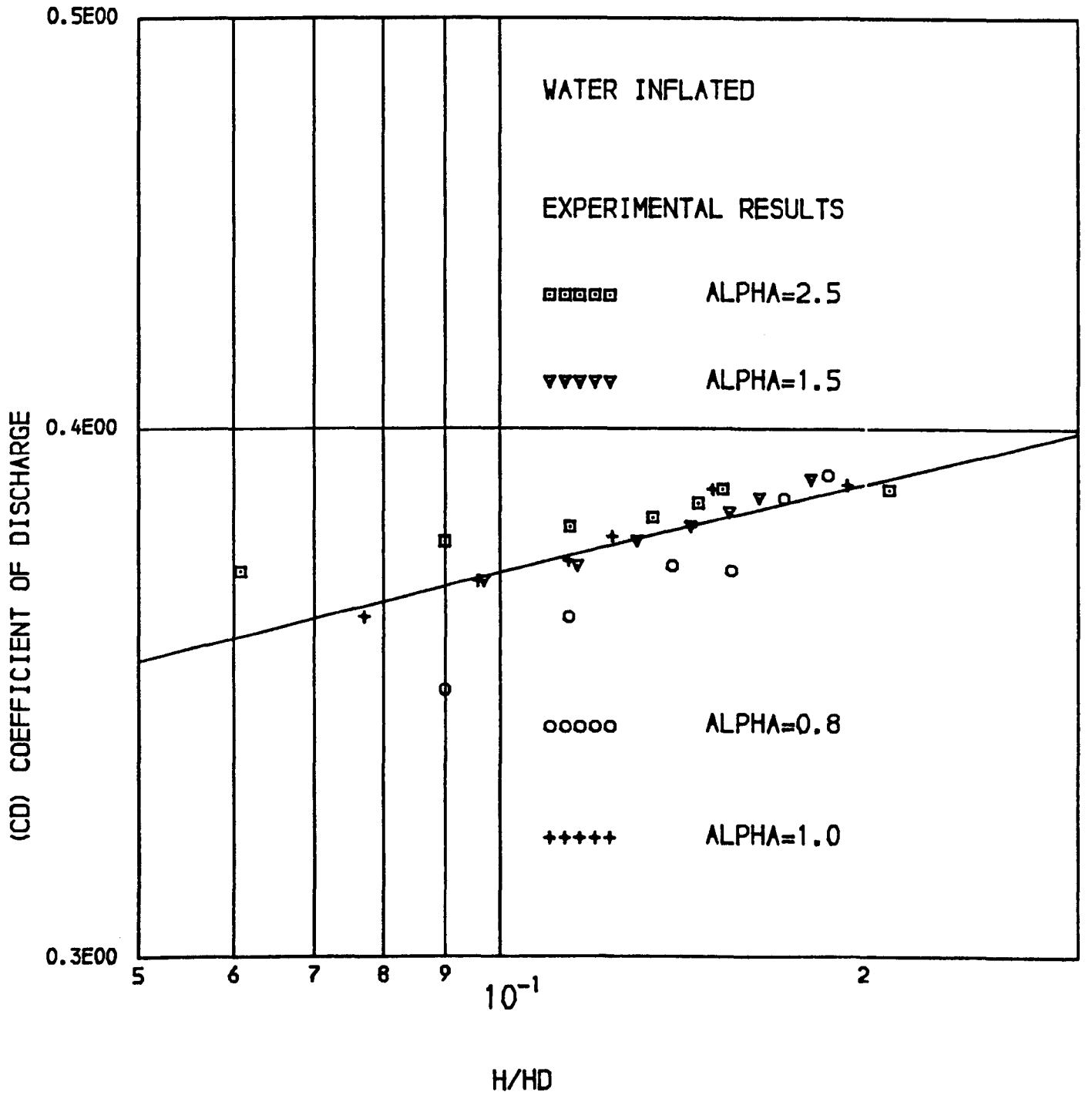

FIG(7-4) VARIATION OF COEFFICIENT OF DISCHARGE WITH RATIO (H/HD)

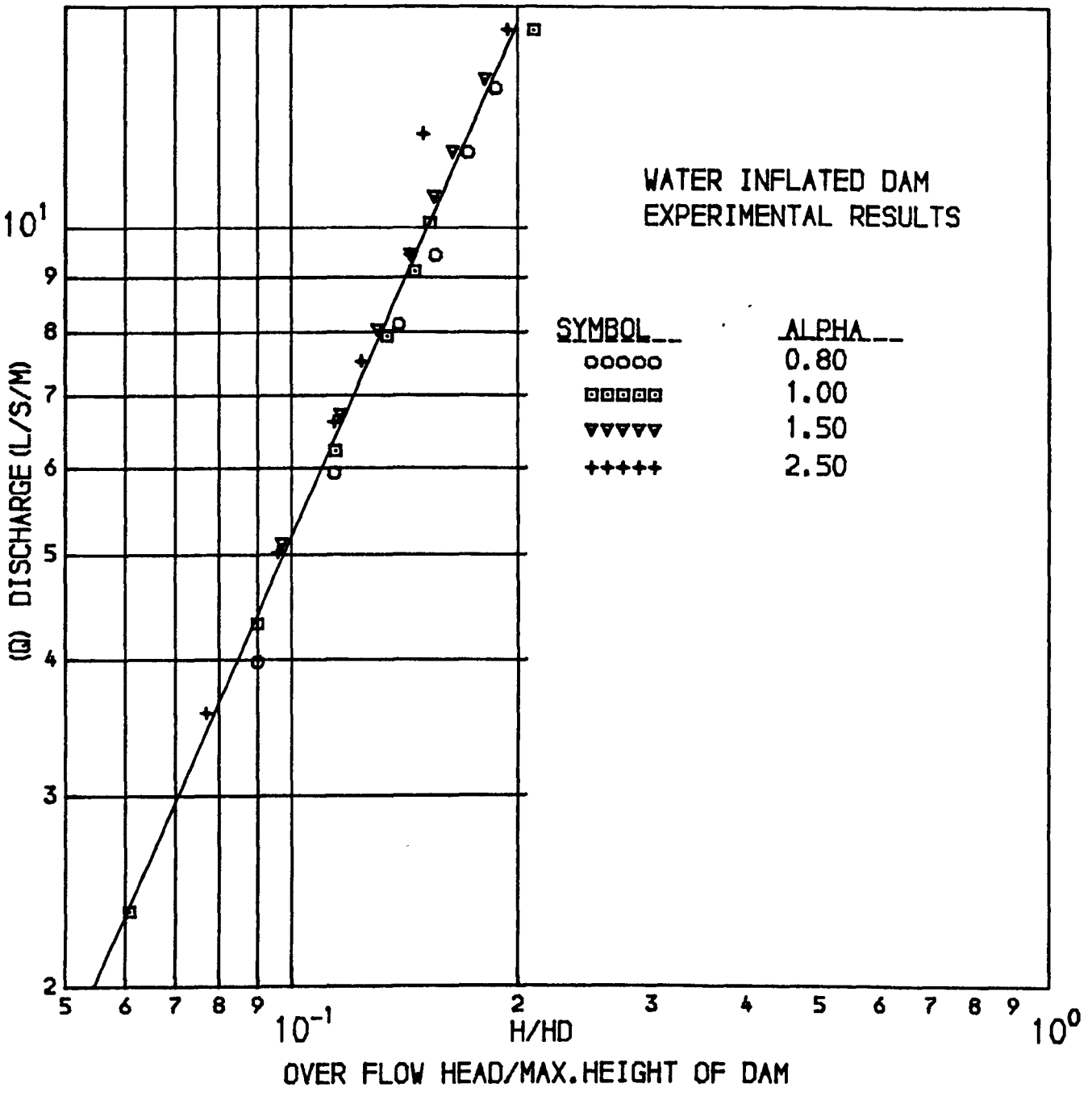

FIG(7-5) VARIATION OF DISCHARGE WITH RATIO (H/HD)

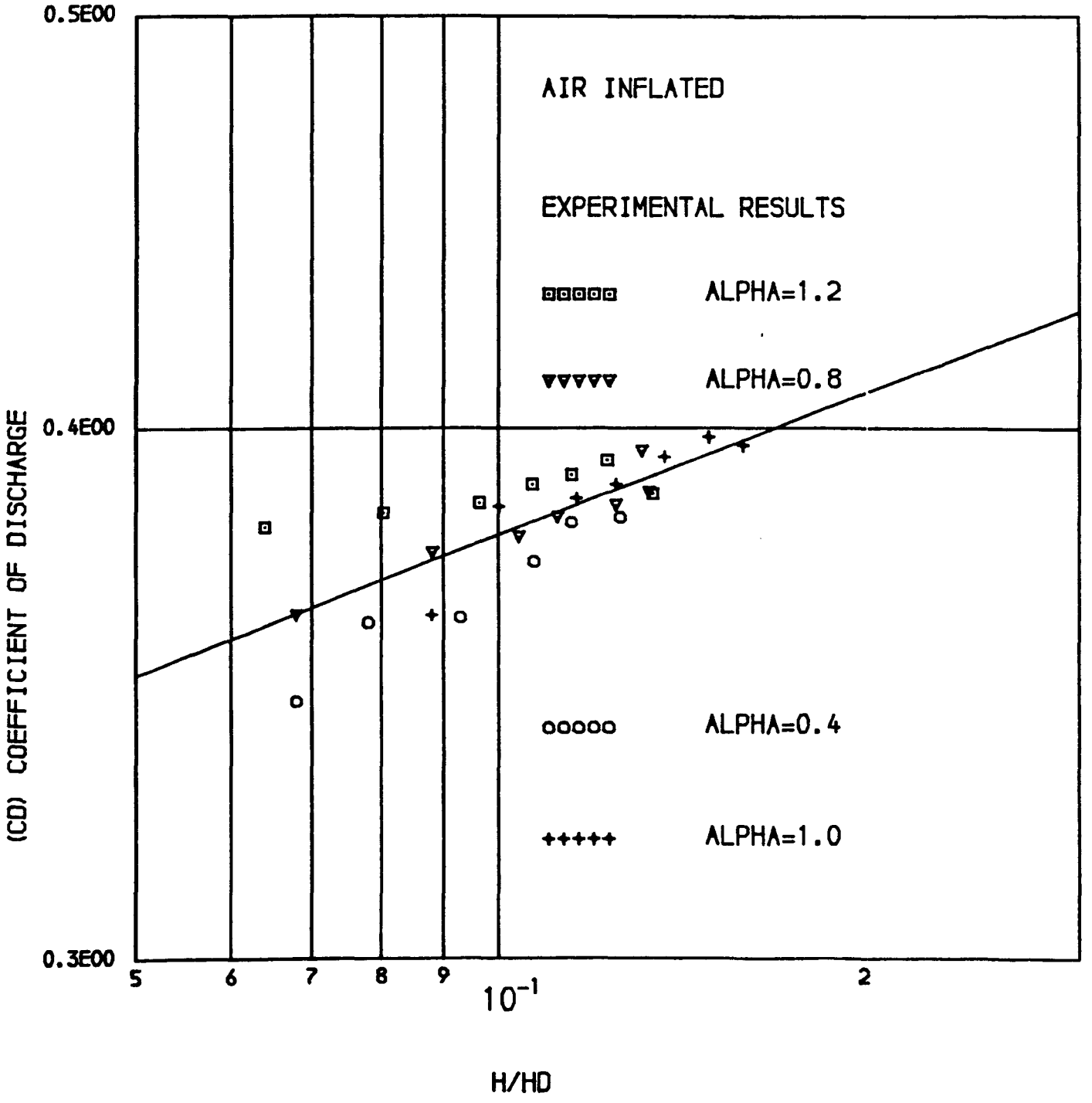

FIG(7-6) VARIATION OF COEFFICIENT OF DISCHARGE WITH RATIO (H/HD)

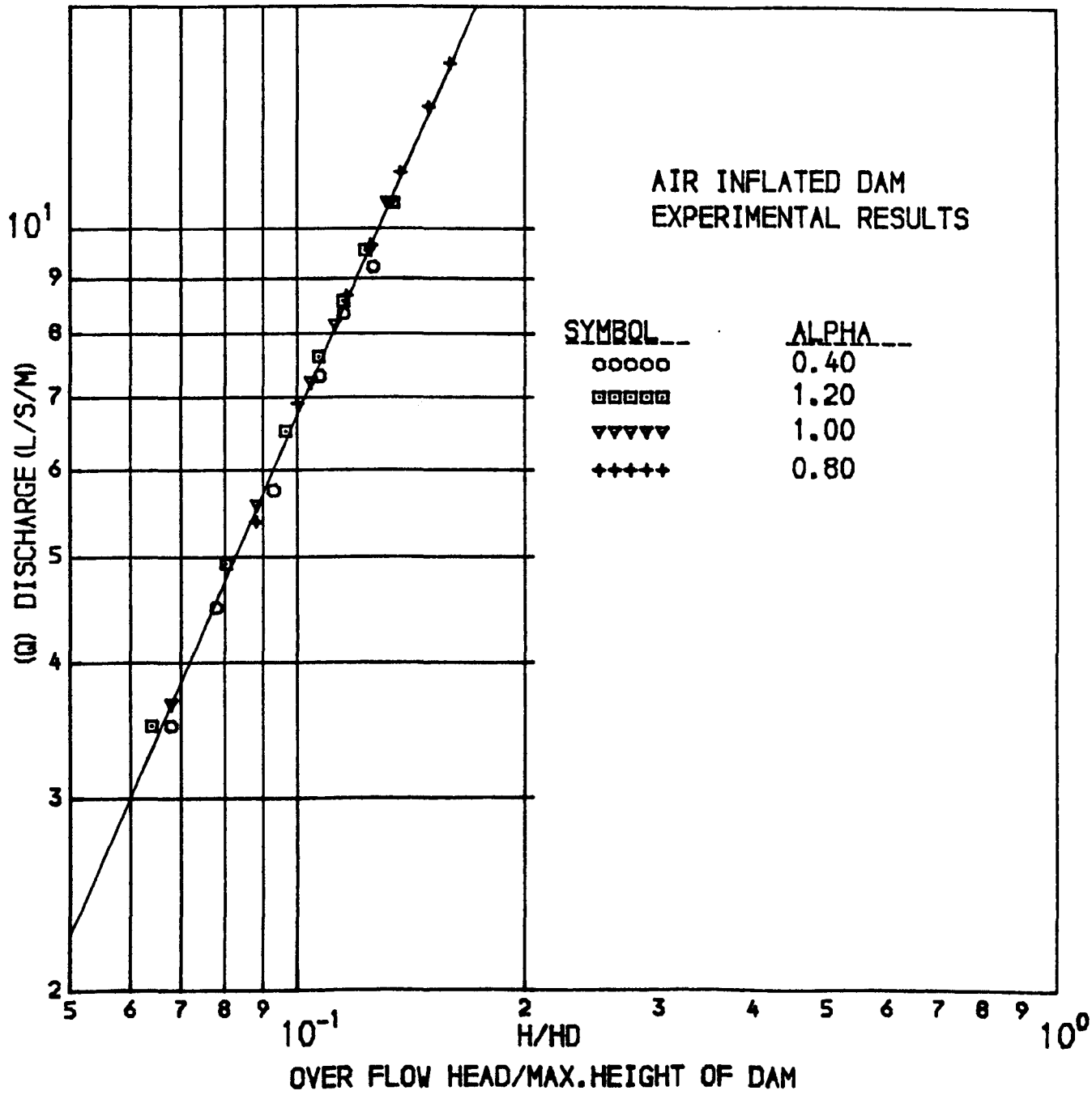

FIG(7-7) VARIATION OF DISCHARGE WITH RATIO (H/HD)

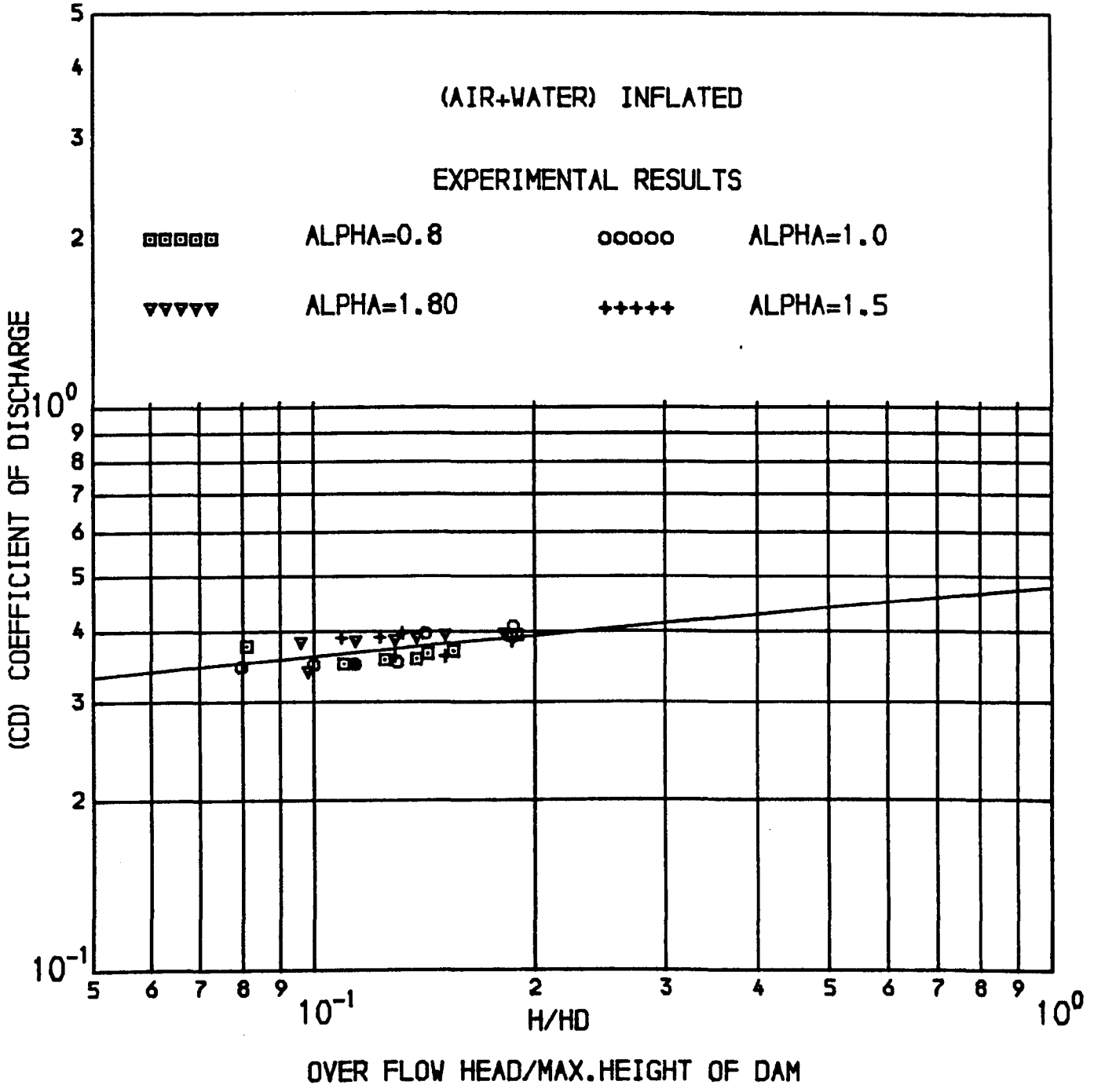

FIG(7-8) VARIATION OF COEFFICIENT OF DISCHARGE WITH PATIO

(H/HD)

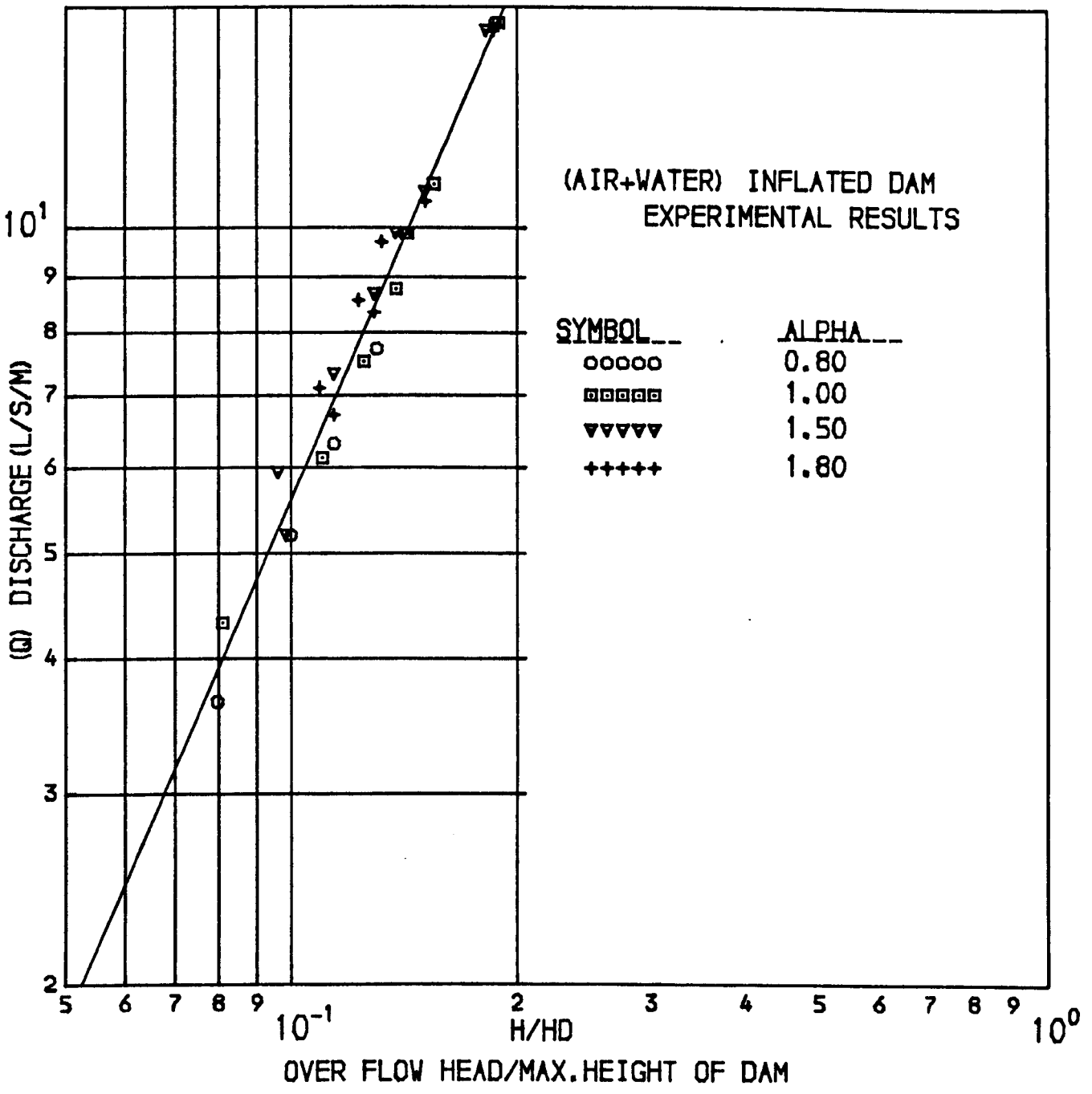

FIG (7-9) VARIATION OF DISCHARGE WITH RATIO (H/HD)

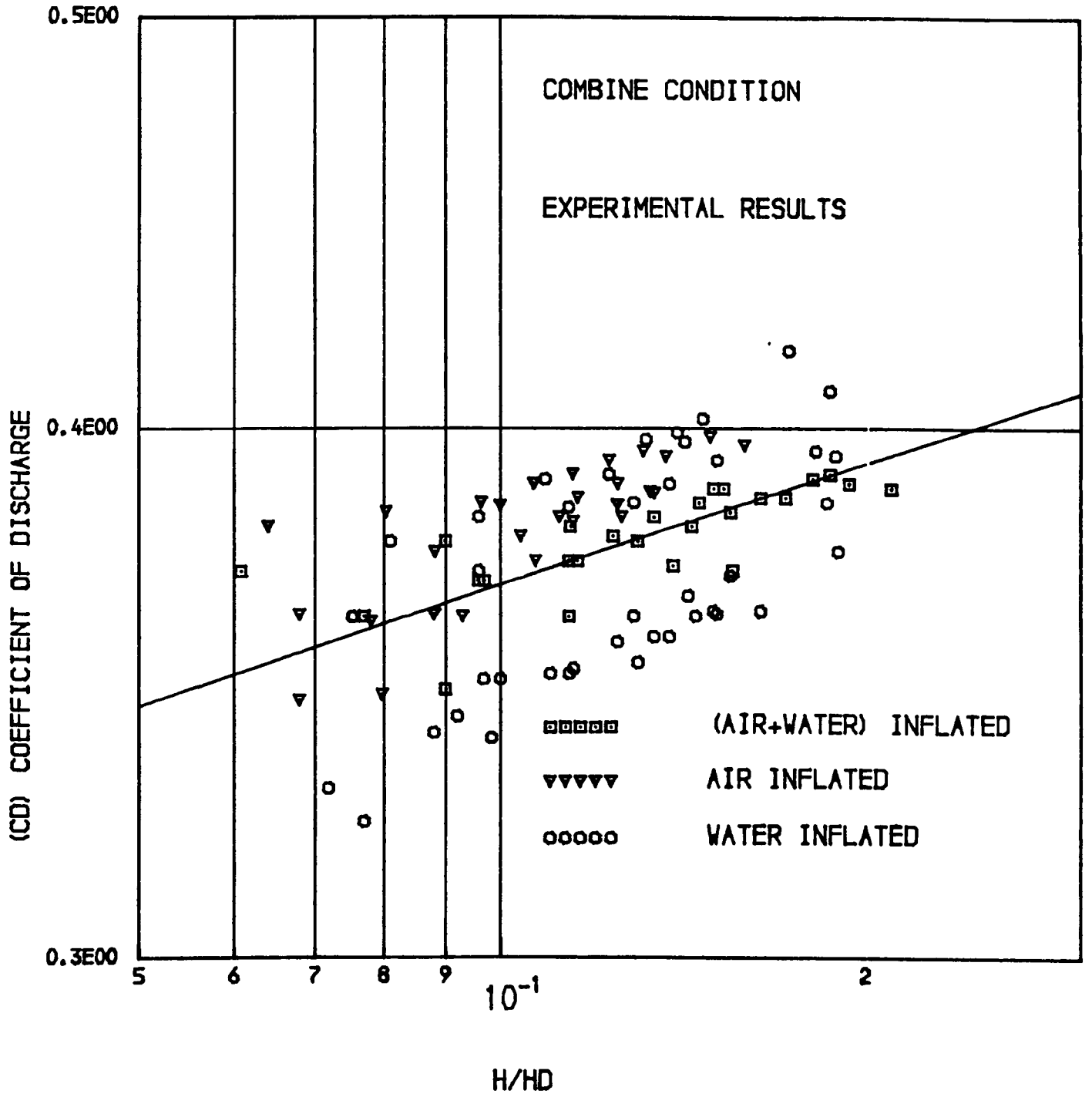

FIG(7-10) VARIATION OF COEFFICIENT OF DISCHARGE WITH RATIO (H/HD)

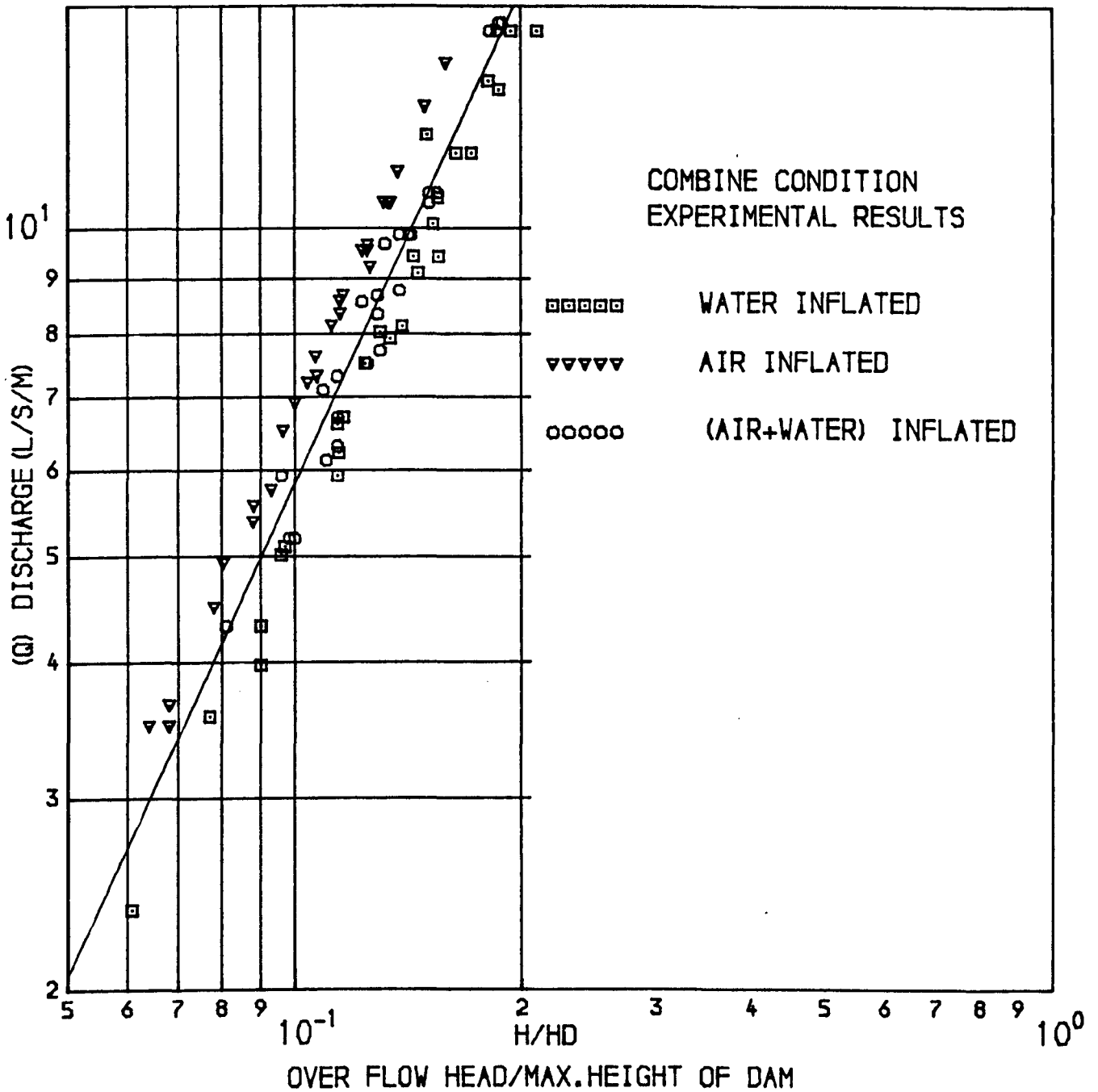

FIG (7-11) VARIATION OF DISCHARGE WITH RATIO (H/HD)

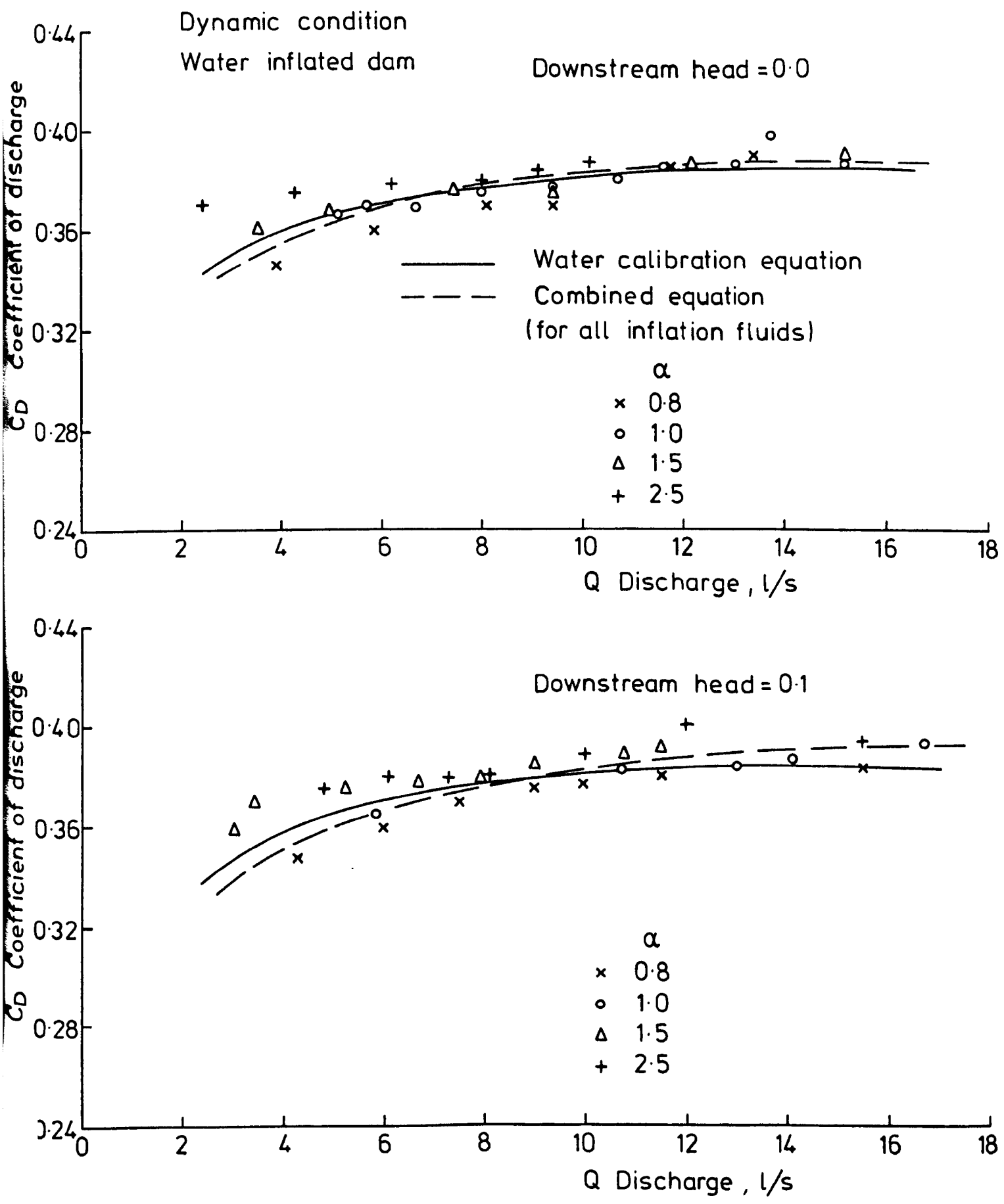

FIG. 7-12 COEFFICIENT OF DISCHARGE Vs. RATE OF FLOW FOR WATER INFLATED DAM

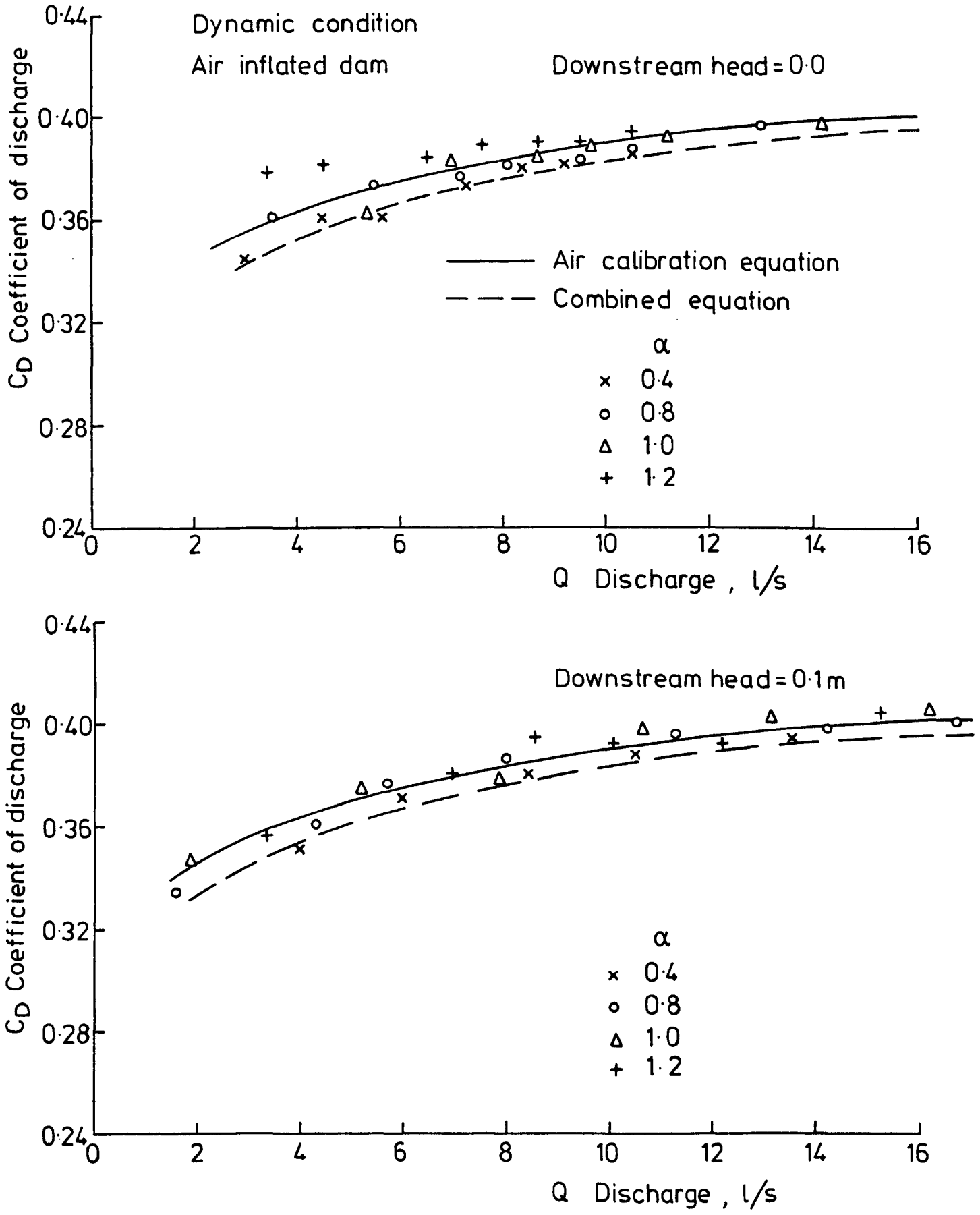

FIG. 7-13 COEFFICIENT OF DISCHARGE Vs. RATE OF FLOW FOR AIR INFLATED DAM

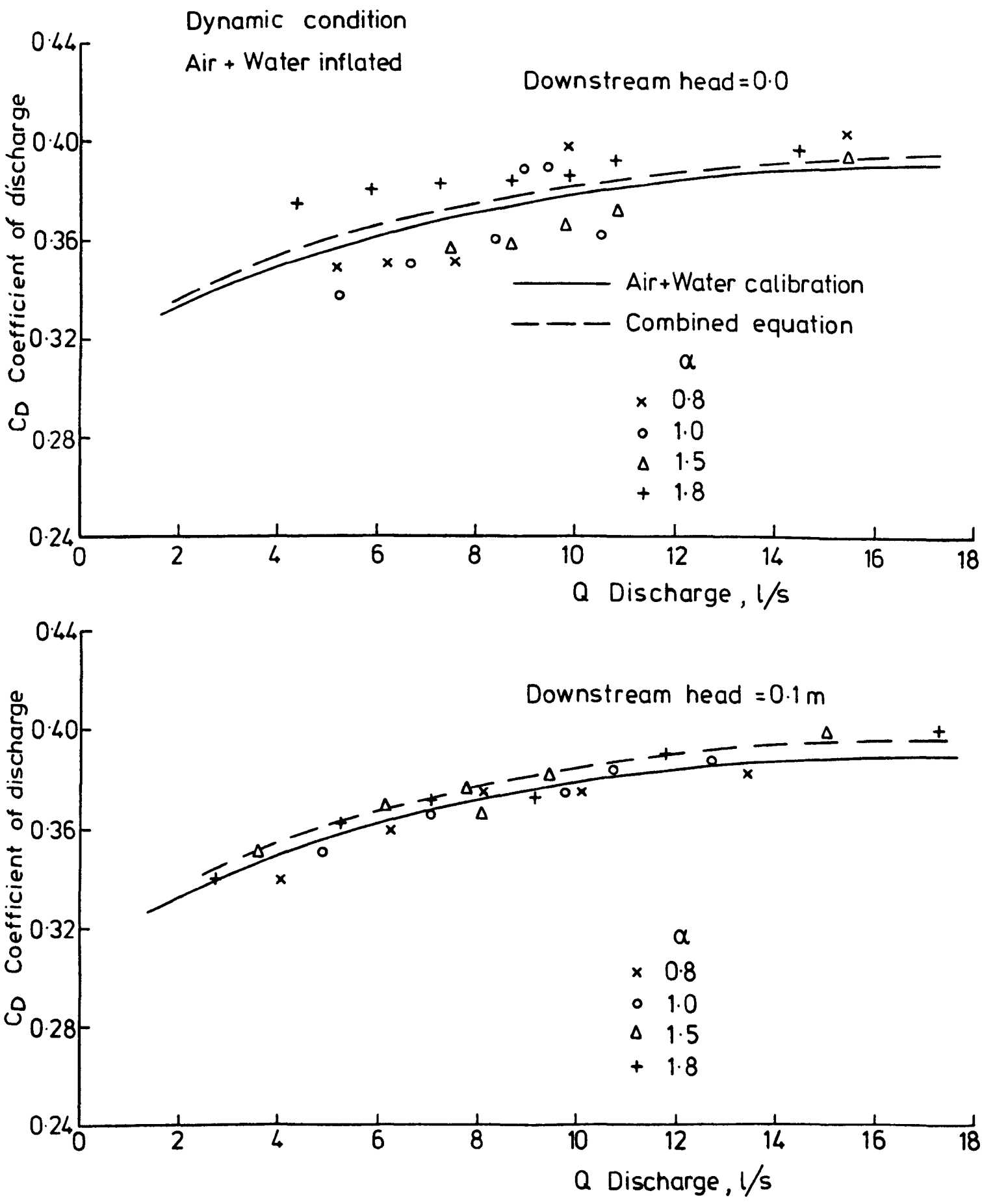

FIG. 7-14 COEFFICIENT OF DISCHARGE Vs. RATE OF FLOW FOR AIR + WATER INFLATED DAM

Table 7.2 Values of the coefficients of equations 7.10 and 7.11 for different inflation fluids.

No.	Type of Inflation fluid	Equation	Correlation coefficient
1	Water	$C_D = 0.4338 \left(\frac{H}{H_D}\right)^{0.0694}$	0.993
		$q = 194.04 \left(\frac{H}{H_D}\right)^{1.5727}$	0.936
2	Air	$C_D = 0.4866 \left(\frac{H}{H_D}\right)^{0.11}$	0.997
		$q = 261.80 \left(\frac{H}{H_D}\right)^{1.588}$	0.957
3	Air+Water	$C_D = 0.479 \left(\frac{H}{H_D}\right)^{0.123}$	0.996
		$q = 223.79 \left(\frac{H}{H_D}\right)^{1.6}$	0.960
4	Combined,i.e., Water, Air (Air+Water)	$C_D = 0.46 \left(\frac{H}{H_D}\right)^{0.095}$	0.994
		$q = 186.84 \left(\frac{H}{H_D}\right)^{1.505}$	0.944

7.6 A comparison of Methods of Determining Discharge.

In this section a comparison is made of the methods of discharge determination as found by Anwar (2), Clare (14) and by Skogero (44), with the equations determined in this study by the author (see table 7.2).

7.6.1 Comparison between Anwar and the author's results.

A comparison has been made by finding the values of the coefficient of discharge C_D from the data of Anwar (2) and the values determined in this study. The dam model used by Anwar was 0.75 feet (229 mm) high and of 2 feet (610 mm) width. The details of the values used are arranged in table 7.3 for a water inflated dam and table 7.4 for an air inflated dam.

Table 7.3 Comparison of the discharge between Anwar and the author for a water inflated dam.

No.	H/H_D	Anwar Method			Author Method		
		Over flow head (H) (mm)	C_D	q(ℓ/s/m)	C_D	q(ℓ/s/m)	% difference in (q)
1	0.19	43.4	0.39	15.64	0.3866	14.24	9.80
2	0.21	48.0	0.40	18.64	0.3892	16.66	11.87
3	0.23	52.6	0.39	20.83	0.3917	19.23	8.30
4	0.24	54.9	0.41	23.34	0.3930	20.60	13.30
5	0.265	60.6	0.42	27.68	0.3960	24.40	13.45
6	0.36	82.3	0.42	43.93	0.4040	38.90	12.90
Mean difference							11.6

Table 7.4 Comparison of the discharge between Anwar and the author for an air inflated dam.

No.	H/H_D	Anwar method			Author Method		
		H (mm)	C_D	q(ℓ/s/m)	C_D	q(ℓ/s/m)	% difference in (q)
1	0.20	51.8	0.39	20.37	0.407	20.32	0.06
2	0.25	64.7	0.42	30.67	0.418	28.97	1.71
3	0.33	85.5	0.43	46.16	0.431	45.02	1.14
4	0.40	103.6	0.44	65.03	0.440	61.00	4.03
5	0.52	134.7	0.47	102.26	0.453	95.52	6.68
6	0.55	167.6	0.48	114.38	0.460	101.19	13.28
Mean difference							5.9

7.6.2 Comparison between Clare's and the author's results.

The discharge determined by the Clare method (14) and the author's method are shown in table 7.5 for a water inflated dam. The coefficients of discharge of Clare's method are taken from his original data. The discharges measured by Clare were determined from a flume of 4 feet (1219 mm) width and the width and the height of the dam were 1.5 feet (457 mm) and 1.125 feet (343 mm) respectively.

Table 7.5 Comparison of the discharge determination between Clare and the author for a water inflated dam.

No.	H/H_D	Clare method		Author method		% diff. in (q)
		C $ft^{0.5}/sec$	q(ℓ/s/m)	C_D	q(ℓ/s/m)	
1	0.125	3.45	17.490	0.390	17.30	1.1
2	0.225	3.55	19.258	0.391	18.58	3.52
3	0.250	3.68	23.399	0.394	21.93	6.7
4	0.255	3.69	24.170	0.395	22.61	6.8
5	0.325	3.73	35.154	0.401	33.12	6.14
6	0.355	3.78	40.670	0.404	38.05	6.87
Mean difference						5.188

7.6.3 Comparison of discharge between Skogerbland and the author's results.

Discharge characteristics were investigated by Skogubo et al. (44) using the data found experimentally by Anwar and their own calibration equation. This equation (7.15) gave considerable differences from the original data

$$q = C_H (H/H_D)^{1.62} \quad \text{.....} \quad 7.15$$

where C_H ranges between 3.6 - 4.0. The comparison shown in table 7.6 is for the data of Anwar, Skogerb et al. and the combined equation (7.13) of the author.

Table 7.6 Comparison of the discharge determination between Anwar, Skogerbo and the author's results.

No.	H/H_D	Anwar q(ℓ/s/m)	Skogerbo q(ℓ/s/m)	Author Eq.(7.13) q(ℓ/s/m)	% diff. between Anwar and Skogerbo	% diff. between Anwar and Author
1	0.19	15.64	22.69	15.346	45	1.9
2	0.21	18.64	26.68	17.840	43	4.5
3	0.23	20.83	30.93	20.458	48	1.8
4	0.24	23.34	33.13	21.810	42	6.8
5	0.265	27.68	38.90	25.725	40	7.6
6	0.36	43.93	63.90	40.100	46	9.5
Mean difference					44	5.35

7.6.4 Comparison of the analysis of the different method.

The discharge and the coefficient of discharge for water, air and for the combination of inflation fluids are compared for different values of the ratio (H/H_D) as shown in table 7.7.

Table 7.7 Comparison of the discharge for different inflation fluids.

No.	H/H_D	q(ℓ/s/m) Water	q(ℓ/s/m) Air	q(ℓ/s/m) Air+Water	C_D Water	C_D Air	C_D Air+Water
1	0.15	9.82	12.88	10.75	0.380	0.395	0.380
2	0.17	11.96	15.70	13.14	0.383	0.400	0.385
3	0.18	13.08	17.19	14.40	0.385	0.403	0.388
4	0.20	15.44	20.32	17.04	0.388	0.408	0.393

This shows that for particular values of H/H_D then the maximum rate of flow is found with an air inflated dam and then for (air+water) and the minimum rate of flow found for a water inflated dam. Also the coefficient of discharge is a maximum for an air inflated dam and minimum for a water inflated dam. These differences in the discharge and coefficient of discharge may be due to the changes in the shape of the crest which is of a low radius of curvature in an air inflated dam whilst of a high radius of curvature in the water inflated dam. The condition for the (air+water) inflated dam gives values in between air and water inflated dam and also the particular value depends mainly on the depth of water inside the dam.

The conclusion is reflected in the results for the coefficient of discharge of the (air+water) dam which is close to that for the water inflated dam, because the depth of water is equal to 75% of the maximum height.

The results of the comparison of the different methods shows differences of the order of 5-11% between earlier work and the calibration method found by the author. The difference may be due to this analysis being for a dam

with one end fixed instead of both ends fixed. The single fixing gives the dam more flexibility to tend to being tangential with the floor and this behaviour will increase the radius of curvature at the crest. So comparing this behaviour with the condition for different inflation fluids, the results show the dam with the highest radius of curvature (i.e. water inflated dam) gives less discharge and a lower coefficient of discharge, than the dam with the lowest radius of curvature (i.e. air inflated dam) which can give high discharges and higher coefficient of discharge. Since the one fixed end dam gives a high radius of curvature the discharges are less than for two ends fixed, (see table 7.3, 7.4, 7.5).

It was also noticed that the rate of flow is affected by the elongation of the material, the discharge over the crest was calculated by using the different calibration equations for two cases, one by considering elongation of the material and the other under constant material length (no elongation). It was observed that the coefficient of discharges was different for the two conditions.

Table 7.8 shows the comparison of the coefficient of discharges and the rates of flow for material considered extensible and inextensible. The results show the difference in the rate of flow for an air inflated dam is 10% more for an inextensible material, 13% for water inflated and 5.56% for an (air+water) inflated dam. The main reason is due to the change in the ratio (H/H_D) due to a change in the radius of curvature which increases for an extensible material relative to an inextensible material. All previous investigators have considered their material as inextensible.

Fig.7.15 shows different profiles of air, water and air+water inflated dams for materials considered as inextensible.

Table 7.8 Comparison of discharge for extensible and inextensible material.

No.	Type of Inflation	Membrane (weight and extensible)							Membrane (weightless and inextensible				
		Propl. factor (α)	U/S Head m	D/S Head m	Max. Height H_D	Over flow head (mm)	C_D	Q ℓ/s/m	Max. Height H_D	Over flow head H	C_D	Q ℓ/s/m	diff. % Q
1	Air	0.8	0.270	0.0	0.227	42.80	0.400	16.43	0.224	45.76	0.410	18.32	11.5
		1.0	0.270	0.0	0.236	34.30	0.395	11.47	0.231	38.55	0.400	13.85	12.0
		1.0	0.280	0.0	0.232	47.40	0.410	19.30	0.228	51.04	0.414	21.80	12.9
		1.2	0.285	0.0	0.237	47.90	0.409	19.63	0.233	51.69	0.414	22.20	13.0
		1.2	0.288	0.0	0.236	51.70	0.414	22.19	0.233	54.9	0.417	24.47	10.3
		0.6	0.279	0.1	0.223	56.28	0.420	25.61	0.220	58.92	0.423	27.61	7.8
		0.6	0.282	0.1	0.221	60.52	0.424	28.80	0.221	60.52	0.424	29.00	0.6
		1.2	0.280	0.1	0.244	35.49	0.395	12.04	0.240	40.0	0.401	14.54	12.0
											Mean difference		10.0
2	Water	1.2	0.221	0.0	0.210	10.72	0.353	1.79	0.208	12.22	0.356	2.20	22.0
		1.2	0.230	0.0	0.206	24.06	0.373	6.35	0.204	25.54	0.375	6.98	9.92
		1.4	0.239	0.0	0.219	19.96	0.367	4.72	0.217	22.16	0.369	5.57	18.0
		1.4	0.244	0.0	0.217	26.53	0.374	7.38	0.215	28.97	0.376	8.25	11.7
		1.2	0.230	0.04	0.208	22.28	0.371	5.63	0.207	23.47	0.373	6.11	8.5
		1.2	0.239	0.04	0.204	34.66	0.382	11.26	0.202	36.64	0.384	12.29	9.0
		1.4	0.245	0.04	0.219	26.30	0.374	7.28	0.216	28.63	0.376	8.31	14.0
		1.4	0.248	0.04	0.217	30.41	0.377	9.14	0.216	32.38	0.379	10.09	10.8
											Mean difference		13.0
3	(Air+Water)	0.8	0.230	0.0	0.199	30.82	0.365	9.02	0.198	32.13	0.366	9.63	6.7
		0.8	0.233	0.0	0.197	35.55	0.368	11.28	0.195	37.50	0.370	12.34	8.5
		1.0	0.248	0.0	0.208	40.21	0.371	13.63	0.206	41.82	0.372	14.50	6.3
		1.0	0.250	0.0	0.206	44.10	0.373	15.76	0.205	44.32	0.373	15.88	0.76
											Mean difference		5.56

U/S HEAD	= 0.2652	METER
D/S HEAD	= 0.1032	METER
AIR PRESSURE	= 3.9840	KN/SQ.M
WATER PRESSURE	= 0.0000	M.W.G.
ORIGINAL LENGTH	= 0.5005	METER
NEW LENGTH	= 0.5005	METER
U/S TENSION	= 0.3618	KN/M
U/S SLOPE	= 101.5261	DEGREE
D/S TENSION	= 0.4635	KN/M
BASE LENGTH	= 0.1243	METER
MAX. HEIGHT	= 0.2255	METER
ALFA	= 0.6000	
AREA	= 0.0473	METER SQ
SILT DEPTH,MS	= 0.0000	METER
OVERFLOW HEAD	= 0.0425	METER
CD	= 0.4066	
RATE OF FLOW	= 16.2447	LET/SEC

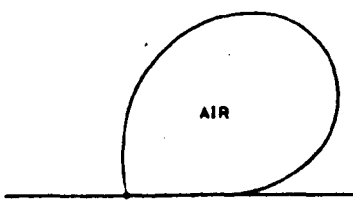

U/S HEAD	= 0.2550	METER
D/S HEAD	= 0.0000	METER
AIR PRESSURE	= 5.7236	KN/SQ.M
WATER PRESSURE	= 0.0000	M.W.G.
ORIGINAL LENGTH	= 0.5005	METER
NEW LENGTH	= 0.5005	METER
U/S TENSION	= 0.5239	KN/M
U/S SLOPE	= 117.0457	DEGREE
D/S TENSION	= 0.7256	KN/M
BASE LENGTH	= 0.1126	METER
MAX. HEIGHT	= 0.2333	METER
ALFA	= 1.2000	
AREA	= 0.0489	METER SQ
SILT DEPTH,MS	= 0.0000	METER
OVERFLOW HEAD	= 0.0517	METER
CD	= 0.4141	
RATE OF FLOW	= 22.2035	LET/SEC

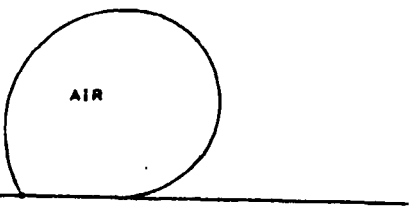

U/S HEAD	= 0.2520	METER
D/S HEAD	= 0.0400	METER
AIR PRESSURE	= 0.0000	KN/SQ.M
WATER PRESSURE	= 0.5004	M.W.G.
ORIGINAL LENGTH	= 0.5107	METER
NEW LENGTH	= 0.5107	METER
U/S TENSION	= 0.3245	KN/M
U/S SLOPE	= 114.3333	DEGREE
D/S TENSION	= 0.4395	KN/M
BASE LENGTH	= 0.1739	METER
MAX. HEIGHT	= 0.2142	METER
ALFA	= 1.4000	
AREA	= 0.0483	METER SQ
SILT DEPTH,MS	= 0.0000	METER
OVERFLOW HEAD	= 0.0378	METER
CD	= 0.3835	
RATE OF FLOW	= 12.8360	LET/SEC

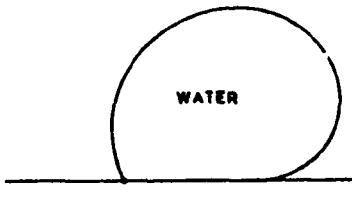

U/S HEAD	= 0.2480	METER
D/S HEAD	= 0.0000	METER
AIR PRESSURE	= 0.0000	KN/SQ.M
WATER PRESSURE	= 0.5004	M.W.G.
ORIGINAL LENGTH	= 0.5107	METER
NEW LENGTH	= 0.5107	METER
U/S TENSION	= 0.3248	KN/M
U/S SLOPE	= 115.5623	DEGREE
D/S TENSION	= 0.4486	KN/M
BASE LENGTH	= 0.1591	METER
MAX. HEIGHT	= 0.2139	METER
ALFA	= 1.4000	
AREA	= 0.0489	METER SQ
SILT DEPTH,MS	= 0.0000	METER
OVERFLOW HEAD	= 0.0341	METER
CD	= 0.3809	
RATE OF FLOW	= 10.9196	LET/SEC

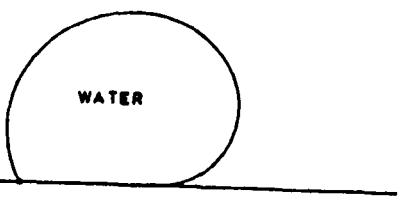

U/S HEAD	= 0.2500	METER
D/S HEAD	= 0.0000	METER
AIR PRESSURE	= 2.5450	KN/SQ.M
WATER PRESSURE	= 0.1575	M.W.G.
ORIGINAL LENGTH	= 0.5009	METER
NEW LENGTH	= 0.5009	METER
U/S TENSION	= 0.3610	KN/M
U/S SLOPE	= 98.7559	DEGREE
D/S TENSION	= 0.5480	KN/M
BASE LENGTH	= 0.1824	METER
MAX. HEIGHT	= 0.2057	METER
ALFA	= 1.0000	
AREA	= 0.0461	METER SQ
SILT DEPTH,MS	= 0.0000	METER
OVERFLOW HEAD	= 0.0443	METER
CD	= 0.3731	
RATE OF FLOW	= 15.0839	LET/SEC

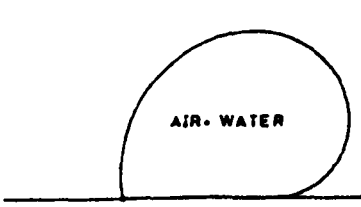

U/S HEAD	= 0.2263	METER
D/S HEAD	= 0.0000	METER
AIR PRESSURE	= 2.0407	KN/SQ.M
WATER PRESSURE	= 0.1575	M.W.G.
ORIGINAL LENGTH	= 0.5000	METER
NEW LENGTH	= 0.5000	METER
U/S TENSION	= 0.2167	KN/M
U/S SLOPE	= 96.5443	DEGREE
D/S TENSION	= 0.2579	KN/M
BASE LENGTH	= 0.1928	METER
MAX. HEIGHT	= 0.2017	METER
ALFA	= 0.5000	
AREA	= 0.0454	METER SQ
SILT DEPTH,MS	= 0.0000	METER
OVERFLOW HEAD	= 0.0243	METER
CD	= 0.3597	
RATE OF FLOW	= 6.2328	LET/SEC

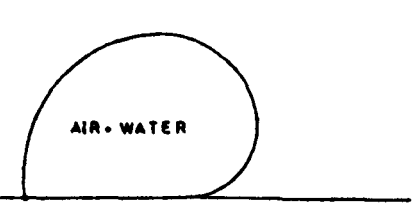

FIG. (7-15) TYPICAL PROFILES OF AIR, WATER AND AIR+WATER INFLATED DAMS FOR INEXTENSIBLE MATERIALS

7.7 Computer program (DYIHSIP).

The rate of flow and the coefficient of discharge were calculated from the subroutine called "Dynamic" and the radius of curvature was calculated from the general equation (45)

$$R = \left[\frac{1 + (dy/dx)^2}{(d^2y/dx^2)}\right]^{-3/2} \quad \ldots\ldots \quad 7.16$$

The input of data for the program is similar to the input for the dynamic condition. Examples of the shapes of the profiles given by this subroutine are shown in fig.7.15 for an inextensible material. The equivalent profiles in figs. 5.37, 5.38 and 5.39 shown in Chapter 5 are on the basis of an extensible material.

7.8 Factors affecting the coefficient of discharge.

The coefficient of discharge (C_D) changes rapidly initially as the overflow increases and then for ever higher overflows the rate of change decreases as can be seen in figs. 7.12 to 7.14.

In this analysis the coefficient of discharges were calculated for different proportional factors and it shows that the coefficient of discharge increases when increasing the proportional factor. This phenomenon was also observed by Anwar (2). This behaviour also may be due to variations in the radius of curvature with high proportional factors giving low values of radius of curvature, thus giving a high coefficient of discharge and the results will be reversed for low proportional factors.

As already discussed the coefficient of discharge for an air inflated dam is higher than for a water inflated dam (see table 7.7) and the main reason is due to changes in the shape of the crest which can be represented by the proportional factor. So for low proportional factor the shape of the crest gives high values of radius of curvature and for high proportional

factor gives low radius of curvature. The radius of curvature was calculated under different conditions of inflation fluids and for different proportional factors. It was found that as the overflow increased the radius of curvature decreased for an air inflated dam for the condition of downstream head equal to zero and also for the downstream head equal to 100 mm as shown in fig.7.16.

A similar behaviour for the radius of curvature for a dam inflated with water is shown in fig.7.17. The results show that the radius of curvature for an air inflated dam are high with downstream head equal to zero than with downstream head equal to 100 mm. It was also noticed that the radius of curvature had a small increase with increasing the overflow for the condition of silt load on the upstream face of the dam as shown in fig.7.16.

Fig.7.17 shows the results of the radius of curvature for a water inflated dam and it appears that the radius of curvature is higher for low proportional factor and vice versa. Also the effects of the downstream head on the radius of curvature reduces as the proportional factor increases. This may be due to the dam becoming more stiff as the proportional factor increases the downstream head will then become less significant. As shown in fig.7.17 for the proportional factors equal to 1.2, 1.4 and 2.5 and for downstream heads equal to zero and 40 mm it can be seen that for $\alpha = 1.2$ the radius of curvature is higher for the condition of D/S = 0.0 than the condition of D/S = 40 mm but as the proportional factor increases to 1.4 the difference in the radius of curvature will be small and as the proportional factor increases to a high of 2.5 the radius of curvature for the two conditions of downstream head is the same.

The behaviour of silt on the upstream face for a particular overflow increases the radius of curvature as shown in fig.7.17. For example for

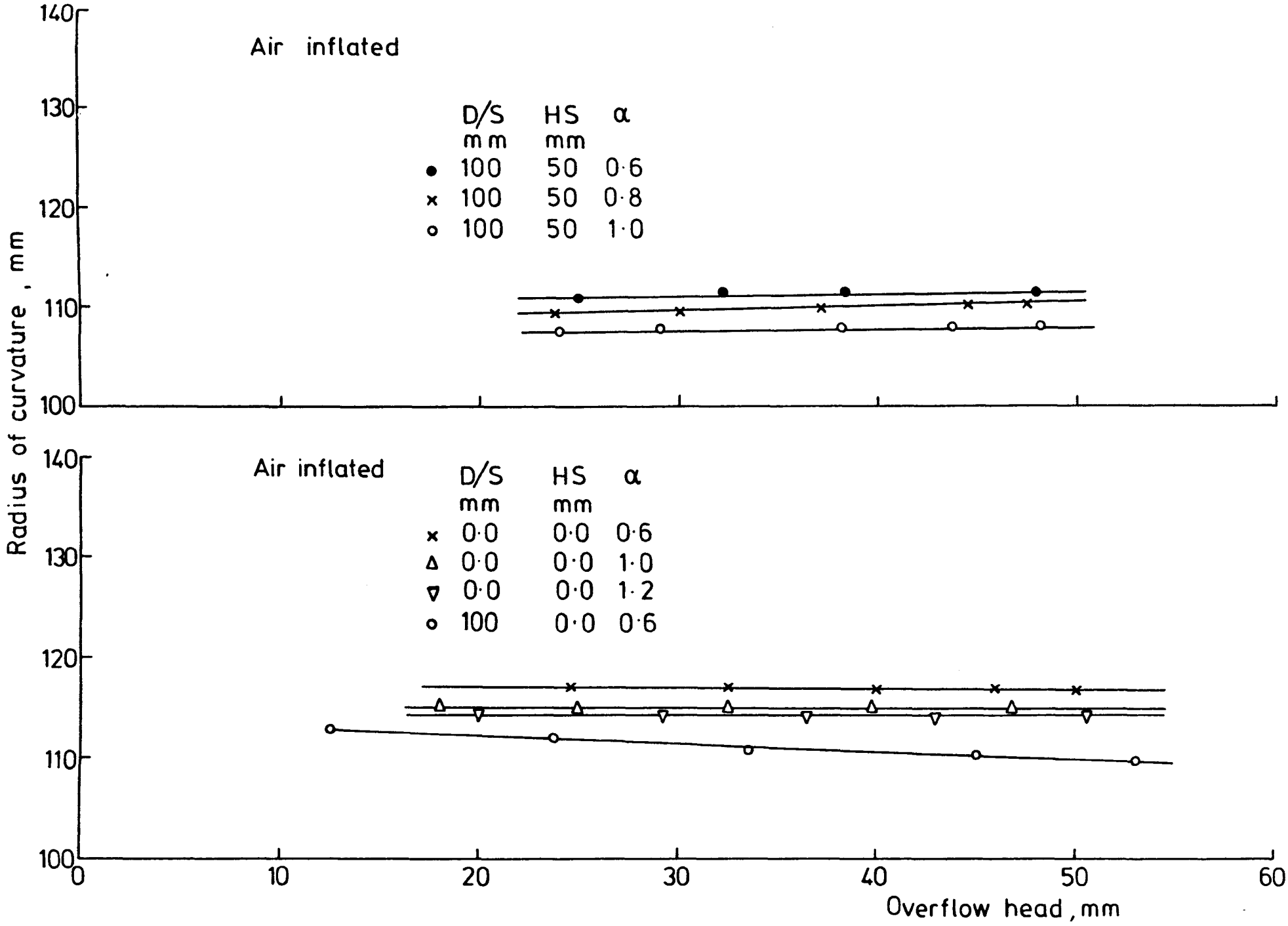

FIG.7-16 OVERFLOW HEAD Vs. RADIUS OF CURVATURE FOR AIR INFLATED DAM

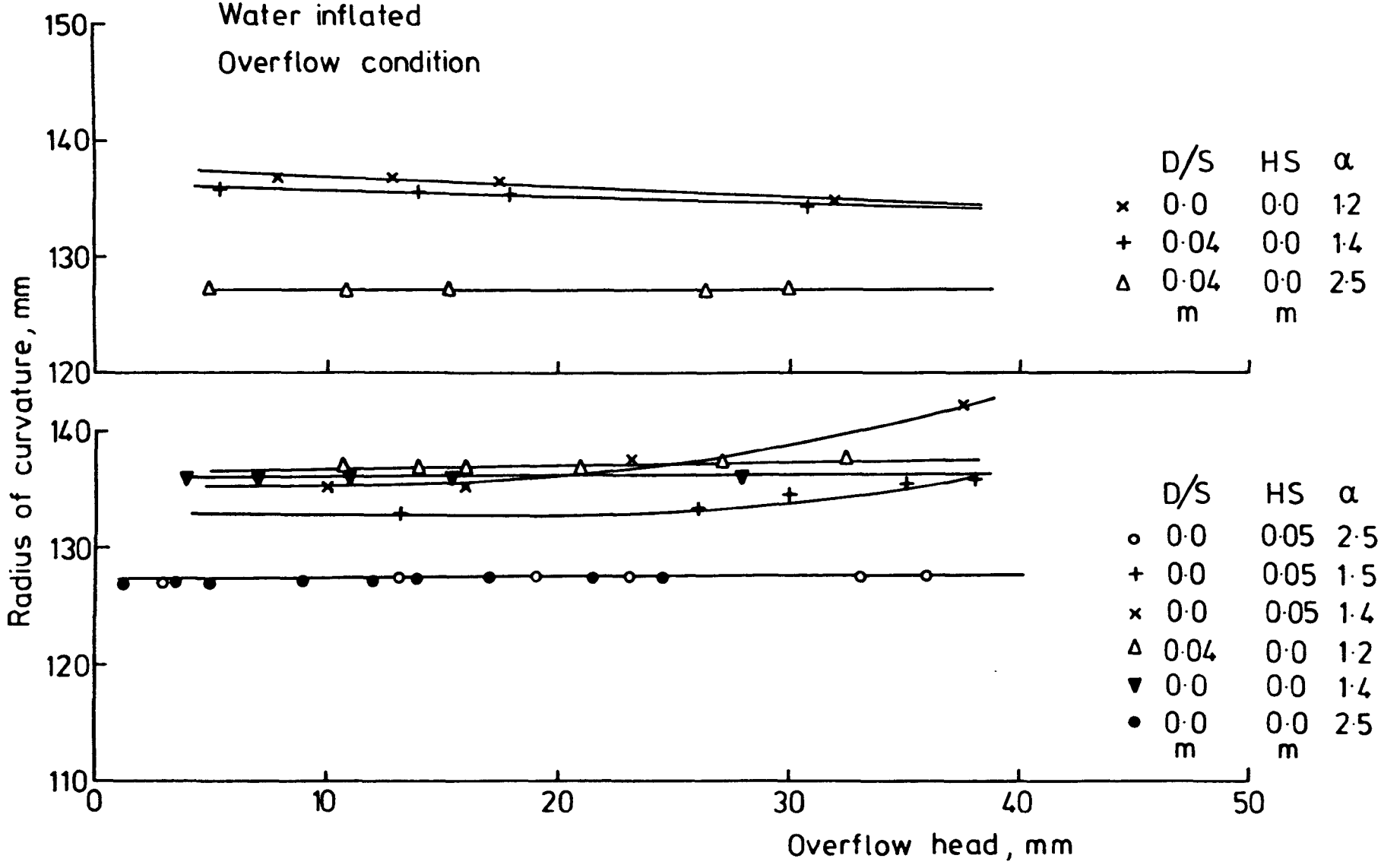

FIG. 7-17 OVERFLOW HEAD Vs. RADIUS OF CURVATURE FOR WATER INFLATED DAM

proportional factors equal to 1.4 and 1.5 the silt causes an increase in the radius of curvature while this effect becomes less significant as the proportional factor increases to 2.5. An increase in the radius of curvature causes a reduction in the coefficient of discharge.

The behaviour of the radius of curvature is similar with respect to the ratio (H/H_D) for a downstream head equal to zero and 40 mm as represented in fig.7.18 and fig.7.19 for both the air and water inflated dams respectively. Since the ratio (H/H_D) changes as the proportional factor changes therefore the ratio H/H_D varies the coefficient of discharge as mentioned earlier in this chapter.

Fig.7.20 shows the variation of the coefficient of discharge with overflow head for water and air inflated dam under different downstream heads. For the air inflated dam it can be seen that for low proportional factors the effect of the downstream head on the coefficient of discharge is very pronounced for low heads, but as the overflow head increases the effect of the downstream head on the radius of curvature will be small and the coefficient of discharge will be constant for both cases of downstream head equal to zero and 100 mm.

The coefficient of discharge for a water inflated dam under different downstream head, shows for low proportional factor ($\alpha = 1.4$) and for a downstream head equal to 40 mm, the coefficient of discharge will be higher than the coefficient of discharge for the same proportional factor but under downstream head equal to zero. As the overflow head increases more, the coefficient of discharge will be the same for both conditions of downstream head. Once the proportional factor increases ($\alpha = 2.5$) the coefficient of discharge will be the same for the condition of downstream head equal to zero and 40 mm which may be due to the dam becoming more stiff and the effect of the downstream head will be less significant on the radius of curvature.

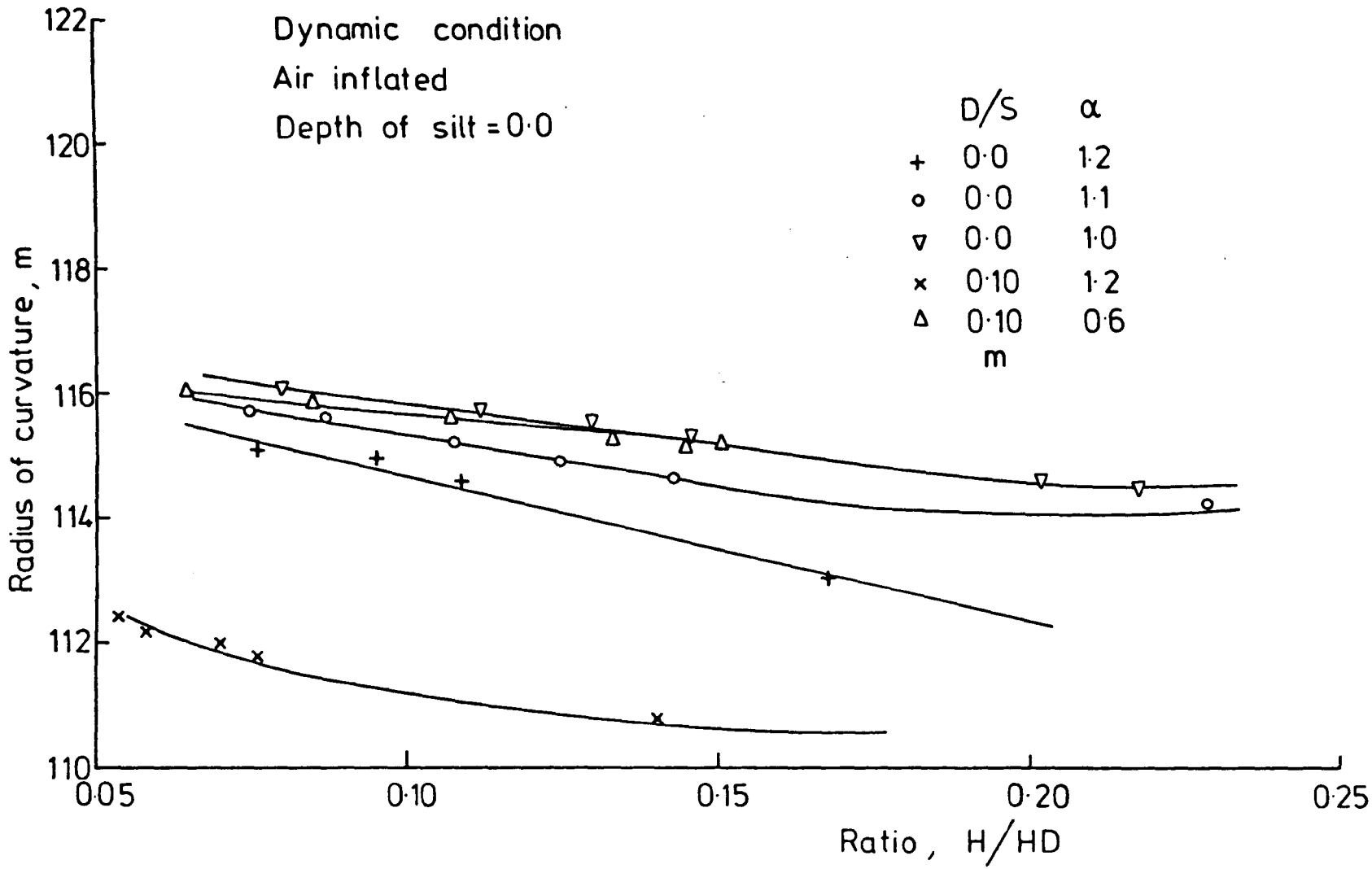

FIG. 7-18 RADIUS OF CURVATURE Vs. RATIO H/HD FOR AIR INFLATED DAM

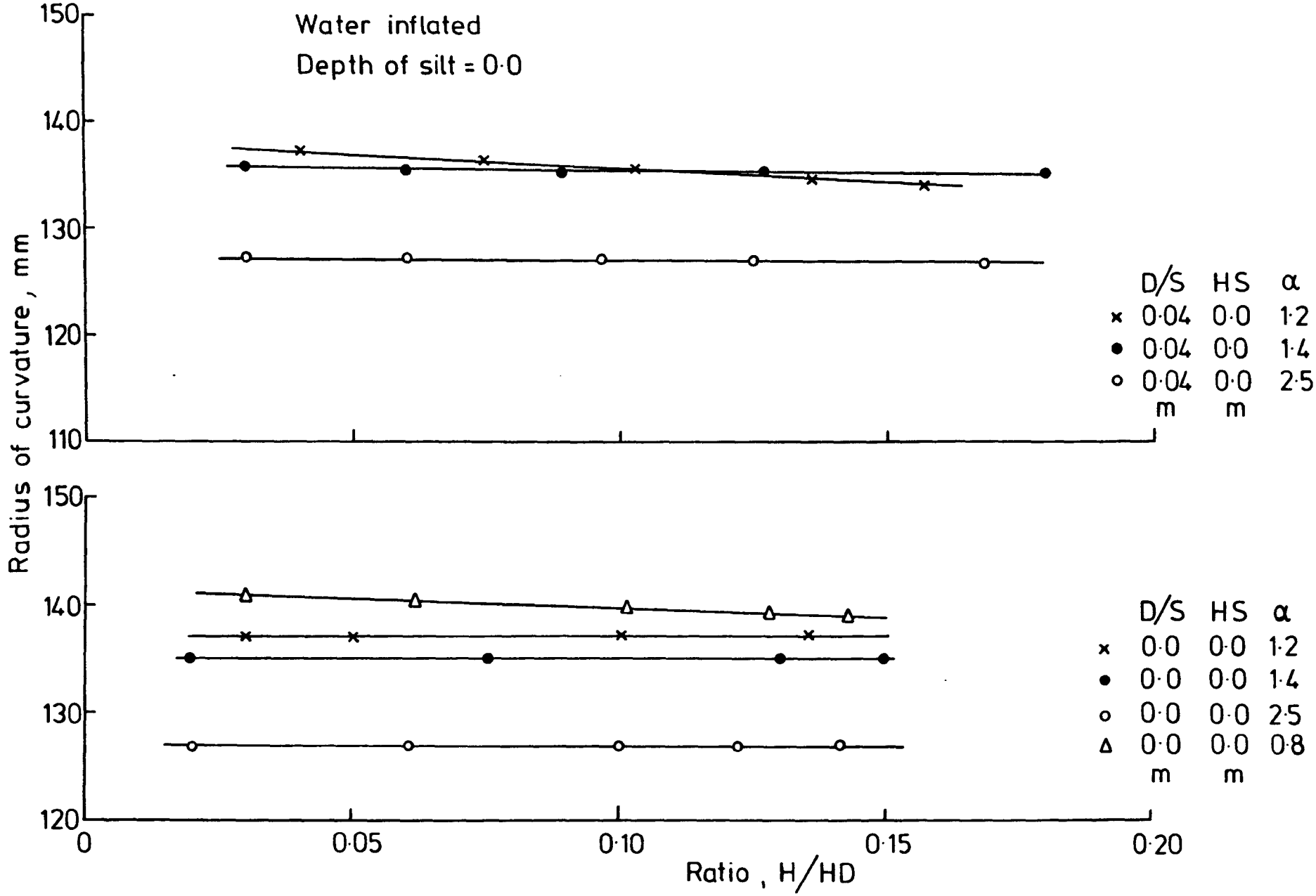

FIG. 7-19 RADIUS OF CURVATURE Vs. RATIO H/HD FOR WATER INFLATED DAM

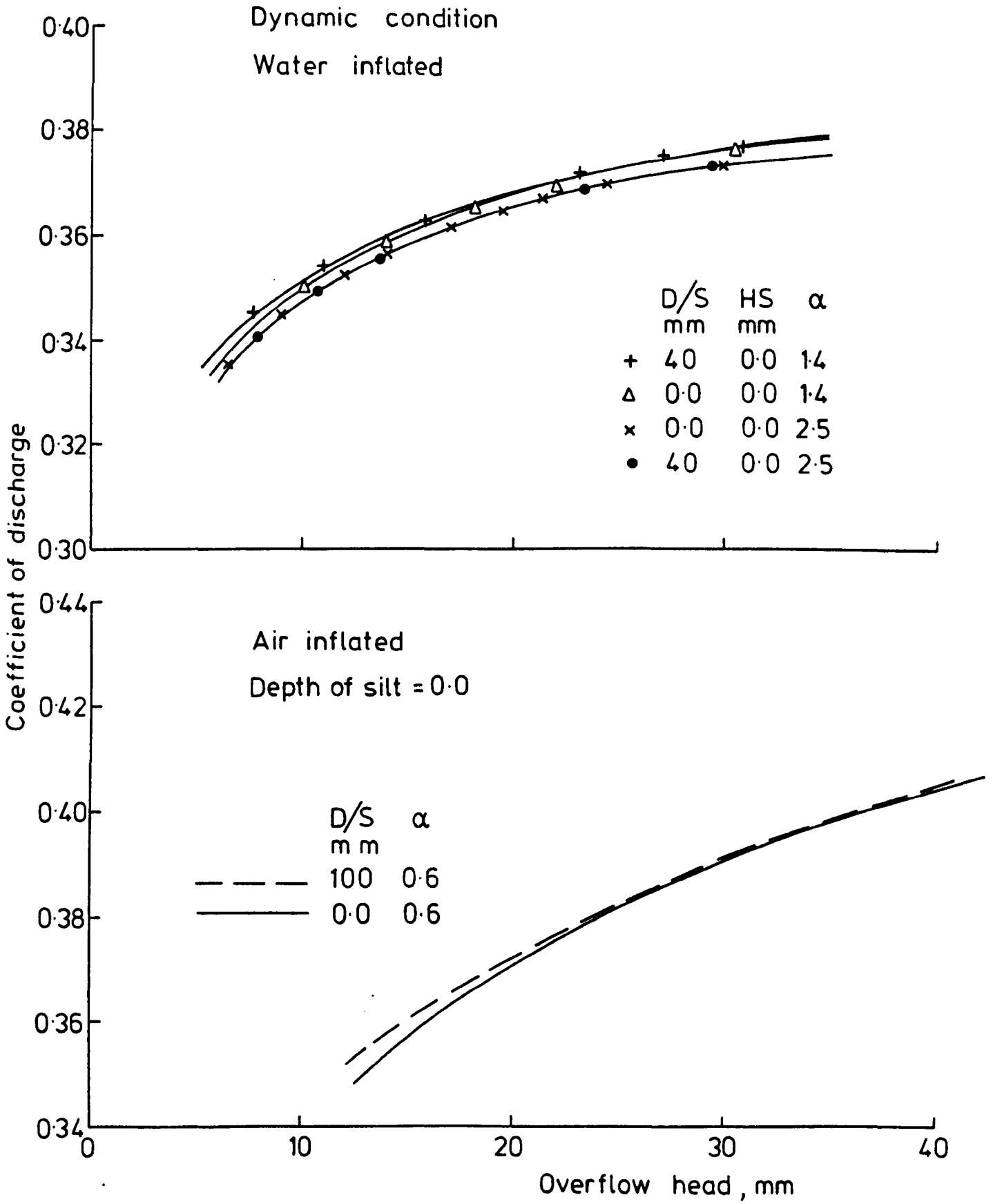

FIG.7-20 COEFFICIENT OF DISCHARGE Vs. OVERFLOW HEAD FOR AIR AND WATER INFLATED DAMS

7.9 Effect of downstream head on the upstream head.

One aspect of the experimental work was to study the effect of the downstream head on the upstream head. This study was carried out for a dam under different pressures and for different inflation fluids.

For an internal air pressure of 3.355 Kn/m^2 for an air inflated dam, the flow was kept constant at 5.56 ℓ/s and the downstream head varied to 70, 90, 100, 120,140 mm and measurements were taken of both upstream head and the maximum height of the dam. It was noticed that as the downstream head increased from 70 mm to 140 mm, the overflow head decreased from 20 mm to 18.5 mm for this particular flow rate. When this procedure was repeated for several rates of flow (7.5, 9.66, 10.67, 11.97 ℓ/s) for the same variation of the downstream head, it was also observed that as the downstream head increased, the upstream head increased. This behaviour causes an increase in the height of the dam and thus decreases the ratio (H/H_D) such that the overflow head decreases, and increases the downstream head causing distortion of the dam on the upstream side decreasing the radius of curvature. This causes an increase in the coefficient of discharge to maintain the constant rate of flow. Similar effects were found for inflation condition changes for water and (air+water) inflated dams.

Fig.7.21, 7.22 and 7.23 show the variations of the upstream head with downstream head under different rates of flow and internal pressures for the condition of air, water and (air+water) inflation respectively.

As the downstream head varied from 70 mm to 140 mm the mean difference of the upstream head and the overflow head for an air inflated dam under a pressure of 3.55 KN/m^2 are 3.1% and 8.64% respectively. While the mean differences reduce to 1.6% for upstream head and 6.1% for the overflow head for a dam inflated with air pressure equal to 5.1 KN/m^2 These variations can be seen in detail in table 7.9.

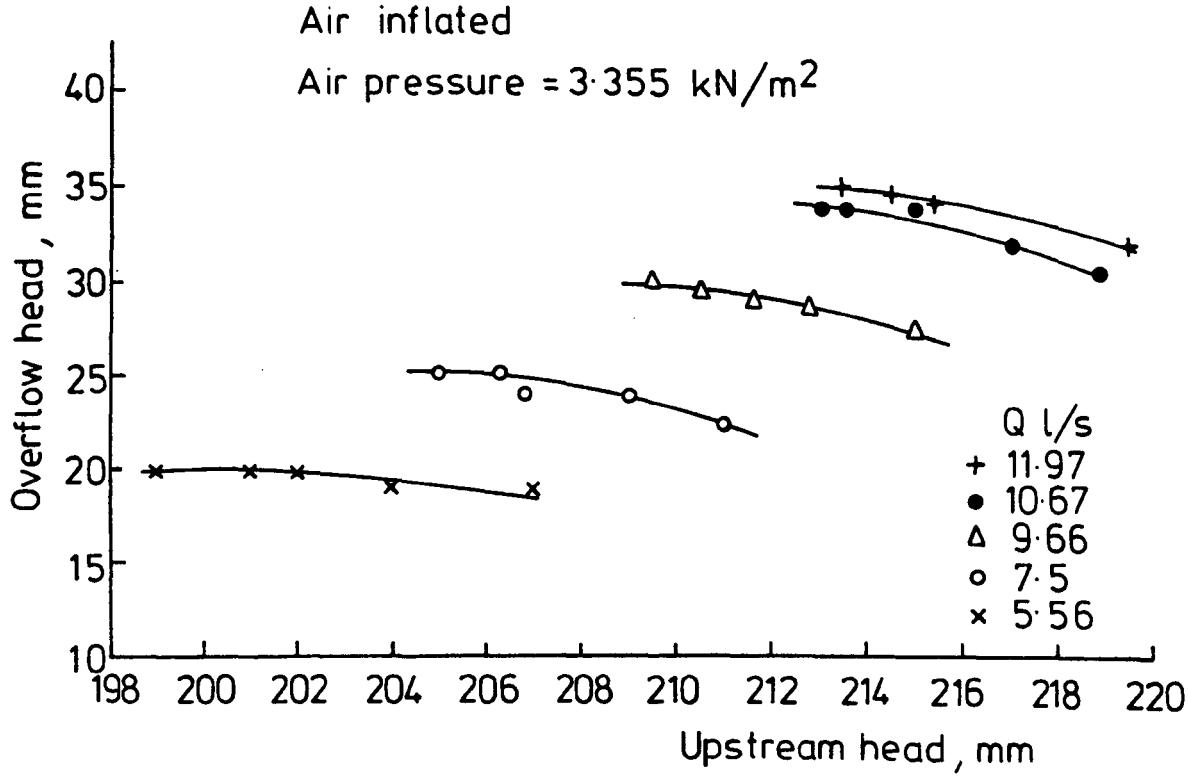

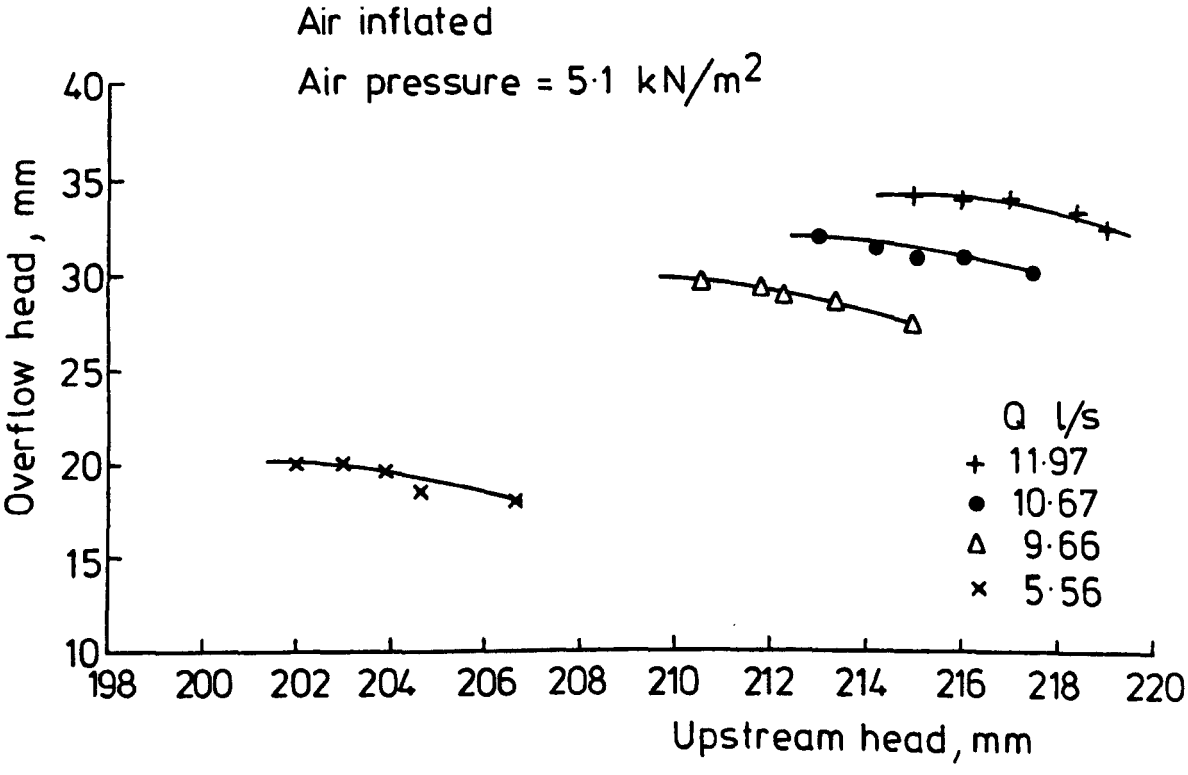

FIG. 7-21 OVERFLOW HEAD Vs. UPSTREAM HEAD FOR DIFFERENT DOWNSTREAM HEADS

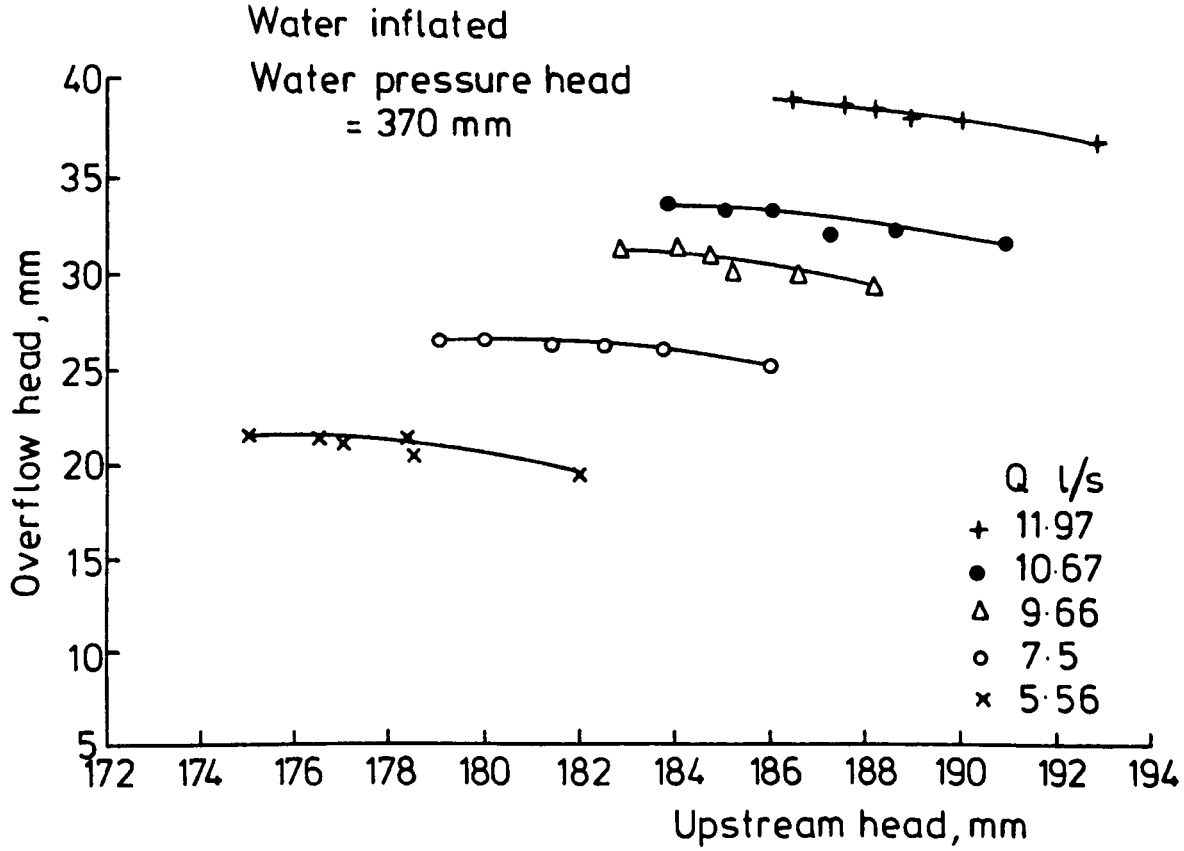

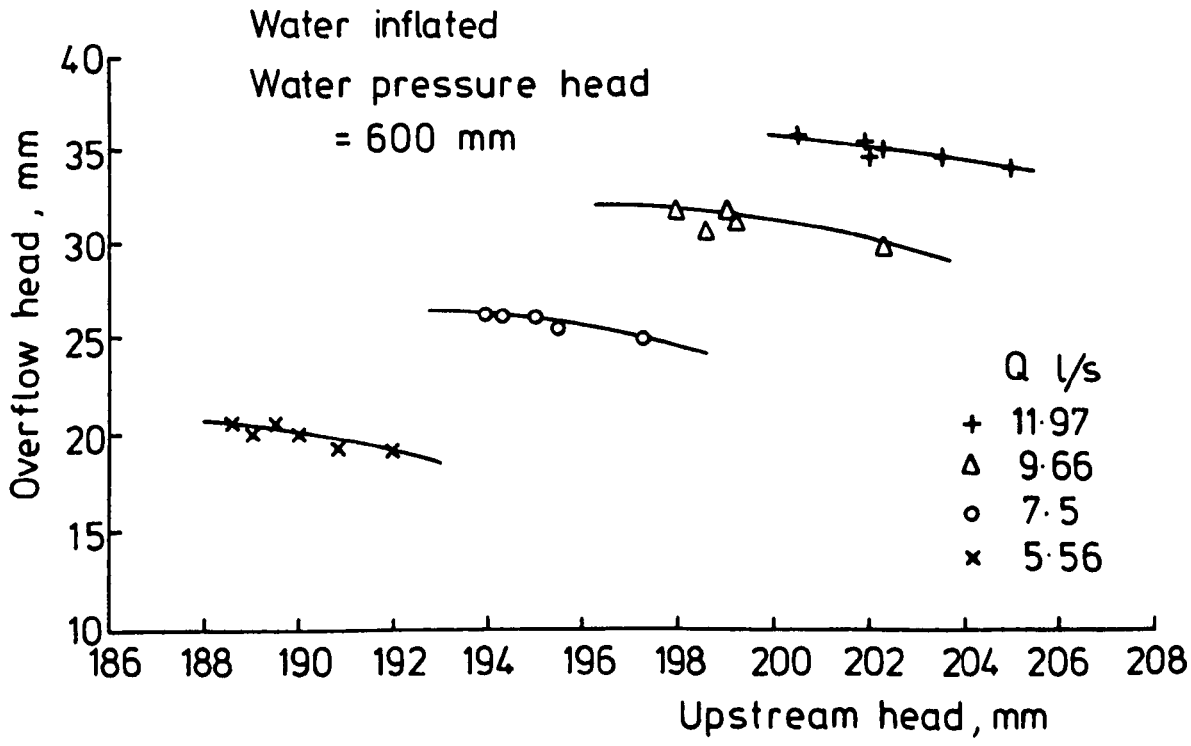

FIG. 7-22 OVERFLOW HEAD Vs. UPSTREAM HEAD FOR DIFFERENT DOWNSTREAM HEADS

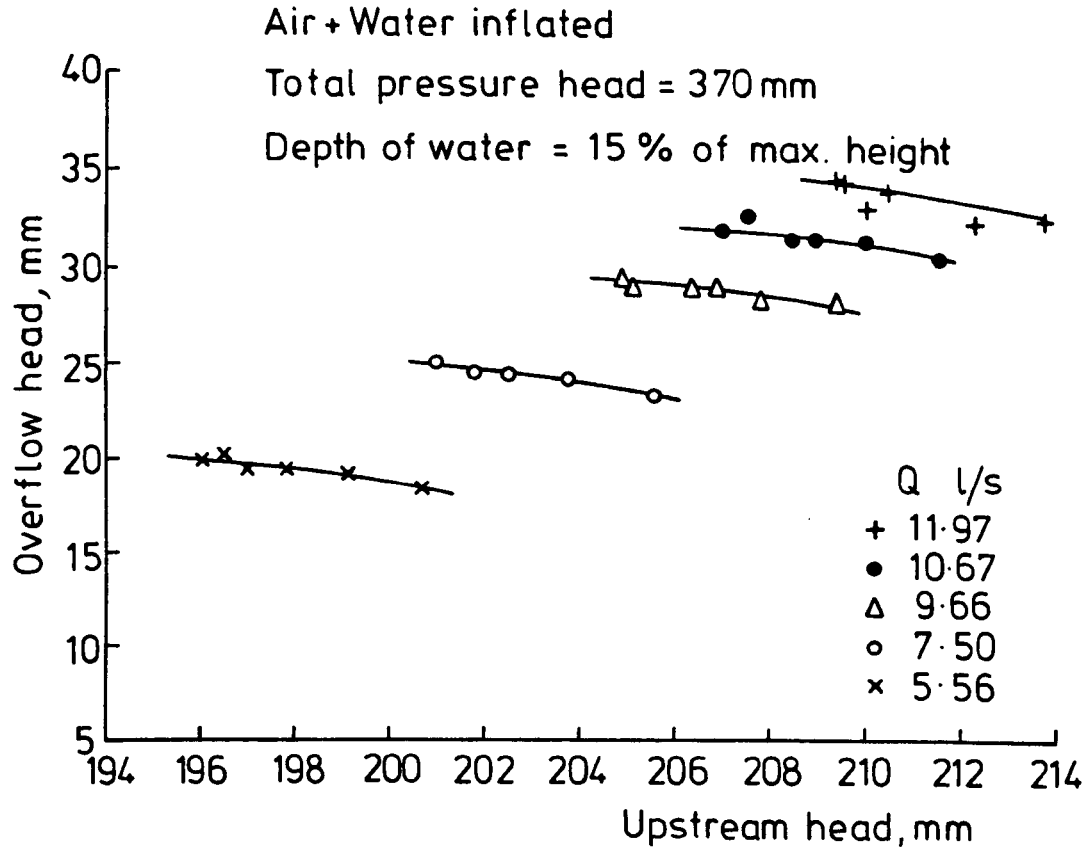

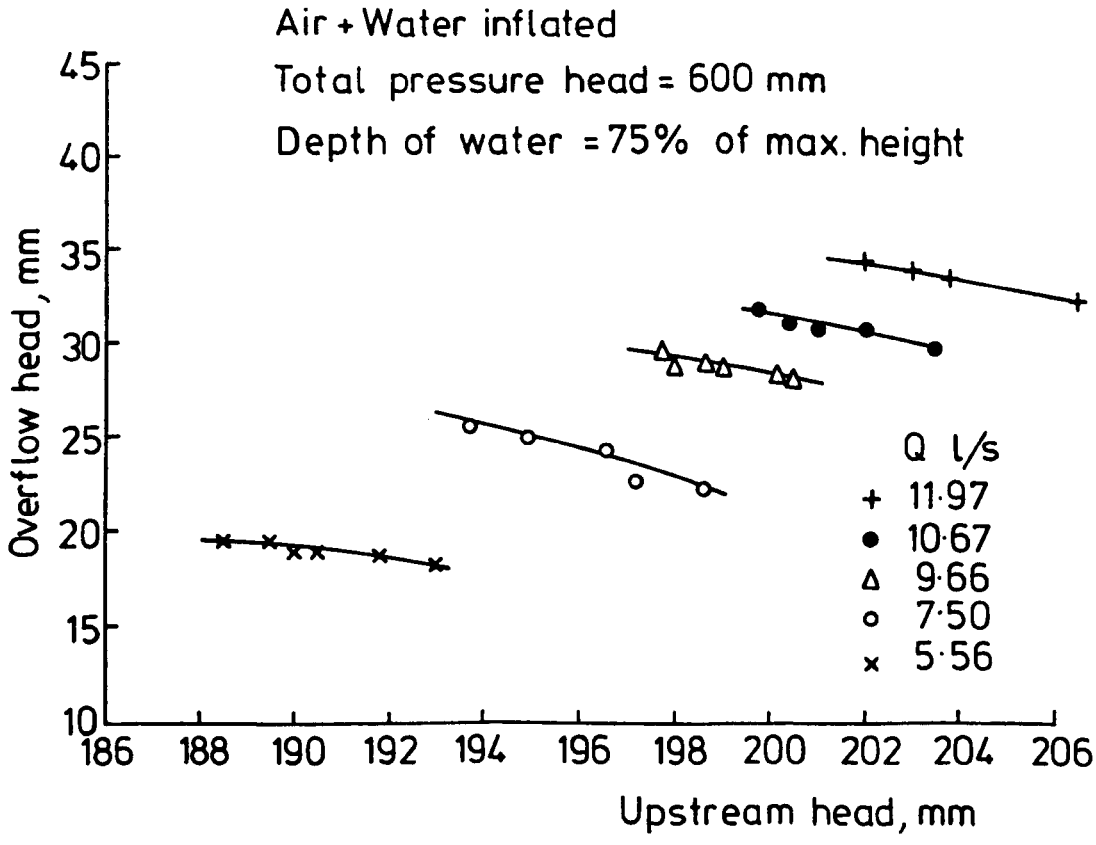

FIG. 7-23 OVERFLOW HEAD Vs. UPSTREAM HEAD FOR DIFFERENT DOWNSTREAM HEADS

The variation for a water inflated dam are similar to those for the air inflated dam, the percentage differences of the upstream head and the overflow head are 3.4% and 7.9% respectively for the condition of water pressure head equal to 370 mm while the differences reduced to 1.6% and 3.4% for the dam inflated with 600 mm head. The details of these differences are shown in table 7.10.

The differences of the upstream head and overflow head for the condition of (air+water) inflated follows a similar pattern to the previous conditions. Table 7.11 shows the detail of the percentage differences in the upstream head and overflow head for a dam inflated to a pressure head equal to 370 mm with a depth of water equal to 15% of the maximum height of the dam. Table 7.11 also shows the difference in the upstream head and the overflow head for a pressure head equal to 600 mm including the depth of water equal to 75% of the maximum height of the dam.

Table 7.9 Effect of downstream head on the upstream and overflow head for an air inflated dam.

No.	Air Press. KN/m^2	Rate of flow ℓ/s	U/S Head (mm)	D.S Head (mm)	Over flow head (mm)	% difference in U/S	% difference in overflow
1	3.355	5.56	199	70	20.0		
		5.56	207	140	18.5	4.0	8.1
2	3.355	7.50	205	70	25.0	2.9	11.1
	3.355	7.50	211	140	22.5		
3	3.55	9.66	209	70	30.0		
	3.55	9.66	215	140	28.0	2.8	7.1
4	3.55	10.67	213	70	34.0	2.7	9.6
			188	140	31.0		
5	3.55	11.97	213	70	35.0	3.05	7.6
			195	140	32.5		
				mean		3.09	8.64
1	5.1	5.56	202	70	20.0		
			206.6	140	18.0	2.2	11.1
2	5.1	9.66	206	70	29.5		
			215	140	27.5	0.48	7.2
3	5.1	10.67	213	70.0	32.0		
			217	140.0	31.0	1.8	3.1
4	5.1	11.97	215	70.0	34.0	1.86	3.0
			219	140.0	33.0		
				Mean		1.585	6.075

Table 7.10 Effect of downstream head on the upstream and overflow head for a water inflated dam.

No.	Water Pressure (mm)	Rate of flow ℓ/s	U/S Head (mm)	D/S Head (mm)	Overflow (mm)	% diff. in U/S	% diff. in overflow
1	370	5.56	175.0	70.0	21.50		
	370	5.56	182.0	140.0	18.50	4	16.2
2	370	7.50	170.0	70.0	26.50		
	370	7.50	186.0	140.0	25.00	3.9	6.0
3	370	9.66	182.9	70.0	31.25	2.7	5.9
	370	9.66	188.0	140.0	29.50		
4	370	10.67	183.9	70.0	33.50	3.3	6.3
	370	10.67	190.0	140.0	31.50		
5	370	11.97	186.5	70.0	38.50	3.3	5.4
	370	11.97	192.8	140.0	36.50		
					Mean	3.40	7.96
1	600	5.56	189.0	70.0	20.50		
	600	5.56	192.0	140.0	19.00	1.6	7.8
2	600	7.50	195.0	70.0	26.00	1.2	4.0
	600	7.50	197.3	140.0	25.00		
3	600	10.67	199.0	70.0	31.25	1.6	5.9
	600	10.67	202.2	140.0	29.50		
4	600	11.97	201.0	70.0	35.05	1.9	3.8
	600	11.97	205.0	140.0	33.75		
					Mean	1.575	5.37

Table 7.11 Effect of downstream head on the upstream and overflow heads for (air+water) inflated dam.

No.	(Air+Water) Pressure	Rate of flow ℓ/s	U/S Head (mm)	D/S Head (mm)	Overflow Head (mm)	% diff. U/S	% diff. in overflow
1	370 mm depth of water = 15% max. Height of the dam.	5.56	196.0	70	20.0		
		5.56	200.8	140	18.3	2.4	9.3
		7.50	201.0	70	25.0		
			205.5	140	23.5	2.2	6.3
		9.66	204.9	70	29.0		
			209.4	140	28.0	2.2	3.5
		10.67	207.0	70	32.0		
			211.5	140	30.1	2.2	6.4
		11.97	209.4	70	34.5		
			213.8	140	32.5	2.1	6.15
					Mean	2.22	6.33
2	600 mm depth of water = 75% of the max. height of the dam.	5.56	18.9	70	19.8		
			193.0	140	18.0	1.8	9.7
		9.66	197.8	70	29.5		
			200.5	140	28.0	1.36	5.3
		10.67	199.8	70	32.0		
			205.0	140	30.0	2.6	6.6
		11.97	202.5	70	34.5	1.7	6.15
			206.0	140	32.5		
					Mean	1.865	6.9

CHAPTER 8.

THE DESIGN LENGTH OF THE MEMBRANE OF AN INFLATABLE STRUCTURE.

8.1 Introduction.

The techniques of other investigators have all been restricted by various limiting conditions.

Anwar (2) has produced closed form solutions for a particular geometrical configuration and for either air inflation or water inflation. In his solution the membrane is assumed weightless and inextensible.

Binnie (5) developed a more general closed form solution for a dam inflated by water pressure which takes account of the physical restriction of base and perimeter length ignored in Anwar's olution. Both these formulations consider only the case where the water level is at the crest of the dam and apply to an idealized weightless inextensible membrane. In addition Binnie considered only an inflation head equal to the height of the dam, i.e. zero pressure at the crest.

In order to avoid these limitations a study was carried out to design the dam using a computer program based on a finite element approach.

The derivation of the design length for the membrane used for an inflatable hydraulic structure is based on two main steps.

1. Find the total length of membrane for a certain maximum upstream head and maximum proportional factor.

2. Using the results from point (1) then design the dam by using a computer program (IHSIP) and by considering the weight and the material as extensible and when the maximum upstream head equals the maximum height of the dam, then the desired length of the membrane has been achieved. (See Sec. 8.5.1).

8.2 Theoretical method of design.

The theoretical method for the design of an inflatable hydraulic structure consists of two parts. The first part is to find the length of the membrane with respect to the maximum proportional factor as described in the following section and the second part deals with a finite element method to design a dam for given conditions (i.e. maximum upstream head and maximum proportional factor) in order to find the condition of maximum upstream head equal to the maximum height of dam by taking into consideration the weight and extensibility of the material.

8.2.1 Design length - assumptions and considerations.

The design length of the membrane is designed by considering the characteristics as shown in fig.8.1 and also makes the following assumption.

1. Material is weightless.

On the basis of this assumption, the tension will be constant around the membrane and using the Parbery (6) equation

$$T_o = T + wy \quad \ldots\ldots \quad 8.1$$

i.e.

$T_o = T$ for a weightless material.

2. The fabric dam is inflated by water and with zero downstream head.

3. The differential pressure is proportional to the maximum storage head (2, 14) and this assumption can be expressed in the following form:

$$h = \alpha H_D \quad \ldots\ldots \quad 8.2$$

where

h = differential pressure head (see fig. 8.1).

α = proportional factor.

H_D = maximum storage head.

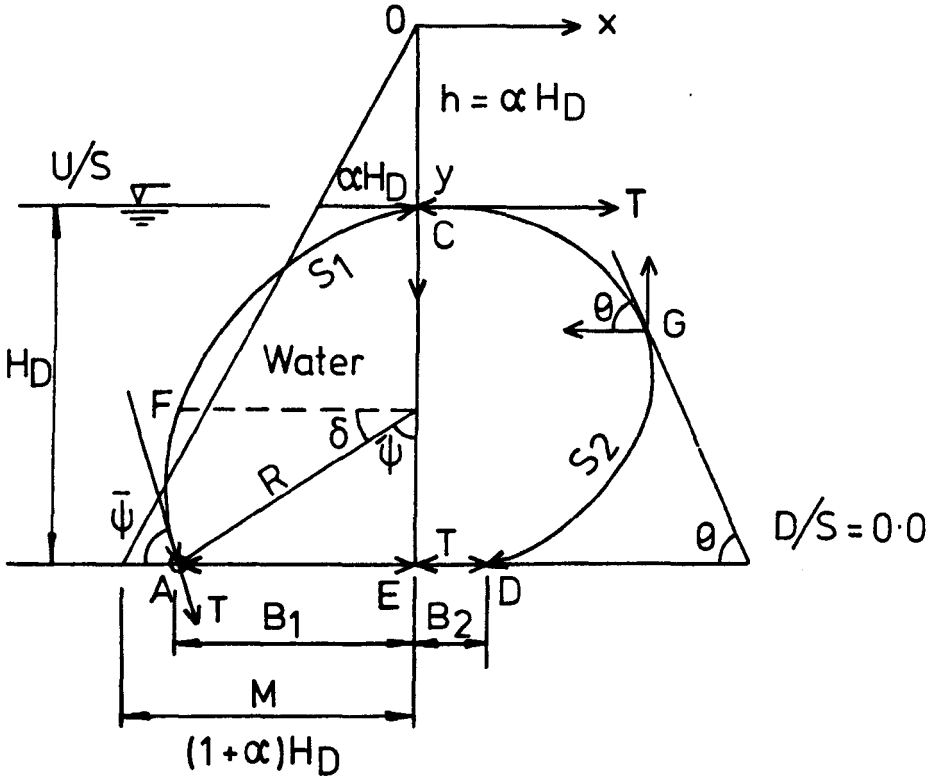

$$S/H_D = S_1/H_D + S_2/H_D$$

$$B/H_D = B_1/H_D + B_2/H_D$$

FIG. (8-1) DESIGN LENGTH OF MEMBRANE

On the basis of the above assumptions the design for the initial tension and membrane length can be considered in two parts i.e.

(1) Downstream side.

(2) Upstream side.

8.3 Downstream side.

The design of the downstream side consists of evaluating the tension and length of membrane in the downstream section.

8.3.1 Tension.

The tension is evaluated by using the general form of the distortion of a strut into a curve known as elastica (23) as was used by Binnie (5) in the following form:

$$T \frac{d\theta}{dS_2} = \rho g y \quad \ldots\ldots \quad 8.3$$

where

T = tension in the membrane.

θ = angle of an arbitrary point on the downstream fabric and tangent through this point (fig.8.1).

S_2 = length of membrane at the downstream side.

g = acceleration due to gravity.

ρ = density of water.

y = co-ordinate (see fig.8.1).

and the general geometric equation can be written as follows:

$$\frac{dy}{dS_2} = \sin\theta \quad \ldots\ldots \quad 8.4$$

Substituting equation 8.4 in 8.3 and integrating for the condition

$$\theta = 0 \quad \text{to} \quad \theta$$

Hence equation 8.3 can be written in the following form

$$\frac{2T}{\rho g}(1 - \cos\theta) = y^2 - h^2 \quad \ldots\ldots \quad 8.5$$

and by substituting the assumption $h = \alpha H_D$ in equation 8.5 and also a $y = h+H_D$, $\theta = \pi$, hence equation 8.5 can be written in the following form:

$$\frac{4T}{\rho g} = (\alpha H_D + H_D)^2 - (\alpha H_D)^2 \quad \ldots\ldots \quad 8.6$$

or

$$\frac{4T}{\rho g M^2} = 1 - \frac{\alpha^2}{(1+\alpha)^2} \quad \ldots\ldots \quad 8.7$$

where

$$M = H_D(1+\alpha)$$

and by considering the value $1 - \frac{\alpha^2}{(1+\alpha)^2} = F_c$ equation 8.6 can be written in the following form:

$$T = \frac{\rho g M^2 FC}{4} \quad \ldots\ldots \quad 8.8$$

or if substituting the value of M and F_c in the equation 8.8 these can be written as:

$$T = \rho g (1+2\alpha) H_D^2/4 \quad \ldots\ldots \quad 8.9$$

Equation 8.9 is used to find the initial value of tension to analyse the dam by using the finite element method by taking into consideration the weight and thickness of the material in the analysis.

8.3.2 Length of the downstream side membrane.

The length of the downstream membrane was divided into two parts as shown in fig.8.1.

a. Length of the base towards the downstream, B_2.

b. Length of the perimeter towards the downstream, S_2.

The length of the membrane of a dam inflated with water was calculated by Clare (14) from the following equation (see Appendix A).

$$B_2/H_D = (1+\alpha)\ (1 - \frac{F_c^2}{2})\ \hat{F} - \hat{E} \quad \ldots\ldots \quad 8.10$$

$$S_2/H_D = \frac{1+\alpha}{2} F_c^2 (\hat{F}) \quad \ldots\ldots \quad 8.11$$

where

B_2 = length of base toward the downstream side.

S_2 = length of perimeter towards the downstream side.

F_c = modulus of elliptic integrals = $\frac{1+2\alpha}{(1+\alpha)^2}$

H_D = maximum height of dam.

α = proportional factor.

$\hat{F}$, $\hat{E}$ = complete elliptic integrals of the first and second kind respectively.

8.4 Upstream side.

For the upstream side of the dam it is also necessary to find the tension and length of the membrane towards the upstream side.

8.4.1 Tension.

It was concluded from previous investigations (2,5) that the upstream face of a dam is a part of a circle and the tension can be found by the following equation:

$$T = PR \quad \ldots\ldots \quad 8.12$$

Since the tension is assumed constant along the membrane, so it can be possible to substitute equation 8.9 in 8.12 to obtain the following:

$$R = \frac{T}{P} = \frac{(1+2\alpha)\ \rho g\ H_D^2}{4\ \rho g\ \alpha H_D} = \left(\frac{1+2\alpha}{4\alpha}\right) H_D \quad \ldots\ldots \quad 8.13$$

where

R = radius of curvature.

P = differential pressure = $\rho g\ H_D$

T = tension in the fabric.

8.4.2 Length of the upstream side of the membrane.

From fig.8.1 the length of the membrane towards the upstream side consists of two parts - see fig.8.1

a. Length of the base towards the upstream side, B_1.

b. Length of the perimeter towards the upstream side, S_1.

Therefore the length of the base B_1 can be found from the relation:

$$B_1 = R \sin \bar{\psi} \quad \ldots\ldots \quad 8.14$$

where $\bar{\psi}$ is the angle of the upstream slope of the fabric from the base.

The angle is found from the equilibrium equation for the upstream side of the dam, i.e.

$$T + T \cos \bar{\psi} = \text{difference in the hydrostatic load per unit width} \quad \ldots\ldots \quad 8.15$$

and can be calculated (see fig.8.1) as the following,

if the difference in the hydrostatic force is ΔF, so

$$\Delta F = \frac{1}{2} \rho g M^2 - \frac{1}{2} \rho g h^2 - \frac{1}{2} \rho g H_D^2 \quad \ldots\ldots \quad 8.16$$

substituting $M = (1+\alpha)\ H_D$, $h = \alpha H_D$

Equation 8.16 becomes

$$\Delta F = \rho g \alpha (H_D^2) \quad \ldots\ldots \quad 8.17$$

If one substitutes equation 8.17 in equation 8.15 it becomes

$$T + T \cos \bar{\psi} = \rho g \alpha\ (H_D^2) \quad \ldots\ldots \quad 8.18$$

Substitute equation 8.9 in equation 8.18

the angle $\bar{\psi}$ is found in the following form:

$$\bar{\psi} = \cos^{-1} \frac{2\alpha-1}{1+2\alpha} \quad \ldots\ldots \quad 8.19$$

Equation 8.19 is used to find the initial slope of the membrane in the analysis of a dam using the finite element method.

Now substituting equation 8.19 in equation 8.14, the length of base B_1 can be found from the following:

$$B_1 = \frac{1+2\alpha}{4\alpha} H_D \sqrt{1 - \left(\frac{2\alpha-1}{1+2\alpha}\right)^2}$$ which simplifies to the following form:

$$B_1/H_D = \frac{1+2\alpha}{4\alpha} \sqrt{1 - \left(\frac{2\alpha-1}{1+2\alpha}\right)^2} \quad \ldots\ldots \quad 8.20$$

The length of the perimeter in the upstream side can be found by considering this part as a part of a circle as concluded by Anwar and Binnie (2,5) and it can be calculated from the following relationship:

$$S_1 = (\pi/2 + \delta)\, R \quad \ldots\ldots \quad 8.21$$

where

S_1 = the length of the arc AFC (see fig.8.1)

δ = angle of the arc AF in radin.

Therefore

$$S_1/H_D = \frac{1+2\alpha}{4} \left[180^o - \cos^{-1}\left(\frac{2\alpha-1}{1+2\alpha}\right)\right] \frac{\pi}{180} \quad \ldots\ldots \quad 8.22$$

Since the length of the perimeter S_1 on the upstream side and the length of the perimeter S_2 on the downstream side are now known, hence the total length S of the perimeter (AFCGD) can be found from the following equation:

$$S/H_D = \frac{S_1}{H_D} + \frac{S_2}{H_D} \quad \ldots\ldots \quad 8.23$$

Similarly for the length of the base, which is equal to

$$B/H_D = \frac{B_1}{H_D} + \frac{B_2}{H_D} \quad \ldots\ldots \quad 8.24$$

Equations 8.10, 8.11, 8.20, 8.22, 8.23 and 8.24 are solved for different proportional factors ranging from 0.1 to 10 in increments of 0.05. The calculations were carried out using a computer program the flow chart of which is given in fig. 8.2. The plotting of the results is shown in figs. 8.3 and 8.4.

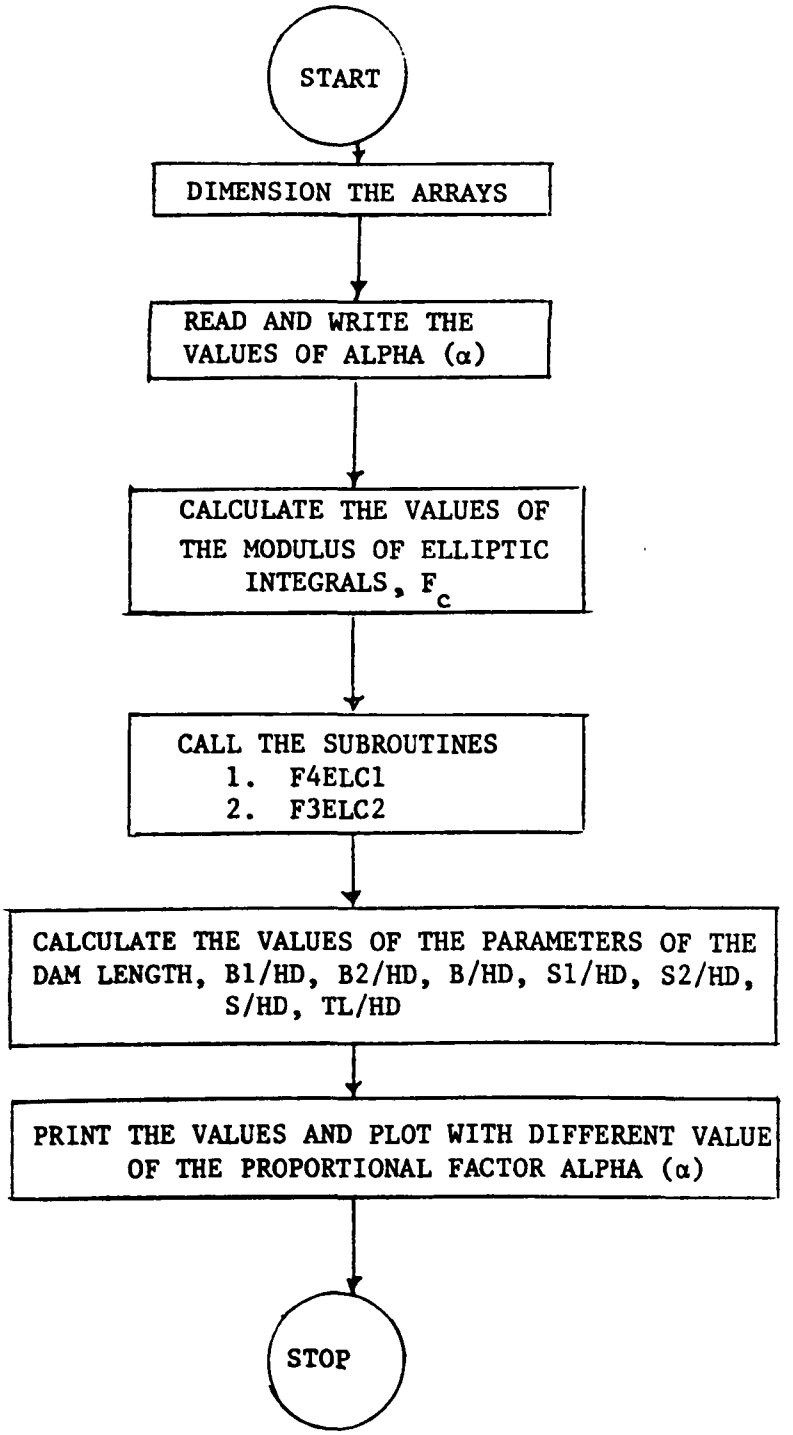

Fig.8.2 Flow chart for calculating the perimeter length ratios.

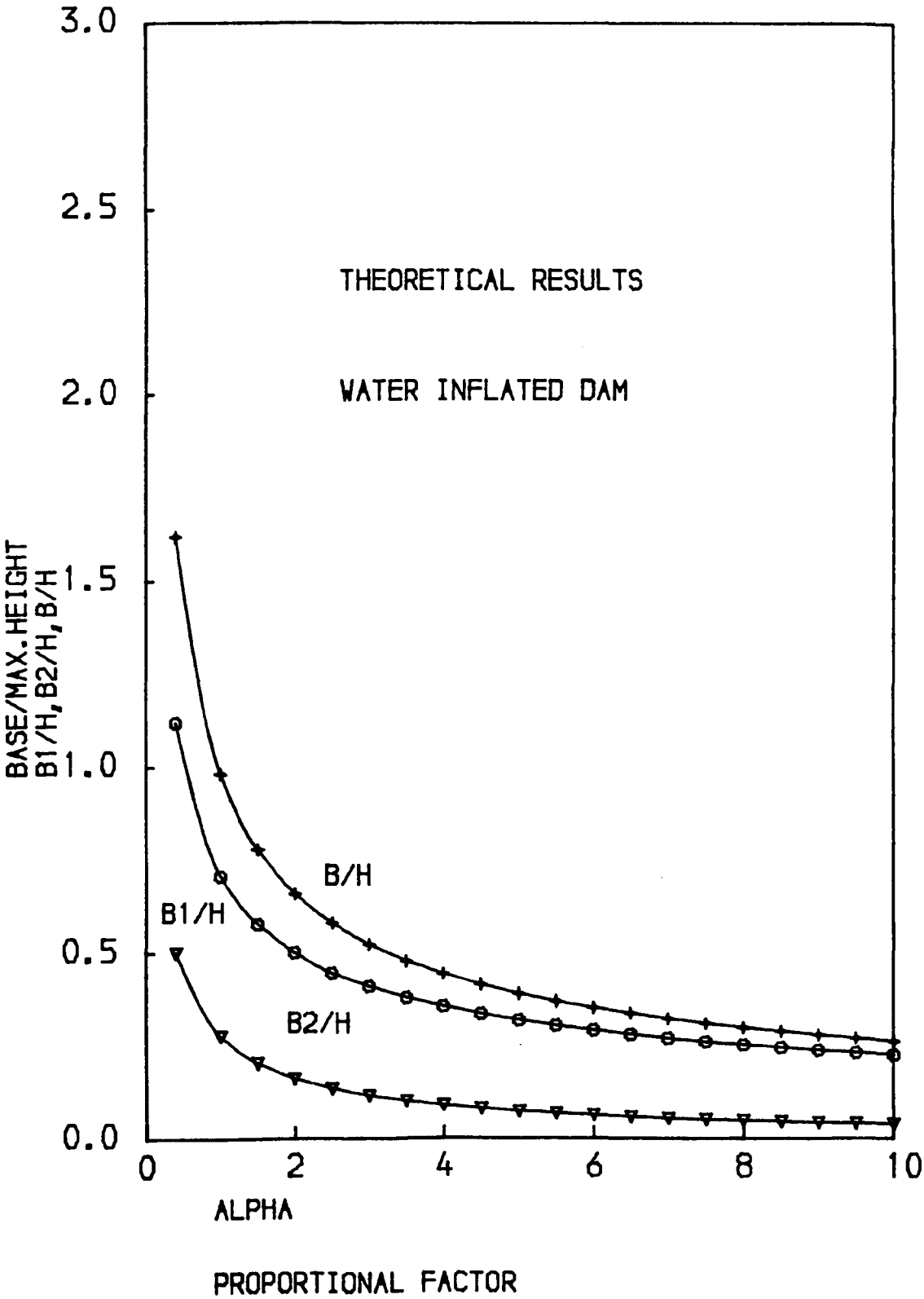

FIG(8-3) VARIATION OF THE BASE LENGTHS RATIO WITH ALPHA

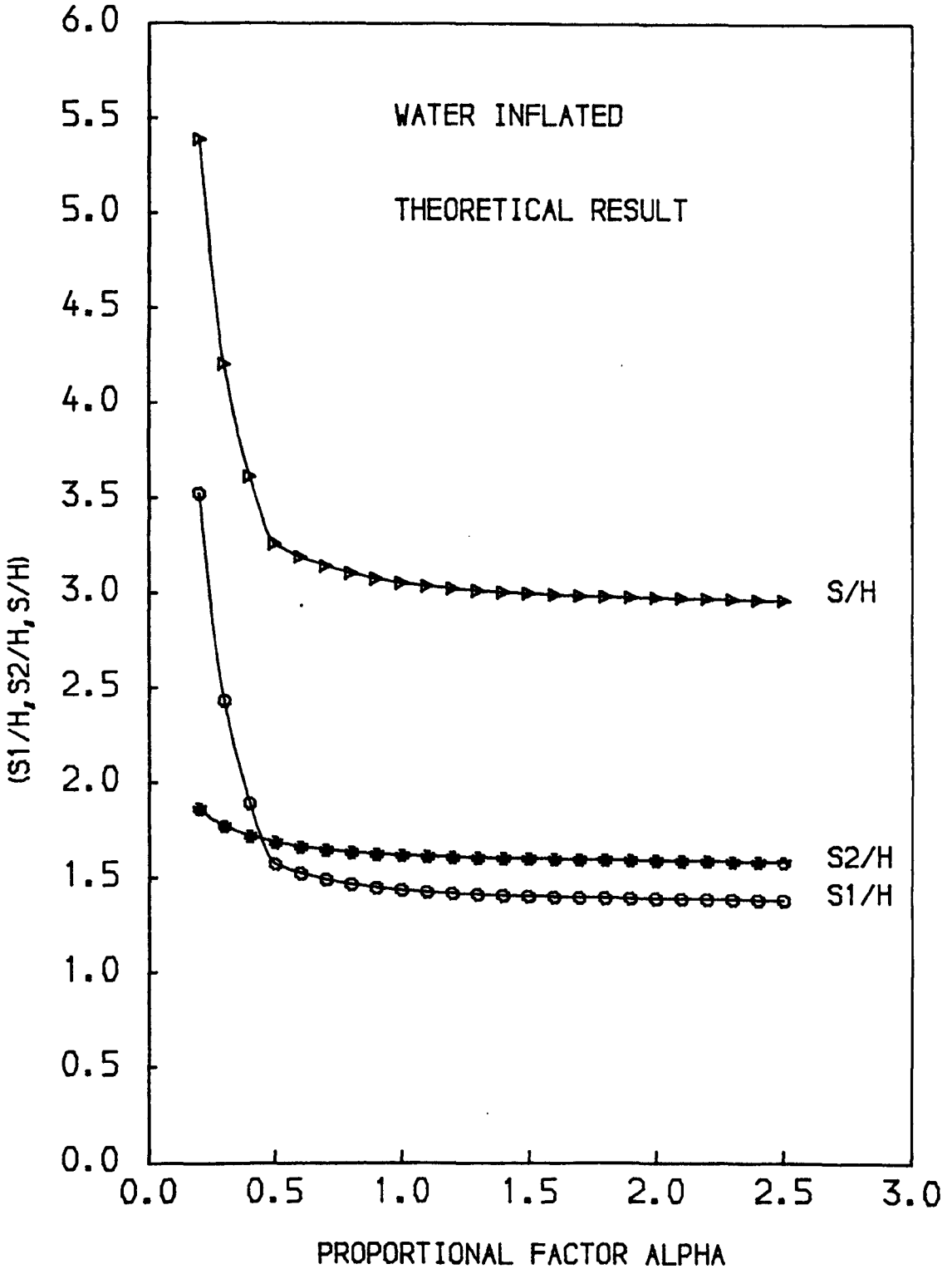

FIG(8-4) VARIATION OF THE PERIMETER LENGTHS RATIO WITH ALPHA

The results of the B/H_D and S/H_D determined experimentally and compared with those theoretical results are shown in fig.8.5 which demonstrates a very good fit.

8.5 Length of the membrane using the least square fitting method.

The results found by the computer program of the lengths ratios (i.e. B_1/H_D, B_2/H_D, B/H_D, S_1/H_D, S_2/H_D, S/H_D) were analysed using a least square method in order to find an equation as a function of proportional factor only and avoiding the use of the modulus of elliptic integrals. So to achieve this purpose, the results of the above equations were fitted using the polynomial fitting technique by using the subroutine available as a central computer subroutine facility to find the best fitting equation with minimum residual between the original data and the values of the fitted equations.

The data was analysed for all length ratios with different values of proportional factors and required high degree polynomial equations with degrees of between 10-13 which is not a very practical form of equation for finding the length ratio for a particular proportional factor. The results of the curve fitting are shown in figs. 8.6 and 8.7 for a water inflated dam.

The results have been plotted on Log-Log Scale and by using the least-square method. A computer program was used to fit and plot the values and the curve fittings were in the form of the following equation:

$$y = m\,\alpha^{n_1} \qquad \ldots\ldots \qquad 8.25$$

The results of fitting the parameters in the form of the above equation can be seen in figs. 8.8 and 8.9 also the values of the coefficients in equation 8.25 are arranged in table 8.1 according to the type of inflation pressure and the limitation of the proportional factors.

The theoretical calculations were compared with the experimental work by using the same form of equation 8.25 and these results were satisfactory as shown in fig.8.10.

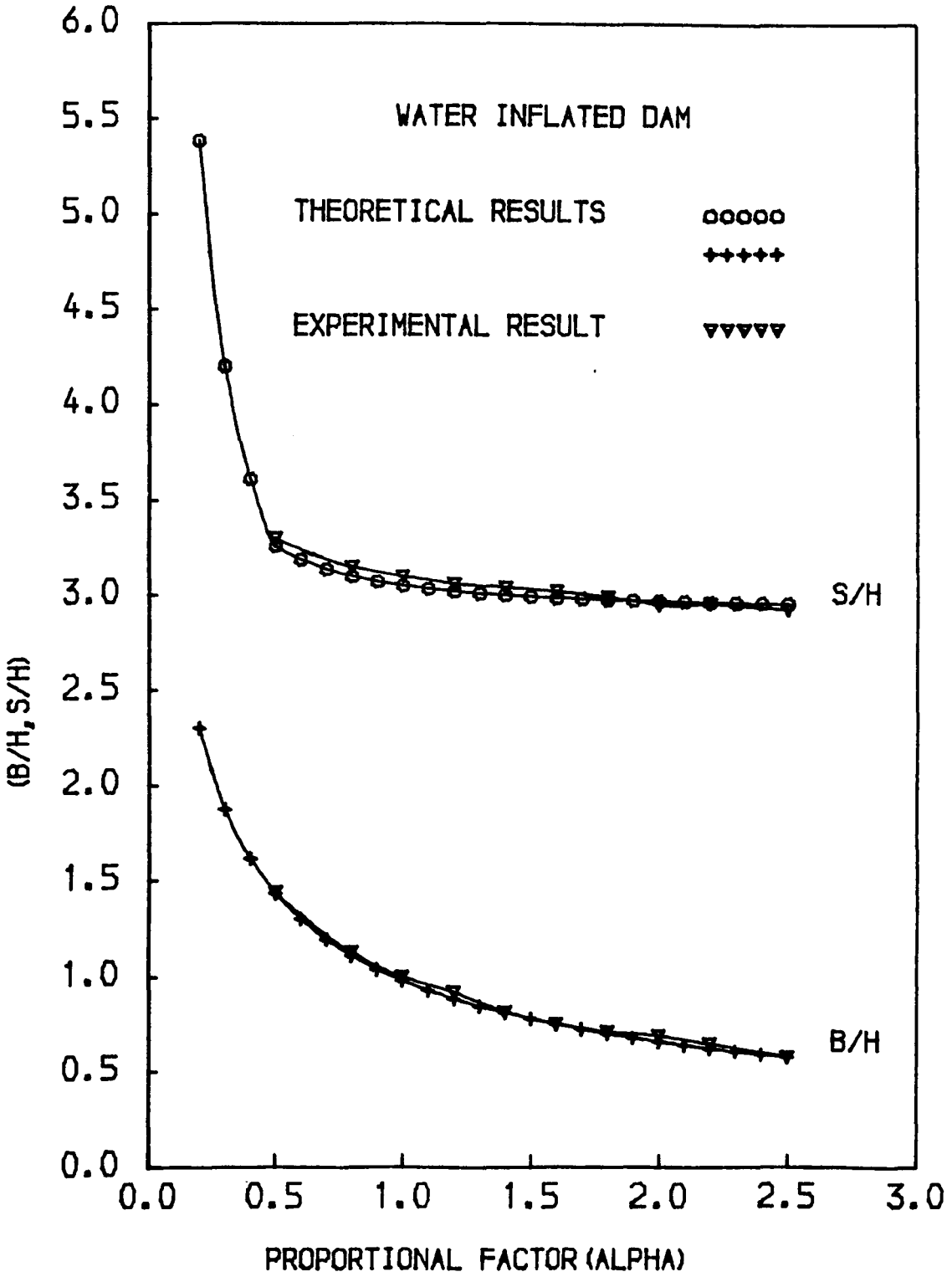

FIG(8-5) VARIATION OF THE LENGTHS PARAMETER RATIO WITH ALPHA

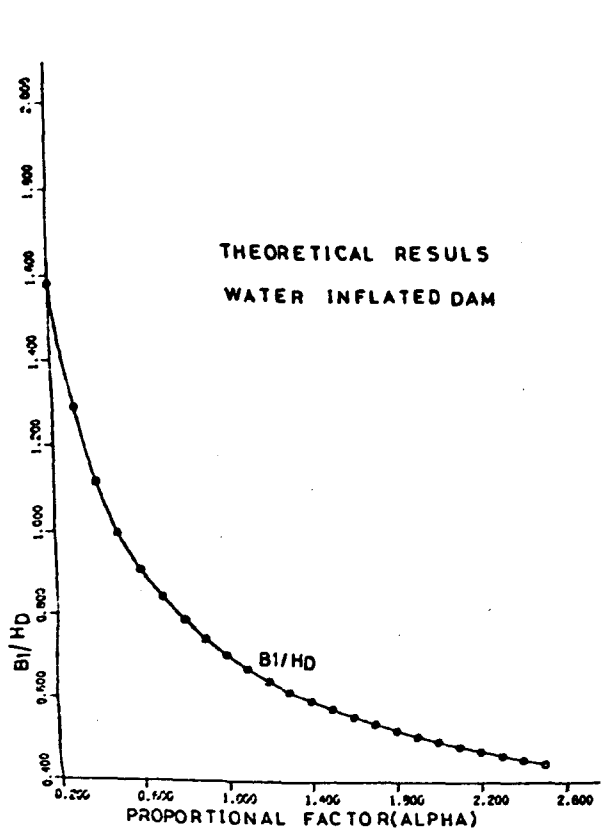

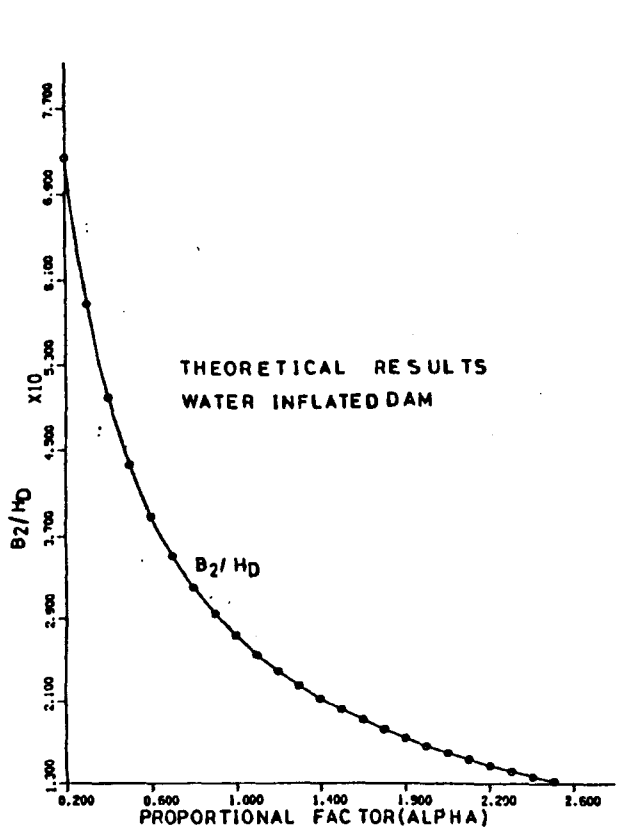

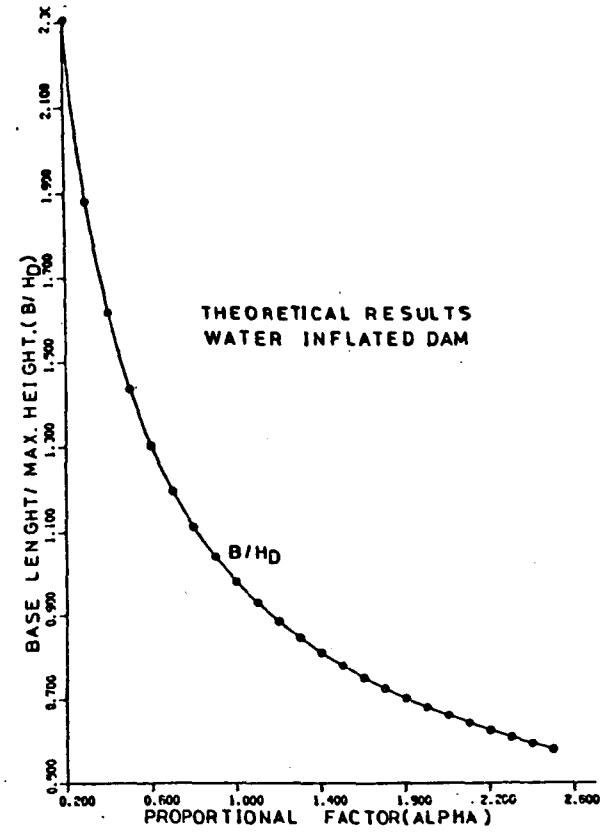

FIG. (8-6) VARIATION OF THE BASE RATIO WITH PROPORTIONAL FACTOR USING A POLYNOMIAL CURVE FITTING FOR WATER INFLATED DAM

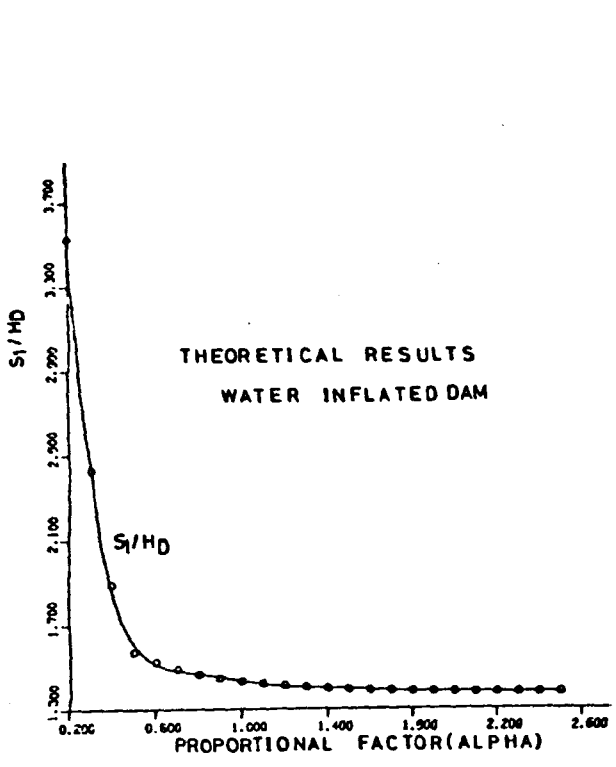

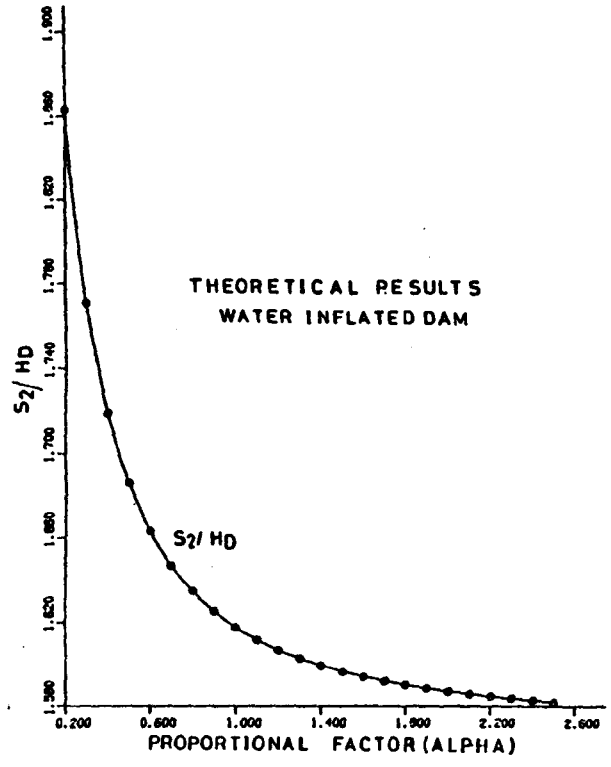

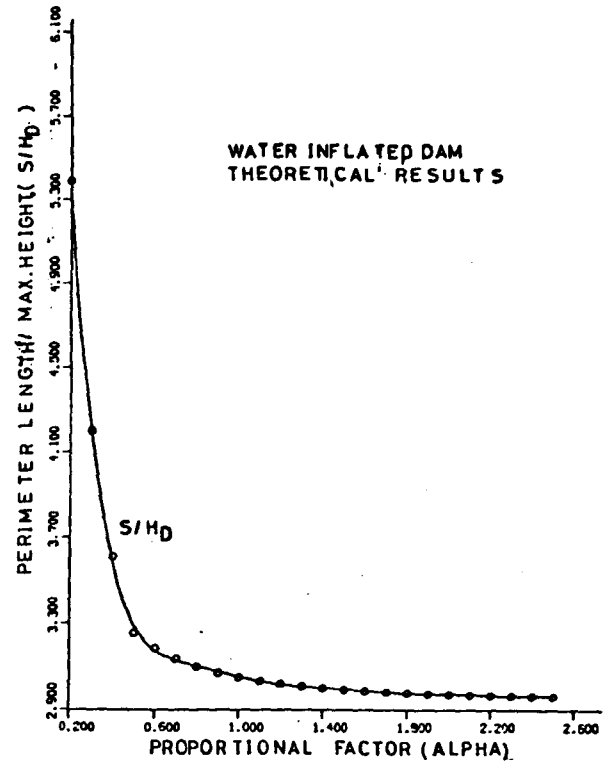

FIG.(8-7) VARIATION OF THE PERIMETER LENGTH RATIO WITH PROPORTIONAL FACTORS USING A POLYNOMIAL CURVE FITTING FOR WATER INFLATED DAM

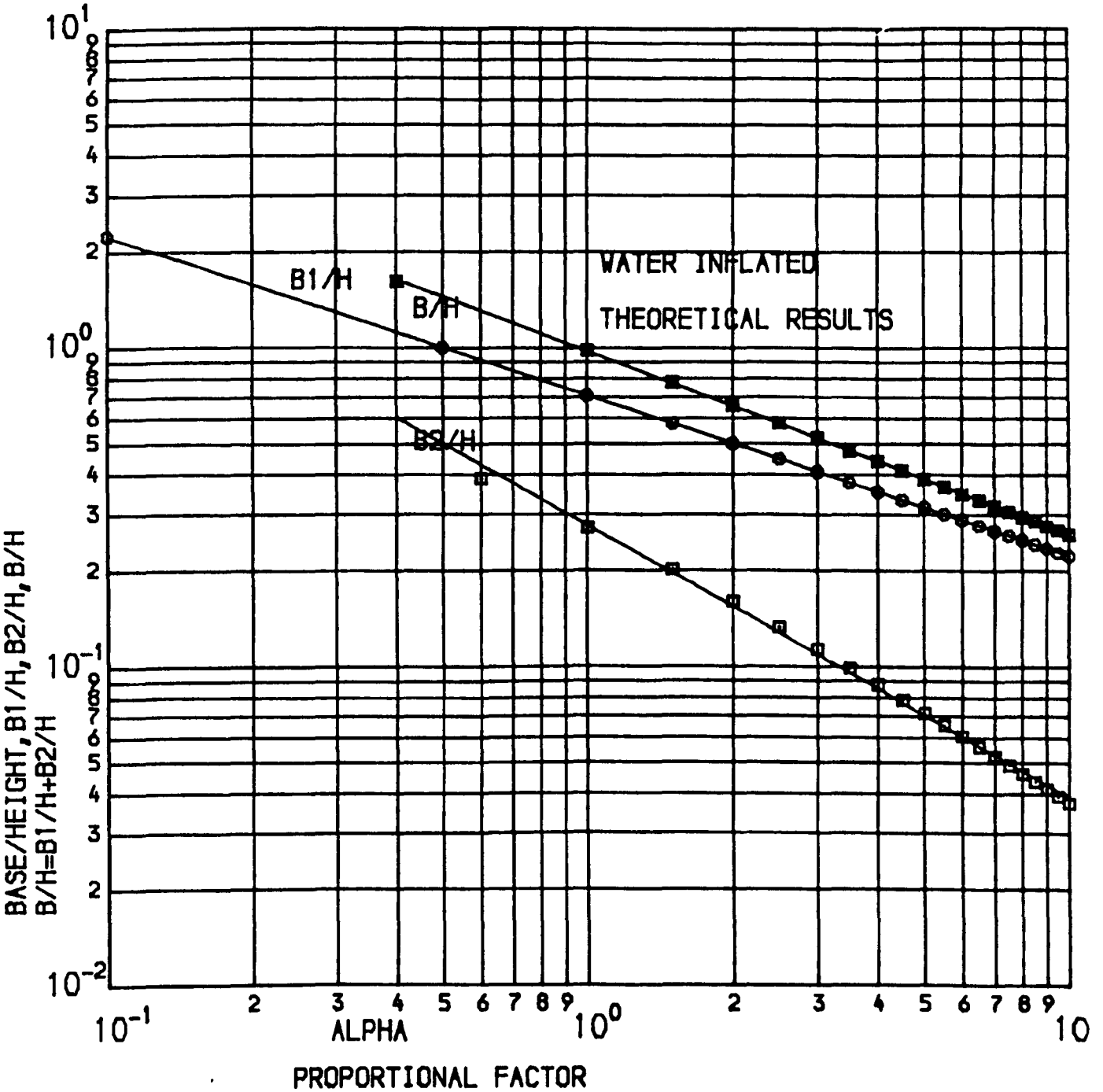

FIG(8-8) VARIATION OF THE LENGTHS RATIO WITH ALPHA

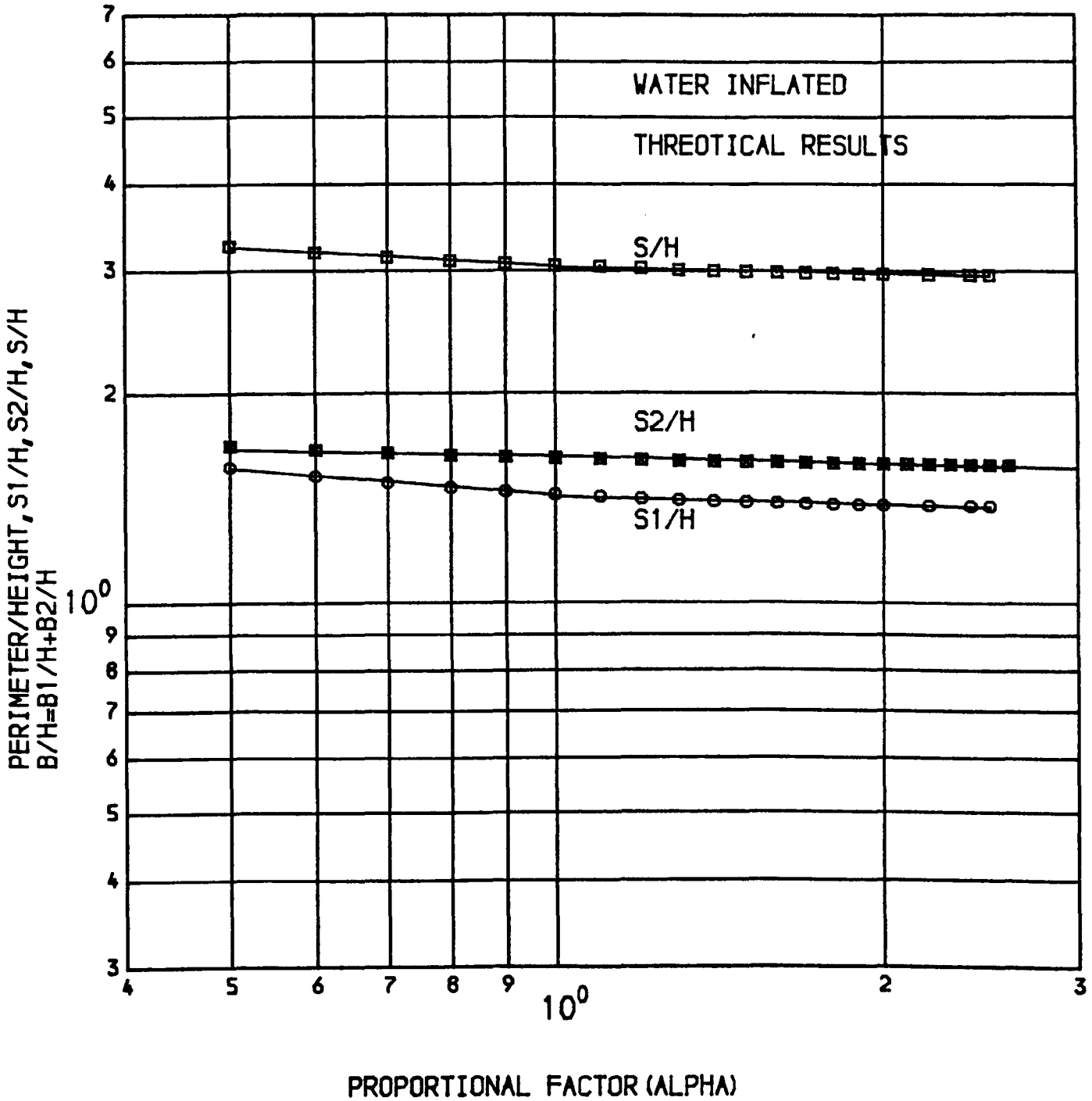

FIG(8-9) VARIATION OF THE PERIMETER LENGTH WITH ALPHA

Table 8.1 Constants of the equation 8.25 of the form $y = m\alpha^{nl}$

S.No.	Parameters (y)	m	n_1	Limitation of alpha (α)	Correlation factors
I	Water inflated				
1	B_1/H	0.707	-0.500	$0.4 \leq \alpha \leq 10$	0.978
2	B_2/H	0.277	-0.852	$0.6 \leq \alpha \leq 10$	0.972
3	B/H	0.973	-0.571	$0.4 \leq \alpha \leq 10$	0.999
1	S_1/H	1.427	-0.132	$0.5 \leq \alpha \leq 1.0$	0.845
2	S_1/H	1.423	-0.039	$1.0 \leq \alpha \leq 2.5$	0.852
3	S_2/H	1.625	-0.035	$0.5 \leq \alpha \leq 2.5$	0.850
4	S/H	3.041	-0.094	$0.5 \leq \alpha \leq 1.0$	0.811
5	S/H	3.040	-0.032	$1.0 < \alpha \leq 2.5$	0.865
II	Air inflated				
1	B/H	0.448	-0.210	$0.2 \leq \alpha \leq 2.5$	0.95
2	S/H	2.662	-0.039	$0.2 \leq \alpha \leq 2.5$	0.96
III	(Air+Water) Inflated				
1	Depth of water inside the dam = 75% max. U/S Head.				
	B/H	0.886	-0.360	$1.0 \leq \alpha \leq 3.0$	0.992
	S/H	3.002	-0.031	$1.0 \leq \alpha \leq 3.0$	0.893
2	Depth of water inside the dam = 30% Max. U/S Head.				
	B/H	0.850	-0.349	$0.3 \leq \alpha \leq 3.0$	0.875
	S/H	2.971	-0.029	$0.3 \leq \alpha \leq 3.0$	0.850
3	Depth of water inside the dam = 15% Max. U/S Head.				
	B/H	0.792	-0.284	$0.3 \leq \alpha \leq 3.0$	0.707
	S/H	2.933	-0.025	$0.3 \leq \alpha \leq 3.0$	0.800

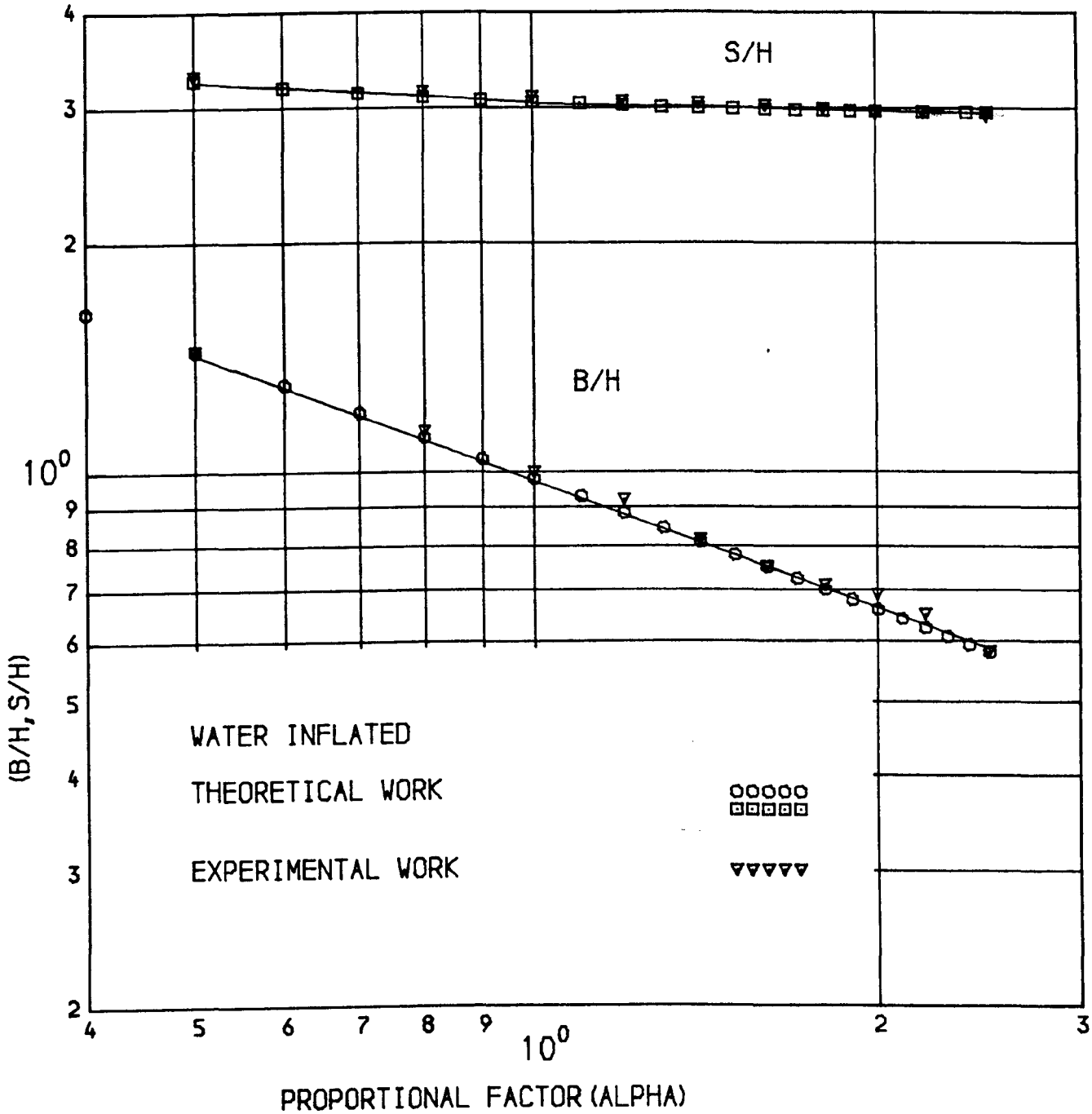

FIG (8-10) COMPARISION OF THE LENGTH RATIO BETWEEN THEORETCAL AND EXPERIMENTAL WORK

The differences in some instances may be due to the assumption of constant tension and weightless material because the material will elongate after applying the loads (i.e. internal pressure head, upstream head, and downstream head).

On the basis of the satisfactory comparison of the theoretical and experimental work for dams inflated with water, the exercise was repeated with air as the inflation fluid.

The results of the experimental work were plotted as shown in fig.8.11 and analysed using the polynomial curve fitting curve technique. Again the fitting required a high degree polynomial as can be seen in fig.8.12, hence the values were fitted in the form of equation 8.25 as for the water inflated dam and the results of this fitting are shown in fig.8.13.

The same procedure was adopted for a dam inflated with (air+water), the depth of water inside the dam ranging between 30-75 percent of the maximum height of the dam and the experimental results plotted as shown in fig.8.14. The curve fitting of the results can be seen in figs. 8.15 and 8.16.

Once one has found the length of material for a particular maximum proportional factor and maximum dam storage height, the dam could be analysed by considering the weight of the membrane and the elongation of the material found from the stress-strain relationship. All the analysis was worked out using the computer program (IHSIP) in order to find the profile of the dam, maximum height, upstream slope, tension along the membrane and the cross-sectional area.

8.5.1 Procedure for design.

1. Assume a maximum proportional factor for a particular type of inflation fluid.

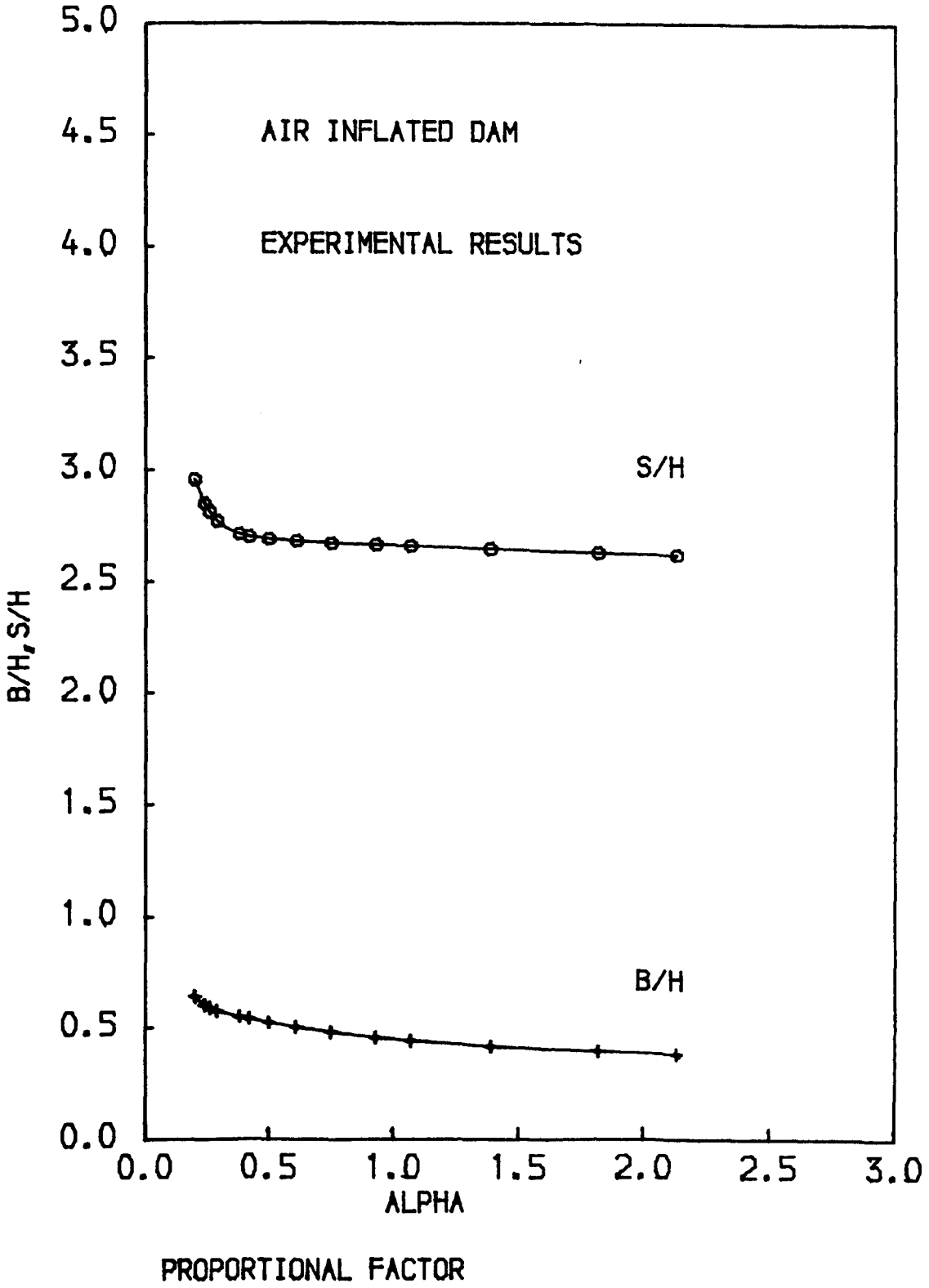

FIG(8-11) VARIATION OF THE LENGHTS RATIO WITH ALPHA

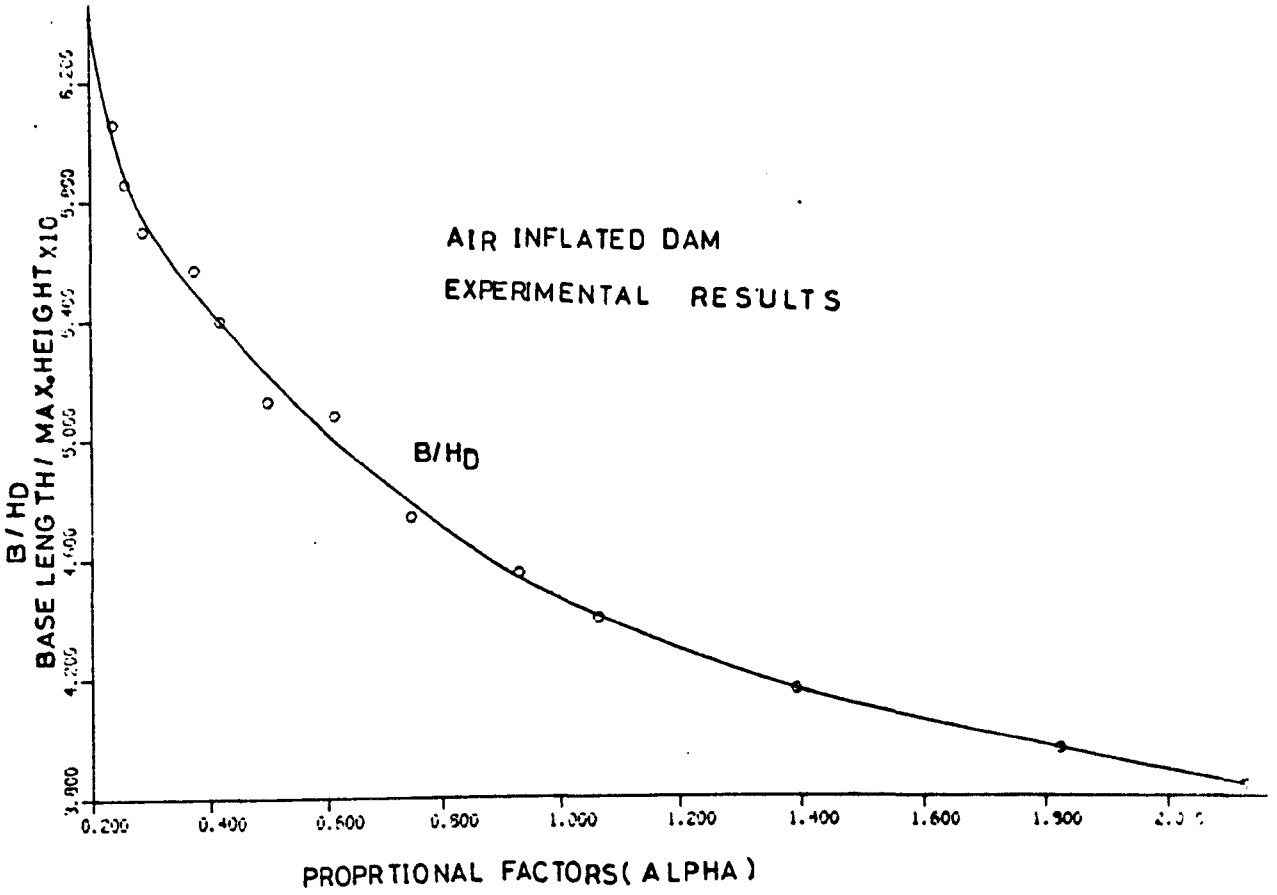

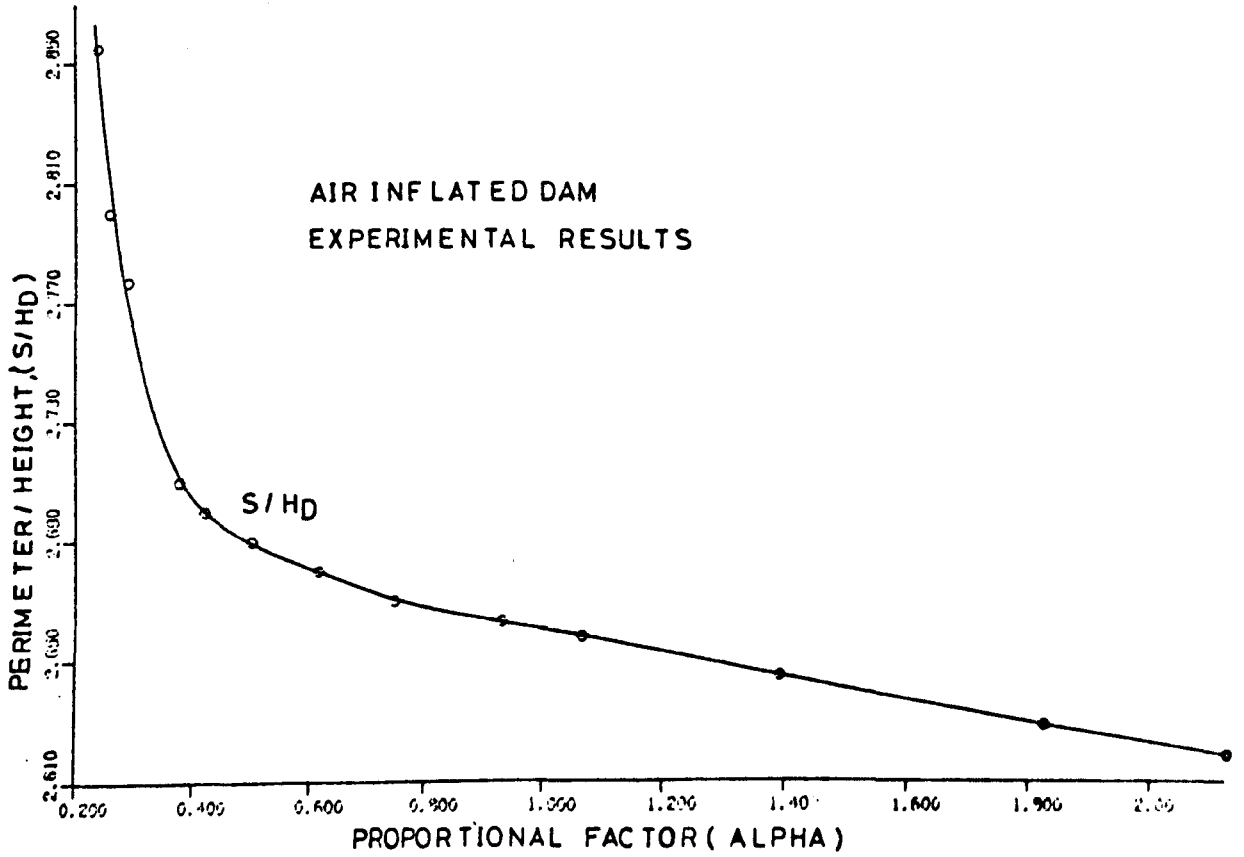

FIG. (8-12) VARIATION OF THE LENGTH RATIO FOR DIFFERENT PROPORTIONAL FACTORS USING POLYNOMIAL CURVE FITTING FOR AIR INFLATED DAM

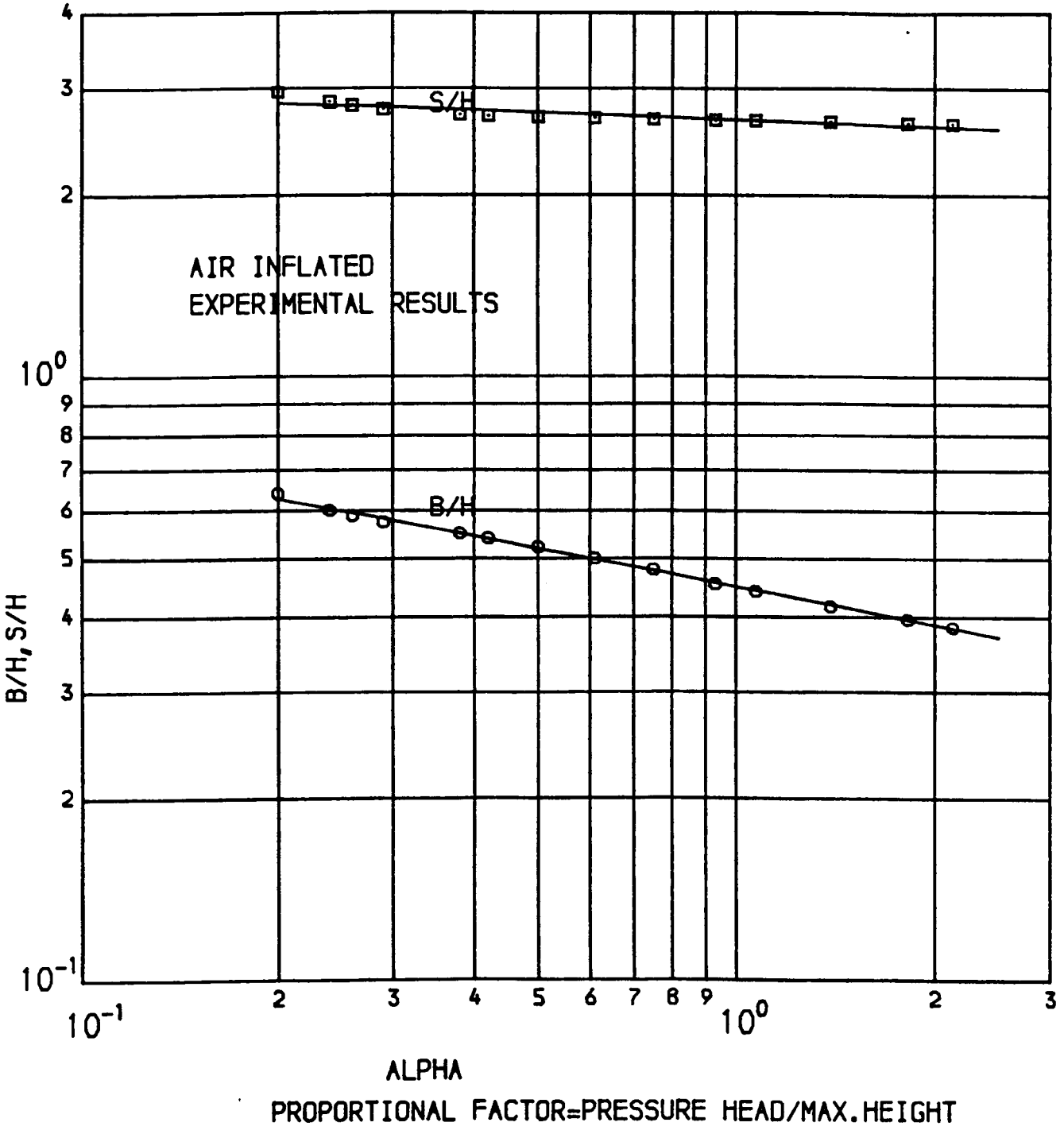

FIG(8-13) VARIATION OF THE LENGTHS RATIO, B/H, S/H, WITH ALPHA

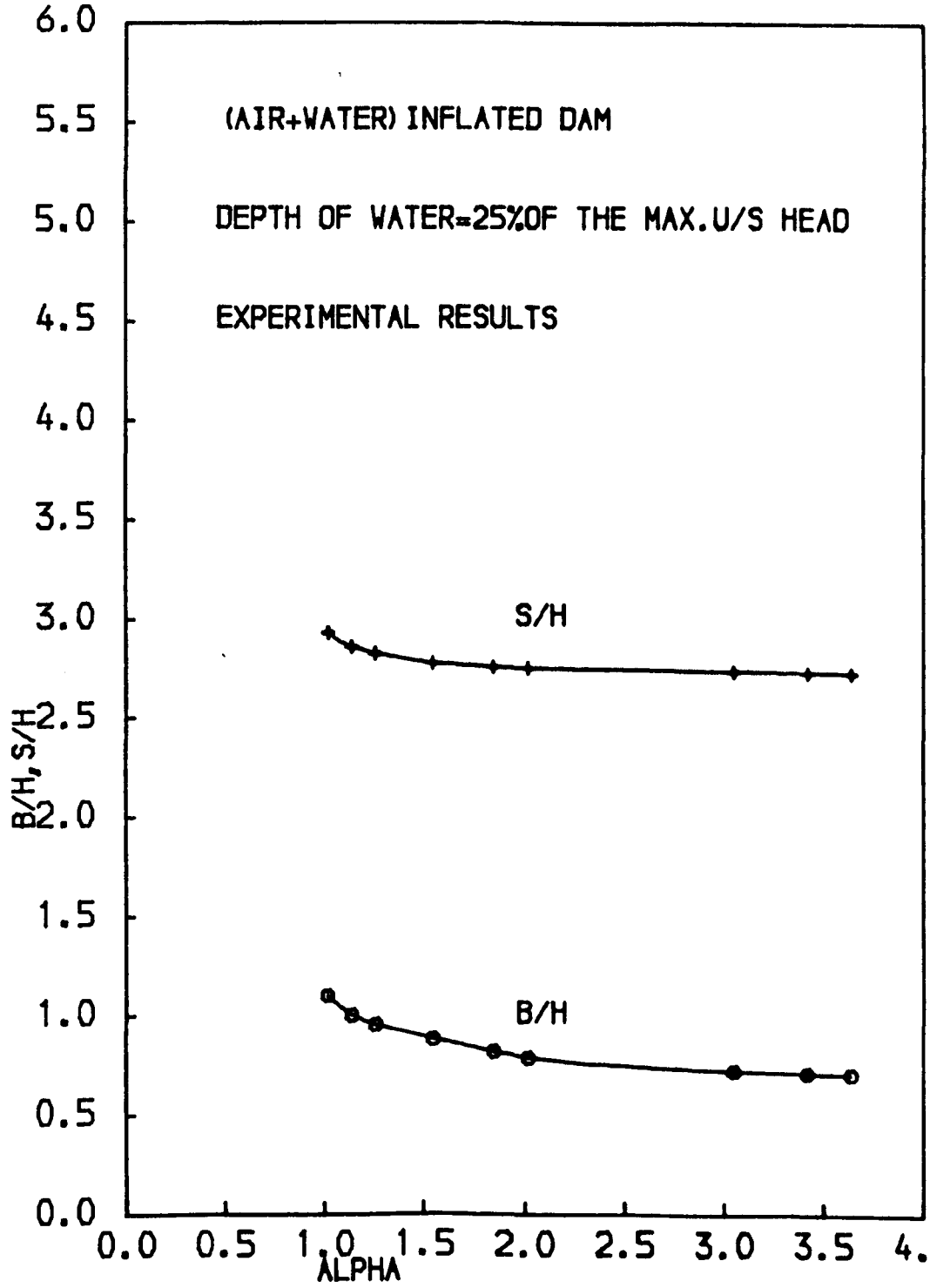

FIG(8-14) VARIATION OF LENGTHS RATIO WITH ALPHA

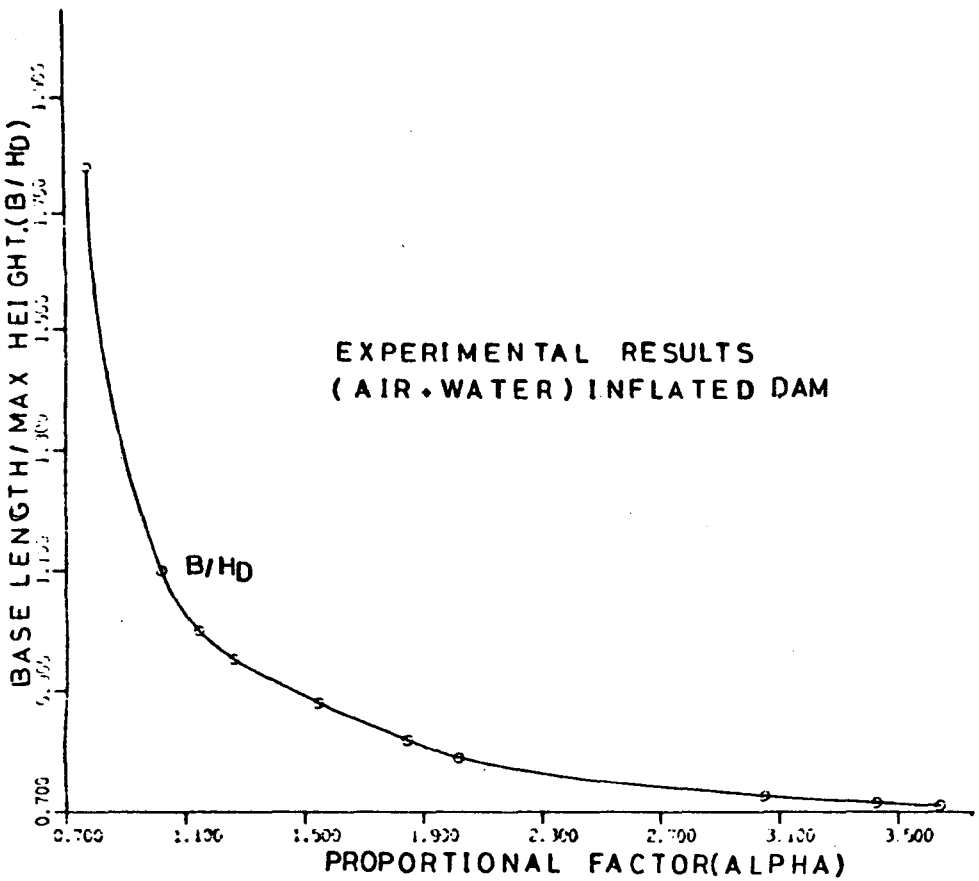

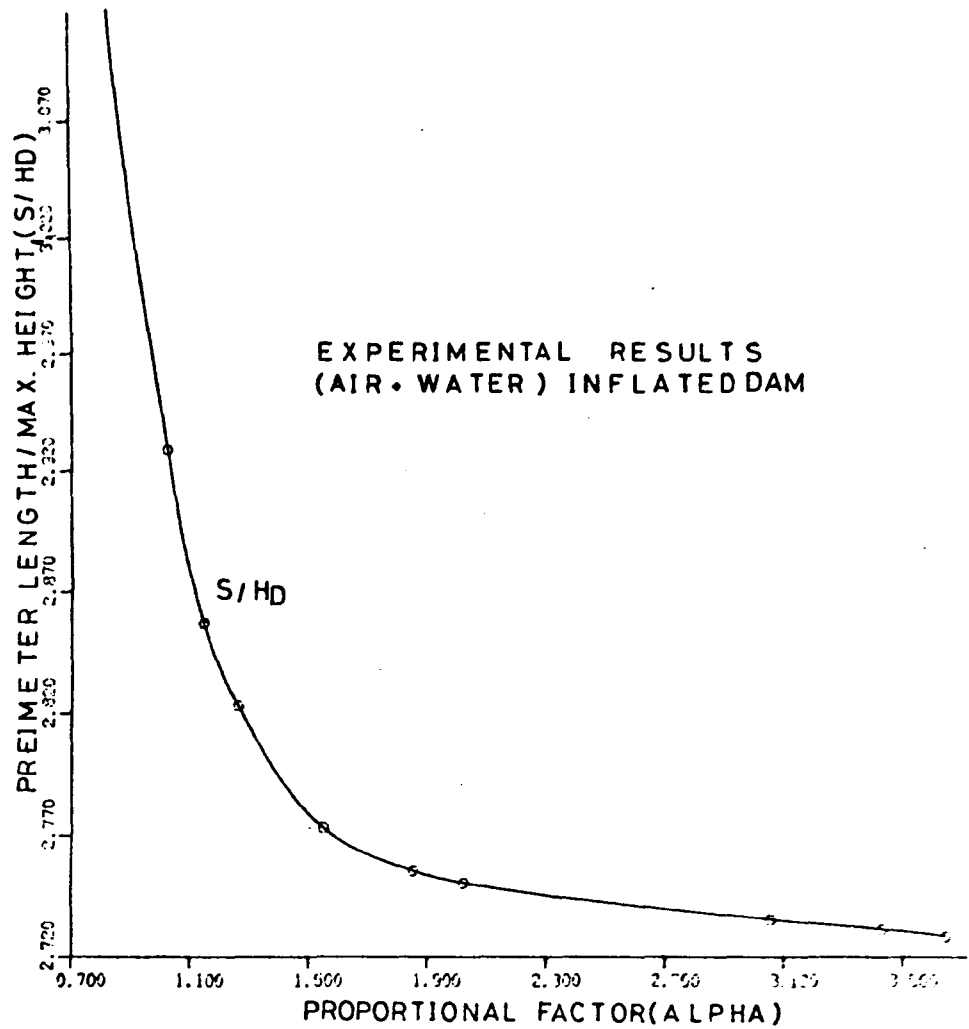

FIG. (8-15) VARIATION OF THE LENGTH RATIO WITH PROPORTIONAL FACTORS USING A POLYNOMIAL CURVE FITTING FOR AIR+WATER INFLATED DAM

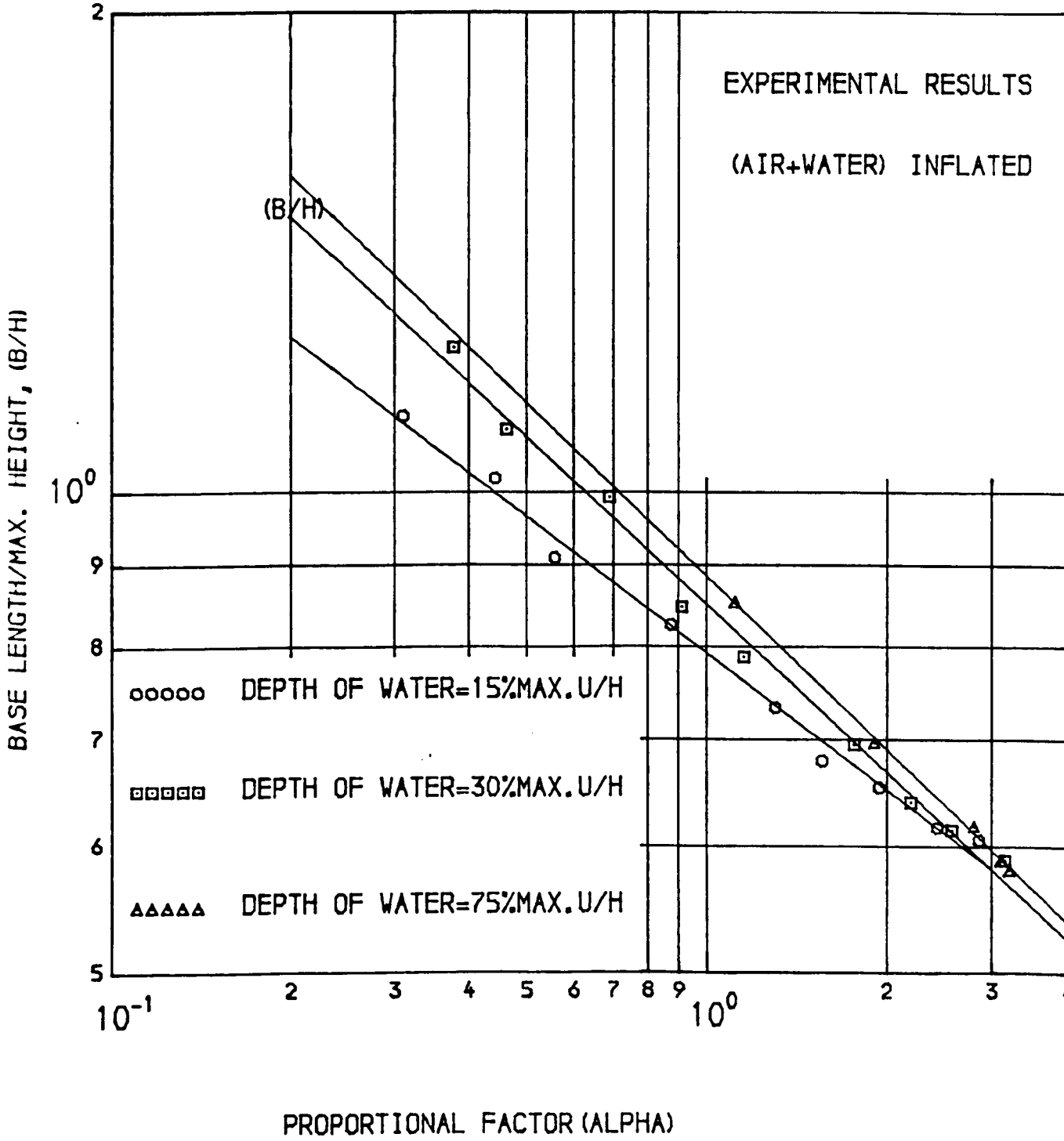

FIG (8-16A) VARIATION OF THE BASE LENGTH RATIO WITH ALPHA

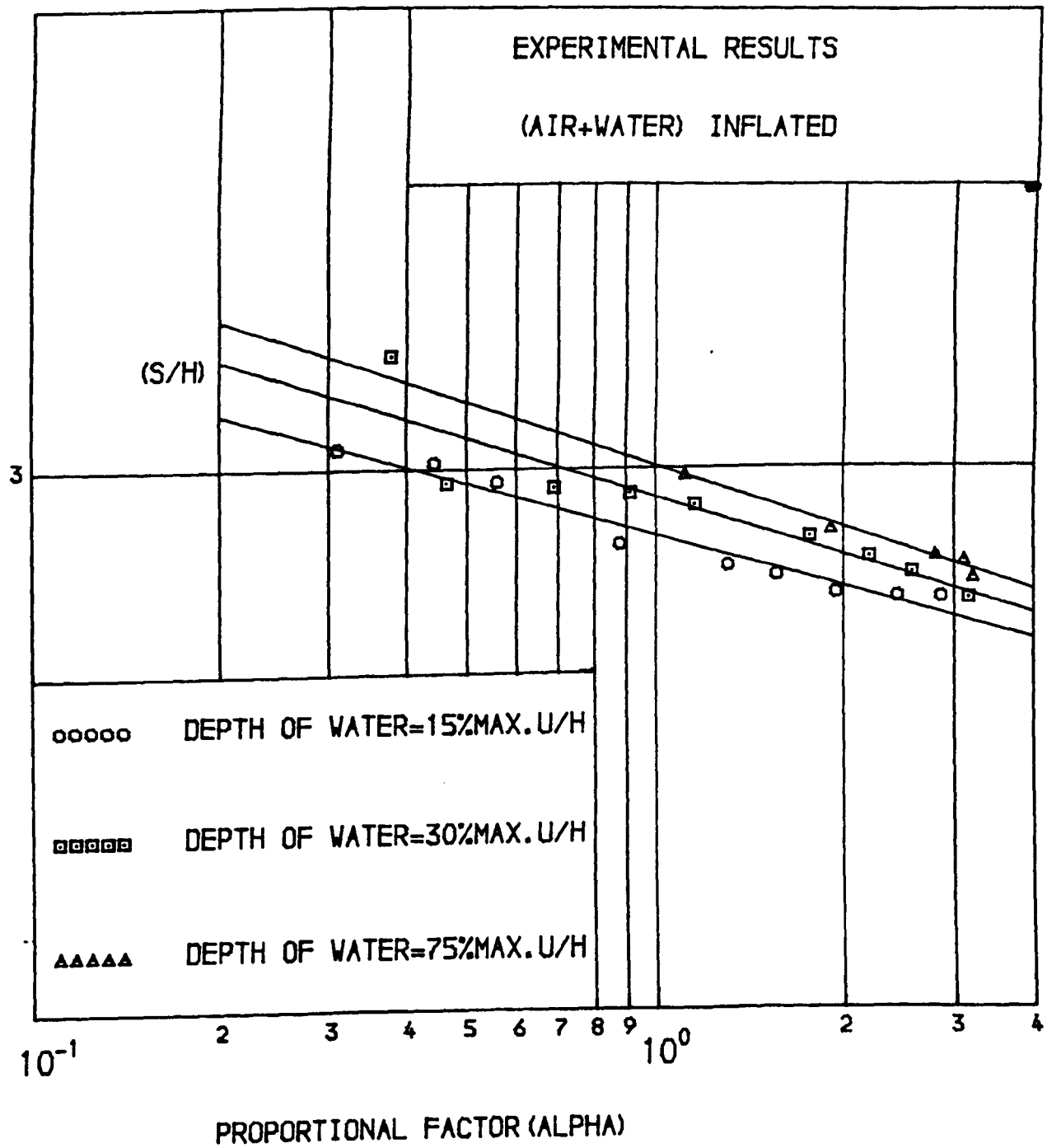

FIG (8-16B) VARIATION OF THE PERIMETER LENGTH RATIO WITH (ALPHA)

2. Determine or assume the maximum storage head required for this dam (i.e. maximum height of dam H_D = maximum upstream head).

3. Find the internal pressure head by using the following relationship (21):

$$\alpha = \frac{h}{H_D} = \frac{H_P - H_D}{H_D}$$

where

H_P = total pressure head.

H_D = maximum height of dam = maximum upstream head.

4. Find the length of membrane for the above values of alpha and maximum upstream head from the equations listed in table 8.1 for a particular type of inflation fluid.

5. Use the program IHSIP to analyse the dam by taking into consideration the weight of the membrane and the elongation in order to find the maximum height of dam.

If the calculated maximum height of dam = maximum upstream head which had been assumed, then the length of the membrane was considered as the optimum length. But if maximum H_D > upstream head, then increase the upstream head by the differences (D) of the upstream head and maximum dam height, i.e.

$$D = H_D - U/S$$

So the new upstream head = U/S + D

and if maximum upstream head > H_D

$$\text{Difference (D)} = U/S - H_D$$

hence the new upstream head = U/S - D

once the maximum upstream head (U/S) equalled the maximum height (H_D) or if any increase in the U/S head will cause decreasing in the maximum height of the dam (H_D), then the U/S head can be considered as maximum and the length of the membrane was considered as the optimum length of membrane.

6. Once the length of the membrane was fixed the analysis of the dam for other proportional factors less than that assumed initially could be carried out to assess the behaviour pattern.

8.5.2 Computer program IHSIP.

The program IHSIP used the equations found by the least square method to calculate the length of the membrane for assumed maximum value of proportional factor and maximum storage head.

The result of using this for a membrane length equal to 0.80 m with maximum proportional factor equal to 2.5 are shown in fig. 3.8.

Two dams of total length of membrane equal to 3.0 m have been designed for different inflation fluids. The maximum heights used were 0.908 and 0.708 m for the air and water inflated dams respectively and the results of the design are shown in figs. 8.17 and 8.18.

8.6 Recommendations for the design of a model and prototype.

In this study the design technique was not based on scale model test of a prototype inflatable dam, but the model test was carried out to check the theoretical output parameters by constructing models of the same dimensions as the design, i.e. the theoretical work was used to design a small dam (lowest size in this study of total membrane length equal to 0.5 m) and a large size of dam as shown in figs. 8.17 and 8.18 with a total length of membrane equal to 3.0 m. Hence using this technique in this study it is possible to design dams of all sizes.

However, if it is decided to study the effects of parameters not including in this theoretical approach for example waves, ice, snow, movement of silt and sediment, vibration, then the construction of a model may be required.

This section outlines the criteria that should be adopted in considering the relationship between a model and prototype inflatable dam. Any model

U/S HEAD	=	0.9084	METER
D/S HEAD	=	0.0000	METER
AIR PRESSURE	=	12.7176	KN/SQ.M
WATER PRESSURE	=	0.0000	M.W.G.
ORIGINAL LENGTH	=	3.0004	METER
NEW LENGTH	=	3.2984	METER
U/S TENSION	=	5.0822	KN/M
U/S SLOPE	=	103.9406	DEGREE
D/S TENSION	=	6.9490	KN/M
BASE LENGTH	=	0.4936	METER
MAX. HEIGHT	=	0.9084	METER
ALFA	=	0.4000	
AREA	=	0.9122	METER SQ
SILT DEPTH, HS	=	0.0000	METER

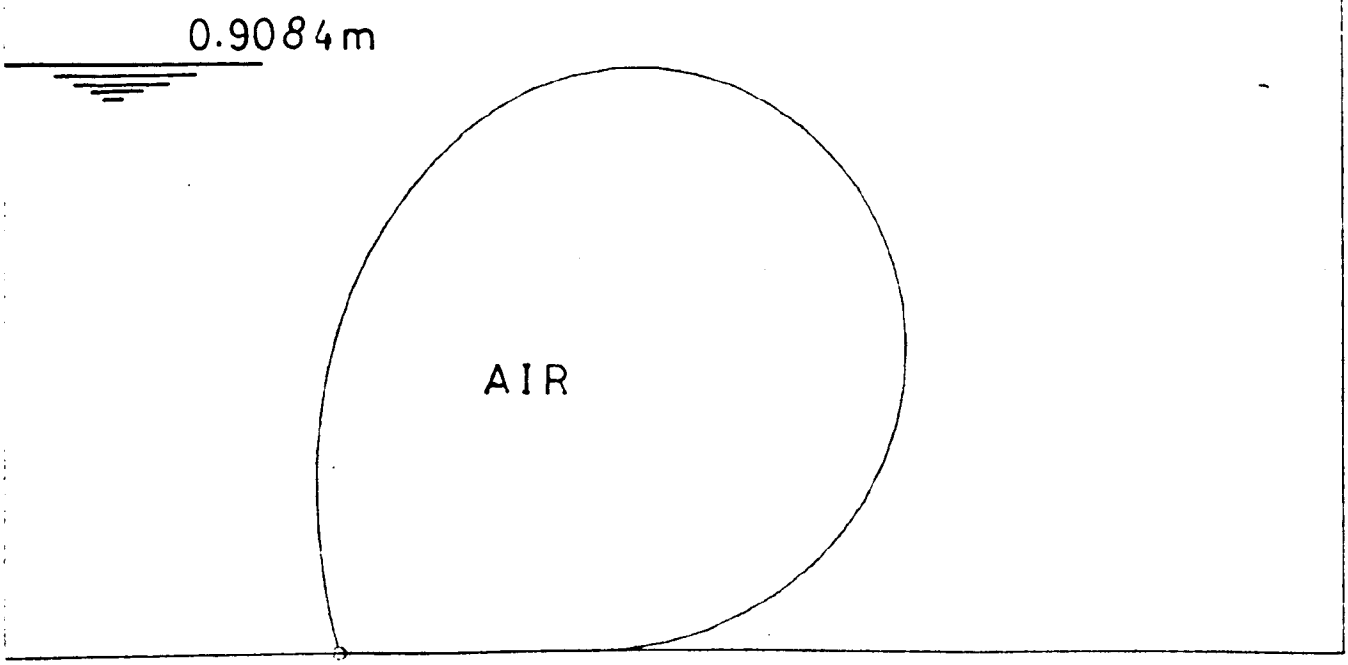

FIG. (8-17) OUTPUT OF AIR INFLATED DAM OF 3·0m LENGTH OF MEMBRANE

U/S HEAD	=	0 7075	MFTER
D/S HEAD	=	0.0000	METER
AIR PRESSURE	=	0.0000	KN/SQ.M
WATER PRESSURE	=	1.4008	M.W.G.
ORIGINAL LENGTH	=	3.0008	METER
NEW LENGTH	=	3.1856	METER
U/S TENSION	=	3.0606	KN
U/S SLOPE	=	130.9630	DEGREE
D/S TENSION	=	4.3081	KN/
BASE LENGTH	=	0.6543	METER
MAX. HEIGHT	=	0.7075	METER
ALFA	=	1.000.	
AREA	=	0.7625	METER SQ
SILT DEPTH, HS	=	0.0000	METER

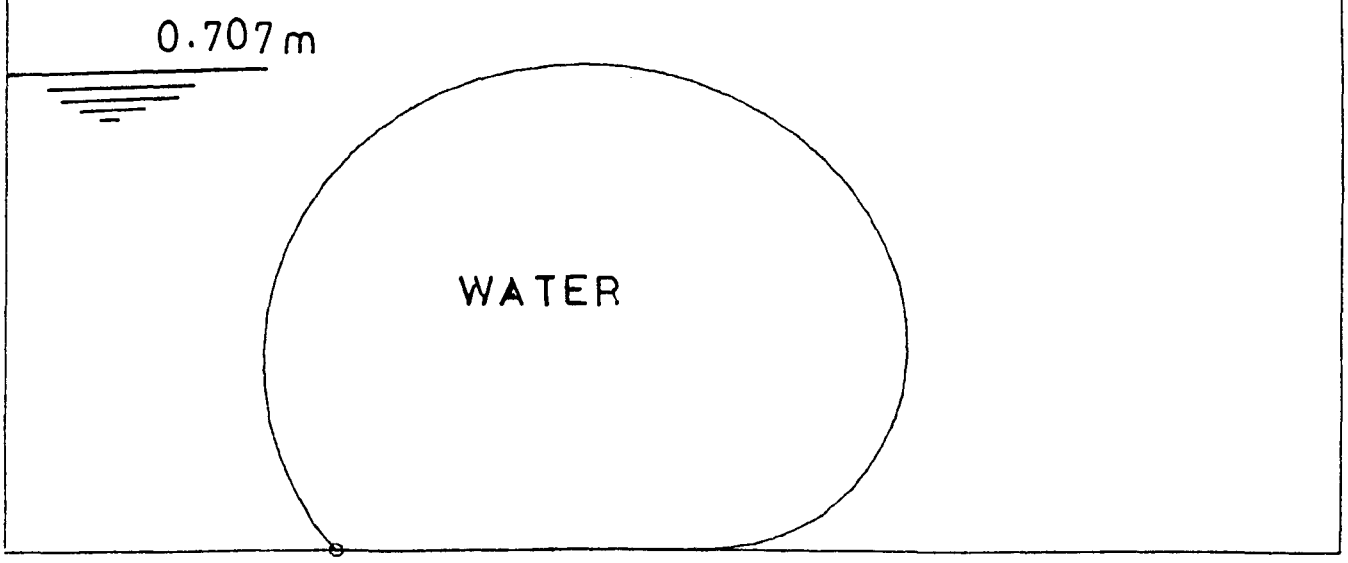

FIG. (8-18) OUTPUT OF WATER INFLATED DAM OF 3·0m LENGTH OF MEMBRANE

should be similar to the prototype in three ways:

a. Geometric similarity.

b. Kinematic similarity.

c. Dynamic similarity.

8.6.1 Design of the model model to be tested under hydrostatic condition.

Geometric similarity exists between model and prototype when the ratio of the corresponding dimensions in the model and prototype are equal, these ratios may be written

Length, $$\frac{L_m}{L_p} = L_r \quad \ldots\ldots \quad 8.26$$

Area, $$\frac{L_m^2}{L_p^2} = L_r^2 \quad \ldots\ldots \quad 8.27$$

where L_r is the scale ratio and subscripts m and p refer to the model and prototype respectively.

In the case of an inflatable dam, the material of the membrane of the model must have similar properties to the material used for the prototype dam, therefore

$$\frac{SU_m}{SU_p} = \frac{\frac{T_{l_m}}{A'_m}}{\frac{T_{l_p}}{A'_p}} = \frac{T_{l_m}}{T_{l_p}} \times \frac{A'_p}{A'_m} \quad \ldots\ldots \quad 8.28$$

or $$\frac{SU_m}{SU_p} = \frac{T_{l_m}}{T_{l_p}} \times \frac{1}{L_r^2} \quad \ldots\ldots \quad 8.29$$

where SU = ultimate stress of the membrane material

T_l = ultimate tension of the membrane material

A' = cross-sectional area of the membrane material.

In order to calculate the relationship of the inflation pressure between the model and the prototype, the validity of assumption No. 3 in this chapter can be used in the model and prototype for the same proportional factor

$$\frac{h_m}{h_p} = \frac{\alpha H_{Dm}}{\alpha H_{Dp}} = L_r \quad \ldots\ldots \quad 8.30$$

or

$$= \frac{h_m}{h_p} = \frac{H_{Dm}}{H_{Dp}} = L_r \quad \ldots\ldots \quad 8.31$$

where

H_D = maximum height of dam.

h = differential pressure head.

α = proportional factor.

8.6.2 Design of the model tested under hydrodynamic condition.

A model which is designed to be tested under hydrodynamic conditions must satisfy the three similarities. To satisfy the geometric similarity of the model to the prototype then one can follow the same approach described in Section 8.6.1.

The second similarity which is kinematic similarity is the similarity of motion, therefore

$$\frac{Q_m}{Q_p} = \frac{V_m A_m}{V_p A_p} \quad \ldots\ldots \quad 8.32$$

or

$$Q_r = V_r A_r \quad \ldots\ldots \quad 8.33$$

where

Q = rate of flow.

v = velocity approach.

A = cross-sectional area of the channel.

The third similarity is dynamic similarity. This similarity of forces (see Appendix B) acting on the surface due to inertia forces, gravity force, viscous forces, pressure forces, surface tension forces, elastic forces. In the case of an inflatable hydraulic structure, the gravity force is predominant and one can neglect the other forces. So when applying dynamic similarity to both model and its prototype then,

$$F_a = M_{,a} \qquad \ldots\ldots \qquad 8.34$$

$$\frac{(F_a)\ m}{(F_a)\ p} = \frac{(M_a)\ m}{(M_a)\ p}$$

$$\frac{(\rho L^3 g)\ m}{(\rho L^3 g)\ p} = \frac{(\rho L^2 v^2) m}{(\rho L^2 U^2) p}$$

$$\frac{V^2{}_m}{g_m\ L_m} = \frac{V^2_p}{g_p\ L_p}$$

$$V_r^{\ 2} = \frac{1}{g_r\ L_r}$$

or

$$\frac{V_r}{\sqrt{g_r\ L_r}} = 1 \qquad \ldots\ldots \qquad 8.35$$

where

F_a = gravity force.

M = mass.

'a = acceleration.

ρ = density of fluid.

g = acceleration due to gravity.

Substituting equations 8.33 into equation 8.35 to yield

$$Q_r = L_r^2 \sqrt{g_r\ L_r} \qquad \ldots\ldots \qquad 8.36$$

and g_r is unity

hence $Q_r = L_r^2 \sqrt{L_r}$

Then from the above equation, it is possible to calculate the corresponding discharge of the model.

CHAPTER 9.

CONCLUSIONS AND RECOMMENDATIONS FOR FUTURE WORK.

9.1 Conclusions.

An inflatable dam constructed from a fabric material can provide a simple and inexpensive way of raising or controlling the water level in a river or canal. Such a dam can be utilised at sites where traditional hydraulic structures are too costly and take too long to construct.

The dam can be inflated with water or air or a combination of the two and anchored to a concrete floor with one end fixed toward the upstream side. The object of this investigation was to obtain a design technique for a dam and to study the behaviour and performance of that dam both for hydrostatic and hydrodynamic conditions. Silt load has been taken into consideration as a static load on the upstream face of the dam.

The theoretical work was developed to use a finite element method to analyse the dam. Models were constructed and tested under hydrostatic and hydrodynamic conditions. The profiles, tension, upstream slope, maximum height of dam and cross-sectional area from the theoretical results were compared with the experimental work. It was found that the maximum percentage differences were 1.3, 5.3, 3.0, 1.5 and 2.8 respectively. For the hydrodynamic conditions the comparison was carried out for the profiles and tension and the maximum percentage differences were 1.97 and 2.9 respectively.

A computer program was written to analyse and design air, water and (air+ water) inflated dams based on the analysis in Chapter 4 for static conditions and for hydrodynamic condition in Chapter 5. The design length of the membrane according to different proportional factors has been developed and detailed as in Chapter 8.

Different relationships for the overflow head were developed to calculate the rate of flow and coefficient of discharge for the dam inflated with different inflation fluids as explained in Chapter 7.

All the above techniques can be used to design such a type of structure which could be used for any of the following purposes (16).

1. Diversion structures.
2. Check structure for flow control.
3. Lock system.
4. Sluice gate.
5. Salinity barriers.
6. Tidal barriers.
7. Raising heights of existing spillways.
8. Raising height of water reservoirs by adding to top of existing gate.
9. Control gate for water treatment plants.
10. Control gates for sewage plants.
11. Replacement of steel gate on concrete structure.
12. Replacement of low concrete dam to 7.5 m in height.
13. Barrier for beach erosion.
14. Breakwaters.

A new technique for deriving the flow rate over an air, water and (air+water) inflated dam has been developed. This leads to a new application of a dam as a device for discharge measurement.

The main conclusions of the behaviour and performance of an inflatable dam (under both hydrostatic and hydrodynamic conditions) resulting from this work are as follows:-

1. For the same internal pressure head different inflation fluids give different dam heights for the same dam.

2. An air inflated dam resulted in a higher maximum height of dam than a water inflated dam for the same internal pressure head while an (air+water) inflated dam gave a higher maximum height than a water inflated dam and

lower height than an air inflated dam for the same internal pressure head.

3. A silt depth on the upstream face of the dam reduced the maximum height of the dam while the downstream head increased the maximum height of the dam.

4. A higher maximum height for an (air+water) inflated dam was achieved for a small internal depth of water relative to the maximum height for a larger proportion of water for the same total internal pressure head.

5. The tension in the membrane was higher for an air inflated dam than for the equivalent water with an equivalent (air+water) dam tension falling between the two.

Higher tension results in longer elongation in the membrane and this may cause a reduction in the dam life which has been suggested as being of the order of 20 years.

6. The tension increased with increasing proportional factors for all dams under different inflation fluids and the upstream tension was lower than the downstream tension.

7. The tension in the membrane increased as the length of the membrane increased for all proportional factors and for all dams inflated with different inflation fluids.

8. The upstream slope increased as the proportional factors increased and also increased as the downstream head increased while the upstream slope decreased as the silt depth increased.

9. The upstream slope remained constant for a particular proportional factor for all different lengths of membrane tested.

10. The downstream slope for all proportional factors was equal to zero i.e. the fabric was tangential to the base.

11. The use of the elliptic integrals to find the length of the membrane for a water inflated dam has been modified using a least square method in

order to avoid the use of the modulus of elliptic integrals.

12. Similar relationships based on least square methods have been used to find the length of membranes for air and (air+water) inflated dam based on the results of the experimental and theoretical work for water inflated dams.

13. For the hydrodynamic condition the height of a dam decreased as the overflow increased.

14. The base width of the dam is increased with increasing the overflow head for a particular proportional factor and inflation fluids and the base width also increased with effect of silt depths.

15. The tension decreased as the overflow increased and this phenomenon was also found experimentally by using strain gauges inside the dam.

16. A dam started to vibrate if the overflow head was increased above a flow limit and this condition was investigated for different dams under different inflation fluids.

17. Different formulae for the coefficient of discharge and discharge with relation to the ratio (H/H_D) were developed; this enables such a structure to be used as a device to measure the discharge. These formulae were related to dams inflated with air, water and (air+water).

18. An increase in the downstream head resulted in an increase in the upstream and decrease in the overflow head,the former being the larger increase overall for dams for different proportional factors and different inflation fluids.

19. The differences in the total average tension between the theoretical and experimental work for the hydrodynamic condition were always less than ± 3%.

20. The thickness of the material had a significant effect on the maximum height of the dam and on the elongation of the material whilst the weight of the material is of little significance.

21. A minimum of 50 elements were required in the analysis to give the best results for the tension and maximum height of dams.

22. A v-notch effect occurred for air inflated dams during deflation for both static and dynamic conditions.

23. Dams become rigid when inflated to high pressures and this resulted in insignificant deformation in shape when downstream, silt depth and overflow changed.

24. The analysis in this study resulted in a technique for the design of different sizes of dam and was demonstrated for dams in the range of 0.5 to 3.0 m.

9.2 Recommendations for future work.

1. To study the behaviour of inflatable dams on mobile beds to see the effect of sediment transport on the dam.

2. Construct a prototype in order to study the behaviour and performance on a large scale dam.

3. To study the effect of differences of downstream head on changing the base width of the dam for different proportional factors and different inflation fluids for static condition.

4. To study the effect of varying hydrostatic and hydrodynamic pressure on the fabric over long periods of time.

5. To study the effect of vibration in detail and to locate the zone of the vibration of the dam and to devise a means of eliminating this.

6. To study other forms of inflatable dams which might be used such as a series of tyre inner tubes, strapped bags, compartment dams.

APPENDIX A.

Equations 8.10 and 8.11 were derived from the following steps. If equation 8.5 is substituted into equation 8.8, we get the following equation

$$\frac{M^2 F_c^{\,2}}{2}(1 - \cos\theta) = y^2 - h^2 \qquad \ldots\ldots \qquad 8.37$$

dividing by M^2 and substitute with the equivalent value of F_c, equation 8.37 can be written

$$y/M = \sqrt{1 - \frac{F_c^{\,2}}{2}\left(\frac{1+\cos\theta}{2}\right)} \qquad \ldots\ldots \qquad 8.38$$

Before going further it is necessary to write the following geometry equations

$$\text{Sin}\,\frac{\lambda}{2} = \sqrt{\frac{1-\cos\lambda}{2}} \qquad \ldots\ldots \qquad 8.39$$

$$\text{Sin}^2\,\frac{\lambda}{2} = \frac{1-\cos\lambda}{2} \qquad \ldots\ldots \qquad 8.40$$

$$\frac{dy}{dx} = \tan\theta \qquad \ldots\ldots \qquad 8.41$$

and if putting $\lambda = \pi - \theta$ 8.42

hence

$$\text{Sin}^2\,\frac{\lambda}{2} = \frac{1 - \cos(\pi-\theta)}{2}$$

or $$\text{Sin}^2\,\frac{\pi-\theta}{2} = \frac{1+\cos\theta}{2} \qquad \ldots\ldots \qquad 8.43$$

if putting $(\pi-\theta)/2 = \phi$

$$\text{Sin}^2\,\phi = \frac{1+\cos\theta}{2} \qquad \ldots\ldots \qquad 8.44$$

Hence equation 8.38 can be written in the following form

$$y/H_D = (1+\alpha)\sqrt{1-F_c^2 \sin^2\phi} \quad \ldots\ldots \quad 8.42$$

Substitute equation 8.42 into equation 8.3 and 8.4 and we get

$$T/\rho g \sin\theta \, d\theta = (1+\alpha)H_D \sqrt{1-F_c^2\sin^2\phi} \quad \frac{\sin\theta}{\cos\theta} \, dx \quad \ldots\ldots \quad 8.43$$

$$\text{or} \qquad \frac{dx}{M} = \frac{F_c^2 \cos\theta \, d\theta}{4\sqrt{1-F_c^2 \sin^2\phi}} \quad \ldots\ldots \quad 8.44$$

From the equation, $\phi = \frac{\pi-\theta}{2}$

or $2\phi = \pi - \theta, \quad \theta = \pi - 2\theta$

$2d\phi = -d\theta, \quad \cos\theta = -\cos 2\phi$

equation 8.44 can be written in the following form

$$\frac{dx}{M} = \frac{2 F_c^2 \cos 2\phi \, d\phi}{4\sqrt{1-F_c^2 \sin^2\phi}} = \frac{F_c^2 (1-2\sin^2\phi)}{2\sqrt{1-F_c^2\sin^2\phi}} \, d\phi$$

$$\frac{1}{M}\int_0^{B_2} dx = \frac{F_c^2}{2}\int_{\pi/2}^{o} \frac{1-2\sin^2\phi}{\sqrt{1-F_c^2\sin^2\phi}} \, d\phi \quad \ldots\ldots \quad 8.44$$

$$\frac{1}{M}\int_0^{B_2} dx = \frac{F_c^2}{2}\int_{\pi/2}^{o} \frac{d\phi}{\sqrt{1-F_c^2\sin^2\phi}} - F_c^2 \int_{\pi/2}^{o} \frac{\sin^2\phi}{\sqrt{1-F_c^2\sin^2\phi}} \, d\phi \quad \ldots. \quad 8.45$$

$$\frac{1}{M}\int_0^{B_2} dx = -\frac{F_c^2}{2}\int_{o}^{\pi/2} \frac{d\phi}{\sqrt{1-F_c^2\sin^2\phi}} - F_c^2 \int_{o}^{\pi/2} \frac{\sin^2\phi}{\sqrt{1-F_c^2\sin^2\phi}} \, d\phi \quad \ldots\ldots \quad 8.46$$

From Appendix (C)

$$B_2/M = \frac{F_c^2}{2}\,\hat{F} + \hat{F}_c^2\left(\frac{\hat{F}-\hat{E}}{F_c^2}\right) \qquad \ldots\ldots \qquad 8.47$$

$$\text{or} \quad \frac{B_2}{H_D} = (1+\alpha)\left(1 - \frac{F_c^2}{2}\right)\hat{F} - \hat{E} \qquad \ldots\ldots \qquad 8.48$$

If apply the following geometry equations

$$\frac{ds}{dx} = \sec \qquad \ldots\ldots \qquad 8.50$$

and from the equation 8.44 we can arrange the following equation

$$\frac{ds}{M} = \frac{F_c^2 \cos^2\phi \, d\phi}{2\sqrt{1-F_c^2 \sin^2\phi}} \quad \text{Sec}\theta \qquad \ldots\ldots \qquad 8.51$$

From the relation between θ and ϕ the equation 8.51 can be written in the following form,

$$\frac{1}{M}\int_0^{S_2} ds = \int_{\pi/2}^{0} \frac{F_c^2 \sin^2\phi \, d\phi}{2\sqrt{1 - F_c^2 \sin^2\phi}} \times \frac{1}{(-\cos\phi)}$$

$$\text{or} \quad \frac{1}{M}\int_0^{S_2} ds = \int_0^{\pi/2} \frac{F_c^2}{2} \frac{d\phi}{\sqrt{1 - F_c^2 \sin^2\phi}} \qquad \ldots\ldots \qquad 8.52$$

and from Appendix (C) equation 8.52 can be written

$$S_2/H_D = \frac{1+\alpha}{2} F_c^2 (\hat{F}) \qquad \ldots\ldots \qquad 8.53$$

APPENDIX B.

FLUID FORCES

The fluid forces that are considered here are those acting on a fluid element whose mass = ρL^3, area = L^2, length = L and velocity = (L/T).

1. Inertia force F_i = (mass)(acceleration) = $(\rho L^3)\ (\frac{L}{T^2})$

$$= \rho L^2\ (\frac{L^2}{T^2}) = \rho L^2 V^2$$

2. Viscous force F_u = (viscous shear stress)(shear area)

$$\tau = L^2 = \mu\rho \frac{du}{dy}\ L^2 = \mu\ (\frac{V}{L})\ L^2 = \mu LV$$

3. Gravity force F_a = (mass) (acceleration due to gravity)

$$= (\rho L^3)\ (g) = \rho L^3 g$$

4. Pressure force F_p = (pressure)(area) pL^2

5. Elastic force F_e = (modulus of elasticity)(area) = EL^2

6. Surface tension force F_σ = (surface tension)(length) = σL

If all fluid forces were acting on a fluid element,

$$F_r = \frac{Fi_m + Fu_m + Fa_m + Fp_m + Fe_m + F\sigma_m}{Fi_p + Fu_p + Fa_p + Fp_p + Fe_p + F\sigma_p}$$

Fortunately in most practical engineering problems, not all of the six forces are involved because they may not be acting, maybe of negligible magnitude or some may be in opposition to each other in such a way as to compensate.

Rouse (45) observed at least 90% of hydraulic model studies the forces connected with surface tension and elastic compression are relatively small and can be neglected. For all practical purposed, therefore, a

particular state of fluid motion can usually be simulated in a model by considering that either gravity forces or viscous forces predominate.

Problems in open channel flow involving overflow and underflow structures (i.e., spillways, diversion dams, sluiceways) it is customary to preserve complete geometric similarity and model heads are adjusted to the values required from equating the ratio of gravitational forces to that of inertial forces and neglecting the other forces.

$$\frac{(Fa)m}{(Fa)p} = \frac{(M'a)m}{(M'a)p}$$

These are the criteria that need to be adopted in considering the relationship between a model and prototype inflatable hydraulic structure.

APPENDIX C.

Elliptic Integrals.

1. Normal elliptic integral of first kind

$$F(F_c, \phi) = \int_0^{\phi} \frac{d\phi}{\sqrt{1 - F_c^2 \sin^2 \theta}} \qquad 0 < F_c < 1$$

2. Complete elliptic integrals of first kind

$$\hat{F}(F_c) = \int_0^{\pi/2} \frac{d\phi}{\sqrt{1 - F_c^2 \sin\phi^2}}$$

3. Normal elliptic integral of second kind.

$$E(F_c, \phi) = \int_0^{\phi} \sqrt{1 - F_c^2 \sin^2\phi} \; d\phi, \quad 0 < F_c < 1$$

4. Complete elliptic integral of second kind

$$\hat{E}(F_c) = \int_0^{\pi/2} \sqrt{1 - F_c^2 \sin^2 \phi} \; d\phi$$

REFERENCES

(1) Connor, L.J. "Fabridam - Their application on flood mitigation project in New South Wales". Journal, Aug. Nat. Committee on large dams, Vol.29, 1969, pp.56-65.

(2) Anwar, H.O. "Inflatable dams". Proc. A.S.C.E., Vol.93, No. Hy3, May 1967, pp.99-115.

(3) Kunihiro Owiwara, et al., "A study on the shape of the Rubber Dam". Transactions of Institute of Civil Engineering, Japan, No. 178, July,1970.

(4) Harrison, H.B. "The analysis and behaviour of inflatable membrane dam under static load". Proc. Inst.Civil Eng. Vol.45, April,1970, pp.661-676.

(5) Binnie, A.M. "The theory of flexible dam inflated by water pressure. Journal of Hydraulic Research, Vol.11, No. 1, 1973.

(6) Parbery, R.D. "A continuous method of analysis for the inflatable dam". Proc.Inst. Civil Eng., part 2, vol.61, Dec.1976, pp.725-736.

(7) Alwan, A.D. "The analysis and design of the inflatable dam". Ph.D. Thesis, University of Sheffield, 1979.

(8) Shepherd, E.M., et al. "The Fabridam extension on Koomboloomba dam of the Tully falls Hydro-electric power project". The Journal of the Institution of Engineers, Australia, Jan.-Feb. 1969, vol.41.

(9) Binnie, G.M. et al. "Inflatable weir used during construction of Mangala Dam". Proceedings I.C.E., Nov. 1973, Vol.54, pp.625-639.

(10) Construction News. 'Inflatable barrage saves low country water table". Construction News, Oct. 15, 1970.

(11) N.R.D.C. News. National Research Development Corporation, 20 July, 1976.

(12) Flexible Structures in Synthetic fabric. Flexible Structures Ltd. A member of the Environmental Division of Leigh Interests Limited.

(13) Imberston, N.M. "Collapsible dam aids Los Angeles water supply". Journal of Civil Engineers, Sept. 1960, pp.42044.

(14) Clare, H.J. "Design of fabric dams". Ph.D. Thesis, University of Liverpool, Oct.1972.

(15) Schofield, A. "A parachute to tame the tide". New Scientist, 8 Oct. 1970, pp.66, Vol.48.

(16) Fabridam General Report, April 23, 1964.

(17) Fenstermacher, Ted "A look at the Inflatable Dam". Report Oct. 1963, Pennsylvania Angler.

(18) Water and Water Engineering "New collapsible dam of Dutch design". Water and Water Engineering, Oct. 1969.

(19) Firestone Tyre & Rubber Co. of California. Fabridam Installation in Los Gatos Creek for the San Jose Water Work, San Jose, California.

(20) Baker, P.J. Model test on a proposed flexible fabric dam for the Mangala Scheme, Pakistan. The British Hydromechanics Research Association, RR 803, March, 1964.

(21) Stodulka, A.M. "The design and analysis of inflatable dams". Thesis submitted to the University of Sydney for the degree of Master of Engineering.

(22) Parbery, R.D. "Factor affecting the membrane dam inflated by air pressure". Proc.Inst.Eng., part 2, Vol.65, Sept. 1978, pp.645-654.

(23) Southwell, R.V. "Theory of elasticity", 1936, p.430, Oxford, Clarendon Press.

(24) Abromowiz, M., et al. Handbook of mathematical functions, 1965, New York, Dover.

(25) Fish, D.C.E. Personal Correspondence. Thos. Hudson (Birmingham) Ltd., Dorset, England.

(26) Butyle Product Ltd. Personal Correspondence.

(27) British Standard, 3424, 1973, "Determination of breaking load breaking extension".

(28) British Standard, 3411, 1971, "Determination of the tensile properties of individual textile fibres".

(29) British Standard, 2576, 1977, "Determination of breaking strength and elongation (strip method).

(30) Willam, P.C., et al. "Engineering for dam", New York, John Wiley & Sons.

(31) Whittaker, E., Robinson, G. "The calculus of observation". Fourth Edition, Blackie and Son.

(32) O'Brien, W.T., Francis, A.J. "Cable movement under two dimensional load". Journal of Structural Div. Proc. A.M.Soc. Civil Eng. 90 No. ST3, pp.-9-123, June 1964.

(33) Harrison, H.B. "Suspension cable movement analysis". The Institution of Engineers, Australia, paper No. 2887, 29th Dec. 1964.

(34) Harrison, H.B. "Computer Method in Structural Analysis".

(35) Harrison, H.B. "The analysis and behaviour of inflatable membrane dam under static loading". (Discussion). Proc. paper No. 7279, pp.131-139.

(36) Henderson,F.M "Open channel flow". The Macmillan Company, New York.

(37) Stodulka, A.M. (Discussion) "A continuous method of analysis of the inflatable dam". Proc. Inst.Engineers, part 2, 1977, Sept. pp.713-714.

(38) Jaeger, C. Engineering Fluid Mechanics, Blackie and Son.

(39) British Standards, 3680 "Method of measurement of liquid flow in open channel", part 4 "Weir and flumes open channel hydraulics".

(40) Chow Ven-Te Open Channel Hydraulics.

(41) Hickoy, G.H. "Areation of spillway". Proc. A.S.C.E., Vol.109, Dec. 1942, pp.537-556.

(42) Langhaar, H.L. "Dimensional analysis and theory of models", New York, John Wiley and Son, 1951.

(43) Rao, S. Shukla "Characteristics of flow over weirs of finite crest width". HY Proc. of A.S.C.E., Nov. 1971.

(44) Skogerboe, U., et al. "Discussion" "Inflatable dam". HY1 Jan. 1968, pp.321-325.

(45) Chawla, C. A Course in Engineering Mathematics.

(46) Rous, H. "Engineering Hydraulics", June, 1949.

(47) Vaughan, John "Strain Measurement", Oct. 1975.

(48) Murdock J.W. Fluid Mechanics and its application.